INL/EXT-19-56215

Light Water Reactor Sustainability Program

Evaluation of the Benefits of ATF, FLEX, and Passive Cooling System for an Enhanced Resilient PWR Model

October 2019

U.S. Department of Energy

Office of Nuclear Energy

INL/EXT-19-56215

Evaluation of the Benefits of ATF, FLEX, and Passive Cooling System for an Enhanced Resilient PWR Model

Zhegang Ma[1], Cliff Davis[1], Carlo Parisi[1], Ryan Dailey[2], Jun Wang[2], Sai Zhang[1], Hongbin Zhang[1], Michael Corradini[2]

[1]Idaho National Laboratory, Idaho Falls, Idaho 83415

[2]University of Wisconsin, Madison, Wisconsin 53706

October 2019

Prepared for the
U.S. Department of Energy
Office of Nuclear Energy

EXECUTIVE SUMMARY

This report, along with report INL/EXT-19-53556 published in August 2019, documents the activities performed by Idaho National Laboratory (INL) during the fiscal year (FY) 2019 for the Department of Energy (DOE) Light Water Reactor Sustainability (LWRS) Program, Risk-Informed System Analysis (RISA) Pathway, Enhanced Resilient Plant (ERP) Systems research. The purpose of the RISA Pathway research and development is to support plant owner-operator decisions with the aim to improve the economics, reliability, and maintain the high levels of safety of current nuclear power plants over periods of extended plant operations. The concept of ERP refers to the combinations of Accident Tolerant Fuel (ATF), optimal use of Diverse and Flexible Coping Strategy (FLEX), enhancements to plant components and systems, and the incorporation of augmented or new passive cooling systems, as well as improved fuel cycle efficiency. The objective of the ERP research effort is to use the RISA methods and toolkit in industry applications, including methods development and early demonstration of technologies, in order to enhance existing reactors' safety features (both active and passive) and to substantially reduce operating costs through risk-informed approaches to plant design modifications to the plant and their characterization.

Compared with the analysis documented in INL/EXT-19-53556, this report includes additional accident scenarios for risk-informed ATF analysis, and examines the risk impacts and benefits of FLEX and passive cooling system on nuclear power plants (NPPs) from other perspectives. The same analysis process, risk analysis approaches, and analysis tools as in FY 2018 were used for near-term ATF cladding (i.e., Iron-Chromium-Aluminum [FeCrAl] cladding and Chromium [Cr]-coated cladding) designs under the small-break loss-of-coolant accident (SBLOCA or SLOCA) including SBLOCA with anticipated transient without scram (ATWS) scenarios, two types of general transients (locked rotor and turbine trip) including locked rotor with ATWS scenarios, and main steam line break (MSLB) scenarios. For benchmarking purpose, University of Wisconsin compared the ATF station blackout (SBO) analysis results using RELAP5-3D as in the FY 2018 report INL/EXT-18-51436 with the results using MELCOR for the same SBO scenarios. In addition, based on the generic probabilistic risk assessment (PRA) model, the risk impacts and benefits of FLEX and the dynamic natural convection (DNC) system on NPPs are evaluated through a case study with the risk-informed decision-making process, i.e., significance determination process (SDP).

In the ATF SBLOCA analysis, eight SBLOCA scenarios were developed based on the generic SAPHIRE PRA model for a Westinghouse three-loop pressurized water reactor (PWR) used in previous ERP analysis, and analyzed using RELAP5-3D for thermal hydraulic analysis with traditional fuel design and near-term ATF designs. The RELAP5-3D simulation results, as presented in Tables ES-1 and ES-2, show that the gain in coping time for FeCrAl varies between 2 and 36 minutes, except for Scenario SBLOCA-2.0 where the gain in coping time is more than 3 hours. The average increase in coping time with the Cr-coated cladding, which is also referred to as Chromite or chromium, is about 3 minutes. A slightly better estimate of the gain in coping time can be obtained by subtracting the time to core uncovery from the time to core damage and averaging. Using this metric, the gain in coping time is about 16 minutes for FeCrAl and 4 minutes for Chromite when Scenario SBLOCA-2.0 is excluded. With these relatively small increases of the time to core damage, the risk benefit to the core damage frequency (CDF) brought by the ATF designs would be very small and was therefore not conducted in this analysis. However, the RELAP5-3D simulation results show the clear benefit in adopting ATFs with much less hydrogen produced at the time of core damage. The SBLOCA with ATWS scenarios are exceptions in that the hydrogen production with the ATF claddings can exceed that with Zircaloy because of longer heatup times. Excluding the ATWS scenarios, the average hydrogen production with FeCrAl was 6.4% of that with Zircaloy. The average hydrogen production with Chromite was 36.9% of that with Zircaloy.

Table ES-1. Time to Core Damage Comparison for SBLOCA Scenarios with ATF Designs.

Scenario	Description	Time to core damage (hr:min)				
		Zircaloy	FeCrAl	Δt (FeCrAl)	Chromite	Δt (Chromite)
SBLOCA-1.0	SBLOCA with AFW, SSC, and HPSI	11:31	11:33	0:02	11:17	-0:14
SBLOCA-1.1	SBLOCA with AFW and HPSI, but no SSC	9:29	10:05	0:36	9:41	0:12
SBLOCA-2.0	SBLOCA with AFW and SSC, but no HPSI	0:59	4:37	3:38	1:05	0:06
SBLOCA-2.1	SBLOCA with AFW, but no SSC and no HPSI	0:58	1:14	0:16	1:02	0:04
SBLOCA-3.0	SBLOCA with no AFW and no FAB	1:01	1:13	0:12	1:07	0:06
SBLOCA-3.1	SBLOCA with FAB, but no AFW	9:44	10:12	0:28	9:36	-0:08
SBLOCA-4.0	SBLOCA with ATWS and no AFW	0:42	0:49	0:07	0:41	-0:01
SBLOCA-4.1	SBLOCA with ATWS and AFW	4:06	4:25	0:19	4:23	0:17

Table ES-2. H_2 Production Comparison for SBLOCA Scenarios with ATF Designs.

Scenario	Description	Total H_2 (kg)			H_2 %	
		Zircaloy	FeCrAl	Chromite	FeCrAl	Chromite
SBLOCA-1.0	SBLOCA with AFW, SSC, and HPSI	10.1	0.7	6.0	6.5	59.3
SBLOCA-1.1	SBLOCA with AFW and HPSI, but no SSC	13.7	1.3	5.8	9.8	42.6
SBLOCA-2.0	SBLOCA with AFW and SSC, but no HPSI	21.2	1.5	7.9	7.1	37.2
SBLOCA-2.1	SBLOCA with AFW, but no SSC and no HPSI	23.9	0.8	9.7	3.3	40.5
SBLOCA-3.0	SBLOCA with no AFW and no FAB	29.7	0.7	9.7	2.5	32.8
SBLOCA-3.1	SBLOCA with FAB, but no AFW	13.9	1.2	1.2	8.9	8.7
SBLOCA-4.0	SBLOCA with ATWS and no AFW	19.8	25.8	14.7	130.6	74.2
SBLOCA-4.1	SBLOCA with ATWS and AFW	33.8	36.8	35.8	108.9	106.0

In the ATF general transient with locked rotor analysis, 10 scenarios were developed based on the generic SAPHIRE PRA model, and analyzed using RELAP5-3D for thermal hydraulic analysis with traditional fuel design and near-term ATF designs. The RELAP5-3D simulation results, as presented in Tables ES-3 and ES-4, show that, on average, the gain in coping time is about 14 minutes for FeCrAl and 7 minutes for Chromite. A slightly better estimate of the gain in coping time can be obtained by subtracting the time to core uncovery from the time to core damage and averaging. Using this metric, the gain in coping time increases to about 16 minutes for FeCrAl and 9 minutes for Chromite. By either measure, the gain in coping time with the ATF designs is modest for the locked rotor scenarios. These tables do not include results from ATWS-1, because the failure was due to high RCS pressure, rather than core damage due to high cladding temperature. With the above relatively small increase of the time to core damage from the RELAP5-3D simulation results, a change to the general transient PRA model (event tree, fault tree, success criteria, or human reliability analysis) is not warranted. The risk benefit on behalf of the CDF brought by the ATF designs would be very small and is not conducted in this analysis. However, the RELAP5-3D

results show a clear benefit in adopting the ATF designs, as much less hydrogen is produced at the time of core damage. The one exception is scenario LOSC-480, where the hydrogen production with FeCrAl is about 80% of that with Zircaloy. However, this result is atypical, because the calculation with Zircaloy was terminated due to severe cladding ballooning rather than maximum cladding temperature. Consequently, the Zircaloy cladding did not reach temperatures as high as those with FeCrAl, which resulted in less hydrogen production than typical for Zircaloy. Excluding scenario LOSC-480, the average hydrogen production with FeCrAl was 3.5% of that with Zircaloy. The average hydrogen production with Chromite was 14.9% of that with Zircaloy.

Table ES-3. Time to Core Damage Comparison for Locked Rotor Scenarios with ATF Designs.

Scenario	Description	Time to core damage (hr:min)				
		Zircaloy	FeCrAl	Δt (FeCrAl)	Chromite	Δt (Chromite)
TRANS-1	General transient, no FW, no HPSI	2:30	2:38	0:08	2:34	0:04
TRANS-2	General transient, no FW, HPSI	14:35	14:41	0:06	14:37	0:02
PORV-1	PORV LOCA with AFW	2:18	2:26	0:08	2:21	0:03
LOSC-182a	RCP seal LOCA, 182 gpm, AFW, SSC	13:26	13:23	-0:03	13:33	0:07
LOSC-182b	RCP seal LOCA, 182 gpm, AFW, no SSC	9:55	10:16	0:21	10:19	0:24
LOSC-76	RCP seal LOCA, 76 gpm, AFW, SSC	13:09	13:38	0:29	13:23	0:14
LOSC-480	RCP seal LOCA, 480 gpm, AFW, SSC	5:46	6:20	0:34	5:51	0:05
ATWS-2	No reactor trip, no AFW	1:17	1:26	0:09	1:21	0:04
ATWS-3	No reactor trip, AFW	2:32	2:46	0:13	2:36	0:04

Table ES-4. H2 Production Comparison for Locked Rotor Scenarios with ATF Designs.

Scenario	Description	Total H_2 (kg)			H_2 %	
		Zircaloy	FeCrAl	Chromite	FeCrAl	Chromite
TRANS-1	General transient, no FW, no HPSI	72.9	1.5	0.7	2.0	1.0
TRANS-2	General transient, no FW, HPSI	108.1	1.9	11.0	1.8	10.2
PORV-1	PORV LOCA with AFW	23.3	2.0	6.5	8.5	27.9
LOSC-182a	RCP seal LOCA, 182 gpm, AFW, SSC	57.7	1.9	16.0	3.3	27.7
LOSC-182b	RCP seal LOCA, 182 gpm, AFW, no SSC	33.1	2.1	8.5	6.3	25.7
LOSC-76	RCP seal LOCA, 76 gpm, AFW, SSC	91.9	1.7	13.5	1.8	14.7
LOSC-480	RCP seal LOCA, 480 gpm, AFW, SSC	0.9	0.7	0.2	81.8	22.7
ATWS-2	No reactor trip, no AFW	88.3	1.5	8.2	1.7	9.3
ATWS-3	No reactor trip, AFW	80.2	1.9	2.1	2.4	2.6

In the ATF general transient with turbine trip analysis, the same seven scenarios developed in the locked rotor analysis other than the three ATWS scenarios were analyzed using RELAP5-3D for thermal hydraulic analysis with traditional fuel design and near-term ATF designs. Both turbine trip and locked rotor are modeled in PRA as general transients with similar plant responses. Turbine trip with ATWS scenarios are

not analyzed as the responses of the ATWS scenarios following locked rotor event and turbine trip event would be similar. The RELAP5-3D simulation results, as presented in Tables ES-5 and ES-6, show that, on average, the gain in coping time is about 13 minutes for FeCrAl. For Chromite, the average loss in coping time is about 2 minutes. A better estimate of the gain in coping time can be obtained by subtracting the time to core uncovery from the time to core damage and averaging. Using this metric, the gain in coping time increases to about 18 minutes for FeCrAl and 6 minutes for Chromite. The gain in coping time with the ATF designs is modest for the turbine trip scenarios. With the above relatively small increase of the time to core damage from the RELAP5-3D simulation results, a change to the general transient PRA model (event tree, fault tree, success criteria, or human reliability analysis) is not warranted. The risk benefit on behalf of the CDF brought by the ATF designs would be very small and is not conducted in this analysis. However, the RELAP5-3D results show a clear benefit in adopting the ATF designs, as much less hydrogen is produced at the time of core damage. The one exception is scenario LOSC-480, where the hydrogen production with FeCrAl is about 75% of that with Zircaloy. However, this result is atypical, as explained in the above paragraph for locked rotor scenario analysis results. Excluding scenario LOSC-480, the average hydrogen production with FeCrAl was 4.1% of that with Zircaloy. The average hydrogen production with Chromite was 16.9% of that with Zircaloy.

Table ES-5. Time to Core Damage Comparison for Turbine Trip Scenarios with ATF Designs.

Scenario	Description	Time to core damage (hr:min)				
		Zircaloy	FeCrAl	Δt (FeCrAl)	Chromite	Δt (Chromite)
TRANS-1	General transient, no FW, no HPSI	2:25	2:32	0:07	2:27	0:02
TRANS-2	General transient, no FW, HPSI	14:51	14:49	-0:02	14:25	-0:26
PORV-1	PORV LOCA with AFW	3:14	3:23	0:09	3:16	0:02
LOSC-182a	RCP seal LOCA, 182 gpm, AFW, SSC	12:49	13:17	0:28	13:01	0:12
LOSC-182b	RCP seal LOCA, 182 gpm, AFW, no SSC	9:37	9:54	0:17	9:44	0:07
LOSC-76	RCP seal LOCA, 76 gpm, AFW, SSC	13:00	13:15	0:15	13:08	0:08
LOSC-480	RCP seal LOCA, 480 gpm, AFW, SSC	6:03	6:17	0:14	5:46	-0:17

Table ES-6. H2 Production Comparison for Turbine Trip Scenarios with ATF Designs.

Scenario	Description	Total H_2 (kg)			H_2 %	
		Zircaloy	FeCrAl	Chromite	FeCrAl	Chromite
TRANS-1	General transient, no FW, no HPSI	90.1	1.5	1.8	1.7	2.0
TRANS-2	General transient, no FW, HPSI	100.6	2.7	2.3	2.7	2.3
PORV-1	PORV LOCA with AFW	18.9	1.4	5.9	7.3	31.0
LOSC-182a	RCP seal LOCA, 182 gpm, AFW, SSC	57.3	1.7	16.6	3.0	29.0
LOSC-182b	RCP seal LOCA, 182 gpm, AFW, no SSC	30.3	2.1	8.9	6.9	29.4
LOSC-76	RCP seal LOCA, 76 gpm, AFW, SSC	83.3	2.7	6.2	3.2	7.5
LOSC-480	RCP seal LOCA, 480 gpm, AFW, SSC	1.0	0.7	0.2	75.0	17.7

In the ATF MSLB analysis, as the generic SAPHIRE PWR model does not include MSLB event, three MSLB scenarios were developed based on information from deterministic safety analysis report instead of PRA inputs, and analyzed using RELAP5-3D for thermal hydraulic analysis with traditional fuel design and near-term ATF designs. The analysis showed that no safety thresholds were violated for all the three different types of claddings. Both departure from nucleate boiling ratio and the clad temperature of the hot rod clad were well below the safety limits. Therefore, no differences have been found in terms of MSLB safety performance between the standard Zircaloy clad and the other near-term ATF claddings.

In the ATF benchmark calculations, University of Wisconsin compared its SBO analysis results using MELCOR to the INL results using RELAP5-3D. Table ES-7 lists the key event timing information from the two codes for Zircaloy cladding under different SBO scenarios. For scenario SBO-7.0, MELCOR and RELAP5-3D produced different timing results for certain parameters; e.g., core water level. It is likely that there exists a difference in certain initial conditions that affects these results. In addition, the observed could also be due to differences between the system code models themselves. Based on the timing behavior of key events (SG water depletion and pressure, core water level), it is surmised that the differences exist in the initial SG inventory, in SG heat transfer, as well as in the flow out of the safety relief valves. Such differences can likely lead to notable differences in the timing of core heatup, peak clad temperatures, and the start of rapid hydrogen generation and so on. To be able to ascertain the root cause of the differences, more information on the RELAP5-3D results need to be acquired and analyzed. For scenario SBO-1.0, the thermal-hydraulic parameter histories, including pressures, core water level, peak cladding temperature, and hydrogen mass were quite similar before 8 hours. This is because the cooling from secondary side is still similar and the events are mostly affected by the accident assumptions. Following the 4-hour window of operability, the differences first arise in the system pressures and then core water inventory. This again leads to the surmise of differences in initial conditions and the system code model differences in flow from the safety relief valves and core and steam generator heat transfer. For scenario SBO-1.3, the events were also similar before 12 hours, when the secondary side can still provide cooling. After this point, RELAP5-3D and MELCOR simulation timing of events diverged for the same key parameters. RELAP5-3D predicted that key events (pressure rise, core water depletion) occurred two to three hours earlier than those predicted by MELCOR. Similar to the SBO 1.0 case, the SBO 1.3 case sees RELAP5-3D predicting core heatup and degradation earlier than in the simulation compared to MELCOR.

Table ES-7. Key Event List Comparison between RELAP5-3D and MELCOR

Event	SBO 1.0 (hr:min)		SBO 1.3 (hr:min)		SBO 7.0 (hr:min)	
	RELAP5-3D	MELCOR	RELAP5-3D	MELCOR	RELAP5-3D	MELCOR
Initiating event – LOOP and failure of the onsite emergency AC power systems	0:00	0:00	0:00	0:00	0:00	0:00
Reactor trip, MSIVs close, RCP seals initially leak at 21 gpm/pump (~1 kg/s)	0:00	0:00	0:00	0:00	00:00	0:00
TDAFW auto initiates at full flow	0:01	0:00	0:01	0:00	N/A	N/A
Operators control AFW to maintain level	0:15	0:15	0:15	0:15	N/A	N/A
First SG SRV opening	0:25	0:04	0:25	0:04	00:06	0:03
Operator performs controlled cooldown of secondary at ~100 F/hr (~55.5 C/hr)	1:30	1:30	1:30	1:30	N/A	N/A
Accumulators begin to inject	2:30	2:25	2:30	2:25	N/A	3:42

Secondary pressure reduced to ~0.9 MPa	3:40	3:46	3:40	3:46	N/A	N/A
DC batteries depleted	4:00	4:00	8:00	8:00	N/A	N/A
SG water depletion	8:16	10:22	12:57	16:14	1:06	1:20
System re-pressurize, pressurizer SRV opens	9:01	11:20	13:34	17:14	1:16	N/A
RPV water level decreases with core uncovery	9:30	12:16	14:28	18:24	1:53	2:19
Core damage	10:32	15:58	15:40	22:44	2:34	4:58

In the ATF benchmark calculation, comparison was also conducted for different cladding designs under the same SBO scenario. As expected, the histories of thermal hydraulic parameters (such as primary pressure, secondary-side pressure, core water level, peak cladding temperature) were initially similar, but there are some differences, particularly in the timing of the core water level and the rate of hydrogen generation. The core water level in the RELAP simulations began to fall below the top of active fuel sooner, resulting in earlier hydrogen generation production. Since no safety systems operate, the rate of water loss from the safety relief valves in the primary system is likely different between the two codes. This needs to be investigated further and seems to drive the later behavior.

In the FLEX analysis, the risk impact and benefits of FLEX was evaluated through conducting an SDP analysis. As a case study, an emergency diesel generator (EDG) is assumed as failed to start and inoperable for nine days. The FLEX SDP analysis results show that the incremental conditional core damage probability (ICCDP) for the event would be 1.36E-6 without FLEX implementation, which would be a white finding for the SDP case. With FLEX implementation, the ICCDP would be decreased to 9.38E-7, which would be a green finding for the case. Also, the maximum days of being inoperable to remain within SDP color zone thresholds are calculated. The results show that by implementing FLEX strategies, 3 additional days could be gained before the event reaches the white zone threshold (1E-6), and 30 additional days could be gained before crossing the yellow zone threshold (1E-5). Such gains could allow more time for plant staff to repair or replace the inoperable equipment, and thus keep the safety significance of this degradation condition in a level as low as possible. The gains could lead to both safety and economic benefits: if not entering a more severe SDP color zone, the plant can be maintained at a safer state while substantial regulatory efforts and associated costs in inspection and investigation can be avoided.

In the passive cooling system analysis, the risk impact and benefits of the DNC system designed by DYNAC Systems was evaluated through conducting a similar SDP analysis. The same case study for FLEX was applied for the DNC system. The DNC SDP analysis results show that while the ICCDP for the event would still be 1.36E-6 and a white finding without DNC implementation, the ICCDP would be decreased to 5.48E-7 and a green finding with DNC implementation. Also, the maximum days of being inoperable to remain within SDP color zone thresholds are calculated. The results show that by replacing the auxiliary feedwater system with the DNC system, 10 additional days could be gained before crossing the white zone threshold (1E-6), and 98 additional days could be gained before crossing the yellow zone threshold (1E-5). Similar to the implications from the FLEX SDP results, such gains could lead to both safety and economic benefits; i.e., allowing more time for repair or replacement of the inoperable equipment, and avoiding the regulatory efforts in inspection and investigation as well as associated costs.

CONTENTS

EXECUTIVE SUMMARY iii

FIGURES xi

TABLES xviii

ACRONYMS xx

1. INTRODUCTION 1

2. ATF EVALUATION 2
   2.1 SBLOCA Scenario Analysis 2
      2.1.1 SBLOCA PRA Model and Scenarios 2
      2.1.2 SBLOCA RELAP5-3D Model 6
      2.1.3 SBLOCA RELAP5-3D Analysis 6
         2.1.3.1 SBLOCA-1.0 6
         2.1.3.2 SBLOCA-1.1 12
         2.1.3.3 SBLOCA-2.0 18
         2.1.3.4 SBLOCA-2.1 23
         2.1.3.5 SBLOCA-3.0 28
         2.1.3.6 SBLOCA-3.1 32
         2.1.3.7 SBLOCA-4.0 38
         2.1.3.8 SBLOCA-4.1 42
      2.1.4 SBLOCA Analysis Results 47
   2.2 General Transient – Locked Rotor Scenario Analysis 50
      2.2.1 General Transient PRA Model and Scenarios 50
      2.2.2 Locked Rotor RELAP5-3D Model 57
      2.2.3 Locked Rotor RELAP5-3D Analysis 57
         2.2.3.1 TRANS-1 58
         2.2.3.2 TRANS-2 63
         2.2.3.3 PORV-1 69
         2.2.3.4 LOSC-182a 75
         2.2.3.5 LOSC-182b 80
         2.2.3.6 LOSC-76 85
         2.2.3.7 LOSC-480 91
         2.2.3.8 ATWS-1 97
         2.2.3.9 ATWS-2 103
         2.2.3.10 ATWS-3 108
      2.2.4 Locked Rotor Analysis Results 115
   2.3 General Transient – Turbine Trip Scenario Analysis 117
      2.3.1 General Transient PRA Model and Scenarios 117
      2.3.2 Turbine Trip RELAP5-3D Model 117
      2.3.3 Turbine Trip RELAP5-3D Analysis 117
         2.3.3.1 TRANS-1 117
         2.3.3.2 TRANS-2 121
         2.3.3.3 PORV-1 127
         2.3.3.4 LOSC-182a 133
         2.3.3.5 LOSC-182b 138

2.3.3.6 LOSC-76 143
2.3.3.7 LOSC-480 148
2.3.4 Turbine Trip Analysis Results 154
2.4 MSLB Scenario Analysis 156
2.4.1 MSLB PRA Model and Scenarios 156
2.4.2 MSLB RELAP5-3D Model 156
2.4.3 MSLB RELAP5-3D Analysis 157
2.4.3.1 MSLB-HFP 158
2.4.3.2 MSLB-HZP-1 163
2.4.3.3 MSLB-HZP-2 169
2.4.4 MSLB Analysis Results 174
2.5 Benchmark Calculations between RELAP5-3D and MELCOR 175
2.5.1 SBO MELCOR Model 175
2.5.2 SBO MELCOR Analysis 176
2.5.2.1 SBO-7.0 177
2.5.2.2 SBO-1.0 178
2.5.2.3 SBO-1.3 179
2.5.3 Comparison Between RELAP5-3D and MELCOR Results 180
2.5.3.1 Comparison of Key Event Lists 180
2.5.3.2 Comparison of Different Scenarios for Zircaloy 181
2.5.3.3 Comparison of a Single Scenario for Three Cladding Designs 184
2.5.3.4 Summary 186

3. FLEX EVALUATION 187
3.1 Overview of FLEX PRA 187
3.2 FLEX Risk Impact – SDP Case 188
3.2.1 Overview of SDP 188
3.2.2 FLEX SDP Analysis 188

4. PASSIVE COOLING SYSTEM EVALUATION 190
4.1 Overview of DNC System PRA 190
4.2 DNC System Risk Impact – SDP Case 191

5. CONCLUSIONS AND FUTURE WORK 192

6. REFERENCES 194

FIGURES

Figure 2-1. Generic PWR SLOCA event tree for SBLOCA. 3
Figure 2-2. Mass flow rate through the break (SBLOCA-1.0). 8
Figure 2-3. Pressure in the pressurizer (SBLOCA-1.0). 8
Figure 2-4. Void fraction at the break (SBLOCA-1.0). 9
Figure 2-5. Collapsed liquid level in the central core channel (SBLOCA-1.0). 9
Figure 2-6. Maximum cladding temperature (SBLOCA-1.0). 10
Figure 2-7. Total HPSI flow into the RCS (SBLOCA-1.0). 10
Figure 2-8. Liquid volume in Accumulator B (SBLOCA-1.0) 11
Figure 2-9. Pressure in SG B (SBLOCA-1.0). 11
Figure 2-10. Collapsed liquid level in SG B (SBLOCA-1.0). 12
Figure 2-11. Mass flow rate through the break (SBLOCA-1.1). 14
Figure 2-12. Pressure in the pressurizer (SBLOCA-1.1). 14
Figure 2-13. Void fraction at the break (SBLOCA-1.1). 15
Figure 2-14. Collapsed liquid level in the central core channel (SBLOCA-1.1). 15
Figure 2-15. Maximum cladding temperature (SBLOCA-1.1). 16
Figure 2-16. Total HPSI flow into the RCS (SBLOCA-1.1). 16
Figure 2-17. Liquid volume in Accumulator B (SBLOCA-1.1) 17
Figure 2-18. Pressure in SG B (SBLOCA-1.1). 17
Figure 2-19. Collapsed liquid level in SG B (SBLOCA-1.1). 18
Figure 2-20. Mass flow rate through the break (SBLOCA-2.0). 20
Figure 2-21. Pressure in the pressurizer (SBLOCA-2.0). 20
Figure 2-22. Collapsed liquid level in the central core channel (SBLOCA-2.0). 21
Figure 2-23. Maximum cladding temperature (SBLOCA-2.0). 21
Figure 2-24. Liquid volume in Accumulator B (SBLOCA-2.0) 22
Figure 2-25. Pressure in SG B (SBLOCA-2.0). 22
Figure 2-26. Collapsed liquid level in SG B (SBLOCA-2.0). 23
Figure 2-27. Mass flow rate through the break (SBLOCA-2.1). 24
Figure 2-28. Pressure in the pressurizer (SBLOCA-2.1). 25
Figure 2-29. Collapsed liquid level in the central core channel (SBLOCA-2.1). 25
Figure 2-30. Maximum cladding temperature (SBLOCA-2.1). 26
Figure 2-31. Liquid volume in Accumulator B (SBLOCA-2.1) 26
Figure 2-32. Pressure in SG B (SBLOCA-2.1). 27
Figure 2-33. Collapsed liquid level in SG B (SBLOCA-2.1). 27

Figure 2-34. Mass flow rate through the break (SBLOCA-3.0). 29
Figure 2-35. Pressure in the pressurizer (SBLOCA-3.0). 29
Figure 2-36. Collapsed liquid level in the central core channel (SBLOCA-3.0). 30
Figure 2-37. Maximum cladding temperature (SBLOCA-3.0). 30
Figure 2-38. Liquid volume in Accumulator B (SBLOCA-3.0). 31
Figure 2-39. Pressure in SG B (SBLOCA-3.0). 31
Figure 2-40. Collapsed liquid level in SG B (SBLOCA-3.0). 32
Figure 2-41. Mass flow rate through the break (SBLOCA-3.1). 34
Figure 2-42. Void fraction at the break (SBLOCA-3.1). 34
Figure 2-43. Pressure in the pressurizer (SBLOCA-3.1). 35
Figure 2-44. Collapsed liquid level in the central core channel (SBLOCA-3.1). 35
Figure 2-45. Maximum cladding temperature (SBLOCA-3.1). 36
Figure 2-46. Total HPSI flow into the RCS (SBLOCA-3.1). 36
Figure 2-47. Liquid volume in Accumulator B (SBLOCA-3.1). 37
Figure 2-48. Collapsed liquid level in SG B (SBLOCA-3.1). 37
Figure 2-49. Mass flow rate through the break (SBLOCA-4.0). 39
Figure 2-50 Reactor power (SBLOCA-4.0). 39
Figure 2-51. Pressure in the pressurizer (SBLOCA-4.0). 40
Figure 2-52. Collapsed liquid level in the central core channel (SBLOCA-4.0). 40
Figure 2-53. Maximum cladding temperature (SBLOCA-4.0). 41
Figure 2-54. Pressure in SG B (SBLOCA-4.0). 41
Figure 2-55. Collapsed liquid level in SG B (SBLOCA-4.0). 42
Figure 2-56. Mass flow rate through the break (SBLOCA-4.1). 43
Figure 2-57. Reactor power (SBLOCA-4.1). 44
Figure 2-58. Pressure in the pressurizer (SBLOCA-4.1). 44
Figure 2-59. Collapsed liquid level in the central core channel (SBLOCA-4.1). 45
Figure 2-60. Maximum cladding temperature (SBLOCA-4.1). 45
Figure 2-61. Liquid volume in Accumulator B (SBLOCA-4.1). 46
Figure 2-62. Pressure in SG B (SBLOCA-4.1). 46
Figure 2-63. Collapsed liquid level in SG B (SBLOCA-4.1). 47
Figure 2-64. Generic PWR TRANS event tree for general transient. 51
Figure 2-65. Generic PWR LOSC event tree – transfer from TRANS. 52
Figure 2-66. Generic PWR ATWS event tree – transfer from TRANS. 53
Figure 2-67. Generic PWR MLOCA event tree – transfer from TRANS&LOSC with 480 gpm/RCP. 54

Figure 2-68. Collapsed liquid level in SG A (TRANS-1). 59
Figure 2-69. Collapsed liquid level in SG B (TRANS-1). 60
Figure 2-70. Pressure in SG A (TRANS-1). 60
Figure 2-71. Pressure in SG B (TRANS-1). 61
Figure 2-72. Pressure in the pressurizer (TRANS-1). 61
Figure 2-73. Collapsed liquid level in the pressurizer (TRANS-1). 62
Figure 2-74. Collapsed liquid level in the central core channel (TRANS-1). 62
Figure 2-75. Maximum cladding temperature (TRANS-1). 63
Figure 2-76. Collapsed liquid level in SG B (TRANS-2). 65
Figure 2-77. Pressure in SG B (TRANS-2). 65
Figure 2-78. Total HPSI flow into the RCS (TRANS-2). 66
Figure 2-79. Containment spray (TRANS-2). 66
Figure 2-80. Pressure in the pressurizer (TRANS-2). 67
Figure 2-81. Collapsed liquid level in the pressurizer (TRANS-2). 67
Figure 2-82. Collapsed liquid level in the central core channel (TRANS-2). 68
Figure 2-83. Maximum cladding temperature (TRANS-2). 68
Figure 2-84. Mass flow rate through the pressurizer PORV (PORV-1). 71
Figure 2-85. Pressure in the pressurizer (PORV-1). 71
Figure 2-86. Collapsed liquid level in the pressurizer (PORV-1). 72
Figure 2-87, Collapsed liquid level in the central core channel (PORV-1). 72
Figure 2-88. Maximum cladding temperature (PORV-1). 73
Figure 2-89. Pressure in SG B (PORV-1). 73
Figure 2-90. Collapsed liquid level in SG B (PORV-1). 74
Figure 2-91. AFW flow rate to SG B (PORV-1). 74
Figure 2-92. Mass flow rate through the seals of RCP B (LOSC-182a). 76
Figure 2-93. Pressure in the pressurizer (LOSC-182a). 77
Figure 2-94. Collapsed liquid level in the pressurizer (LOSC-182a). 77
Figure 2-95, Collapsed liquid level in the central core channel (LOSC-182a). 78
Figure 2-96. Maximum cladding temperature (LOSC-182a). 78
Figure 2-97. Pressure in SG B (LOSC-182a). 79
Figure 2-98. Collapsed liquid level in SG B (LOSC-182a). 79
Figure 2-99. AFW flow rate to SG B (LOSC-182a). 80
Figure 2-100. Mass flow rate through the seals of RCP B (LOSC-182b). 81
Figure 2-101. Pressure in the pressurizer (LOSC-182b). 82
Figure 2-102. Collapsed liquid level in the pressurizer (LOSC-182b). 82

Figure 2-103. Collapsed liquid level in the central core channel (LOSC-182b). 83
Figure 2-104. Maximum cladding temperature (LOSC-182b). 83
Figure 2-105. Pressure in SG B (LOSC-182b). 84
Figure 2-106. Collapsed liquid level in SG B (LOSC-182). 84
Figure 2-107. AFW flow rate to SG B (LOSC-182b). 85
Figure 2-108. Mass flow rate through the seals of RCP B (LOSC-76). 87
Figure 2-109. Pressure in the pressurizer (LOSC-76). 88
Figure 2-110. Collapsed liquid level in the pressurizer (LOSC-76). 88
Figure 2-111. Collapsed liquid level in the central core channel (LOSC-76). 89
Figure 2-112. Maximum cladding temperature (LOSC-182a). 89
Figure 2-113. Pressure in SG B (LOSC-76). 90
Figure 2-114. Collapsed liquid level in SG B (LOSC-76). 90
Figure 2-115. AFW flow rate to SG B (LOSC-76). 91
Figure 2-116. Mass flow rate through the seals of RCP B (LOSC-480). 93
Figure 2-117. Pressure in the pressurizer (LOSC-480). 93
Figure 2-118. Collapsed liquid level in the pressurizer (LOSC-480). 94
Figure 2-119, Collapsed liquid level in the central core channel (LOSC-480). 94
Figure 2-120. Maximum cladding temperature (LOSC-480). 95
Figure 2-121. Pressure in SG B (LOSC-480). 95
Figure 2-122. Collapsed liquid level in SG B (LOSC-480). 96
Figure 2-123. AFW flow rate to SG B (LOSC-480). 96
Figure 2-124. Flow rate in the cold leg of Loop A (ATWS-1). 98
Figure 2-125. Total flow rate at the vessel inlet (ATWS-1). 98
Figure 2-126. Power-squared weighted average moderator temperature (ATWS-1). 99
Figure 2-127. Reactor power (ATWS-1). 99
Figure 2-128. Power-squared weighted average fuel temperature (ATWS-1). 100
Figure 2-129. Pressure in the pressurizer (ATWS-1). 100
Figure 2-130. Collapsed liquid level in the pressurizer (ATWS-1). 101
Figure 2-131, Collapsed liquid level in the central core channel (ATWS-1). 101
Figure 2-132. Maximum cladding temperature (ATWS-1). 102
Figure 2-133. Pressure in SG B (ATWS-1). 102
Figure 2-134. Collapsed liquid level in SG B (ATWS-1). 103
Figure 2-135. Reactor power (ATWS-2). 104
Figure 2-136. Power-squared weighted average moderator temperature (ATWS-2). 105
Figure 2-137. Pressure in the pressurizer (ATWS-2). 105

Figure 2-138. Collapsed liquid level in the pressurizer (ATWS-2). 106
Figure 2-139, Collapsed liquid level in the central core channel (ATWS-2). 106
Figure 2-140. Maximum cladding temperature (ATWS-2). 107
Figure 2-141. Pressure in SG B (ATWS-2). 107
Figure 2-142. Collapsed liquid level in SG B (ATWS-2). 108
Figure 2-143. Reactor power (ATWS-3). 110
Figure 2-144. Power-squared weighted average moderator temperature (ATWS-3). 110
Figure 2-145. Pressure in the pressurizer (ATWS-3) 111
Figure 2-146. Collapsed liquid level in the pressurizer (ATWS-3). 111
Figure 2-147, Collapsed liquid level in the central core channel (ATWS-3). 112
Figure 2-148. Maximum cladding temperature (ATWS-3). 112
Figure 2-149. Pressure in SG B (ATWS-3). 113
Figure 2-150. Collapsed liquid level in SG B (ATWS-3). 113
Figure 2-151. Total AFW flow rate to SG B (ATWS-3). 114
Figure 2-152. Pressure in SG B (TRANS-1). 119
Figure 2-153. Collapsed liquid level in SG B (TRANS-1). 119
Figure 2-154. Pressure in the pressurizer (TRANS-1). 120
Figure 2-155. Collapsed liquid level in the pressurizer (TRANS-1). 120
Figure 2-156. Collapsed liquid level in the central core channel (TRANS-1). 121
Figure 2-157. Maximum cladding temperature (TRANS-1). 121
Figure 2-158. Pressure in SG B (TRANS-2). 123
Figure 2-159. Collapsed liquid level in SG B (TRANS-2). 123
Figure 2-160. Total HPSI flow into the RCS (TRANS-2) 124
Figure 2-161. Containment spray (TRANS-2) 124
Figure 2-162. Pressure in the pressurizer (TRANS-2). 125
Figure 2-163. Collapsed liquid level in the pressurizer (TRANS-2). 125
Figure 2-164. Collapsed liquid level in the central core channel (TRANS-2). 126
Figure 2-165. Maximum cladding temperature (TRANS-2). 126
Figure 2-166. Mass flow rate through the pressurizer PORV (PORV-1). 129
Figure 2-167. Pressure in the pressurizer (PORV-1). 129
Figure 2-168. Collapsed liquid level in the pressurizer (PORV-1). 130
Figure 2-169. Collapsed liquid level in the central core channel (PORV-1). 130
Figure 2-170. Maximum cladding temperature (PORV-1). 131
Figure 2-171. Pressure in SG B (PORV-1). 131
Figure 2-172. Collapsed liquid level in SG B (PORV-1). 132

Figure 2-173. AFW flow rate to SG B (PORV-1). 132
Figure 2-174. Mass flow rate through the seals of RCP B (LOSC-182a). 134
Figure 2-175. Pressure in the pressurizer (LOSC-182a). 135
Figure 2-176. Collapsed liquid level in the pressurizer (LOSC-182a). 135
Figure 2-177. Collapsed liquid level in the central core channel (LOSC-182a). 136
Figure 2-178. Maximum cladding temperature (LOSC-182a). 136
Figure 2-179. Pressure in SG B (LOSC-182a). 137
Figure 2-180. Collapsed liquid level in SG B (LOSC-182a). 137
Figure 2-181. AFW flow rate to SG B (LOSC-182a). 138
Figure 2-182. Mass flow rate through the seals of RCP B (LOSC-182b). 139
Figure 2-183. Pressure in the pressurizer (LOSC-182b). 140
Figure 2-184. Collapsed liquid level in the pressurizer (LOSC-182b). 140
Figure 2-185. Collapsed liquid level in the central core channel (LOSC-182b). 141
Figure 2-186. Maximum cladding temperature (LOSC-182b). 141
Figure 2-187. Pressure in SG B (LOSC-182b). 142
Figure 2-188. Collapsed liquid level in SG B (LOSC-182b). 142
Figure 2-189. AFW flow rate to SG B (LOSC-182b). 143
Figure 2-190. Mass flow rate through the seals of RCP B (LOSC-76). 145
Figure 2-191. Pressure in the pressurizer (LOSC-76). 145
Figure 2-192. Collapsed liquid level in the pressurizer (LOSC-76). 146
Figure 2-193. Collapsed liquid level in the central core channel (LOSC-76). 146
Figure 2-194. Maximum cladding temperature (LOSC-182a). 147
Figure 2-195. Pressure in SG B (LOSC-76). 147
Figure 2-196. Collapsed liquid level in SG B (LOSC-76). 148
Figure 2-197. AFW flow rate to SG B (LOSC-76). 148
Figure 2-198. Mass flow rate through the seals of RCP B (LOSC-480). 150
Figure 2-199. Pressure in the pressurizer (LOSC-480). 151
Figure 2-200. Collapsed liquid level in the pressurizer (LOSC-480). 151
Figure 2-201, Collapsed liquid level in the central core channel (LOSC-480). 152
Figure 2-202. Maximum cladding temperature (LOSC-480). 152
Figure 2-203. Pressure in SG B (LOSC-480). 153
Figure 2-204. Collapsed liquid level in SG B (LOSC-480). 153
Figure 2-205. AFW flow rate to SG B (LOSC-480). 154
Figure 2-206. Modeling of MSLB on SG C. 156
Figure 2-207. Steam line nodalization for MSLB transient. 157

Figure 2-208. Total mass flow at the break (MSLB-HFP). 159
Figure 2-209. RCS average temperature (MSLB-HFP). 159
Figure 2-210. PRZ pressure (MSLB-HFP). 160
Figure 2-211. RCP-A velocity (MSLB-HFP). 160
Figure 2-212. Containment pressure (MSLB-HFP). 161
Figure 2-213. Normalized power (MSLB-HFP). 161
Figure 2-214. Reactivity (MSLB-HFP). 162
Figure 2-215. Maximum clad temperature (MSLB-HFP). 162
Figure 2-216. Hot rod DNBR at level 5 (MSLB-HFP). 163
Figure 2-217. Total mass flow at the break (MSLB-HZP-1). 164
Figure 2-218. RCS average temperature (MSLB-HZP-1). 165
Figure 2-219. PRZ pressure (MSLB-HZP-1). 165
Figure 2-220. RCP-A velocity (MSLB-HZP-1) 166
Figure 2-221. Containment pressure (MSLB-HZP-1). 166
Figure 2-222. Normalized power (MSLB-HZP-1). 167
Figure 2-223. Reactivity (MSLB-HZP-1). 167
Figure 2-224. Maximum clad temperature (MSLB-HZP-1). 168
Figure 2-225. Hot rod DNBR at level 5 (MSLB-HZP-1). 168
Figure 2-226. Total mass flow at the break (MSLB-HZP-2). 169
Figure 2-227. RCS average temperature (MSLB-HZP-2). 170
Figure 2-228. PRZ pressure (MSLB-HZP-2). 170
Figure 2-229. RCP-A velocity (MSLB-HZP-2) 171
Figure 2-230. Containment pressure (MSLB-HZP-2). 171
Figure 2-231. Normalized power (MSLB-HZP-2). 172
Figure 2-232. Reactivity (MSLB-HZP-2). 172
Figure 2-233. Maximum clad temperature (MSLB-HZP-2). 173
Figure 2-234. Hot rod DNBR at level 5 (MSLB-HZP-2). 173
Figure 2-235. Nodalization of Surry Plant (a Westinghouse three-loop PWR) by MELCOR. 176
Figure 2-236. MELCOR thermal hydraulic outputs with three cladding options (SBO 7.0). 178
Figure 2-237. MELCOR thermal hydraulic outputs with three cladding options (SBO 1.0). 179
Figure 2-238. MELCOR thermal hydraulic outputs with three cladding options (SBO 1.3). 180
Figure 2-239. Comparison between RELAP5-3D and MELCOR – Zircaloy cladding (SBO 7.0). 182
Figure 2-240. Comparison between RELAP5-3D and MELCOR – Zircaloy cladding (SBO 1.0). 183
Figure 2-241. Comparison between RELAP5-3D and MELCOR – Zircaloy cladding (SBO 1.3). 184

Figure 2-242. Comparison between RELAP5-3D and MELCOR – three cladding options (SBO 7.0). 185
Figure 4-1. Schematic of the DNC system. 190

TABLES

Table 2-1. Overview of SLOCA Event Tree Quantification Results. 2
Table 2-2. SBLOCA Scenarios for RELAP-5 3D Analysis. 5
Table 2-3. Sequence of Events for Scenario SBLOCA-1.0. 7
Table 2-4. Sequence of Events for Scenario SBLOCA-1.1 12
Table 2-5. Sequence of Events for Scenario SBLOCA-2.0. 18
Table 2-6. Sequence of Events for Scenario SBLOCA-2.1. 23
Table 2-7. Sequence of Events for Scenario SBLOCA-3.0. 28
Table 2-8. Sequence of Events for Scenario SBLOCA-3.1. 32
Table 2-9. Sequence of Events for Scenario SBLOCA-4.0. 38
Table 2-10. Sequence of Events for Scenario SBLOCA-4.1. 42
Table 2-11. Summary of RELAP5-3D Time Results for SBLOCA Scenarios with Zircaloy and ATF Claddings. 47
Table 2-12. Time to Core Damage Comparisons for SBLOCA Scenarios with ATF Designs. 48
Table 2-13. H2 Production Comparisons for SBLOCA Scenarios with ATF Designs. 49
Table 2-14. Overview of TRANS Event Trees Quantification Results. 50
Table 2-15. TRANS Scenarios for RELAP-5 3D Analysis. 56
Table 2-16. Sequence of Events for Scenario TRANS-1 58
Table 2-17. Sequence of Events for Scenario TRANS-2. 64
Table 2-18. The Effects of Feed and Bleed Cooling in Scenario TRANS-2 with Zircaloy Cladding 69
Table 2-19. Sequence of Events for Scenario PORV-1. 70
Table 2-20. Sequence of Events for Scenario LOSC-182a. 75
Table 2-21. Sequence of Events for Scenario LOSC-182b 80
Table 2-22. Sequence of Events for Scenario LOSC-76 86
Table 2-23. Sequence of Events for Scenario LOSC-480 92
Table 2-24. Sequence of Events for Scenario ATWS-1. 97
Table 2-25. Sequence of Events for Scenario ATWS-2. 103
Table 2-26. Sequence of Events for Scenario ATWS-3. 108
Table 2-27. Summary of RELAP5-3D Time Results for Locked Rotor Scenarios with Zircaloy and ATF Claddings. 115
Table 2-28. Time to Core Damage Comparisons for Locked Rotor Scenarios with ATF Designs. 116

Table 2-29. H2 Production Comparisons for Locked Rotor Scenarios with ATF Designs. 116
Table 2-30. Sequence of Events for Scenario TRANS-1..... 118
Table 2-31. Sequence of Events for Scenario TRANS-2..... 122
Table 2-32. The Effects of Feed and Bleed Cooling in Scenario TRANS-2 with Zircaloy Cladding..... 127
Table 2-33. Sequence of Events for Scenario PORV-1. 128
Table 2-34. Sequence of Events for Scenario LOSC-182a..... 133
Table 2-35. Sequence of Events for Scenario LOSC-182b..... 138
Table 2-36. Sequence of Events for Scenario LOSC-76..... 144
Table 2-37. Sequence of Events for Scenario LOSC-480..... 149
Table 2-38. Summary of RELAP5-3D Time Results for Turbine Trip Scenarios with Zircaloy and ATF Claddings. 154
Table 2-39. Time to Core Damage Comparisons for Turbine Trip Scenarios with ATF Designs. 155
Table 2-40. H2 Production Comparisons for Turbine Trip Scenarios with ATF Designs..... 155
Table 2-41. Peaking Factors for HZP and HFP. 157
Table 2-42. Sequence of Events for Scenario MSLB-HFP..... 158
Table 2-43. Sequence of Events for Scenario MSLB-HZP-1. 164
Table 2-44. Sequence of Events for Scenario MSLB-HZP-2. 169
Table 2-45. SBO Scenarios for MELCOR Analysis..... 177
Table 2-46. Key Event List of MELCOR Analysis. 177
Table 2-47. Key Event List Comparison between RELAP5-3D and MELCOR. 180
Table 3-1. SDP Color versus Safety Significance and NRC Action Matrix. 188
Table 3-2. FLEX SDP Analysis Results. 189
Table 3-3. Max Days of Being Inoperable to Remain Within SDP Color Zone Thresholds (FLEX)..... 189
Table 4-1. DNC System SDP Analysis Results. 191
Table 4-2. Max Days of Being Inoperable to Remain Within SDP Color Zone Thresholds (DNC). 191

ACRONYMS

AC	alternating current
AFW	auxiliary feedwater
ATF	accident tolerant fuel
ATWS	anticipated transient without scram
BDBEE	beyond-design-basis external event
BWR	boiling water reactor
CCF	common cause failure
CDF	core damage frequency
CRA	control rod assembly
DC	direct current
DG	diesel generator
DID	defense-in-depth
DNB	departure from nucleate boiling
DNBR	departure from nucleate boiling ratio
DNC	dynamic natural convection
DOE	Department of Energy
ECCS	emergency core cooling system
ECST	emergency condensate storage tank
EDG	emergency diesel generator
ELAP	extended loss of AC power
EPS	emergency power system
ERP	enhanced resilient plant
ERPS	enhanced resilient plant systems
FA	fuel assembly
FAB	feed and bleed
FLEX	diverse and flexible coping strategy
FSAR	final safety analysis report
FTR	failure to run
FTS	failure to start
FY	fiscal year
HEP	human error probability

HFP	hot full power
HPI	high pressure injection
HPIS	high pressure injection system
HPR	high pressure recirculation
HPSI	high pressure safety injection
HRA	human reliability analysis
HX	heat exchanger
HZP	hot zero power
ICCDP	incremental conditional core damage probability
IE	initiating event
IGPWR	INL Generic PWR
INL	Idaho National Laboratory
LBLOCA	large break loss of coolant accident
LCO	limiting condition for operation
LERF	large early release frequency
LOCA	loss of coolant accident
LOFW	loss of feedwater
LOOP	loss of offsite power
LOSC	loss of seal cooling
LPI	low pressure injection
LPR	low pressure recirculation
LTSBO	long-term station blackout
LUHS	loss of normal access to the ultimate heat sink
LWR	light water reactor
LWRS	light water reactor sustainability
MCP	main coolant pump
MDAFP	motor-driven auxiliary feedwater pump
MFW	main feedwater
MLOCA	medium-break loss-of-coolant accident
MSIV	main steam isolation valves
MSLB	main steam line break
MSPI	mitigating systems performance index
NEI	Nuclear Energy Institute
NOED	notices of enforcement discretion
NPP	nuclear power plant

NRC	Nuclear Regulatory Commission
NUREG	nuclear regulatory report
PCT	peak clad temperature
PORV	power-operated relief valve
PRA	probabilistic risk assessment
PRT	pressurizer relief tank
PRZ	pressurizer
PWR	pressurized water reactor
R&D	research and development
RCP	reactor coolant pump
RCS	reactor cooling system
RELAP5-3D	Reactor Excursion and Leak Analysis Program 5 – 3D
RHR	residual heat removal
RISA	risk-informed system analysis
RISMC	risk informed safety margin characterization
RITS	risk-informed technical specifications
RPS	reactor protection system
RPV	reactor pressure vessel
RWST	reactor water storage tank
SBO	station blackout
SBLOCA	Small-break loss-of-coolant accident
SDP	significance determination process
SG	steam generator
SGTR	steam generator rupture
SI	safety injection
SIAS	safety injection actuation signal
SRV	safety relief valve
SSC	secondary side cooldown
STSBO	short-term station blackout
TDAFP	turbine driven auxiliary feedwater pump
TDAFW	turbine driven auxiliary feedwater
TH	thermal-hydraulic
TSV	turbine stop valve
U.S.	United States

Risk-Informed Analysis for an Enhanced Resilient PWR with Additional Accident Scenarios

1. INTRODUCTION

This report, along with report INL/EXT-19-53556, Risk-Informed Analysis for an Enhanced Resilient PWR with ATF, FLEX, and Passive Cooling (Ma, et al., 2019) published in August 2019, documents the activities performed by Idaho National Laboratory (INL) during fiscal year (FY) 2019 for the U.S. Department of Energy (DOE) Light Water Reactor Sustainability (LWRS) Program, Risk-Informed Systems Analysis (RISA) Pathway, Enhanced Resilient Plant (ERP) Systems research (INL, 2018). The LWRS Program is a research and development (R&D) program that provides technical foundations for the continued operation of the nation's nuclear power plants (NPPs), develops methods to support safe and economical long-term management and operation of existing NPPs, and investigates new technologies to address enhanced NPP performance, economics, and safety. The RISA Pathway is one of the primary technical areas of R&D under the LWRS Program. This pathway supports decision-making related to economics, reliability, and safety by providing integrated plant system analysis and solutions through collaborative demonstrations to enhance economic competitiveness of operating NPPs.

One of the research efforts under the RISA Pathway is the ERP system analysis, which supports the DOE and industry initiatives including Accident Tolerant Fuel (ATF), Diverse and Flexible Coping Strategy (FLEX), and passive cooling system designs, in order to improve the safety and economic performance of the current fleet of nuclear power plants. The ATF, combined with the optimal use of FLEX, the enhancements to plant components and systems, the incorporation of augmented or new passive cooling systems, and the improved fuel cycle efficiency are called ERP Systems. The objective of the ERP research effort is to use the RISA methods and toolkit in industry applications, including methods development and early demonstration of technologies, in order to enhance existing reactors' safety features (both active and passive) and to substantially reduce operating costs through risk-informed approaches.

The purpose of the FY 2019 ERP R&D efforts is to demonstrate additional safety margins or risk benefits available to industry by integrating individual design and operational enhancements, such as near-term ATF concepts, FLEX equipment, and passive cooling systems through risk analysis for a more resilient plant. As an "add-on" project report to the first part of FY 2019 ERP efforts (Ma, et al., 2019) as documented in INL/EXT-19-53556, this report includes additional accident scenarios for risk-informed ATF analysis, and examines the risk impacts and benefits of FLEX and passive cooling systems on NPPs from additional perspectives. The same analysis process, risk analysis approaches, and analysis tools, including SAPHIRE (Smith & Wood, 2011) and RELAP5-3D (RELAP5-3D Code Development Team, 2018) codes, as in FY 2018 were used for near-term ATF cladding (i.e., Iron-Chromium-Aluminum [FeCrAl] cladding and Chromium [Cr]-coated cladding) designs under the small-break loss-of-coolant accident (SBLOCA or SLOCA) including SBLOCA with anticipated transient without scram (ATWS) scenarios, two types of general transients (locked rotor and turbine trip) including locked rotor with ATWS scenarios, and main steam line break (MSLB) scenarios. Benchmark calculations for ATF analysis using RELAP5-3D and MELCOR are also presented. In addition, based on the generic probabilistic risk assessment (PRA) model, the risk impacts and benefits of FLEX and the dynamic natural convection (DNC) system on NPPs are evaluated through a case study within a risk-informed decision-making process, i.e., significance determination process (SDP).

The remaining sections of the report are organized as below: Section 2 presents risk-informed ATF analysis for SBLOCA, general transient, and MSLB scenarios, as well as the benchmark calculations between RELAP5-3D and MELCOR. Sections 3 and 4 provide benefit analysis through SDP case study for FLEX and the DNC system, respectively. Section 5 provides a summary and the future work planning for ERP.

2. ATF EVALUATION

This section presents a risk-informed analysis on ATF with the same generic SAPHIRE PRA model and INL Generic PWR (IGPWR) RELAP5-3D model for a Westinghouse three-loop PWR used in FY 2018 activities (Ma, et al., 2018). Compared to the first part of FY 2019 activities as documented in INL/EXT-19-53556 (Ma, et al., 2019), the ATF analysis documented in this report covers the following additional accident scenarios: SBLOCA including SBLOCA with ATWS scenarios, two types of general transients (locked rotor and turbine trip) including locked rotor with ATWS scenarios, and MSLB scenarios. Also, a comparison of ATF analysis results using RELAP5-3D and MELCOR under certain station blackout (SBO) scenarios are presented. These accident scenarios are developed by reviewing the PRA model and then analyzed by RELAP5-3D code for two near-term ATF designs, i.e., FeCrAl, and Cr-coated cladding.

2.1 SBLOCA Scenario Analysis

2.1.1 SBLOCA PRA Model and Scenarios

The generic PRA model represents SBLOCA by the SLOCA event tree, as shown in Figure 2-1. The SLOCA event tree was quantified with SAPHIRE 8 using a truncation level of 1E-12. Table 2-1 presents the quantification results. The total SLOCA core damage frequency (CDF) is 7.78E-8/year. There are 7 non-zero CDF sequences out of a total of 10 SLOCA accident sequences (i.e., the sequence end state is core damage). SLOCA Sequence 3 is the most risk-significant sequence with a CDF of 6.43E-8/year and contributes 82.6% of the total SLOCA CDF. In this sequence, the reactor protection system (RPS) trips the reactor, secondary cooling and safety injection are available, primary and secondary side depressurization and cooldown are successful. Core damage, however, still occurs, as long-term cooling cannot be established. SLOCA Sequence 9 is the second-most risk-significant sequence with a CDF of 7.39E-9/year, contributing 9.5% of the total SLOCA CDF. In this sequence, core damage occurs as neither high pressure injection (HPI) nor low pressure injection (LPI) could provide makeup water to the reactor coolant system (RCS). Other significant SLOCA sequences include SLOCA Sequence 5 (contributing 3.5% of total SLOCA CDF) and Sequence 19 (contributing 3.3% of the total SLOCA CDF).

Table 2-1. Overview of SLOCA Event Tree Quantification Results.

Sequence	CDF	Cut Set Count	% CDF
SLOCA:03	6.43E-08	564	82.6%
SLOCA:05	2.87E-09	97	3.7%
SLOCA:08	0.00E+00	0	0.0%
SLOCA:09	7.39E-09	142	9.5%
SLOCA:10	1.37E-10	5	0.2%
SLOCA:13	0.00E+00	0	0.0%
SLOCA:15	0.00E+00	0	0.0%
SLOCA:17	1.55E-11	3	0.0%
SLOCA:18	5.34E-10	27	0.7%
SLOCA:19	2.57E-09	5	3.3%
SLOCA Total	7.78E-08	843	100%

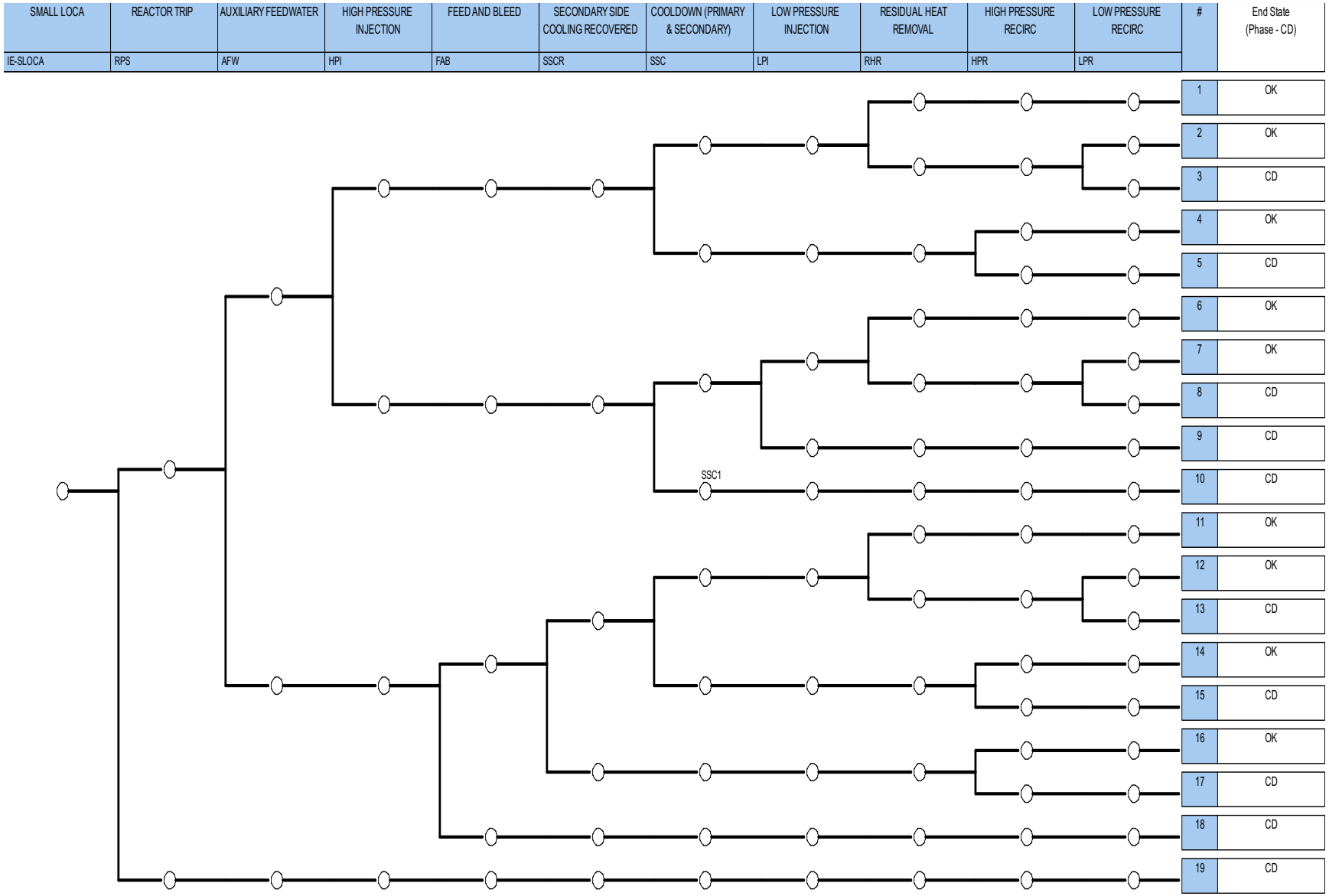

Figure 2-1. Generic PWR SLOCA event tree for SBLOCA.

The following SBLOCA scenarios were developed as input for RELAP5-3D thermal hydraulic analysis with traditional fuel design and near-term ATF designs. The scenarios can be grouped into three categories: (1) SBLOCA with auxiliary feedwater (AFW) available scenarios; (2) SBLOCA with AFW unavailable scenarios; and (3) SBLOCA with ATWS scenarios.

SBLOCA with AFW Available Scenarios

SBLOCA-1.0: This is an SBLOCA with AFW available scenario. An SBLOCA initiating event occurs, RPS trips the reactor, AFW is available to provide secondary cooling, safety injection is provided by either HPI or LPI, primary and secondary side depressurization and cooldown are successful; however, residual heat removal (RHR) and low-pressure recirculation (LPR) fail to provide long-term RCS makeup after reactor water storage tank (RWST) depletes, core damage occurs.

SBLOCA-1.1: This scenario is similar with SBLOCA-1.0, except that there is no primary- and secondary side depressurization and cooldown. Although HPI is available to provide short-term makeup to RCS, high-pressure recirculation (HPR) fails to provide long-term RCS makeup after RWST depletes, core damage occurs.

SBLOCA-2.0: This is an SBLOCA with AFW available but no safety injection (SI) scenario. An SBLOCA initiating event occurs, RPS trips the reactor, AFW is available to provide secondary cooling, primary- and secondary-side depressurization and cooldown are successful, but neither HPI nor LPI could provide safety injection function, core damage occurs with no RCS makeup.

SBLOCA-2.1: This scenario is similar with SBLOCA-2.0, except that there is no primary and secondary side depressurization and cooldown. HPI fails to provide safety injection function, core damage occurs with no RCS makeup.

SBLOCA with AFW Unavailable Scenarios

SBLOCA-3.0: This is a short-term unmitigated SBLOCA with no AFW or feed-and-bleed (FAB) scenario. An SBLOCA initiating event occurs, RPS trips the reactor, AFW is unavailable to provide secondary cooling, FAB also fails to provide mitigation, core damage occurs.

SBLOCA-3.1: This is a mitigated SBLOCA with no AFW but with successful FAB scenario. An SBLOCA initiating event occurs, RPS trips the reactor, AFW is unavailable to provide secondary cooling, FAB is successful to provide primary safety injection and secondary cooldown, but HPR fails to provide long-term RCS makeup after RWST depletes, core damage occurs.

SBLOCA with ATWS Scenarios

SBLOCA-4.0: This is an SBLOCA with ATWS scenario. An SBLOCA initiating event occurs, RPS fails to trip the reactor, no feedwater is available, and core damage is assumed.

SBLOCA-4.1: This scenario is similar with SBLOCA-4.1, except that AFW is assumed available.

Table 2-2 presents an overview of the SBLOCA scenarios developed for RELAP5-3D analysis. All scenarios would be run with RELAP5-3D, first with the current Zr-based fuel cladding design as the base case, and then with the ATF design (the FeCrAl design or the Cr-coated design). The times of peak cladding temperature (PCT) to reach melting point, the times to generate a half kilogram hydrogen, and the total amount of hydrogen generated when the run is terminated, are compared between different cladding designs for each scenario. The estimated time differences for PCT to reach melting point from RELAP5-3D are then considered for PRA model changes to evaluate the risk impacts from the proposed ATF design.

Table 2-2. SBLOCA Scenarios for RELAP-5 3D Analysis.

RELAP-5 Scenario	Scenario Description	SLOCA										ATWS
		RPS	AFW	FAB	SSCR	SSC	HPI	LPI	RHR	HPR	LPR	AFW
SBLOCA-1.0	SBLOCA with AFW	Trip	AFW			SSC	HPI		No RHR		No LPR	
SBLOCA-1.1	SBLOCA with AFW and No Depressurization	Trip	AFW			No SSC	HPI			No HPR		
SBLOCA-2.0	SBLOCA with AFW and No Safety Injection	Trip	AFW			SSC	No HPI	No LPI				
SBLOCA-2.1	SBLOCA with AFW, No Depressurization, and No Safety Injection	Trip	AFW			No SSC	No HPI					
SBLOCA-3.0	SBLOCA with No AFW and No FAB	Trip	No AFW	No FAB								
SBLOCA-3.1	SBLOCA with FAB and No AFW	Trip	No AFW	FAB	No SSCR					No HPR		
SBLOCA-4.0	SBLOCA ATWS with No AFW	No Trip										No AFW
SBLOCA-4.1	SBLOCA ATWS with AFW	No trip										AFW

2.1.2 SBLOCA RELAP5-3D Model

The same RELAP5-3D IGPWR model as in (Ma, et al., 2018) was used in this analysis. The details of this are described in (Parisi, et al., 2016). The model is based on a generic Westinghouse three-loop PWR.

2.1.3 SBLOCA RELAP5-3D Analysis

The SBLOCA was assumed to be initiated by a 2-inch diameter break in the cold leg of Loop A between the Reactor Coolant Pump (RCP) and the reactor vessel. Offsite power was assumed to be available. The early response of all the analyzed scenarios was similar. The reactor trip was initiated by low reactor pressure (12.69 MPa [1840 psia]). Reactor scram occurred 1.0 second later for those cases in which the reactor trip system was assumed to work.

Main feedwater (MFW) was assumed to terminate normally following reactor trip, delivering the equivalent of 5 seconds of full flow after the scram before coasting down to zero. The Main Steam Isolation Valves (MSIVs) in the model were assumed to close 1.0 second after the reactor scram to simulate closure of the turbine stop valves (TSVs). The SG power-operated relief valves (PORVs) were assumed to operate as necessary to control SG pressure.

For the scenarios with feedwater, one motor-driven auxiliary feedwater pump (MDAFP) was assumed to be available. The operators were assumed to control the SG levels to near the level of the feedwater ring. The injected volume of AFW never exceeded the minimum operating volume of the ECST, so AFW was not terminated due to low ECST level in any of the SBLOCA scenarios.

The safety injection actuation signal (SIAS) was initiated on low-low reactor pressure (12.34 MPa [1789.7 psia]). For the scenarios in which pumped safety injection was credited, one high pressure safety injection (HPSI) pump was assumed to be available. The high pressure safety injection was terminated when the water source for the safety injection automatically switches from the RWST to the containment sump because the automatic switch was assumed to fail. Containment spray and fan coolers were assumed to be available because the containment spray uses a significant amount of RWST water and results in an earlier loss of HPSI flow.

The RCPs were assumed to trip when average void fraction in the vicinity of the pumps exceeded 0.1. This trip could be due to a pump failure in two-phase flow or to an operator action in response to pump vibrations.

The calculations were terminated when the maximum cladding temperature reached 2099 K for cases with Zircaloy and 1804 K for cases with FeCrAl and Chromite. These temperatures were assumed to correspond to core damage.

The calculated results for the SBLOCA scenarios described in Table 2-2 are summarized in the following sections.

2.1.3.1 SBLOCA-1.0

This scenario assumed that one MDAFP and one HPSI pump were available, and that the operators manually initiated secondary side cooldown (SSC) at 30 minutes. The PORVs were opened as necessary to obtain a 56°C/hr (100°F/hr) cooldown rate in the steam generators. The cooldown was terminated when the SGs reached 0.93 MPa (134.7 psia), so that the turbine-driven AFW pumps would be available if needed. Thereafter, the PORVs opened as needed to control the SG pressure between 0.93 MPa (134.7 psia) and 1.27 MPa (184.7 psia). The HPSI was terminated when the water source for the safety injection automatically switched from the RWST to the containment sump, because the automatic switch was assumed to fail.

The calculated sequences of events are shown in Table 2-3. The break was assumed to open at 0.0 second. The reactor scram, termination of MFW, closure of the TSVs, and SIAS all occurred within the first minute. Motor-driven AFW and HPSI were initiated 30 seconds after the SIAS. The RCPs were tripped at about 9 minutes. The

operators manually initiated SSC at 30 minutes. Accumulator injection began at about 70 minutes and ended at about 140 minutes. HPSI flow was terminated at about 550 minutes when the RWST reached the level at which the automatic switchover to sump injection occurred. The core began to uncover about 80 minutes after the HPSI flow was terminated. Note that rupture was not calculated with FeCrAl cladding. Core damage occurred at about 680 minutes. The time of core damage varied by about 16 minutes among the calculations, but part of this difference is attributed to numerical causes rather than the differences between claddings. The time between when the core began to uncover and the termination of the calculations is judged to be a more reasonable measure of the effects of the claddings. The time between when the core began to uncover and core damage occurred was 52 minutes with Zircaloy, 75 minutes with FeCrAl, and 54 minutes with Chromite. The calculated amount of hydrogen produced during the transients varied significantly between claddings. The amount of hydrogen produced was 0.7 kg for FeCrAl, 6.0 kg for Chromite, and 10.1 kg for Zircaloy.

Table 2-3. Sequence of Events for Scenario SBLOCA-1.0.

	Time (hr:min)		
Event	**Zircaloy**	**FeCrAl**	**Chromite**
Break opens	0:00	0:00	0:00
Reactor scram	0:00	0:00	0:00
SIAS	0:00	0:00	0:00
RCPs tripped	0:09	0:08	0:08
High containment pressure	0:24	0:24	0:26
SSC begins	0:30	0:30	0:30
Accumulator flow initiated	1:06	1:09	1:10
Accumulator flow terminated	2:20	2:21	2:21
SSC ends	2:32	2:34	2:32
RWST switchover	9:07	9:07	9:07
Core begins to uncover	10:39	10:18	10:23
First cladding rupture	11:15	NA	10:55
0.5 kg H_2 generation	11:19	11:33	11:03
Calculated terminated	11:31	11:33	11:17

The following figures illustrate the effects of the cladding on various parameters. The mass flow through the break is illustrated in Figure 2-2. The mass flow rate responds to both the changes in pressure (Figure 2-3) and void fraction at the break (Figure 2-4). The break was venting mostly liquid for the first 30 minutes of the transient and mostly steam after 560 minutes. The pressurizer and SG pressures were closely coupled during most of the transient, which indicates that the SGs were generally removing heat from the RCS.

The break caused some voiding in the core within a few minutes of the start of the transient, as shown in Figure 2-5. The level in the core then remained roughly constant until the cover began to uncover near 620 minutes. The core began to heat up a few minutes later, as shown in Figure 2-6.

The total HPSI flow into the RCS is shown in Figure 2-7. The flow began at about 1 min in response to the SIAS on low-low pressurizer pressure. The HPSI flow was terminated at 547 minutes, when the automatic switchover to sump recirculation mode was assumed to fail. Figure 2-8 shows that the accumulators injected relatively rapidly, and nearly continuously, between about 70 and 160 minutes.

The performance of the SGs is illustrated in Figure 2-9 and Figure 2-10, which show pressure and level in the B steam generator. The SG pressure generally remained between the open and close setpoints of the PORV until SSC began at 30 minutes. The pressure then decreased until the cooldown was terminated near 150 minutes. The pressure remained roughly constant for the remainder of the transient. The SG level remained relatively high throughout the transient. AFW was still available at the end of the calculations because the ECST was not yet depleted of liquid.

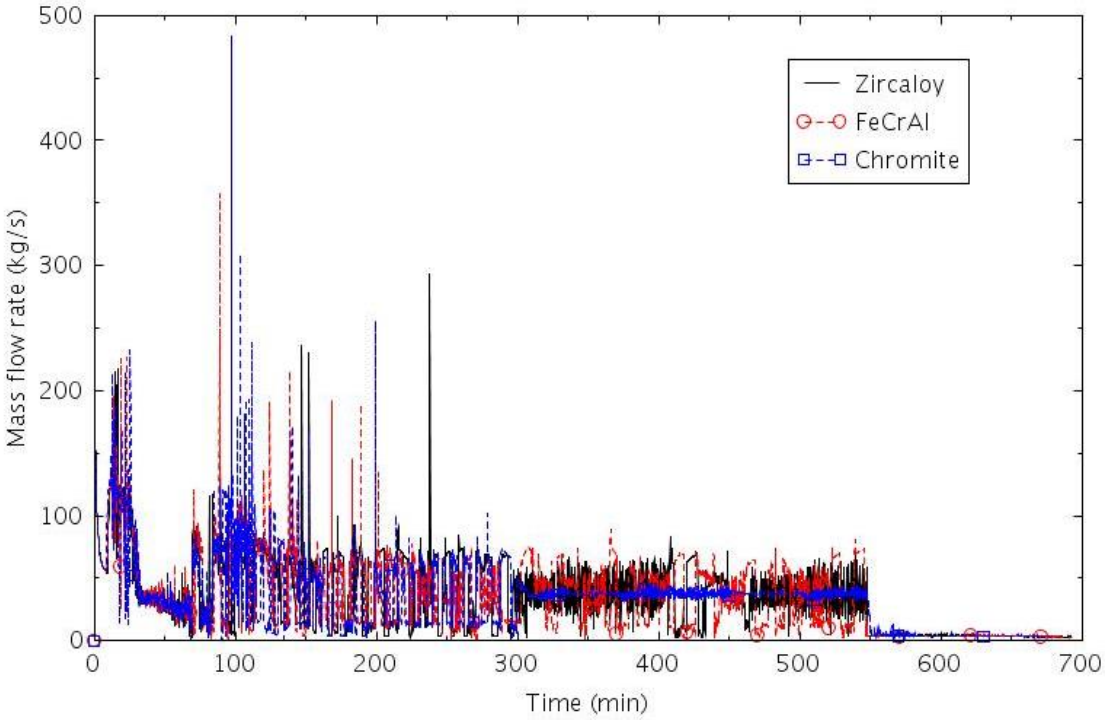

Figure 2-2. Mass flow rate through the break (SBLOCA-1.0).

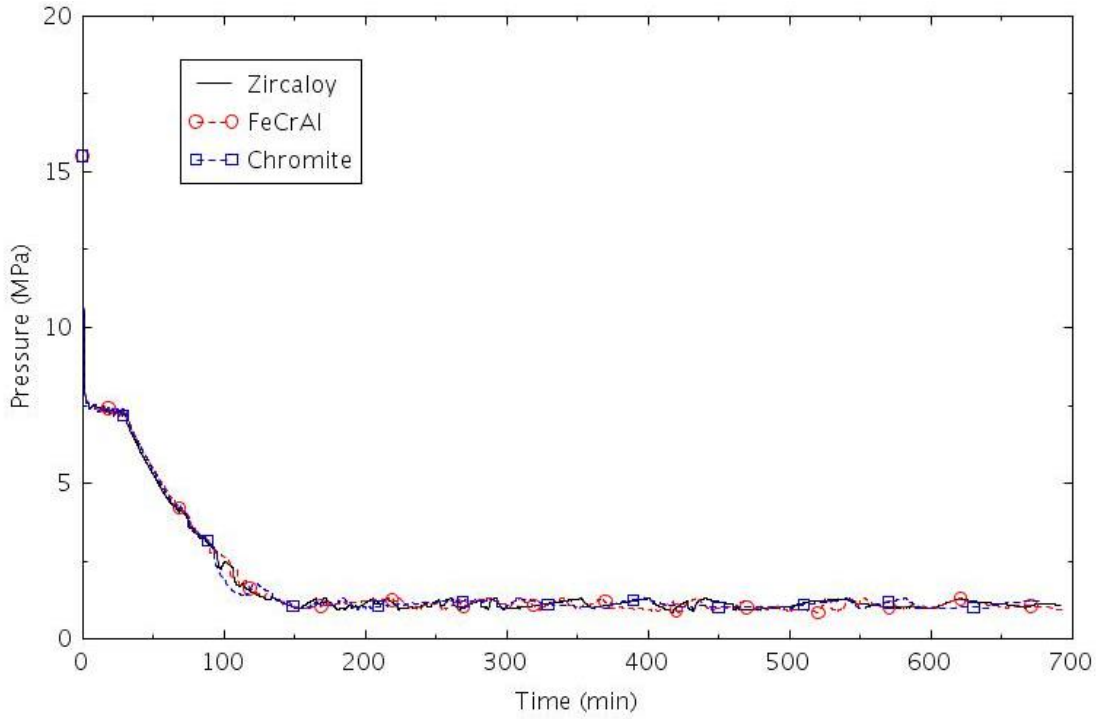

Figure 2-3. Pressure in the pressurizer (SBLOCA-1.0).

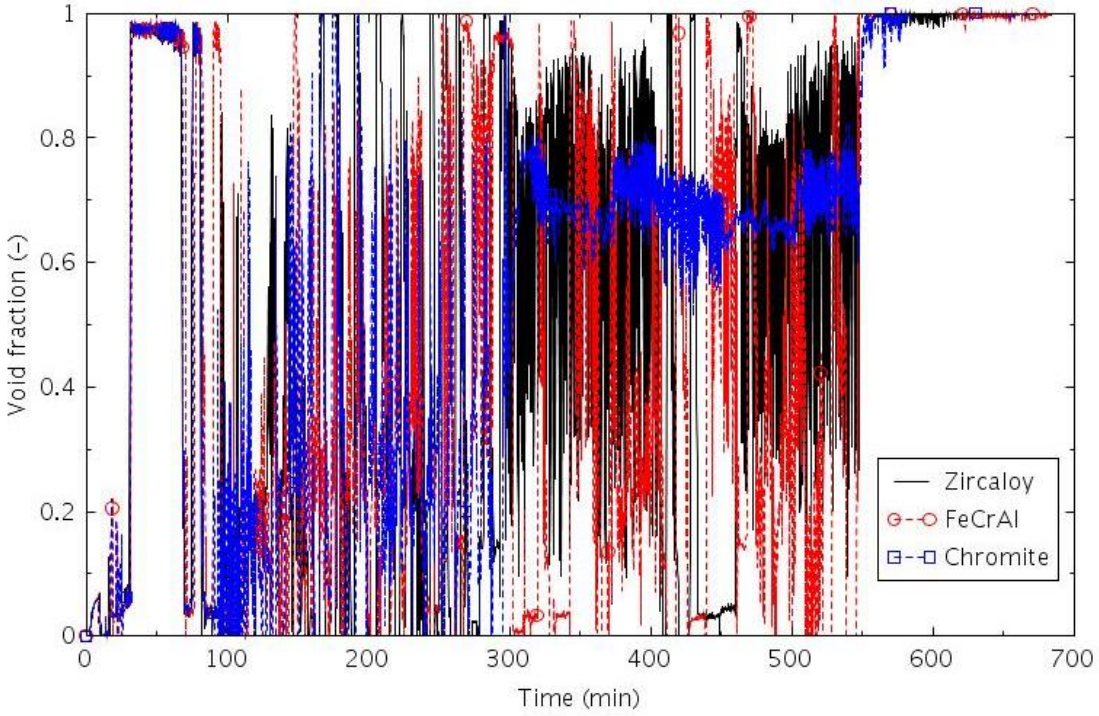

Figure 2-4. Void fraction at the break (SBLOCA-1.0).

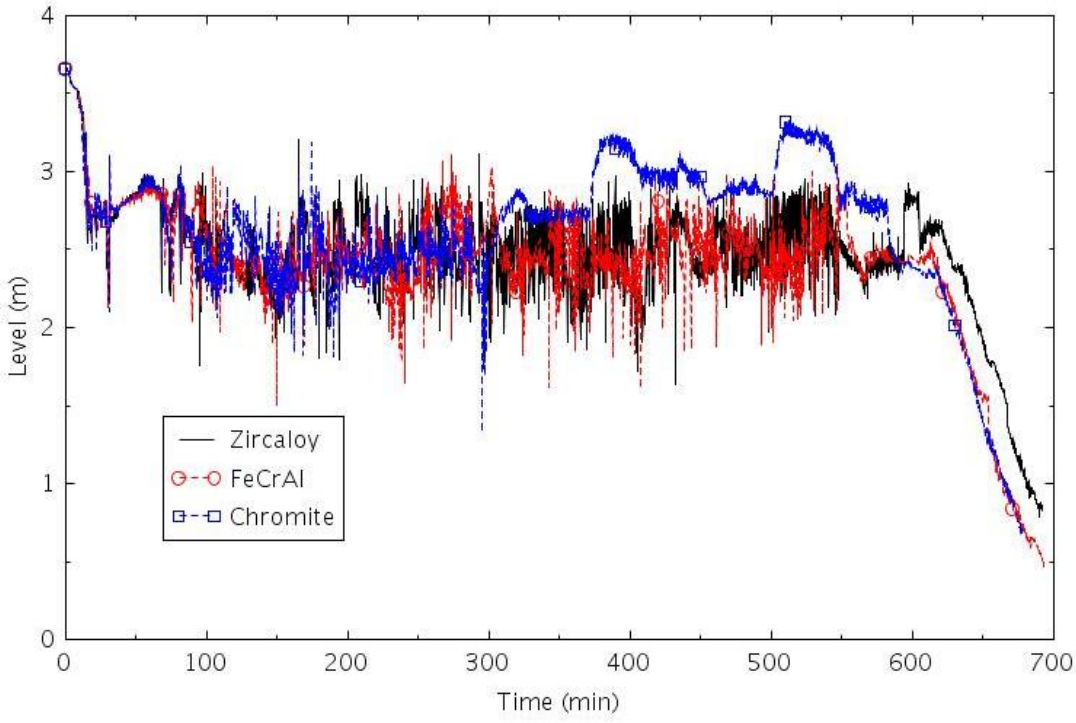

Figure 2-5. Collapsed liquid level in the central core channel (SBLOCA-1.0).

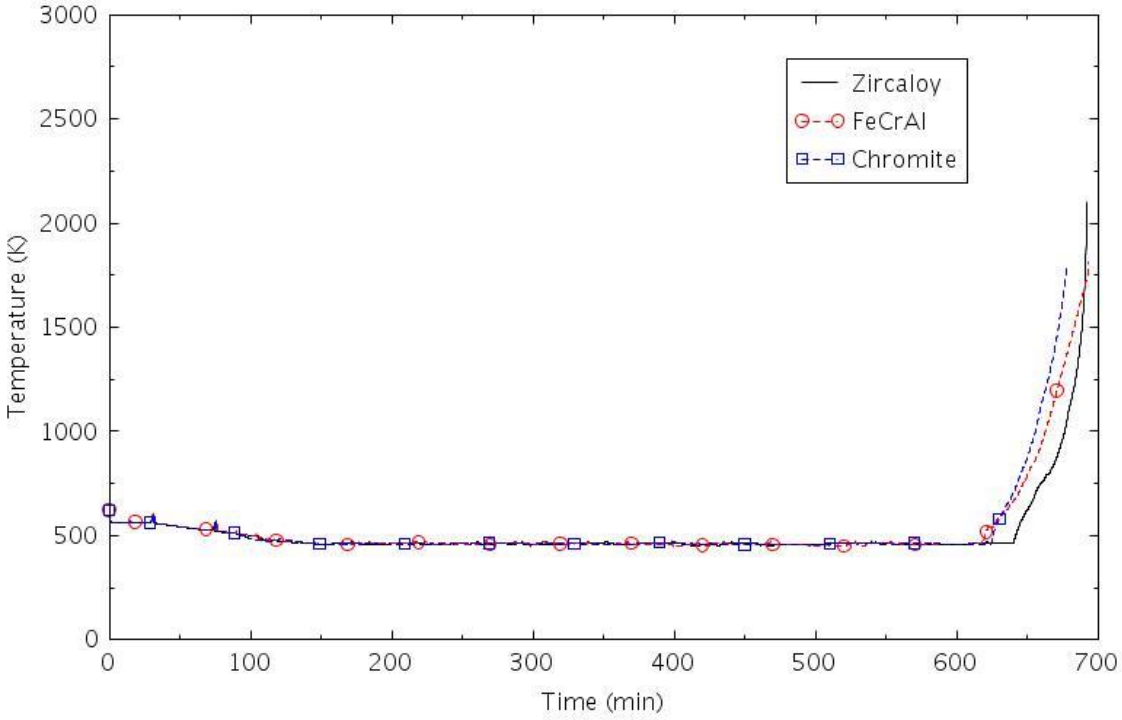

Figure 2-6. Maximum cladding temperature (SBLOCA-1.0).

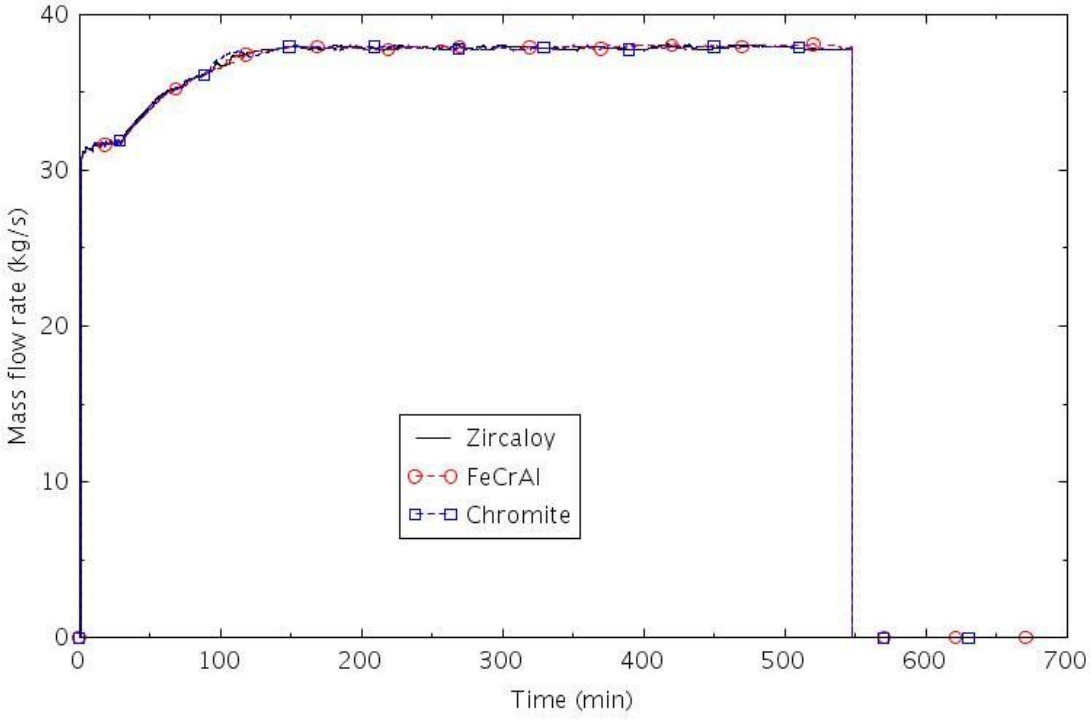

Figure 2-7. Total HPSI flow into the RCS (SBLOCA-1.0).

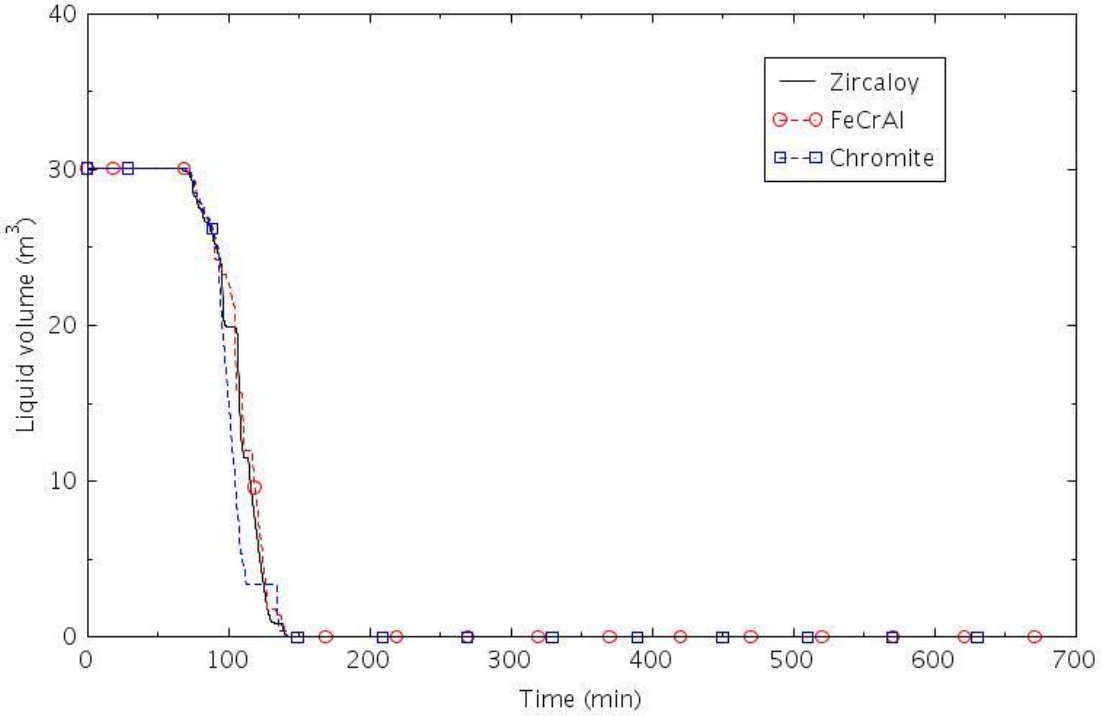

Figure 2-8. Liquid volume in Accumulator B (SBLOCA-1.0)

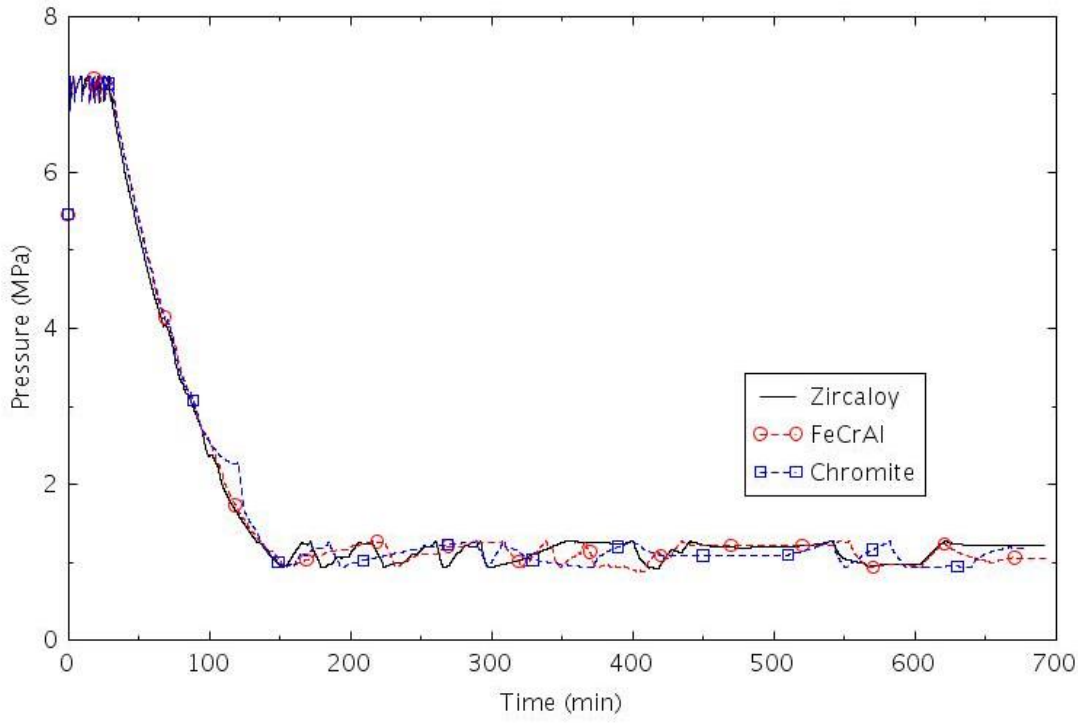

Figure 2-9. Pressure in SG B (SBLOCA-1.0).

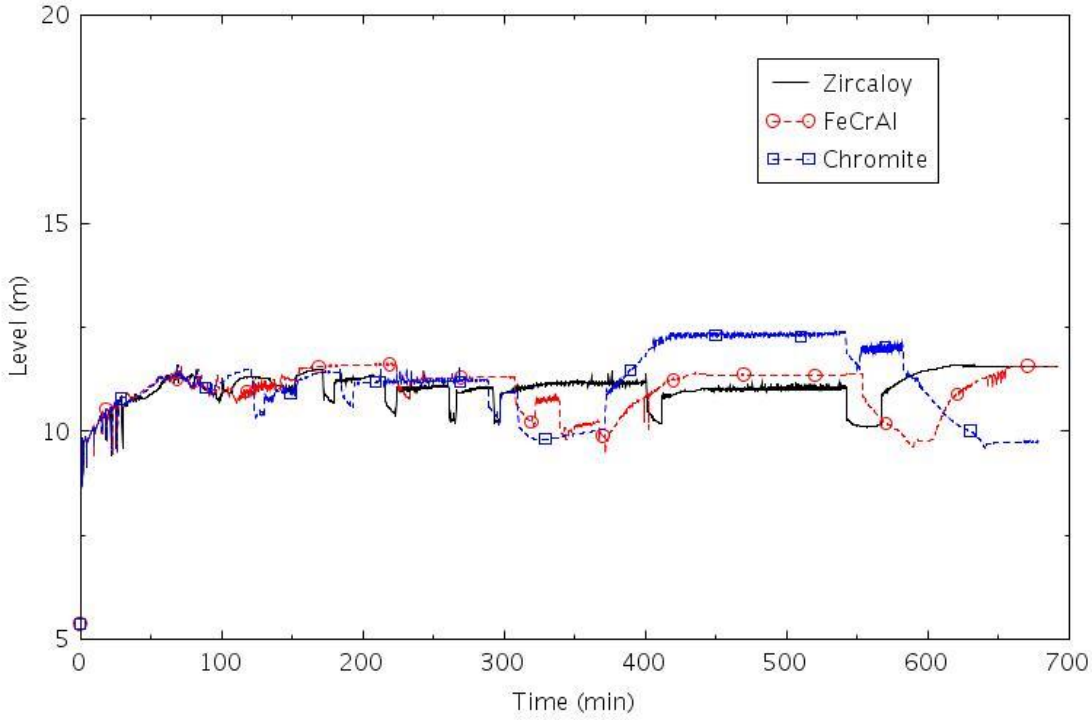

Figure 2-10. Collapsed liquid level in SG B (SBLOCA-1.0).

2.1.3.2 SBLOCA-1.1

This scenario was the same as SBLOCA-1.0, except that the operators did not manually initiate SSC.

The calculated sequences of events are shown in Table 2-4. The break was assumed to open at 0.0 second. The reactor scram, termination of MFW, closure of the TSVs, and SIAS all occurred within the first minute. Motor-driven AFW and HPSI were initiated 30 seconds after the SIAS. The RCPs were tripped at about 9 minutes. Accumulator injection began at about 90 minutes. HPSI flow was terminated at about 500 minutes, when the RWST reached the level at which the automatic switchover to sump injection occurred. The core began to uncover within an hour after the HPSI flow was terminated. Core damage occurred at about 580 minutes. The time of core damage varied by about 30 minutes among the calculations, but part of this difference is attributed to numerical causes rather than the differences between claddings. The time between the onset of core uncovery and the termination of the calculations is judged to be a more reasonable measure of the effects of the claddings. The time between when the core began to uncover and core damage occurred was 35 minutes with Zircaloy, 50 minutes with FeCrAl, and 40 minutes with Chromite. The calculated amount of hydrogen produced during the transients varied significantly between claddings. The amount of hydrogen produced was 1.3 kg for FeCrAl, 5.8 kg for Chromite, and 13.7 kg for Zircaloy.

Table 2-4. Sequence of Events for Scenario SBLOCA-1.1

	Time (hr:min)		
Event	**Zircaloy**	**FeCrAl**	**Chromite**
Break opened	0:00	0:00	0:00
Reactor scram	0:00	0:00	0:00
SIAS	0:00	0:00	0:00
RCPs tripped	0:09	0:08	0:08
High containment pressure	0:24	0:24	0:26

Accumulator flow initiated	1:30	1:30	1:33
Containment spray first actuated	3:04	3:07	3:06
RWST switchover	8:34	8:23	8:34
Core begins to uncover	8:54	9:15	9:01
First cladding rupture	9:16	9:35	9:24
0.5 kg H_2 generation	9:17	10:05	9:30
Calculated terminated	9:29	10:05	9:41

The following figures illustrate the effects of the cladding on various parameters. The mass flow through the break is illustrated in Figure 2-11. The mass flow rate responds to both the changes in pressure (Figure 2-12) and void fraction at the break (Figure 2-13). The break was venting mostly liquid for the first 30 minutes of the transient, and mostly steam after 500 minutes. In between, the fluid at the break oscillated between mostly liquid and mostly steam. These oscillations in the void fraction caused oscillations in many parameters, including the pressurizer pressure and the break mass flow.

The break caused some voiding in the core within a few minutes of the start of the transient, as indicated by the relatively rapid decrease in the collapsed core level, as shown in Figure 2-14. The level then remained roughly constant until the core began to uncover near 550 minutes. The core began to heat up a few minutes later, as shown in Figure 2-15.

The total HPSI flow into the RCS is shown in Figure 2-16. The flow began at about 1 min in response to the SIAS on low-low pressurizer pressure. The HPSI flow was terminated near 500 minutes, when the automatic switchover to sump recirculation mode was assumed to fail. The behavior of the accumulators is illustrated in Figure 2-17. The liquid volume decreased relatively slowly between 90 and 250 minutes. The liquid volume decreased rapidly in the calculation with the Zircaloy cladding near 250 minutes. Similar rapid decreases occurred later with the other two claddings. The variability of the response of the accumulators in this scenario contributed to a larger numerical variability of this scenario compared to that described previously for Scenario SBLOCA-1.0.

The performance of the SGs is illustrated in Figure 2-18 and Figure 2-19, which show pressure and level in the B steam generator. The SG pressure generally remained between the open and close setpoints of the PORV until about 30 minutes, when steam reached the break (see Figure 2-13). The resulting decrease in primary pressure resulted in a decrease in SG pressure until the two systems thermally decoupled near 60 minutes. The SG pressure remained roughly constant for the remainder of the transient. The SG level remained relatively high throughout the transient. AFW was still available at the end of the calculations because the ECST was not yet depleted of liquid.

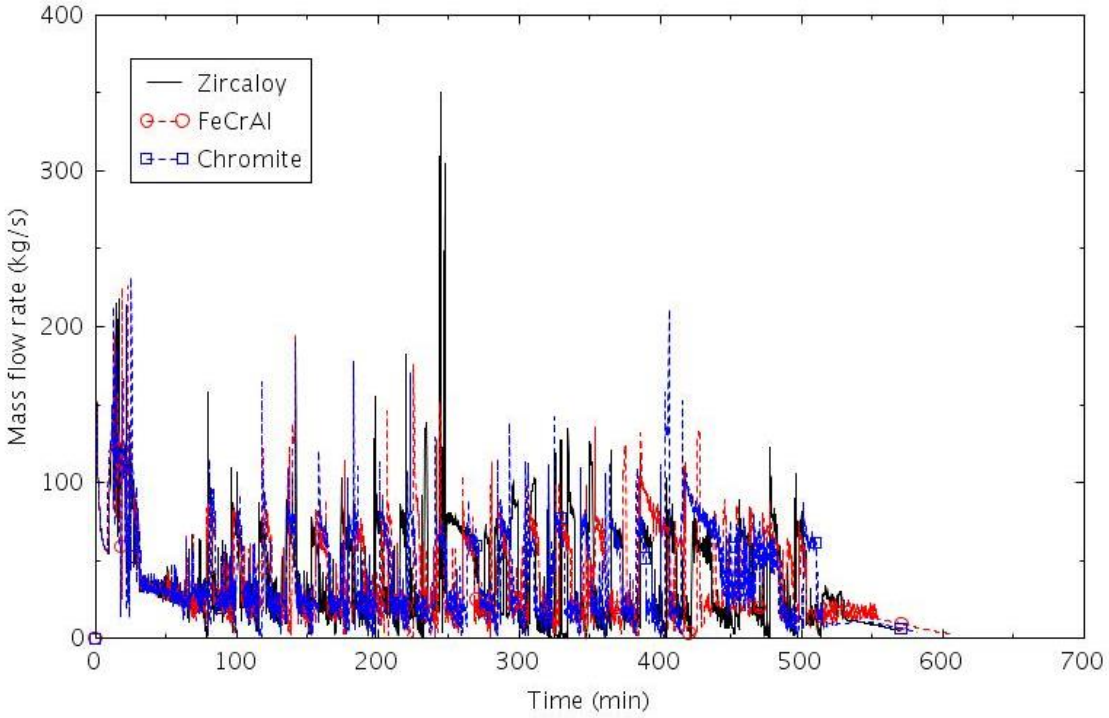

Figure 2-11. Mass flow rate through the break (SBLOCA-1.1).

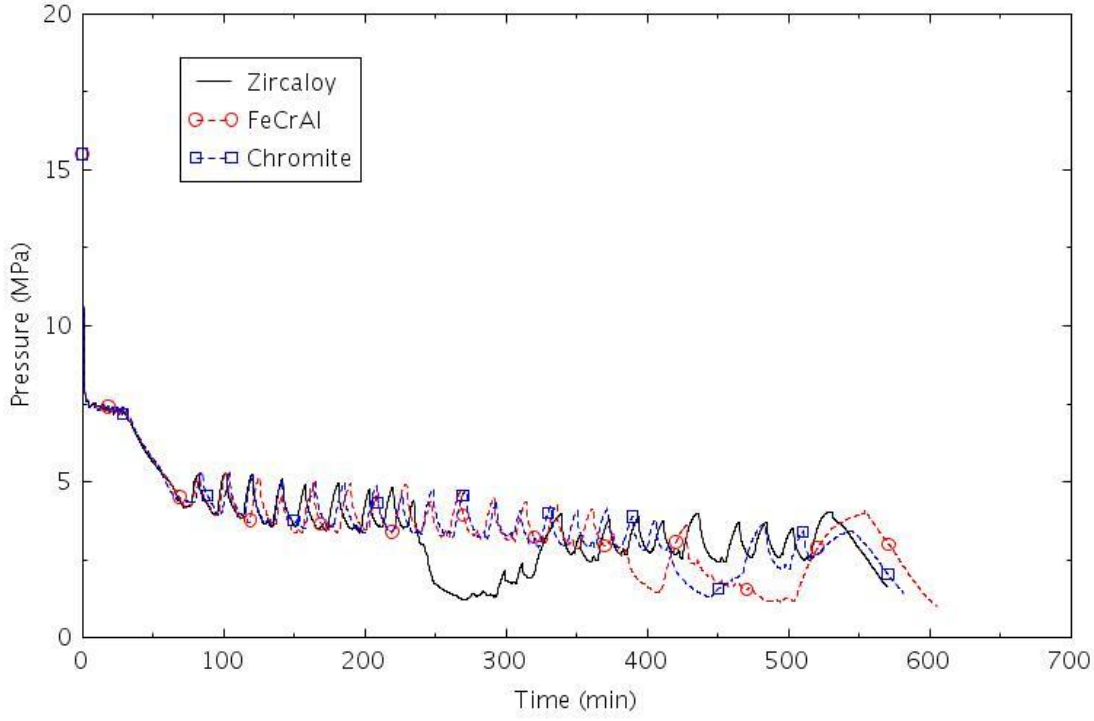

Figure 2-12. Pressure in the pressurizer (SBLOCA-1.1).

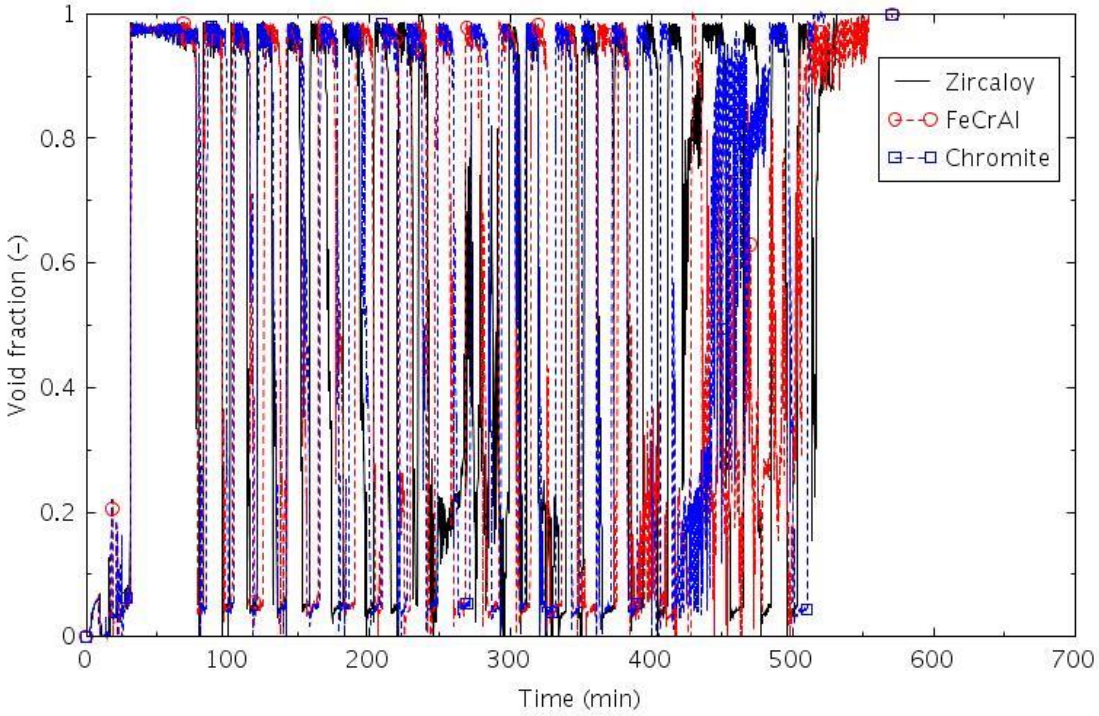

Figure 2-13. Void fraction at the break (SBLOCA-1.1).

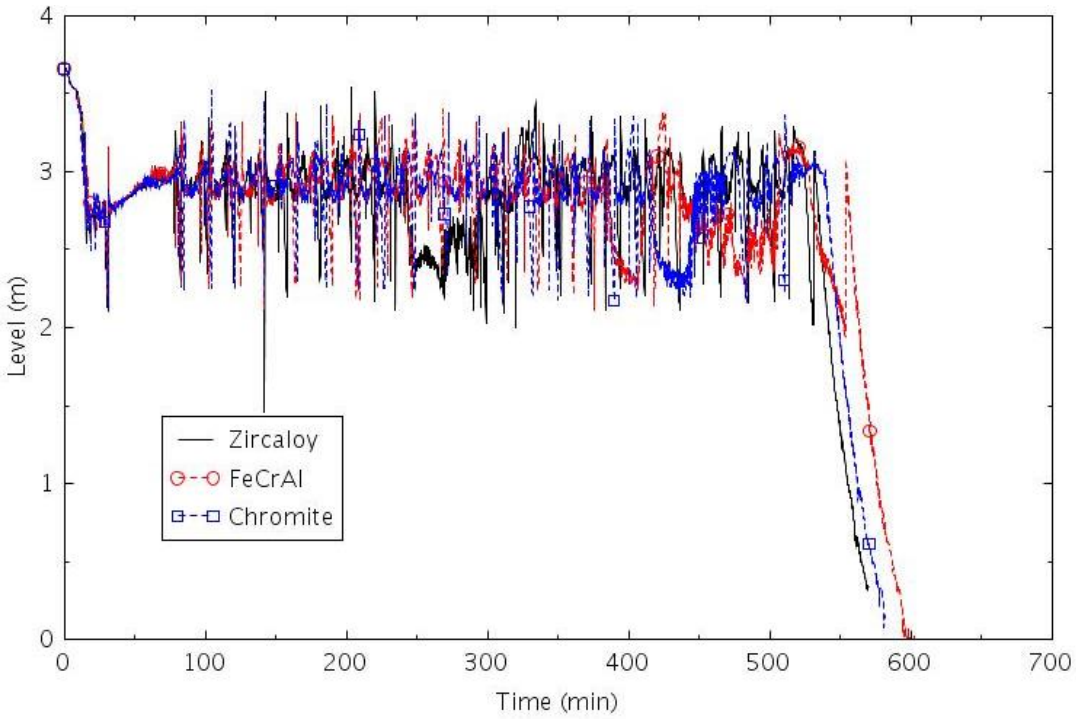

Figure 2-14. Collapsed liquid level in the central core channel (SBLOCA-1.1).

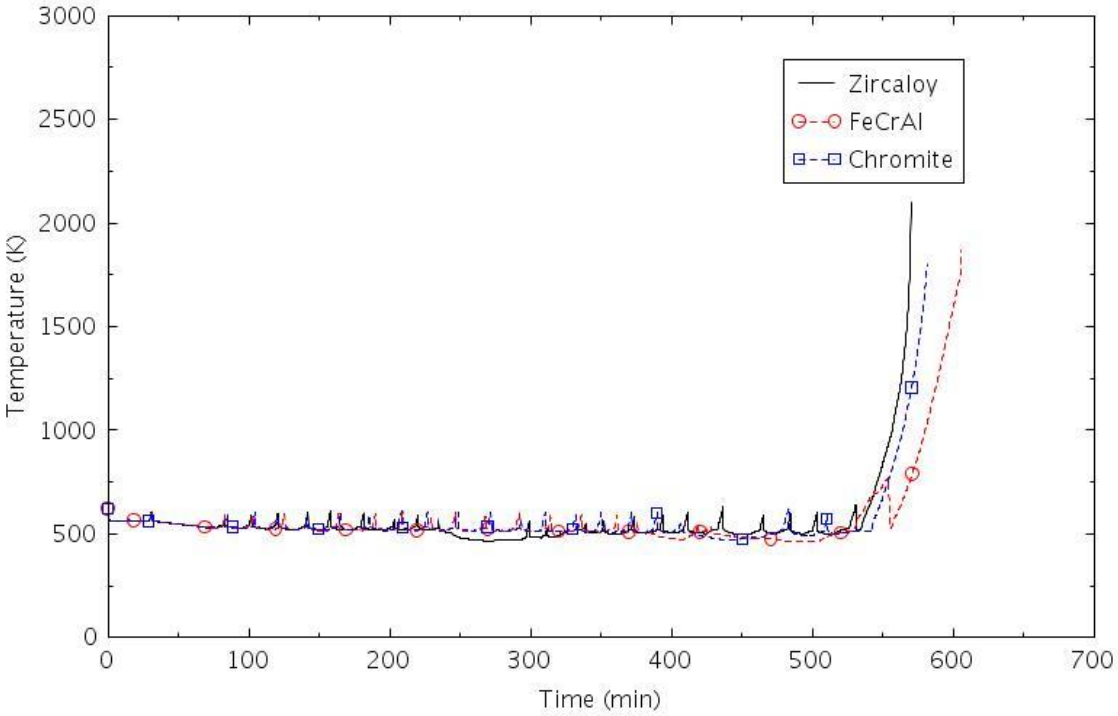

Figure 2-15. Maximum cladding temperature (SBLOCA-1.1).

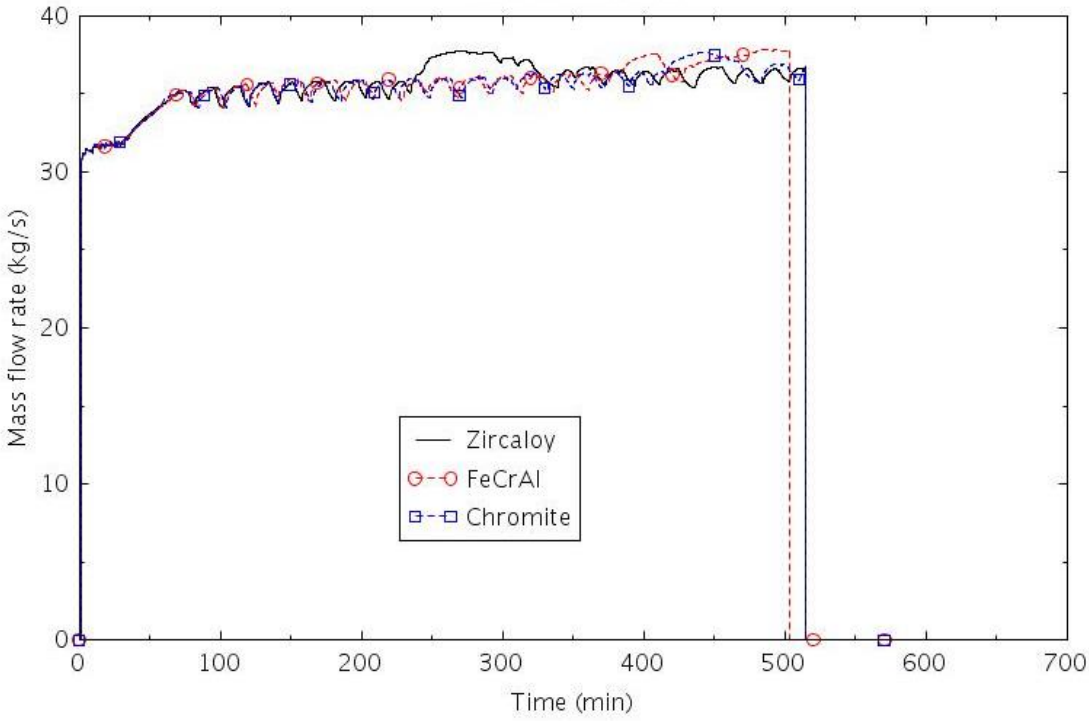

Figure 2-16. Total HPSI flow into the RCS (SBLOCA-1.1).

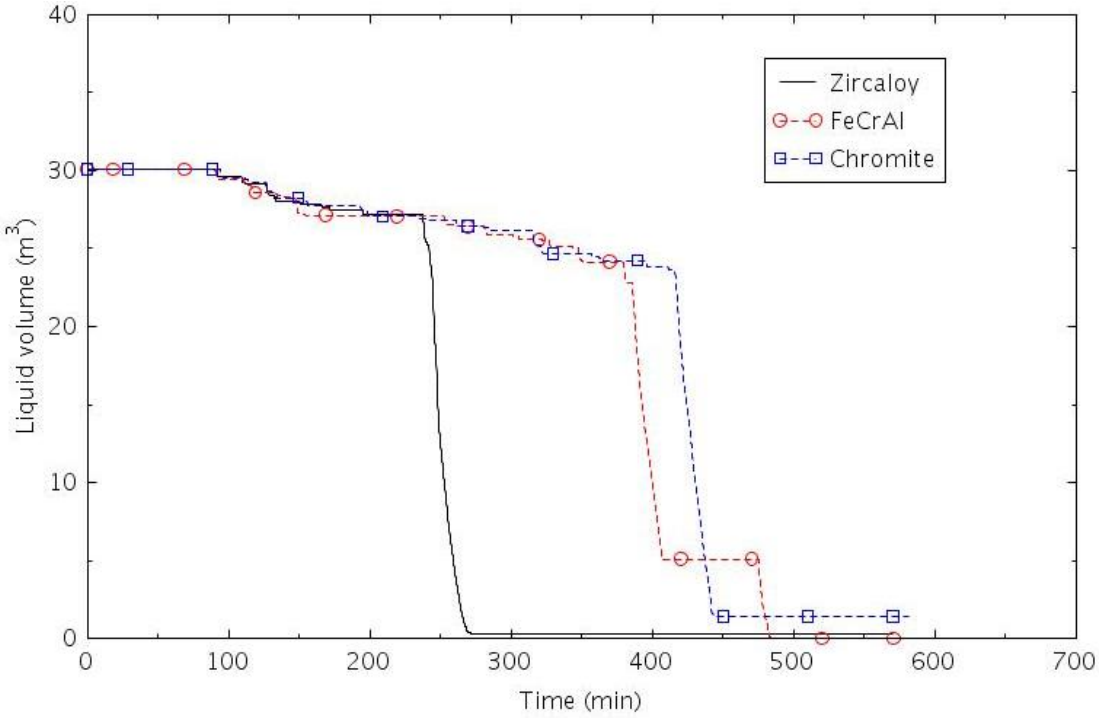

Figure 2-17. Liquid volume in Accumulator B (SBLOCA-1.1)

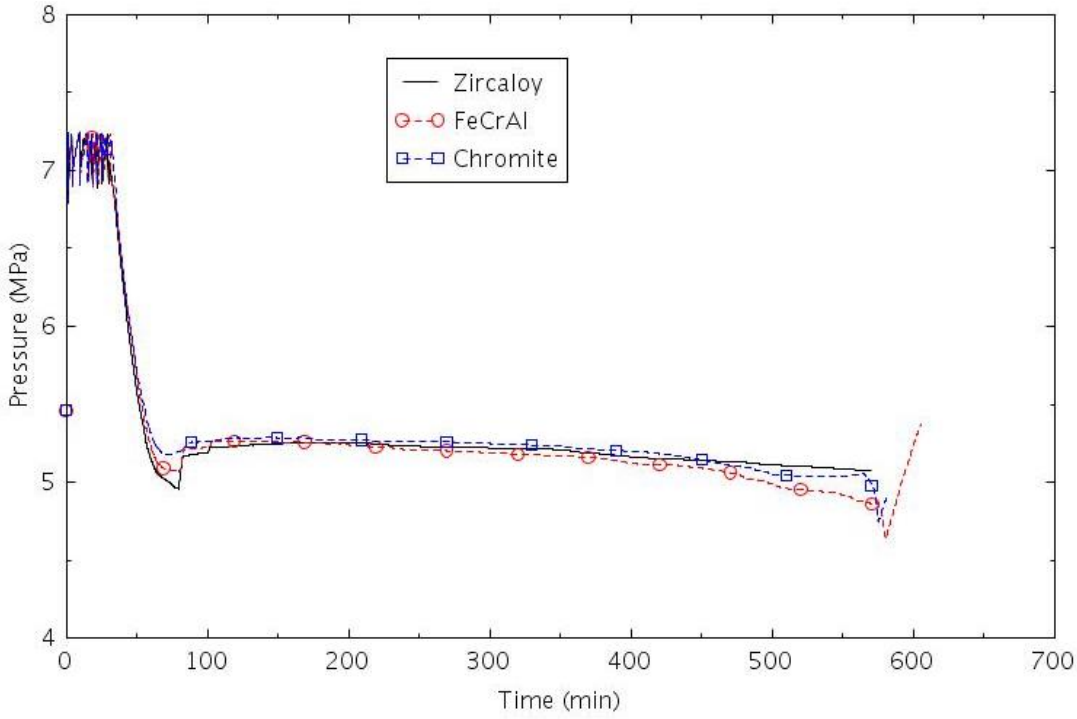

Figure 2-18. Pressure in SG B (SBLOCA-1.1).

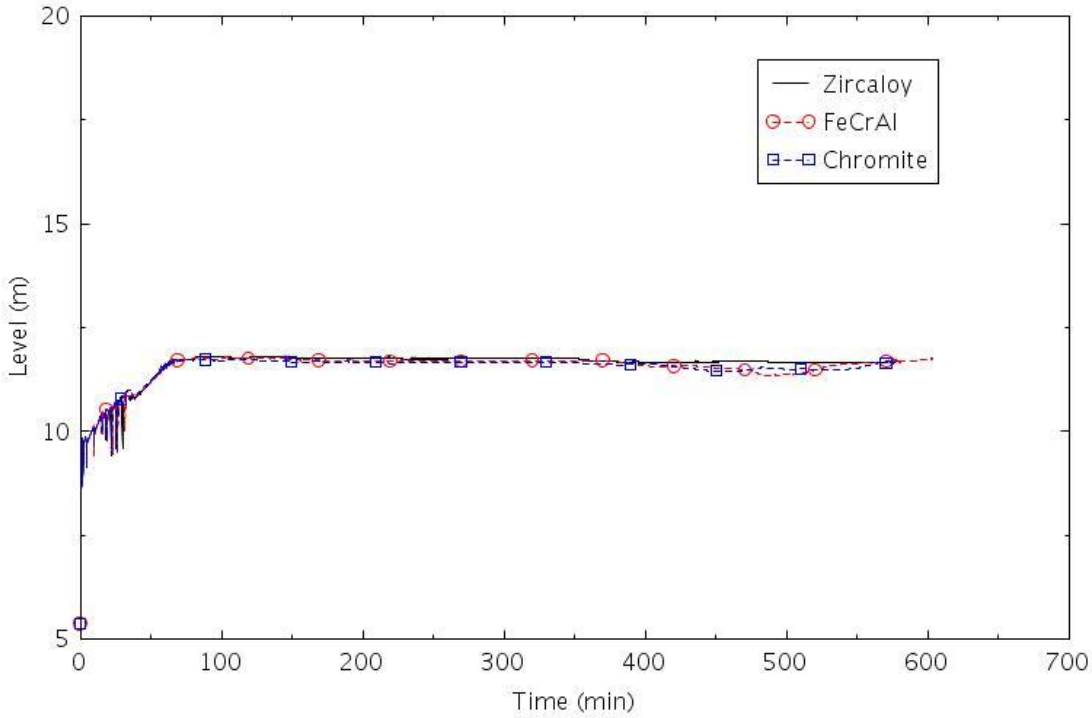

Figure 2-19. Collapsed liquid level in SG B (SBLOCA-1.1).

2.1.3.3 SBLOCA-2.0

This scenario assumed that one motor-driven AFW pump was available and that the operators manually initiated SSC at 30 minutes. This scenario was identical to Scenario SBLOCA-1.0, except that HPSI was assumed to fail. LPSI was also assumed to fail so no pumped injection into the RCS was available during this transient.

The calculated sequences of events are shown in Table 2-5. The break was assumed to open at 0.0 s. The reactor scram, termination of MFW, closure of the TSVs, and SIAS all occurred within the first minute. Motor-driven AFW was initiated 30 seconds after the SIAS. The HPSI was assumed to fail. The RCPs were tripped at about 4 minutes. The operators manually initiated SSC at 30 minutes. The core began to uncover at about 36 minutes. Accumulator injection began at 53 minutes, just 6 minutes before core damage occurred in the calculation with Zircaloy. Although the heat transfer from the hottest cladding improved somewhat after accumulator injection began, the accumulators were not able to prevent early core damage for the calculations with Zircaloy and Chromite. The FeCrAl cladding was a little cooler than the other claddings, and the improved heat transfer due to the accumulator injection was sufficient to quench the core. Although the FeCrAl cladding was within 100 K of the damage criterion, the accumulator injection came just in the nick of time to prevent early core damage. As a result, the initially small difference in cladding temperature with FeCrAl provided more than 200 minutes of additional coping time. The calculated amount of hydrogen produced during the transients varied significantly between claddings. The amount of hydrogen produced was 1.5 kg for FeCrAl, 7.90 kg for Chromite, and 21.2 kg for Zircaloy.

Table 2-5. Sequence of Events for Scenario SBLOCA-2.0.

	Time (min)		
Event	**Zircaloy**	**FeCrAl**	**Chromite**
Break opens	0.0	0.0	0.0
Reactor scram	0.7	0.7	0.7
SIAS	0.7	0.7	0.7
RCPs tripped	4.4	4.4	4.5

SSC begins	30.0	30.0	30.0
High containment pressure	32.9	32.8	32.8
Core begins to uncover	36.0	35.6	35.8
First cladding rupture	49.3	48.0	49.2
0.5 kg H_2 generation	49.3	276.9	52.0
Accumulator flow initiated	53.2	53.2	53.2
Accumulator flow terminated	NA	147.1	NA
SSC ends	NA	164.6	NA
Calculated terminated	59.2	277.4	66.0

The following figures illustrate the effects of the cladding on various parameters. The mass flow through the break is illustrated in Figure 2-20. RCS pressure is shown in Figure 2-21.

The break caused some voiding in the core within a few minutes of the start of the transient, as shown in Figure 2-22. The level in the core then remained roughly constant until the cover began to uncover near 35 minutes. The level then decreased until the core began to heat up near 36 minutes, as shown in Figure 2-23.

The onset of accumulator injection near 50 minutes caused the level to increase, but not enough to quench the core, except in the calculation with FeCrAl. The core began to heat up again near 230 minutes with FeCrAl cladding. The RCS pressure was low enough in that case that LPSI flow would have occurred had it not been assumed to fail. Figure 2-24 shows that a relatively small fraction of the liquid inventory in the accumulators was injected in the cases with Zircaloy and Chromite, but the entire inventory was injected in the calculation with FeCrAl.

The performance of the SGs is illustrated in Figure 2-25 and Figure 2-26, which show pressure and level in the B steam generator. The SG pressure generally remained between the open and close setpoints of the PORV until SSC began at 30 minutes. The cooldown was completed only in the case with FeCrAl cladding. The SG level remained relatively high throughout the transient. AFW was still available at the end of all the calculations because the ECST was not yet depleted of liquid.

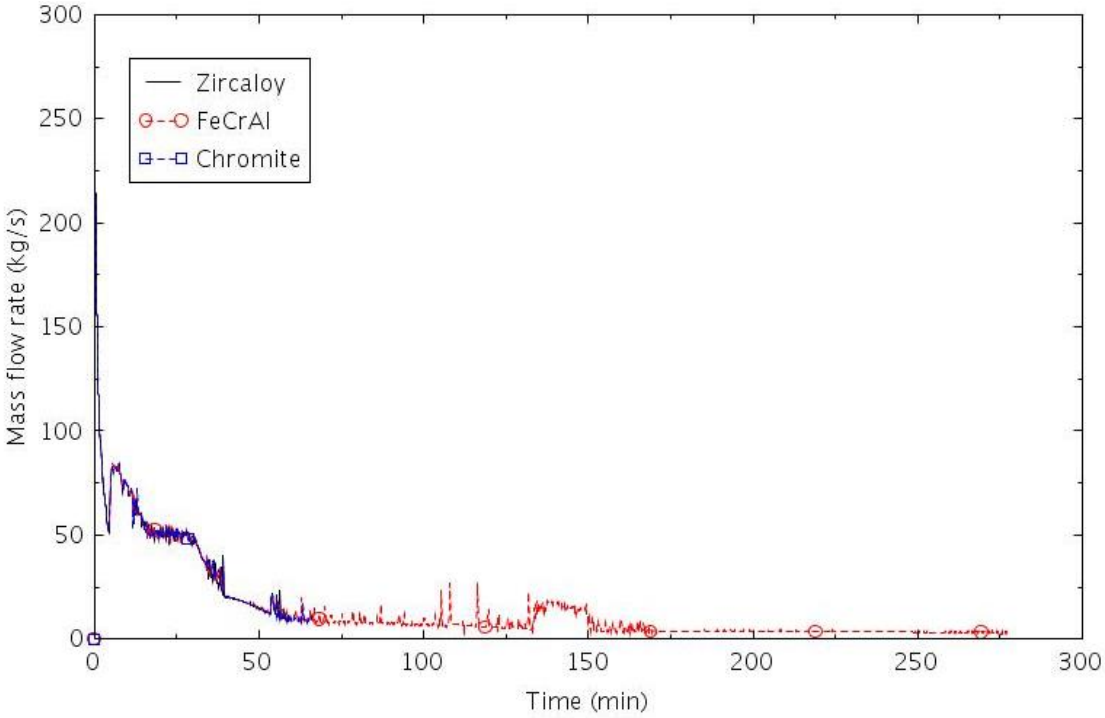

Figure 2-20. Mass flow rate through the break (SBLOCA-2.0).

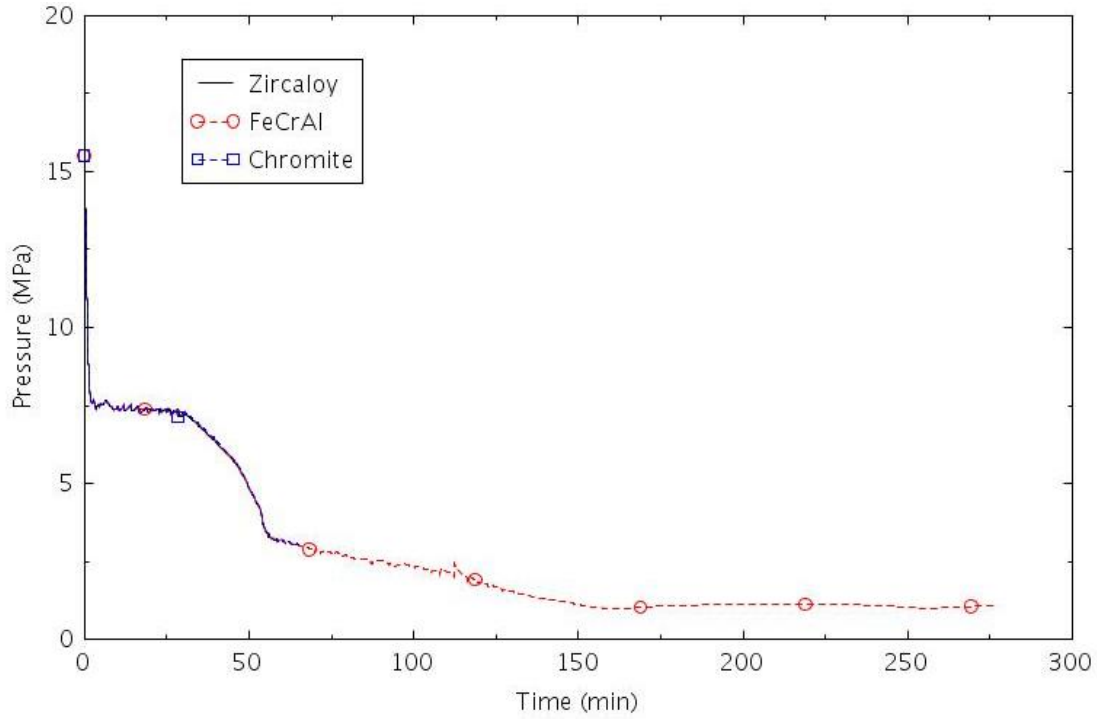

Figure 2-21. Pressure in the pressurizer (SBLOCA-2.0).

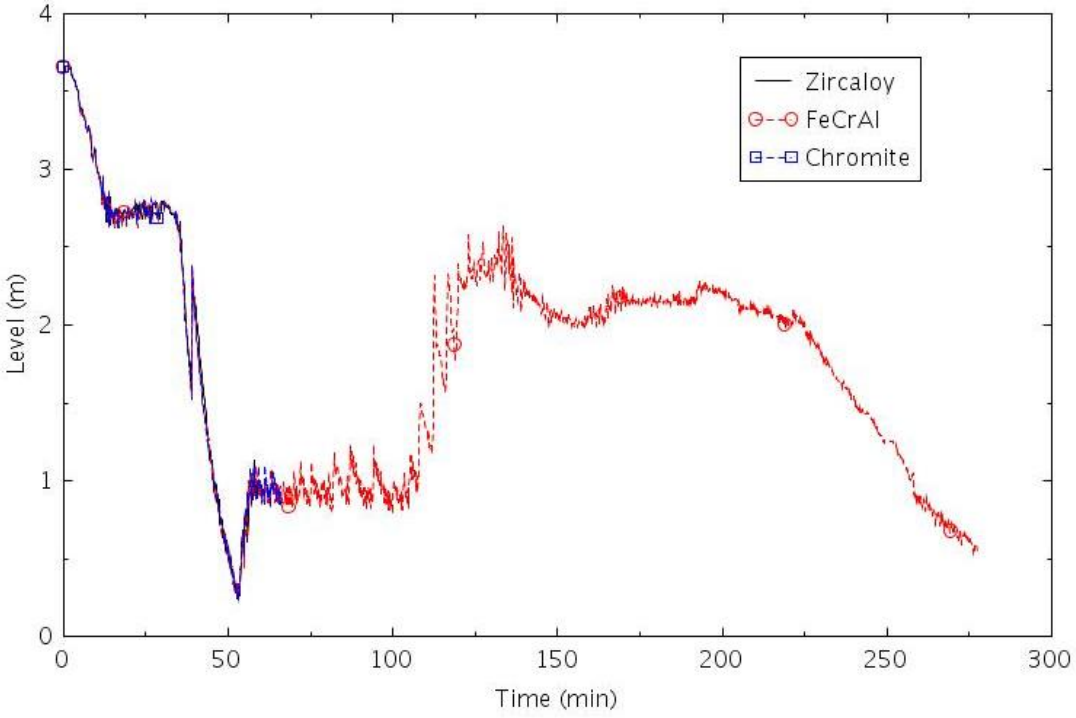

Figure 2-22. Collapsed liquid level in the central core channel (SBLOCA-2.0).

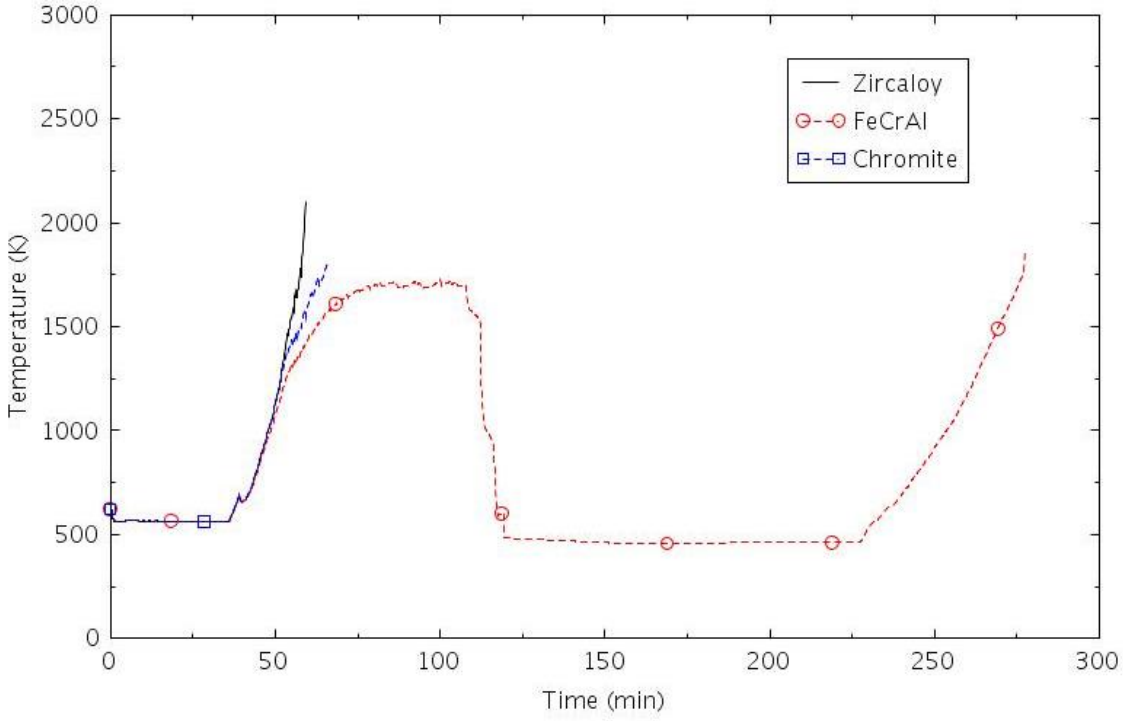

Figure 2-23. Maximum cladding temperature (SBLOCA-2.0).

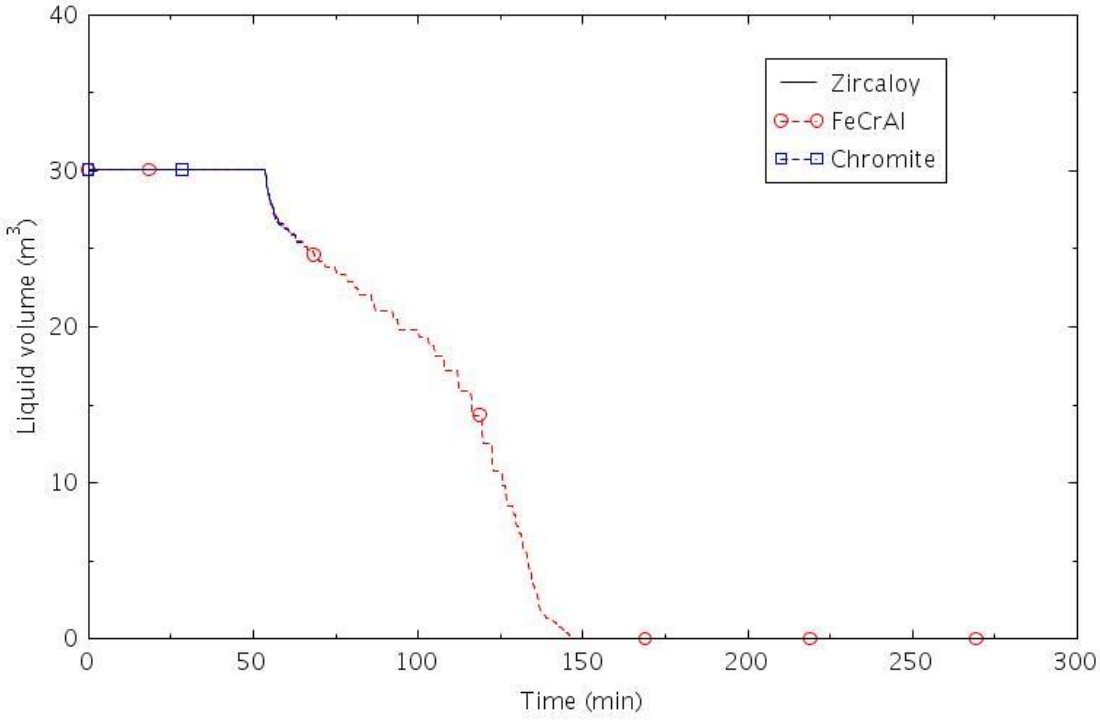

Figure 2-24. Liquid volume in Accumulator B (SBLOCA-2.0)

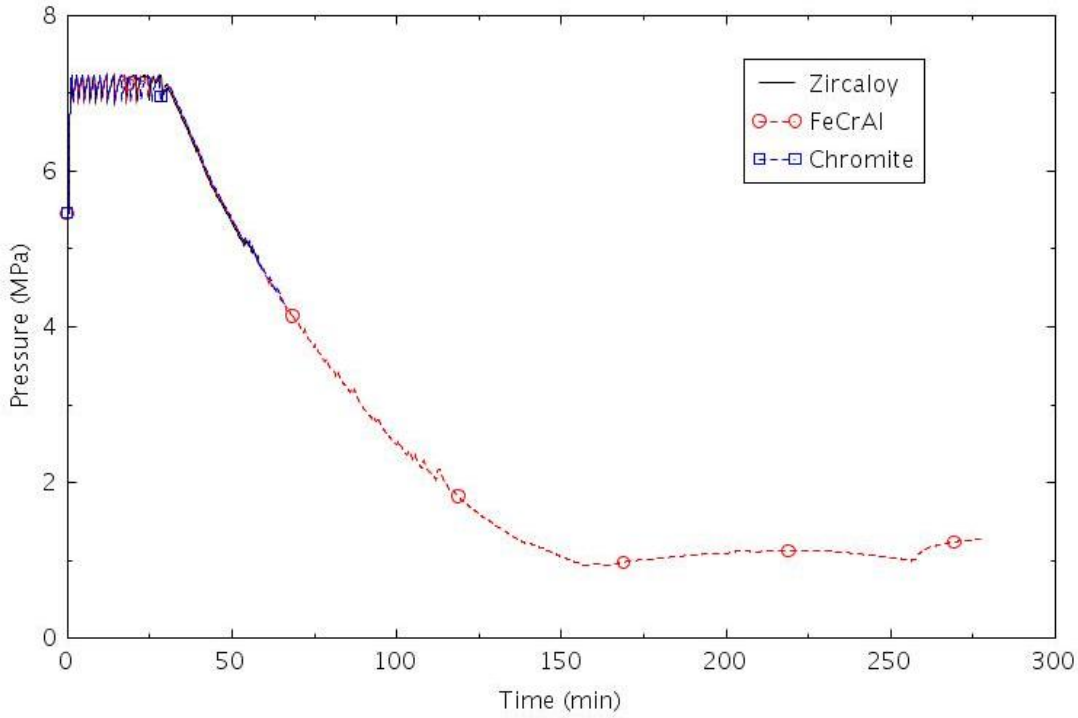

Figure 2-25. Pressure in SG B (SBLOCA-2.0).

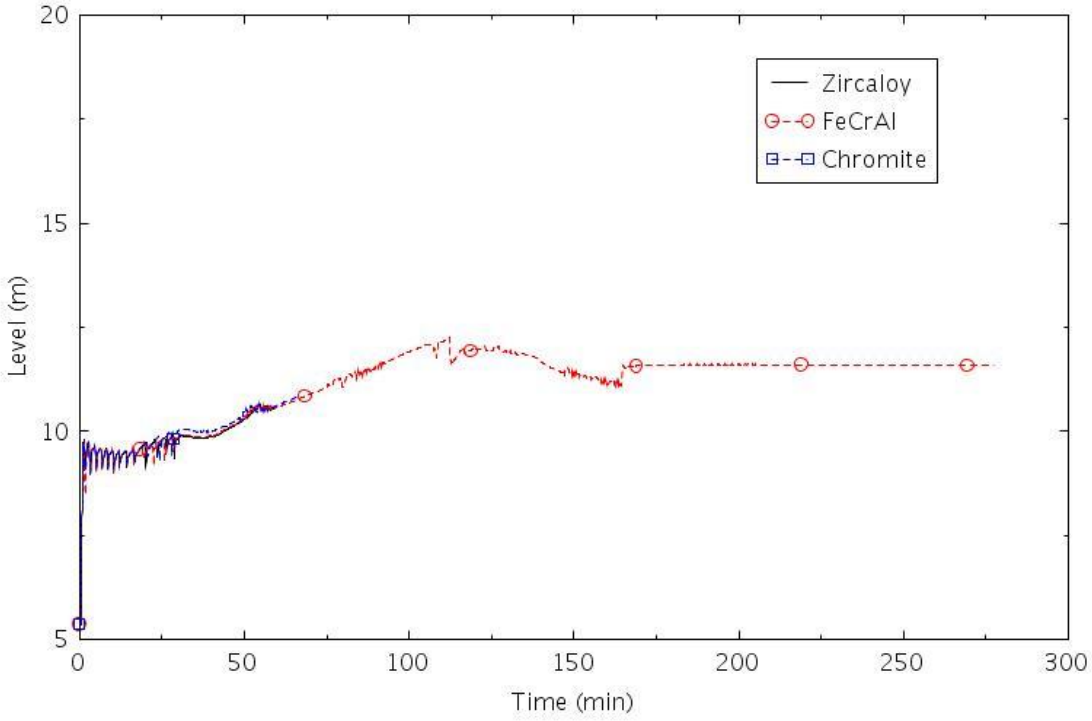

Figure 2-26. Collapsed liquid level in SG B (SBLOCA-2.0).

2.1.3.4 SBLOCA-2.1

This scenario assumed that one motor-driven AFW pump was available, but that HPSI failed. This scenario was identical to Scenario SBLOCA-2.0, except that the operators were not assumed to manually initiate SSC.

The calculated sequences of events are shown in Table 2-6. The break was assumed to open at 0.0 s. The reactor scram, termination of MFW, closure of the TSVs, and SIAS all occurred within the first minute. Motor-driven AFW was initiated 30 seconds after the SIAS. The HPSI was assumed to fail. The RCPs were tripped at about 4 minutes. The core began to uncover at about 38 minutes. Accumulator injection began at about 54 minutes, just 5 minutes before core damage occurred in the calculation with Zircaloy. Although the heat transfer from the hottest cladding improved somewhat after accumulator injection began, the accumulators were not able to prevent early core damage for any of the calculations. The calculated amount of hydrogen produced during the transients varied significantly between claddings. The amount of hydrogen produced was 0.8 kg for FeCrAl, 9.7 kg for Chromite, and 23.9 kg for Zircaloy.

Table 2-6. Sequence of Events for Scenario SBLOCA-2.1.

	Time (min)		
Event	**Zircaloy**	**FeCrAl**	**Chromite**
Break opens	0.0	0.0	0.0
Reactor scram	0.7	0.7	0.7
SIAS	0.7	0.7	0.7
RCPs tripped	4.4	4.4	4.5
High containment pressure	32.6	32.6	32.7
Core begins to uncover	37.9	38.3	37.9
First cladding rupture	49.0	48.2	49.0

0.5 kg H_2 generation	48.7	74.9	51.6
Accumulator flow initiated	53.9	54.3	53.9
Calculated terminated	58.6	74.9	62.2

The following figures illustrate the effects of the cladding on various parameters. The mass flow through the break is illustrated in Figure 2-27. RCS pressure is shown in Figure 2-28.

The break caused some voiding in the core within a few minutes of the start of the transient, as shown in Figure 2-29. The level in the core then remained roughly constant until 35 minutes. The core rapid core level decrease between 35 and 37 minutes and the rapid increase at 37 minutes were associated with the liquid level in the pump suction piping in Loop A dropping to the bottom of the U-shaped piping and the subsequent clearing of the loop seal, which allowed steam to flow directly from the reactor core through the B loop and to the break. A minor heatup occurred in the core between 35 and 37 minutes, as shown in Figure 2-30. The minor heatup was terminated by the clearing of the loop seal at 37 minutes. The level then decreased again due to the loss of fluid out the break until a sustained heatup of the core began near 38 minutes.

The onset of accumulator injection near 54 minutes caused the level to increase, but not enough to quench the core. Based on the results shown previously for Scenario SBLOCA-2.0, the maximum temperature with FeCrAl was probably very close to turning around before the core damage criterion was reached. Figure 2-31 shows that a relatively small fraction of the liquid inventory in the accumulators was injected in each calculation.

The performance of the SGs is illustrated in Figure 2-32 and Figure 2-33, which show pressure and level in the B steam generator. The SG pressure generally remained between the open and close setpoints of the PORV until about 38 minutes. The SG pressure then decreased, but not as much as the RCS pressure. The SG level remained relatively high throughout the transient. AFW was still available at the end of all the calculations because the ECST was not yet depleted of liquid.

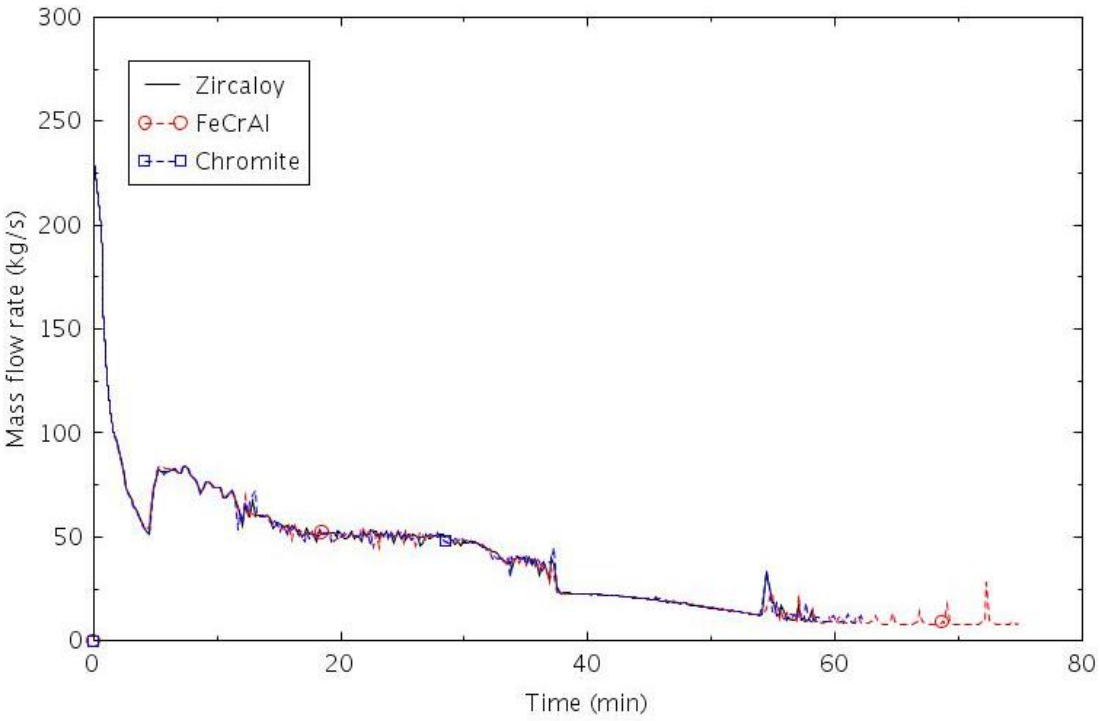

Figure 2-27. Mass flow rate through the break (SBLOCA-2.1).

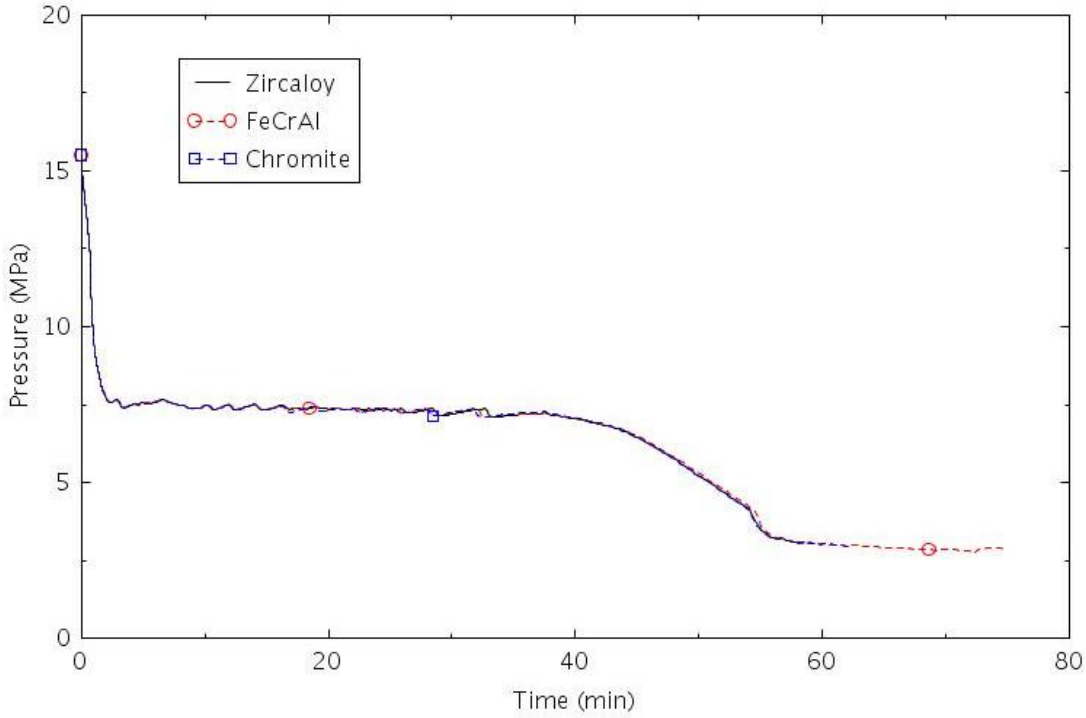

Figure 2-28. Pressure in the pressurizer (SBLOCA-2.1).

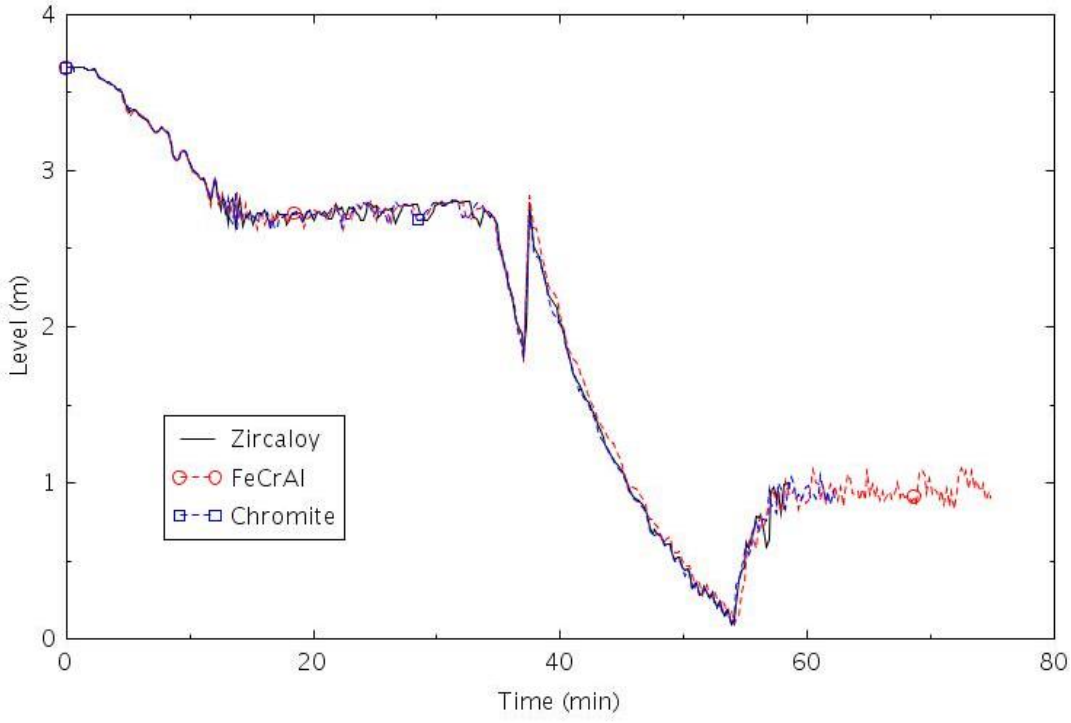

Figure 2-29. Collapsed liquid level in the central core channel (SBLOCA-2.1).

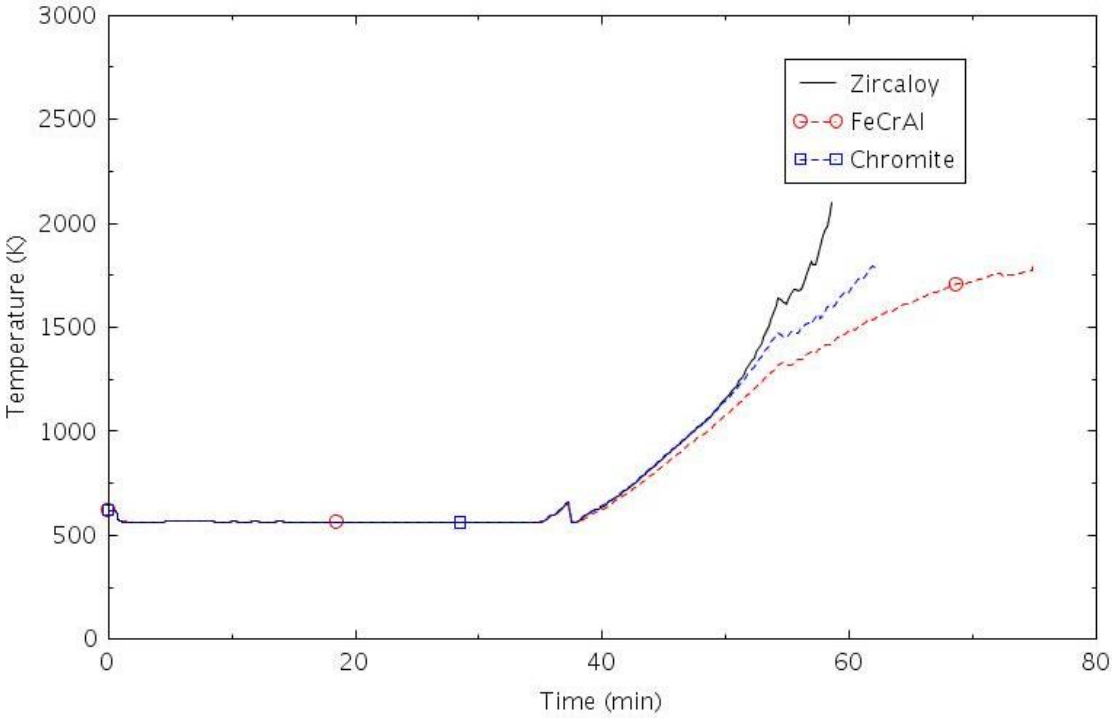

Figure 2-30. Maximum cladding temperature (SBLOCA-2.1).

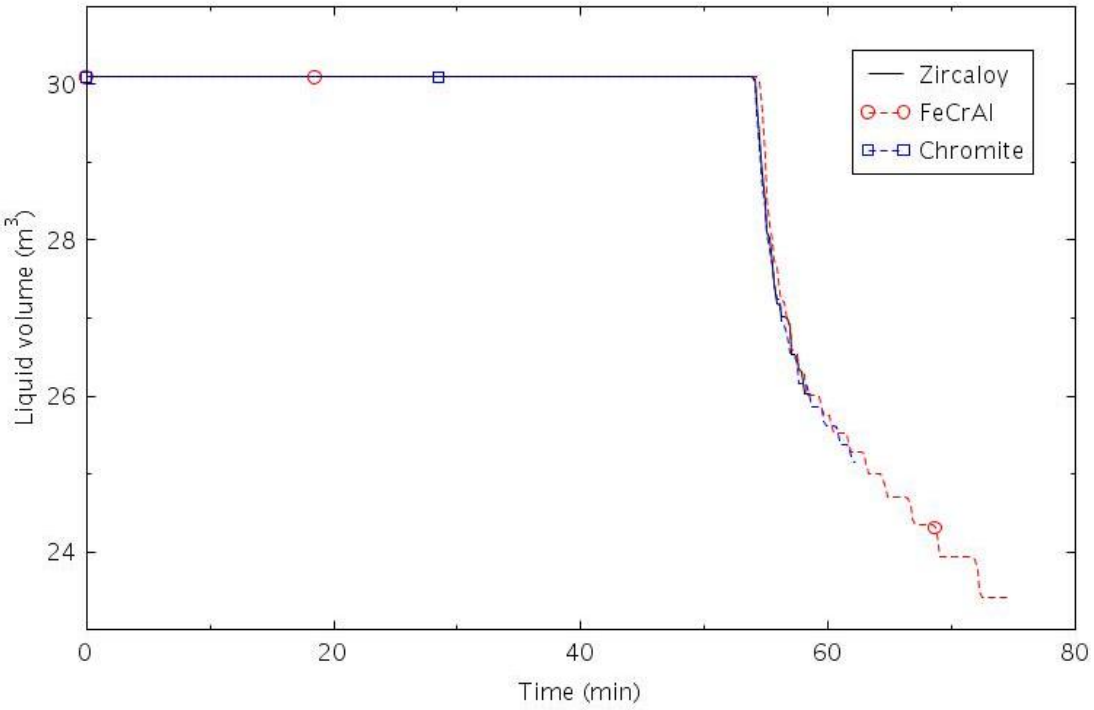

Figure 2-31. Liquid volume in Accumulator B (SBLOCA-2.1)

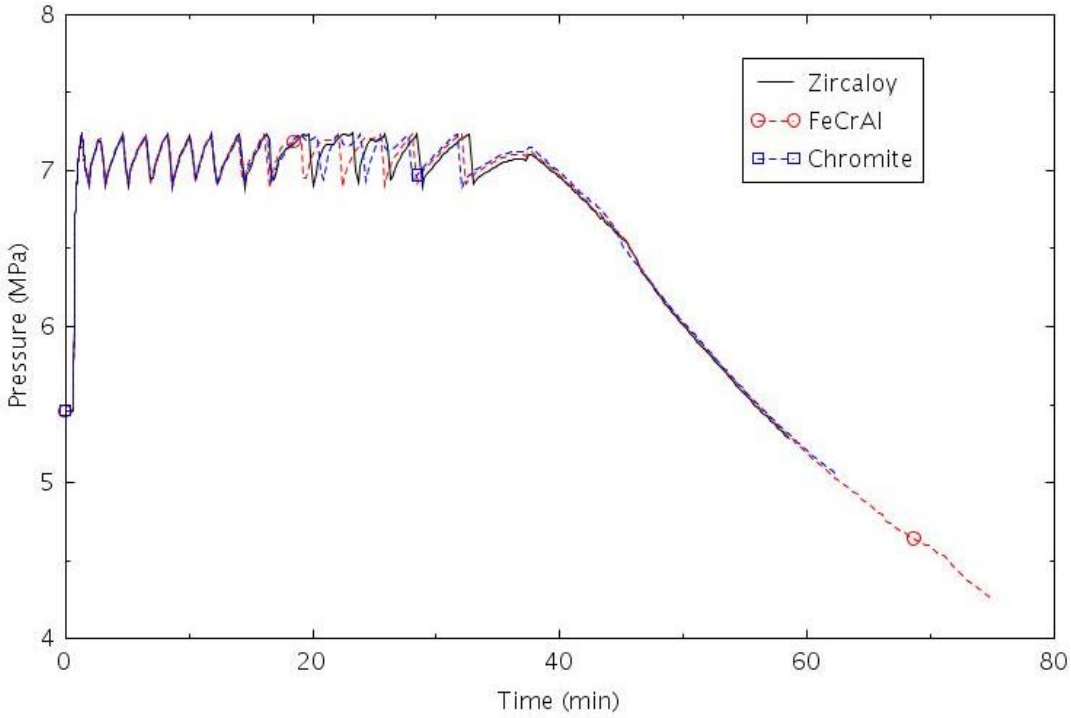

Figure 2-32. Pressure in SG B (SBLOCA-2.1).

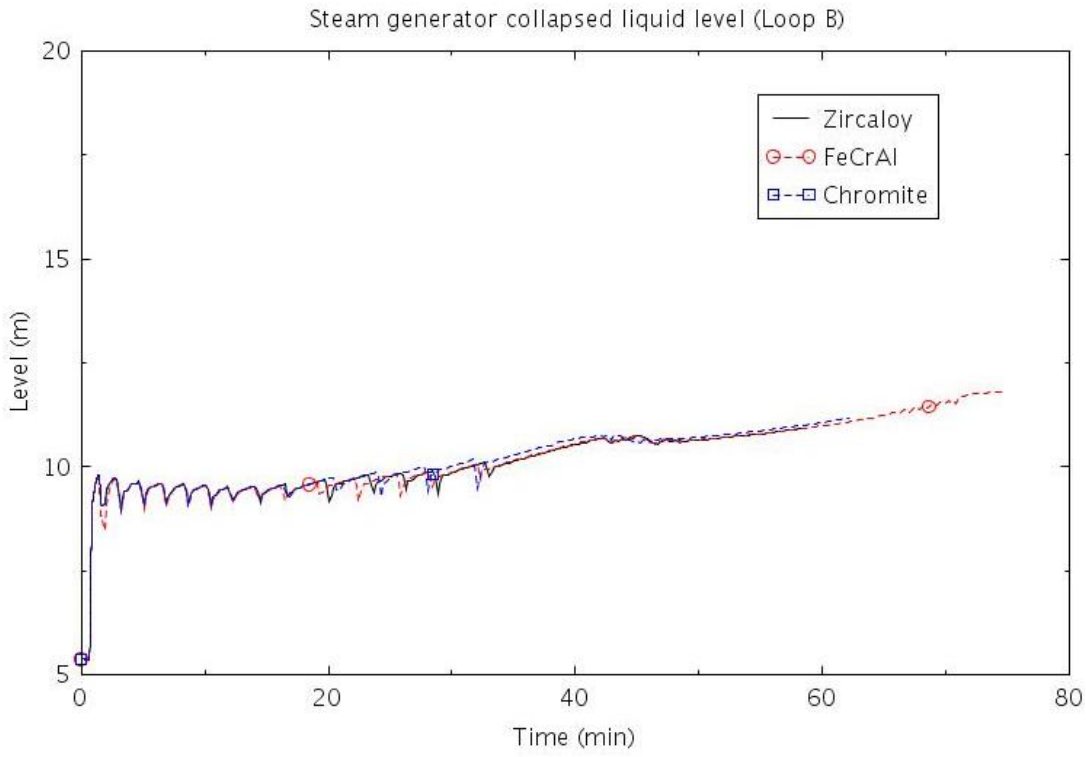

Figure 2-33. Collapsed liquid level in SG B (SBLOCA-2.1).

2.1.3.5 SBLOCA-3.0

This scenario assumed that the AFW and HPSI both failed. This scenario was identical to Scenario SBLOCA-2.1, except that HPSI was not available in this scenario.

The calculated sequences of events are shown in Table 2-7. The break was assumed to open at 0.0 s. The reactor scram, termination of MFW, closure of the TSVs, and SIAS all occurred within the first minute. The AFW and HPSI was assumed to fail. The RCPs were tripped at about 4 minutes. The core began to uncover at about 38 minutes. Accumulator injection began at about 55 minutes, just 7 minutes before core damage occurred in the calculation with Zircaloy. Although the heat transfer from the hottest cladding improved somewhat after accumulator injection began, the accumulators were not able to prevent early core damage for any of the calculations. The calculated amount of hydrogen produced during the transients varied significantly between claddings. The amount of hydrogen produced was 0.7 kg for FeCrAl, 9.7 kg for Chromite, and 29.7 kg for Zircaloy.

Table 2-7. Sequence of Events for Scenario SBLOCA-3.0.

	Time (min)		
Event	**Zircaloy**	**FeCrAl**	**Chromite**
Break opens	0.0	0.0	0.0
Reactor scram	0.7	0.7	0.7
SIAS	0.7	0.7	0.7
RCPs tripped	4.3	4.3	4.3
High containment pressure	32.5	32.5	32.5
Core begins to uncover	38.1	38.3	37.7
0.5 kg H_2 generation	48.9	73.9	51.7
First cladding rupture	49.3	48.5	49.1
Accumulator flow initiated	54.5	54.7	54.1
Calculated terminated	61.4	73.9	67.5

The following figures illustrate the effects of the cladding on various parameters. The mass flow through the break is illustrated in Figure 2-34. RCS pressure is shown in Figure 2-35.

The break caused some voiding in the core within a few minutes of the start of the transient, as shown in Figure 2-36. The level in the core then remained roughly constant until 34 minutes. The rapid core level decrease between 34 and 37 minutes and the rapid increase at 37 minutes were associated with loop seal phenomena, as described previously in Section 2.1. The level then decreased again due to the loss of fluid out the break, until a sustained heatup of the core began near 38 minutes. The onset of accumulator injection near 54 minutes caused the level to increase, but not enough to quench the core, as shown in Figure 2-37. Figure 2-38 shows that a relatively small fraction of the liquid inventory in the accumulators was injected in each calculation.

The performance of the SGs is illustrated in Figure 2-39 and Figure 2-40, which show pressure and level in the B steam generator. The SG pressure generally remained between the open and close setpoints of the PORV. The SG level decreased during the transient, but none of the SGs dried out before core damage occurred. The behavior of the SGs differed after about 40 minutes in the calculations. Prior to 40 minutes, all three SGs were actively removing heat from the RCS with the PORVs cycling between open and closed and the level decreasing. After 40 minutes, only one steam generator was actively removing heat in each calculation, but which SG was active varied between calculations. The active steam generators were SG C for the calculation with Zircaloy, SG B for the calculation with FeCrAl, and SG A for the calculation with Chromite. The PORVs quit cycling, causing the pressure to remain nearly constant, and the level quit decreasing in the SGs that were not actively removing heat.

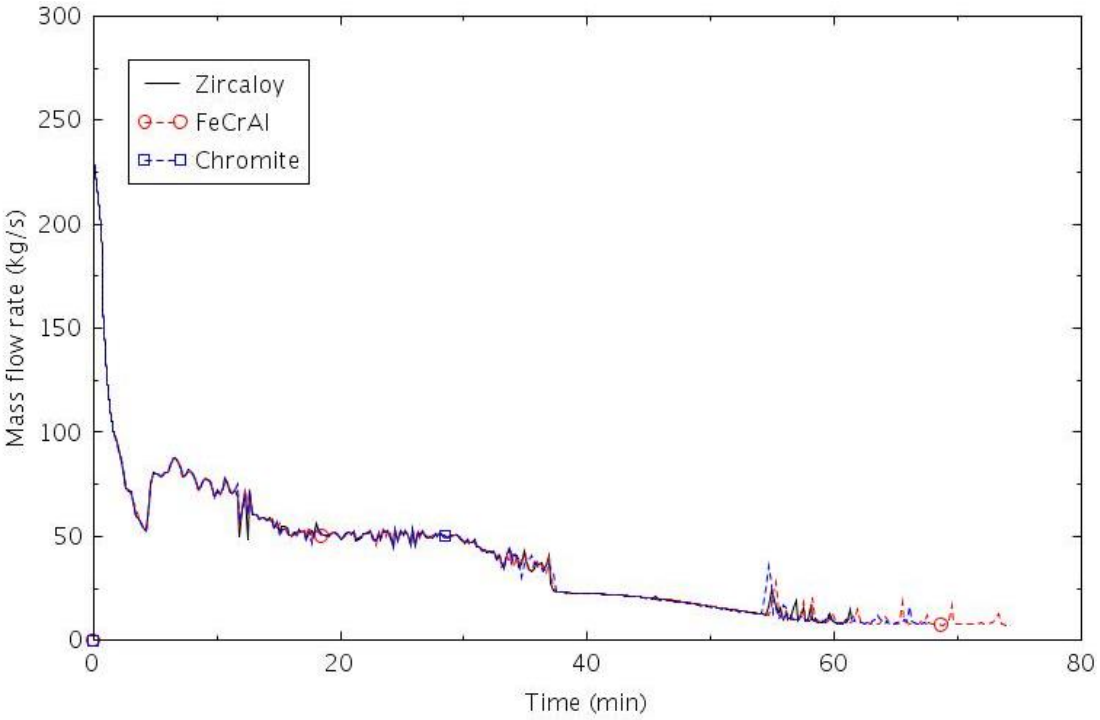

Figure 2-34. Mass flow rate through the break (SBLOCA-3.0).

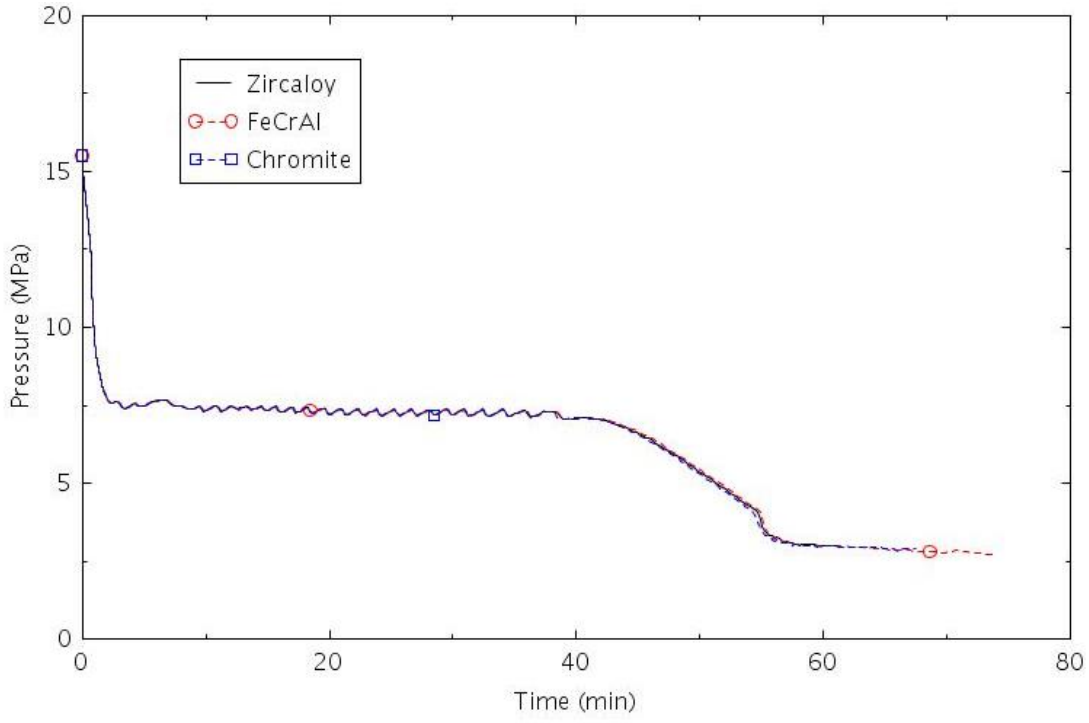

Figure 2-35. Pressure in the pressurizer (SBLOCA-3.0).

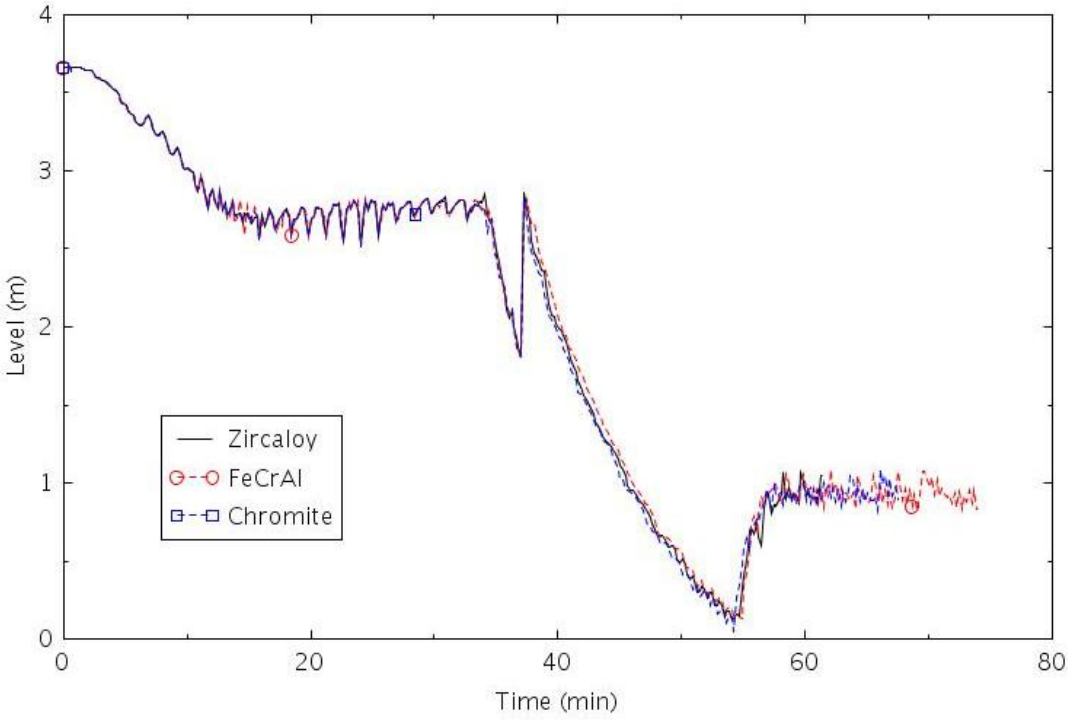

Figure 2-36. Collapsed liquid level in the central core channel (SBLOCA-3.0).

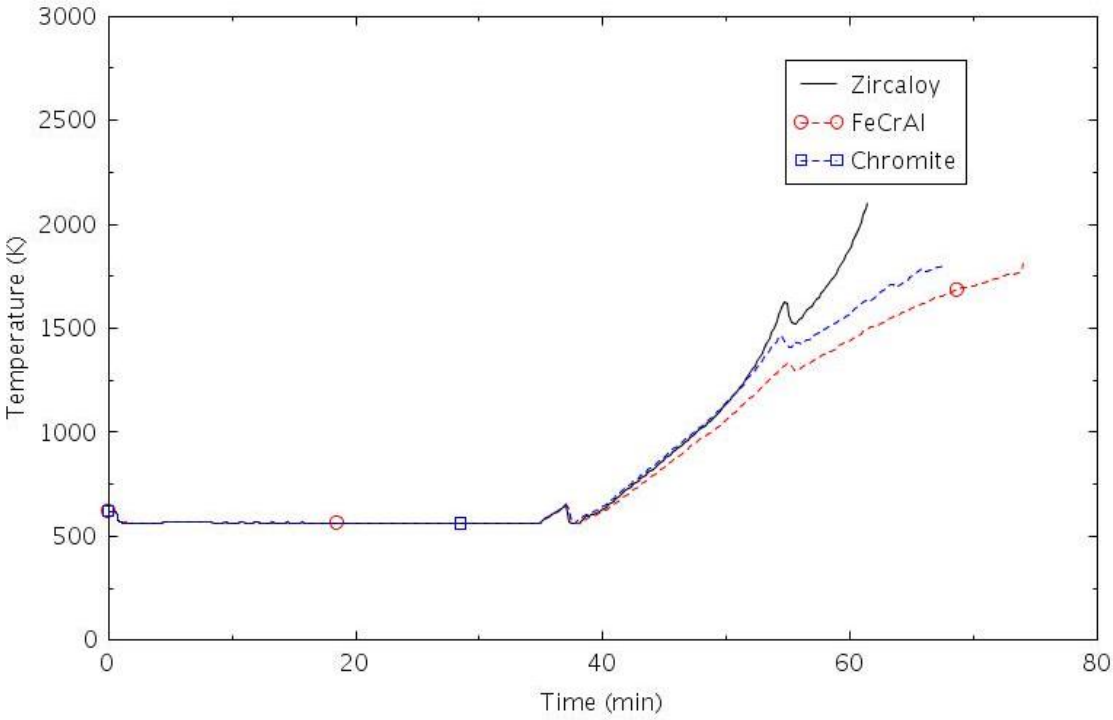

Figure 2-37. Maximum cladding temperature (SBLOCA-3.0).

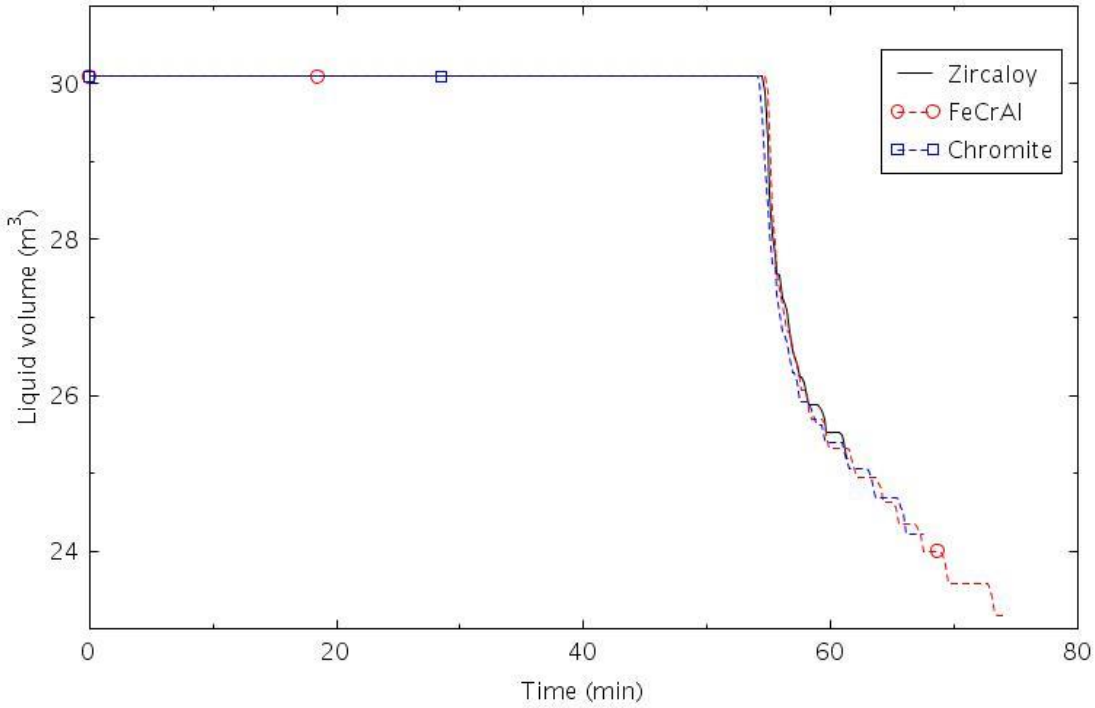

Figure 2-38. Liquid volume in Accumulator B (SBLOCA-3.0).

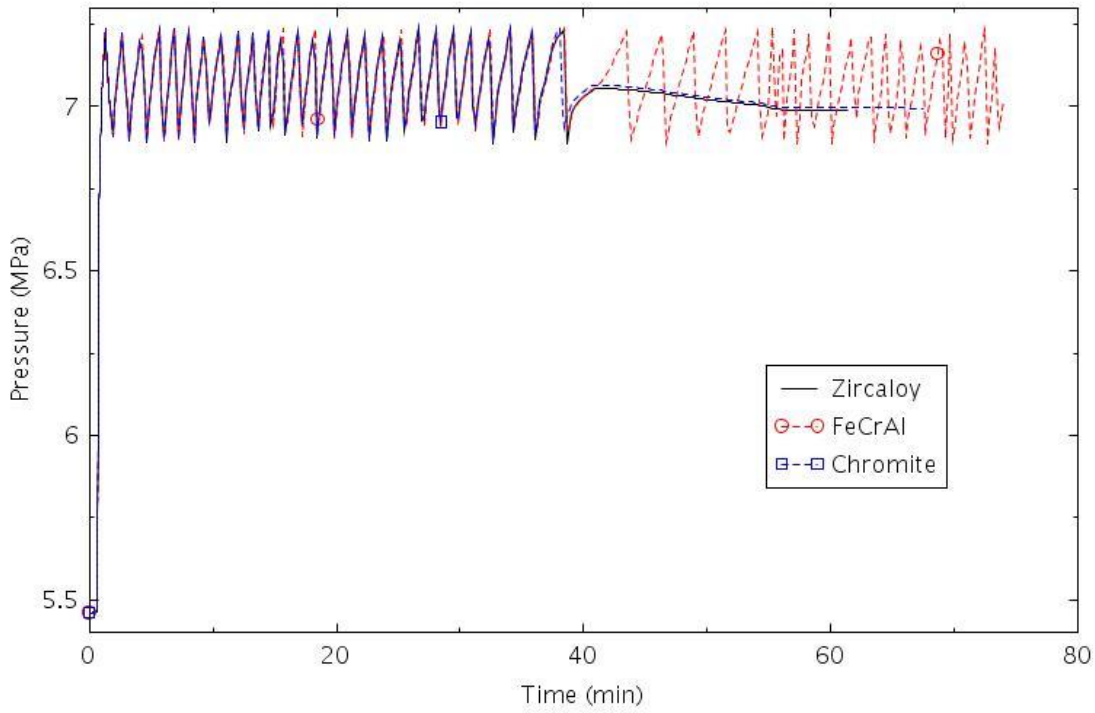

Figure 2-39. Pressure in SG B (SBLOCA-3.0).

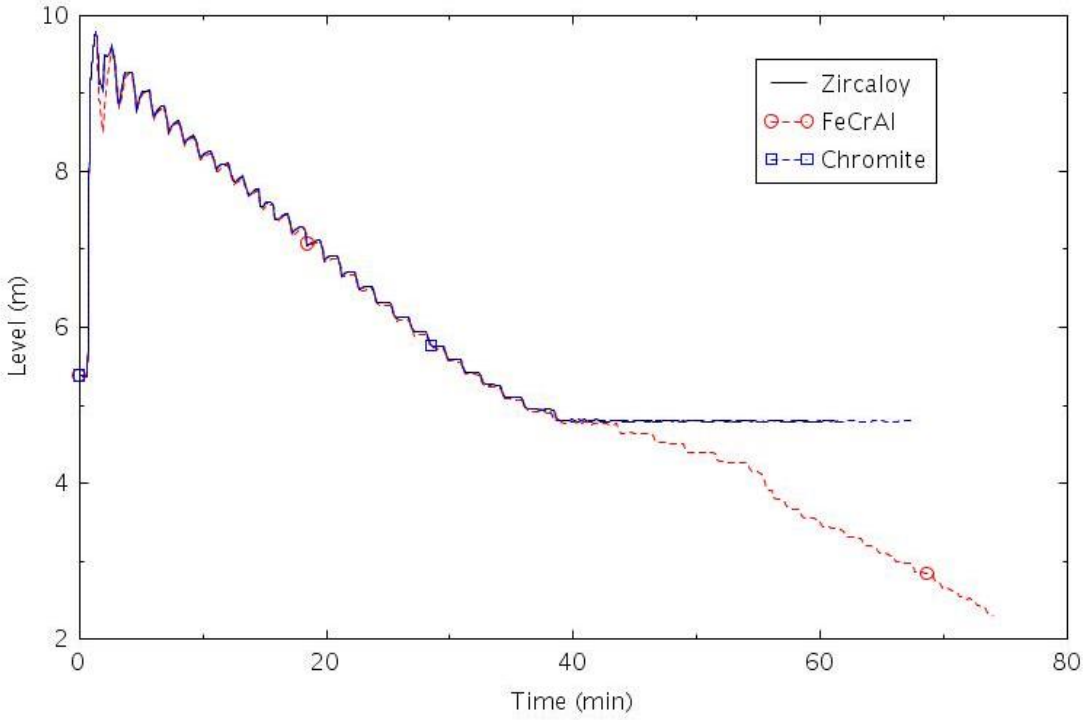

Figure 2-40. Collapsed liquid level in SG B (SBLOCA-3.0).

2.1.3.6 SBLOCA-3.1

This scenario assumed that the AFW failed, but the HPSI was available. The operators were assumed to lock open the pressurizer PORV to initiate feed and bleed cooling at 60 minutes.

The calculated sequences of events are shown in Table 2-8. The break was assumed to open at 0.0 s. The reactor scram, termination of MFW, closure of the TSVs, and SIAS all occurred within the first minute. The AFW was assumed to fail. HPSI flow began 30 seconds after the SIAS. The RCPs were tripped at 7 minutes. The pressurizer PORV was locked open at 60 minutes. Accumulator injection began at about 65 minutes. HPSI flow was terminated at about 500 minutes, when the RWST reached the level at which the automatic switchover to sump injection occurred. The core began to uncover about 40 minutes later. Core damage occurred at about 600 minutes. The time of core damage varied by about 30 minutes among the calculations, but part of this difference is attributed to numerical causes rather than the differences between claddings. The time between the onset of core uncovery and the termination of the calculations is judged to be a more reasonable measure of the effects of the claddings. The time between when the core began to uncover and core damage occurred was 46 minutes with Zircaloy, 66 minutes with FeCrAl, and 41 minutes with Chromite. The calculated amount of hydrogen produced during the transients varied significantly between claddings. The amount of hydrogen produced was 1.2 kg for FeCrAl, 1.2 kg for Chromite, and 13.9 kg for Zircaloy.

Table 2-8. Sequence of Events for Scenario SBLOCA-3.1.

	Time (min)		
Event	**Zircaloy**	**FeCrAl**	**Chromite**
Break opens	0:00	0:00	0:00
Reactor scram	0:00	0:00	0:00
SIAS	0:00	0:00	0:00
RCPs tripped	0:07	0:07	0:07
High containment pressure	0:23	0:23	0:23

Pressurizer PORV locked open	1:00	1:00	1:00
PRT rupture disk opens	1:00	1:14	1:00
Accumulator flow initiated	1:05	1:05	1:05
Containment spray first actuated	2:37	3:08	2:56
RWST switchover	8:11	8:23	8:28
Core begins to uncover	8:58	9:06	8:55
First cladding rupture	9:26	9:27	9:22
0.5 kg H_2 generation	9:28	10:12	9:31
Calculated terminated	9:44	10:12	9:36

The following figures illustrate the effects of the cladding on various parameters. The mass flow through the break is illustrated in Figure 2-41. The break was venting mostly liquid for the first 30 minutes of the transient and mostly steam after 500 minutes as shown in Figure 2-42. The oscillations in between were primarily due to oscillations in the void fraction at the break. The oscillations in the void fraction at the break were also responsible for oscillations in the RCS pressure as shown in Figure 2-43.

The break caused some voiding in the core within a few minutes of the start of the transient, as shown in Figure 2-44 . The level then remained roughly constant until the core began to uncover near 540 minutes. The core began to heat up about 50 minutes later, as shown in Figure 2-45.

The total HPSI flow into the RCS is shown in Figure 2-46. The flow began at about 1 min in response to the SIAS on low-low pressurizer pressure. The HPSI flow was terminated near 500 minutes, when the automatic switchover to sump recirculation mode was assumed to fail. The behavior of the accumulators is illustrated in Figure 2-47. The liquid volume decreased rapidly near 160 minutes in the calculation with Zircaloy cladding. A similar rapid decrease occurred near 400 minutes with FeCrAl cladding, but did not occur with Chromite cladding. The variability of the response of the accumulators in this scenario contributed to a larger numerical variability of this scenario, compared to that described previously for Scenario SBLOCA-1.0.

The level in the B steam generator is shown in Figure 2-48. The level decreased rapidly for about 30 minutes. Although AFW was not available in this scenario, the SGs did not dry out, which indicates that the SGs were not actively removing heat for most of the transient.

In the calculations described previously, the operators were assumed to lock open a pressurizer PORV at 60 minutes. Sensitivity calculations were performed in which the operators were assumed to not initiate feed and bleed cooling. On average, core damage occurred about one hour earlier without feed and bleed. Thus, the manual initiation of feed and bleed cooling added about one hour to the coping time for this scenario.

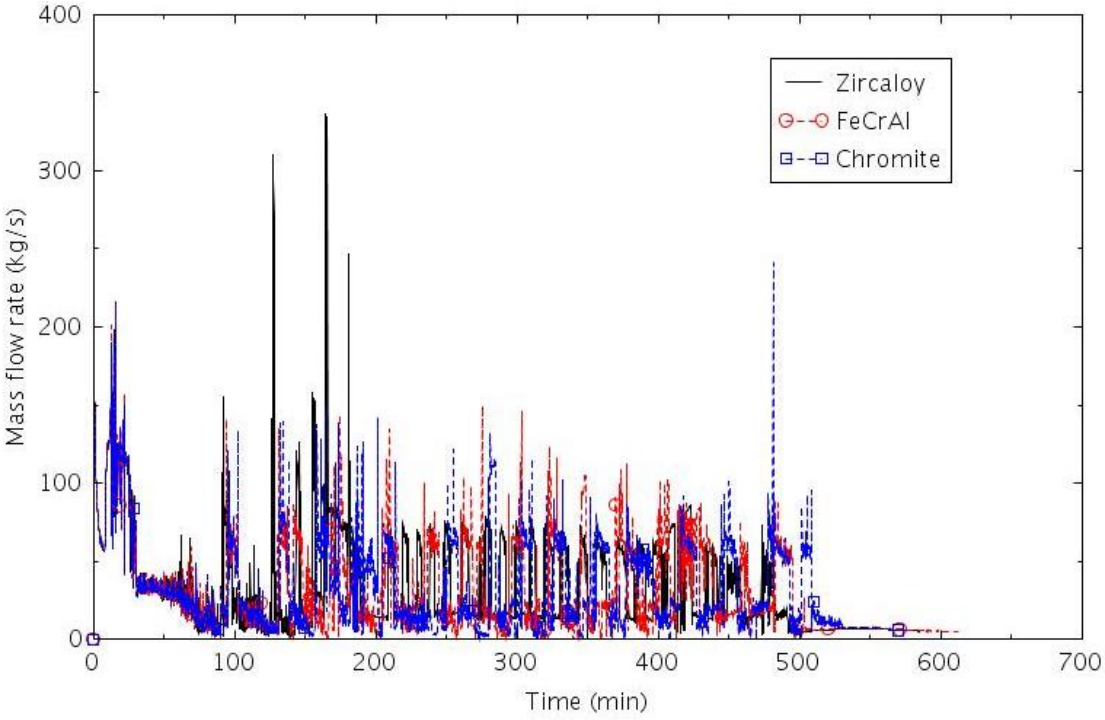

Figure 2-41. Mass flow rate through the break (SBLOCA-3.1).

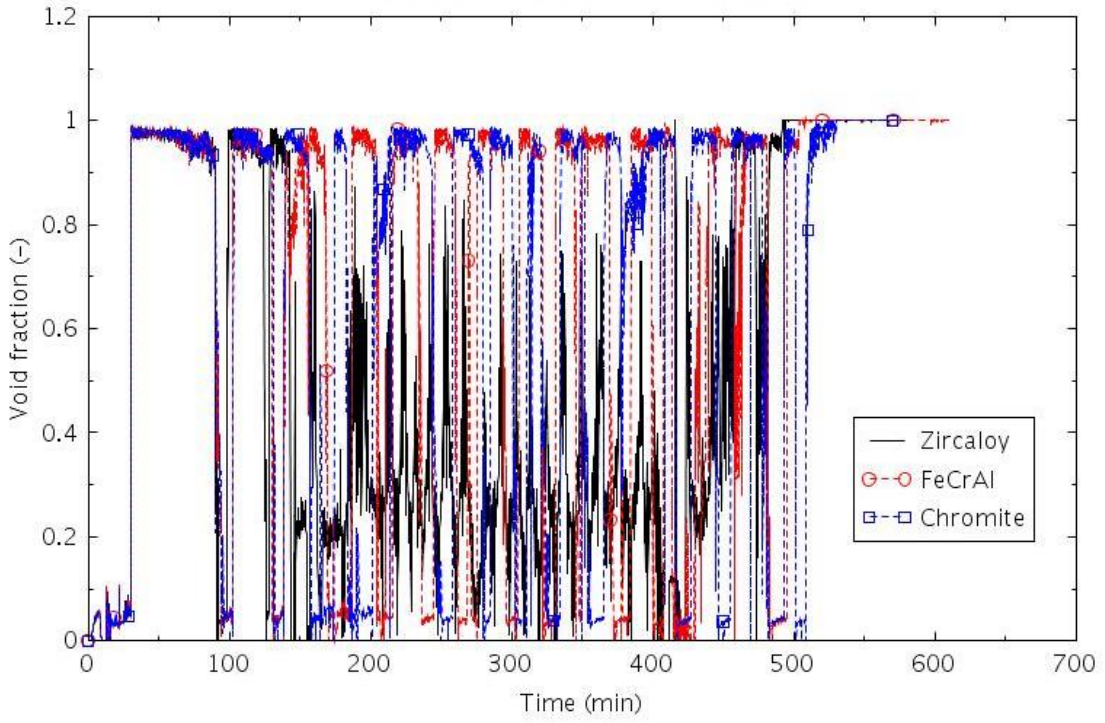

Figure 2-42. Void fraction at the break (SBLOCA-3.1).

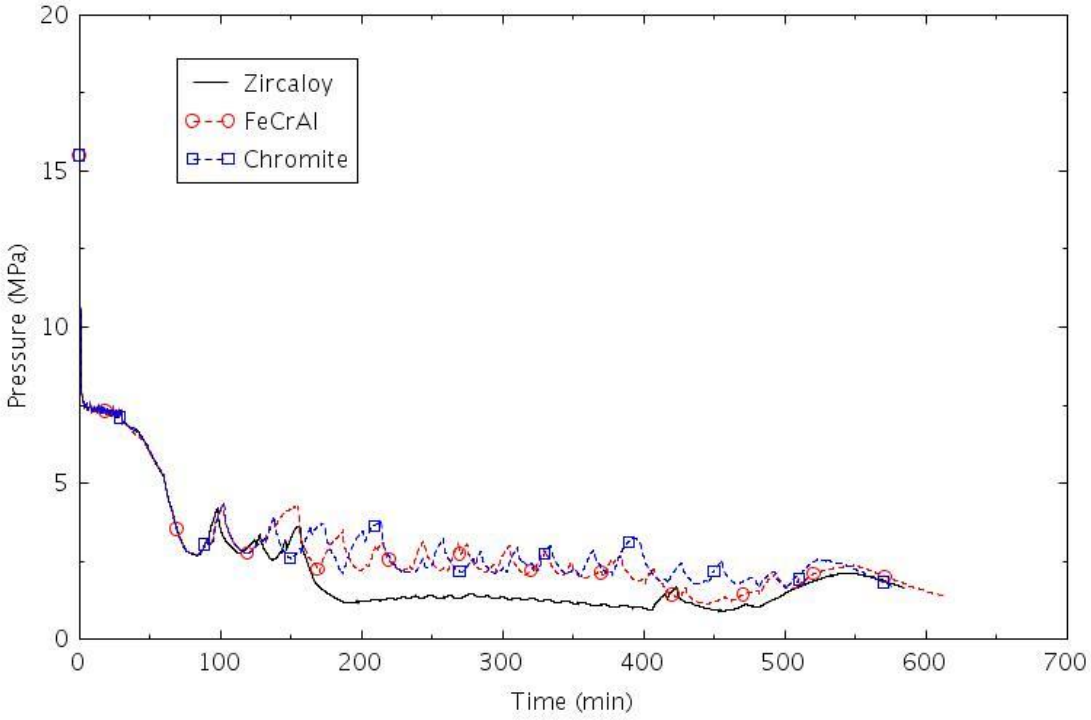

Figure 2-43. Pressure in the pressurizer (SBLOCA-3.1).

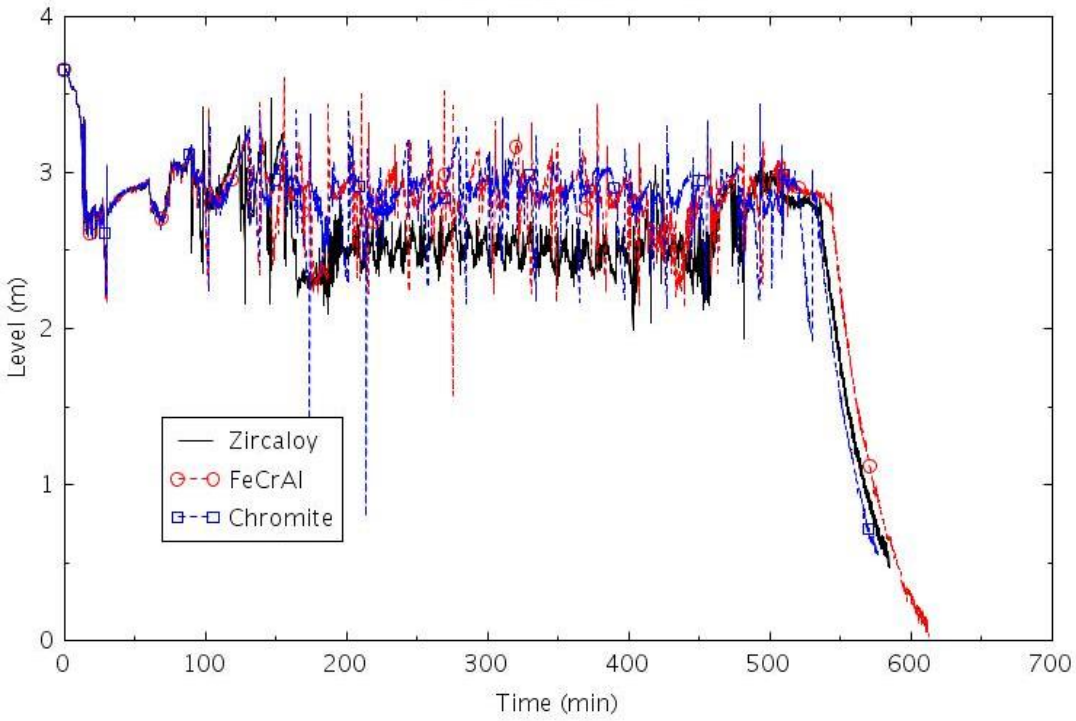

Figure 2-44. Collapsed liquid level in the central core channel (SBLOCA-3.1).

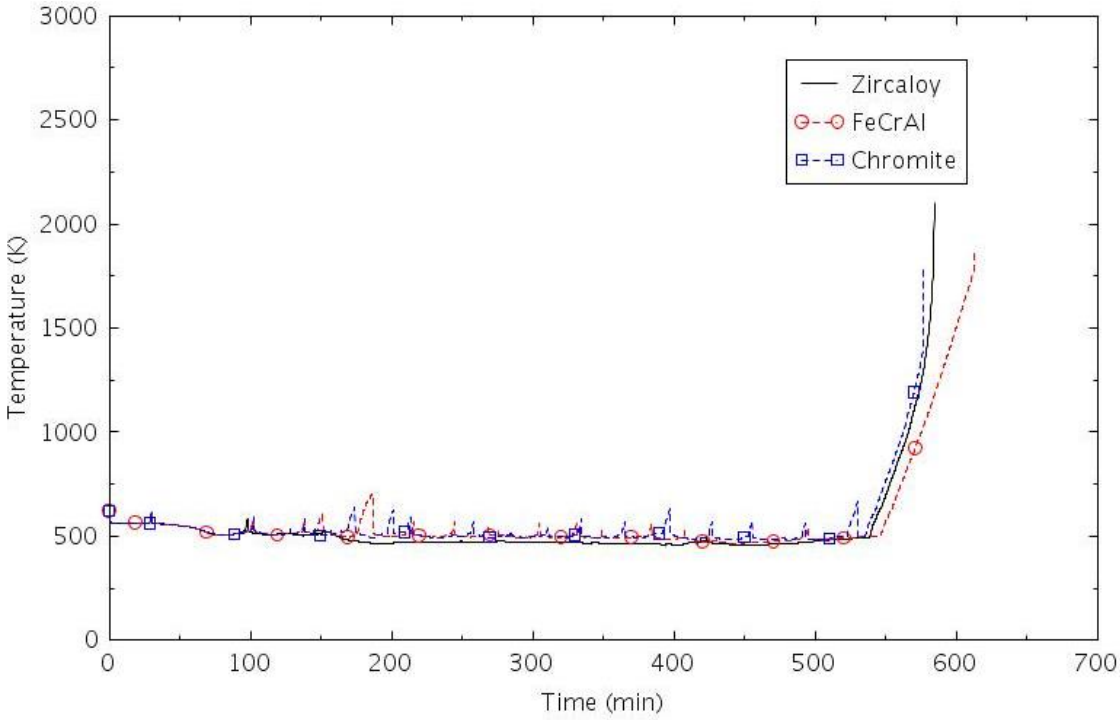

Figure 2-45. Maximum cladding temperature (SBLOCA-3.1).

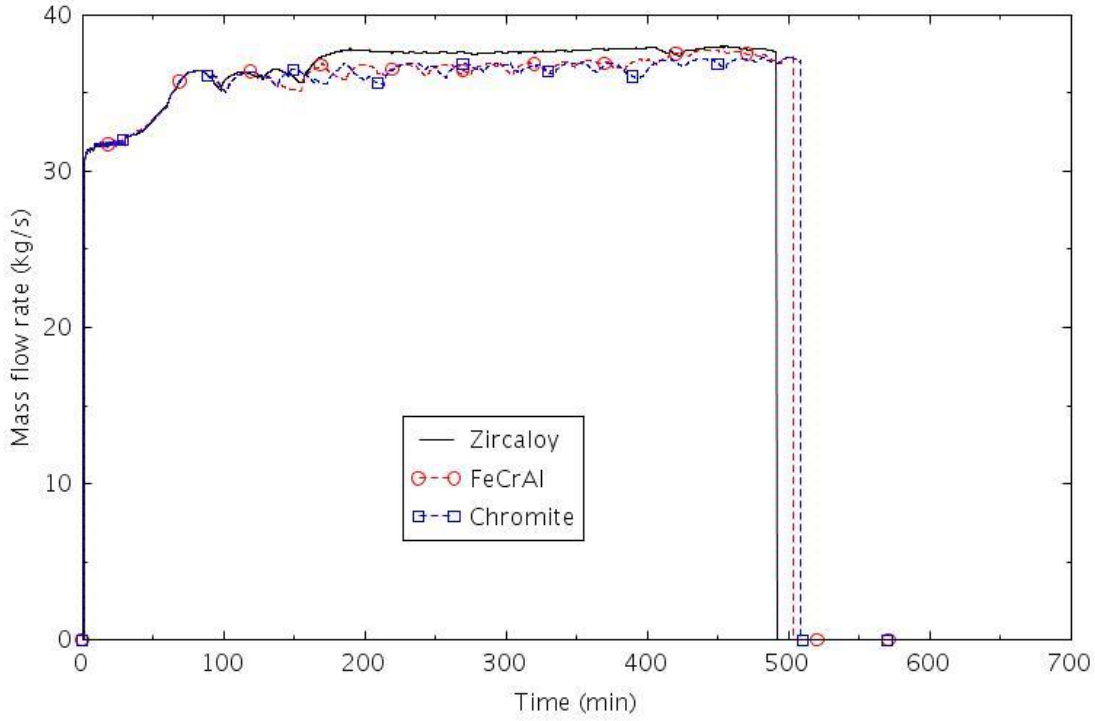

Figure 2-46. Total HPSI flow into the RCS (SBLOCA-3.1).

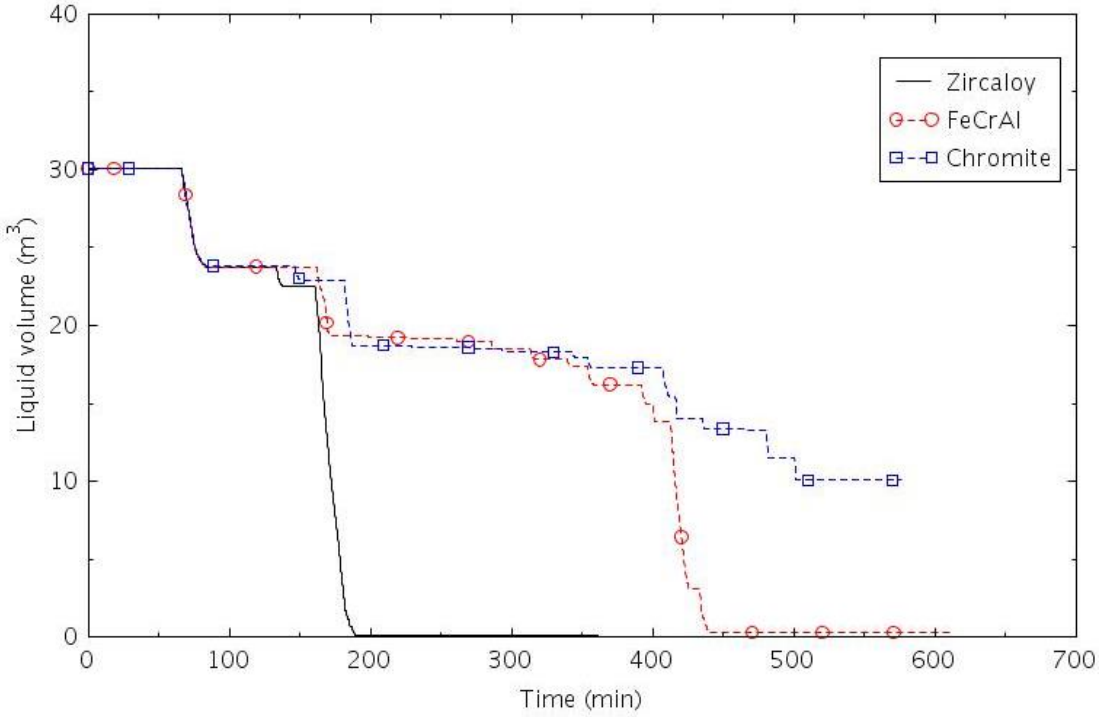

Figure 2-47. Liquid volume in Accumulator B (SBLOCA-3.1).

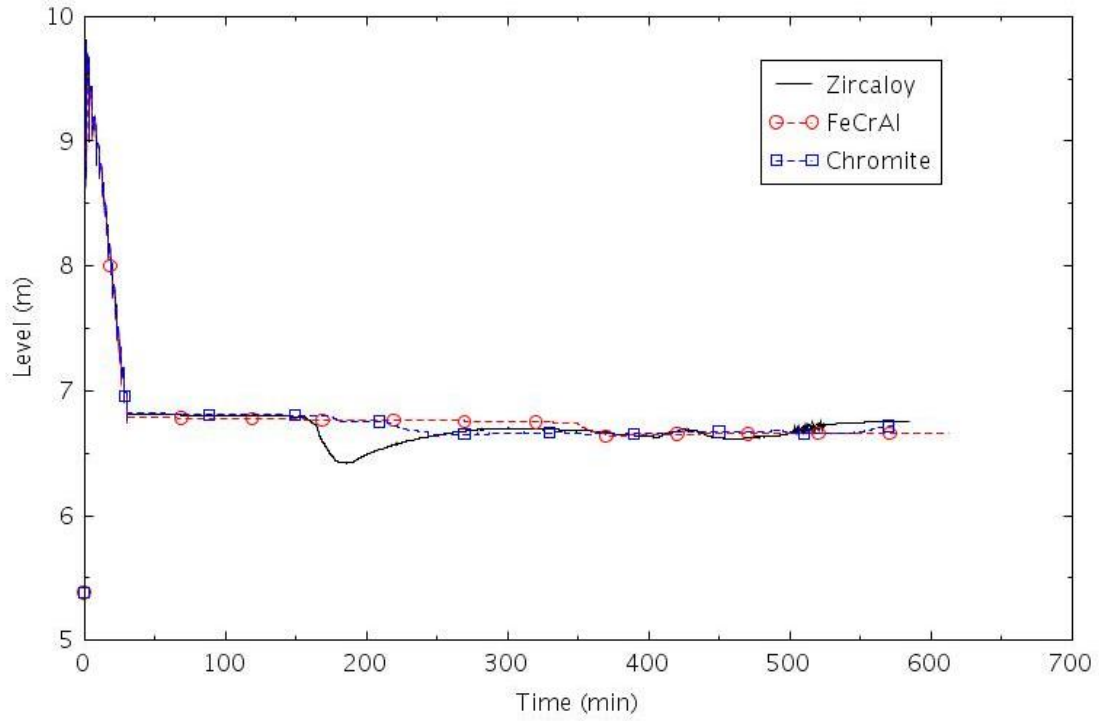

Figure 2-48. Collapsed liquid level in SG B (SBLOCA-3.1).

2.1.3.7 SBLOCA-4.0

This scenario assumed that the reactor trip system failed to scram the reactor and that no feedwater was available. The TSVs were assumed to close 2.0 seconds after the reactor trip signal. The MFW was terminated 6.5 seconds after the reactor trip signal.

The calculated sequences of events are shown in Table 2-9. The reactor trip signal was generated at 0.6 min after the start of the event. The reactor scram was assumed to fail. The TSVs and MFW valves were assumed to close normally following the reactor trip signal. The SIAS was generated at 1.2 minutes, but the HPSI and AFW systems were assumed to fail. The SGs dried out at about 5 minutes. The core began to uncover at about 23 minutes and core damage occurred at about 45 minutes. The amount of hydrogen produced was 14.7 kg for Chromite, 19.8 kg for Zircaloy, and 25.8 kg for FeCrAl. The larger amount of hydrogen produced for FeCrAl was due to a longer heatup time, as discussed later.

Table 2-9. Sequence of Events for Scenario SBLOCA-4.0.

	Time (min)		
Event	**Zircaloy**	**FeCrAl**	**Chromite**
Break opens	0.0	0.0	0.0
Scram signal	0.6	0.6	0.6
SIAS	1.2	1.2	1.2
RCPs tripped	4.6	4.6	4.6
All SGs empty	5.4	5.2	5.3
High containment pressure	14.5	14.6	14.6
Core begins to uncover	22.6	22.7	22.4
0.5 kg H_2 generation	34.5	35.1	34.3
First cladding rupture	36.0	36.6	35.9
Accumulator flow initiated	NA	42.8	NA
Calculated terminated	42.7	49.1	42.0

The following figures illustrate the effects of the cladding on various parameters. The mass flow through the break is shown in Figure 2-49. The flow out the break caused voiding in the RCS, which caused the reactor power (see Figure 2-50) to decrease due to moderator density feedback. The break flow initially caused the RCS to depressurize, as shown in Figure 2-51. The pressure increased after the SGs emptied near 5 minutes, but not enough to challenge the pressurizer PORVs or SRVs. The RCS pressure decreased again after 20 minutes when steam began exiting the break. The pressure increase near 45 minutes with FeCrAl cladding was due to a brief period of accumulator injection, which caused an increase in the liquid level in the core as shown in Figure 2-52, and a decrease in maximum cladding temperature, as shown in Figure 2-53. The accumulator injection was not able to quench the core, but the additional heat removed pressurized the RCS somewhat and gave a few additional minutes of heatup time before core damage occurred. The accumulators were within a minute or two injecting in the cases with Zircaloy and Chromite cladding.

The pressure in SG B is shown in Figure 2-54. Pressure in SG B (SBLOCA-4.0). The SG PORV opened near 1 minute, but it did not have enough relief capacity to prevent the pressure from reaching the SRV setpoint. The SRVs quit cycling after the SGs dried out near 5 minutes, and the PORVs cycled occasionally thereafter.

The collapsed liquid level in the boiler of SG B is shown in Figure 2-55. The collapsed level increased following the closure of the TSVs because of a redistribution of liquid between the downcomer and boiler sides of the SG and the additional mass added to the SG during the coastdown of the MFW. The SGs dried out at about 5 minutes.

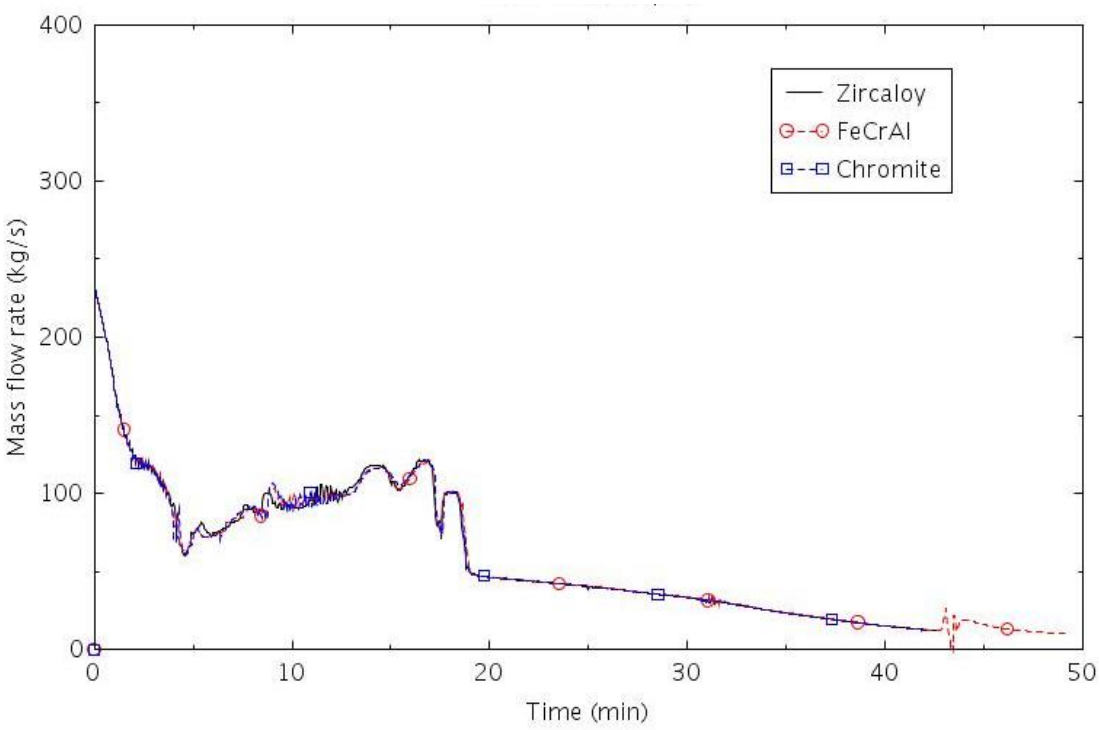

Figure 2-49. Mass flow rate through the break (SBLOCA-4.0).

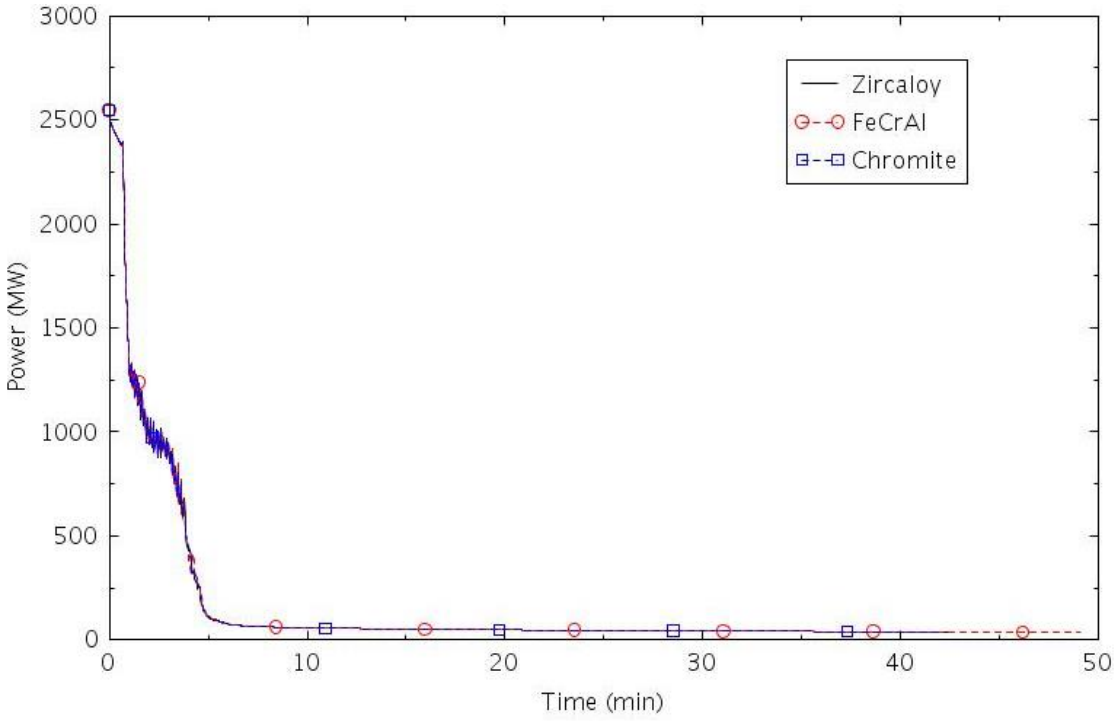

Figure 2-50 Reactor power (SBLOCA-4.0).

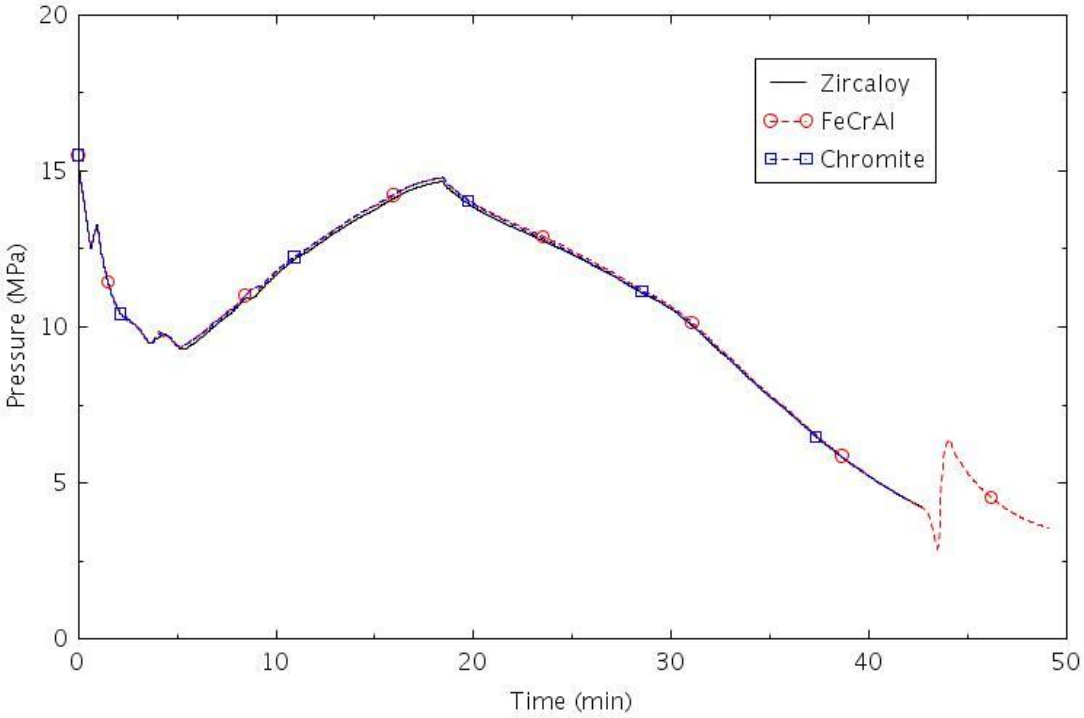

Figure 2-51. Pressure in the pressurizer (SBLOCA-4.0).

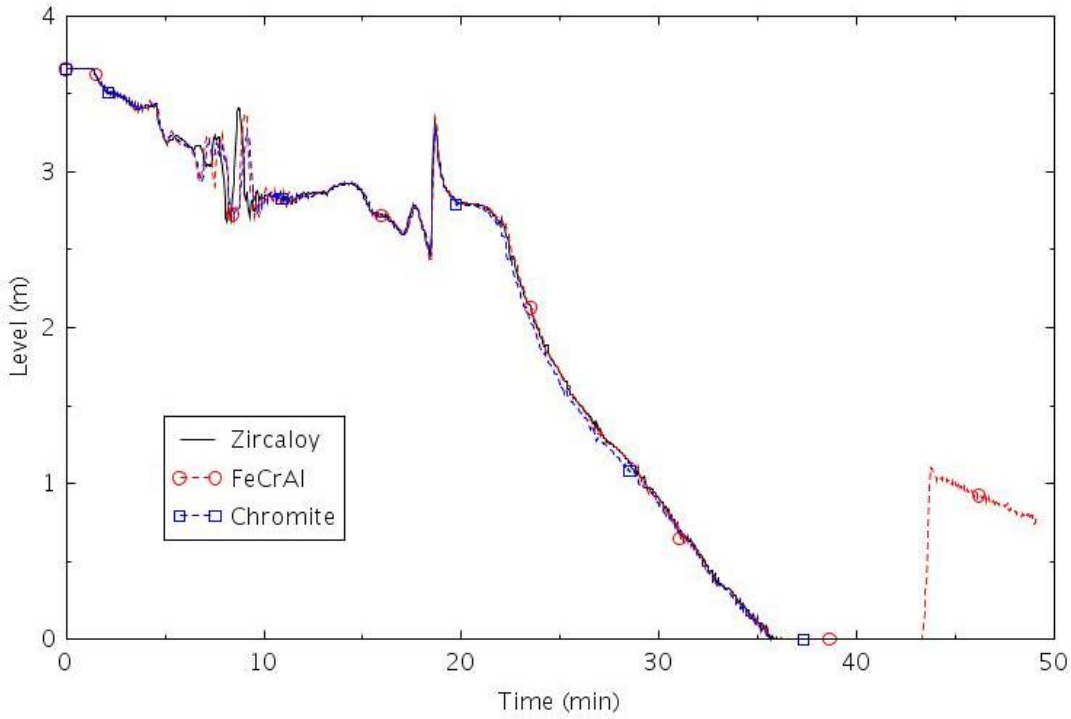

Figure 2-52. Collapsed liquid level in the central core channel (SBLOCA-4.0).

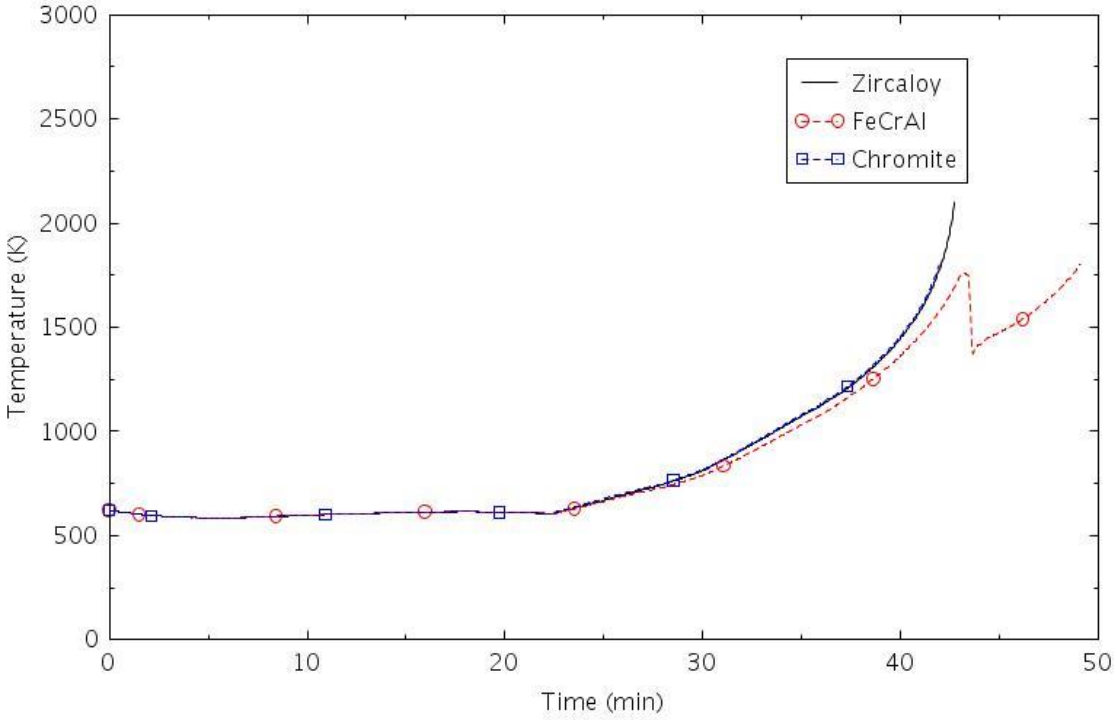

Figure 2-53. Maximum cladding temperature (SBLOCA-4.0).

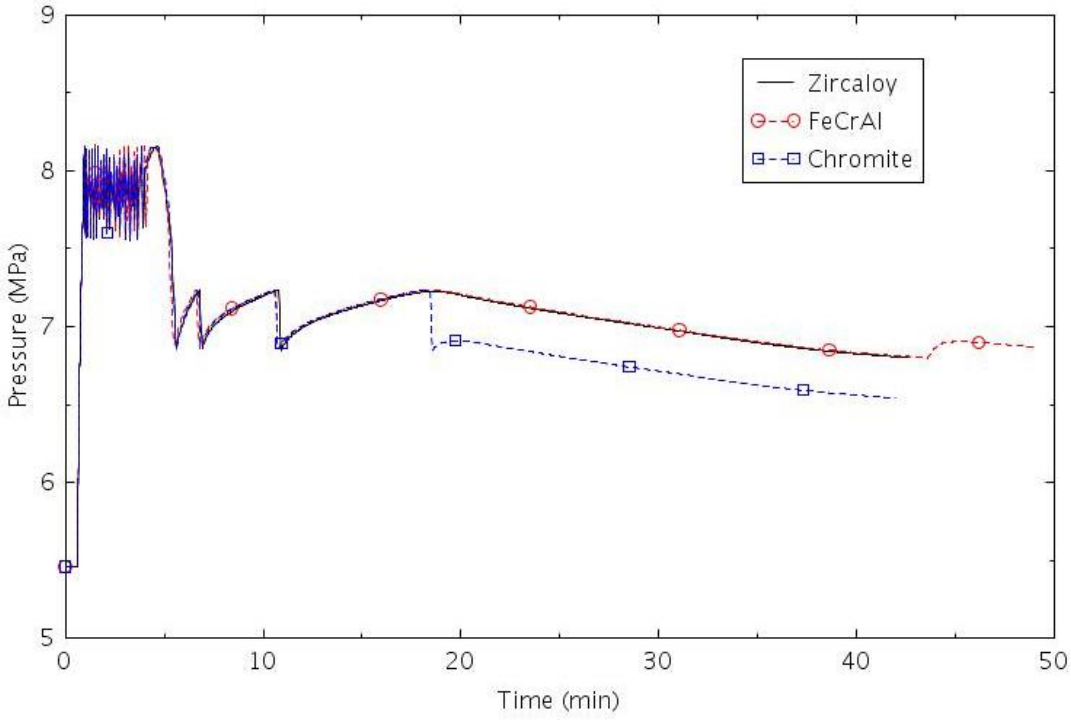

Figure 2-54. Pressure in SG B (SBLOCA-4.0).

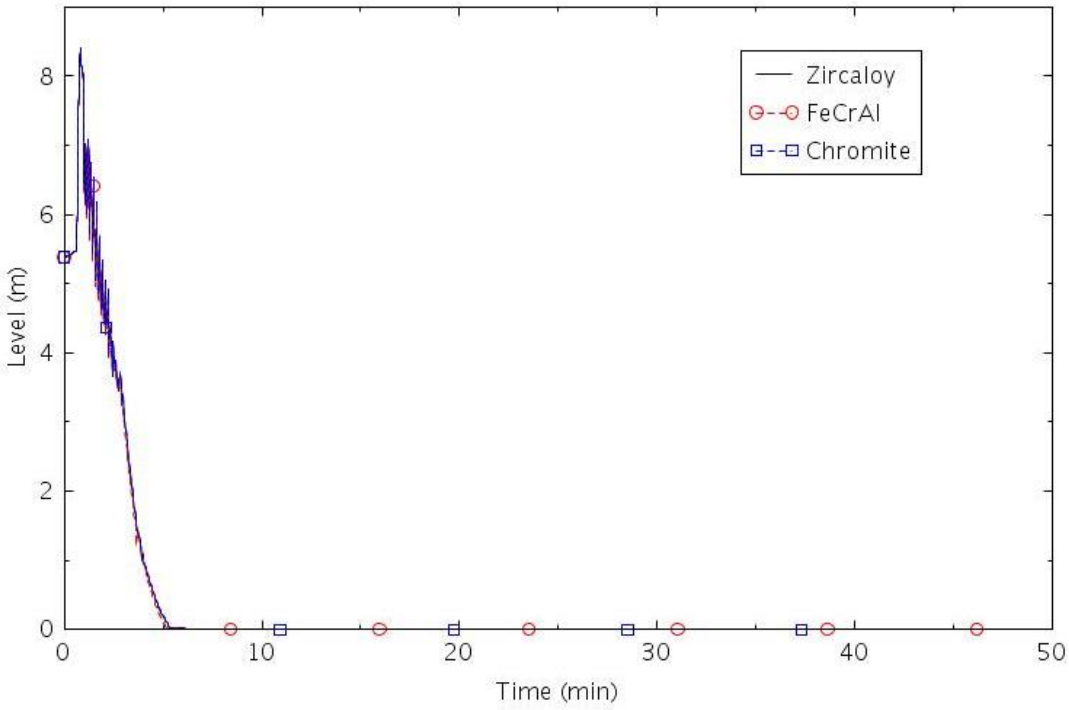

Figure 2-55. Collapsed liquid level in SG B (SBLOCA-4.0).

2.1.3.8 SBLOCA-4.1

This scenario assumed that the reactor trip system failed to scram the reactor, that one motor-driven AFW pump was available, and that HPSI failed. The TSVs were assumed to close 2.0 seconds after the reactor trip signal. The MFW was terminated 6.5 seconds after the reactor trip signal.

The calculated sequences of events are shown in Table 2-10. The reactor trip signal was generated about 0.6 min after the start of the event. The reactor scram was assumed to fail. The TSVs and MFW valves were assumed to close normally following the reactor trip signal. The SIAS was generated at about 1.2 minutes and AFW was initiated 30 seconds later. The HPSI was assumed to fail. The core began to uncover at about 72 minutes and core damage occurred after 4 hours. The amount of hydrogen produced was 33.8 kg for Zircaloy, 35.8 kg for Chromite, and 36.8 kg for FeCrAl. The time between the onset of core uncovery and core damage was relatively long for this scenario due to accumulator injection. The heatup times for FeCrAl and Chromite were longer than for Zircaloy, which resulted in more hydrogen production.

Table 2-10. Sequence of Events for Scenario SBLOCA-4.1.

	Time (hr:min)		
Event	**Zircaloy**	**FeCrAl**	**Chromite**
Break opens	0:00	0:00	0:00
Scram signal	0:00	0:00	0:00
SIAS	0:01	0:01	0:01
AFW initiated	0:01	0:01	0:01
RCPs tripped	0:04	0:04	0:04
Accumulator flow initiated	0:33	0:33	0:33
Core begins to uncover	1:12	1:13	1:13
High containment pressure	1:21	1:22	1:22
First cladding rupture	1:35	1:38	1:36

0.5 kg H_2 generation	1:36	1:39	1:37
Core damage	4:06	4:25	4:23

The following figures illustrate the effects of the cladding on various parameters. The mass flow through the break is shown in Figure 2-56. The flow out of the break caused voiding in the RCS, which caused the reactor power (see Figure 2-57) to decrease due to moderator density feedback. The break flow caused the RCS to depressurize, as shown in Figure 2-58. The brief pressure increases after 150 minutes were due to accumulator injection, which caused increases in the liquid level in the core, as shown in Figure 2-59, and a decrease in maximum cladding temperature, as shown in Figure 2-60. The accumulator injection was not able to quench the core, but the additional heat removed pressurized the RCS somewhat. The sporadic accumulator injection resulted in a relatively long time between the onset of core uncovery and core damage for this scenario. Figure 2-61 shows that the accumulators began injecting near 30 minutes and were nearly empty by the end of the calculations.

The pressure in SG B is shown in Figure 2-62. The SG PORV opened near 1 minute, but it did not have enough relief capacity to prevent the pressure from reaching the SRV setpoint. The SRVs quit cycling after 4 minutes and the PORVs quit cycling near six minutes. The SG in the A loop removed most of the core decay power after about 90 minutes.

The collapsed liquid level in the boiler of SG B is shown in Figure 2-63. The level eventually increased due to the shutdown of fission power due to reactivity feedback and the AFW flow. AFW was still available at the end of the calculations because the ECST was not depleted of liquid.

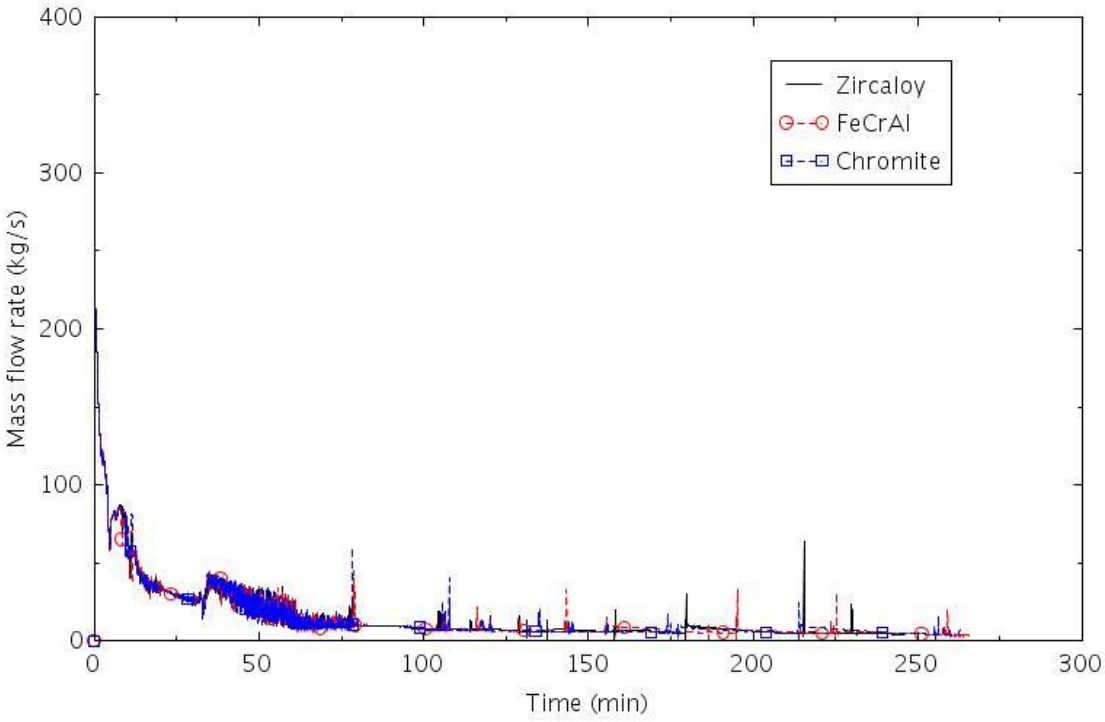

Figure 2-56. Mass flow rate through the break (SBLOCA-4.1).

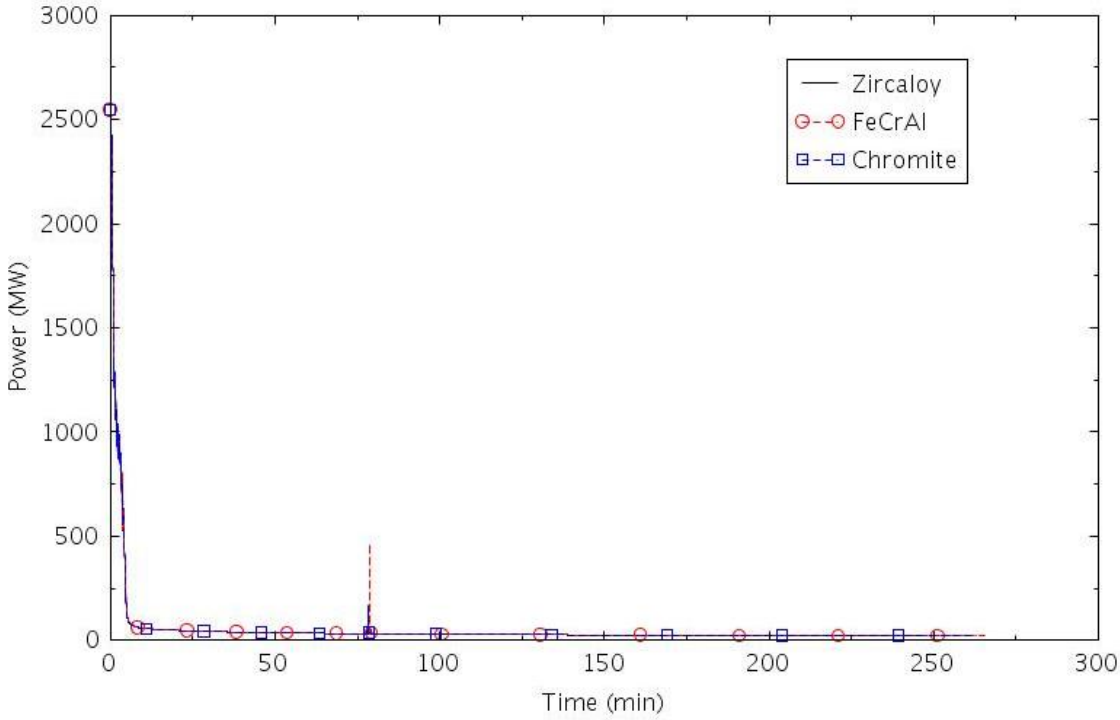

Figure 2-57. Reactor power (SBLOCA-4.1).

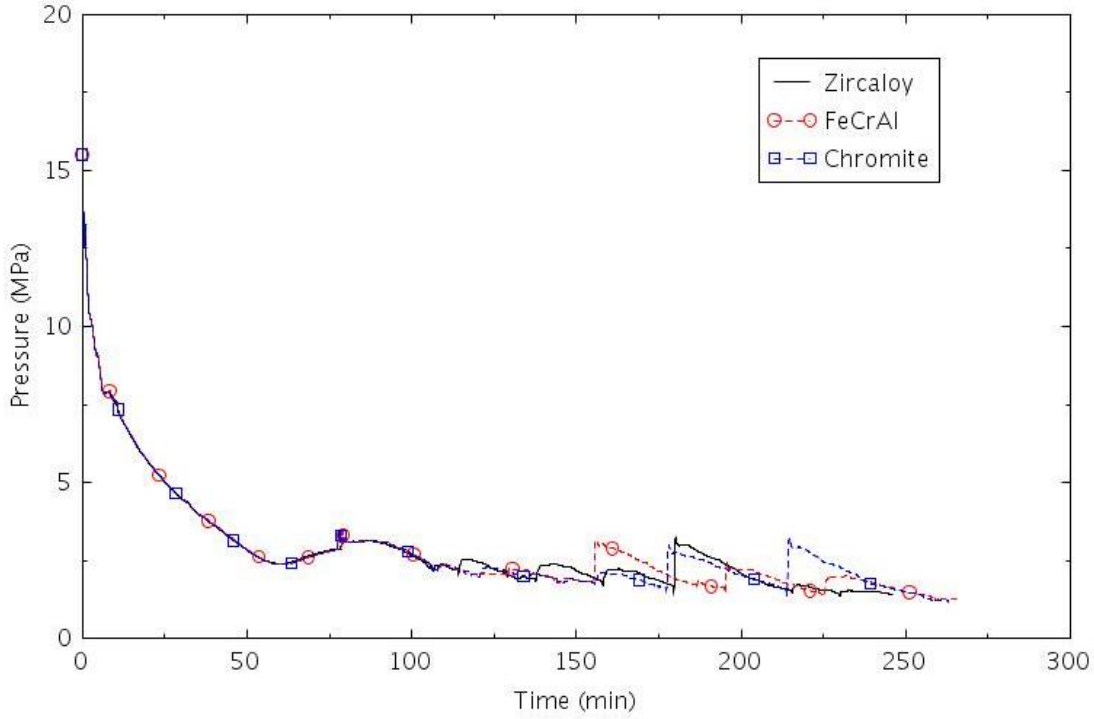

Figure 2-58. Pressure in the pressurizer (SBLOCA-4.1).

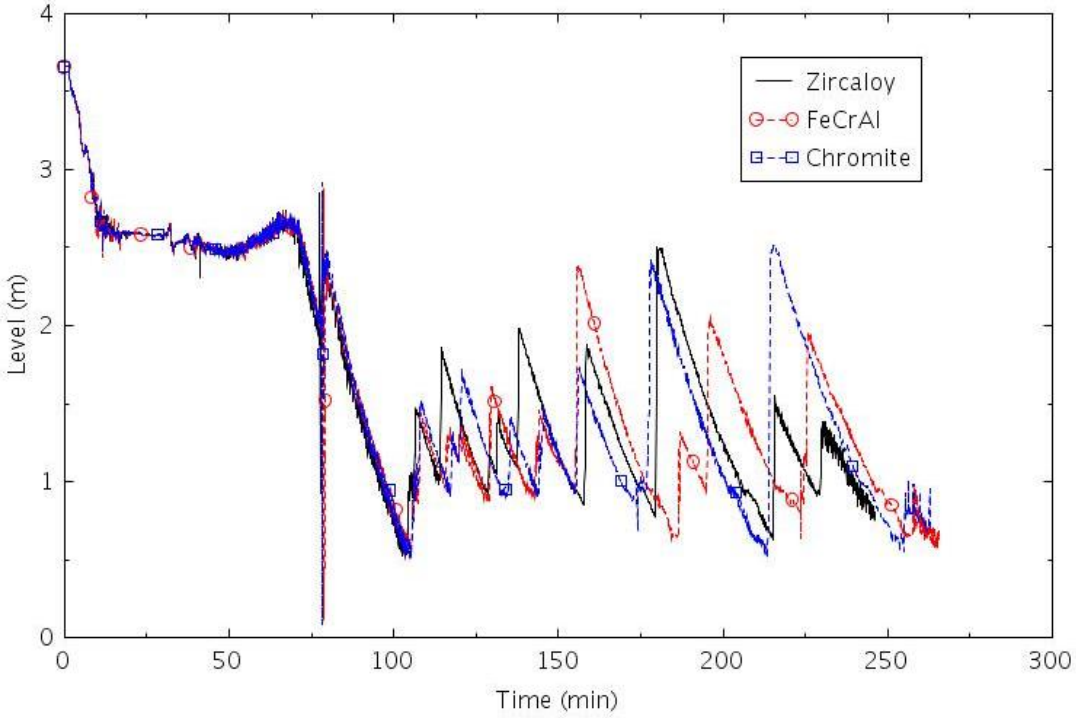

Figure 2-59. Collapsed liquid level in the central core channel (SBLOCA-4.1).

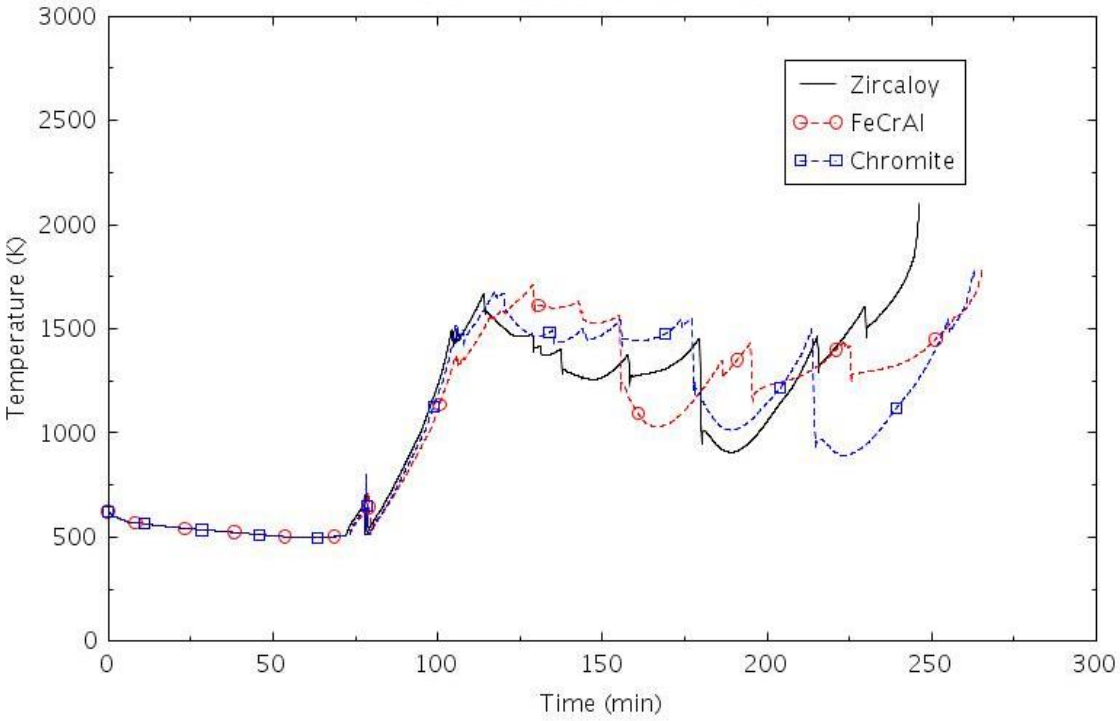

Figure 2-60. Maximum cladding temperature (SBLOCA-4.1).

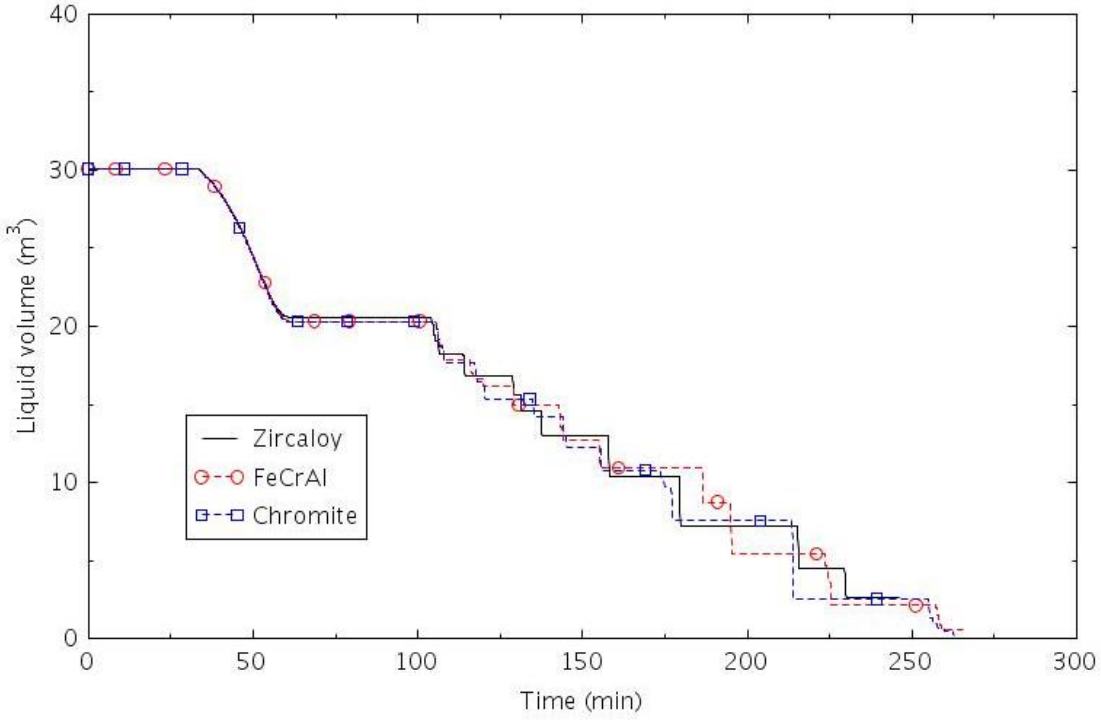

Figure 2-61. Liquid volume in Accumulator B (SBLOCA-4.1).

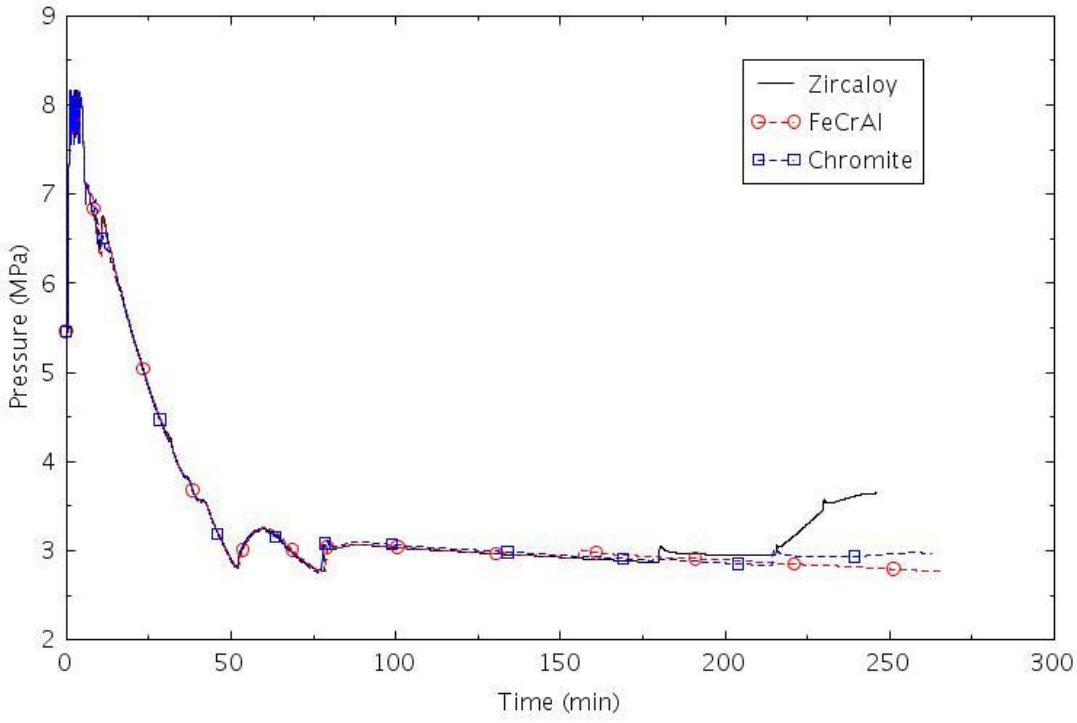

Figure 2-62. Pressure in SG B (SBLOCA-4.1).

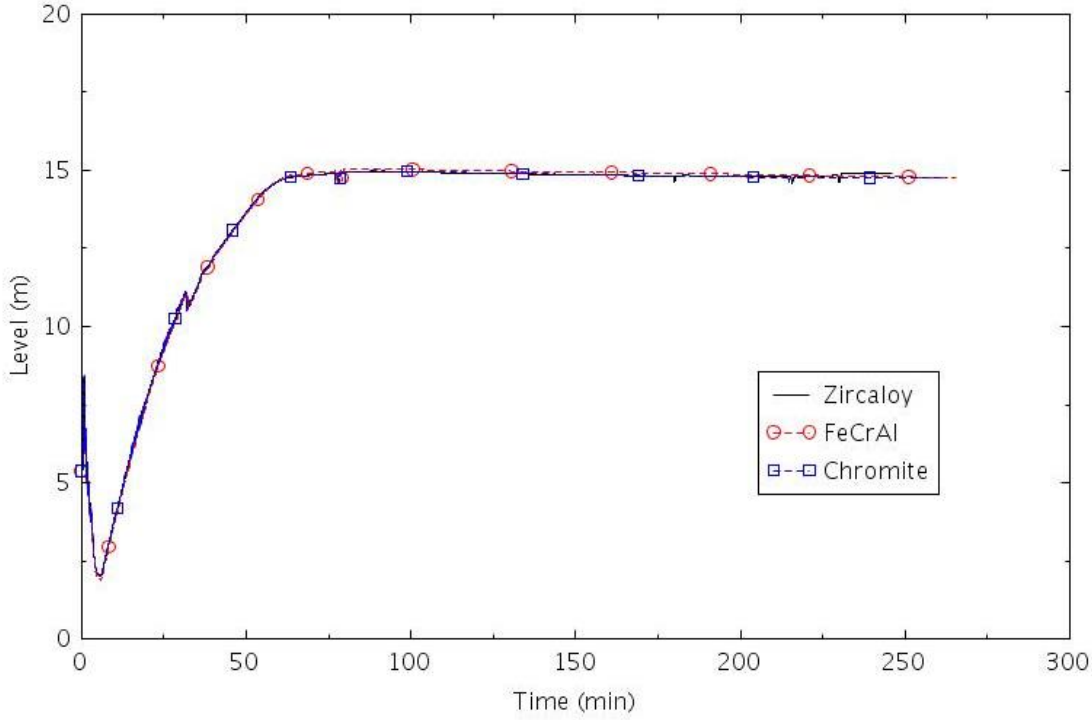

Figure 2-63. Collapsed liquid level in SG B (SBLOCA-4.1).

2.1.4 SBLOCA Analysis Results

Table 2-11 presents a summary of the RELAP5-3D results for time to core uncovery, time to 0.5 kg of hydrogen production, and time to core damage for SBLOCA scenarios with Zircaloy and ATF claddings. The results show that HPSI is far more important than AFW for SBLOCA scenarios with respect to core damage time. The most severe scenarios in terms of the shortest time to core damage, SBLOCA-2.0, SBLOCA-2.1, SBLOCA-3.0, SBLOCA-4.0, and SBLOCA-4.1, had no pumped safety injection. A comparison of SBLOCA-2.1 and SBLOCA-3.0 shows that AFW did not have a significant effect on core damage times for scenarios with reactor trip. However, the effect of AFW is much more significant for scenarios without reactor trip, as shown by a comparison of SBLOCA-4.0 and SBLOCA-4.1.

Table 2-11. Summary of RELAP5-3D Time Results for SBLOCA Scenarios with Zircaloy and ATF Claddings.

Scenario	Time to core uncovery (hr:min)			Time to 0.5 kg H_2 (hr:min)			Time to core damage (hr:min)		
	Zircaloy	FeCrAl	Chromite	Zircaloy	FeCrAl	Chromite	Zircaloy	FeCrAl	Chromite
SBLOCA-1.0	10:39	10:18	10:23	11:19	11:33	11:03	11:31	11:33	11:17
SBLOCA-1.1	8:54	9:15	9:01	9:17	10:05	9:30	9:29	10:05	9:41
SBLOCA-2.0	0:36	0:35	0:35	0:49	4:36	0:52	0:59	4:37	1:05
SBLOCA-2.1	0:37	0:38	0:37	0:48	1:14	0:51	0:58	1:14	1:02
SBLOCA-3.0	0:38	0:38	0:37	0:48	1:13	0:51	1:01	1:13	1:07
SBLOCA-3.1	8:58	9:06	8:55	9:28	10:12	9:31	9:44	10:12	9:36
SBLOCA-4.0	0:22	0:22	0:22	0:34	0:35	0:34	0:42	0:49	0:41
SBLOCA-4.1	1:12	1:13	1:13	1:36	1:39	1:37	4:06	4:25	4:23

Table 2-12 compares the times to core damage for the ATF designs with those for the existing design with Zircaloy cladding in different SBLOCA scenarios. The results show that the gain in coping time for FeCrAl varies between 2 and 36 minutes, except for Scenario SBLOCA-2.0, where the gain in coping time is more than 3 hours. As described previously for Scenario SBLOCA-2.0 with FeCrAl, accumulator injection quenched the core just in the nick of time to prevent core damage. These results indicate that it is possible to obtain large increases in coping times with ATF claddings for selected scenarios. However, the increase in coping time is generally much more modest. For example, if Scenario SBLOCA-2.0 is excluded, the average gain in coping time for FeCrAl is 17 minutes. The average increase in coping time with Chromite cladding is about 3 minutes. A slightly better estimate of the gain in coping time can be obtained by subtracting the time to core uncovery from the time to core damage in Table 2-11 and averaging. Using this metric, the gain in coping time is about 16 minutes for FeCrAl and 4 minutes for Chromite when Scenario SBLOCA-2.0 is excluded. The gain in coping time with the ATF designs is generally modest for SBLOCAs but can be much larger for selected scenarios.

With the above relatively small increase of the time to core damage from the RELAP5-3D simulation results, a change to the general transient PRA model (event tree, fault tree, success criteria, or human reliability analysis [HRA]) is not warranted. The risk benefit on behalf of the CDF brought by the ATF designs would be very small and is not conducted in this analysis.

However, the RELAP5-3D results show a clear benefit in adopting the ATF designs, as much less hydrogen is produced at the time of core damage. Table 2-13 compares the hydrogen production for the ATF designs with those for the existing Zircaloy clad design in different SBLOCA scenarios. The hydrogen production is generally significantly smaller with the ATF claddings. The ATWS scenarios are exceptions in that the hydrogen production with the ATF claddings can exceed that with Zircaloy due to longer heatup times. Excluding the ATWS scenarios, the average hydrogen production with FeCrAl was 6.4% of that with Zircaloy. The average hydrogen production with Chromite was 36.9% of that with Zircaloy.

Table 2-12. Time to Core Damage Comparisons for SBLOCA Scenarios with ATF Designs.

Section	Scenario	Description	Time to core damage (hr:min)				
			Zircaloy	FeCrAl	Δt (FeCrAl)	Chromite	Δt (Chromite)
2.1.3.1	SBLOCA-1.0	SBLOCA with AFW, SSC, and HPSI	11:31	11:33	0:02	11:17	-0:14
2.1.3.2	SBLOCA-1.1	SBLOCA with AFW and HPSI, but no SSC	9:29	10:05	0:36	9:41	0:12
2.1.3.3	SBLOCA-2.0	SBLOCA with AFW and SSC, but no HPSI	0:59	4:37	3:38	1:05	0:06
2.1.3.4	SBLOCA-2.1	SBLOCA with AFW, but no SSC and no HPSI	0:58	1:14	0:16	1:02	0:04
2.1.3.5	SBLOCA-3.0	SBLOCA with no AFW and no FAB	1:01	1:13	0:12	1:07	0:06
2.1.3.6	SBLOCA-3.1	SBLOCA with FAB, but no AFW	9:44	10:12	0:28	9:36	-0:08
2.1.3.7	SBLOCA-4.0	SBLOCA with ATWS and no AFW	0:42	0:49	0:07	0:41	-0:01
2.1.3.8	SBLOCA-4.1	SBLOCA with ATWS and AFW	4:06	4:25	0:19	4:23	0:17

Table 2-13. H2 Production Comparisons for SBLOCA Scenarios with ATF Designs.

Section	Scenario	Description	Total H_2 (kg)			H_2 %	
			Zircaloy	FeCrAl	Chromite	FeCrAl	Chromite
2.1.3.1	SBLOCA-1.0	SBLOCA with AFW, SSC, and HPSI	10.1	0.7	6.0	6.5	59.3
2.1.3.2	SBLOCA-1.1	SBLOCA with AFW and HPSI, but no SSC	13.7	1.3	5.8	9.8	42.6
2.1.3.3	SBLOCA-2.0	SBLOCA with AFW and SSC, but no HPSI	21.2	1.5	7.9	7.1	37.2
2.1.3.4	SBLOCA-2.1	SBLOCA with AFW, but no SSC and no HPSI	23.9	0.8	9.7	3.3	40.5
2.1.3.5	SBLOCA-3.0	SBLOCA with no AFW and no FAB	29.7	0.7	9.7	2.5	32.8
2.1.3.6	SBLOCA-3.1	SBLOCA with FAB, but no AFW	13.9	1.2	1.2	8.9	8.7
2.1.3.7	SBLOCA-4.0	SBLOCA with ATWS and no AFW	19.8	25.8	14.7	130.6	74.2
2.1.3.8	SBLOCA-4.1	SBLOCA with ATWS and AFW	33.8	36.8	35.8	108.9	106.0

2.2 General Transient – Locked Rotor Scenario Analysis

2.2.1 General Transient PRA Model and Scenarios

The generic PRA model represents general transient by the TRANS event tree and a series of sub event trees that are transferred from the main event tree. Figure 2-64 shows the TRANS event tree. Figure 2-65 shows the loss of seal cooling (LOSC) for RCP event tree that is transferred from TRANS Sequences 2 and 10. Figure 2-66 shows the AWTS event tree that is transferred from TRANS Sequence 21. Sequences of the LOSC event tree also transfer to SLOCA event tree (Figure 2-1) for SBLOCA and MLOCA event tree (Figure 2-67) for medium-break loss-of-coolant accident (MLOCA).

The TRANS event tree was quantified with SAPHIRE 8 using a truncation level of 1E-12. Table 2-14 presents the quantification results. The total TRANS CDF is 7.96E-7/year. There are 10 non-zero CDF sequences out of a total of 145 TRANS accident sequences (i.e., the sequence end state is core damage). TRANS Sequence 21:16 is the most risk-significant sequence with a CDF of 5.39E-07/year and contributes 67.7% of the total TRANS CDF. In this sequence, the RPS fails to trip the reactor following the general transient IE, the sequence transfers from the TRANS Sequence 21 to the ATWS event tree. In the ATWS event, if the RCS pressure exceeds the design pressure of the reactor vessel (ATWS Sequence 16), core damage is assumed. TRANS Sequence 20 is the second-most risk-significant sequence, with a CDF of 1.45e-07/year, contributing 18.2% of the total TRANS CDF. In this sequence, RPS trips the reactor successfully, but neither MFW nor AFW could provide enough cooling water to at least one steam generator. When FAB cooling also fails to provide decay heat removal, core damage cannot be prevented. Other significant TRANS sequences include another ATWS sequence (TRANS:21-14, contributing 9.1% of total TRANS CDF) and a loss of RCP seal cooling sequence (TRANS:02-02-09, contributing 4.3% of the total TRANS CDF).

Table 2-14. Overview of TRANS Event Trees Quantification Results.

Sequence	CDF	Cut Set Count	% CDF
TRANS:02-02-09	3.39E-08	1265	4.3%
TRANS:02-02-10	4.54E-10	126	0.1%
TRANS:02-03-09	1.41E-09	283	0.2%
TRANS:02-04-10	2.43E-10	77	0.0%
ITRANS:02-14-10	6.99E-11	39	0.0%
TRANS:19	2.80E-09	159	0.4%
TRANS:20	1.45E-07	984	18.2%
TRANS:21-14	7.24E-08	47	9.1%
TRANS:21-15	8.18E-10	99	0.1%
TRANS:21-16	5.39E-07	51	67.7%
TRANS Total	7.96E-07	3130	100.0%

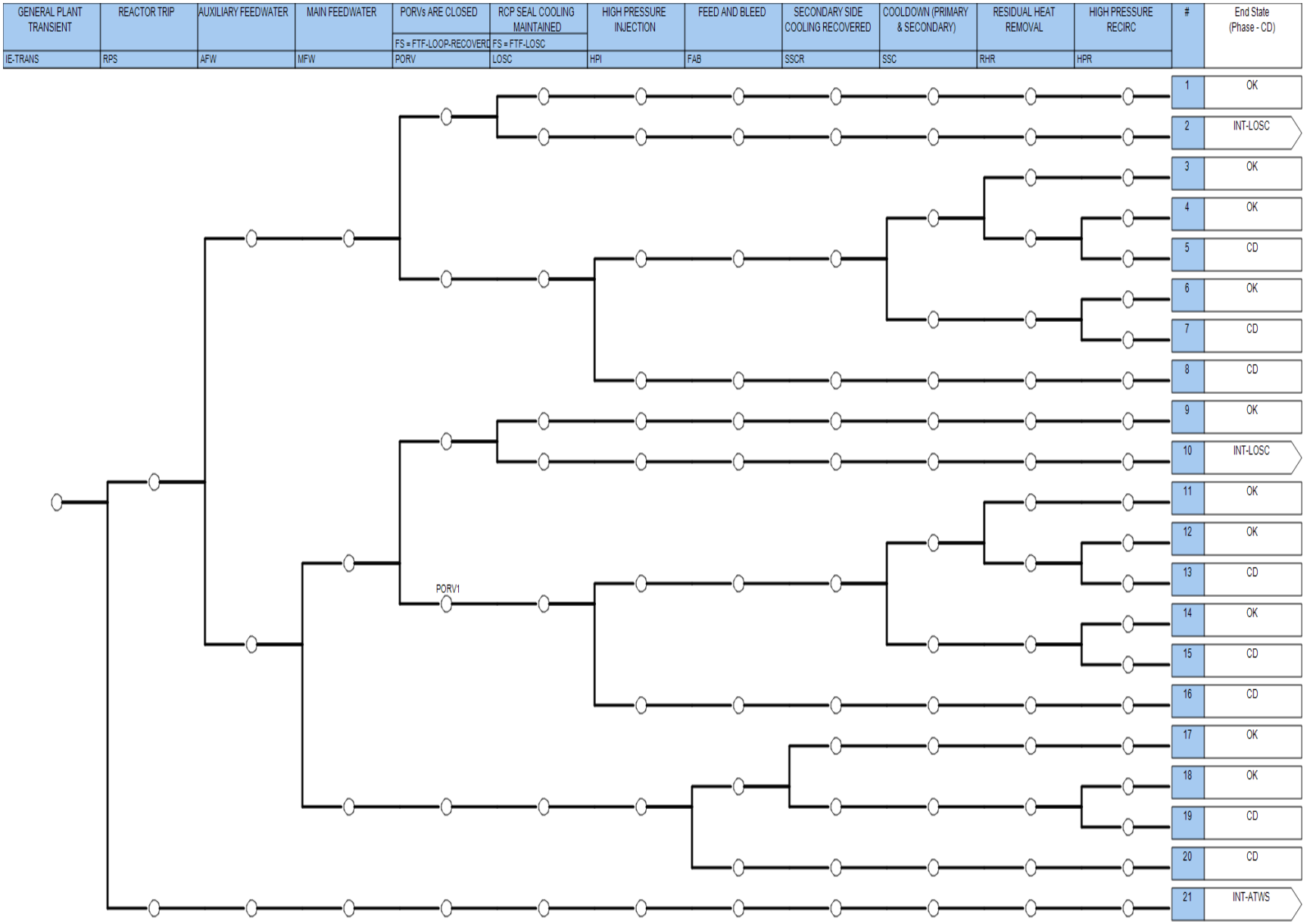

Figure 2-64. Generic PWR TRANS event tree for general transient.

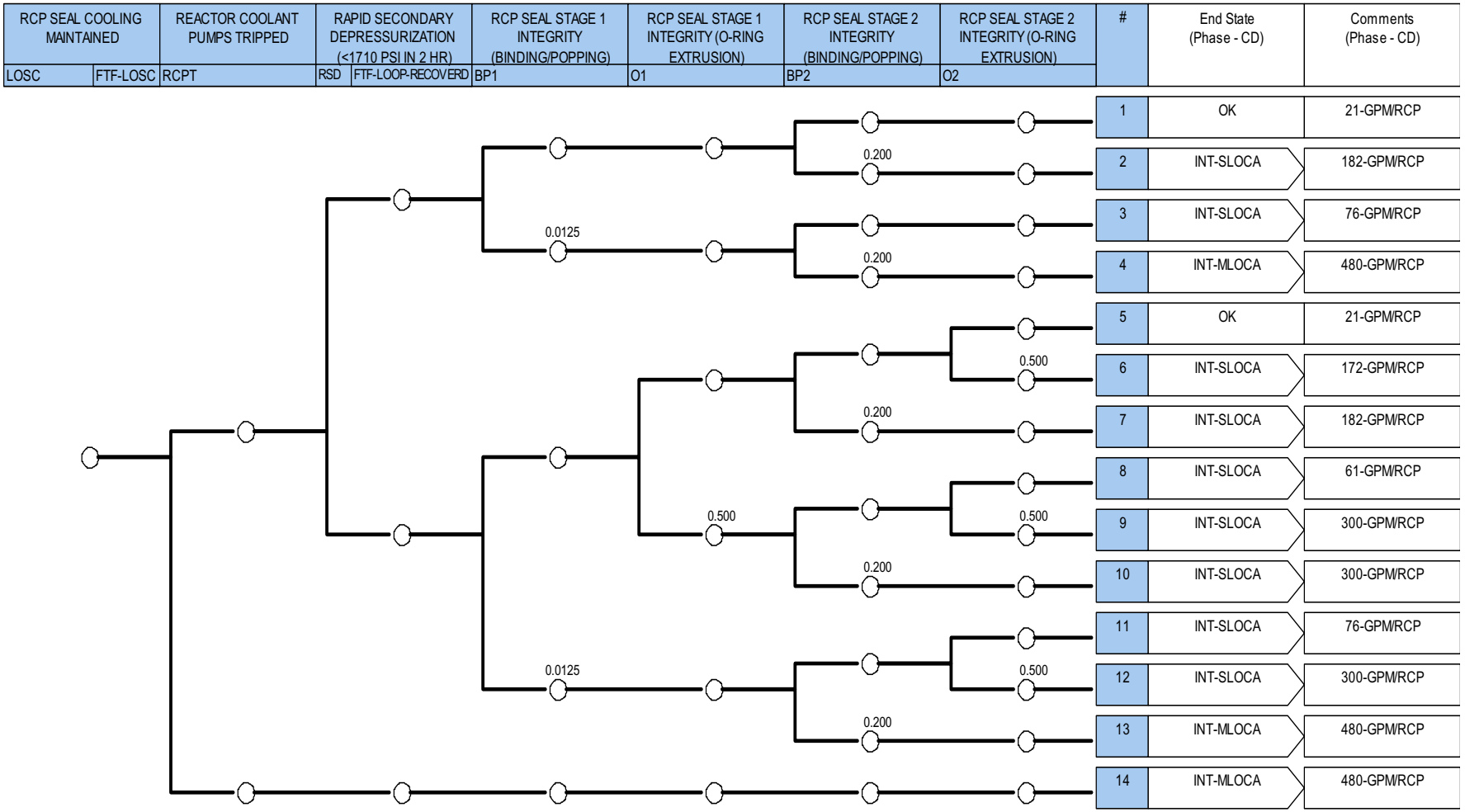

Figure 2-65. Generic PWR LOSC event tree – transfer from TRANS.

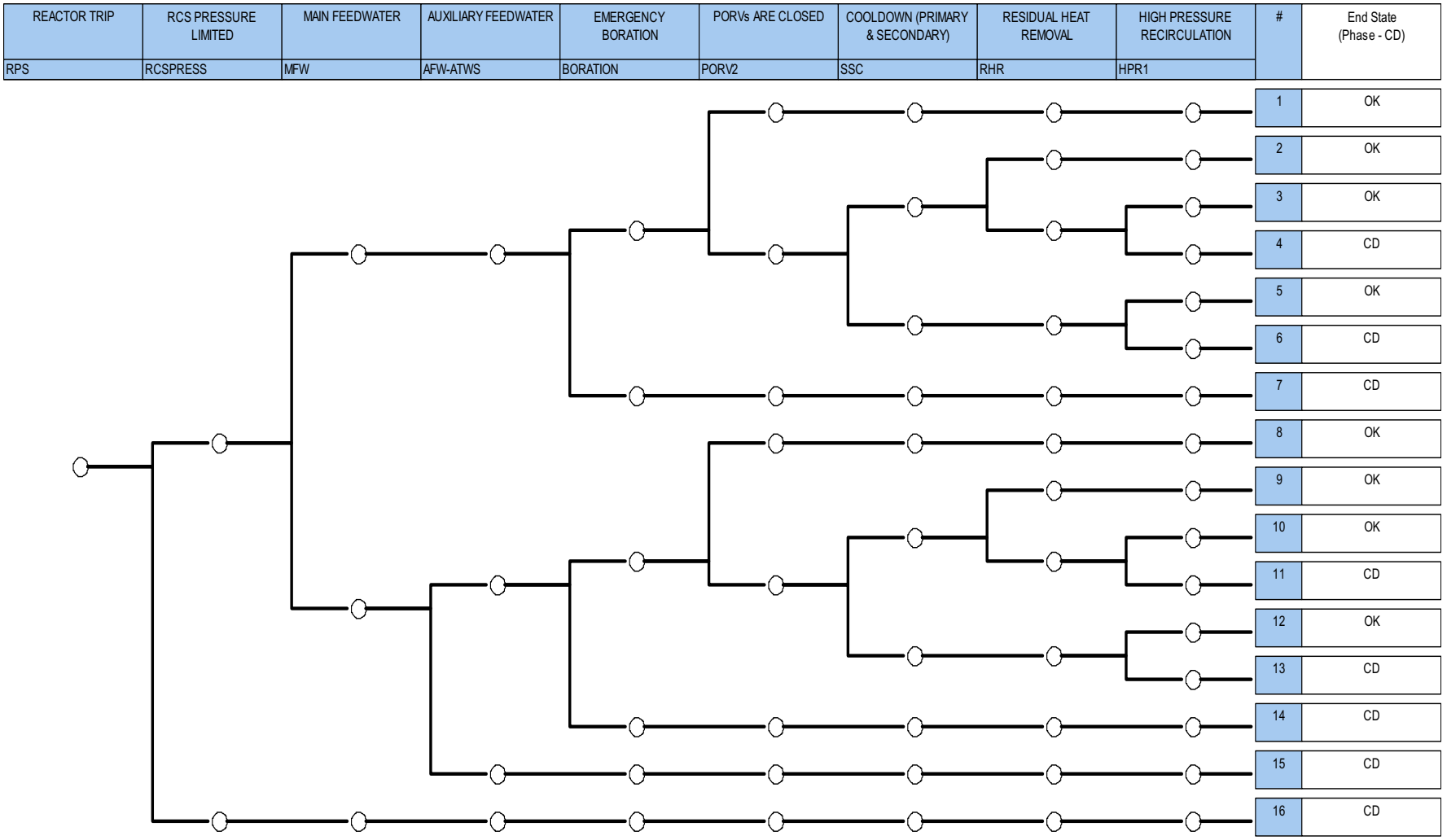

Figure 2-66. Generic PWR ATWS event tree – transfer from TRANS.

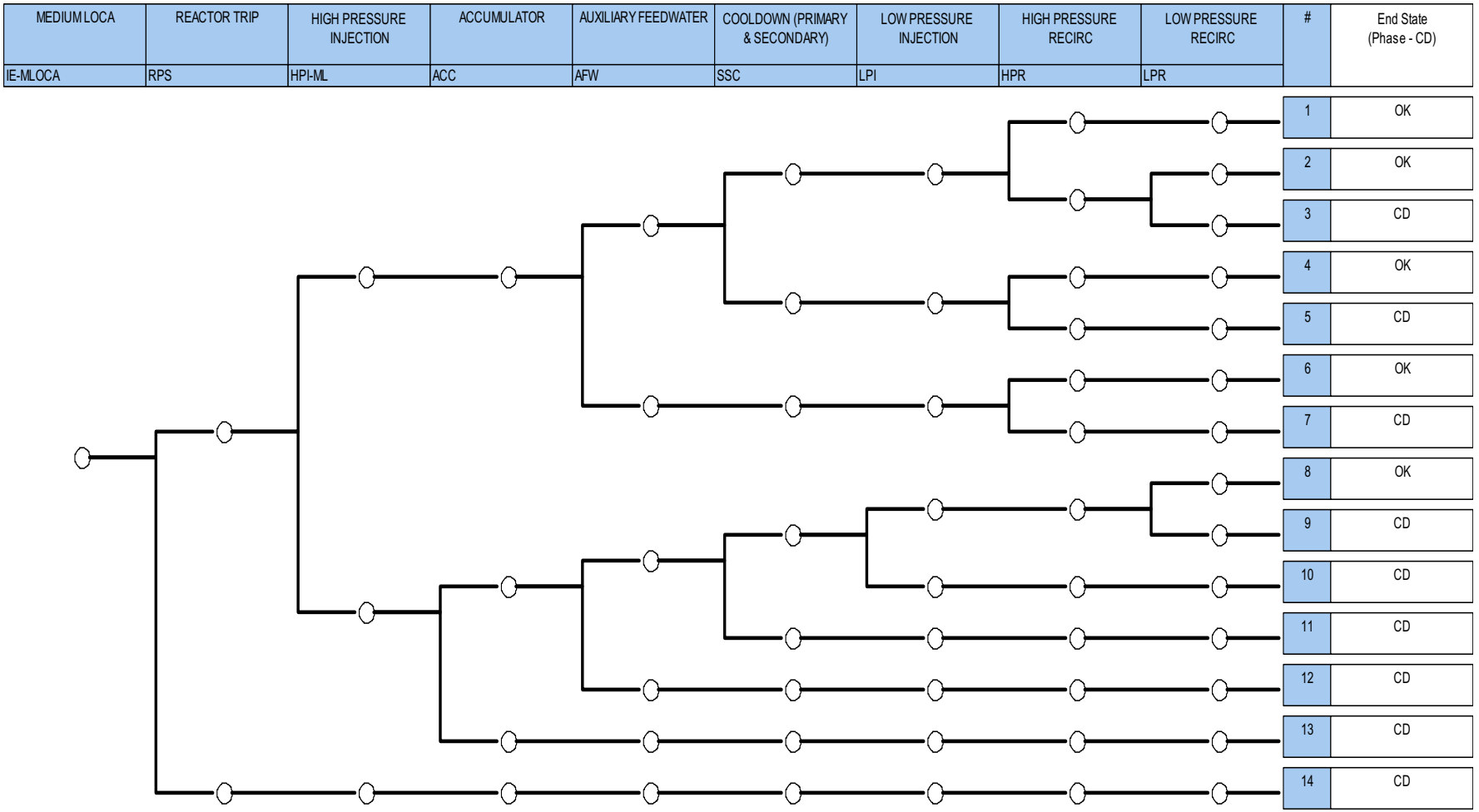

Figure 2-67. Generic PWR MLOCA event tree – transfer from TRANS&LOSC with 480 gpm/RCP.

The following TRANS scenarios were developed as input for RELAP5-3D thermal hydraulic analysis with traditional fuel design and near-term ATF designs.

TRANS-1: A general transient IE occurs, the reactor automatically shuts down; however, neither MFW nor AFW supplies enough cooling water to at least one steam generator. When FAB cooling also fails to remove decay heat, core damage occurs.

TRANS-2: This scenario is similar with TRANS-1, except that FAB cooling succeeds. Secondary cooling is not recovered and HPR fails to provide long-term RCS makeup after RWST depletes, core damage occurs.

PORV-1: A general transient IE occurs, the reactor automatically shuts down, feedwater is available. The pressurizer PORV, however, stuck open after its first lift, and no HPI is available.

LOSC-182a: A general transient IE occurs, the RPS trips the reactor, feedwater is available, no PORVs are open; however, RCP seal cooling is not maintained, leading to an LOSC accident. The RCP is tripped, the RCS depressurization is successful; however, the RCP seal fails at the second stage, leading to a SBLOCA with a leak rate of 182 gallon per minute (gpm). Secondary side cooldown is successful, however, neither HPI nor LPI is available to provide makeup water to the RCS, core damage occurs.

LOSC-182b: This scenario is similar with LOSC-182a, except that secondary side cooldown fails.

LOSC-76: This scenario is similar with LOSC-182a, except that the RCP seal leak rate is 76 gpm.

LOSC-480: This scenario is similar with LOSC-182a, except that the RCP seal leak rate is 480 gpm which corresponds a MLOCA. Accumulators and auxiliary feedwater are available to mitigate the accident. Secondary side cooldown is successful, however, neither HPI nor LPI is available to provide makeup water to the RCS, core damage occurs.

ATWS-1: A generic transient IE occurs, the RPS fails to trip the reactor, leading to an ATWS. As the RCS pressure exceeds the design pressure of the reactor vessel, core damage is assumed.

ATWS-2: A generic transient IE occurs, the RPS fails to trip the reactor, leading to an ATWS. The RCS pressure remains under the reactor vessel design pressure boundary; however, no feedwater is available and core damage occurs.

ATWS-3: This scenario is similar with ATWS-2, except that AFW is available. Due to a failure in providing borated water to the reactor core, core damage still occurs.

Table 2-15 presents an overview of the TRANS scenarios developed for RELAP5-3D analysis. All these scenarios would be run with RELAP5-3D, first with the current Zr-based fuel cladding design as the base case, and then with the ATF design (the FeCrAl design or the Cr-coated design). The times of PCT to reach melting point, the times to generate a half kilogram hydrogen, and the total amount of hydrogen generated when the run is terminated, are compared between different cladding designs for each scenario. The estimated time differences for PCT to reach melting point from RELAP5-3D are then considered for PRA model changes to evaluate the risk impacts from the proposed ATF design.

Table 2-15. TRANS Scenarios for RELAP-5 3D Analysis.

RELAP-5 Scenario	Scenario Description	TRANS					PORV or RCP Seal LOCA							ATWS		
		RPS	FW	FAB	SSCR	HPR	PORV	RCP Seal	HPI	ACC	AFW	SSC	LPI	RCS-P	AFW	Boration
TRANS-1	General Transient, No FW, No F&B	Trip	No FW	No FAB												
TRANS-2	General Transient, No FW, with F&B	Trip	No FW	FAB	No SSCR	No HPR										
PORV-1	PORV LOCA	Trip	FW				PORV LOCA		No HPI							
LOSC-182a	RCP Seal LOCA 182 gpm, SLOCA	Trip	FW				PORV OK	182 gpm	No HPI			SSC	No LPI			
LOSC-182b	RCP Seal LOCA 182 gpm, SLOCA	Trip	FW				PORV OK	182 gpm	No HPI			No SSC				
LOSC-76	RCP Seal LOCA 76 gpm, SLOCA	Trip	FW				PORV OK	76 gpm	No HPI			SSC	No LPI			
LOSC-480	RCP Seal LOCA 480 gpm, MLOCA	Trip	FW				PORV OK	480 gpm	No HPI	ACC	AFW	SSC	No LPI			
ATWS-1	ATWS	No Trip												RCS-P Fail		
ATWS-2	ATWS	No Trip												RCS-P Good	No AFW	
ATWS-3	ATWS	No Trip												RCS-P Good	AFW	No Boration

2.2.2 Locked Rotor RELAP5-3D Model

The same RELAP5-3D IGPWR model as in (Ma, et al., 2018) was used in this analysis. The details of this are described in (Parisi, et al., 2016). The model is based on a generic Westinghouse three-loop PWR.

2.2.3 Locked Rotor RELAP5-3D Analysis

The locked rotor event is initiated by a seizure of an RCP motor due to a mechanical failure. The event is described in Section 14.2.9.2 of the Surry Power Station Final Safety Analysis Report (FSAR) (Dominion, 2007). The event was simulated by instantly decreasing the speed of the RCP in Loop A to zero. Offsite power is assumed to be available. The early response of the all the analyzed scenarios was similar. The reactor trip signal was generated when the flow in Loop A decreased to 87% of the steady-state value, based on Section 14.2.8.2.2 of the FSAR (Dominion, 2007). Reactor scram, which is defined as the release of the control rods, was assumed to occur 1 second later for those cases in which the reactor trip system was assumed to work. MFW was assumed to terminate normally following reactor trip, delivering the equivalent of 5 seconds of full flow after the scram before coasting down to zero. The MSIVs in the model were assumed to close 1 second after the reactor scram to simulate closure of the TSVs. The steam generator (SG) power operated relief valves (PORVs) were assumed to operate as necessary to control SG pressure. The decrease in heat removal by the affected SG in Loop A caused a rapid pressure increase in the RCS that reached the open setpoint of the pressurizer PORV. The PORV generally lifted once a few seconds after the start of the event for those transients in which it was assumed to be available.

For the scenarios with feedwater, one MDAFP was generally assumed to be available. The operators were assumed to control the SG levels to near the level of the feedwater ring. The AFW was terminated after the injected volume exceeded the minimum operating volume of the emergency condensate storage tank (ECST), which was 96,000 gallons, based on page 10.2-29 of (Dominion, 2007).

The SIAS was initiated either on high containment pressure (P > 122 kPa [17.7 psia]) or low-low reactor pressure (12.34 MPa [1789.7 psia]), based on Page A-2 of (NRC, 2011). For the one scenario in which pumped safety injection was credited, one high pressure safety injection (HPSI) pump was assumed to be available. The high pressure safety injection was terminated when the water source for the safety injection automatically switches from the RWST to the containment sump, based on Page 9 of (NRC, 2011) because the automatic switch was assumed to fail. Containment spray and fan coolers were assumed to be available because the containment spray uses a significant amount of RWST water and results in an earlier loss of HPSI flow.

The RCPs in the unaffected loops were assumed to trip when average void fraction in the vicinity of the pumps exceeded 0.1. This trip could be due to a pump failure in two-phase flow or to an operator action in response to pump vibrations. The time of core damage would have been delayed if the RCPs had been tripped sooner.

Most of the calculations were terminated when the maximum cladding temperature reached 2099 K for cases with Zircaloy and 1804 K for cases with FeCrAl and Chromite. The temperatures were assumed to correspond to core damage.

Three anticipated transients without scram (ATWS) scenarios were simulated. A point kinetics model was used to calculate the reactor power during these scenarios. For convenience, the point kinetics model was taken from the H. B. Robinson Unit 2 model described in (Fletcher, et al., 1985). H. B. Robinson is a three-loop Westinghouse pressurized water reactor that is similar to Surry. Reactivity feedbacks due to changes in moderator density and fuel temperature at the end of life were modeled using a powered-squared weighting scheme. The point kinetics model from H. B. Robinson was judged to be sufficiently representative of Surry to determine the relative effects of different claddings during the various scenarios.

The calculated results for the general transient scenarios described in Table 2-15 are summarized in the following sections.

2.2.3.1 TRANS-1

This scenario assumed that no feedwater was available after the initial coastdown of the MFW and that no high-pressure injection was available. The only cooling mechanisms present were due to the inventory of water stored in the SGs and the reactor coolant system (RCS) at the beginning of the transient.

The calculated sequences of events are shown in Table 2-16. The reactor trip signal was generated 0.1 seconds after the start of the event. The reactor scram, termination of MFW, closure of the TSVs, the first lift of the pressurizer PORV and the SG PORVs all occurred within 10 s. Heat from the core and the RCPs was transferred to the SGs, boiling liquid to steam, which was then vented out of the SG PORVs. The pressurizer PORV began to cycle at 58 minutes, shortly before all of the SGs were empty. The RCPs in the unaffected loops were tripped at 90 minutes. The SIAS occurred near 100 minutes, but the HPSI pumps were assumed to fail. The core began to uncover near 110 minutes. The differences between calculations due to the different claddings were negligible before the core began to uncover and were relatively small after the onset of core uncovery. The calculations were terminated when the hottest cladding reached its maximum temperature. The termination times varied by less than 10 minutes. The calculated amount of hydrogen produced during the transients varied significantly between claddings. The amount of hydrogen produced was 0.7 kg for Chromite, 1.5 kg for FeCrAl, and 72.9 kg for Zircaloy.

Table 2-16. Sequence of Events for Scenario TRANS-1.

	Time (hr:min)		
Event	**Zircaloy**	**FeCrAl**	**Chromite**
RCP A locked	0:00	0:00	0:00
Pressurizer PORV begins to cycle	0:58	0:58	0:58
All SGs dried out	1:03	1:03	1:03
PRT rupture disk opens	1:18	1:18	1:19
RCP B and C tripped	1:30	1:30	1:30
SIAS	1:37	1:42	1:41
Core begins to uncover	1:52	1:52	1:52
0.5 kg H_2 generated	2:06	2:36	2:34
First cladding rupture	2:27	2:29	2:33
Core damage	2:30	2:38	2:34

The following figures illustrate the effects of the cladding on various parameters. The differences between calculations are generally small before the core began to uncover as expected, based on Table 2-16. A comparison of the collapsed liquid levels in the SGs in Figure 2-68 and Figure 2-69 shows that the affected and unaffected loops respond differently. This is because the locked RCP rotor in Loop A results in an asymmetric flow pattern in the RCS, with positive flow in Loops B and C and negative flow in Loop A. The fluid entering the U-tubes in Loop A is colder than in Loops B and C, which results in less heat transfer to SG A and a slower decrease in the level. SG B runs out of liquid at 38 min, while SG A is empty at 63 minutes. The large asymmetry between loops disappears after the RCPs in the unaffected loops are tripped at 90 minutes.

The calculated pressures in the A and B steam generators are shown in Figure 2-70 and Figure 2-71. The pressures are generally oscillating between the open and close setpoints of the SG PORVs. In Loop A, the SG PORVs do not open until 22 minutes, whereas the PORVs in Loop B begin opening and closing almost immediately after the start of the transient. The frequency with which the valves in each SG open slows significantly after the SG dries out.

The calculated response of the pressurizer is shown in Figure 2-72 and Figure 2-73, which show pressure and collapsed liquid level, respectively. The pressure increases near 38 minutes, because the SGs in the unaffected loops dry out. The pressurizer PORV begins cycling shortly before the SG in the affected loop dries out. The RCS temperature begins to increase after all the SGs have dried out, which causes the level and pressure in the pressurizer to increase rapidly. After the pressurizer fills with liquid, the first PORV is no longer able to relieve the pressure,

and the pressure increases enough to open the second pressurizer PORV and the safety relief valves. The pressure falls after the pressurizer begins to void. The pressurizer is depleted of liquid near140 minutes.

The collapsed liquid level in the core and the maximum cladding temperature are shown in Figure 2-74 and Figure 2-75, respectively. The collapsed liquid level in the core begins to decrease near 90 minutes, which is about the same time as the RCPs in the unaffected loops are tripped, based on voiding. The collapsed level begins to decrease rapidly at about 110 minutes, when the top of the core begins to uncover and the maximum cladding temperature begins to increase. The maximum cladding temperatures then begin to diverge. The highest temperatures occur with the Zircaloy cladding, but the difference in timing is relatively small.

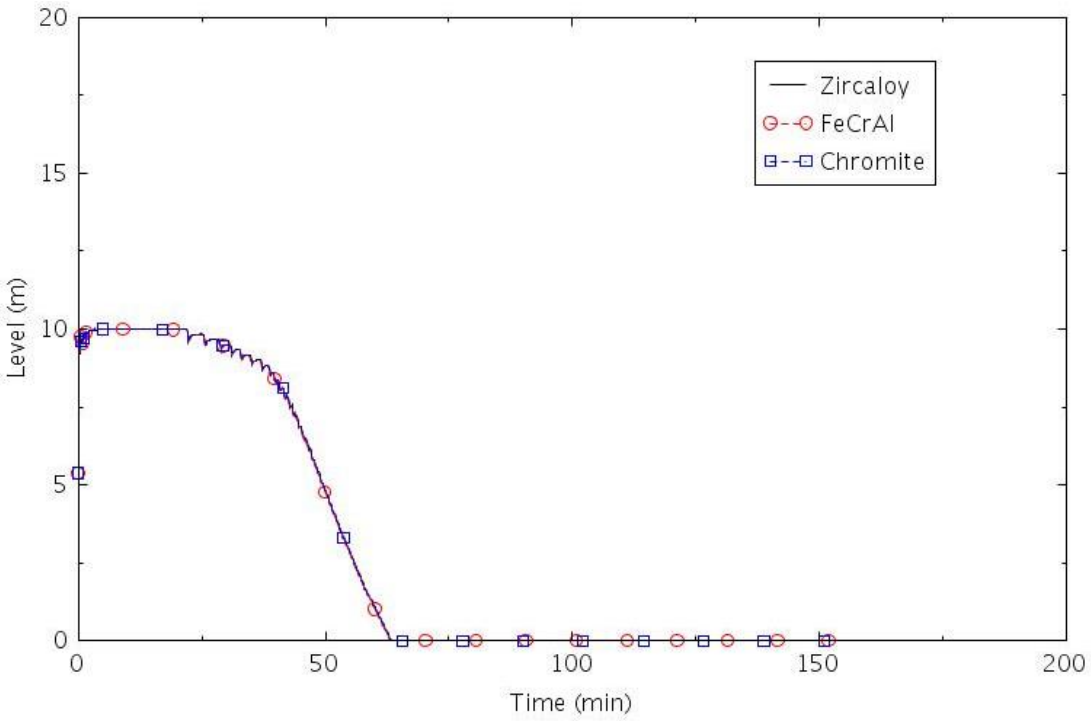

Figure 2-68. Collapsed liquid level in SG A (TRANS-1).

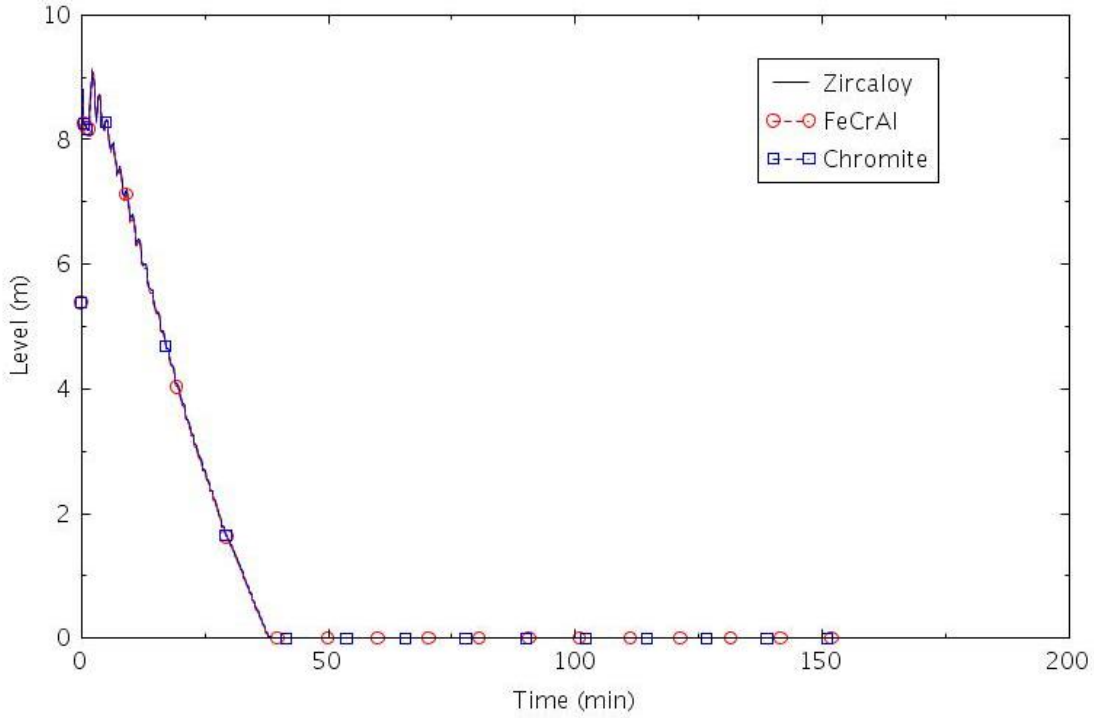

Figure 2-69. Collapsed liquid level in SG B (TRANS-1).

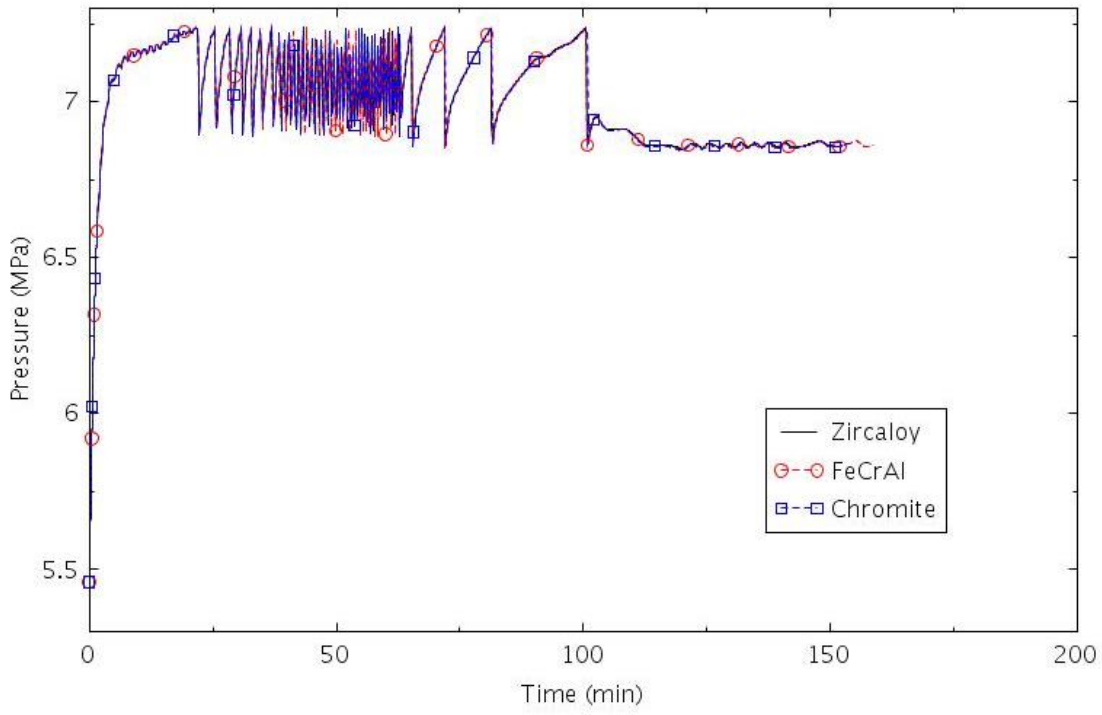

Figure 2-70. Pressure in SG A (TRANS-1).

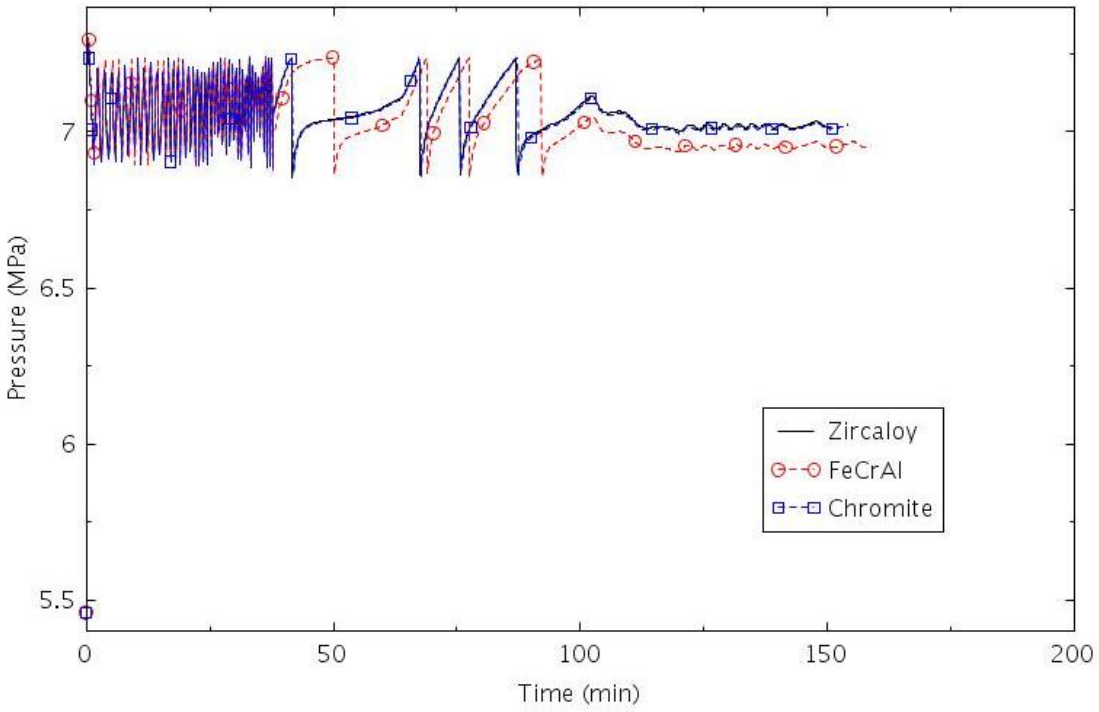

Figure 2-71. Pressure in SG B (TRANS-1).

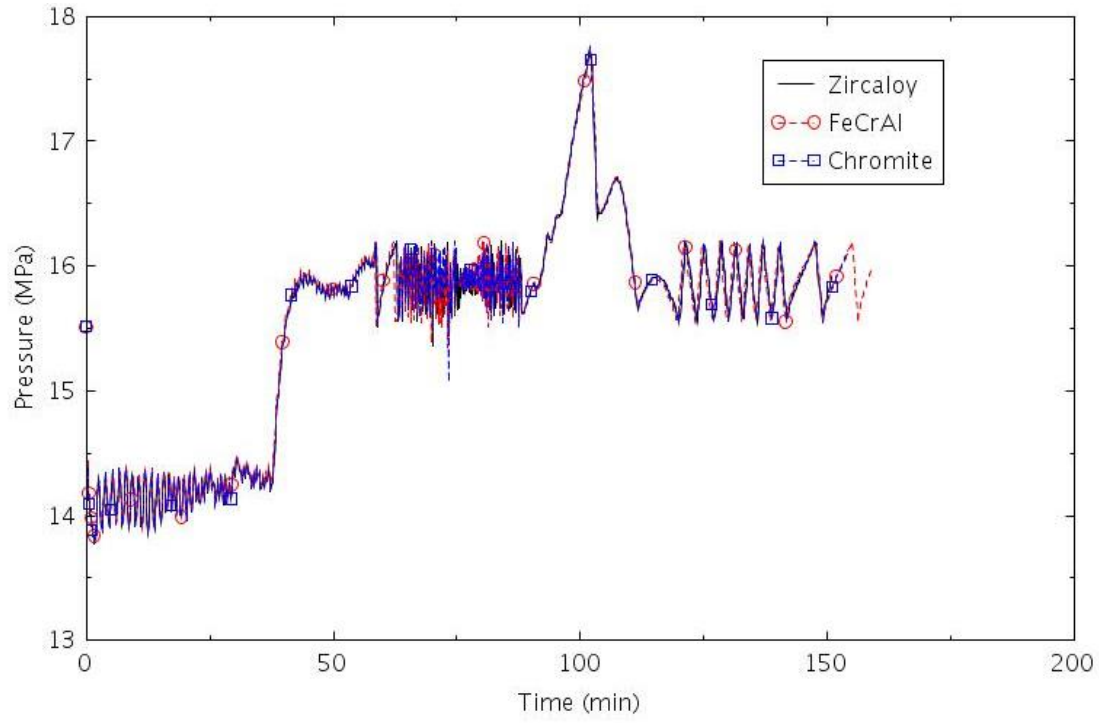

Figure 2-72. Pressure in the pressurizer (TRANS-1).

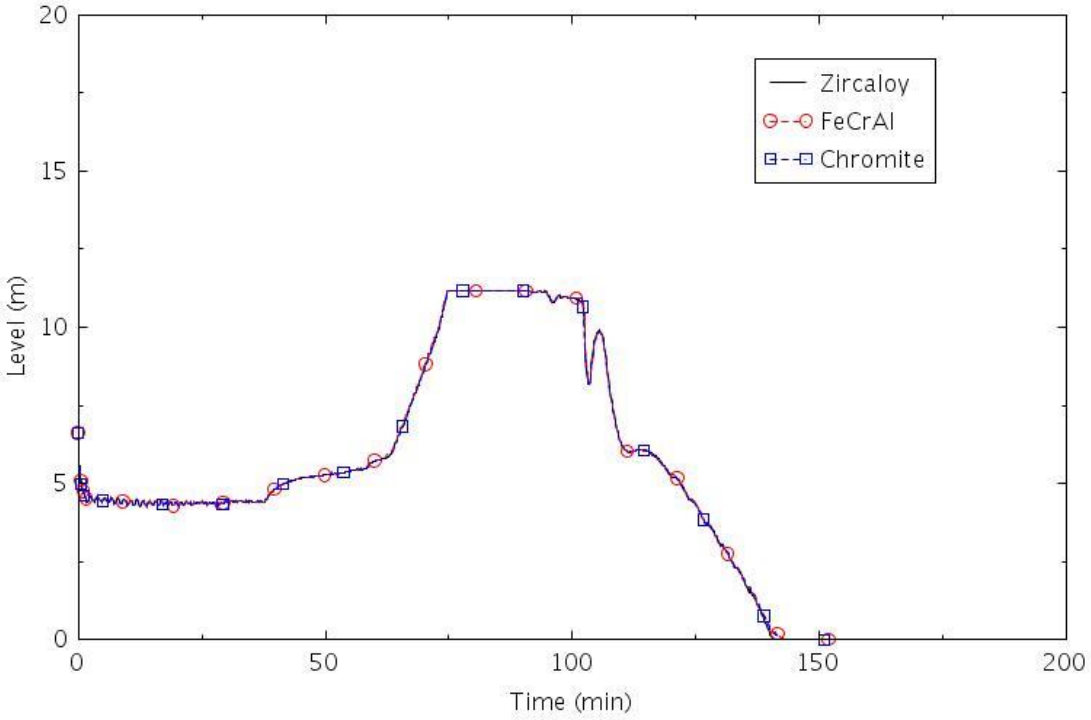

Figure 2-73. Collapsed liquid level in the pressurizer (TRANS-1).

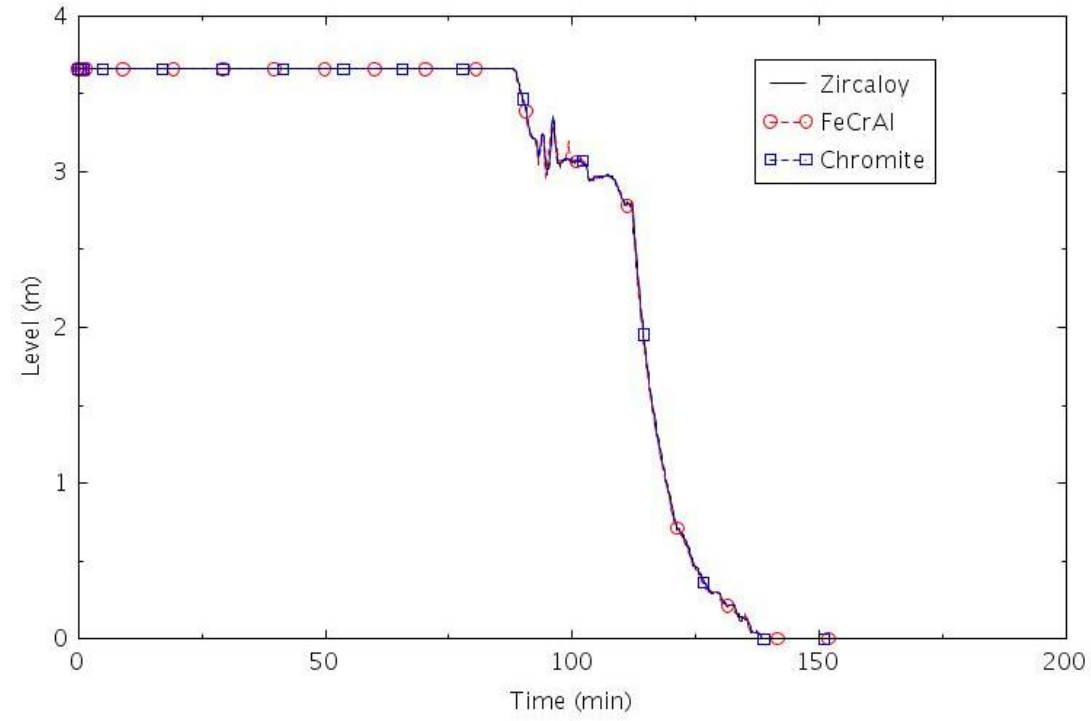

Figure 2-74. Collapsed liquid level in the central core channel (TRANS-1).

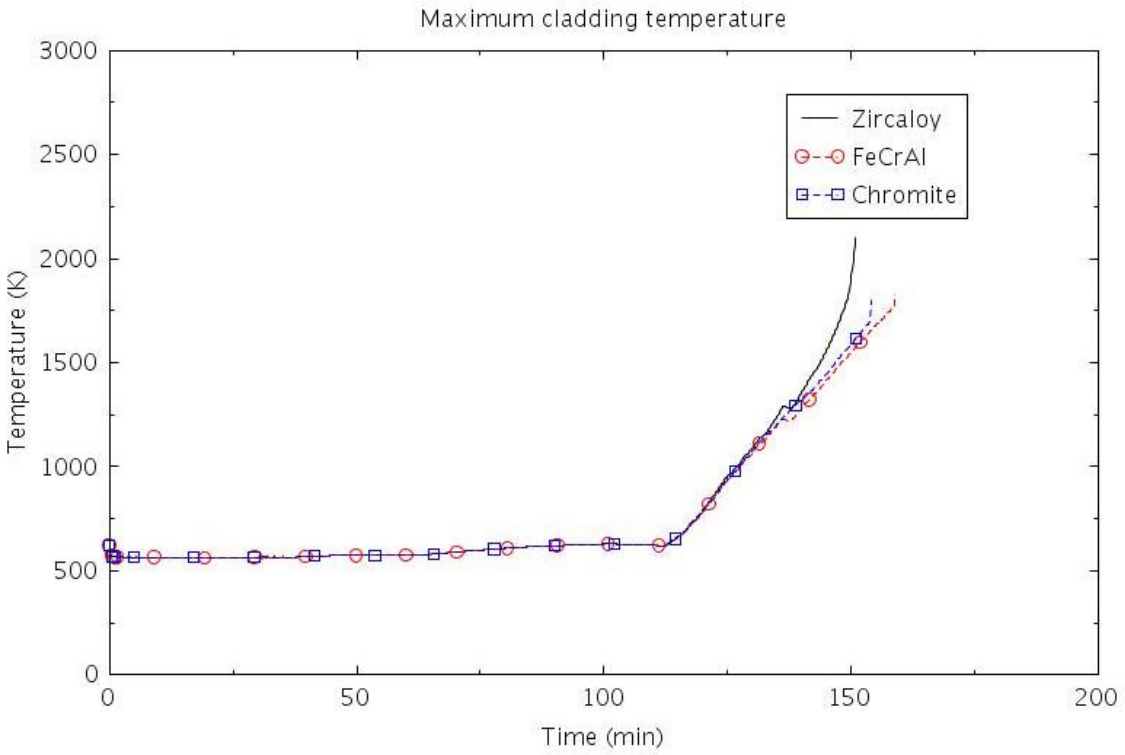

Figure 2-75. Maximum cladding temperature (TRANS-1).

2.2.3.2 TRANS-2

This scenario assumed that no feedwater was available after the initial coastdown of the MFW and that one HPSI pump actuated normally following the SIAS. The HPSI was terminated when the water source for the safety injection was supposed to automatically switch from the RWST to the containment sump; the automatic switch was assumed to fail.

The calculated sequences of events are shown in Table 2-17. The reactor trip signal was generated 0.1 seconds after the start of the event. The reactor scram, termination of MFW, closure of the TSVs, the first lift of the pressurizer PORV and the SG PORVs all occurred within 10 s. Heat from the core and the RCPs was transferred to the SGs, boiling liquid to steam, which was then vented out of the SG PORVs. The pressurizer PORV began to cycle at 58 minutes, shortly before the all of the SGs were empty. The RCPs in the unaffected loops were tripped at 90 minutes. The SIAS occurred near 100 minutes, and flow from one HPSI pump was initiated 30 seconds later. The containment spray was first actuated near 3 hours and then operated intermittently as needed to control the containment pressure between 172 kPa (25 psia) and 83 kPa (12 psia). The HPSI flow was terminated near 12 hours, when the level in the RWST dropped to the setpoint for the automatic switchover to sump recirculation mode. Without any HPSI flow, the water inventory in the RCS began to boil off through the PORV. The core began to uncover at about 13 hours. The calculations were terminated with high cladding temperatures around 15 hours. The differences between calculations due to the different claddings were negligible prior to the actuation of containment spray and were generally small afterwards. The increased variability thereafter was more likely due to numerical causes than to the differences between claddings. However, the time between the onset of core uncovery and the termination of the calculations is judged to be reasonable. The time between when the core began to uncover and core damage occurred was 70 minutes with Zircaloy, 91 minutes with FeCrAl, and 87 minutes with Chromite. The calculated amount of hydrogen produced during the transients varied significantly between claddings. The amount of hydrogen produced was 1.9 kg for FeCrAl, 11 kg for Chromite, and 108 kg for Zircaloy.

Table 2-17. Sequence of Events for Scenario TRANS-2.

	Time (hr:min)		
Event	**Zircaloy**	**FeCrAl**	**Chromite**
RCP A locked	0:00	0:00	0:00
Pressurizer PORV begins to cycle	0:58	0:58	0:58
All SGs dried out	1:03	1:03	1:03
PRT rupture disk opens	1:18	1:18	1:18
RCP B and C tripped	1:30	1:30	1:30
SIAS	1:42	1:42	1:42
HPSI begins	1:43	1:43	1:43
Containment spray actuated	3:14	3:14	3:13
HPSI terminated	12:14	11:54	11:57
Core begins to uncover	13:25	13:10	13:10
0.5 kg H_2 generated	13:54	14:29	14:26
First cladding rupture	14:29	14:23	14:26
Core damage	14:35	14:41	14:37

The following figures illustrate the effects of the cladding on various parameters. The response prior to the onset of HPSI flow near 100 minutes was identical to that discussed previously for Scenario TRANS-1. Since they had already dried out before HPSI was actuated, the SGs did not significantly affect the response of the RCS after 100 minutes. The response of SG B is illustrated in Figure 2-76 and Figure 2-77.

The total HPSI flow into the RCS is shown in Figure 2-78. The flow began at about 100 min in response to the SIAS on high containment pressure. The HPSI flow was terminated near 720 minutes, when the automatic switchover to sump recirculation mode was assumed to fail.

The containment spray is shown in Figure 2-79. Although intermittent, the maximum spray flow rate greatly exceeds that of the HPSI. Slightly more than half of the total injection had gone to the containment at the time of the failed automatic switch to sump injection.

The calculated response of the pressurizer is shown in Figure 2-80 and Figure 2-81, which show pressure and collapsed liquid level, respectively. The pressure generally stayed between the open and close setpoints of the pressurizer PORV after the initiation of HPSI flow near 100 min. HPSI flow eventually refilled the pressurizer. The pressurizer emptied after HPSI was terminated near 660 minutes.

The collapsed liquid level in the core and the maximum cladding temperature are shown in Figure 2-82 and Figure 2-83, respectively. The core stayed nearly full until after HPSI was terminated near 660 minutes. The level began to decrease rapidly near 750 minutes, and the maximum cladding temperature began to increase shortly thereafter.

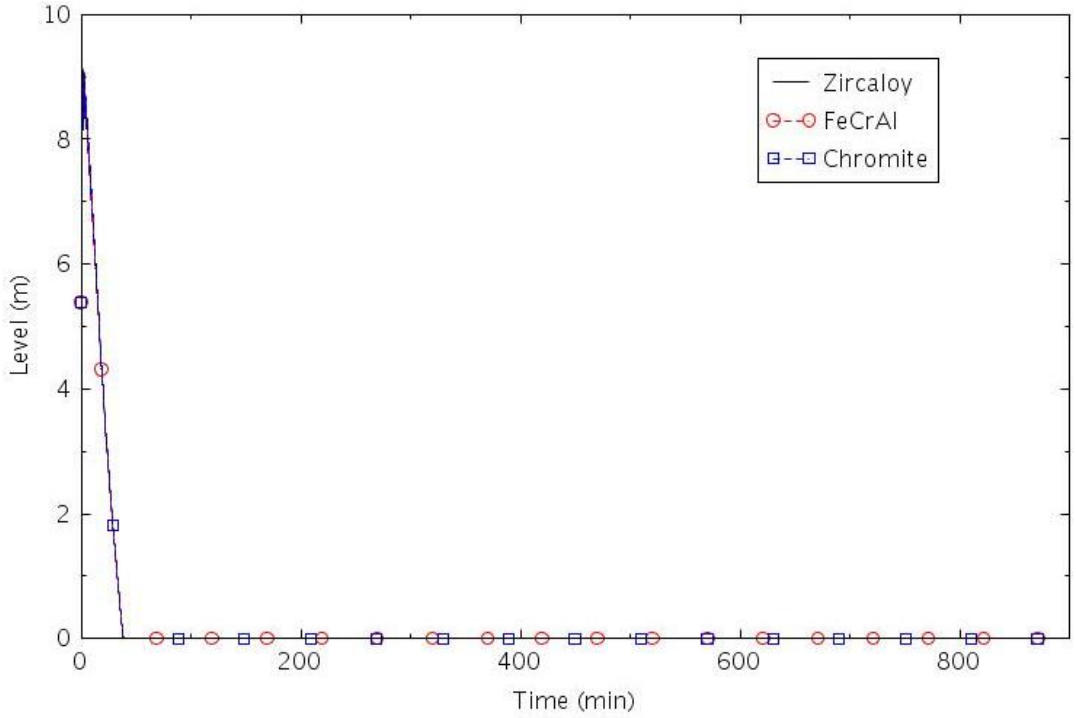

Figure 2-76. Collapsed liquid level in SG B (TRANS-2).

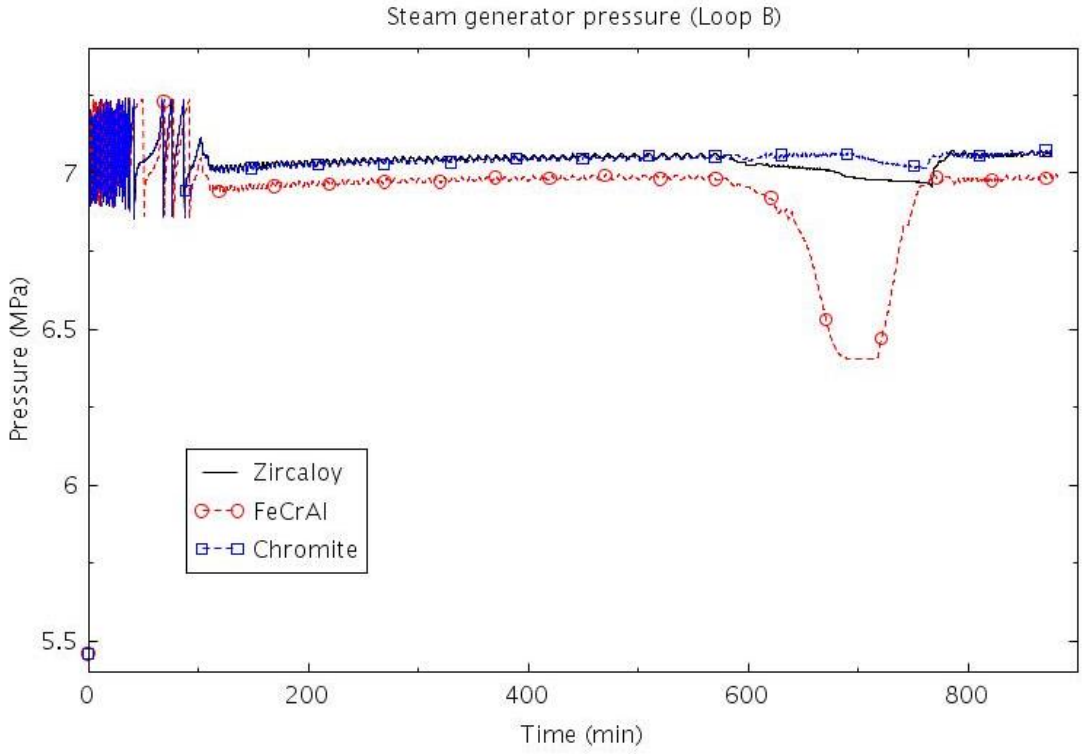

Figure 2-77. Pressure in SG B (TRANS-2).

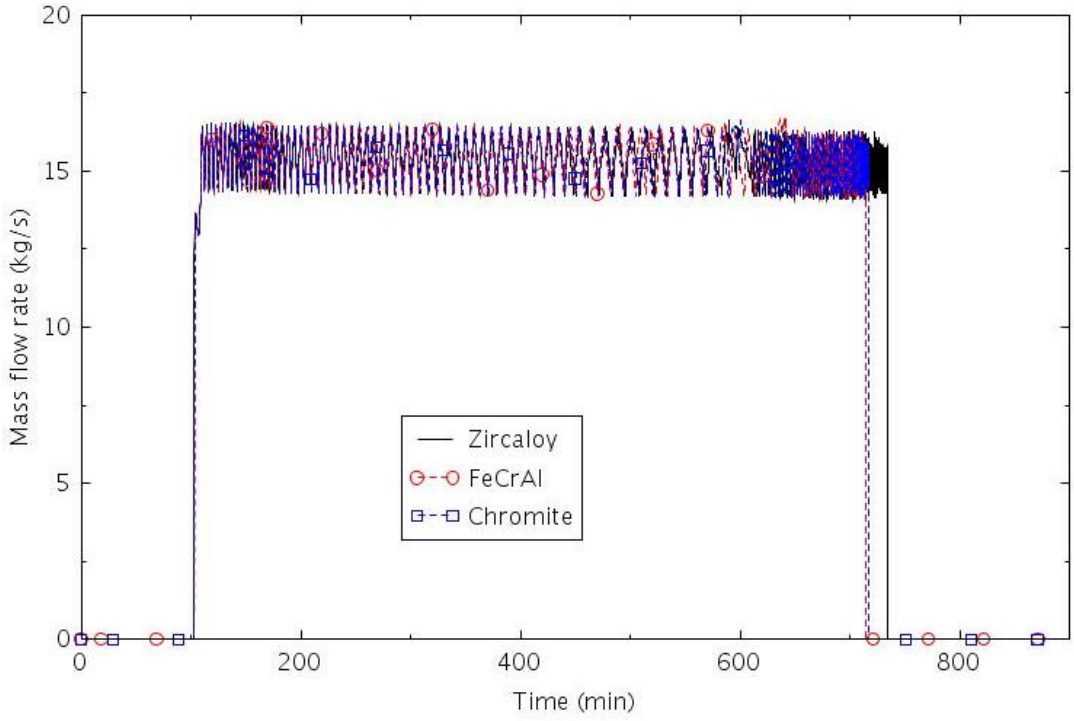

Figure 2-78. Total HPSI flow into the RCS (TRANS-2).

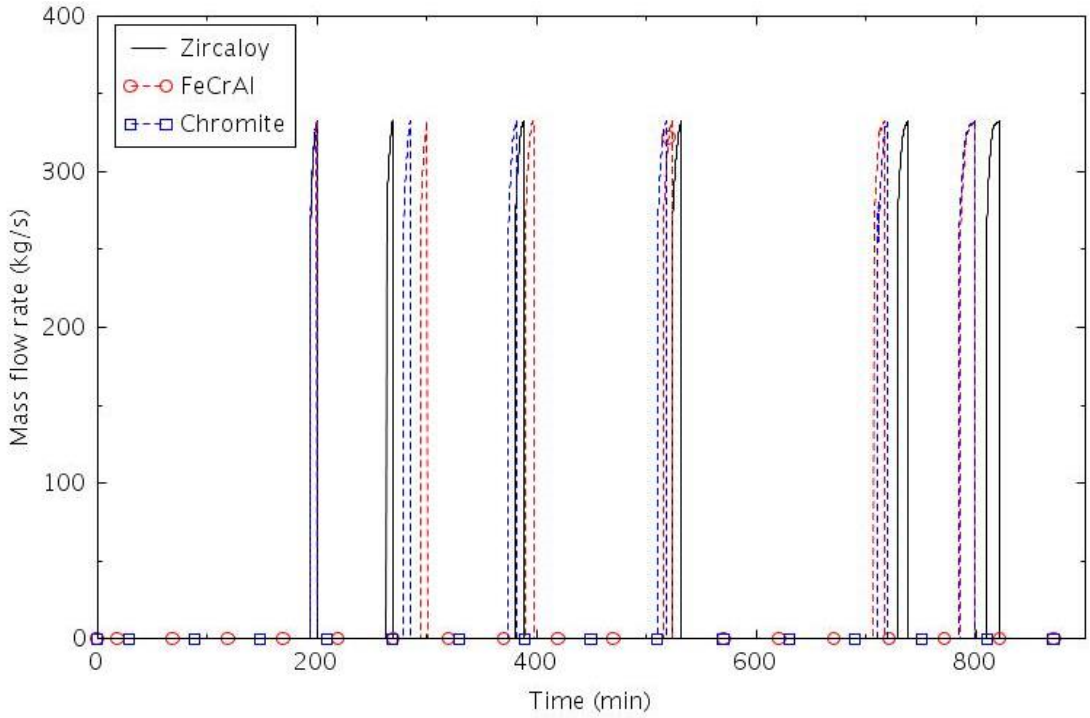

Figure 2-79. Containment spray (TRANS-2).

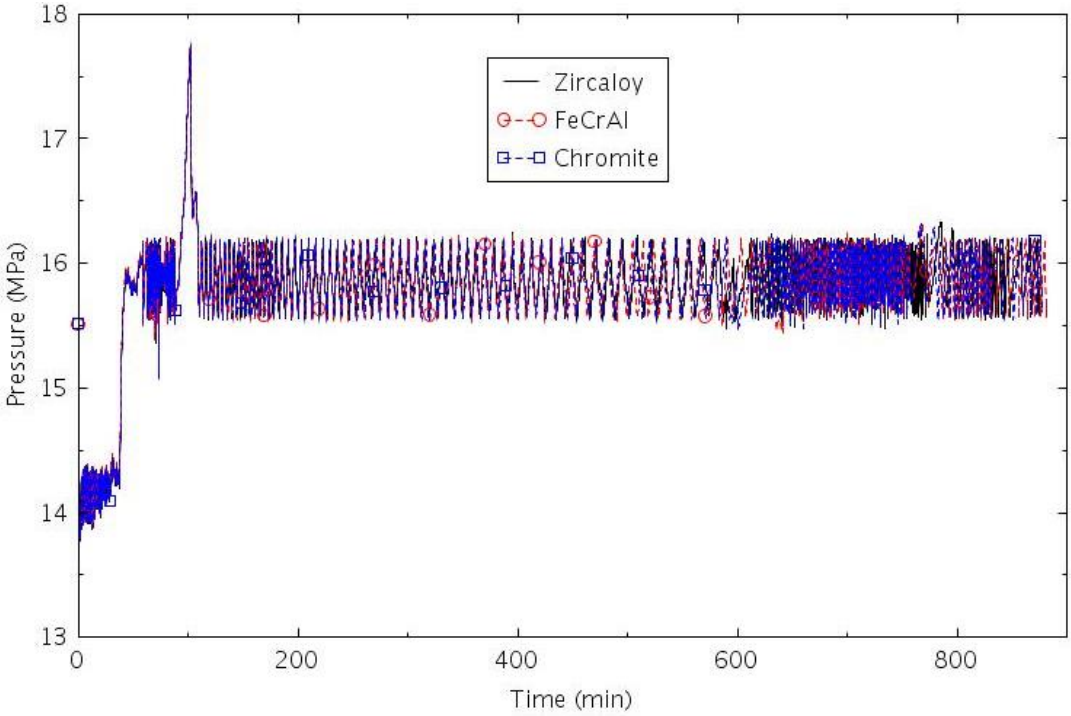

Figure 2-80. Pressure in the pressurizer (TRANS-2).

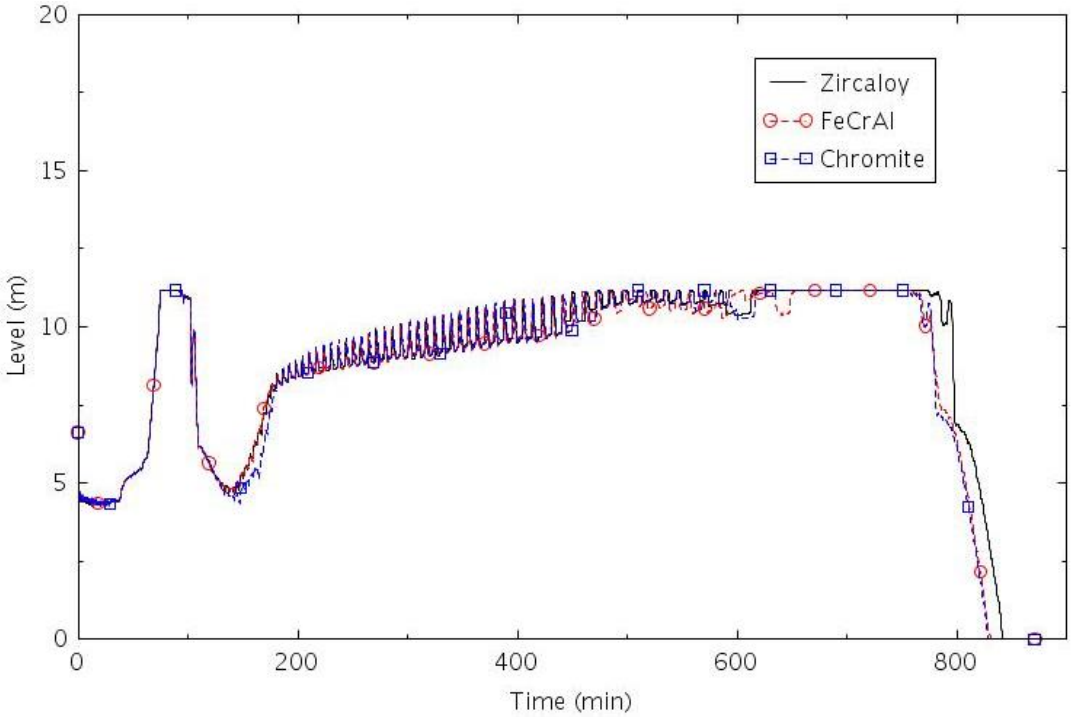

Figure 2-81. Collapsed liquid level in the pressurizer (TRANS-2).

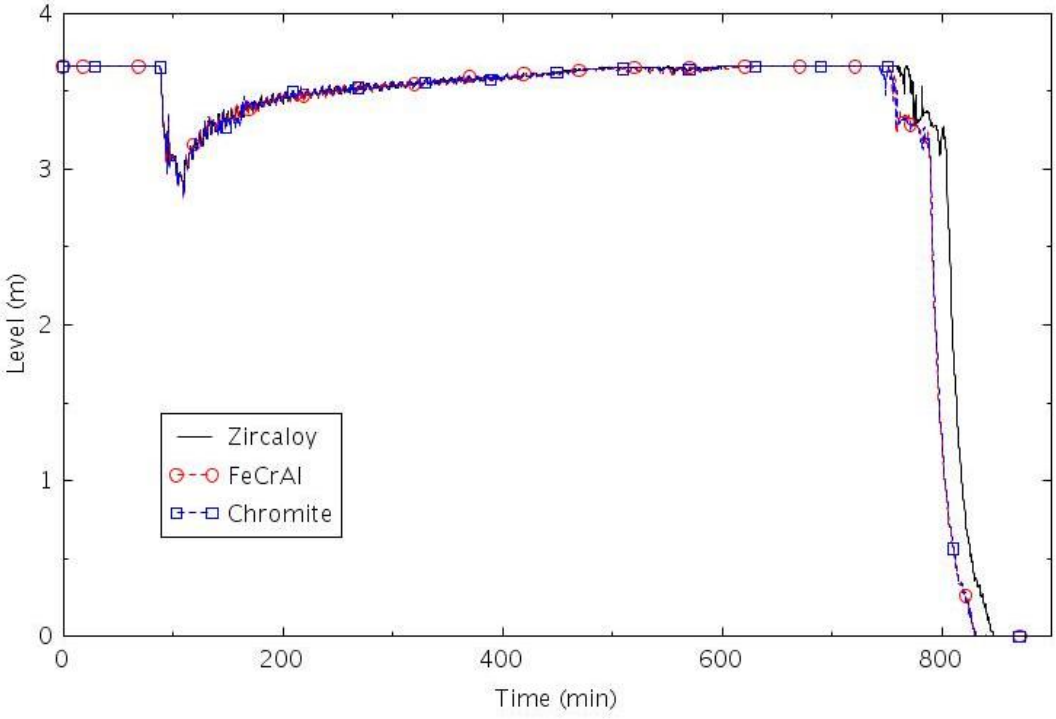

Figure 2-82. Collapsed liquid level in the central core channel (TRANS-2).

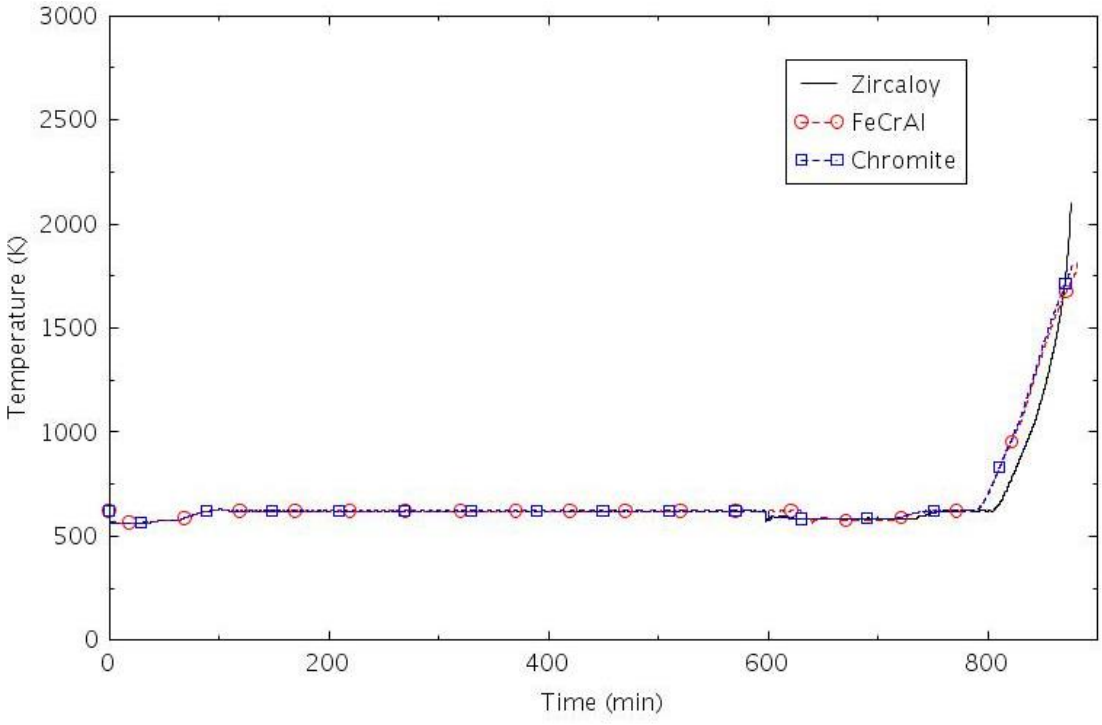

Figure 2-83. Maximum cladding temperature (TRANS-2).

Sensitivity calculations were performed in which three HPSI pumps were assumed to be available instead of just one. The additional HPSI flow suppressed boiling in the core, which resulted in a higher mass flow rate through the pressurizer PORV and a more rapid depletion of the inventory in the RWST. The core began to uncover about 100 minutes earlier in the sensitivity calculations, because the RWST inventory was not used as efficiently as in the base calculations.

In the calculations described previously, the pressurizer PORVs were assumed to operate automatically. Sensitivity calculations were performed in which the operators were assumed to lock open one pressurizer PORV at 1 hour to initiate feed and bleed cooling. The effects of the operator action on the sequence of events for the case with Zircaloy cladding are shown in Table 2-18. The SIAS occurred almost immediately after the PORV was locked open in the sensitivity calculation due to low-low pressurizer pressure rather than high containment pressure as in the base case. The other most significant differences were that the RCPs in the B and C loops were tripped about 7 hours later, the HPSI flow was terminated about 4 hours earlier, and core damage occurred about 5 hours earlier with feed and bleed. The earlier core damage was a result of the RWST inventory not being used as efficiently as in the base calculation, and the additional power added to the RCS due to the longer operation of the RCPs.

Table 2-18. The Effects of Feed and Bleed Cooling in Scenario TRANS-2 with Zircaloy Cladding.

	Time (hr:min)	
Event	**Without feed and bleed**	**With feed and bleed**
RCP A locked	0:00	0:00
Pressurizer PORV begins to cycle	0:58	0:58
Pressurizer PORV locked open	NA	1:00
All SGs dried out	1:03	1:18
PRT rupture disk opens	1:18	1:05
RCP B and C tripped	1:30	8:08
SIAS	1:42	1:00
HPSI begins	1:43	1:01
Containment spray actuated	3:14	4:13
HPSI terminated	12:14	8:01
Core begins to uncover	13:25	9:14
0.5 kg H_2 generated	13:54	9:37
First cladding rupture	14:29	9:42
Core damage	14:35	9:58

2.2.3.3 PORV-1

This scenario assumed that the pressurizer PORV stuck open after its first lift, one motor-driven AFW pump was available, and that no high-pressure injection was available. AFW was assumed to start 30 seconds after the SIAS.

The calculated sequences of events are shown in Table 2-19. The reactor trip signal was generated 0.1 seconds after the start of the event. The reactor scram, termination of MFW, closure of the TSVs, the first lift of the pressurizer PORV and the SG PORVs all occurred within 10 s. The pressurizer PORV was assumed to stick open initiating a loss-of-coolant accident. The SIAS occurred at about 50 seconds and motor-driven AFW was initiated 30 seconds later. The HPSI was assumed to fail. The RCPs in the unaffected loops were tripped at 5 minutes. The PRT rupture disk opened at about 6 minutes. The RCS coolant inventory decreased continuously due to flow through

the stuck-open PORV and the HPSI failure. The core began to uncover about 100 minutes. The differences between calculations due to the different claddings were negligible before the core began to uncover and were relatively small afterwards. The calculations were terminated when the hottest cladding reached its failure temperature. The termination times varied by less than 10 minutes. The calculated amount of hydrogen produced during the transients varied significantly between claddings. The amount of hydrogen produced was 2.0 kg for FeCrAl, 6.5 kg for Chromite, and 23.3 kg for Zircaloy.

Table 2-19. Sequence of Events for Scenario PORV-1.

	Time (hr:min)		
Event	**Zircaloy**	**FeCrAl**	**Chromite**
RCP A locked	0:00	0:00	0:00
AFW initiated	0:01	0:01	0:01
RCP B and C tripped	0:05	0:05	0:05
PRT rupture disk opens	0:06	0:06	0:06
Core begins to uncover	1:42	1:41	1:41
0.5 kg H_2 generated	2:04	2:25	2:10
First cladding rupture	2:07	2:05	2:07
Core damage	2:18	2:26	2:21

The following figures illustrate the effects of the cladding on various parameters. The mass flow through the stuck-open PORV is illustrated in Figure 2-84. The PORV flow rate responds to both the changes in pressurizer pressure (Figure 2-85) and level (Figure 2-86). The PORV was venting nearly pure steam until about 6 minutes, when the level got high enough to allow some liquid to exit the PORV. The PORV was relieving nearly pure steam again after 100 minutes. The pressurizer and SG pressures were closely coupled during most of the transient, but the pressurizer pressure decreased below the SG pressure near 115 minutes, which indicates that the SGs were no longer removing heat from the RCS.

The stuck-open PORV caused some voiding in the core within a few minutes of the start of the transient, as shown in Figure 2-87. The level in the core began decreasing rapidly at about 100 minutes. The core began to heat up a few minutes later, as shown in Figure 2-88. The maximum cladding temperatures then begin to diverge. The difference in the timing of the termination of the calculations on high temperature is less than 10 minutes.

The performance of the SGs is illustrated in Figure 2-89 and Figure 2-90, which show pressure and level in the B steam generator. The AFW flow is shown in Figure 2-91. The AFW flow is terminated because the SG level is high enough, not because the ECST is empty.

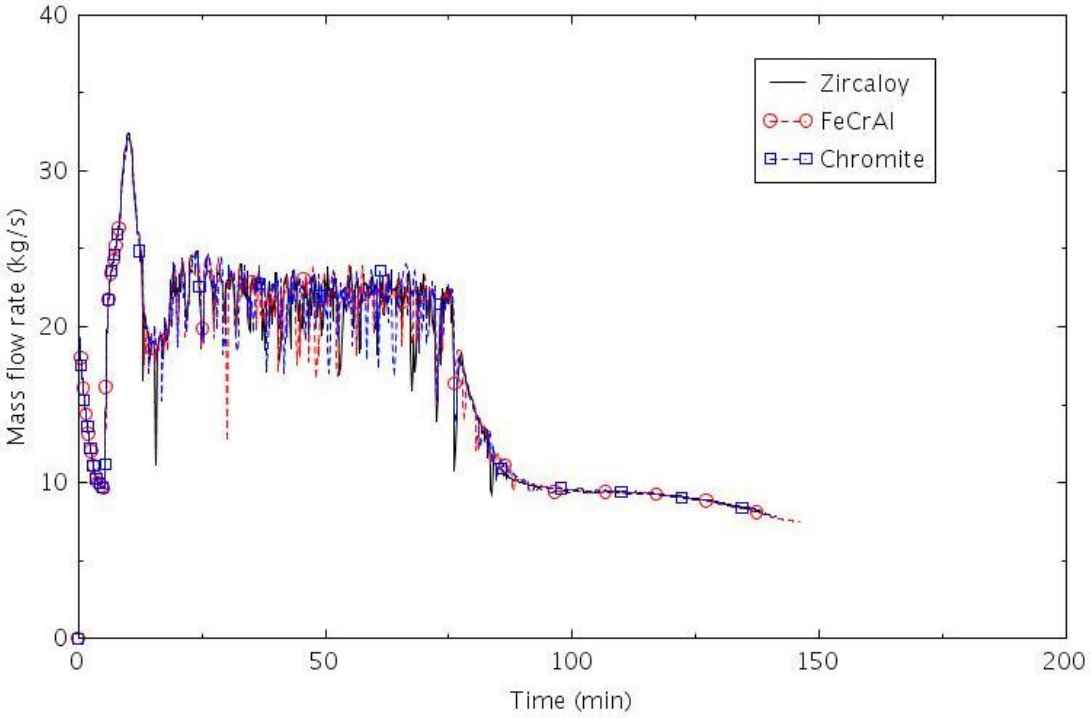

Figure 2-84. Mass flow rate through the pressurizer PORV (PORV-1).

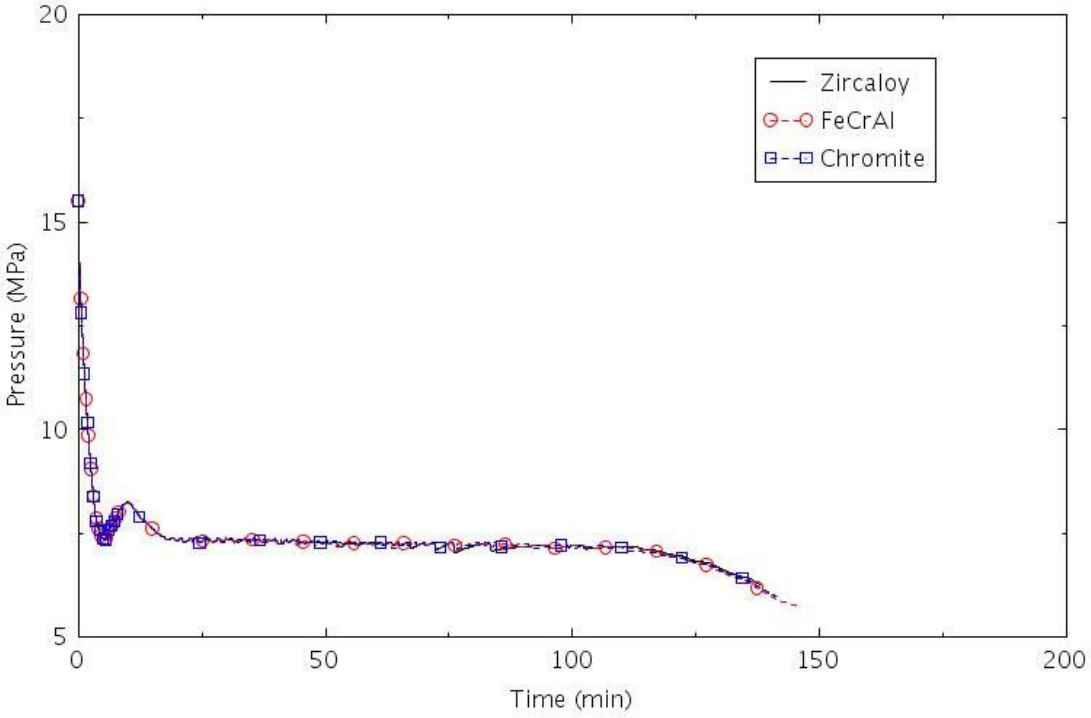

Figure 2-85. Pressure in the pressurizer (PORV-1).

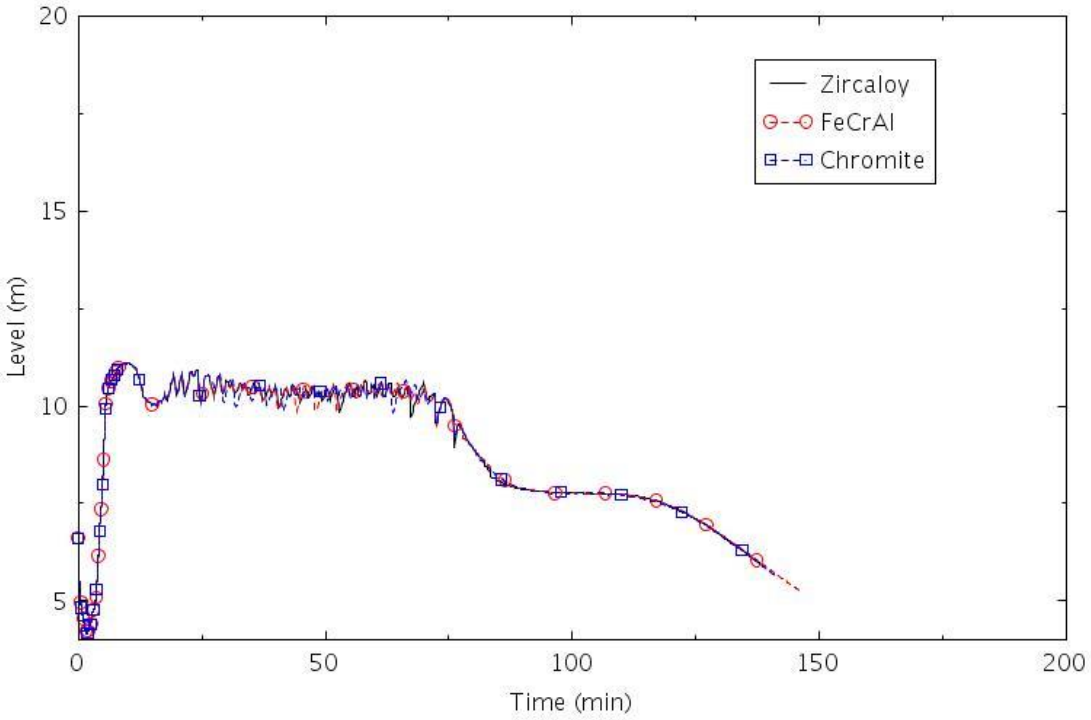

Figure 2-86. Collapsed liquid level in the pressurizer (PORV-1).

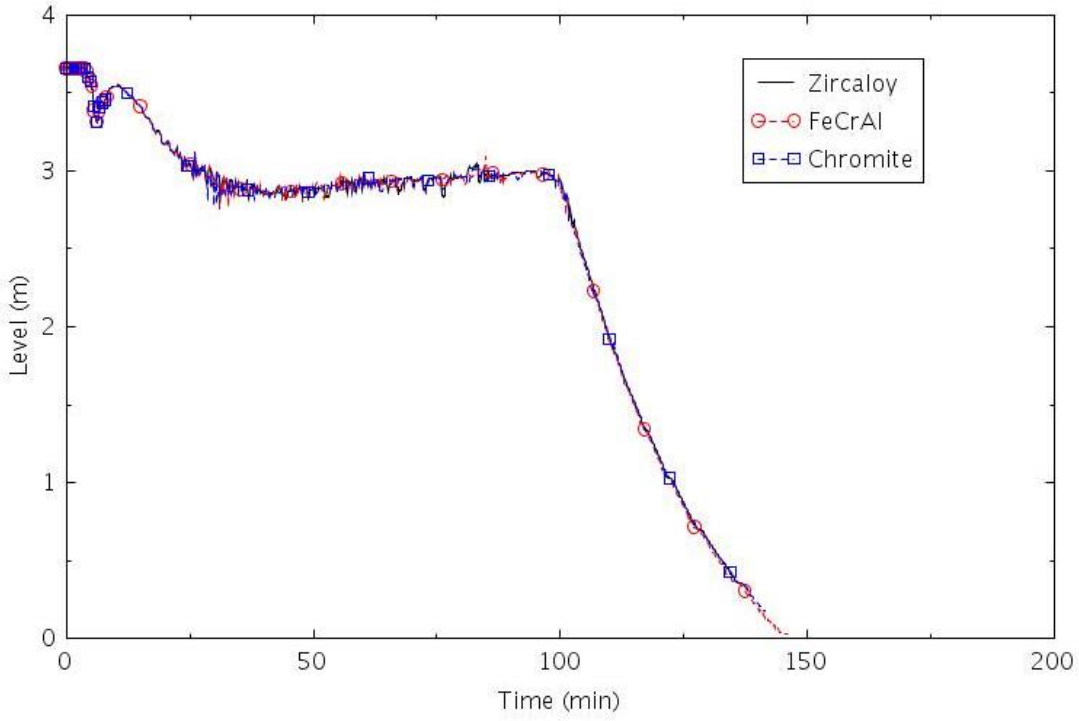

Figure 2-87, Collapsed liquid level in the central core channel (PORV-1).

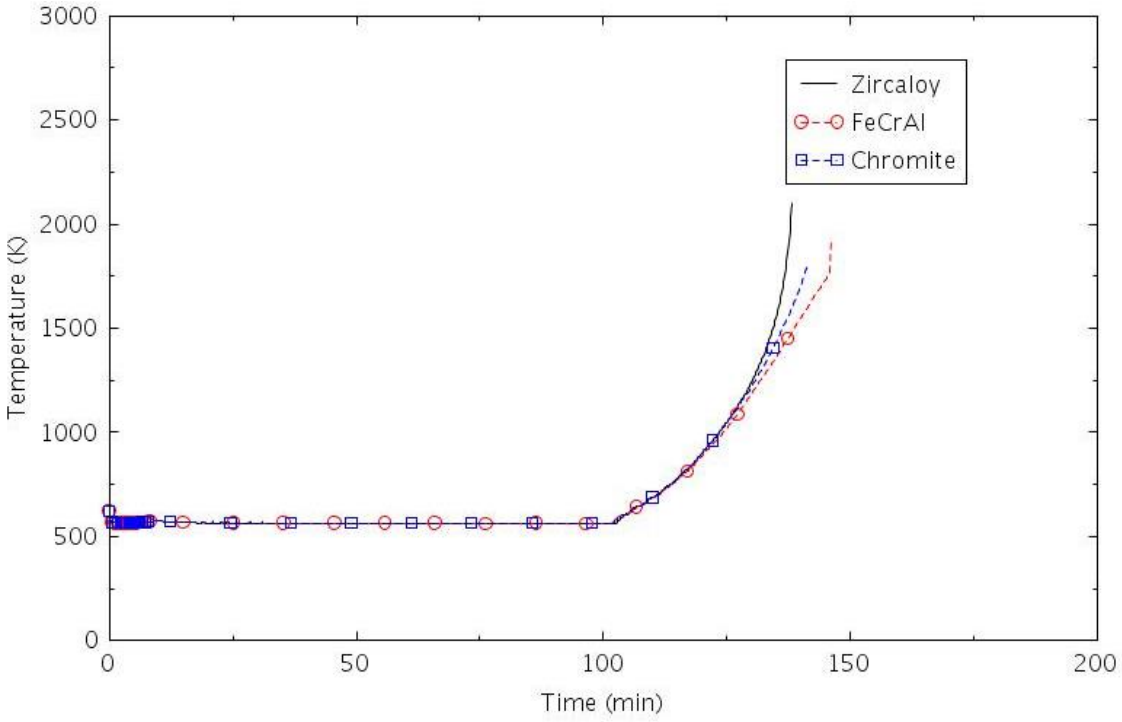

Figure 2-88. Maximum cladding temperature (PORV-1).

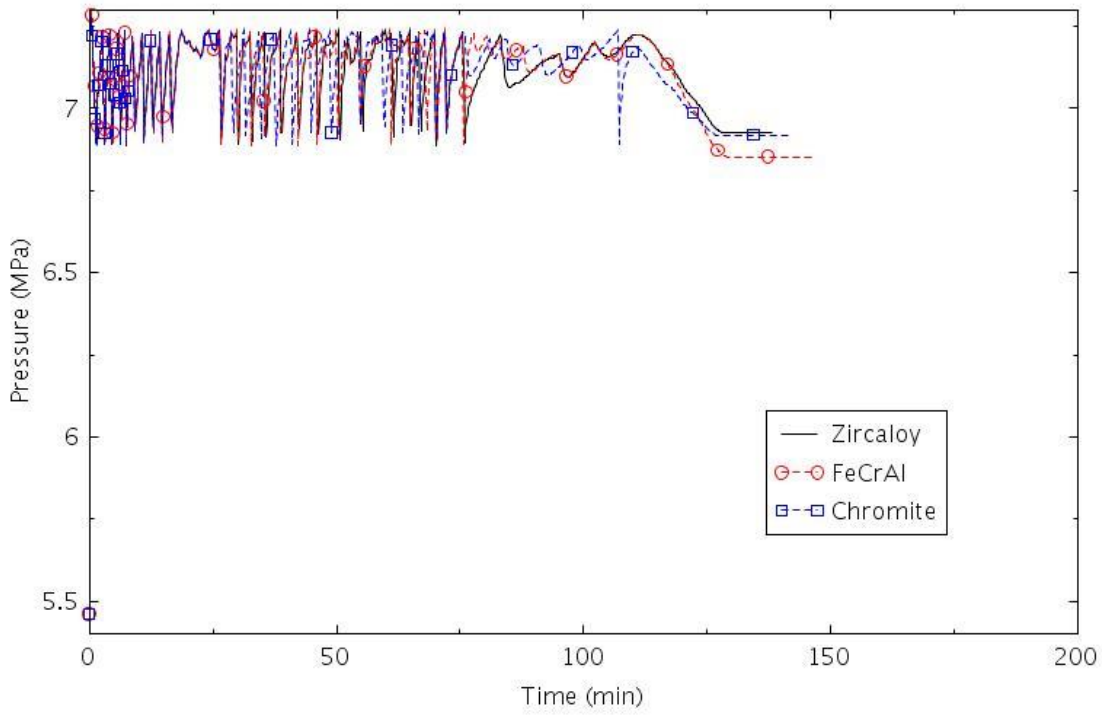

Figure 2-89. Pressure in SG B (PORV-1).

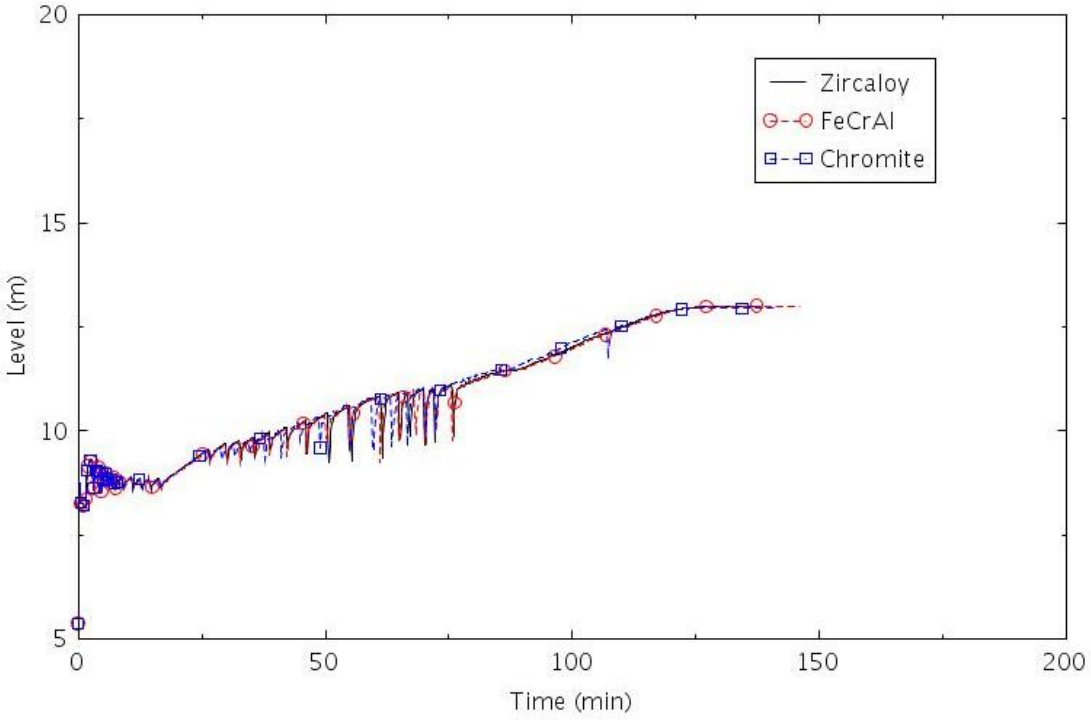

Figure 2-90. Collapsed liquid level in SG B (PORV-1).

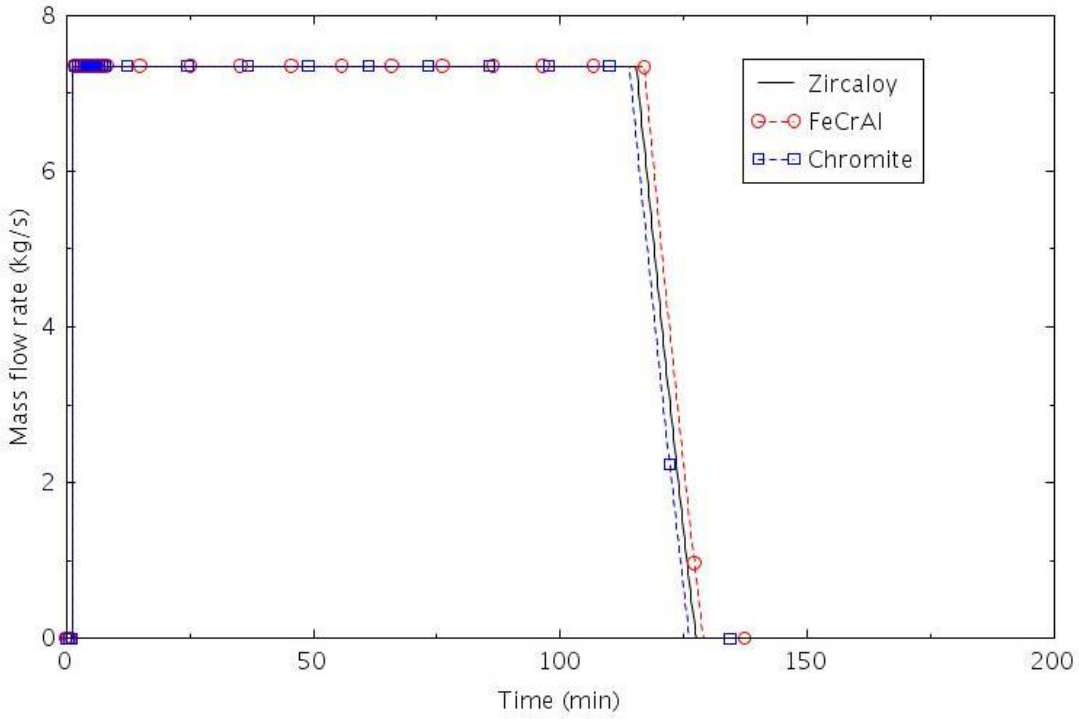

Figure 2-91. AFW flow rate to SG B (PORV-1).

2.2.3.4 LOSC-182a

This scenario assumes that one motor-driven AFW pump is available, that the RCP pump seals fail, that no high-pressure injection is available, and that the operators manually initiate a secondary side cooldown. The pump seal failures produce an initial leakage of 0.011 m^3/s (182 gpm) per pump. Since power is available in this scenario, the cause of the seal failure is not mechanistic due to overheating, as is generally modeled in an SBO. The seal failure was assumed to conservatively occur simultaneously with the reactor trip. The SSC was assumed to begin at 1.5 hours, the same time as assumed in Section 3.1.4.1 of (NRC, 2012). The PORVs were opened as necessary to obtain a 56°C/hr (100°F/hr) cooldown rate in the steam generators. The cooldown was terminated when the SGs reached 0.93 MPa (134.7 psia), so that the turbine-driven AFW pumps would be available if needed. Thereafter, the PORVs opened as needed to control the SG pressure between 0.93 MPa (134.7 psia) and 1.27 MPa (184.7 psia).

The calculated sequences of events are shown in Table 2-20. The reactor trip signal was generated 0.1 seconds after the start of the event. The reactor scram, termination of MFW, closure of the TSVs, the first lift of the pressurizer PORV and the SG PORVs all occurred within 10 s. The RCP pump seals were assumed to fail simultaneously with the reactor trip. The SIAS occurred at about 4 minutes on low reactor pressure and the AFW was initiated 30 seconds later. The HPSI was assumed to fail. The RCPs in the unaffected loops were tripped at about 50 minutes. The RCS coolant inventory decreased continuously due to flow through the ruptured pump seals and lack of HPSI. The operators were assumed to manually initiate a controlled cooldown of the SGs beginning at 90 minutes. The resulting depressurization of the RCS resulted in accumulator injection at 130 minutes. The AFW flow was terminated near 5 hours, because the ECST was depleted. The SGs were empty near 10 hours. The core began to uncover near 12 hours. The differences between calculations were generally negligible before the SGs emptied of liquid. The increased variability thereafter was more likely due to numerical issues than to the differences between claddings. However, the time between the onset of core uncovery and the termination of the calculations is judged to be reasonable. The time between when the core began to uncover and core damage occurred was 62 minutes with Zircaloy, 84 minutes with FeCrAl, and 75 minutes with Chromite. The calculated amount of hydrogen produced during the transients varied significantly between claddings. The amount of hydrogen produced was 1.9 kg for FeCrAl, 16.0 kg for Chromite, and 57.7 kg for Zircaloy.

Table 2-20. Sequence of Events for Scenario LOSC-182a.

	Time (hr:min)		
Event	**Zircaloy**	**FeCrAl**	**Chromite**
RCP A locked	0:00	0:00	0:00
SIAS	0:04	0:04	0:04
AFW initiated	0:04	0:04	0:04
RCP B and C tripped	0:54	0:53	0:53
SSC begins	1:30	1:30	1:30
Accumulator flow initiated	2:13	2:13	2:13
SSC ends	3:37	3:36	3:36
Accumulator flow terminated	4:09	4:06	4:05
AFW terminated	4:48	4:48	4:48
All SGs empty	10:26	10:03	10:09
Core begins to uncover	12:24	11:59	12:18
0.5 kg H_2 generation	12:53	13:16	13:14
First cladding rupture	13:19	12:52	13:13
Core damage	13:26	13:23	13:33

The following figures illustrate the effects of the cladding on various parameters. The mass flow through the seals in RCP B is illustrated in Figure 2-92. The flow rate increased after accumulator flow was initiated near 130 minutes. The accumulators emptied near 250 minutes and the mass flow eventually decreased. The increase in mass

flow near 650 minutes was due to an increase in pressure. Pressurizer pressure is shown in Figure 2-93. The loss of coolant accident (LOCA) initiated by the rupture of the pump seals caused the pressure to decrease until the RCS and SG pressures were nearly the same near 15 minutes. The decrease in pressure at 90 minutes was due to the SSC. The RCS and SG pressures were closely coupled until all the SGs were empty near 600 minutes. Thereafter, boiling in the core caused the pressure to increase until the core began to uncover. The collapsed liquid level in the pressurizer is shown in Figure 2-94. The LOCA caused the pressurizer to empty near 10 minutes. After all the SGs were empty, boiling in the core caused the pressurizer to partially refill.

The LOCA caused some voiding in the core within a few minutes of the start of the transient, as shown in Figure 2-95. The onset of accumulator injection near 130 minutes nearly refilled the core. The level decreased somewhat after accumulator injection was terminated near 250 minutes and continued to decrease until all the SGs were empty near 600 minutes. The level decreased sharply near 800 minutes. The core began to heat up a few minutes later, as shown in Figure 2-96.

The pressure in SG B is illustrated in Figure 2-97. The pressure was generally between the open and close setpoints of the SG PORVs until 90 minutes, when the manual SSC was initiated. After the cooldown was terminated near 220 minutes, the operators were assumed to open and close the PORVs as necessary to maintain the pressure between 0.93 MPa (134.7 psia) and 1.27 MPa (184.7 psia).

The collapsed liquid level in SG B is shown in Figure 2-98 and the AFW flow is shown in Figure 2-99. Even though the AFW flow was initiated at 4 minutes, the collapsed liquid level decreased until the unaffected RCPs were tripped near 54 minutes. The levels then increased until the AFW was terminated near 290 minutes. The collapsed levels then decreased, although there was considerable variation in the calculated levels.

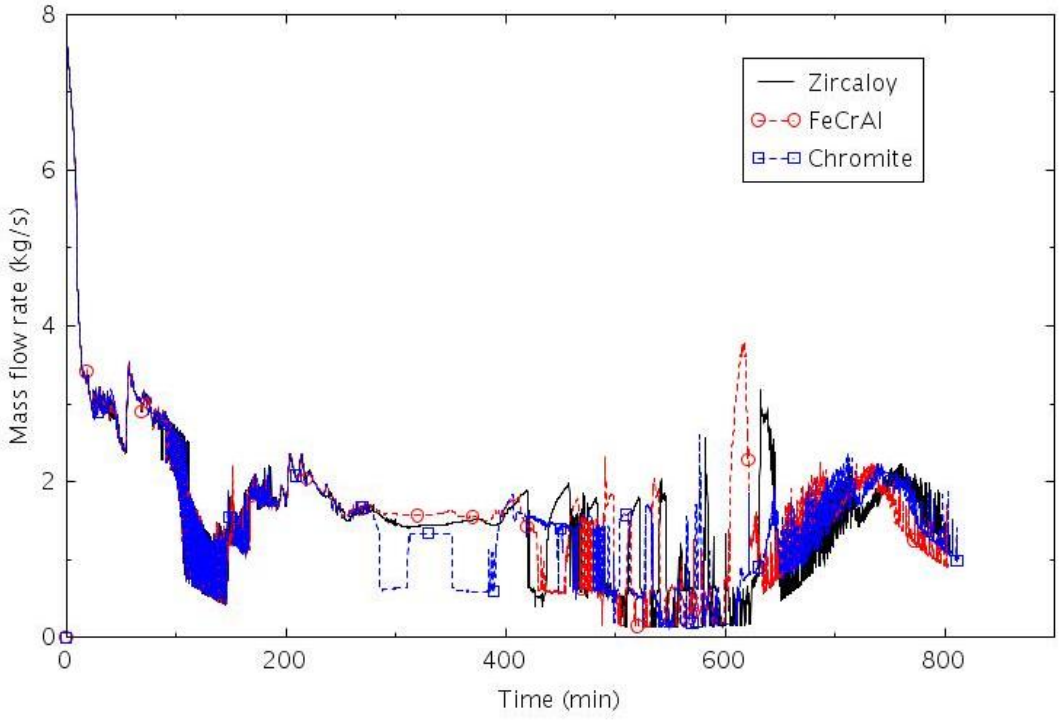

Figure 2-92. Mass flow rate through the seals of RCP B (LOSC-182a).

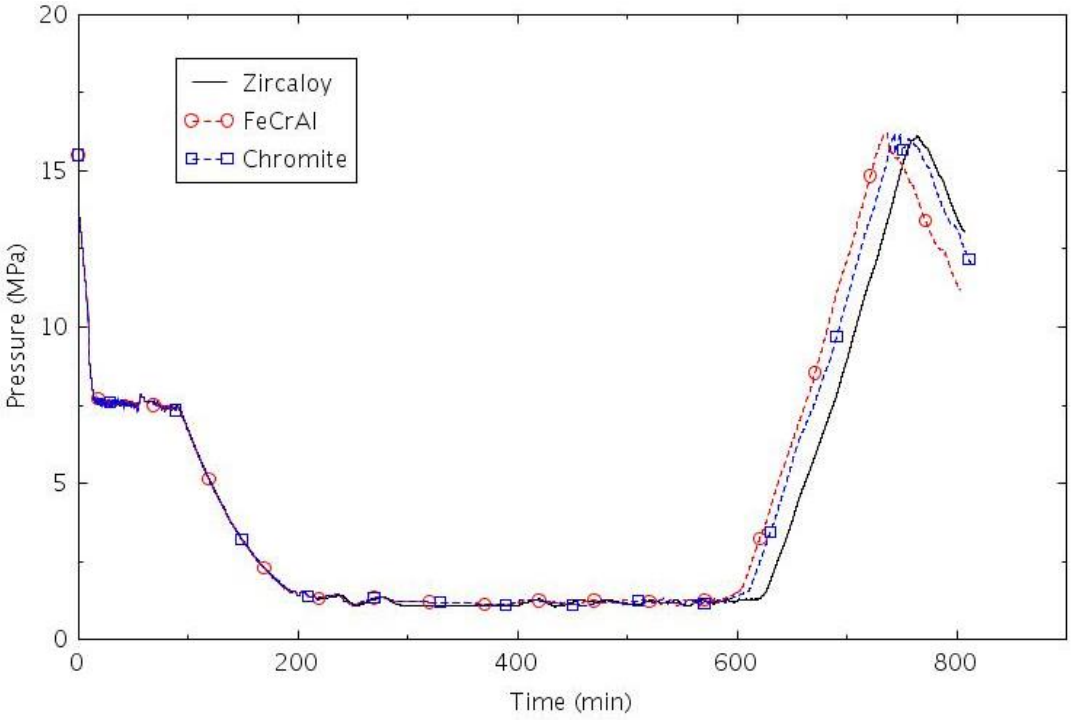

Figure 2-93. Pressure in the pressurizer (LOSC-182a).

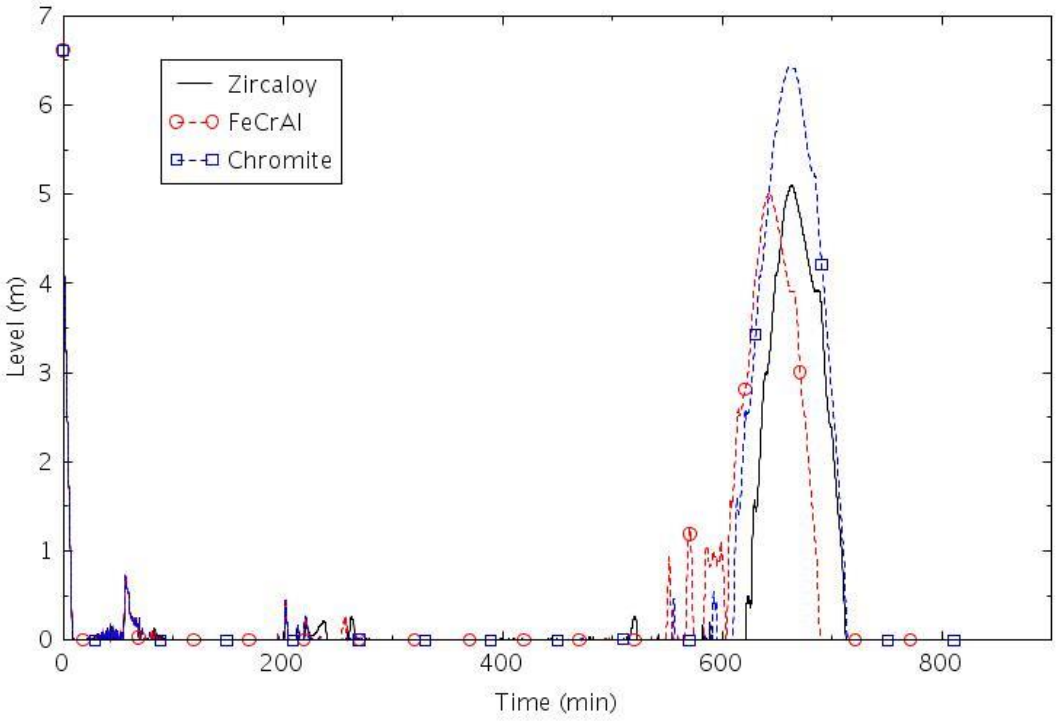

Figure 2-94. Collapsed liquid level in the pressurizer (LOSC-182a).

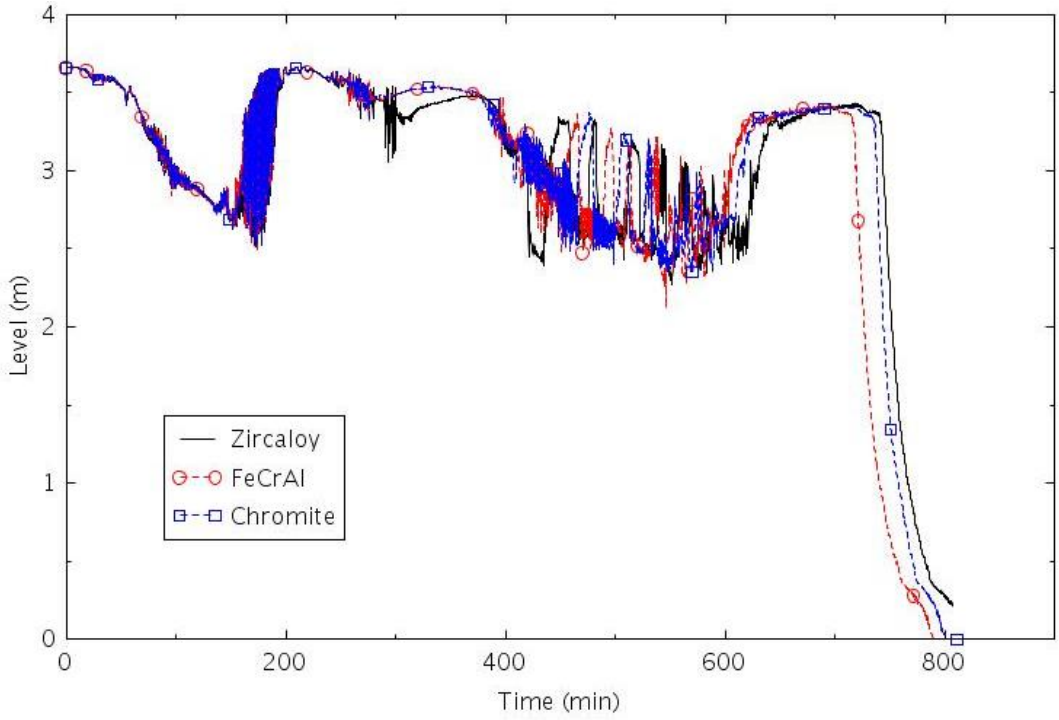

Figure 2-95, Collapsed liquid level in the central core channel (LOSC-182a).

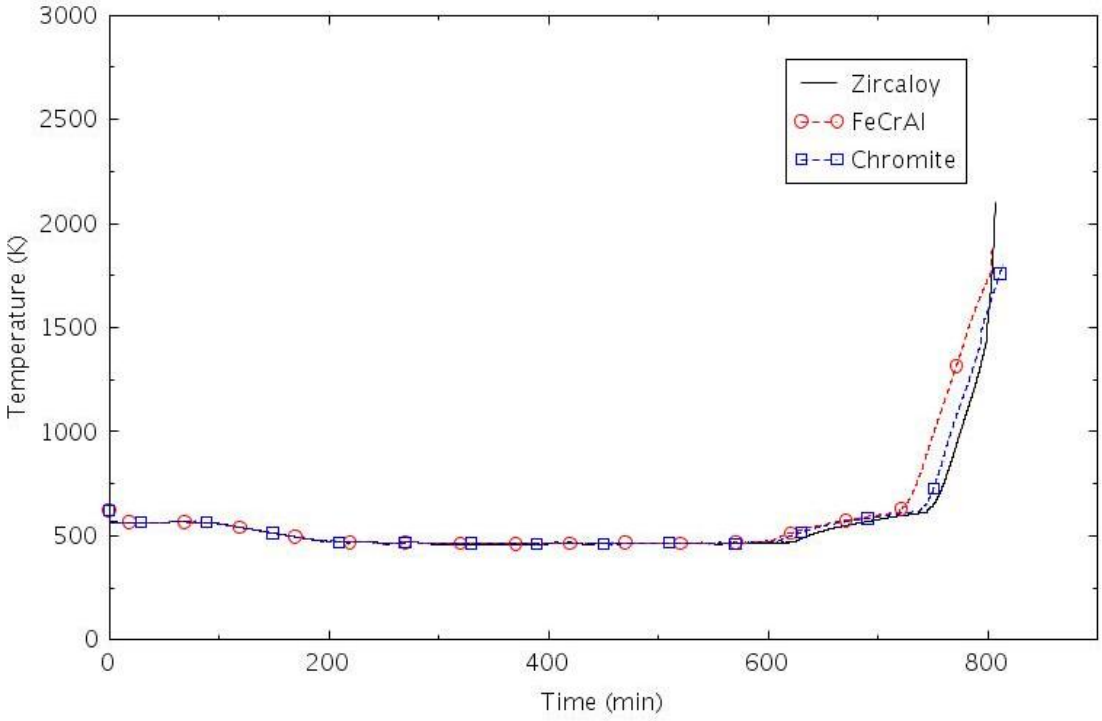

Figure 2-96. Maximum cladding temperature (LOSC-182a).

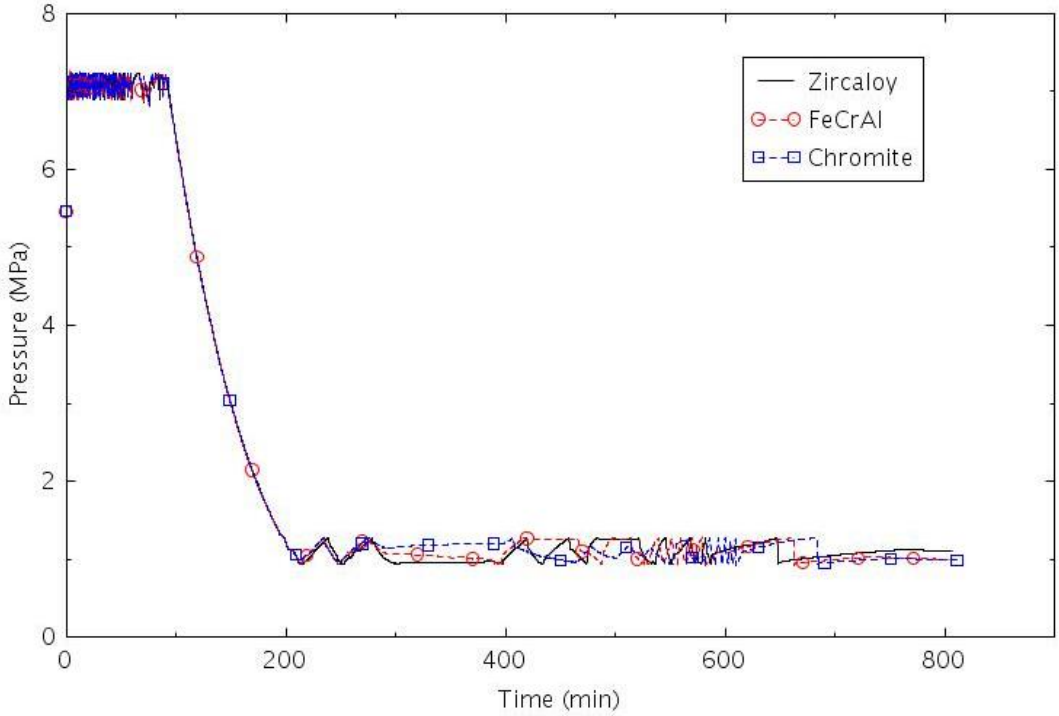

Figure 2-97. Pressure in SG B (LOSC-182a).

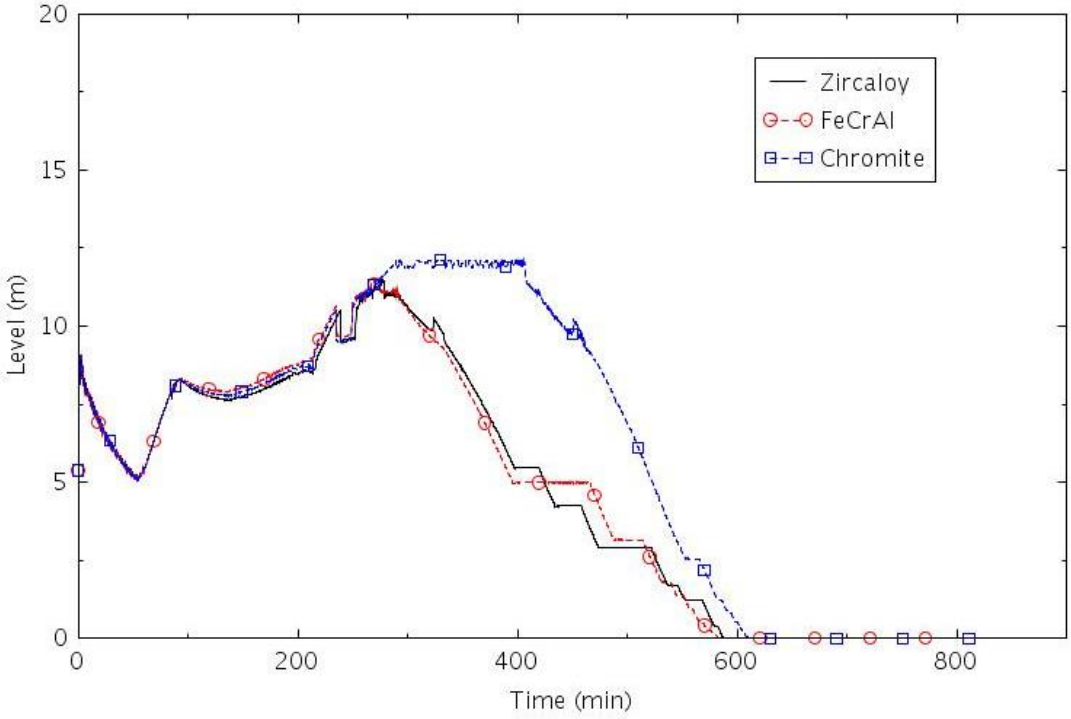

Figure 2-98. Collapsed liquid level in SG B (LOSC-182a).

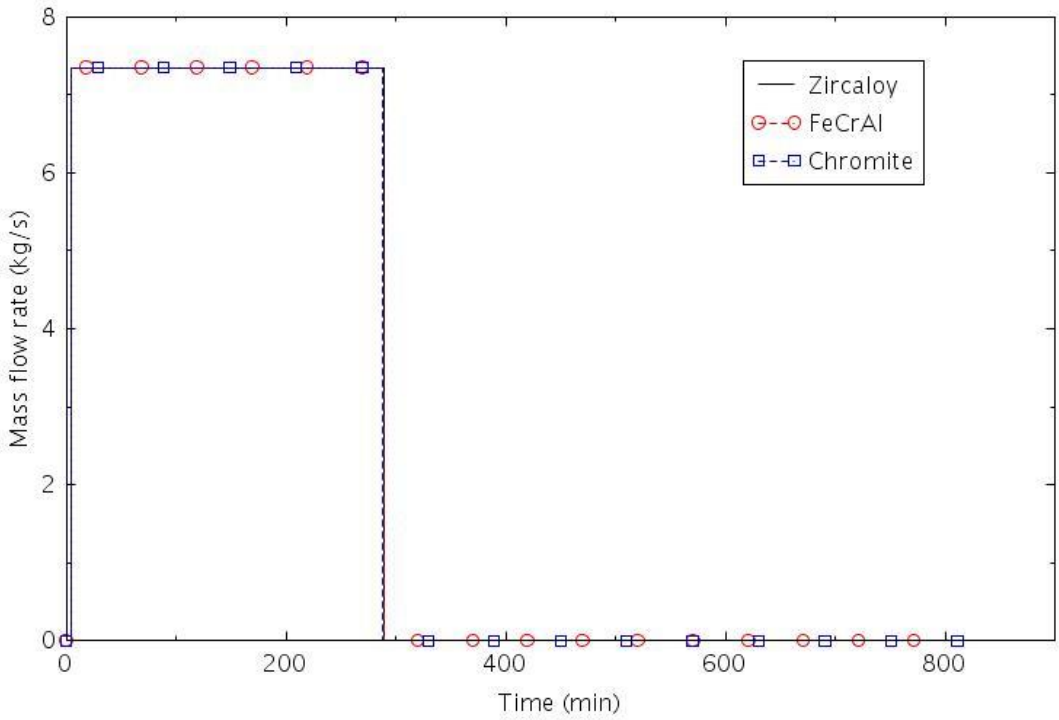

Figure 2-99. AFW flow rate to SG B (LOSC-182a).

2.2.3.5 LOSC-182b

This scenario assumes that one motor-driven AFW pump is available, that the RCP pump seals fail, and that no high-pressure injection is available. The pump seal failures produce an initial leakage of 0.011 m^3/s (182 gpm) per pump. Since power is available in this scenario, the cause of the seal failure is not mechanistic due to overheating as is generally modeled in an SBO. The seal failure was assumed to conservatively occur simultaneously with the reactor trip.

The calculated sequences of events are shown in Table 2-21. The reactor trip signal was generated 0.1 seconds after the start of the event. The reactor scram, termination of MFW, closure of the TSVs, the first lift of the pressurizer PORV and the SG PORVs all occurred within 10 s. The RCP pump seals were assumed to fail simultaneously with the reactor trip. The SIAS occurred at about 4 minutes on low reactor pressure and the AFW was initiated 30 seconds later. The HPSI was assumed to fail. The RCPs in the unaffected loops were tripped at about 54 minutes. The RCS coolant inventory decreased continuously due to flow through the ruptured pump seals and lack of HPSI. The core began to uncover near 9 hours. The AFW was terminated near 9 hours because the ECST was depleted. The calculations were terminated near 10 hours. The differences between calculations were generally negligible before the core began to uncover. The time between when the core began to uncover and core damage occurred was 84 minutes with Zircaloy, 97 minutes with FeCrAl, and 93 minutes with Chromite. The calculated amount of hydrogen produced during the transients varied significantly between claddings. The amount of hydrogen produced was 2.1 kg for FeCrAl, 8.5 kg for Chromite, and 33.1 kg for Zircaloy.

Table 2-21. Sequence of Events for Scenario LOSC-182b.

	Time (hr:min)		
Event	**Zircaloy**	**FeCrAl**	**Chromite**

RCP A locked	0:00	0:00	0:00
SIAS	0:04	0:04	0:04
AFW initiated	0:04	0:04	0:04
RCP B and C tripped	0:54	0:53	0:54
Core begins to uncover	8:31	8:39	8:47
AFW terminated	9:06	9:10	9:13
0.5 kg H_2 generation	9:32	10:16	10:00
First cladding rupture	9:38	9:43	9:55
Core damage	9:55	10:16	10:19

The following figures illustrate the effects of the cladding on various parameters. The mass flow through the seals in RCP B is illustrated in Figure 2-100. The fluid going out through the pump seals was mostly liquid before 110 minutes and mostly vapor afterwards. Pressurizer pressure is shown in Figure 2-101. The LOCA initiated by the rupture of the pump seals caused the pressure to decrease until the RCS and SG pressures were nearly the same after 15 minutes. The collapsed liquid level in the pressurizer is shown in Figure 2-102. The LOCA caused the pressurizer to empty within 10 minutes.

The LOCA caused some voiding in the core within a few minutes of the start of the transient, as shown in Figure 2-103. The collapsed level remained nearly constant between 100 and 500 minutes, when the level began to decrease sharply. The core began to heat up a few minutes later, as shown in Figure 2-104.

The pressure in SG B is shown in Figure 2-105. The pressure was generally between the open and close setpoints of the SG PORVs. The collapsed liquid level in SG B is shown in Figure 2-106 and the AFW flow is shown in Figure 2-107. Although the AFW flow was initiated at 4 minutes, the collapsed liquid level decreased until the unaffected RCPs were tripped near 54 minutes. The levels then increased until the AFW was manually shut off near 270 minutes. The collapsed levels then decreased until about 510 minutes, when the AFW was manually restarted. The AFW was terminated near 730 minutes, because the ECST was depleted of liquid.

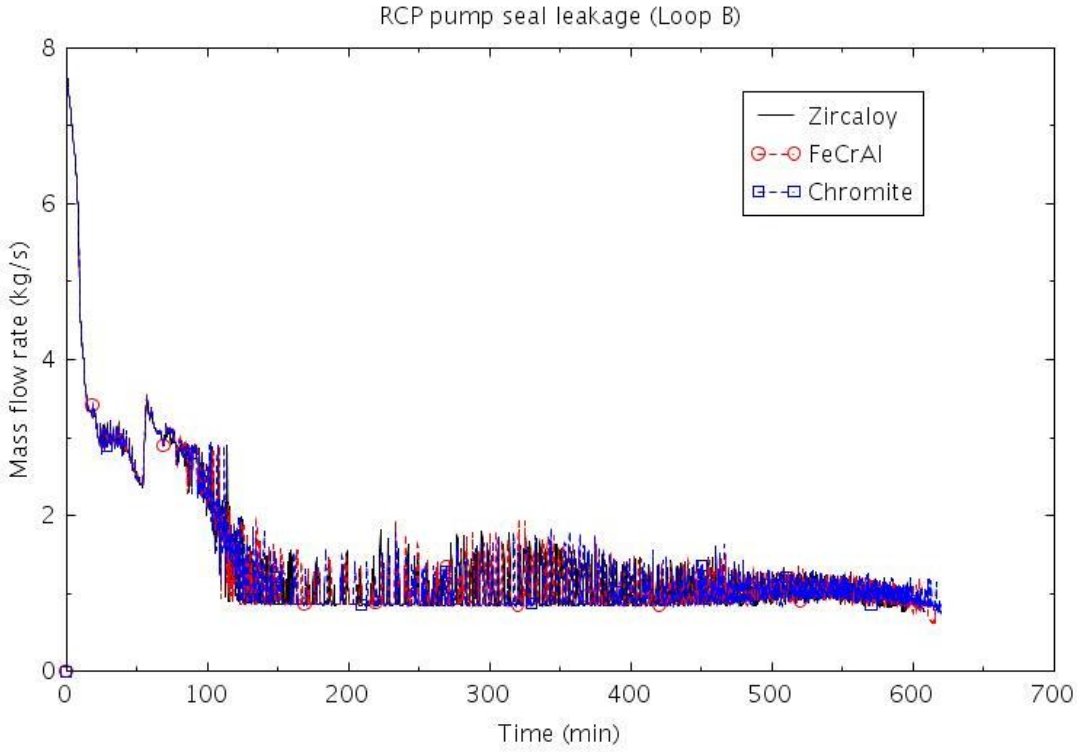

Figure 2-100. Mass flow rate through the seals of RCP B (LOSC-182b).

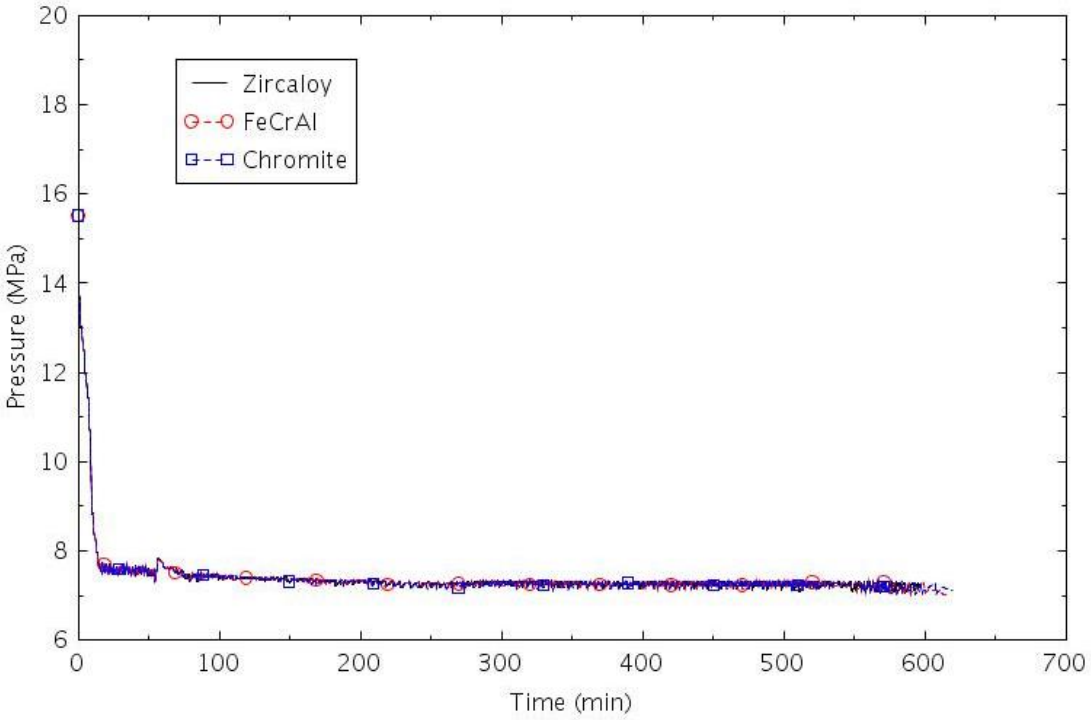

Figure 2-101. Pressure in the pressurizer (LOSC-182b).

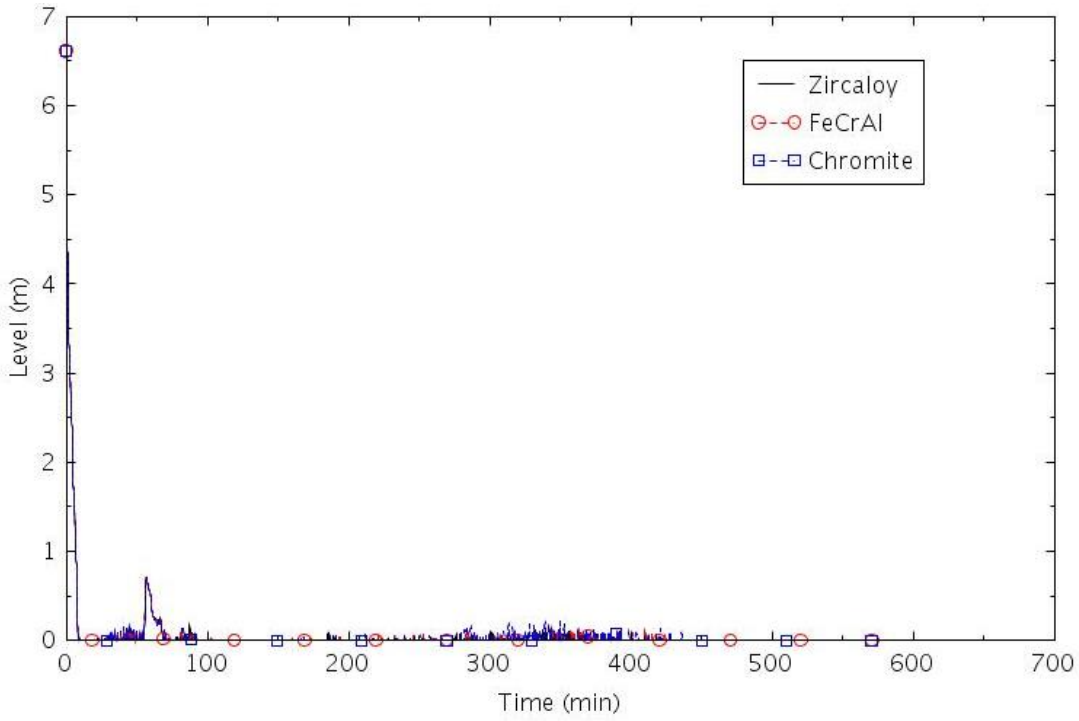

Figure 2-102. Collapsed liquid level in the pressurizer (LOSC-182b).

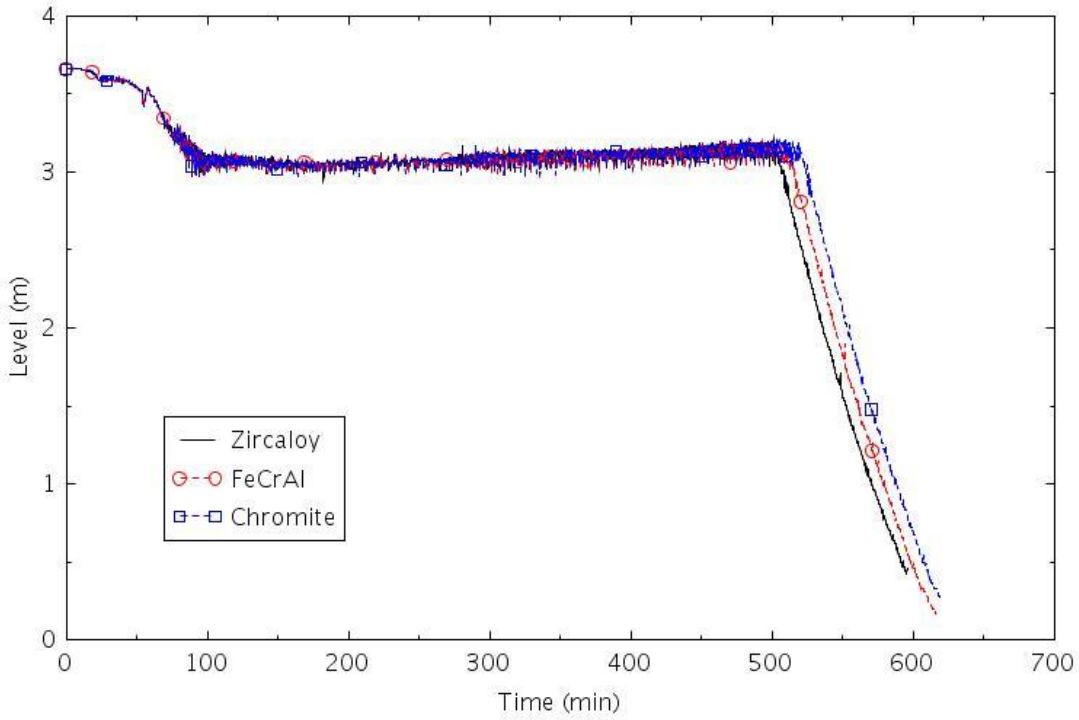

Figure 2-103. Collapsed liquid level in the central core channel (LOSC-182b).

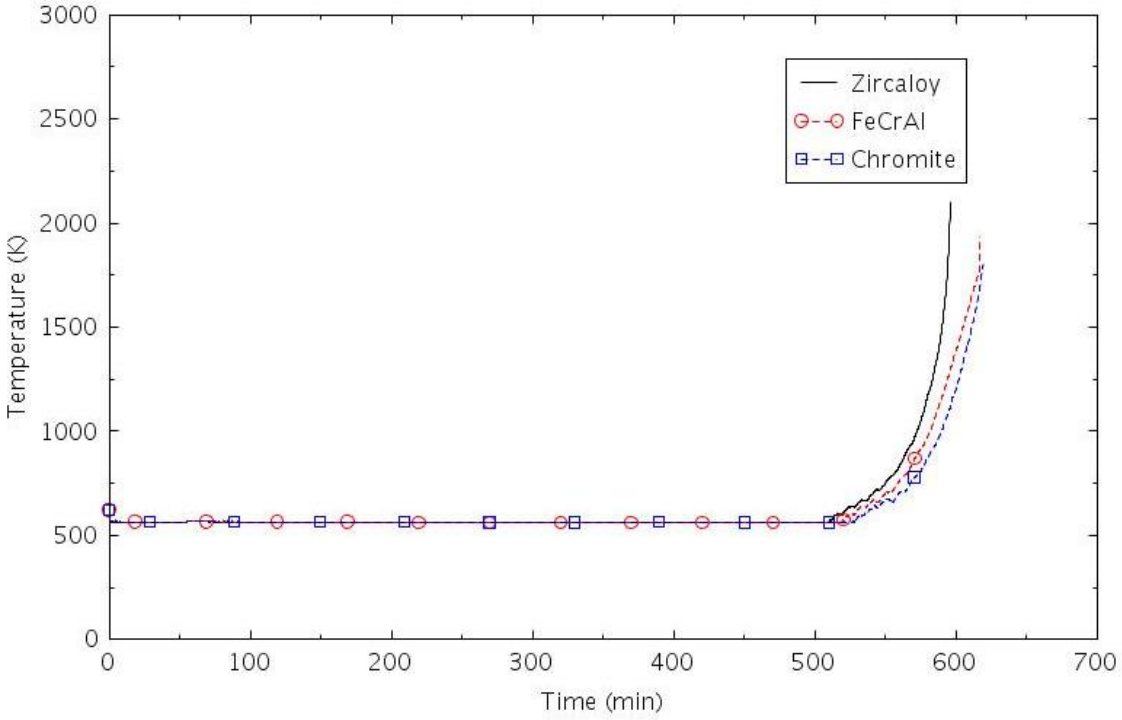

Figure 2-104. Maximum cladding temperature (LOSC-182b).

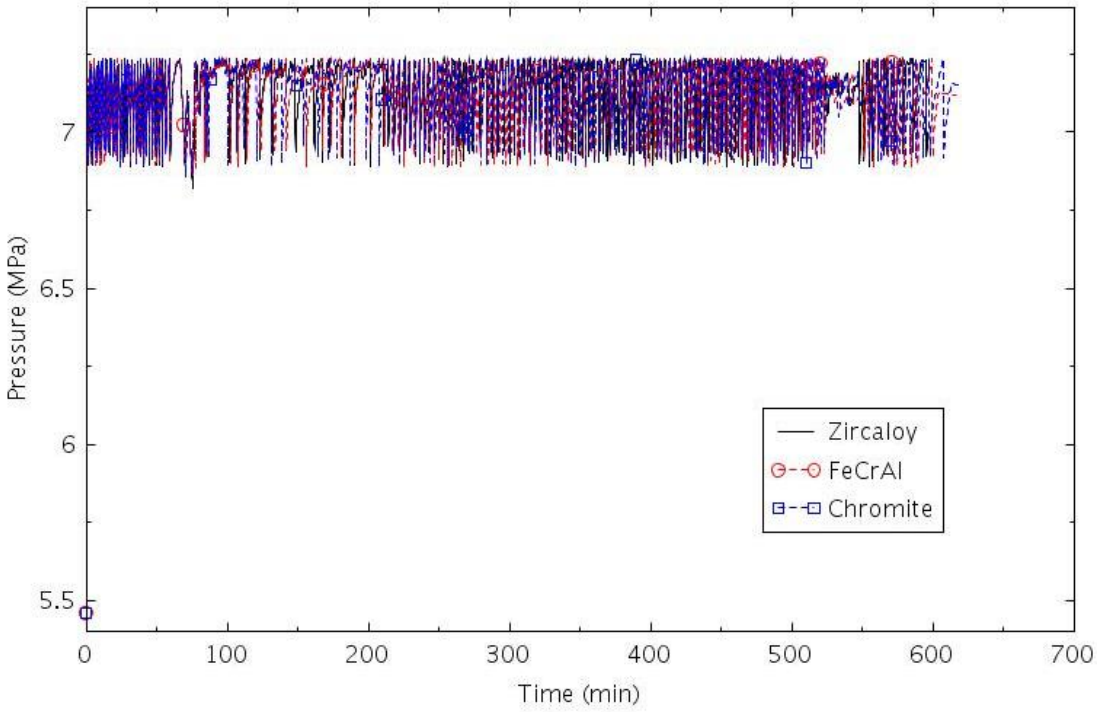

Figure 2-105. Pressure in SG B (LOSC-182b).

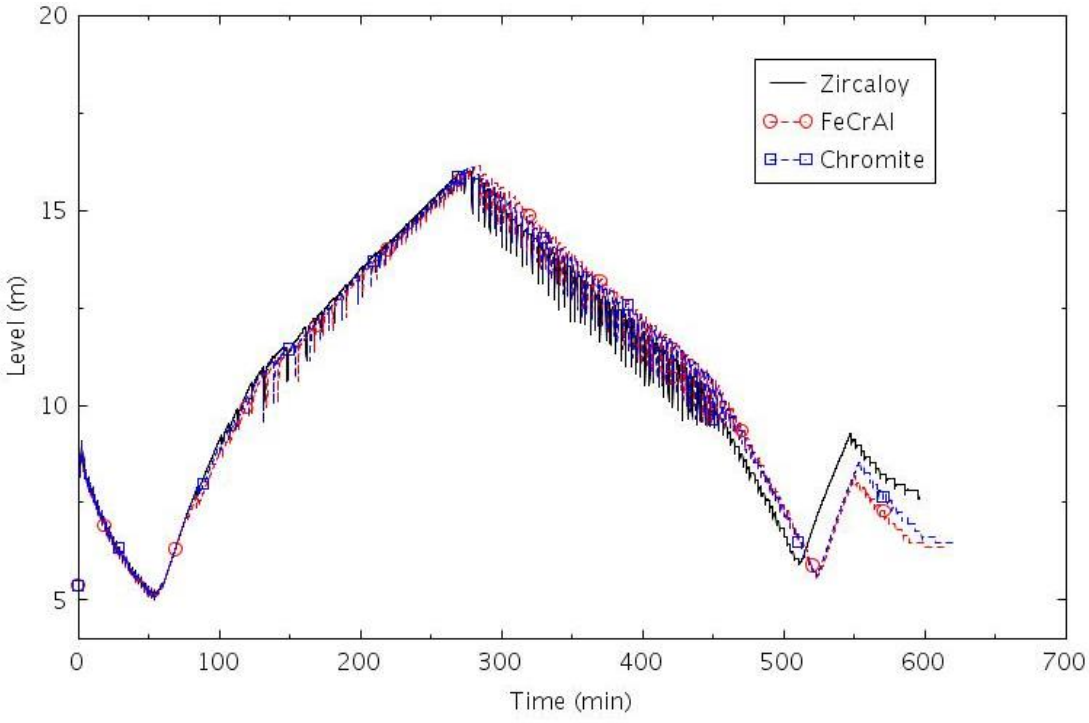

Figure 2-106. Collapsed liquid level in SG B (LOSC-182).

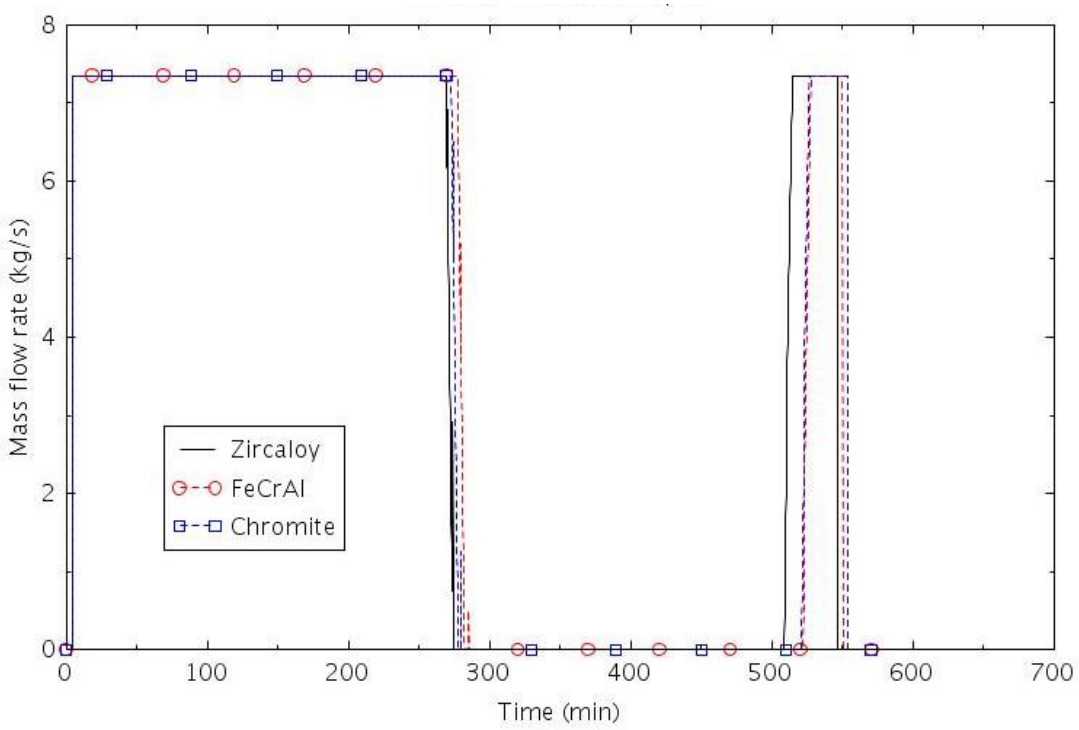

Figure 2-107. AFW flow rate to SG B (LOSC-182b).

2.2.3.6 LOSC-76

This scenario assumes that one motor-driven AFW pump is available, that the RCP pump seals fail, that no high-pressure injection is available, and that the operators manually initiate SSC at 1.5 hours, the same time as assumed in Section 3.1.4.1 of (NRC, 2012). The pump seal failures produce an initial leakage of 0.0048 m^3/s (76 gpm) per pump. Since power is available in this scenario, the cause of the seal failure is not mechanistic due to overheating as is generally modeled in an SBO. The seal failure was assumed to conservatively occur simultaneously with the reactor trip. The PORVs were opened as necessary to obtain a 56°C/hr (100°F/hr) cooldown rate in the steam generators. The cooldown was terminated when the SGs reached 0.93 MPa (134.7 psia) so that the turbine-driven AFW pumps would be available if needed. Thereafter, the PORVs opened as needed to control the SG pressure between 0.93 MPa (134.7 psia) and 1.27 MPa (184.7 psia).

The calculated sequences of events are shown in Table 2-22. The reactor trip signal was generated 0.1 seconds after the start of the event. The reactor scram, termination of MFW, closure of the TSVs, the first lift of the pressurizer PORV and the SG PORVs all occurred within 10 s. The RCP pump seals were assumed to fail simultaneously with the reactor trip. The SIAS occurred at about 9 minutes on low reactor pressure and the AFW was initiated 30 seconds later. The HPSI was assumed to fail. The RCPs in the unaffected loops were tripped at about 110 minutes. The RCS coolant inventory decreased continuously due to flow through the ruptured pump seals and lack of HPSI. The operators were assumed to manually initiate a controlled cooldown of the SGs beginning at 90 minutes. The resulting depressurization of the RCS resulted in accumulator injection near 140 minutes. The AFW was terminated near 5 hours because the ECST was depleted. The SGs were empty near 9 hours. The core began to uncover near 12 hours. The differences between calculations were generally small before the core began to uncover. The time between when the core began to uncover and core damage occurred was 71 minutes with Zircaloy, 91 minutes with FeCrAl, and 84 minutes with Chromite. The calculated amount of hydrogen produced

during the transients varied significantly between claddings. The amount of hydrogen produced was 1.7 kg for FeCrAl, 13.5 kg for Chromite, and 91.9 kg for Zircaloy.

Table 2-22. Sequence of Events for Scenario LOSC-76.

	Time (hr:min)		
Event	**Zircaloy**	**FeCrAl**	**Chromite**
RCP A locked	0:00	0:00	0:00
SIAS	0:09	0:10	0:09
AFW initiated	0:10	0:10	0:10
SSC begins	1:30	1:30	1:30
RCP B and C tripped	1:47	1:48	1:48
Accumulator flow initiated	2:20	2:20	2:19
SSC ends	3:35	3:35	3:35
AFW terminated	5:02	5:02	5:02
Accumulator flow terminated	7:20	7:56	7:34
All SGs empty	9:21	9:32	9:24
Pressurizer PORV begins to cycle	11:33	11:43	11:35
PRT rupture disk opens	11:34	11:44	11:36
Core begins to uncover	11:58	12:07	11:59
0.5 kg H_2 generation	12:30	13:31	13:13
First cladding rupture	13:04	13:19	13:12
Core damage	13:09	13:38	13:23

The following figures illustrate the effects of the cladding on various parameters. The mass flow through the seals in RCP B is illustrated in Figure 2-108. The increase in mass flow near560 minutes was due to an increase in RCS pressure. The leakage was small enough that mostly liquid passed through the seals until about 700 minutes. Pressurizer pressure is shown in Figure 2-109. The LOCA initiated by the rupture of the pump seals caused the pressure to decrease until the RCS and SG pressures were nearly the same near 30 minutes. The decrease in pressure at 90 minutes was due to the SSC. The RCS and SG pressures were closely coupled until all the SGs were empty near 570 minutes. Thereafter, boiling in the core caused the pressure to increase until the pressurizer PORV began to cycle near 700 minutes. As shown in Figure 2-110, the pressurizer completely filled with liquid shortly before the PORV began to cycle. The pressurizer then began to drain again and was empty by the end of the calculation.

The LOCA caused some voiding in the core within 20 minutes of the start of the transient, as shown in Figure 2-111. The onset of accumulator injection near 140 minutes eventually refilled the core. The level decreased somewhat after accumulator injection was terminated near 450 minutes. The level decreased sharply near 700 minutes. The core began to heat up near 720 minutes, as shown in Figure 2-112.

The pressure in SG B is illustrated in Figure 2-113. The pressure was generally between the open and close setpoints of the SG PORVs until 90 minutes, when the manual SSC was initiated. After the cooldown was terminated near 200 minutes, the operators were assumed to open and close the PORVs as necessary to maintain the pressure between 0.93 MPa (134.7 psia) and 1.27 MPa (184.7 psia).

The collapsed liquid level in SG B is shown in Figure 2-114 and the AFW flow is shown in Figure 2-115. Even though the AFW flow was initiated at 10 minutes, the collapsed liquid level decreased until the unaffected RCPs were tripped near110 minutes. The levels then increased until the AFW was terminated near 300 minutes. The collapsed levels then decreased.

Scenario LOSC-76 was identical to Scenario LOSC-182a, except that there was less leakage through the pump seals. A comparison of Table 2-20 and Table 2-22 shows that the core uncovered about 10 minutes earlier, on average, with the smaller leakage. This unexpected result can be explained as follows. The smaller leakage in Scenario LOSC-76 resulted in less energy removal through the break, which required additional heat transfer to the SGs in order to remove core decay heat and cool down the RCS. Consequently, the SGs were empty about 50

minutes earlier, on average, in Scenario LOSC-76. The earlier dryout of the SGs resulted in an earlier pressurization of the RCS and a period of increased leakage through the seals compared to Scenario 182a. RCS mass was also lost out the PORV near the end of the calculation in Scenario LOSC-76, which did not occur in Scenario LOSC-182a. This additional mass loss was responsible for the earlier dryout of the core in Scenario LOSC-76.

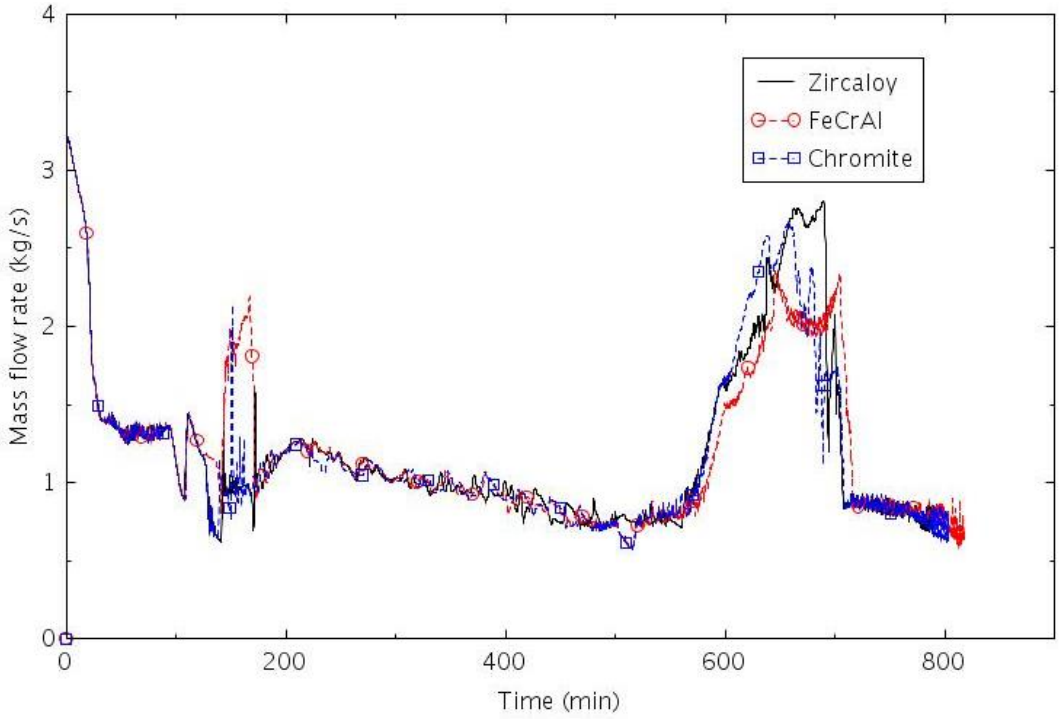

Figure 2-108. Mass flow rate through the seals of RCP B (LOSC-76).

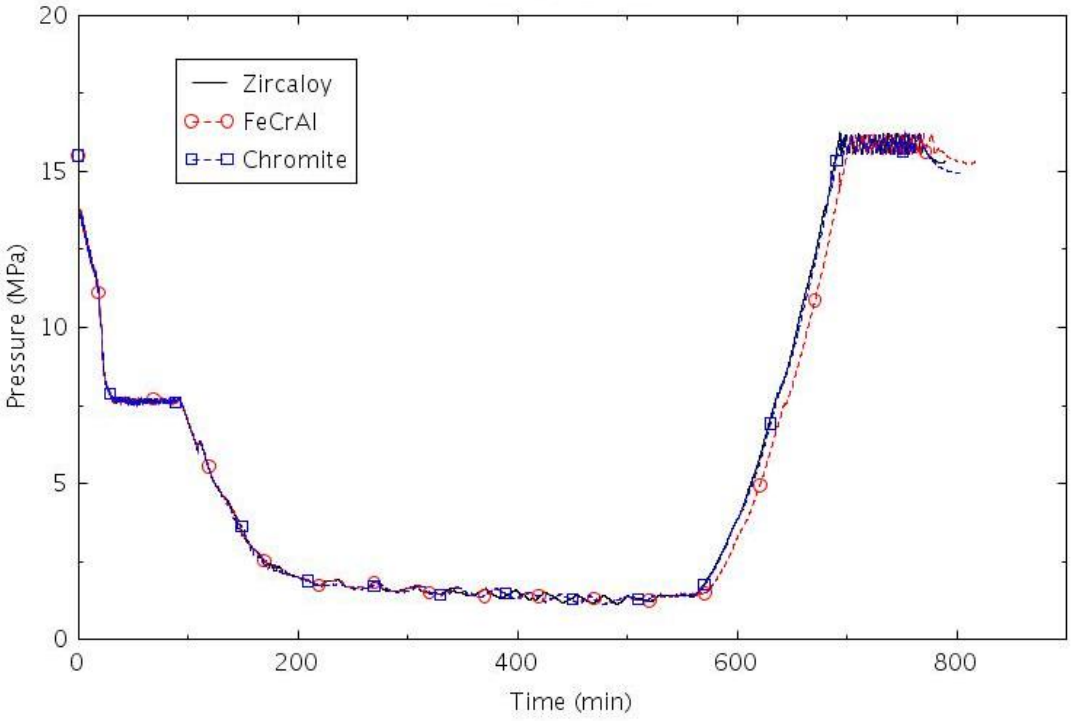

Figure 2-109. Pressure in the pressurizer (LOSC-76).

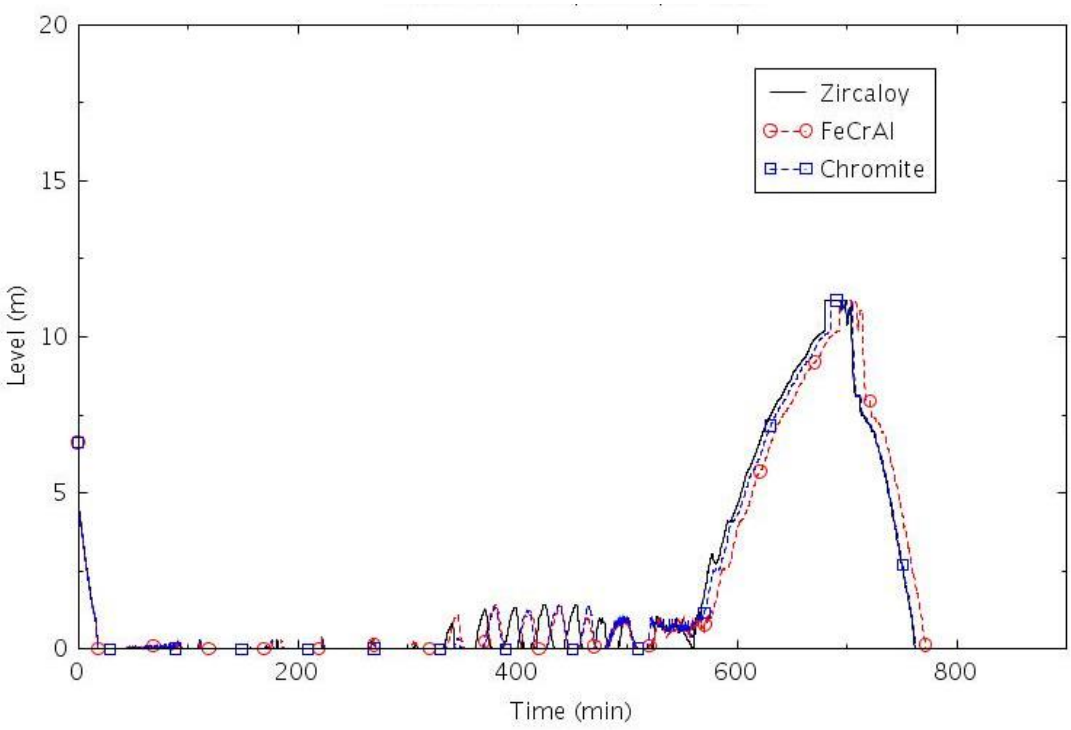

Figure 2-110. Collapsed liquid level in the pressurizer (LOSC-76).

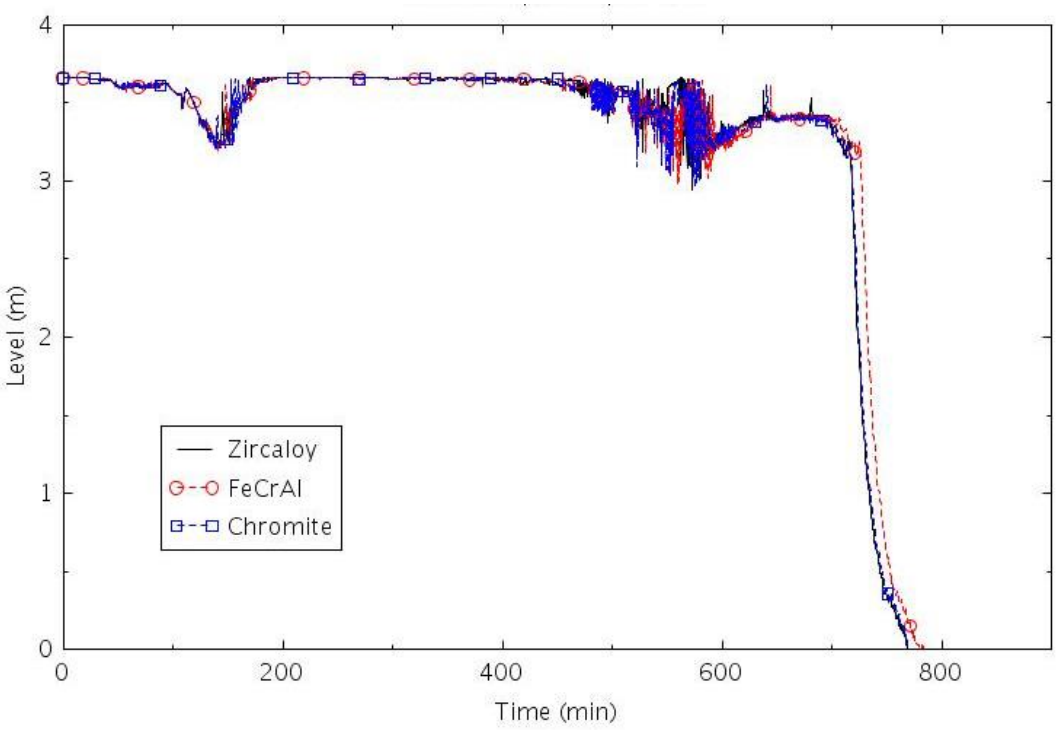

Figure 2-111. Collapsed liquid level in the central core channel (LOSC-76).

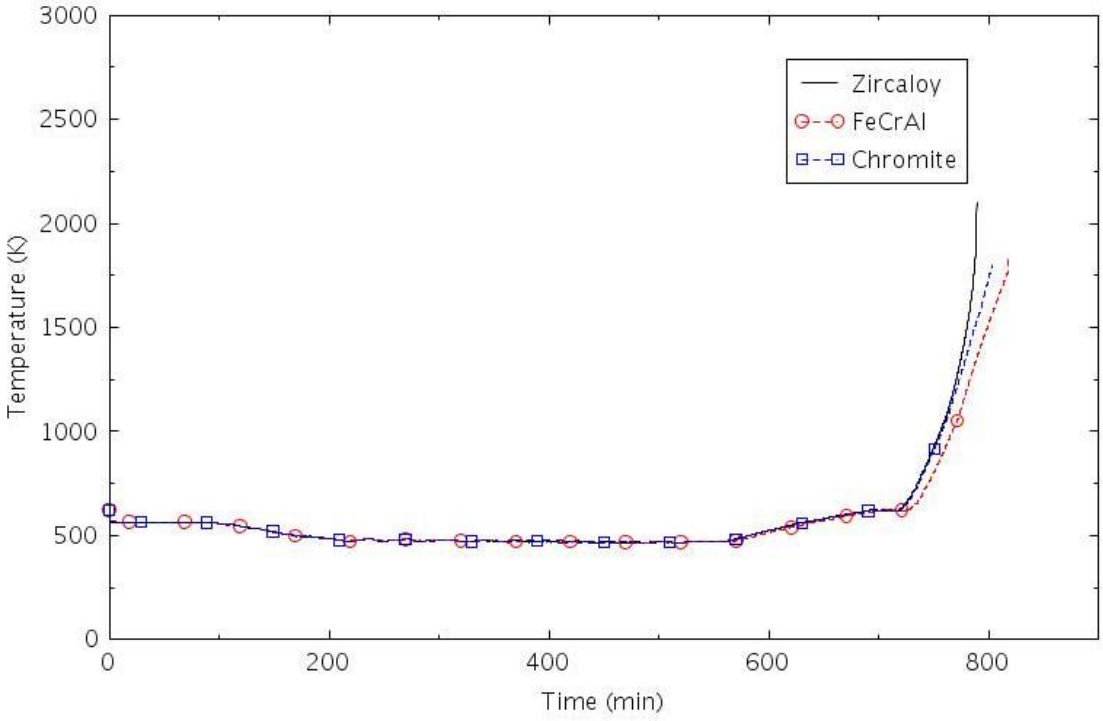

Figure 2-112. Maximum cladding temperature (LOSC-182a).

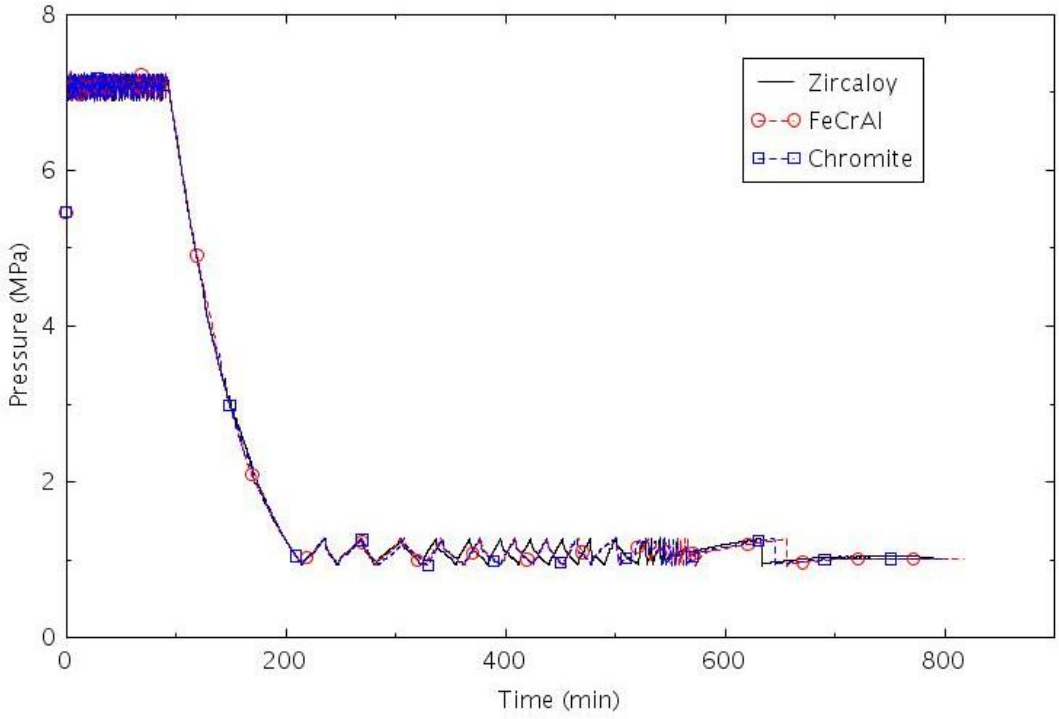

Figure 2-113. Pressure in SG B (LOSC-76).

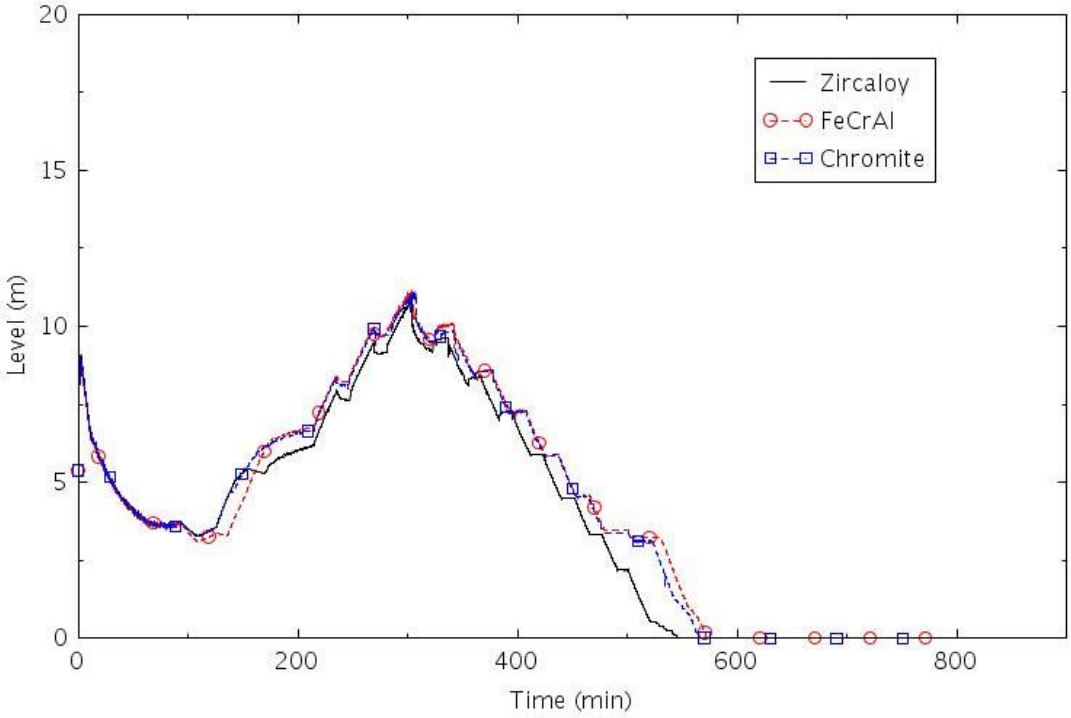

Figure 2-114. Collapsed liquid level in SG B (LOSC-76).

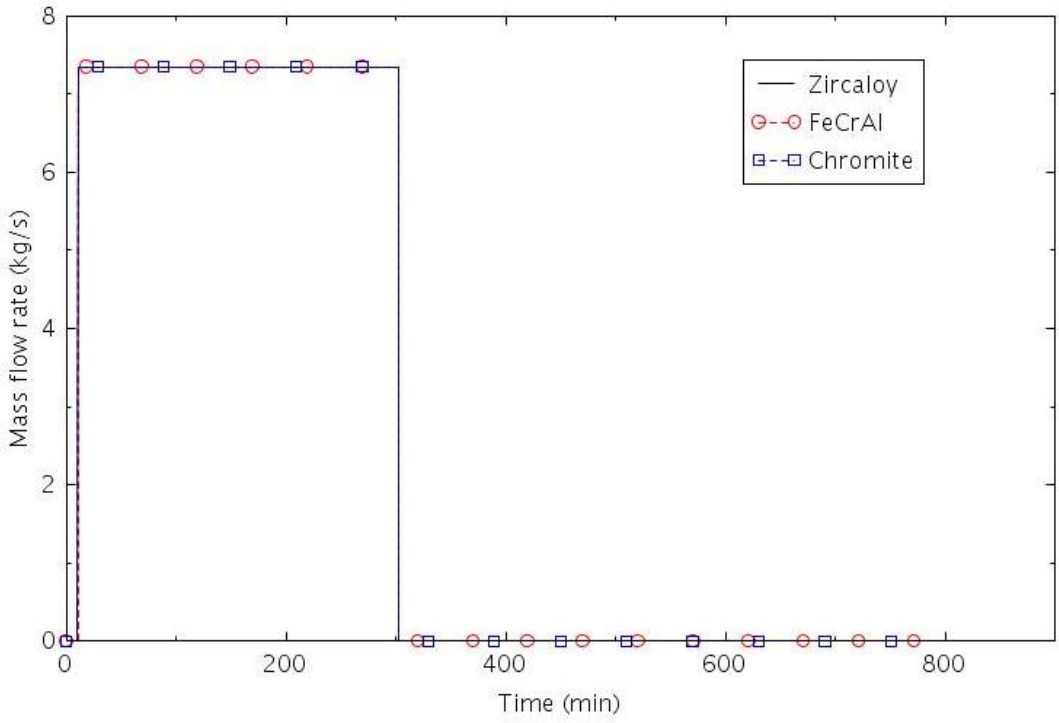

Figure 2-115. AFW flow rate to SG B (LOSC-76).

2.2.3.7 LOSC-480

This scenario assumes that one motor-driven AFW pump is available, that the RCP pump seals fail, that no high-pressure injection is available, and that the operators manually initiate SSC. The pump seal failures produce an initial leakage of 0.030 m^3/s (480 gpm) per pump. Since power is available in this scenario, the cause of the seal failure is not mechanistic due to overheating as is generally modeled in an SBO. The seal failure was assumed to conservatively occur simultaneously with the reactor trip. The SSC was assumed to begin at 1.5 hours, the same time as assumed in Section 3.1.4.1 of (NRC, 2012). The PORVs were opened as necessary to obtain a 56°C/hr (100°F/hr) cooldown rate in the steam generators. The cooldown was terminated when the SGs reached 0.93 MPa (134.7 psia) so that the turbine-driven AFW pumps would be available if needed. Thereafter, the PORVs opened as needed to control the SG pressure between 0.93 MPa (134.7 psia) and 1.27 MPa (184.7 psia).

The calculated sequences of events are shown in Table 2-23. The reactor trip signal was generated 0.1 seconds after the start of the event. The reactor scram, termination of MFW, closure of the TSVs, the first lift of the pressurizer PORV and the SG PORVs all occurred within 10 s. The RCP pump seals were assumed to fail simultaneously with the reactor trip. The SIAS occurred at about 1minute on low reactor pressure and the AFW was initiated 30 seconds later. The HPSI was assumed to fail. The RCPs in the unaffected loops were tripped at 21 minutes. The RCS coolant inventory decreased continuously due to flow through the ruptured pump seals and lack of HPSI. The operators were assumed to manually initiate a controlled cooldown of the SGs beginning at 90 minutes. The resulting depressurization of the RCS resulted in accumulator injection at 131 minutes. The AFW flow was terminated near5 hours because the ECST was depleted. However, the SGs were not empty at the end of the calculations. The core began to uncover near 5 hours. The calculations were terminated by either high cladding temperature or severe fuel rod ballooning at the top of the core. The differences between calculations were negligible before the SSC ended and were generally small afterwards. The increased variability after the SSC ended was more likely due to numerical issues than to the differences between claddings. The calculations with the Zircaloy and

Chromite claddings were terminated due to severe cladding ballooning in the middle core channel. Consequently, the cladding in those calculations did not reach temperatures as high as obtained in the previous calculations and less hydrogen was produced. The amount of hydrogen produced was 0.2 kg for Chromite, 0.7 kg for FeCrAl, and 0.9 kg for Zircaloy.

Table 2-23. Sequence of Events for Scenario LOSC-480.

	Time (hr:min)		
Event	**Zircaloy**	**FeCrAl**	**Chromite**
RCP A locked	0:00	0:00	0:00
SIAS	0:01	0:01	0:01
AFW initiated	0:02	0:02	0:02
RCP B and C tripped	0:21	0:21	0:21
SSC begins	1:30	1:30	1:30
Accumulator flow initiated	2:11	2:11	2:11
Accumulator flow terminated	3:25	3:25	3:25
SSC ends	3:37	3:37	3:40
AFW terminated	4:42	4:41	5:02
Core begins to uncover	5:12	5:13	4:59
First cladding rupture	5:38	5:39	5:42
0.5 kg H_2 generation	5:43	6:20	NA
Core damage	5:46	6:20	5:51

The following figures illustrate the effects of the cladding on various parameters. The mass flow through the seals in RCP B is illustrated in Figure 2-116. The flow rate increased after accumulator flow was initiated near 130 minutes. The accumulators emptied near 290 minutes and the mass flow decreased shortly thereafter.

Pressurizer pressure is shown in Figure 2-117. The LOCA initiated by the rupture of the pump seals caused the pressure to decrease until the RCS and SG pressures were nearly the same near 5 minutes. The decrease in pressure at 90 minutes was due to the SSC. The RCS and SG pressures were closely coupled for the remainder of the calculations. The collapsed liquid level in the pressurizer is shown in Figure 2-118. The LOCA caused the pressurizer to empty within a few minutes.

The LOCA caused some voiding in the core within a few minutes of the start of the transient as shown in Figure 2-119. Although the collapsed liquid level was considerably lower than in the previous calculations, the core did not begin to heat up until about 300 minutes, as shown in Figure 2-120. The cladding did not reach the termination temperatures of 2099 K for Zircaloy and 1804 K for Chromite before the calculations were terminated, due to severe ballooning of the cladding that reduced the flow area of the middle channel to near zero.

The pressure in SG B is illustrated in Figure 2-121. The pressure was generally between the open and close setpoints of the SG PORVs until 90 minutes, when the manual SSC was initiated. After the cooldown was terminated near 220 minutes, the operators were assumed to open and close the PORVs as necessary to maintain the pressure between 0.93 MPa (134.7 psia) and 1.27 MPa (184.7 psia).

The collapsed liquid level in SG B is shown in Figure 2-122 and the AFW flow is shown in Figure 2-123. Even though the AFW flow was initiated at 2 minutes, the collapsed liquid level decreased until the unaffected RCPs were tripped near 20 minutes. The level then increased until the SSC was initiated at 90 minutes. The levels remained nearly constant until the SSC ended near 220 minutes. The levels then increased until AFW was terminated near 290 minutes. The collapsed levels then generally decreased although there was considerable variation in the calculated levels within a single SG. The calculated levels were decreasing at the end of the Zircaloy and Chromite calculations but were nearly constant in the FeCrAl calculation. These results indicate that the B SG was removing decay heat in the Zircaloy and Chromite calculations, but not in the Chromite calculation. The C steam generator was removing the decay heat at the end of the Chromite calculation. The break was big enough in all these calculations that the SGs were not empty when the calculations were terminated.

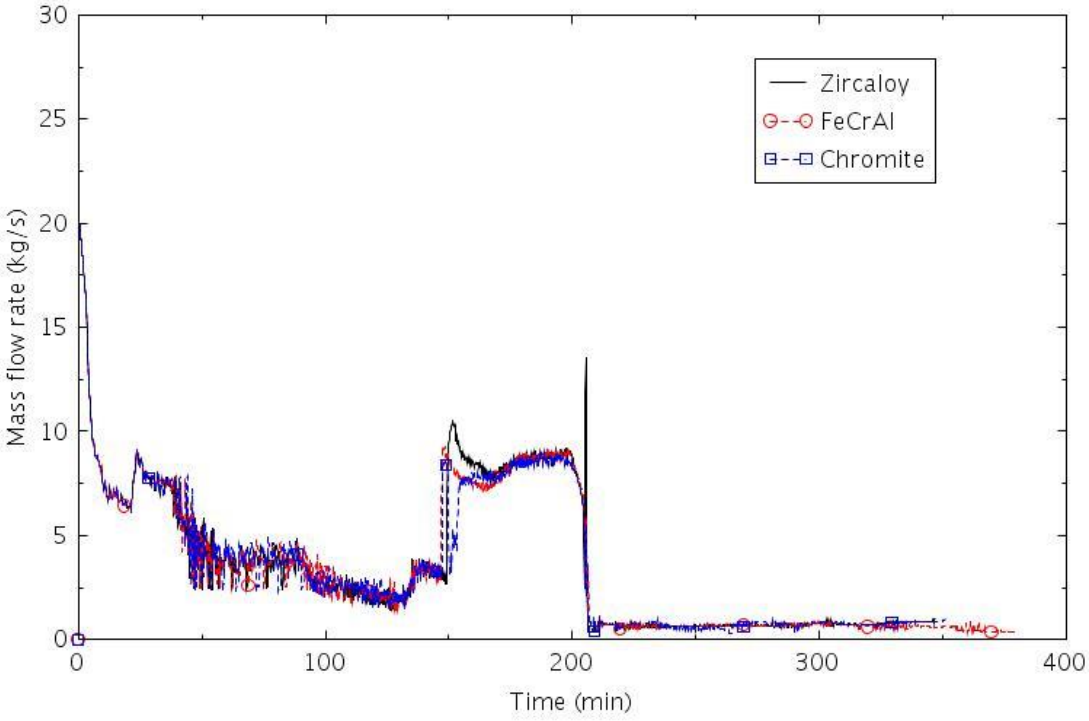

Figure 2-116. Mass flow rate through the seals of RCP B (LOSC-480).

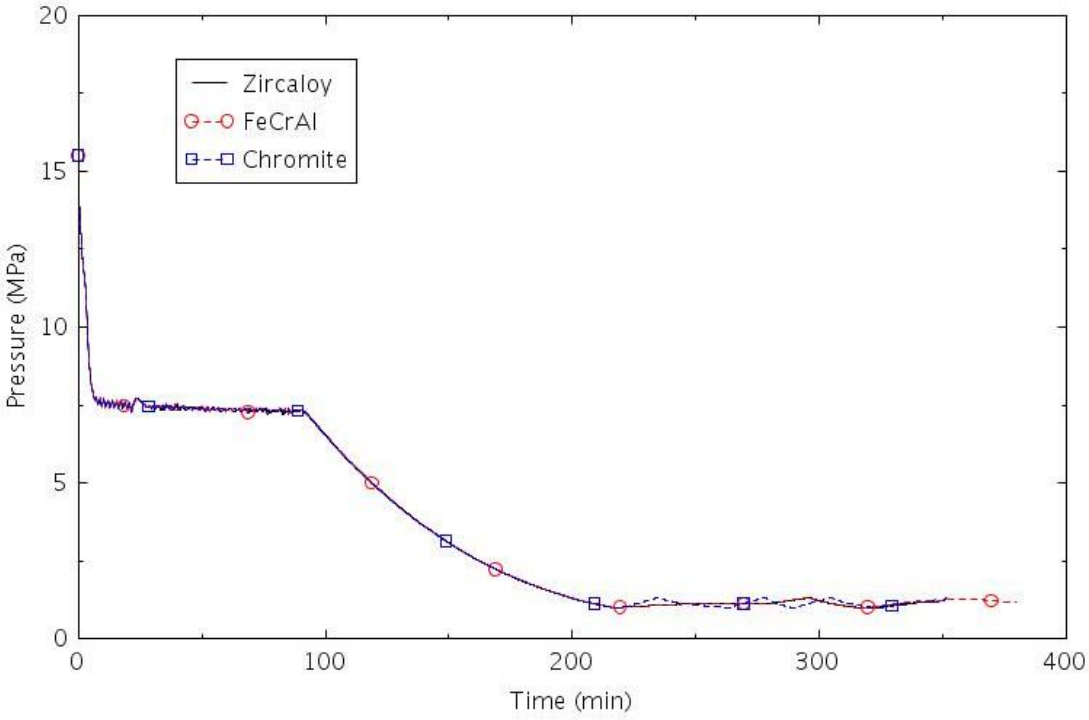

Figure 2-117. Pressure in the pressurizer (LOSC-480).

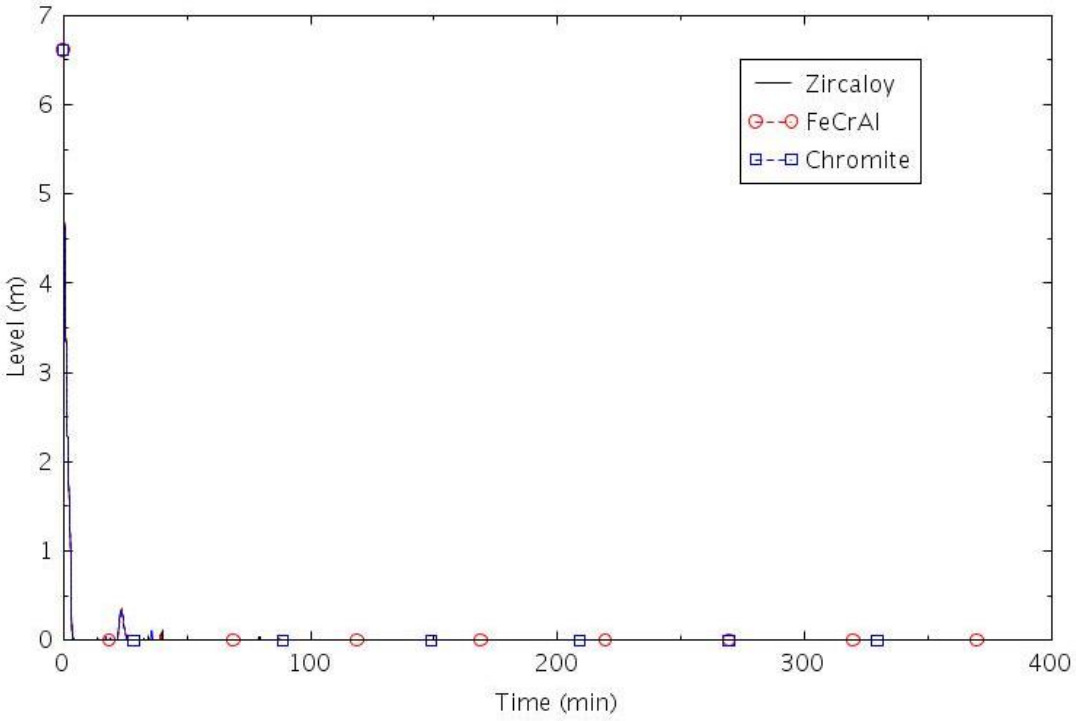

Figure 2-118. Collapsed liquid level in the pressurizer (LOSC-480).

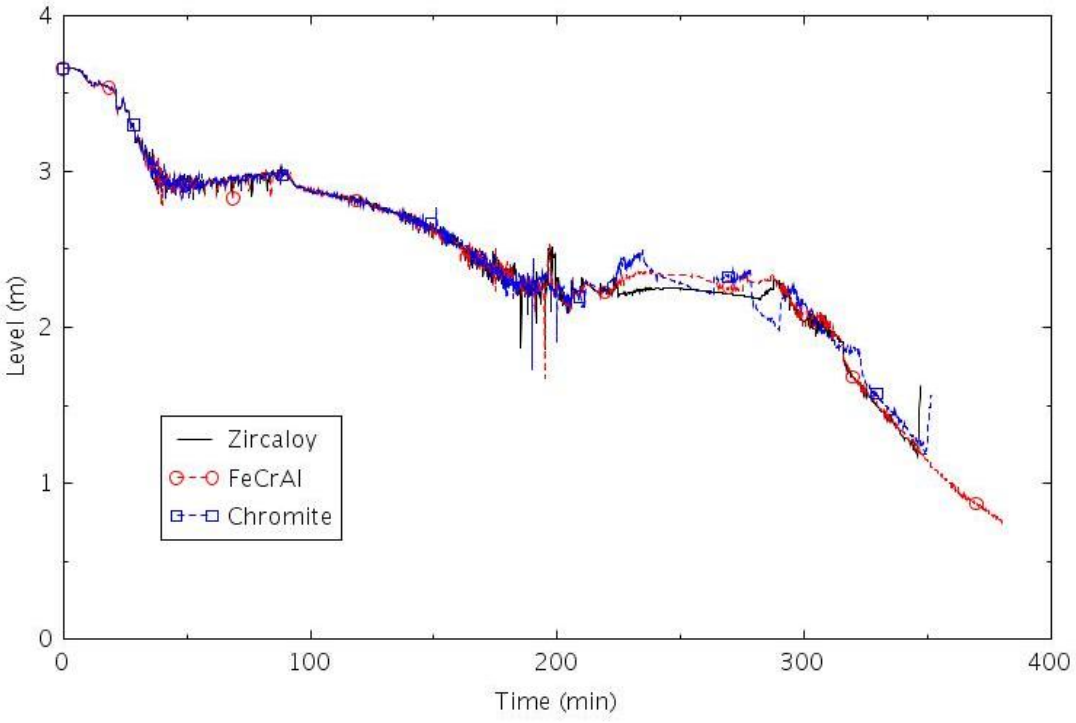

Figure 2-119, Collapsed liquid level in the central core channel (LOSC-480).

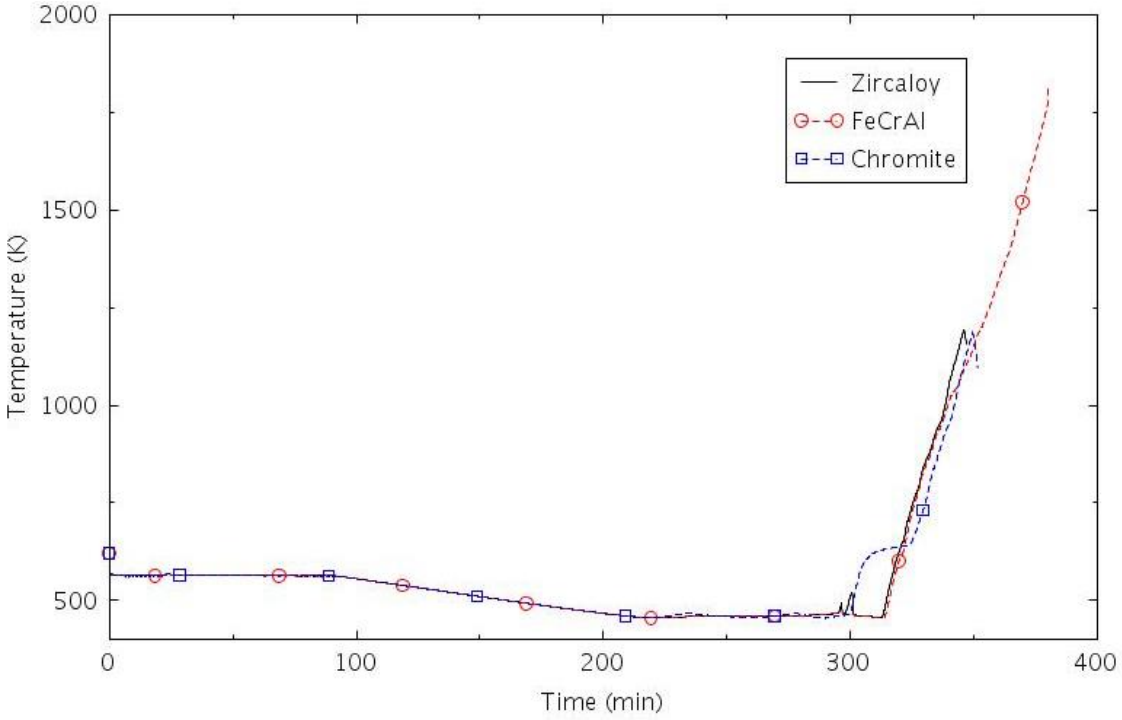

Figure 2-120. Maximum cladding temperature (LOSC-480).

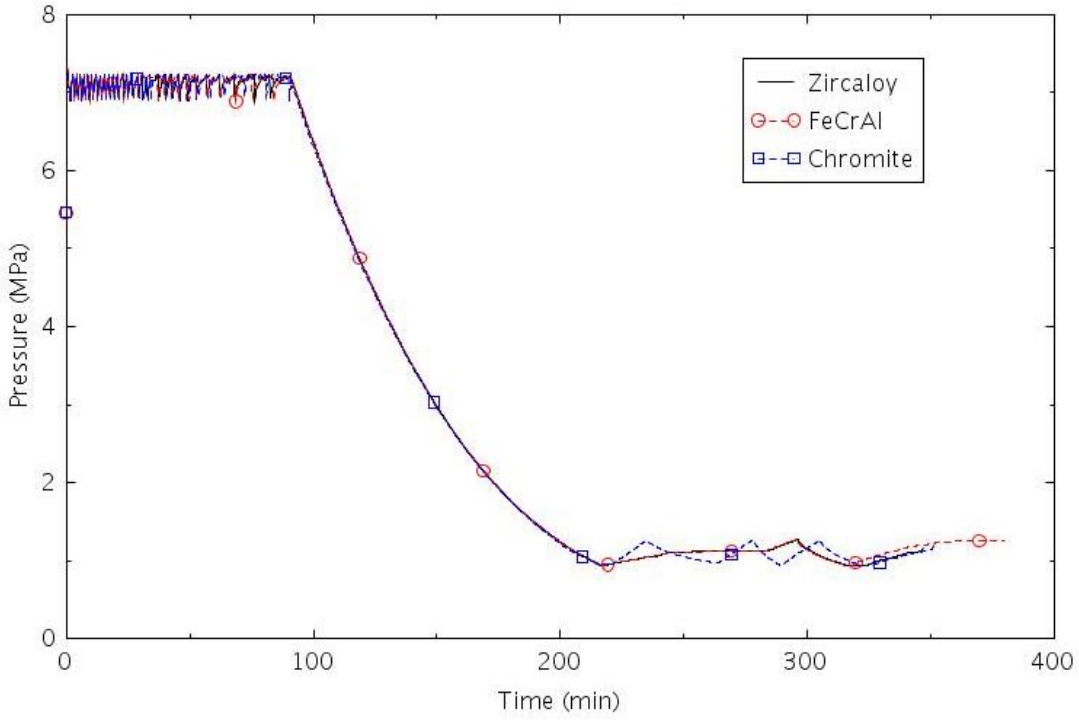

Figure 2-121. Pressure in SG B (LOSC-480).

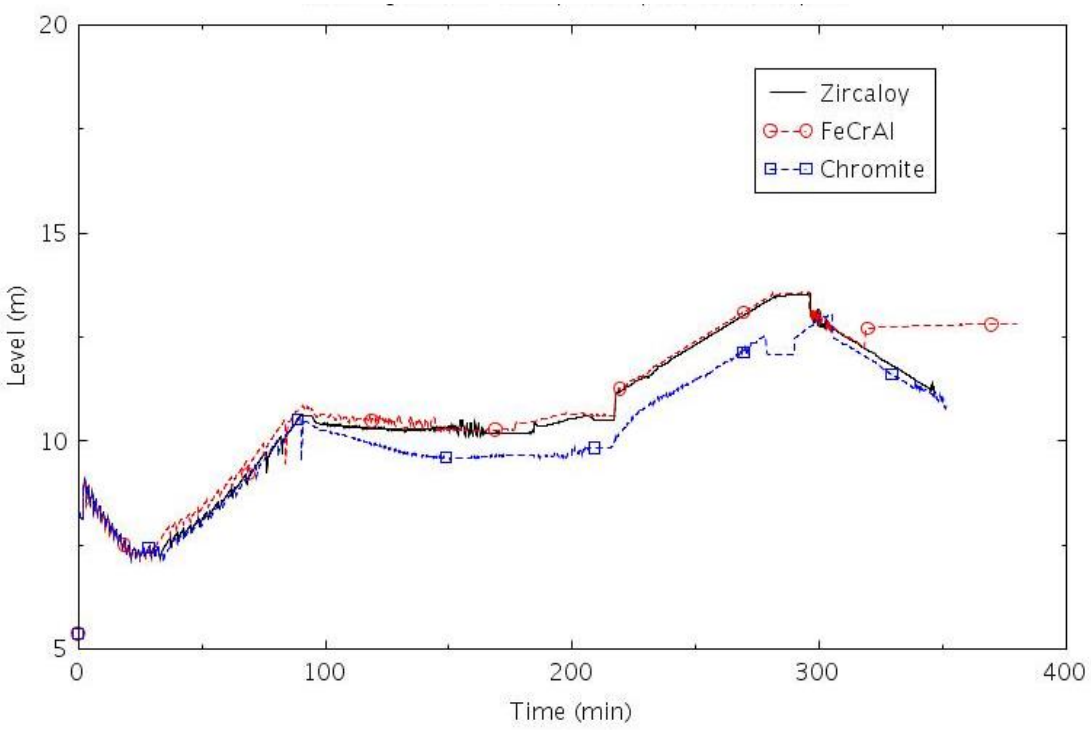

Figure 2-122. Collapsed liquid level in SG B (LOSC-480).

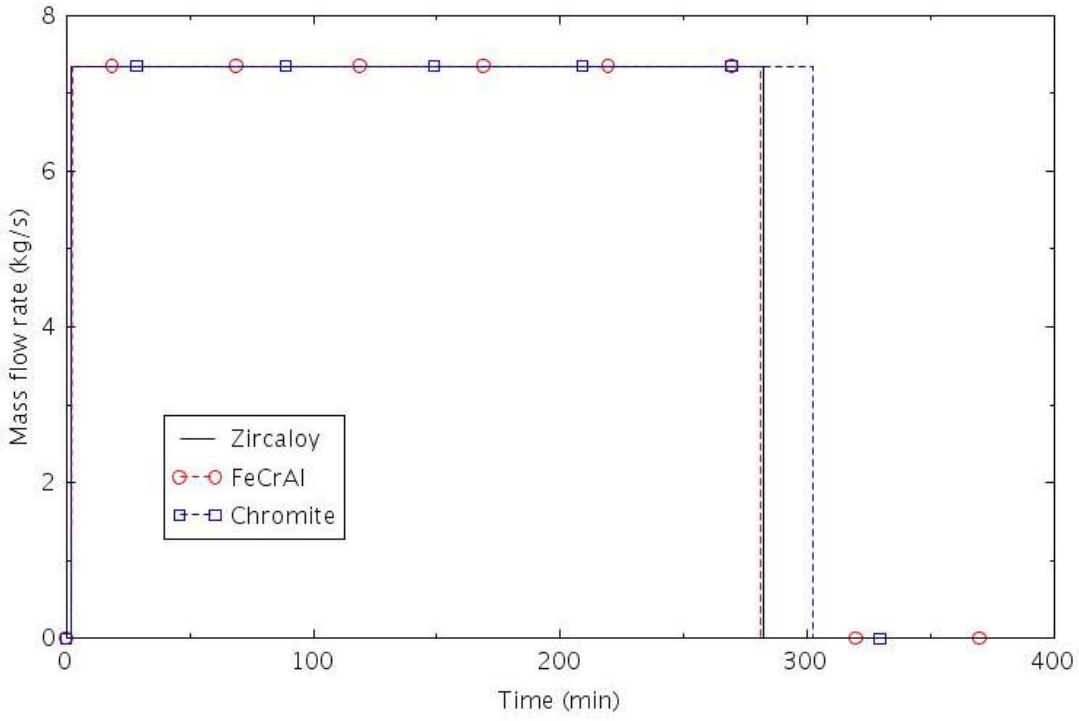

Figure 2-123. AFW flow rate to SG B (LOSC-480).

2.2.3.8 ATWS-1

This scenario assumed that the reactor trip system failed to scram the reactor, that the RCS pressure relief valves failed to function, and that no feedwater was available. The TSVs were assumed to close 2.0 seconds after the reactor trip signal. The MFW was terminated 6.5 seconds after the reactor trip signal. The failed relief valves included two PORVs and three safety relief valves (SRVs) on the pressurizer. The calculation was terminated when the pressure in the RCS exceeded 19.0 MPa [2750 psia], which corresponds to 110% of the design pressure, based on Section 14.2.2.3 of (Dominion, 2007).

The calculated sequences of events are shown in Table 2-24. The reactor trip signal was generated 0.1 seconds after the start of the event. The reactor scram was assumed to fail. The TSVs and MFW valves were assumed to close normally following the reactor trip signal. The RCS pressure quickly rose above the setpoint of the pressurizer PORVs and SRVs, but these relief valves were assumed to fail to open. The pressure exceeded 110% of the design pressure in 15 seconds.

Table 2-24. Sequence of Events for Scenario ATWS-1.

	Time (s)		
Event	**Zircaloy**	**FeCrAl**	**Chromite**
RCP A locked	0.0	0.0	0.0
Scram signal	0.1	0.1	0.1
TSVs closed	2.1	2.1	2.1
MFW terminated	6.6	6.6	6.6
SG PORVs open	9.5	9.5	9.5
RCS above design pressure	15.0	15.4	15.0

The following figures illustrate the effects of the cladding on various parameters. The flow in the cold leg in Loop A is shown in Figure 2-124. The flow rate through the affected loop decreases quickly in response to the locked rotor and reverses within 2 s. The total vessel inlet flow, which is shown in Figure 2-125, decreases by a little more than 33% in response to the loss of one of three RCPs because of the reverse flow through the affected loop. The reduced flow through the reactor vessel causes the powered-squared weighted average moderator temperature in the core to generally increase, as shown in Figure 2-126. The reactivity feedback associated with the increasing moderator temperature causes the reactor power to generally decrease, as shown in Figure 2-127. The power with the FeCrAl cladding was generally a little lower than in the other cases, because the thinner cladding and thicker fuel pellet resulted in a slightly slower cooldown of the fuel (see Figure 2-128) and less reactivity insertion due to the cooling of the fuel.

Pressurizer pressure is shown in Figure 2-129. The heating of the reactor coolant caused the pressure to increase. The pressurizer PORVs and SRVs were all assumed to fail. The pressure reached 110% of the design pressure at about 15 s. The collapsed liquid level in the pressurizer is shown in Figure 2-130.

The collapsed liquid level in the central core channel is shown in Figure 2-131. No voiding in the core was calculated during this scenario. Consequently, the maximum cladding temperature remained relatively low, as shown in Figure 2-132.

The pressure in SG B is illustrated in Figure 2-133. The PORV in SG B opened near 10 s, but did not have enough relief capacity to prevent the pressure from continuing to rise. The SRVs did not open before the calculation was terminated.

The collapsed liquid level in the boiler of SG B is shown in Figure 2-134. The collapsed level increased following the closure of the TSVs, due to a redistribution of liquid between the downcomer and boiler sides of the SG and the additional mass added to the SG during the coastdown of the MFW.

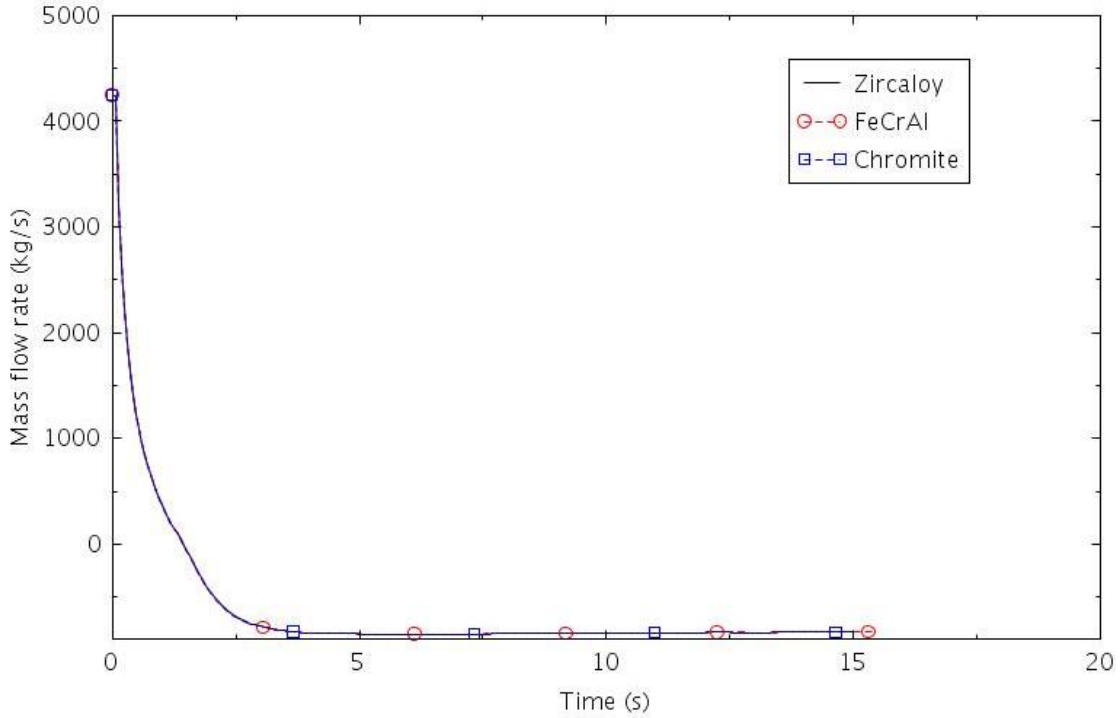

Figure 2-124. Flow rate in the cold leg of Loop A (ATWS-1).

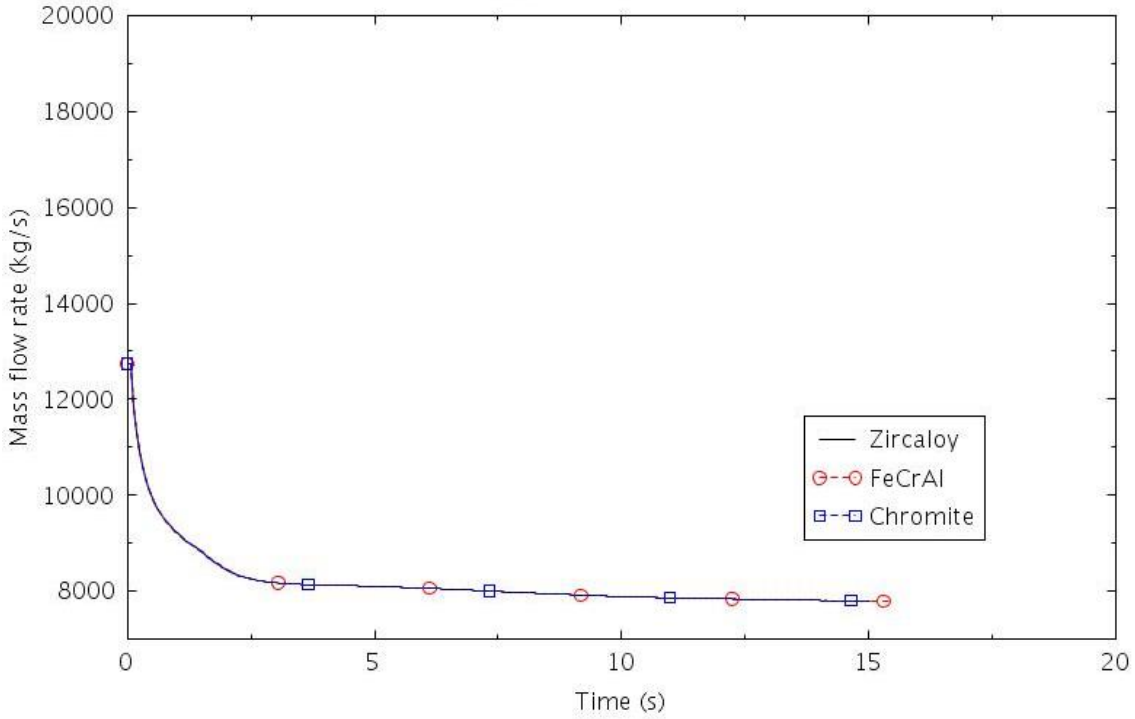

Figure 2-125. Total flow rate at the vessel inlet (ATWS-1).

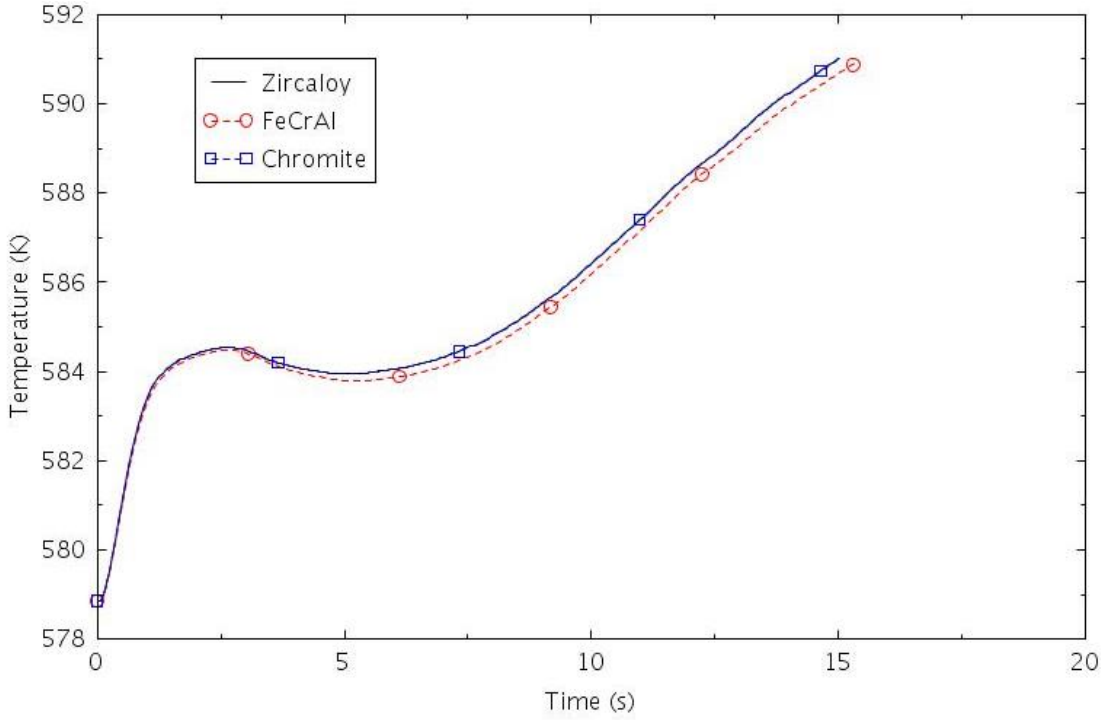

Figure 2-126. Power-squared weighted average moderator temperature (ATWS-1).

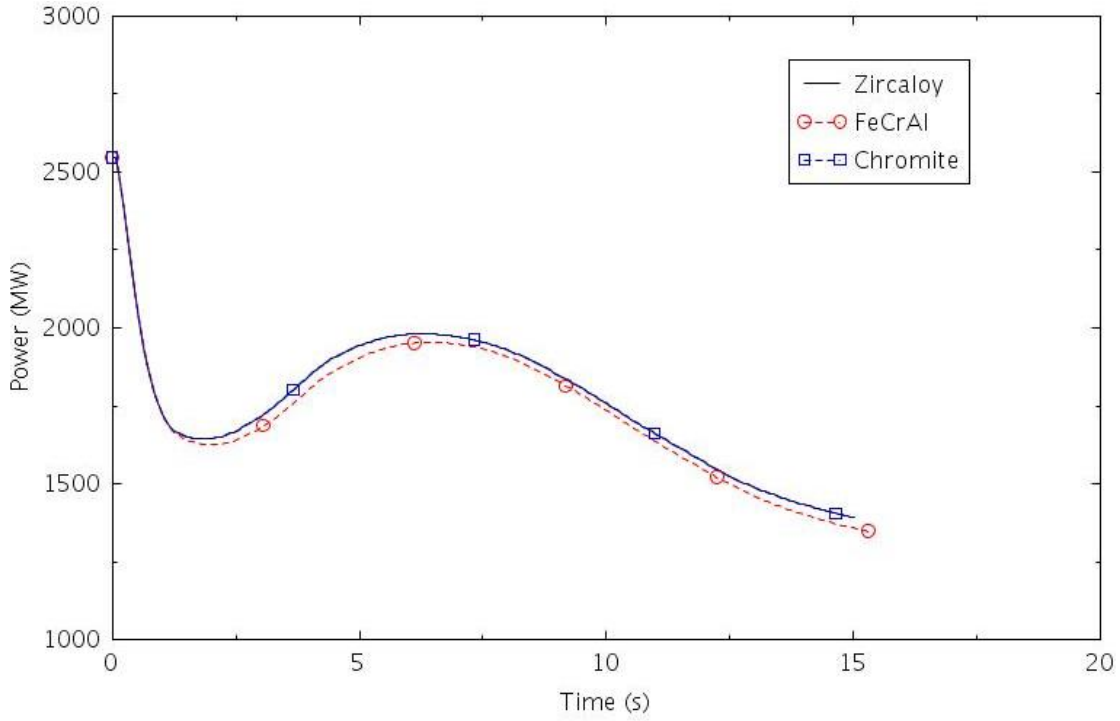

Figure 2-127. Reactor power (ATWS-1).

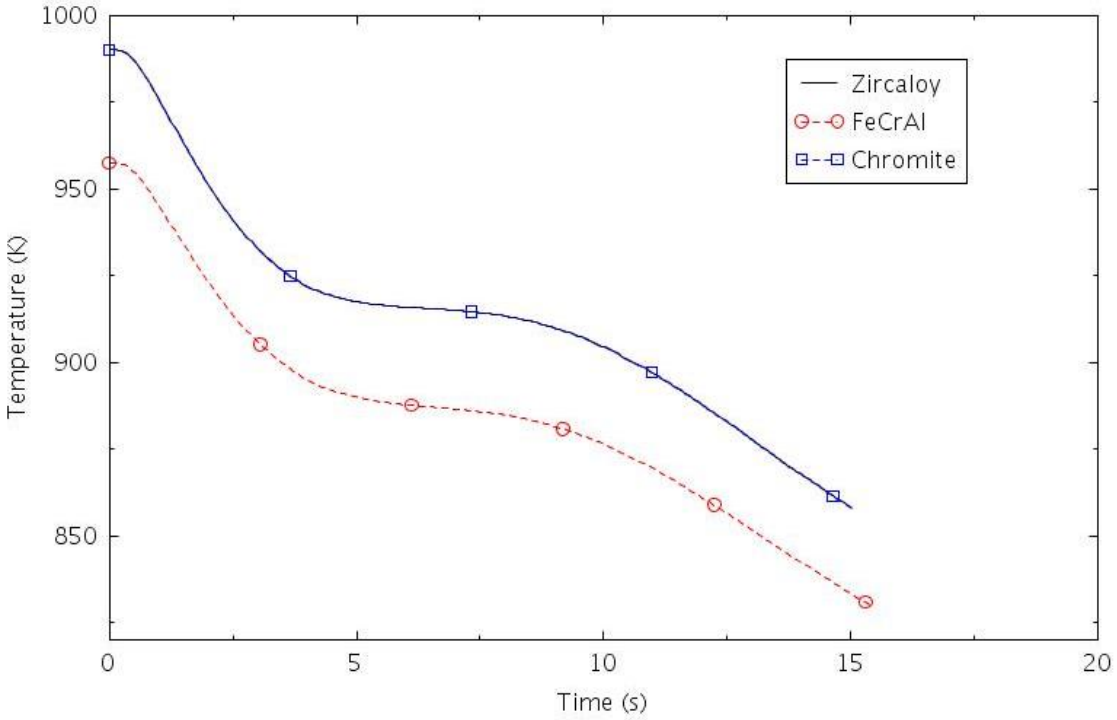

Figure 2-128. Power-squared weighted average fuel temperature (ATWS-1).

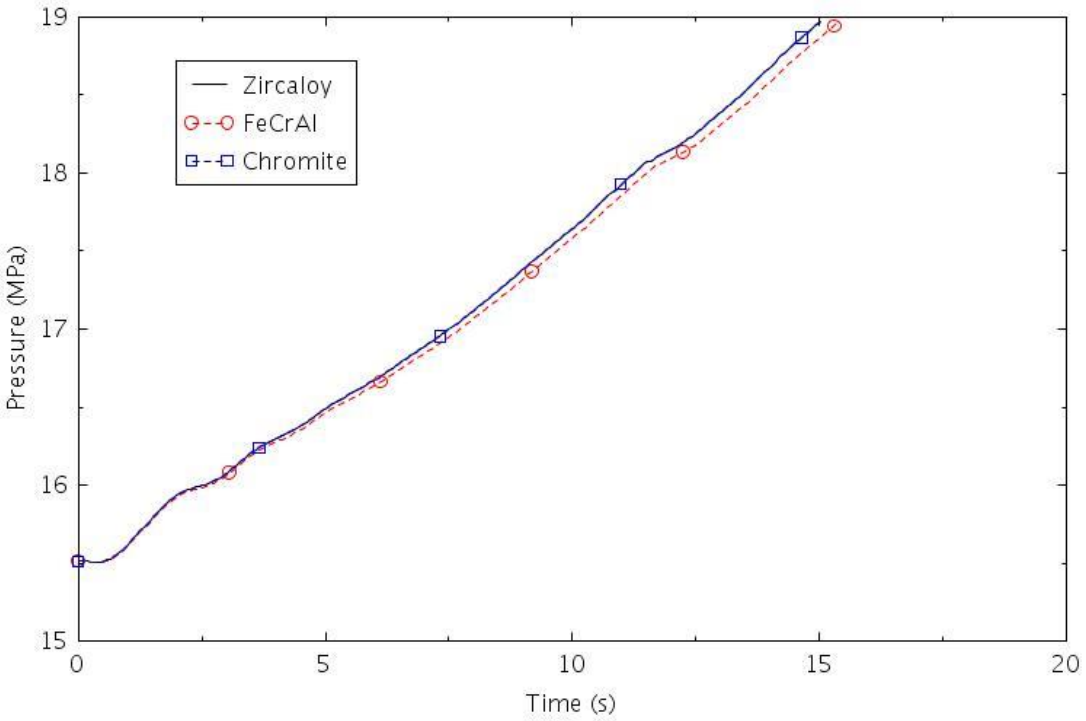

Figure 2-129. Pressure in the pressurizer (ATWS-1).

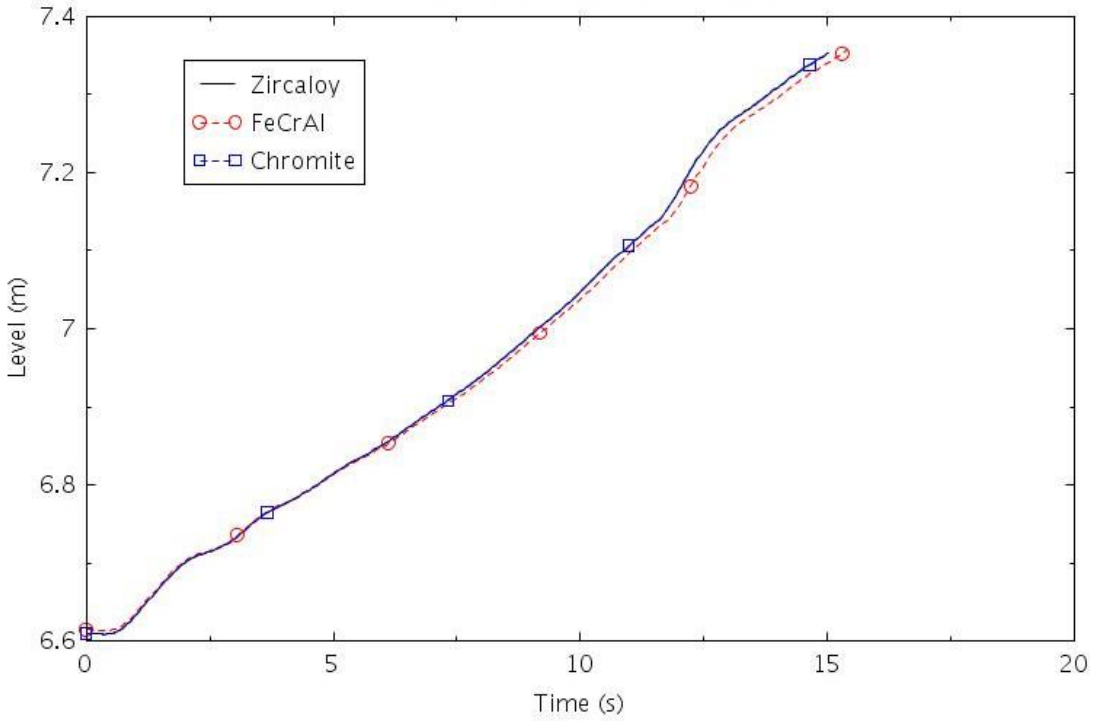

Figure 2-130. Collapsed liquid level in the pressurizer (ATWS-1).

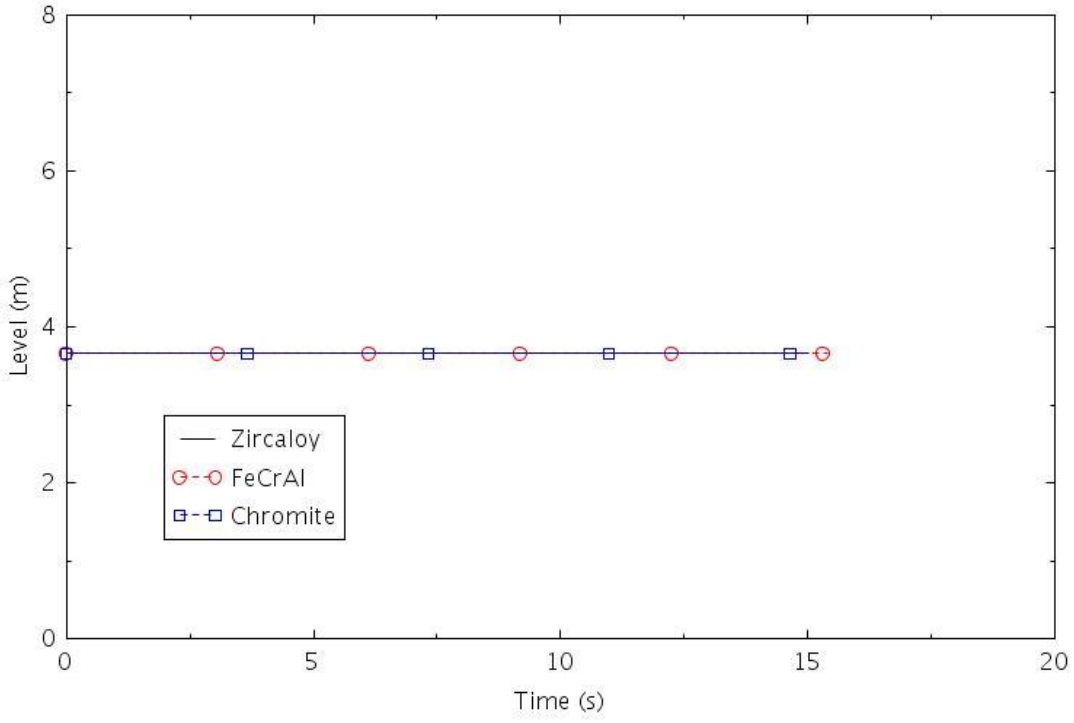

Figure 2-131, Collapsed liquid level in the central core channel (ATWS-1).

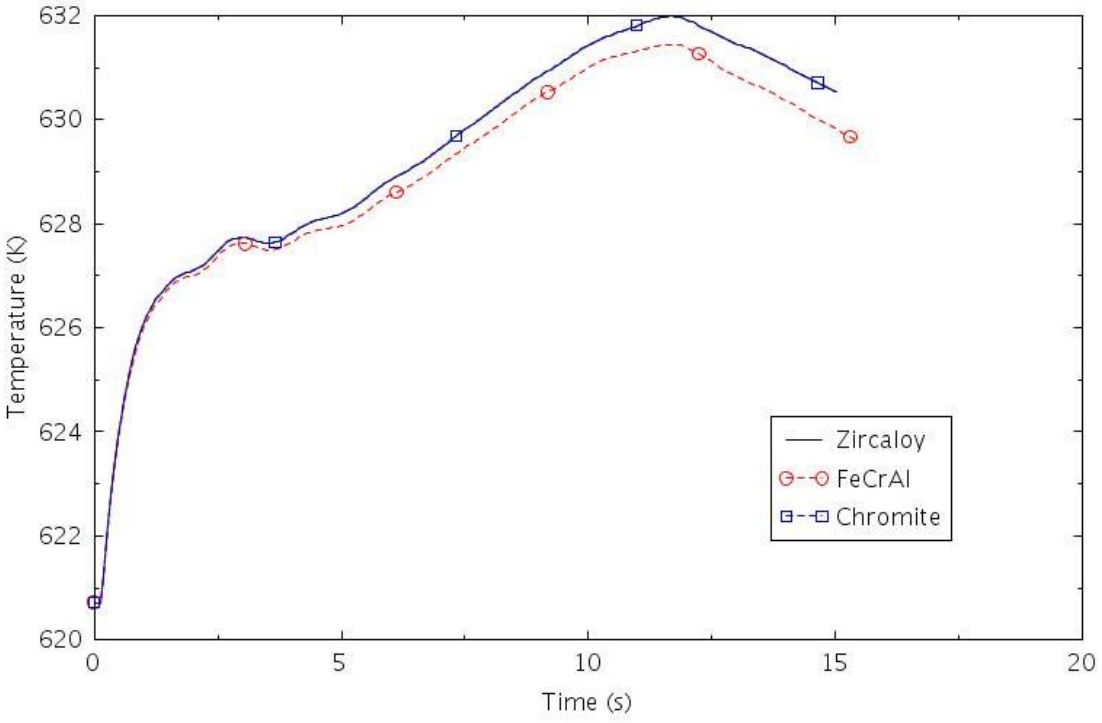

Figure 2-132. Maximum cladding temperature (ATWS-1).

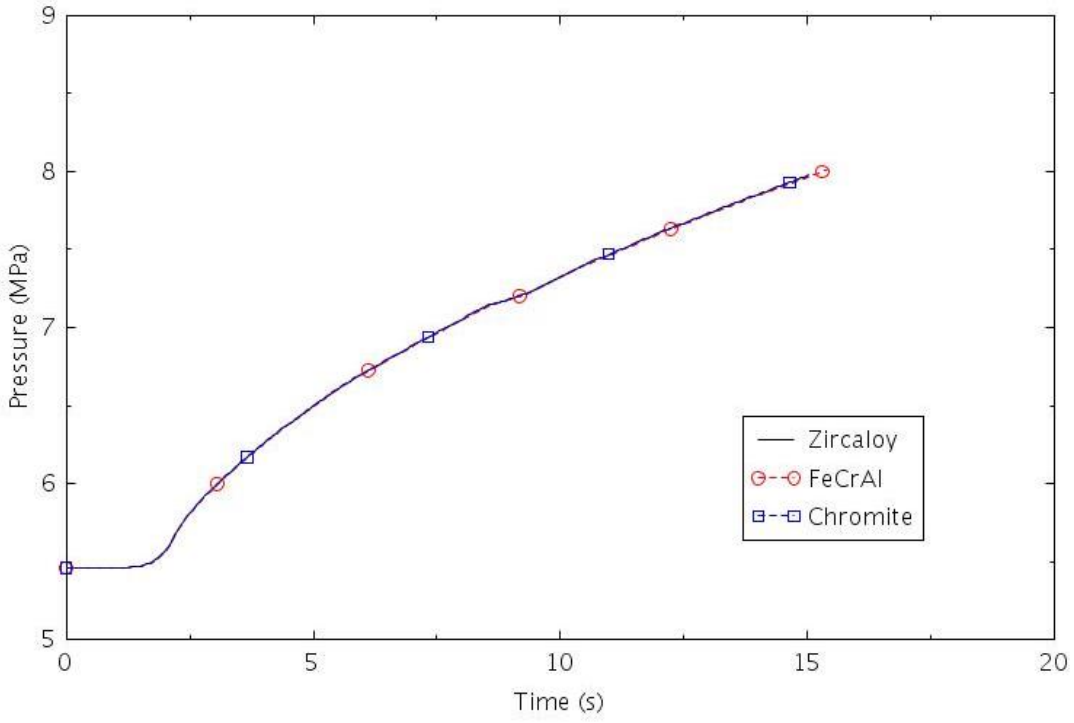

Figure 2-133. Pressure in SG B (ATWS-1).

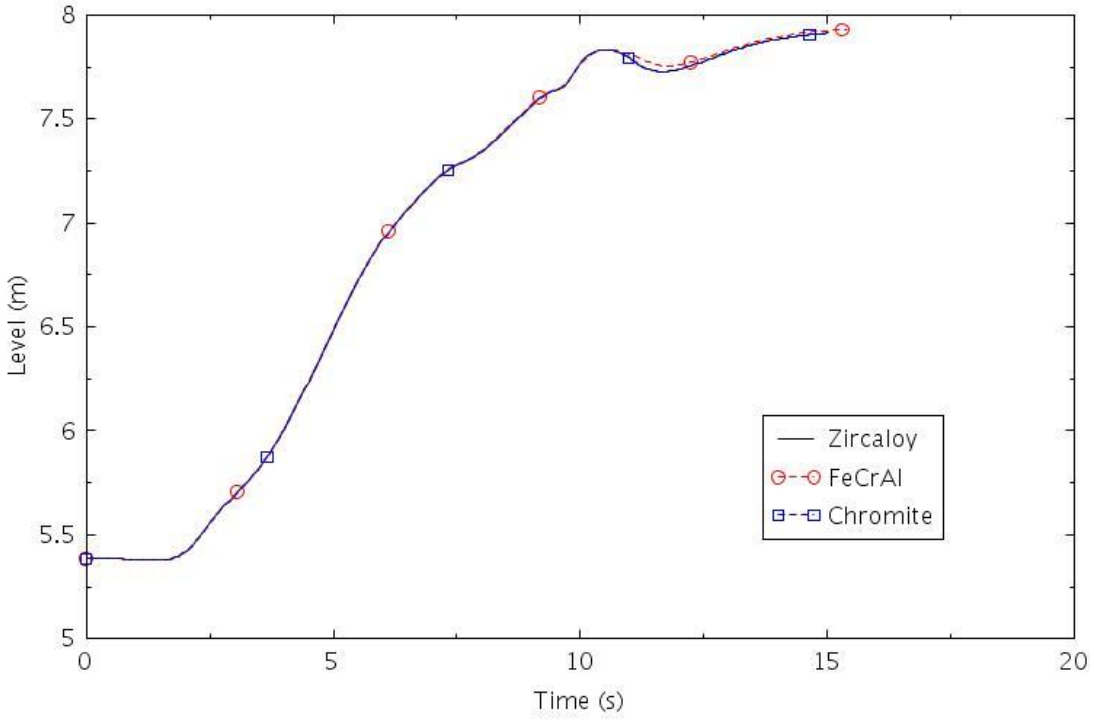

Figure 2-134. Collapsed liquid level in SG B (ATWS-1).

2.2.3.9 ATWS-2

This scenario assumed that the reactor trip system failed to scram the reactor and that no feedwater was available. The pressurizer PORVs and SRVs were assumed to function normally. The TSVs were assumed to close 2.0 seconds after the reactor trip signal. The MFW was terminated 6.5 seconds after the reactor trip signal.

The calculated sequences of events are shown in Table 2-25. The reactor trip signal was generated 0.1 seconds after the start of the event, but the reactor trip was assumed to fail. The termination of MFW, closure of the TSVs, the first lift of the pressurizer PORV and the SG PORVs all occurred within 10 s. All the SGs emptied within 12 minutes, but the B and C SGs emptied significantly earlier than SG A. The RCPs in the unaffected loops were tripped at about 25 minutes. The SIAS occurred at about 33 minutes on high containment pressure, but no high-pressure injection was credited. The core began to uncover near 43 minutes. The time between when the core began to uncover and core damage occurred was 34 minutes with Zircaloy, 41 minutes with FeCrAl, and 38 minutes with Chromite. The calculated amount of hydrogen produced during the transients varied significantly between claddings. The amount of hydrogen produced was 1.5 kg for FeCrAl, 8.2 kg for Chromite, and 88.3 kg for Zircaloy.

Table 2-25. Sequence of Events for Scenario ATWS-2.

	Time (hr:min)		
Event	**Zircaloy**	**FeCrAl**	**Chromite**
RCP A locked	0:00	0:00	0:00
SGs B and C empty	0:02	0:02	0:02
SG A empty	0:12	0:12	0:12
PRT rupture disk opens	0:14	0:15	0:14
RCP B and C tripped	0:25	0:26	0:25
SIAS	0:33	0:34	0:33

Core begins to uncover	0:43	0:45	0:43
0.5 kg H_2 generation	0:54	1:23	1:20
First cladding rupture	1:13	1:17	1:19
Core damage	1:17	1:26	1:21

The following figures illustrate the effects of the cladding on various parameters. The reactor power is shown in Figure 2-135. The reactor power primarily responded to the changes in moderator temperature, which is shown in Figure 2-136. The temperature initially increased in response to the locked rotor and then increased again after SGs B and C emptied near 2 minutes. The power decreased sharply at 2 minutes in response to the negative reactivity feedback. The core power was mostly due to decay heat after 20 minutes.

Pressurizer pressure and level are shown in Figure 2-137 and Figure 2-138, respectively. The heating of the reactor coolant caused the pressure to increase. The pressurizer generally stayed between the open and close setpoints of the PORV, approximately 16.2 MPa (2350 psia) and 15.5 MPa (2255 psia) except near 5 minutes, when the pressure decreased following the reduction in reactor power and between about 25 and 40 minutes, when the pressure increased due to boiling in the core (see Figure 2-139). The pressurizer SRVs opened briefly near 30 minutes. The collapsed liquid level in the core began to decrease sharply near 40 minutes, and the fuel rods began to heat up near 43 minutes, as shown in Figure 2-140.

The pressure and collapsed liquid level in SG B are shown in Figure 2-141 and Figure 2-142, respectively. The PORV in SG B was generally open and the SRVs were intermittently open before the steam generator ran out of liquid near two minutes. The pressure was generally between the open and close setpoints of the PORV after the steam generator emptied.

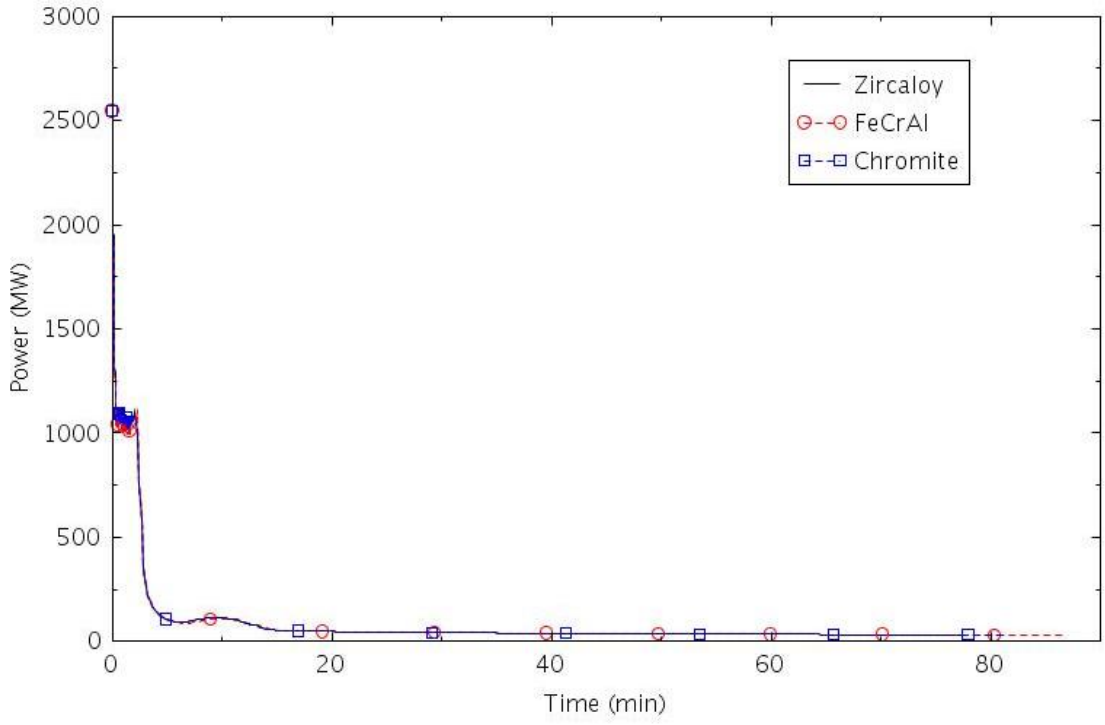

Figure 2-135. Reactor power (ATWS-2).

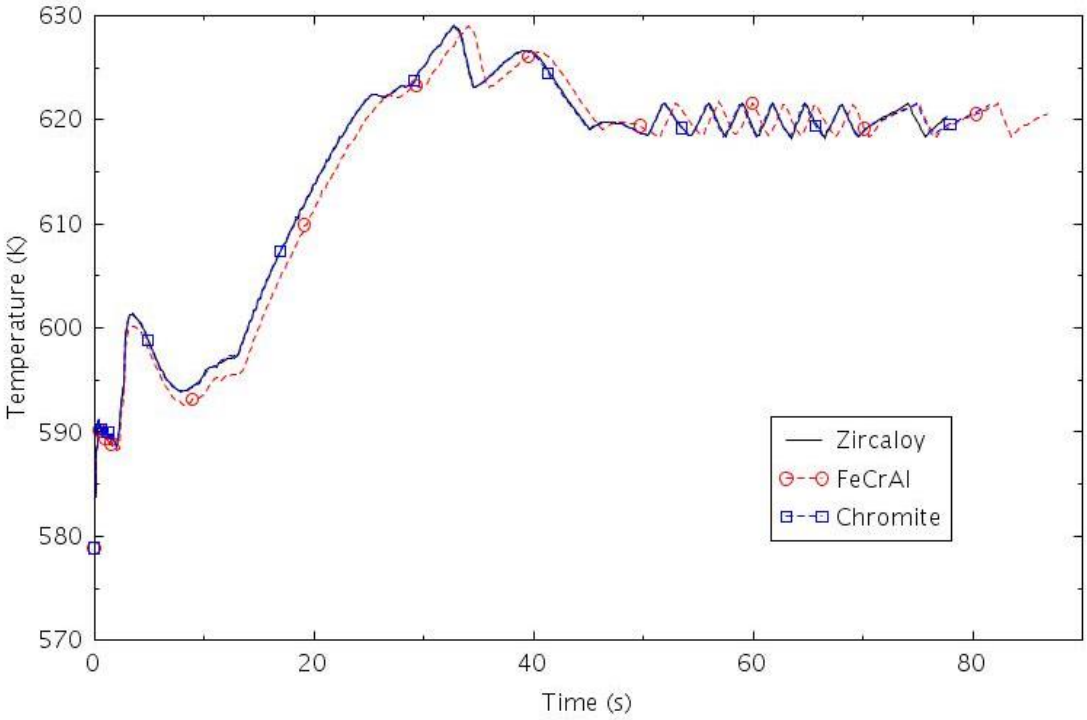

Figure 2-136. Power-squared weighted average moderator temperature (ATWS-2).

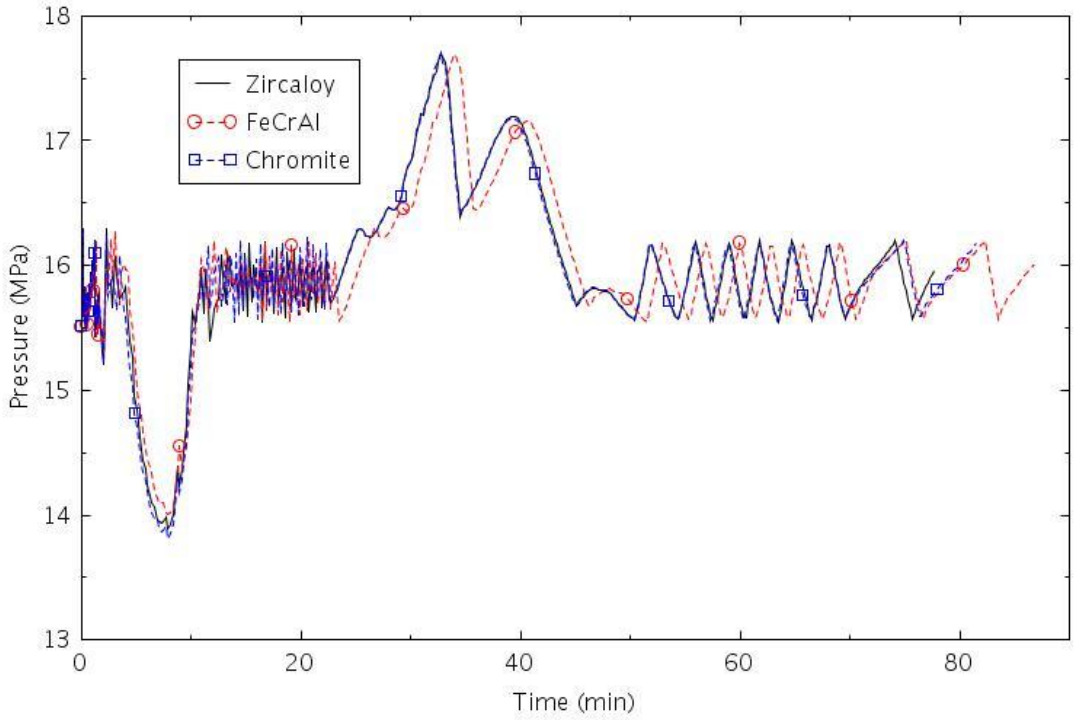

Figure 2-137. Pressure in the pressurizer (ATWS-2).

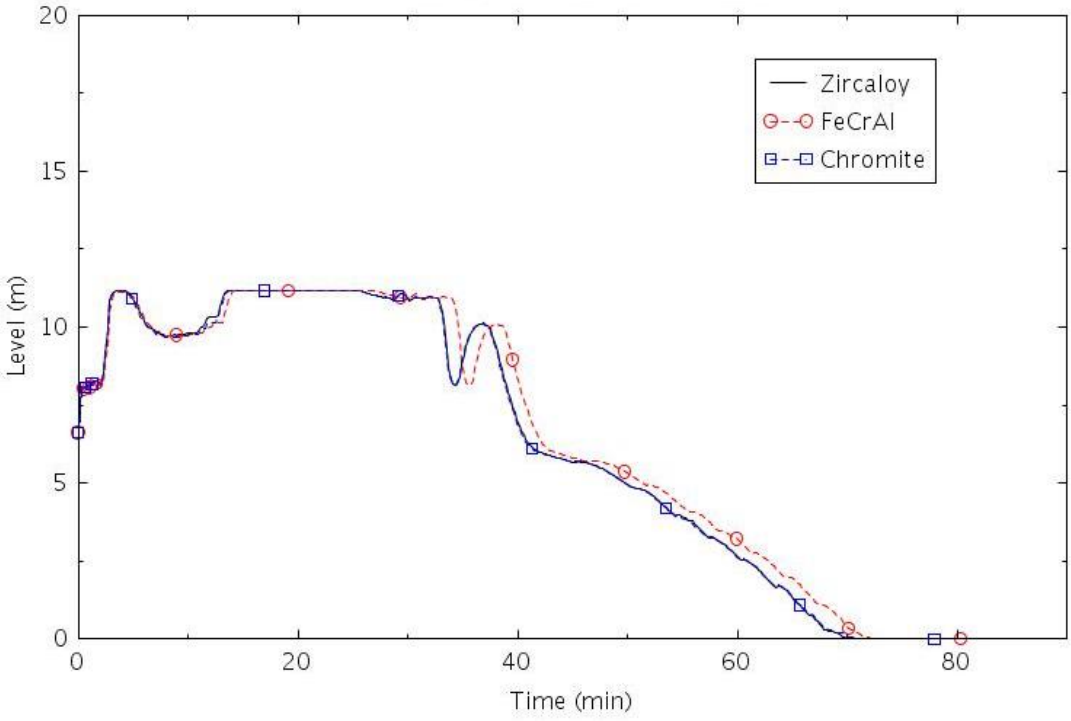

Figure 2-138. Collapsed liquid level in the pressurizer (ATWS-2).

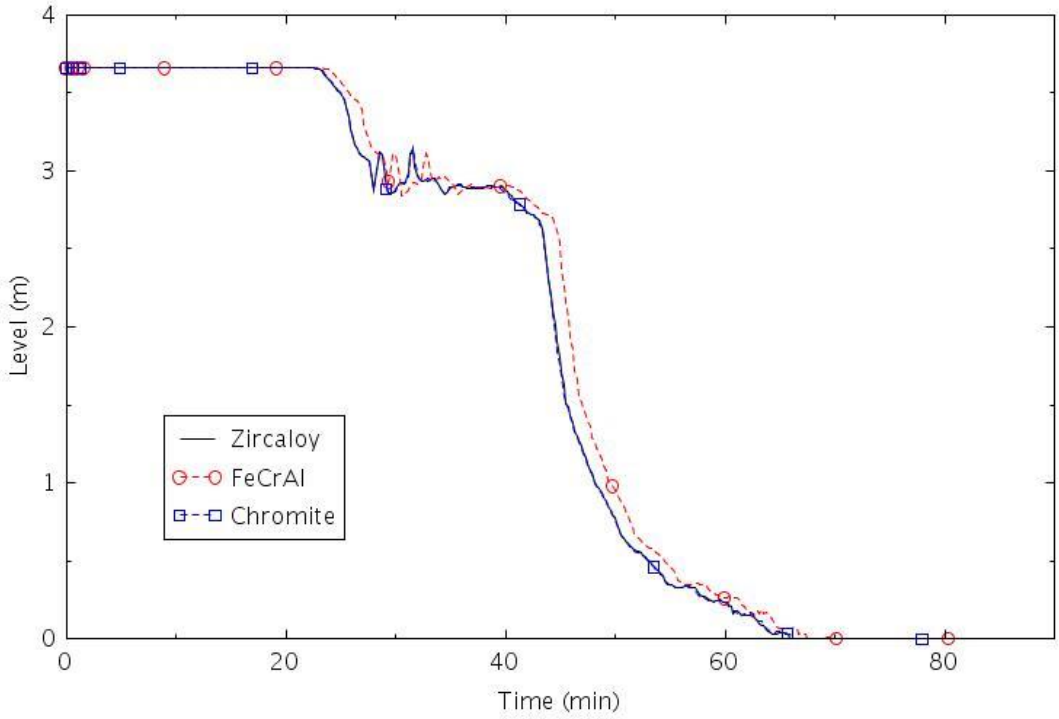

Figure 2-139, Collapsed liquid level in the central core channel (ATWS-2).

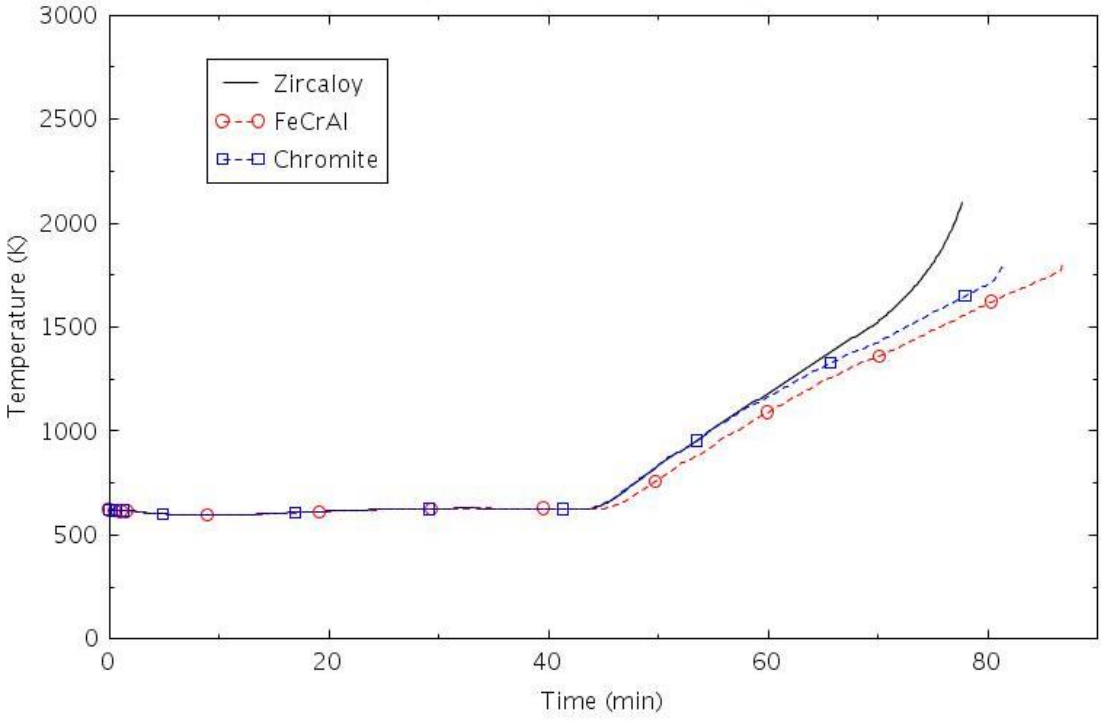

Figure 2-140. Maximum cladding temperature (ATWS-2).

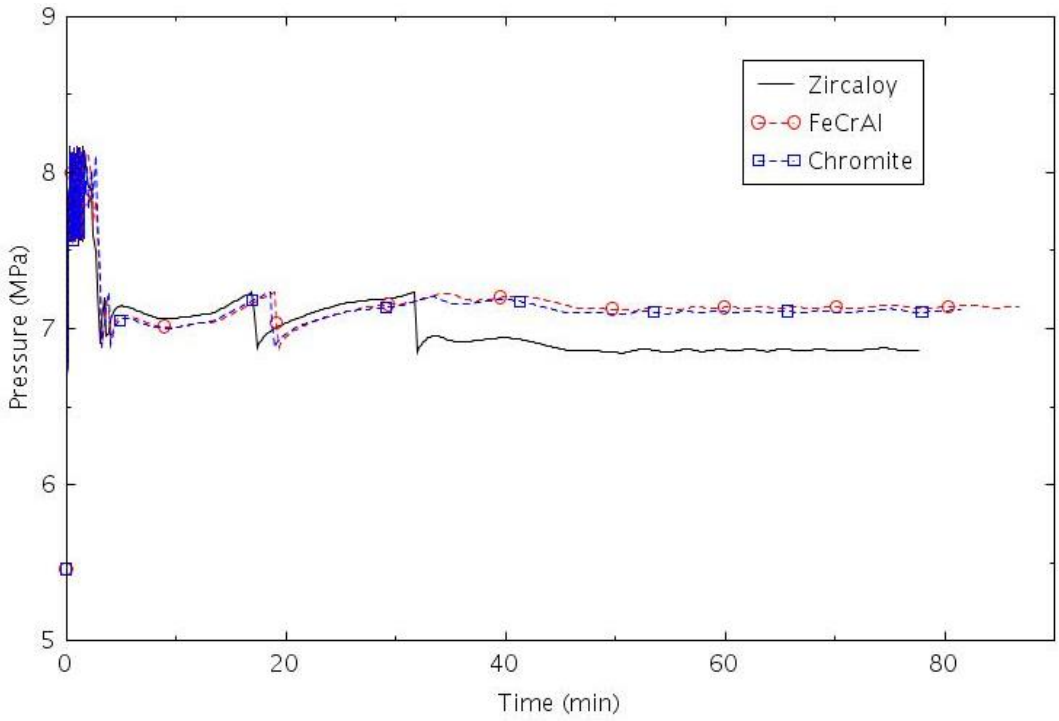

Figure 2-141. Pressure in SG B (ATWS-2).

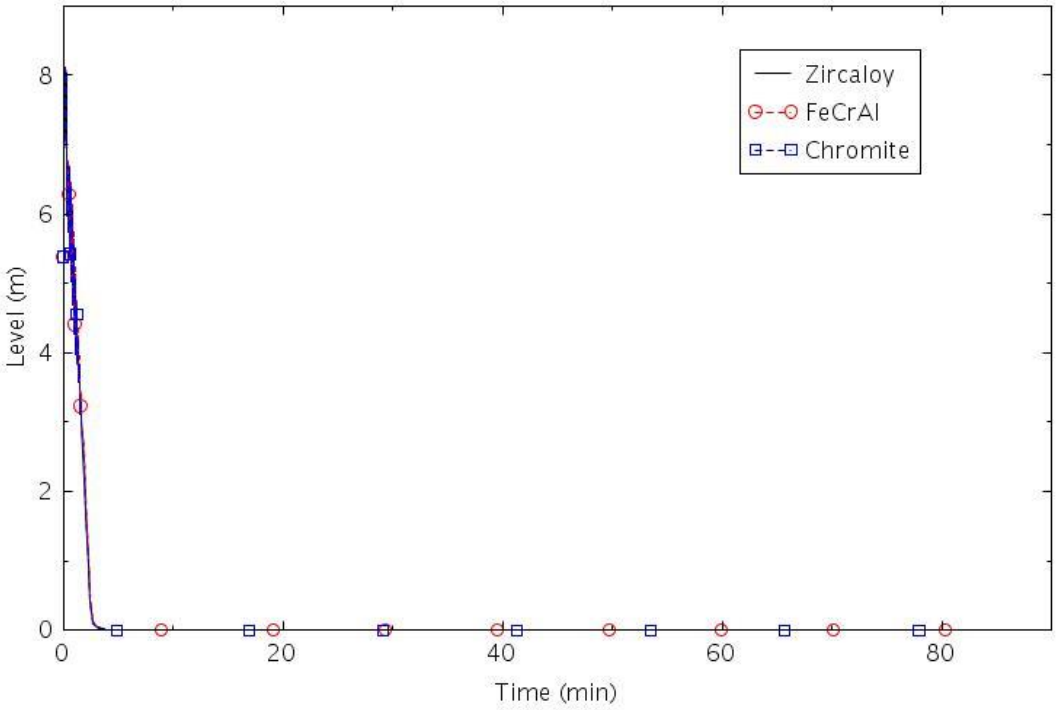

Figure 2-142. Collapsed liquid level in SG B (ATWS-2).

2.2.3.10 ATWS-3

This scenario assumed that the reactor trip system failed to scram the reactor and that AFW was available. The pressurizer PORVs and SRVs were assumed to function normally. The TSVs were assumed to close 2.0 seconds after the reactor trip signal. The MFW was terminated 6.5 seconds after the reactor trip signal. The turbine-driven AFW pump and both motor-driven AFW pumps were assumed to be available.

The calculated sequences of events are shown in Table 2-26. The reactor trip signal was generated 0.1 seconds after the start of the event, but the reactor trip was assumed to fail. The termination of MFW, closure of the TSVs, the first lift of the pressurizer PORV and the SG PORVs all occurred within 10 s. AFW was assumed to start at 30 s. The AFW flow was terminated at 69 minutes, because the ECST was depleted. The SGs were empty within a couple of minutes of the termination of AFW flow. The RCPs in the unaffected loops were tripped at about 86 minutes. The SIAS occurred at about 107 minutes on high containment pressure, but no high-pressure injection was credited. The core began to uncover near 117 minutes. The time between when the core began to uncover and core damage occurred was 45 minutes with Zircaloy, 57 minutes with FeCrAl, and 49 minutes with Chromite. The calculated amount of hydrogen produced during the transients varied significantly between claddings. The amount of hydrogen produced was 1.9 kg for FeCrAl, 2.1 kg for Chromite, and 80.2 kg for Zircaloy.

Table 2-26. Sequence of Events for Scenario ATWS-3.

	Time (hr:min)		
Event	**Zircaloy**	**FeCrAl**	**Chromite**
RCP A locked	0:00	0:00	0:00
AFW initiated	0:00	0:00	0:00
AFW terminated	1:09	1:09	1:09
PRT rupture disk opens	1:10	1:11	1:10
All SGs empty	1:11	1:11	1:11

RCP B and C tripped	1:26	1:26	1:25
SIAS	1:37	1:39	1:37
Core begins to uncover	1:47	1:49	1:47
0.5 kg H_2 generation	2:04	2:41	2:35
First cladding rupture	2:28	2:35	2:35
Core damage	2:32	2:46	2:36

The following figures illustrate the effects of the cladding on various parameters. The reactor power is shown in Figure 2-143. The reactor power primarily responded to the changes in moderator temperature, which is shown in Figure 2-144. The temperature initially increased in response to the locked rotor, and then reached a quasi-steady point between about 5 minutes and 69 minutes. Consequently, the reactor power was also nearly steady during this time period. The AFW was terminated at 69 minutes, the SGs dried out shortly thereafter, causing the moderator temperature to increase and the reactor power to decrease, due to the negative reactivity feedback. The core power was mostly due to decay heat after 75 minutes.

Pressurizer pressure and level are shown in Figure 2-145 and Figure 2-146, respectively. The initial heating of the reactor coolant caused the pressure to increase enough to open the pressurizer PORV during the first several minutes of the transient. Thereafter, the pressurizer PORV opened only a few times until the AFW was terminated at 69 minutes. Thereafter, the PORV opened frequently and the pressure stayed between the open and close setpoints of the PORV, except between about 80 and 105 minutes, when the pressure increased due to boiling in the core (see Figure 2-147). The pressurizer SRVs opened briefly near 100 minutes. The collapsed liquid level in the core began to decrease sharply near 108 minutes, and the fuel rods began to heat up near 117 minutes, as shown in Figure 2-148.

The pressure and collapsed liquid level in SG B are shown in Figure 2-149 and Figure 2-150, respectively. The pressure was generally between the open and close setpoints of the SG SRVs, 8.16 MPa (1184 psia) and 7.53 MPa (1092 psia), respectively, during the first three minutes of the transient. The SG SRVs closed after the reduction in core power at 3 minutes, and the pressure generally remained between the open and close setpoints of the SG PORVs thereafter. The PORVs opened much less frequently after AFW was terminated, and the SGs emptied near 70 minutes. The total AFW flow rate, which includes output from the motor-driven and turbine-driven pumps, is shown in Figure 2-151.

Sensitivity calculations were performed in which only the motor-driven AFW pumps were used rather than both the motor-driven and turbine-driven pumps. The AFW flow rate in the sensitivity calculations was about half of that in the base calculations. The reduced AFW flow rate in the sensitivity calculations resulted in a lower quasi-steady level in the SGs, a higher moderator temperature, and a reduced core power. The lower AFW flow rate in the sensitivity calculations caused the ECST to be depleted 68 minutes later than in the base calculations. As a result, the core began to uncover 75 minutes later, and the limiting cladding temperatures were reached 87 minutes later in the sensitivity calculations than in the base calculations. The ECST water inventory was used more efficiently in the sensitivity calculations, allowing the operators more time to recover the ECST inventory before core damage occurs.

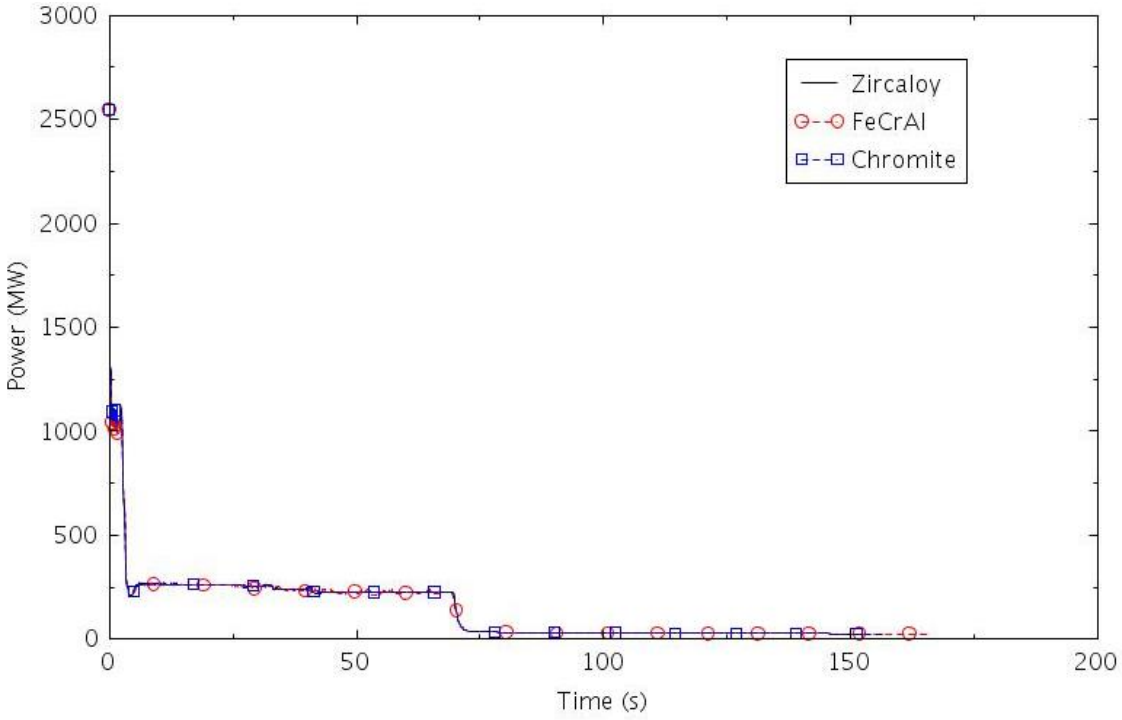

Figure 2-143. Reactor power (ATWS-3).

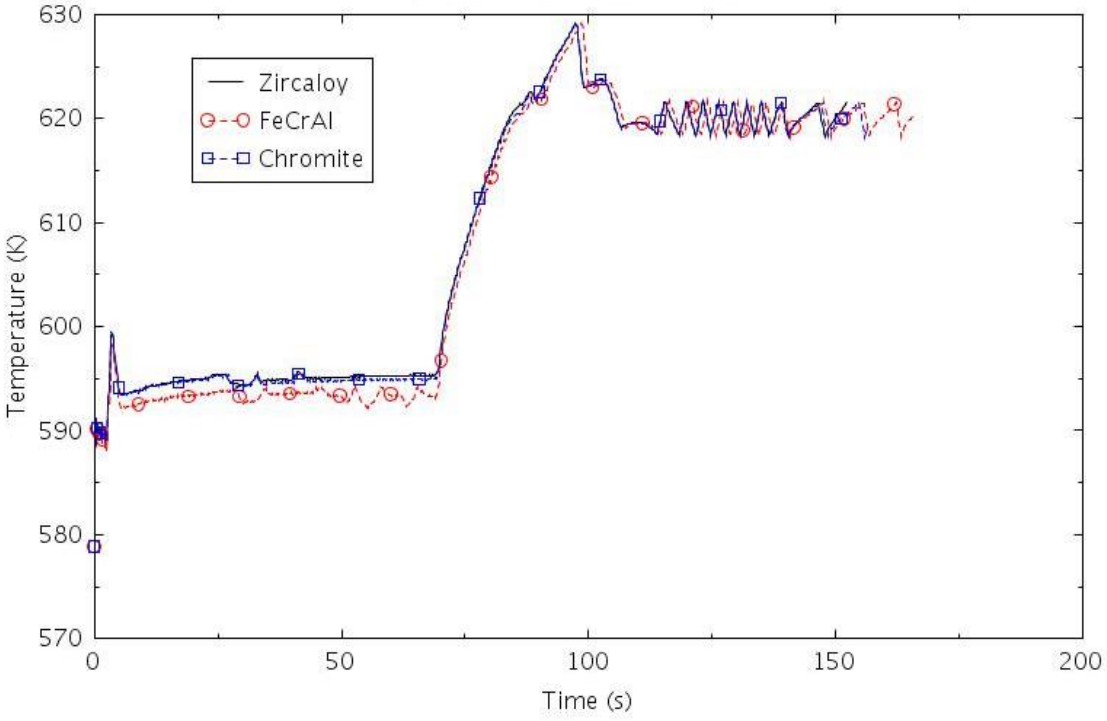

Figure 2-144. Power-squared weighted average moderator temperature (ATWS-3).

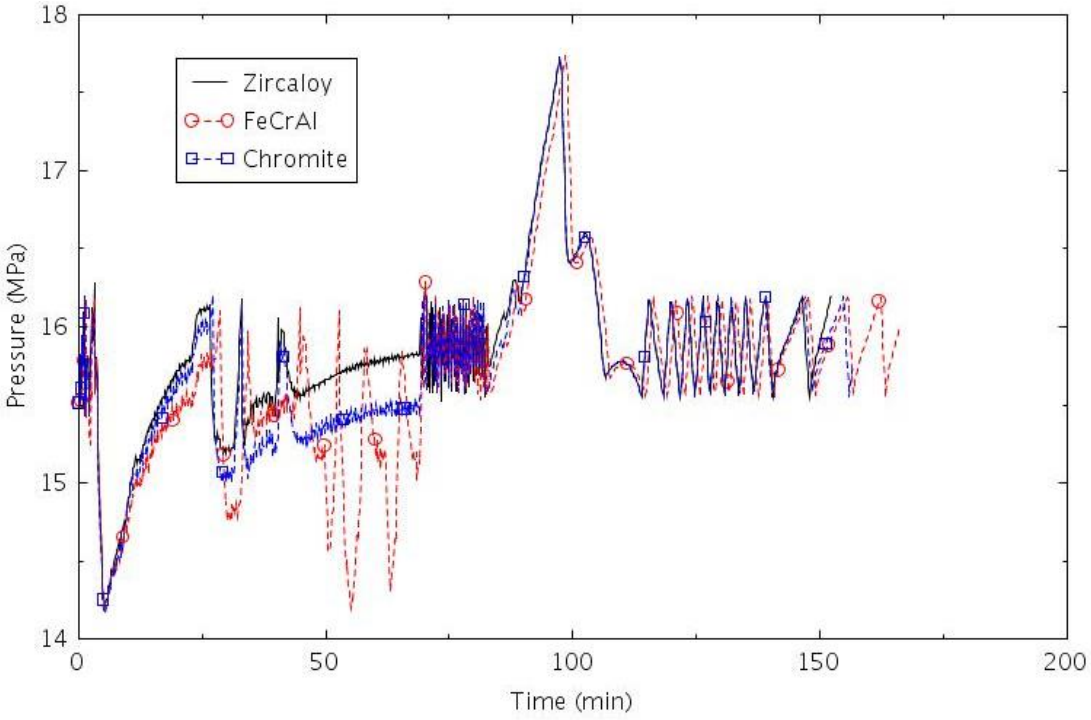

Figure 2-145. Pressure in the pressurizer (ATWS-3).

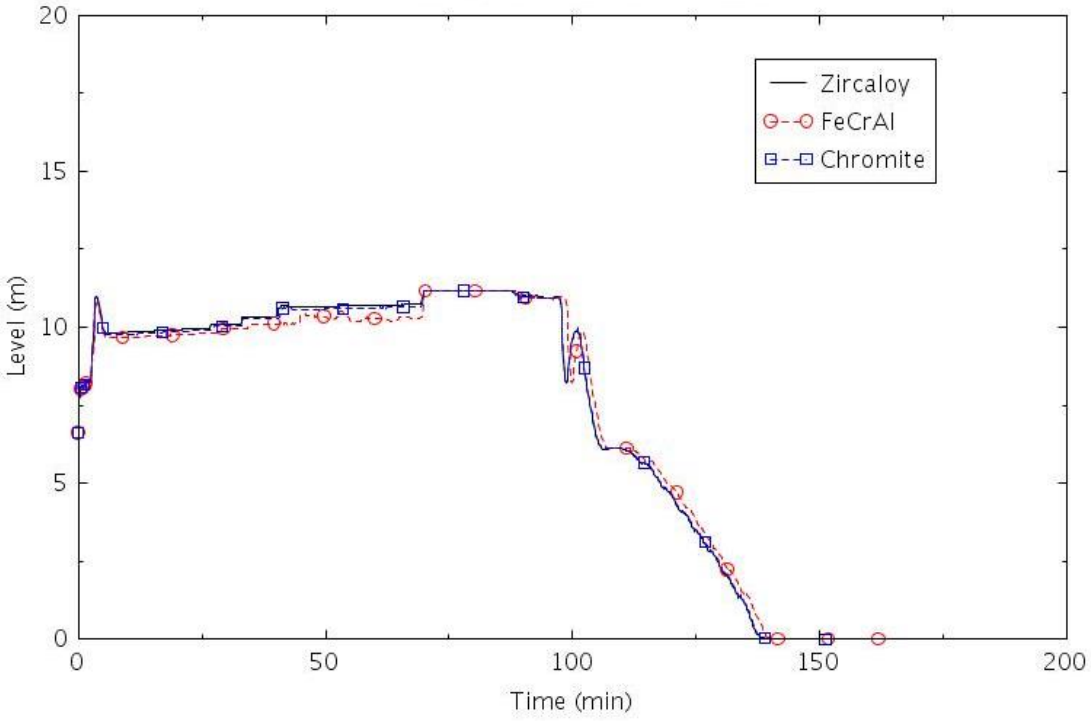

Figure 2-146. Collapsed liquid level in the pressurizer (ATWS-3).

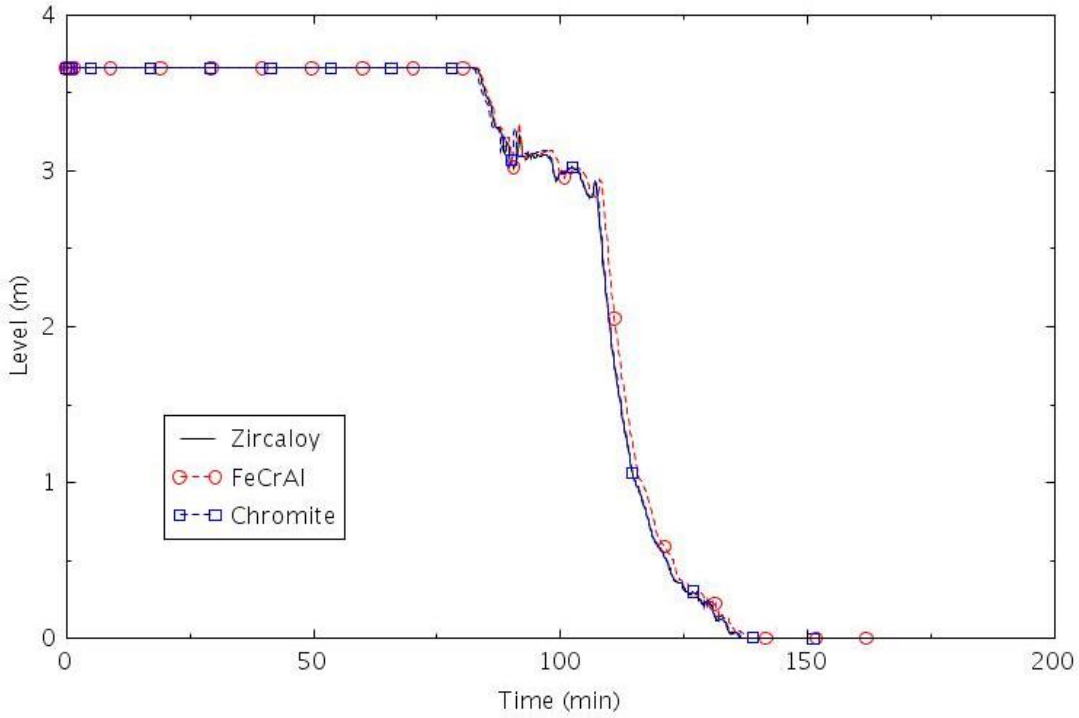

Figure 2-147, Collapsed liquid level in the central core channel (ATWS-3).

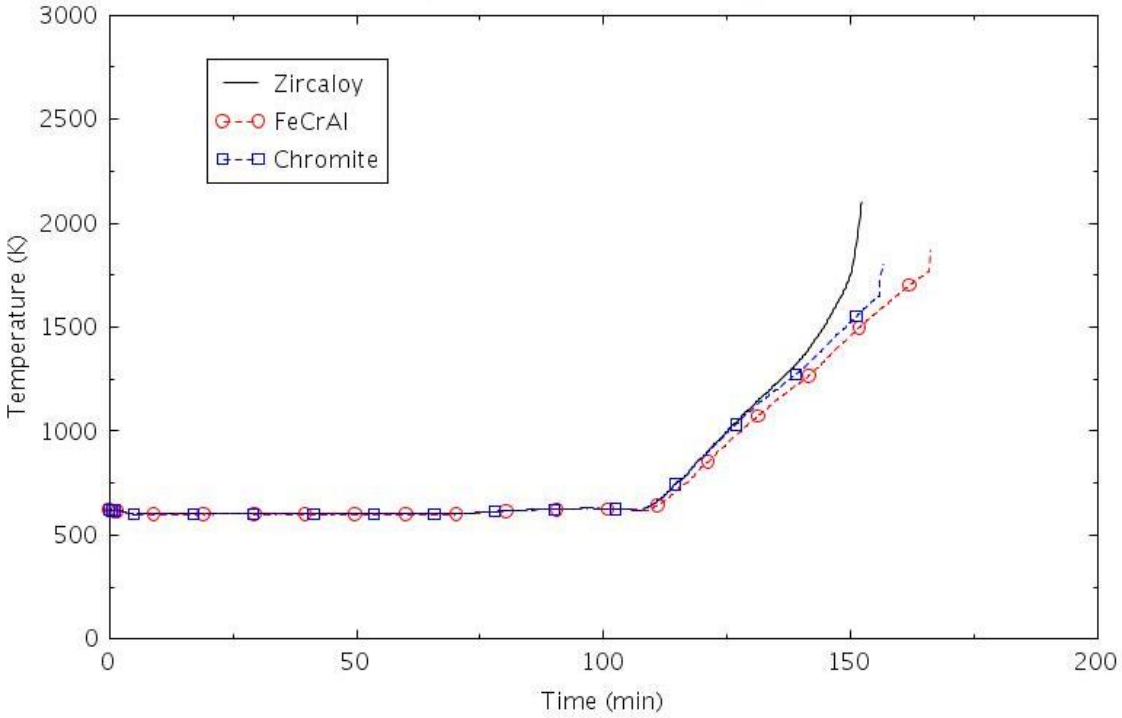

Figure 2-148. Maximum cladding temperature (ATWS-3).

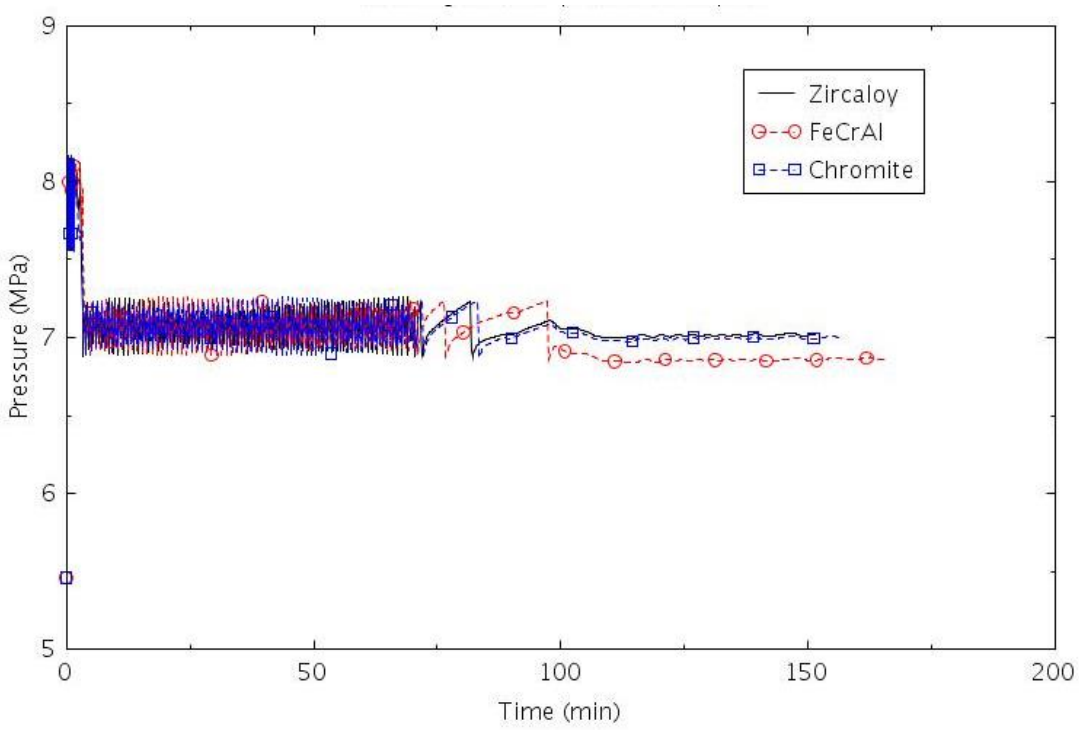

Figure 2-149. Pressure in SG B (ATWS-3).

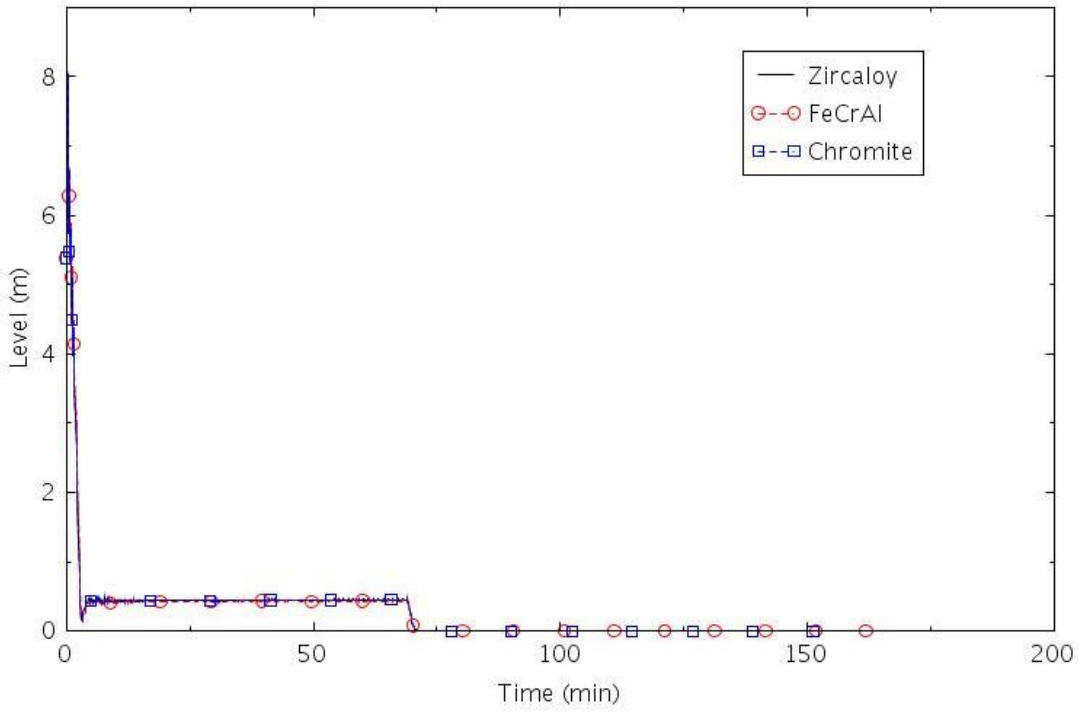

Figure 2-150. Collapsed liquid level in SG B (ATWS-3).

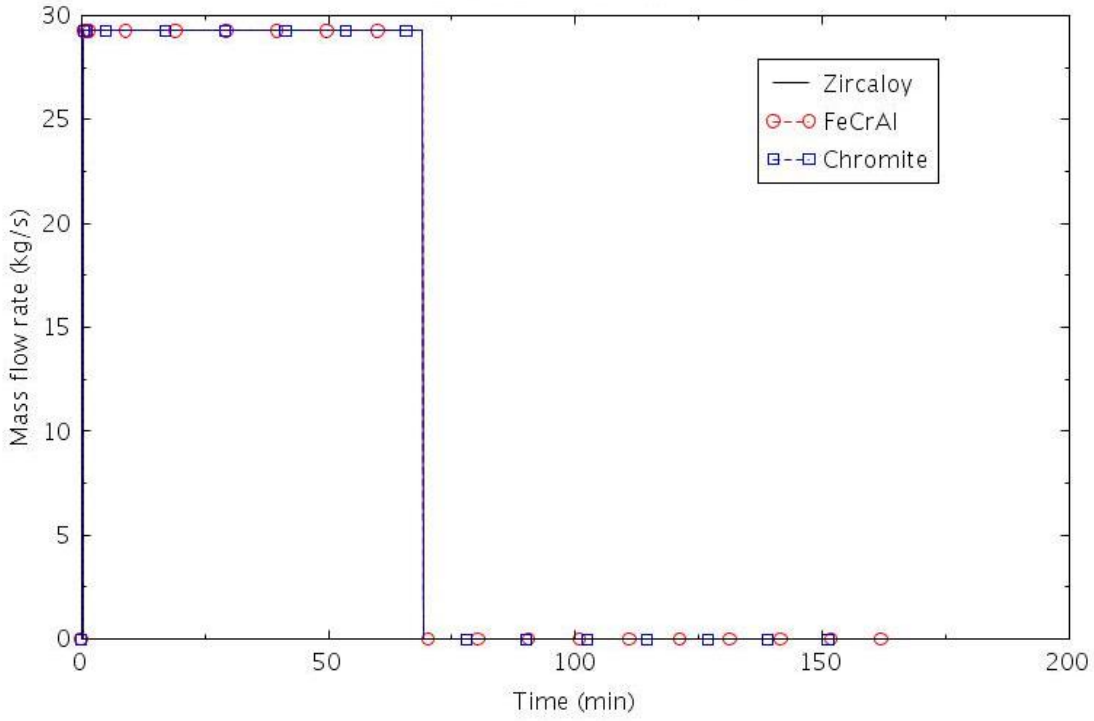

Figure 2-151. Total AFW flow rate to SG B (ATWS-3).

2.2.4 Locked Rotor Analysis Results

Table 2-27 presents a summary of the RELAP5-3D results for time to core uncovery, time to 0.5 kg of hydrogen production, and time to core damage for locked rotor scenarios with Zircaloy and ATF claddings. The most severe scenarios in terms of the shortest time to core damage are PORV-1, in which AFW is available but an PORV LOCA occurs without safety injection; TRANS-1, in which there is no feedwater and no safety injection; and the two ATWS scenarios. The table does not include results from ATWS-1, because the failure was due to high RCS pressure rather than core damage due to high cladding temperature.

Table 2-27. Summary of RELAP5-3D Time Results for Locked Rotor Scenarios with Zircaloy and ATF Claddings.

Scenario	Time to core uncovery (hr:min)			Time to 0.5 kg H_2 (hr:min)			Time to core damage (hr:min)		
	Zircaloy	FeCrAl	Chromite	Zircaloy	FeCrAl	Chromite	Zircaloy	FeCrAl	Chromite
TRANS-1	1:52	1:52	1:52	2:06	2:36	2:34	2:30	2:38	2:34
TRANS-2	13:25	13:10	13:10	13:54	14:29	14:26	14:35	14:41	14:37
PORV-1	1:42	1:41	1:41	2:04	2:25	2:10	2:18	2:26	2:21
LOSC-182a	12:24	11:59	12:18	12:53	13:16	13:14	13:26	13:23	13:33
LOSC-182b	8:31	8:39	8:47	9:32	10;16	10:00	9:55	10:16	10:19
LOSC-76	11:58	12:07	11:59	12:30	13:31	13:13	13:09	13:38	13:23
LOSC-480	5:12	5:13	4:59	5:43	6:20	6:06	5:46	6:20	5:51
ATWS-2	0:43	0:45	0:43	0:54	1:23	1:20	1:17	1:26	1:21
ATWS-3	1:47	1:49	1:47	2:04	2:41	2:35	2:32	2:46	2:36

Table 2-28 compares the times to core damage for the ATF designs with those for the existing design with Zircaloy cladding in different locked rotor scenarios. On average, the gain in coping time is about 14 minutes for FeCrAl and 7 minutes for Chromite. There is some variability in the results due to numerical causes. A slightly better estimate of the gain in coping time can be obtained by subtracting the time to core uncovery from the time to core damage in Table 2-27 and averaging. Using this metric, the gain in coping time increases to about 16 minutes for FeCrAl and 9 minutes for Chromite. By either measure, the gain in coping time with the ATF designs is modest for the locked rotor scenarios.

With the above relatively small increase of the time to core damage from the RELAP5-3D simulation results, a change to the general transient PRA model (event tree, fault tree, success criteria, or human reliability analysis) is not warranted. The risk benefit on behalf of the CDF brought by the ATF designs would be very small and is not conducted in this analysis.

However, the RELAP5-3D results show a clear benefit in adopting the ATF designs as much less hydrogen is produced at the time of core damage. Table 2-29 compares the hydrogen production for the ATF designs with those for the existing Zircaloy clad design in different locked rotor scenarios. The hydrogen production is generally significantly smaller with the ATF claddings. The one exception is Scenario LOSC-480, where the hydrogen production with FeCrAl is about 80% of that with Zircaloy. However, this result is atypical because the calculation with Zircaloy was terminated due to severe cladding ballooning, rather than maximum cladding temperature. Consequently, the Zircaloy cladding did not reach temperatures as high as those with FeCrAl, which resulted in less hydrogen production than typical for Zircaloy. Excluding Scenario LOSC-480, the average hydrogen production with FeCrAl was 3.5% of that with Zircaloy. The average hydrogen production with Chromite was 14.9% of that with Zircaloy.

Table 2-28. Time to Core Damage Comparisons for Locked Rotor Scenarios with ATF Designs.

Section	Scenario	Description	Time to core damage (hr:min)				
			Zircaloy	FeCrAl	Δt (FeCrAl)	Chromite	Δt (Chromite)
2.2.3.1	TRANS-1	General transient, no FW, no HPSI	2:30	2:38	0:08	2:34	0:04
2.2.3.2	TRANS-2	General transient, no FW, HPSI	14:35	14:41	0:06	14:37	0:02
2.2.3.3	PORV-1	PORV LOCA with AFW	2:18	2:26	0:08	2:21	0:03
2.2.3.4	LOSC-182a	RCP seal LOCA, 182 gpm, AFW, SSC	13:26	13:23	-0:03	13:33	0:07
2.2.3.5	LOSC-182b	RCP seal LOCA, 182 gpm, AFW, no SSC	9:55	10:16	0:21	10:19	0:24
2.2.3.6	LOSC-76	RCP seal LOCA, 76 gpm, AFW, SSC	13:09	13:38	0:29	13:23	0:14
2.2.3.7	LOSC-480	RCP seal LOCA, 480 gpm, AFW, SSC	5:46	6:20	0:34	5:51	0:05
2.2.3.9	ATWS-2	No reactor trip, no AFW	1:17	1:26	0:09	1:21	0:04
2.2.3.10	ATWS-3	No reactor trip, AFW	2:32	2:46	0:13	2:36	0:04

Table 2-29. H2 Production Comparisons for Locked Rotor Scenarios with ATF Designs.

Section	Scenario	Description	Total H_2 (kg)			H_2 %	
			Zircaloy	FeCrAl	Chromite	FeCrAl	Chromite
2.2.3.1	TRANS-1	General transient, no FW, no HPSI	72.9	1.5	0.7	2.0	1.0
2.2.3.2	TRANS-2	General transient, no FW, HPSI	108.1	1.9	11.0	1.8	10.2
2.2.3.3	PORV-1	PORV LOCA with AFW	23.3	2.0	6.5	8.5	27.9
2.2.3.4	LOSC-182a	RCP seal LOCA, 182 gpm, AFW, SSC	57.7	1.9	16.0	3.3	27.7
2.2.3.5	LOSC-182b	RCP seal LOCA, 182 gpm, AFW, no SSC	33.1	2.1	8.5	6.3	25.7
2.2.3.6	LOSC-76	RCP seal LOCA, 76 gpm, AFW, SSC	91.9	1.7	13.5	1.8	14.7
2.2.3.7	LOSC-480	RCP seal LOCA, 480 gpm, AFW, SSC	0.9	0.7	0.2	81.8	22.7
2.2.3.9	ATWS-2	No reactor trip, no AFW	88.3	1.5	8.2	1.7	9.3
2.2.3.10	ATWS-3	No reactor trip, AFW	80.2	1.9	2.1	2.4	2.6

2.3 General Transient – Turbine Trip Scenario Analysis

2.3.1 General Transient PRA Model and Scenarios

For ATF general transient with turbine trip analysis, the same seven scenarios developed in the locked rotor analysis other than the three ATWS scenarios (see Section 2.2.1) were analyzed using RELAP5-3D for thermal hydraulic analysis with traditional fuel design and near-term ATF designs. Both turbine trip and locked rotor are modeled in PRA as general transients with similar plant responses. Turbine trip with ATWS scenarios are not analyzed as the responses of the ATWS scenarios following locked rotor event and turbine trip event would be similar.

2.3.2 Turbine Trip RELAP5-3D Model

The same RELAP5-3D IGPWR model as in (Ma, et al., 2018) was used in this analysis. The details of this are described in (Parisi, et al., 2016). The model is based on a generic Westinghouse three-loop PWR.

2.3.3 Turbine Trip RELAP5-3D Analysis

The turbine trip event is initiated by a closure of the TSVs. Offsite power is assumed to be available. The early response of all the analyzed scenarios was similar. The MSIVs in the model were assumed to close 1 second after the turbine trip to simulate closure of the TSVs. The turbine trip was assumed to cause a direct reactor trip, based on Section 14.2.10 of the Surry Power Station FSAR (Dominion, 2007). MFW was assumed to terminate normally following reactor trip, delivering the equivalent of 5 seconds of full flow after the scram, before coasting down to zero. The SG PORVs were assumed to operate as necessary to control SG pressure.

For the scenarios with feedwater, one motor-driven AFW pump was assumed to be available. The operators were assumed to control the SG levels to near the level of the feedwater ring. The AFW was terminated after the injected volume exceeded the minimum operating volume of the ECST, which was 96,000 gallons, based on p. 10.2-29 of (Dominion, 2007).

The SIAS was initiated either on high containment pressure (P > 122 kPa [17.7 psia]) or low-low reactor pressure (12.34 MPa [1789.7 psia]), based on Page A-2 of (NRC, 2011). For the one scenario in which pumped safety injection was credited, one HPSI pump was assumed to be available. The high-pressure safety injection was terminated when the water source for the safety injection automatically switches from the RWST to the containment sump, based on Page 9 of (NRC, 2011), because the automatic switch was assumed to fail. Containment spray and fan coolers were assumed to be available, because the containment spray uses a significant amount of RWST water and results in an earlier loss of HPSI flow.

The RCPs were assumed to trip when average void fraction in the vicinity of the pumps exceeded 0.1. This trip could be due to a pump failure in two-phase flow, or to an operator action in response to pump vibrations. The time of core damage would have been delayed if the RCPs had been tripped sooner.

Most of the calculations were terminated when the maximum cladding temperature reached 2099 K for cases with Zircaloy and 1804 K for cases with FeCrAl and Chromite. These temperatures were assumed to correspond to core damage.

The calculated results for the general transient scenarios described in Table 2-15 are summarized in the following sections.

2.3.3.1 TRANS-1

This scenario assumed that no feedwater was available after the initial coastdown of the MFW and that no high-pressure injection was available. The only cooling mechanisms present were due to the inventory of water stored in the SGs and the RCS at the beginning of the transient.

The calculated sequences of events are shown in Table 2-30. The event was initiated by the turbine trip at 0.0 s, which caused the TSVs to close and a direct reactor trip. The first lift of the SG PORVs occurred within 30 s. Heat from the core and the RCPs was transferred to the SGs, boiling liquid to steam, which was then vented out of the SG PORVs. The steam generators were depleted of liquid at about 55 minutes. The pressurizer PORV began cycling shortly thereafter. The RCPs were tripped at 85 minutes. The SIAS occurred near 100 minutes, but the HPSI pumps were assumed to fail. The core began to uncover near 105 minutes. The differences between calculations due to the different claddings were negligible before the core began to uncover and were relatively small after the onset of core uncovery. The calculations were terminated when the hottest cladding reached the temperature corresponding to assumed core damage. The timing of core damage varied by less than 10 minutes. The calculated amount of hydrogen produced during the transients varied significantly between claddings. The amount of hydrogen produced was 1.5 kg for FeCrAl, 1.8 kg for Chromite, and 90.1 kg for Zircaloy.

Table 2-30. Sequence of Events for Scenario TRANS-1.

	Time (hr:min)		
Event	**Zircaloy**	**FeCrAl**	**Chromite**
Turbine trip	0:00	0:00	0:00
All SGs dried out	0:55	0:54	0:55
Pressurizer PORV begins to cycle	0:57	0:57	0:57
PRT rupture disk opens	1:13	1:13	1:13
RCPs tripped	1:25	1:25	1:25
SIAS	1:36	1:36	1:36
Core begins to uncover	1:46	1:46	1:46
0.5 kg H_2 generated	2:00	2:29	2:26
First cladding rupture	2:21	2:23	2:26
Core damage	2:25	2:32	2:27

The following figures illustrate the effects of the cladding on various parameters. The differences between calculations are generally small before the core began to uncover, as expected, based on Table 2-30.

The behavior of SG B is illustrated in Figure 2-152 and Figure 2-153, which show pressure and collapsed liquid level, respectively. The other SGs behaved similarly. The SG PORVs opened shortly after the turbine trip and the pressure was maintained between the open and closing setpoints of the PORVs for the remainder of the transient. The SGs emptied near 55 minutes.

The calculated response of the pressurizer is shown in Figure 2-154 and Figure 2-155, which show pressure and collapsed liquid level, respectively. The pressure increases near 55 minutes, because the SGs dry out. The pressurizer PORV begins cycling shortly thereafter. The RCS temperature begins to increase after all the SGs have dried out, which causes the level and pressure in the pressurizer to increase rapidly. After the pressurizer fills with liquid, the first PORV is no longer able to relieve the pressure, and the pressure increases enough to open the second pressurizer PORV and the safety relief valves. The pressure falls after the pressurizer begins to void. The pressurizer is depleted of liquid near 135 minutes.

The collapsed liquid level in the core and the maximum cladding temperature are shown in Figure 2-156 and Figure 2-157, respectively. The collapsed liquid level in the core begins to decrease near 80 minutes, which is about the same time as the RCPs are tripped, based on voiding. The collapsed level begins to decrease rapidly at about 106 minutes, when the top of the core begins to uncover and the maximum cladding temperature begins to increase. The maximum cladding temperatures then begin to diverge. The highest temperatures occur with the Zircaloy cladding, but the difference in the timing of core damage is relatively small.

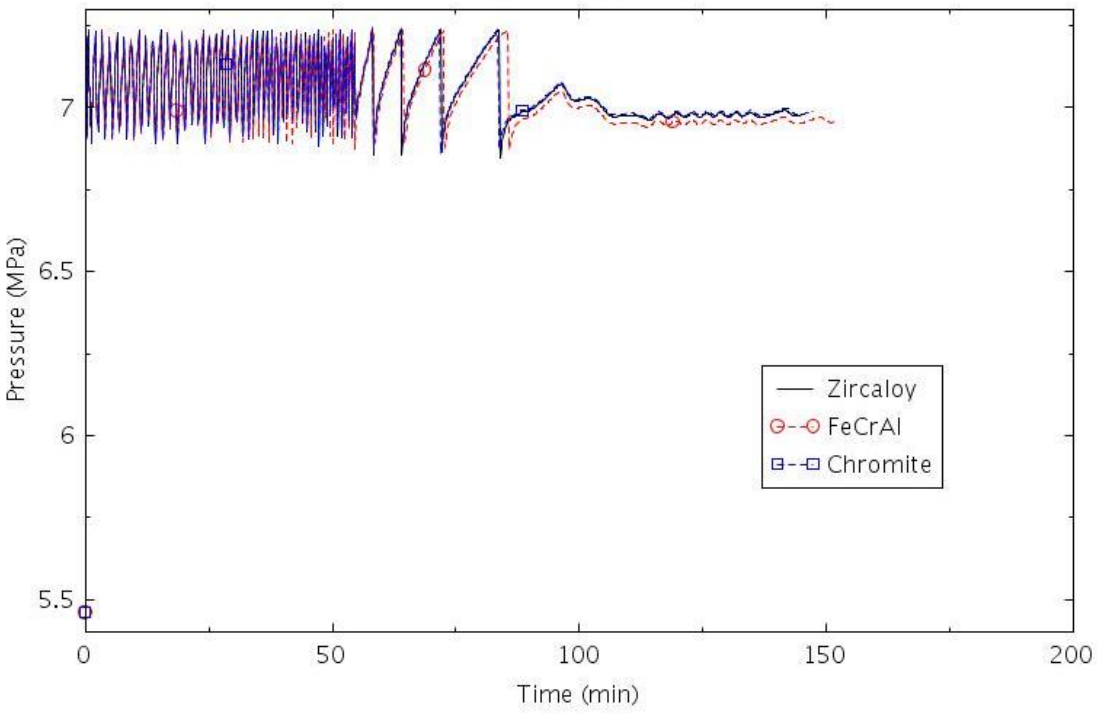

Figure 2-152. Pressure in SG B (TRANS-1).

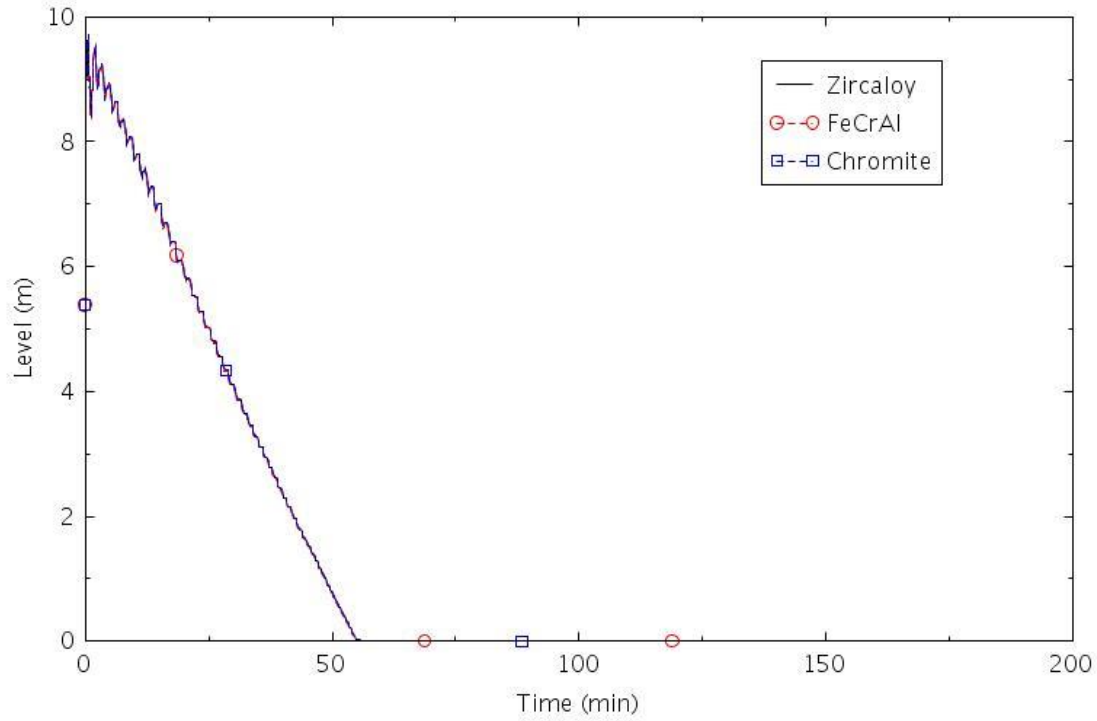

Figure 2-153. Collapsed liquid level in SG B (TRANS-1).

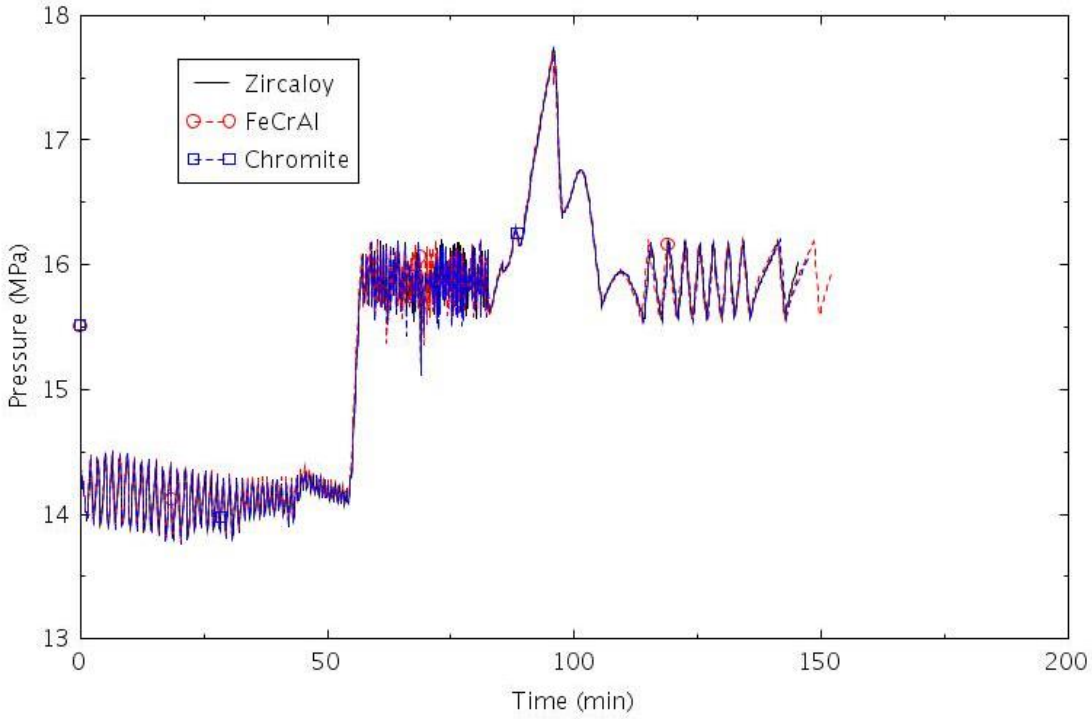

Figure 2-154. Pressure in the pressurizer (TRANS-1).

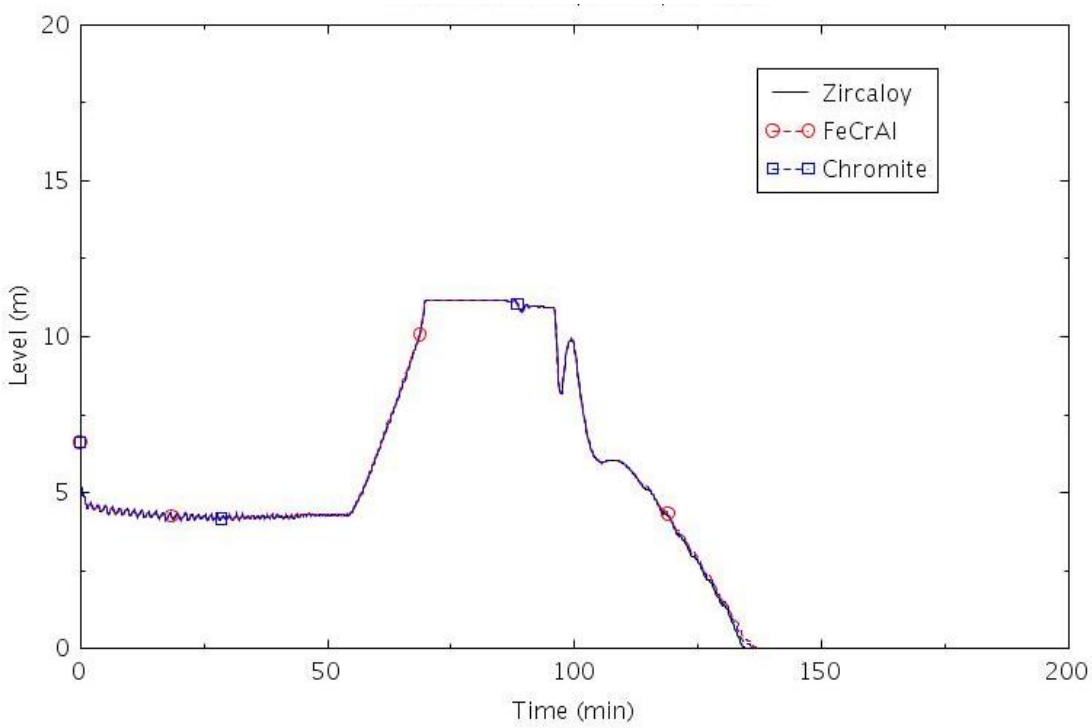

Figure 2-155. Collapsed liquid level in the pressurizer (TRANS-1).

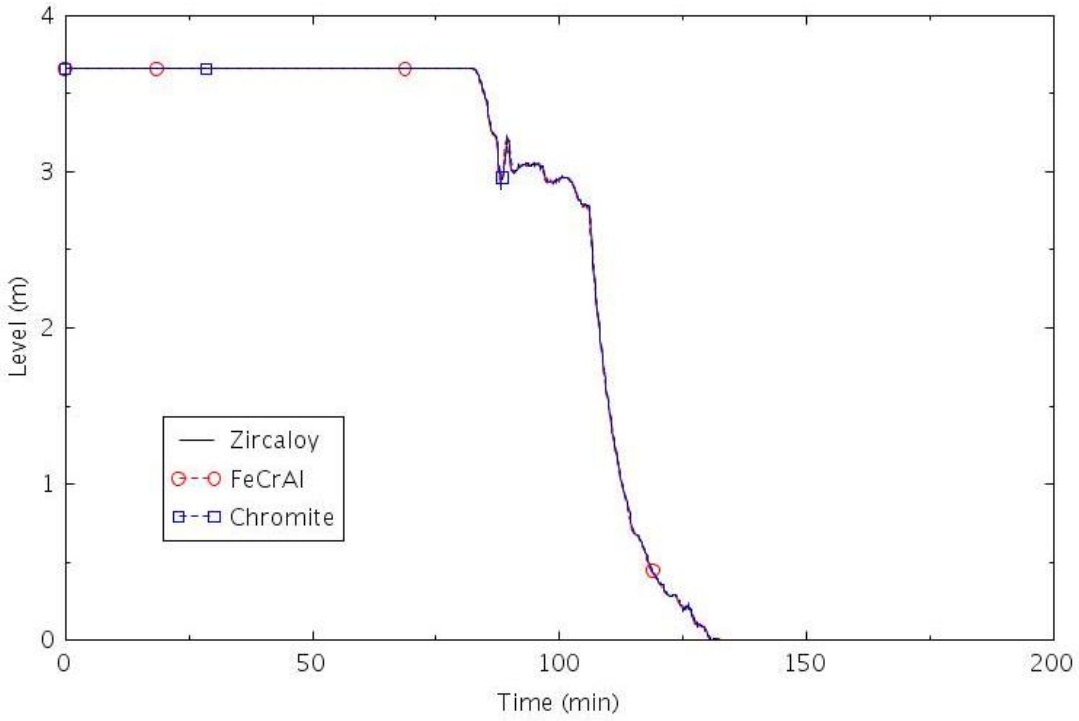

Figure 2-156. Collapsed liquid level in the central core channel (TRANS-1).

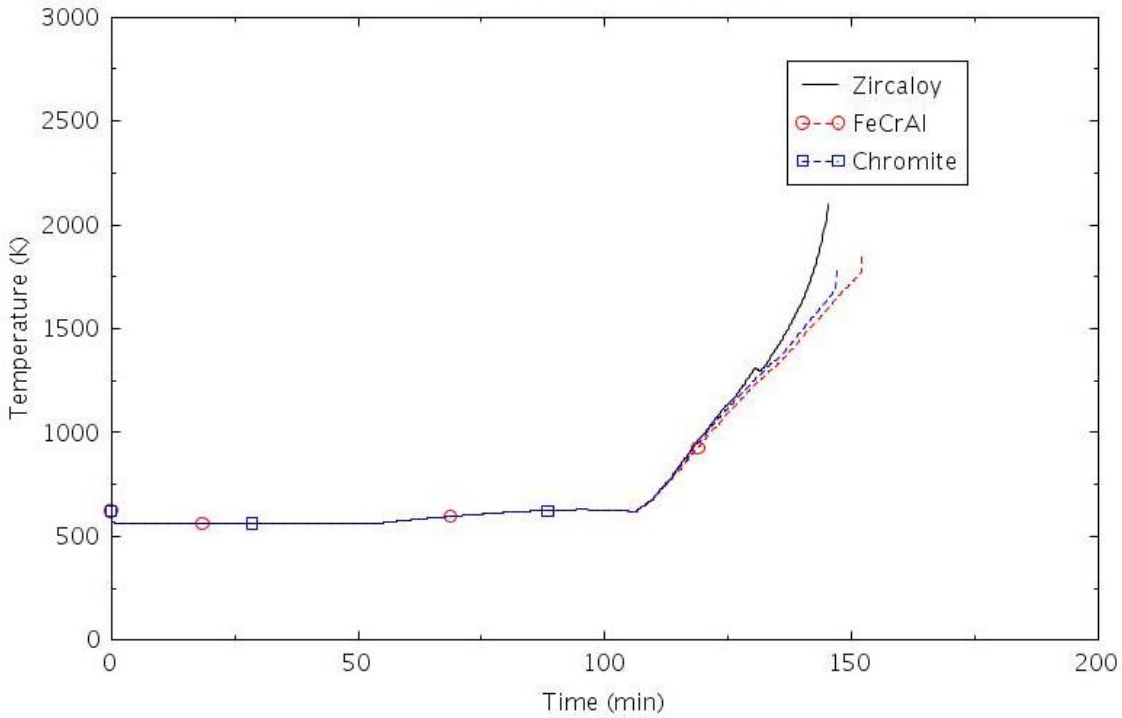

Figure 2-157. Maximum cladding temperature (TRANS-1).

2.3.3.2 TRANS-2

This scenario assumed that no feedwater was available after the initial coastdown of the MFW, and that one HPSI pump actuated normally following the SIAS. The HPSI was terminated when the water source

for the safety injection was supposed to automatically switch from the RWST to the containment sump; the automatic switch was assumed to fail.

The calculated sequences of events are shown in Table 2-31. Event times were identical to those shown previously in Table 2-30, until HPSI flow began at 96 minutes. The containment spray was first actuated near 3 hours, and then operated intermittently as needed to control the containment pressure between 172 kPa (25 psia) and 83 kPa (12 psia). The HPSI flow was terminated near 12 hours, when the level in the RWST dropped to the setpoint for the automatic switchover to sump recirculation mode. Without any HPSI flow, the water inventory in the RCS began to boil off through the PORV. The core began to uncover at about 13 hours. The calculations were terminated with high cladding temperatures around 15 hours. The differences between calculations due to the different claddings were negligible prior to the actuation of containment spray, and were generally small afterwards. The increased variability thereafter was more likely due to numerical causes than to the differences between claddings. However, the time between the onset of core uncovery and the termination of the calculations is judged to be reasonable. The time between when the core began to uncover and core damage occurred was 70 minutes with Zircaloy, 91 minutes with FeCrAl, and 79 minutes with Chromite. The calculated amount of hydrogen produced during the transients varied significantly between claddings. The amount of hydrogen produced was 2.3 kg for Chromite, 2.7 kg for FeCrAl, and 100.6 kg for Zircaloy.

Table 2-31. Sequence of Events for Scenario TRANS-2.

	Time (hr:min)		
Event	**Zircaloy**	**FeCrAl**	**Chromite**
Turbine trip	0:00	0:00	0:00
All SGs dried out	0:55	0:54	0:55
Pressurizer PORV begins to cycle	0:57	0:57	0:57
PRT rupture disk opens	1:13	1:13	1:13
RCPs tripped	1:25	1:25	1:25
SIAS	1:36	1:36	1:36
HPSI begins	1:36	1:36	1:36
Containment spray actuated	2:54	3:04	3:02
HPSI terminated	12:11	12:01	11:53
Core begins to uncover	13:40	13:19	13:06
0.5 kg H_2 generated	14:09	14:36	14:25
First cladding rupture	14:45	14:32	14:25
Core damage	14:51	14:49	14:25

The following figures illustrate the effects of the cladding on various parameters. The response prior to the onset of HPSI flow near 96 minutes was identical to that discussed previously for Scenario TRANS-1. Since they had already dried out before HPSI was actuated, the SGs did not significantly affect the response of the RCS after 96 minutes. The response of SG B is illustrated in Figure 2-158 and Figure 2-159.

The total HPSI flow into the RCS is shown in Figure 2-160. The flow began at 96 min in response to the SIAS on high containment pressure. The HPSI flow was terminated near 720 minutes, when the automatic switchover to sump recirculation mode was assumed to fail.

The containment spray is shown in Figure 2-161. Although intermittent, the maximum spray flow rate greatly exceeds that of the HPSI. Slightly more than half of the total injection had gone to the containment at the time of the failed automatic switch to sump injection.

The calculated response of the pressurizer is shown in Figure 2-162 and Figure 2-163, which show pressure and collapsed liquid level, respectively. The pressure generally stayed between the open and close setpoints of the pressurizer PORV after the initiation of HPSI flow at 96 min. HPSI flow eventually refilled the pressurizer. The pressurizer emptied after HPSI was terminated near 720 minutes.

The collapsed liquid level in the core and the maximum cladding temperature are shown in Figure 2-164 and Figure 2-165, respectively. The core stayed nearly full until after HPSI was terminated near 720 minutes. The maximum cladding temperature began to increase near 800 minutes.

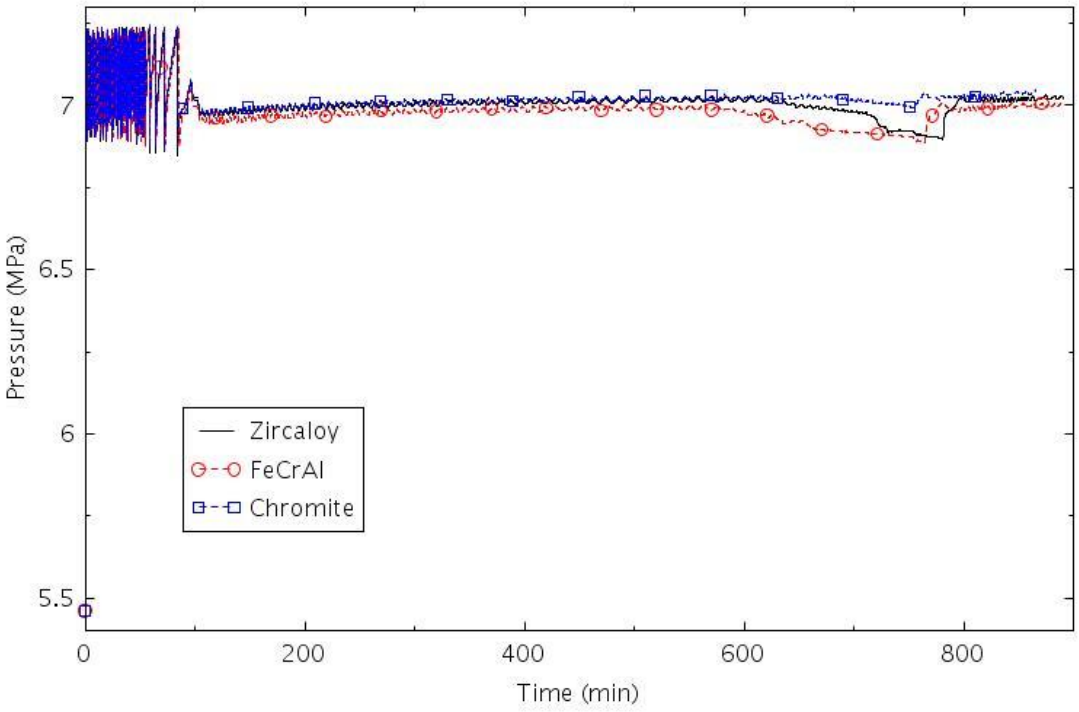

Figure 2-158. Pressure in SG B (TRANS-2).

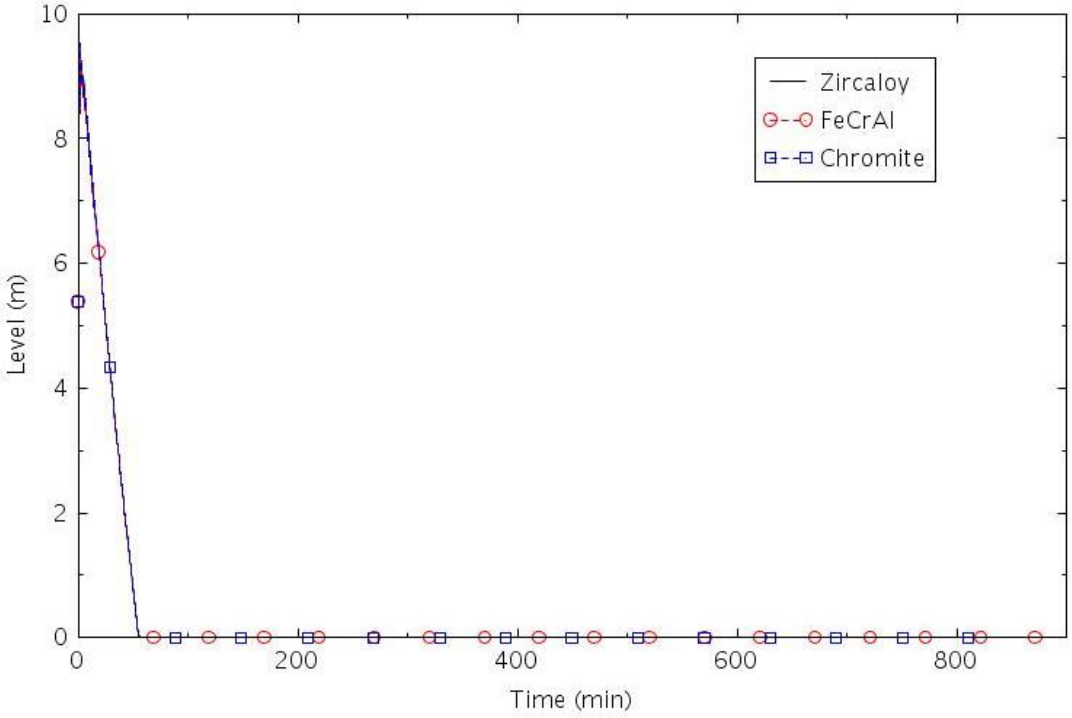

Figure 2-159. Collapsed liquid level in SG B (TRANS-2).

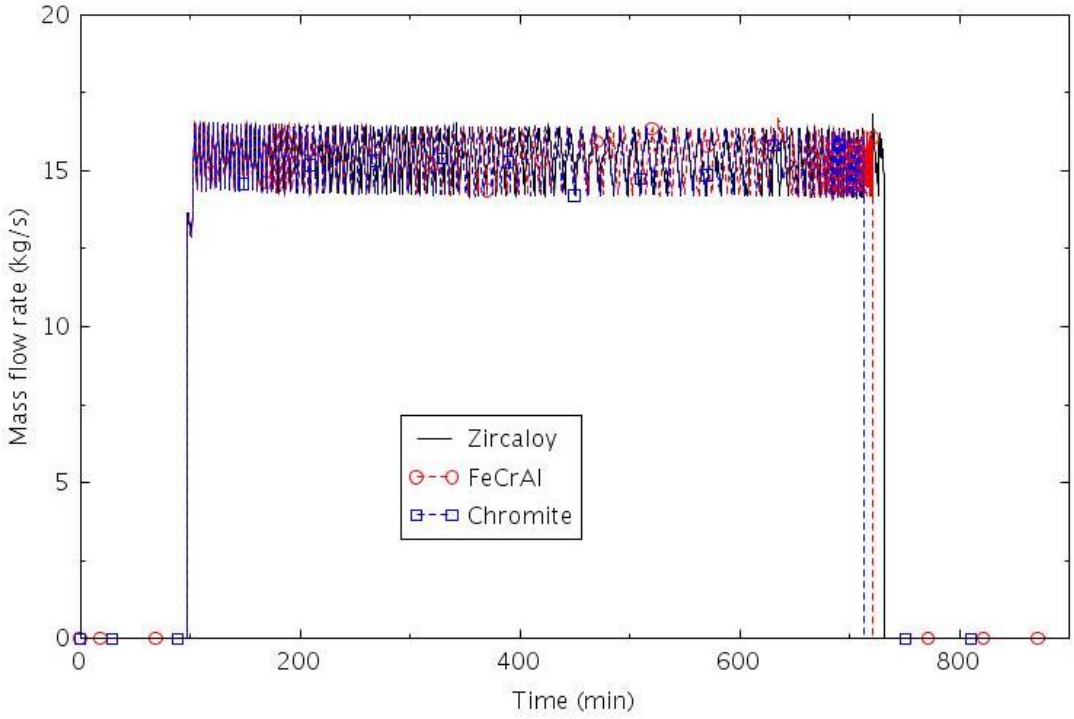

Figure 2-160. Total HPSI flow into the RCS (TRANS-2)

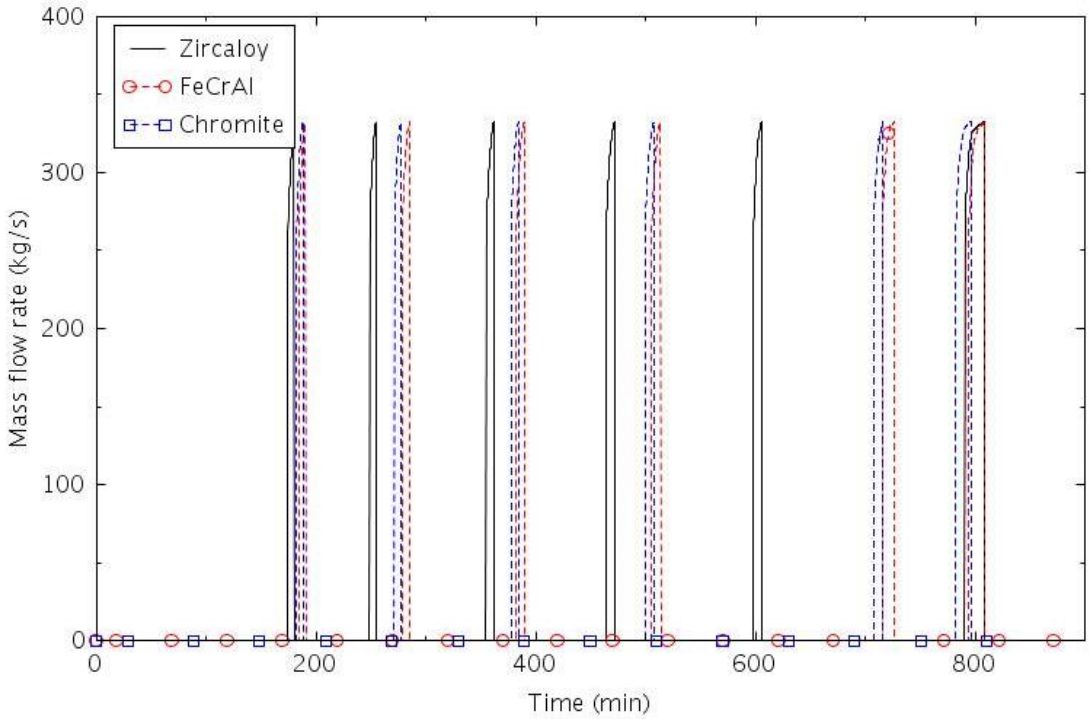

Figure 2-161. Containment spray (TRANS-2).

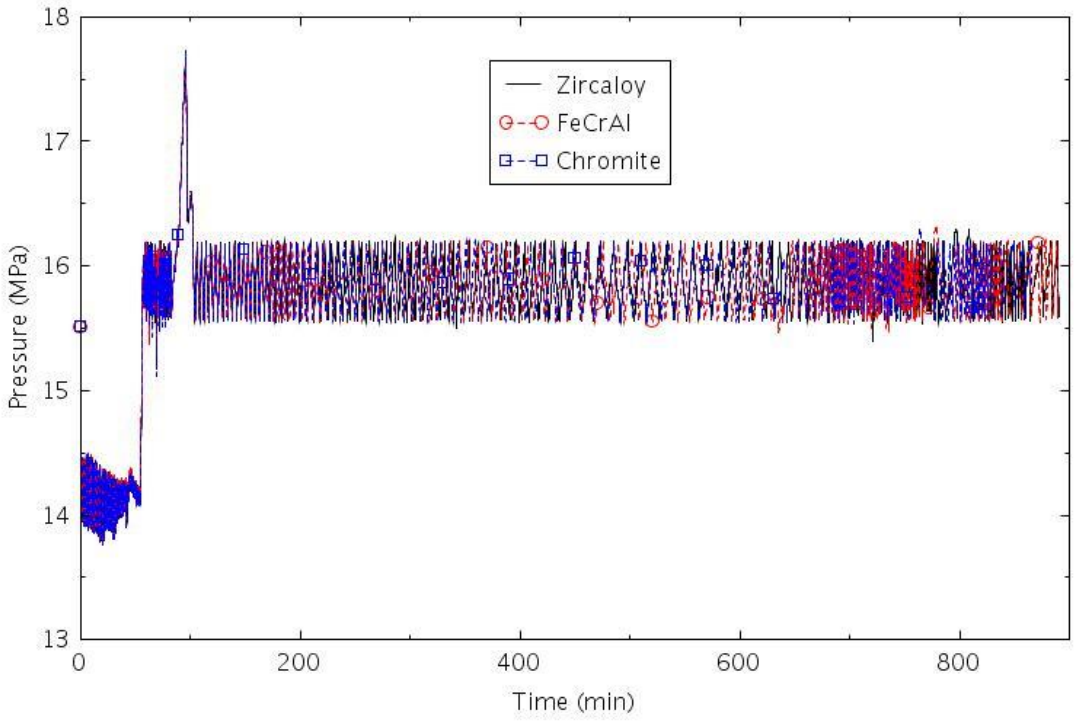

Figure 2-162. Pressure in the pressurizer (TRANS-2).

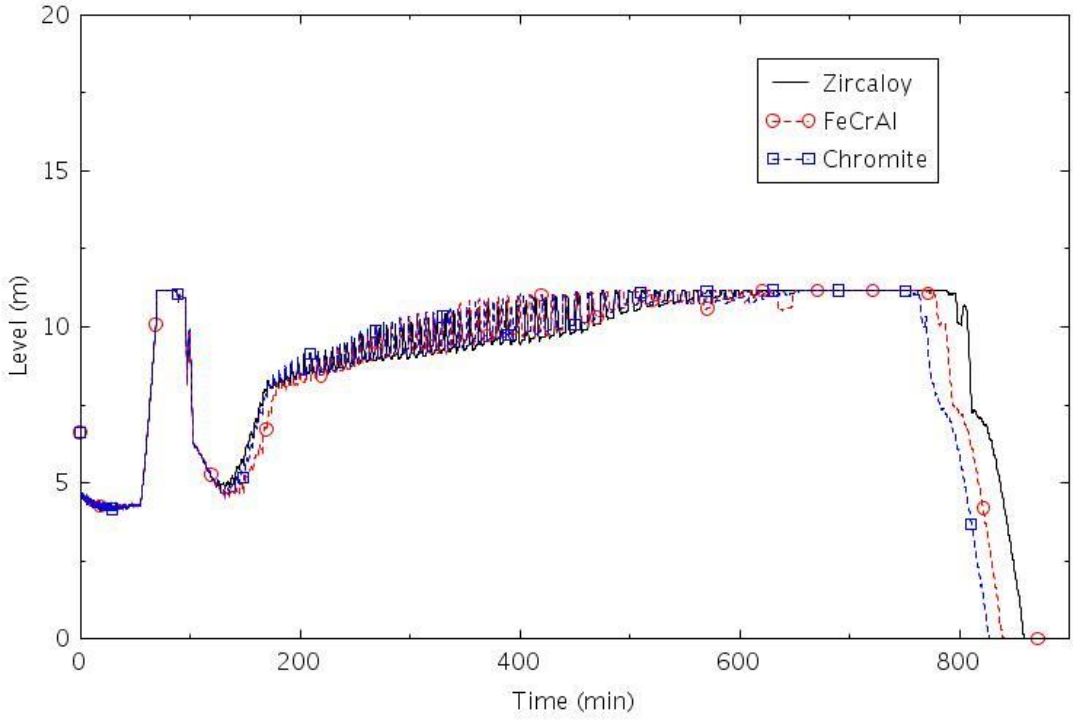

Figure 2-163. Collapsed liquid level in the pressurizer (TRANS-2).

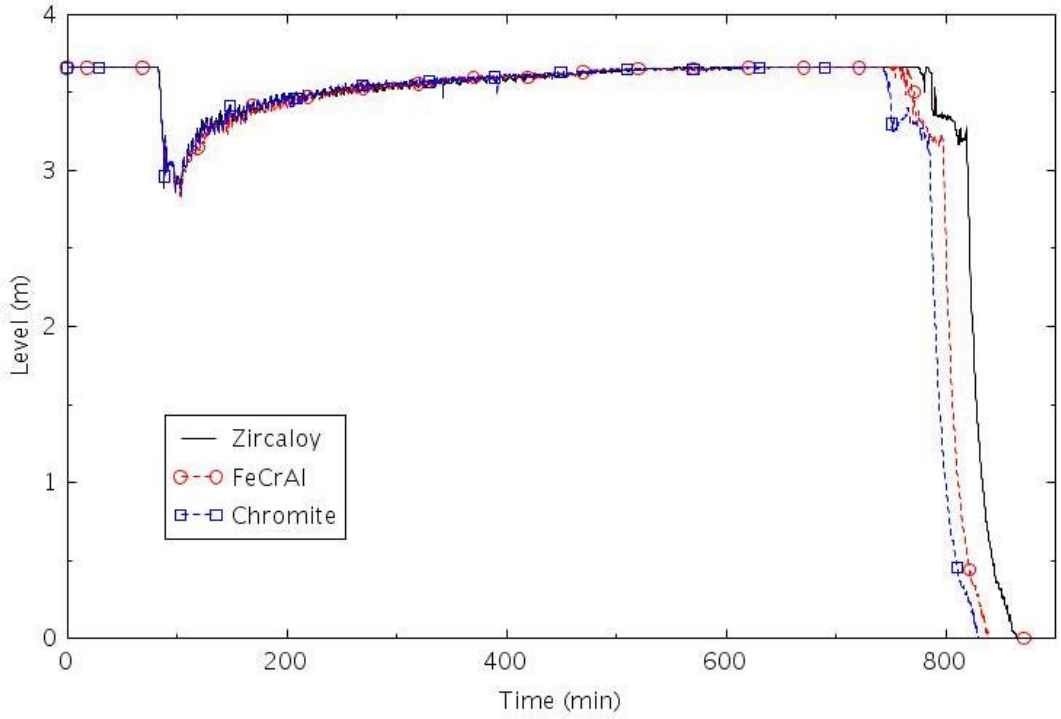

Figure 2-164. Collapsed liquid level in the central core channel (TRANS-2).

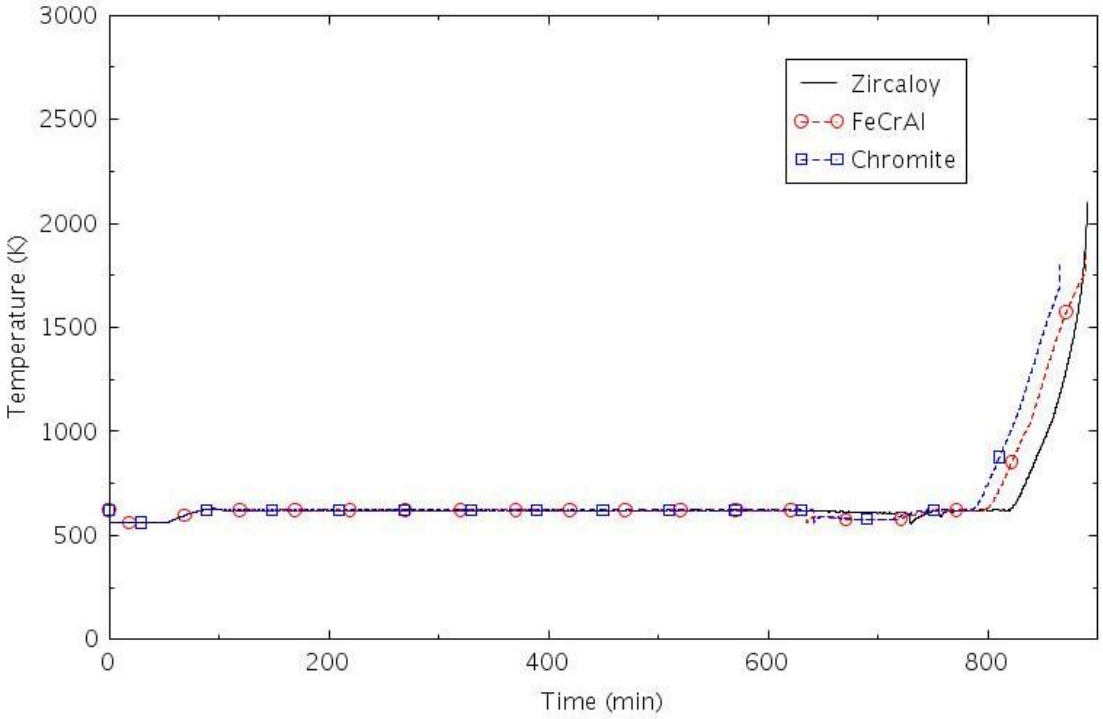

Figure 2-165. Maximum cladding temperature (TRANS-2).

In the calculations described previously, the pressurizer PORVs were assumed to operate automatically. Sensitivity calculations were performed in which the operators were assumed to lock open one pressurizer PORV at 1 hour to initiate feed and bleed cooling. The effects of the operator action on the sequence of events for the case with Zircaloy cladding are shown in Table 2-32. The SIAS occurred almost immediately

after the PORV was locked open in the sensitivity calculation, due to low-low pressurizer pressure rather than high containment pressure as in the base case. The other most significant differences were that the RCS pressure decreased enough to initiate flow from the accumulators, the HPSI flow was terminated about 3 hours earlier, and core damage occurred about 3 hours earlier with feed and bleed. Even though feed and bleed allowed much of the accumulator water to be injected, earlier core damage occurred, because the RWST liquid inventory not used as efficiently as in the base calculation. In the base calculation, the periodic opening and closing of the PORV resulted in oscillations in the fluid state at the PORV between steam and liquid. In the sensitivity calculation, the lower RCS pressure resulted in increased HPSI flow into the RCS and mostly liquid flow out the PORV.

Table 2-32. The Effects of Feed and Bleed Cooling in Scenario TRANS-2 with Zircaloy Cladding.

	Time (hr:min)	
Event	**Without feed and bleed**	**With feed and bleed**
Turbine trip	0:00	0:00
All SGs dried out	0:55	0:55
Pressurizer PORV begins to cycle	0:57	0:57
Pressurizer PORV locked open	NA	1:00
PRT rupture disk opens	1:13	1:04
RCPs tripped	1:25	2:02
SIAS	1:36	1:00
HPSI begins	1:36	1:00
Containment spray actuated	2:54	3:44
Accumulator flow initiated	NA	6:00
HPSI terminated	12:11	8:47
Core begins to uncover	13:40	10:47
0.5 kg H_2 generated	14:09	11:16
First cladding rupture	14:45	11:19
Core damage	14:51	11:34

2.3.3.3 PORV-1

This scenario assumed that the pressurizer PORV stuck open after its first lift, one motor-driven AFW pump was available, and that no high-pressure injection was available. AFW was assumed to start 30 seconds after the SIAS.

The calculated sequences of events are shown in Table 2-33. Event times were identical to those shown previously in Table 2-30, until the pressurizer PORV stuck open at 57 minutes and initiated a loss-of-coolant accident. The SIAS occurred on low pressurizer pressure shortly about 30 seconds later, and motor-driven AFW was initiated 30 seconds after that. The HPSI was assumed to fail. The RCPs were tripped at 60 minutes. The PRT rupture disk opened at 63 minutes. The RCS coolant inventory decreased continuously due to flow through the stuck-open PORV and the HPSI failure. The core began to uncover at about 155 minutes. The differences between calculations due to the different claddings were negligible before the core began to uncover, and were relatively small afterwards. The calculations were terminated when the hottest cladding reached its failure temperature and core damage was assumed to occur. The termination times varied by less than 10 minutes. The calculated amount of hydrogen produced during the transients varied significantly between claddings. The amount of hydrogen produced was 1.4 kg for FeCrAl, 5.9 kg for Chromite, and 18.9 kg for Zircaloy.

Table 2-33. Sequence of Events for Scenario PORV-1.

	Time (hr:min)		
Event	**Zircaloy**	**FeCrAl**	**Chromite**
Turbine trip	0:00	0:00	0:00
All SGs dried out	0:55	0:54	0:55
PORV sticks open	0:57	0:57	0:57
SIAS	0:57	0:57	0:57
AFW initiated	0:58	0:58	0:58
RCPs tripped	1:00	1:00	1:00
PRT rupture disk opens	1:03	1:03	1:03
Core begins to uncover	2:36	2:35	2:35
0.5 kg H_2 generated	3:01	3:23	3:06
First cladding rupture	3:03	3:00	3:02
Core damage	3:14	3:23	3:16

The following figures illustrate the effects of the cladding on various parameters. The mass flow through the stuck-open PORV is illustrated in Figure 2-166. The PORV flow rate responds to both the changes in pressurizer pressure (Figure 2-167) and level (Figure 2-168). The PORV stuck open at 57 minutes and vented nearly pure steam until about 61 minutes when the level got high enough to allow some liquid to exit the PORV. The PORV was relieving nearly pure steam again after145 minutes.

Some voiding occurred in the core within a few minutes after the PORV stuck open as shown in Figure 2-169. The level in the core began decreasing rapidly at about 150 minutes. The core began to heat up a few minutes later as shown in Figure 2-170. The maximum cladding temperatures then begin to diverge. The difference in the timing of core damage is less than 10 minutes.

The performance of the SGs is illustrated in Figure 2-171 and Figure 2-172, which show pressure and level in the B steam generator. The SG pressure was being controlled by the SG PORVs until about 130 minutes, when the pressure began to decrease due to the decreasing pressurizer pressure shown previously. The SG and RCS pressures were closely coupled after 130 minutes, which is common during small-break loss-of-coolant accidents when the SGs are removing heat and two-phase fluid is present on both the tube and shell sides of the SGs. The AFW flow is shown in Figure 2-173. Although AFW flow was not terminated during this transient, AFW was not able to prevent core damage because no emergency core coolant was injected into the RCS to make up for the loss of coolant through the stuck-open PORV.

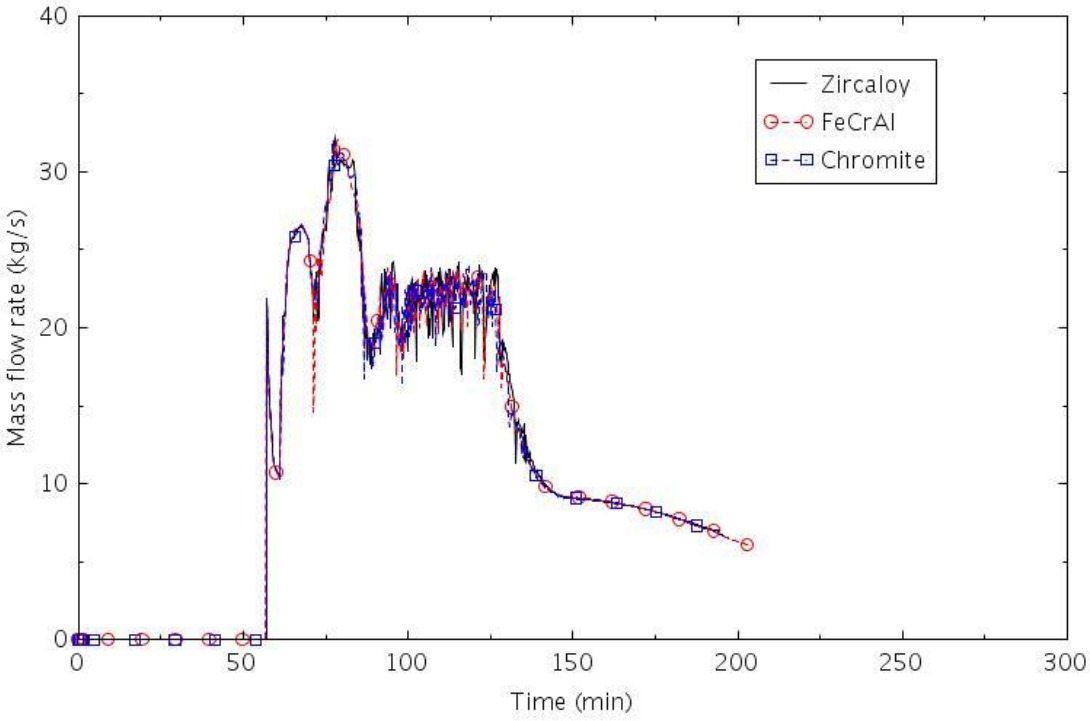

Figure 2-166. Mass flow rate through the pressurizer PORV (PORV-1).

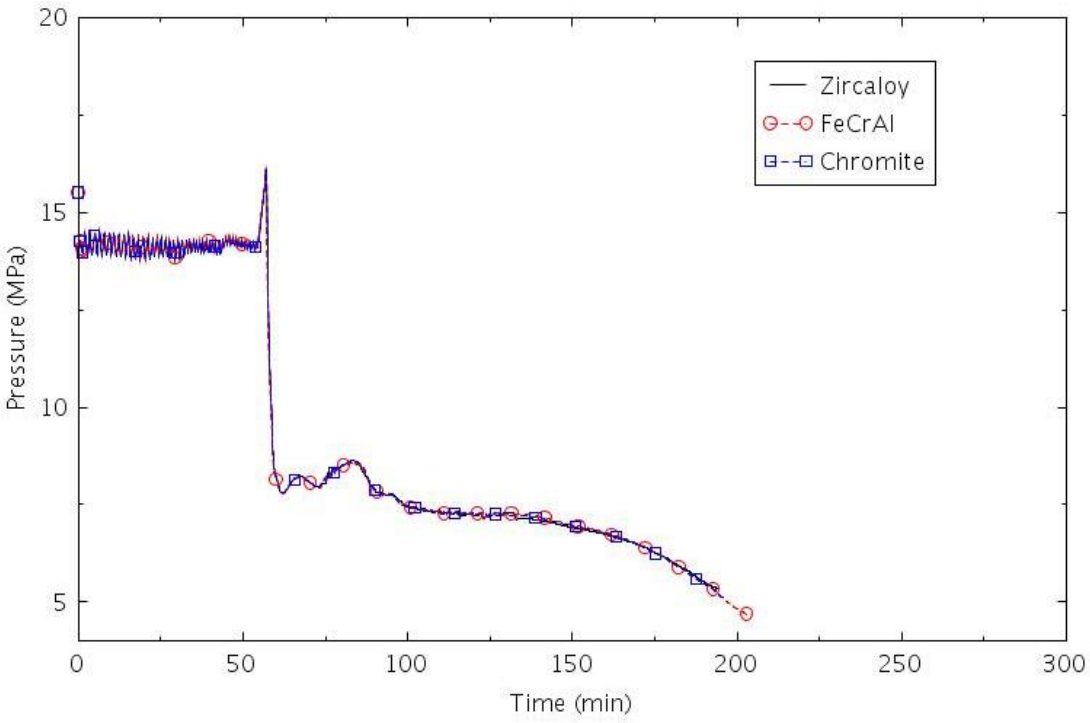

Figure 2-167. Pressure in the pressurizer (PORV-1).

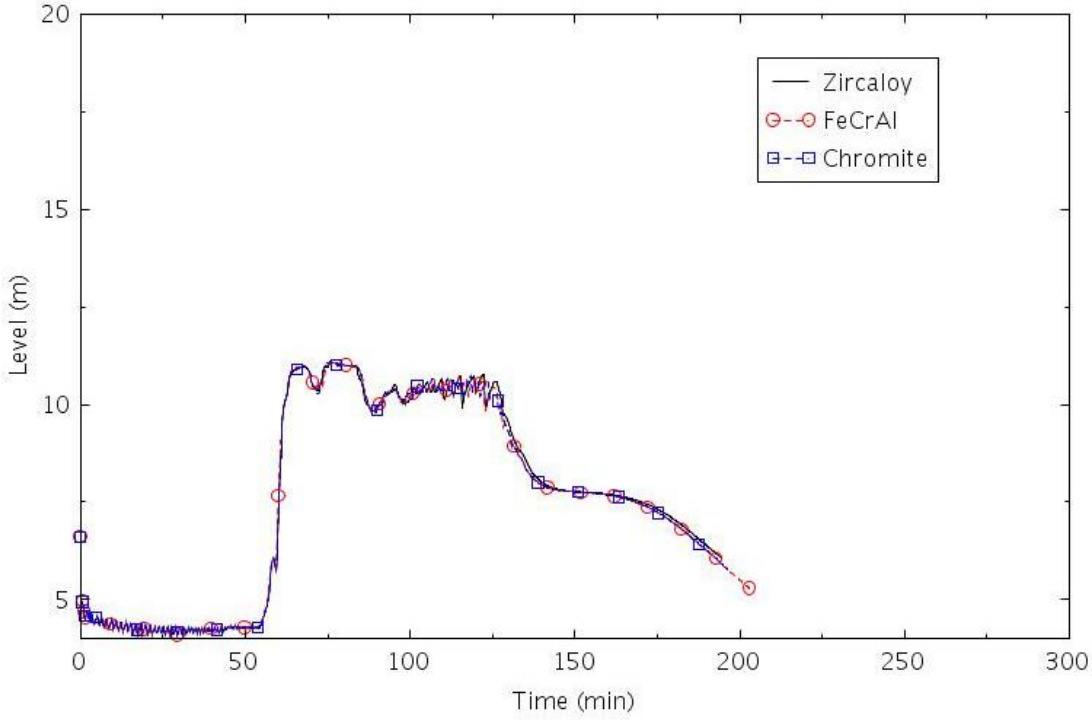

Figure 2-168. Collapsed liquid level in the pressurizer (PORV-1).

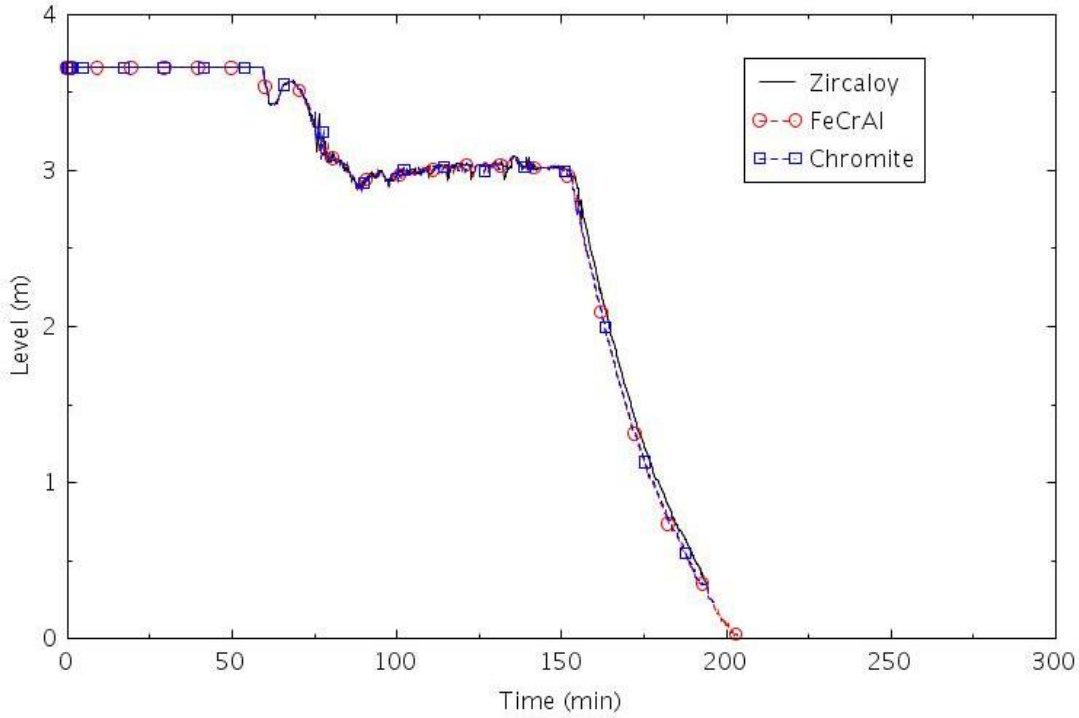

Figure 2-169. Collapsed liquid level in the central core channel (PORV-1).

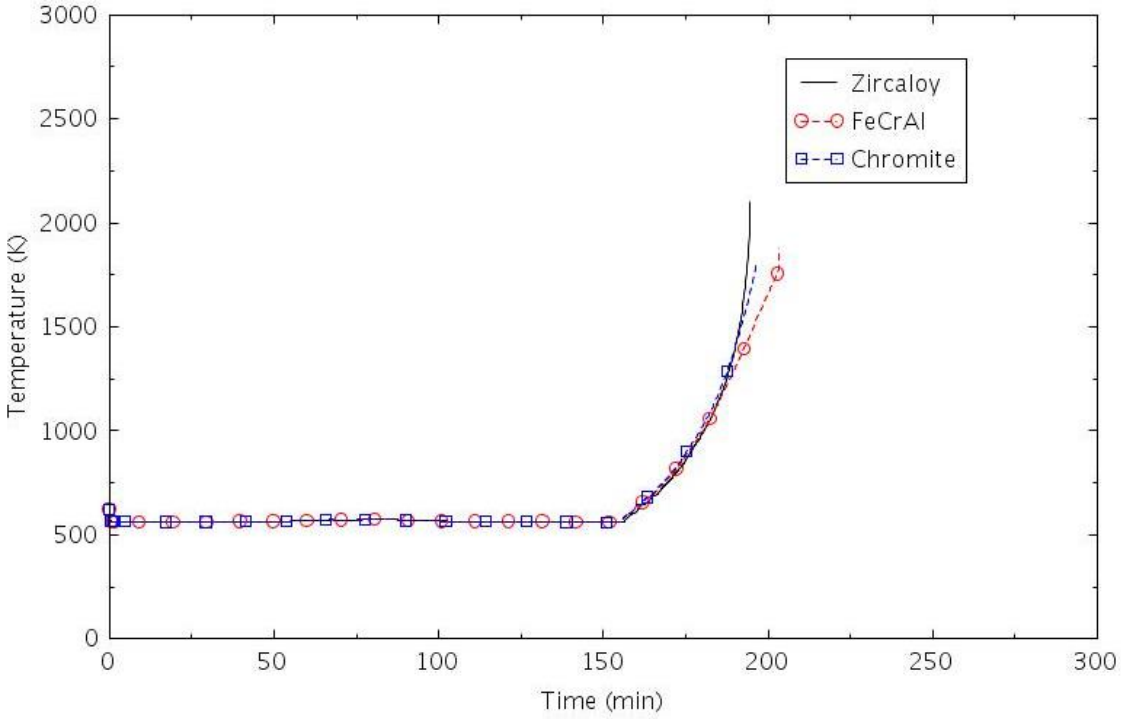

Figure 2-170. Maximum cladding temperature (PORV-1).

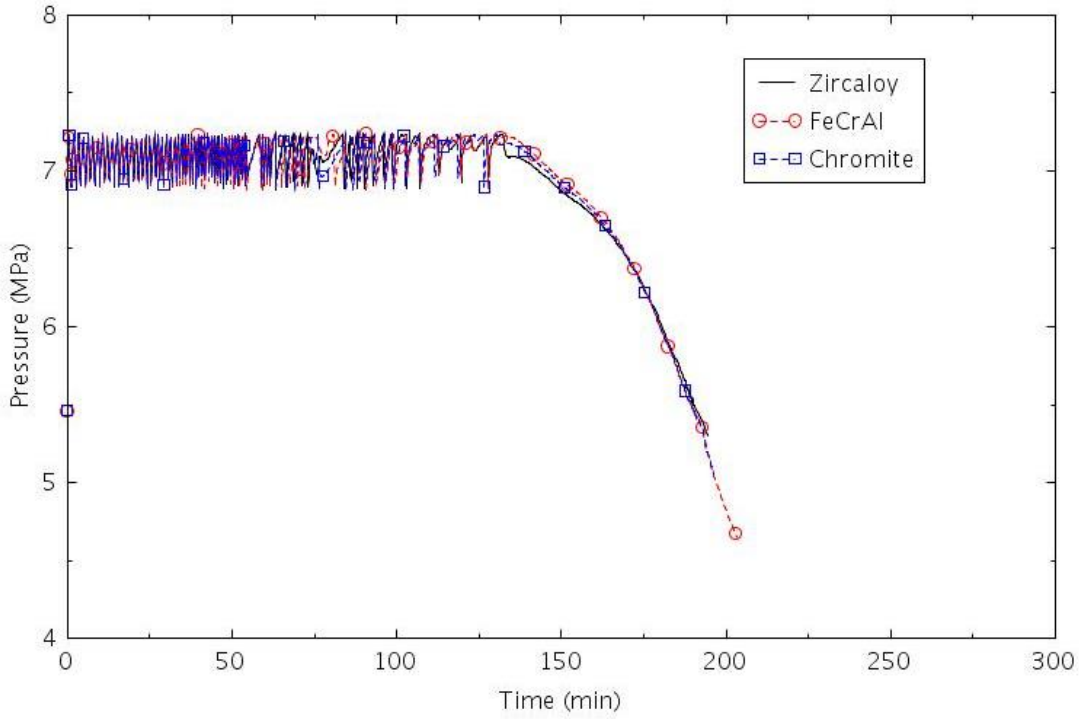

Figure 2-171. Pressure in SG B (PORV-1).

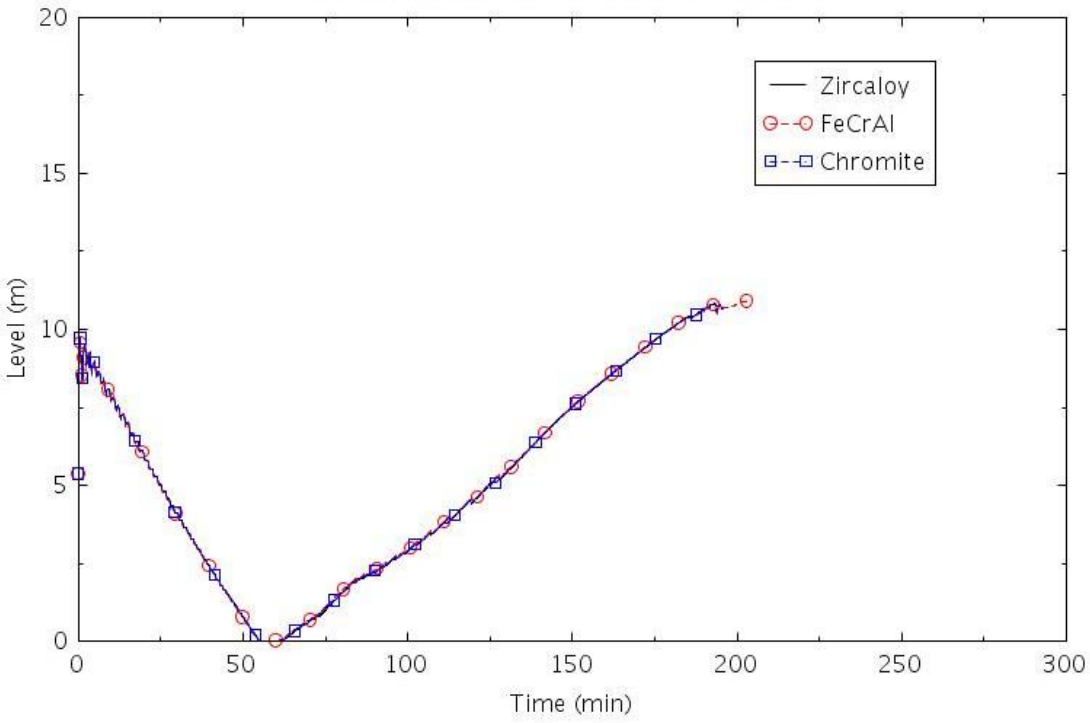

Figure 2-172. Collapsed liquid level in SG B (PORV-1).

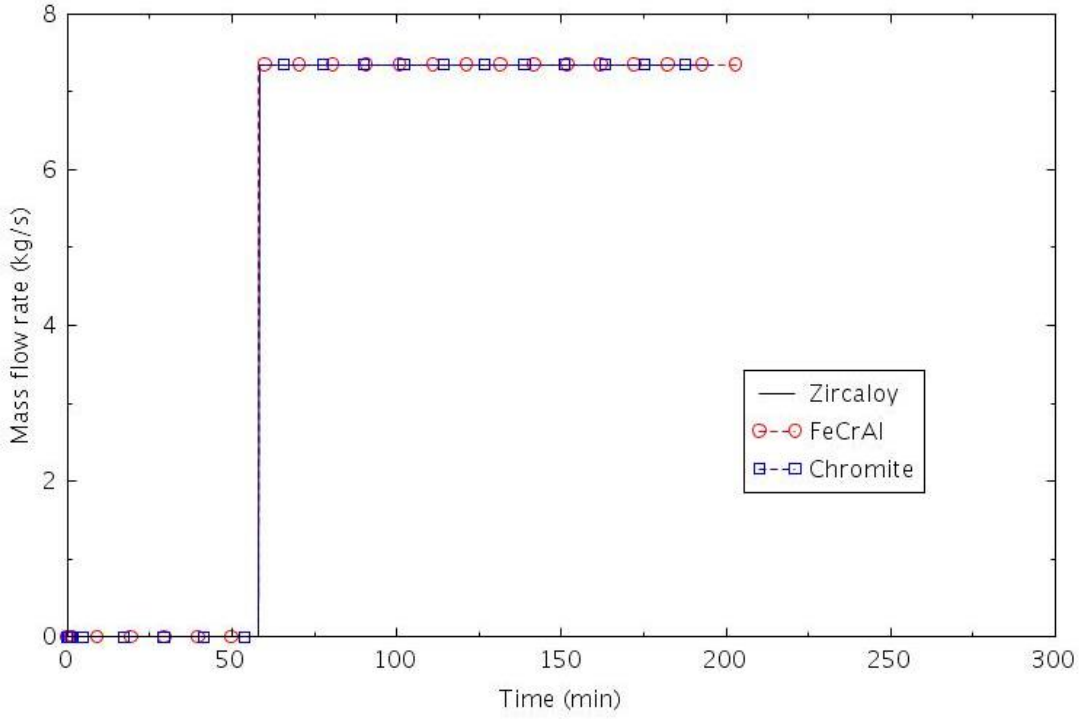

Figure 2-173. AFW flow rate to SG B (PORV-1).

2.3.3.4 LOSC-182a

This scenario assumes that one motor-driven AFW pump is available, that the RCP pump seals fail, that no high-pressure injection is available, and that the operators manually initiate an SSC. The pump seal failures produce an initial leakage of 0.011 m^3/s (182 gpm) per pump. Since power is available in this scenario, the cause of the seal failure is not mechanistic due to overheating, as is generally modeled in an SBO. The seal failure was assumed to conservatively occur simultaneously with the turbine trip. The SSC was assumed to begin at 1.5 hours, the same time as assumed in Section 3.1.4.1 of (NRC, 2012). The PORVs were opened as necessary to obtain a 56°C/hr (100°F/hr) cooldown rate in the steam generators. The cooldown was terminated when the SGs reached 0.93 MPa (134.7 psia), so that the turbine-driven AFW pumps would be available if needed. Thereafter, the PORVs opened as needed to control the SG pressure between 0.93 MPa (134.7 psia) and 1.27 MPa (184.7 psia).

The calculated sequences of events are shown in Table 2-34. The event was initiated by the turbine trip at 0.0 s, which caused the TSVs to close and a direct reactor trip. The first lift of the SG PORVs occurred within 30 s. The RCP pump seals were assumed to fail simultaneously with the turbine trip. The SIAS occurred at about 4 minutes on low reactor pressure and the AFW was initiated 30 seconds later. The HPSI was assumed to fail. The RCPs were tripped at 52 minutes. The RCS coolant inventory decreased continuously due to flow through the ruptured pump seals and lack of HPSI. The operators were assumed to manually initiate a controlled cooldown of the SGs beginning at 90 minutes. The resulting depressurization of the RCS resulted in accumulator injection between 130 minutes and about 240 minutes. The AFW flow was terminated near 5 hours, because the ECST was depleted. The SGs were empty near 10 hours. The core began to uncover near 12 hours. The differences between calculations were generally negligible before the accumulators emptied of liquid, and generally small thereafter. The time between the onset of core uncovery and the termination of the calculations was 62 minutes with Zircaloy, 84 minutes with FeCrAl, and 73 minutes with Chromite. The calculated amount of hydrogen produced during the transients varied significantly between claddings. The amount of hydrogen produced was 1.7 kg for FeCrAl, 16.6 kg for Chromite, and 57.3 kg for Zircaloy.

Table 2-34. Sequence of Events for Scenario LOSC-182a.

	Time (hr:min)		
Event	**Zircaloy**	**FeCrAl**	**Chromite**
Turbine trip	0:00	0:00	0:00
SIAS	0:04	0:04	0:04
AFW initiated	0:04	0:04	0:04
RCPs tripped	0:52	0:52	0:52
SSC begins	1:30	1:30	1:30
Accumulator flow initiated	2:12	2:12	2:13
Accumulator flow terminated	3:35	4:07	4:10
SSC ends	3:37	3:36	3:36
AFW terminated	4:37	4:36	4:36
All SGs empty	9:59	9:56	9:54
Core begins to uncover	11:47	11:53	11:48
0.5 kg H_2 generation	12:16	13:10	12:44
First cladding rupture	12:41	12:46	12:43
Core damage	12:49	13:17	13:01

The following figures illustrate the effects of the cladding on various parameters. The mass flow through the seals in RCP B is illustrated in Figure 2-174. The flow rate increased after accumulator flow was initiated near 130 minutes. The accumulators emptied near 240 minutes and the mass flow eventually decreased. The increase in mass flow near 600 minutes was due to an increase in pressure. Pressurizer pressure is shown in Figure 2-175. The LOCA initiated by the rupture of the pump seals caused the pressure to decrease until the RCS and SG pressures were nearly the same near 15 minutes. The decrease in pressure at 90 minutes was due to the SSC. The RCS and SG pressures were closely coupled until all the SGs were empty near 600 minutes. Thereafter, boiling in the core caused the pressure to increase until the core began

to uncover. The collapsed liquid level in the pressurizer is shown in Figure 2-176. The LOCA caused the pressurizer to empty near 10 minutes. After all the SGs were empty, boiling in the core caused the pressurizer to partially refill.

The LOCA caused some voiding in the core within a few minutes of the start of the transient, as shown in Figure 2-177. The onset of accumulator injection near 130 minutes nearly refilled the core. The level decreased somewhat after accumulator injection was terminated near 240 minutes, and continued to decrease until all the SGs were empty near 600 minutes. The level decreased sharply near 700 minutes. The core began to heat up a few minutes later, as shown in Figure 2-178.

The pressure in SG B is illustrated in Figure 2-179. The pressure was generally between the open and close setpoints of the SG PORVs until 90 minutes, when the manual SSC was initiated. After the cooldown was terminated near 220 minutes, the operators were assumed to open and close the PORVs as necessary to maintain the pressure between 0.93 MPa (134.7 psia) and 1.27 MPa (184.7 psia).

The collapsed liquid level in SG B is shown in Figure 2-180 and the AFW flow is shown in Figure 2-181. Even though the AFW flow was initiated at 4 minutes, the collapsed liquid level did not increase significantly until after the RCPs were tripped at 52 minutes. The levels then increased until the AFW was terminated near 280 minutes. The collapsed levels then decreased, although there was considerable variation in the calculated levels.

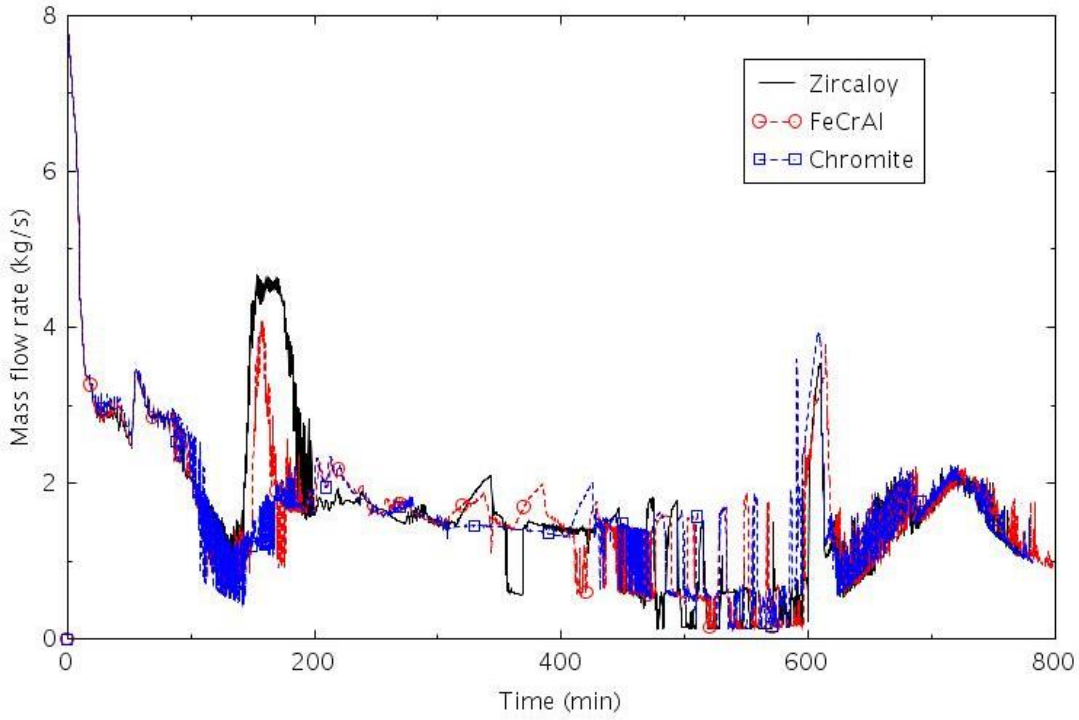

Figure 2-174. Mass flow rate through the seals of RCP B (LOSC-182a).

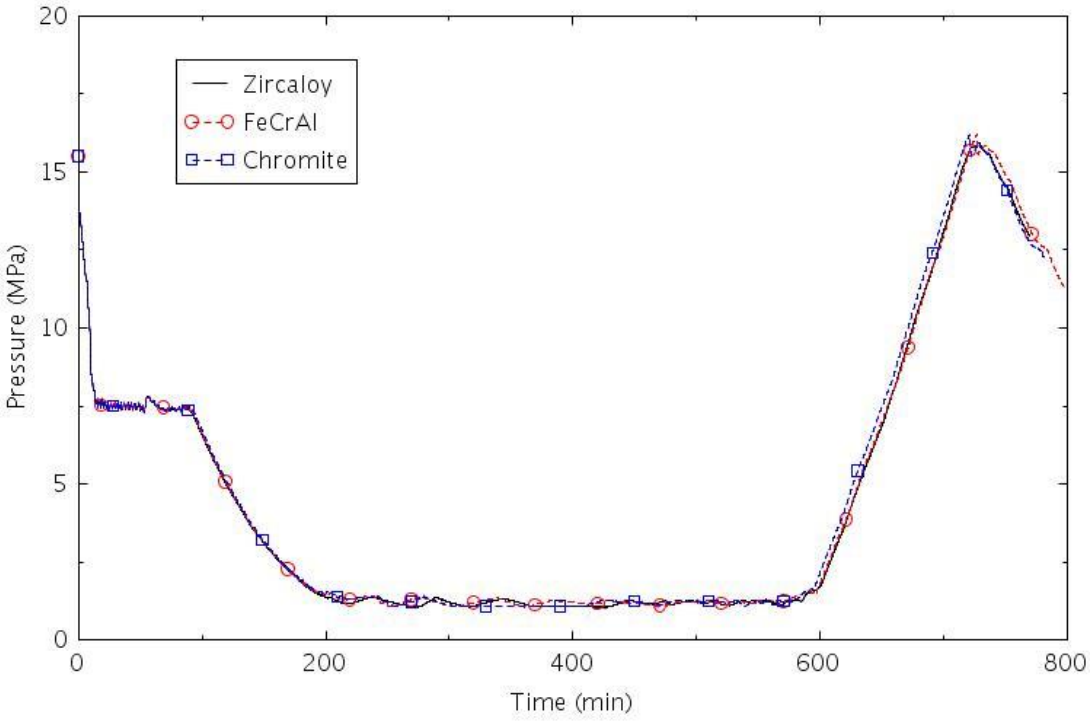

Figure 2-175. Pressure in the pressurizer (LOSC-182a).

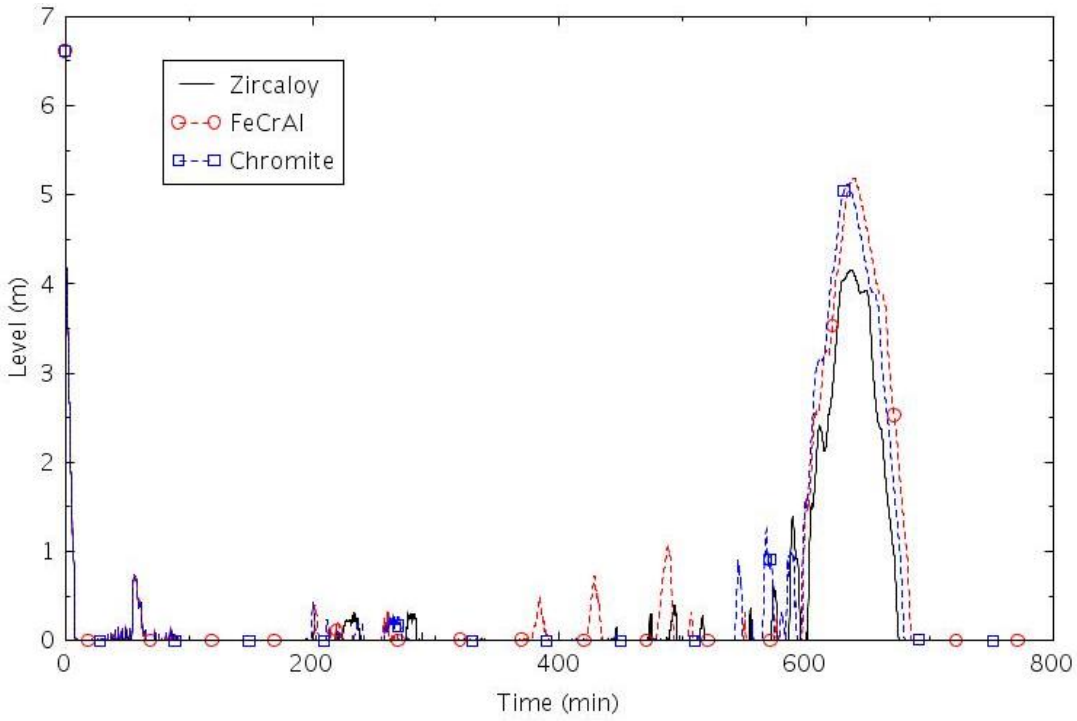

Figure 2-176. Collapsed liquid level in the pressurizer (LOSC-182a).

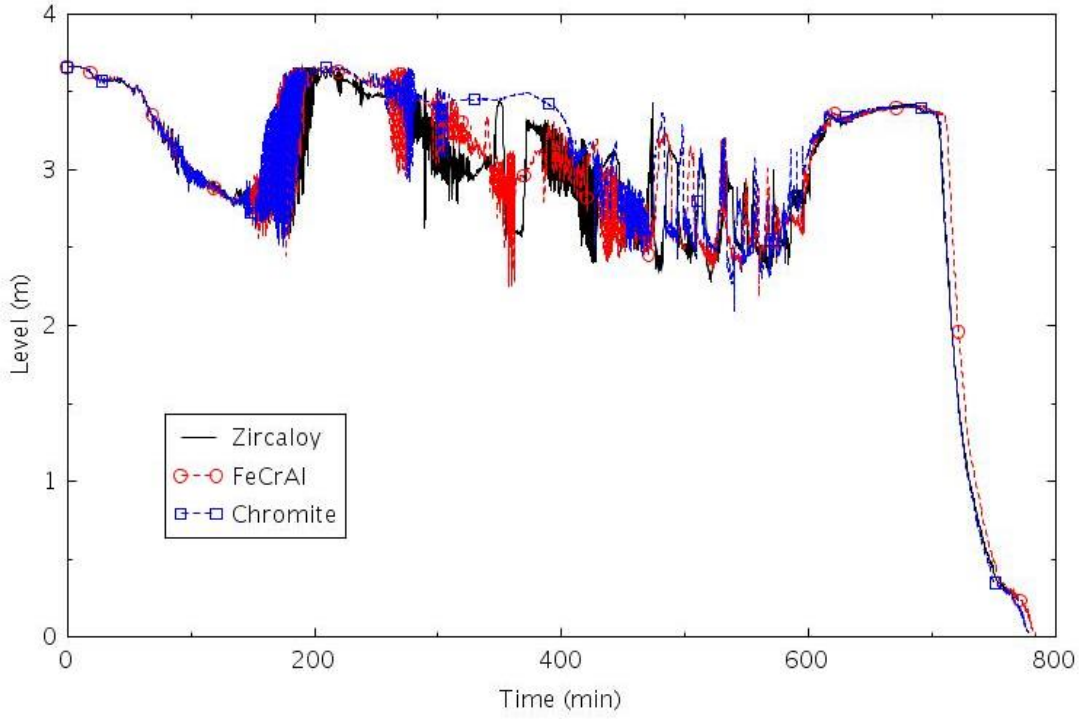

Figure 2-177. Collapsed liquid level in the central core channel (LOSC-182a).

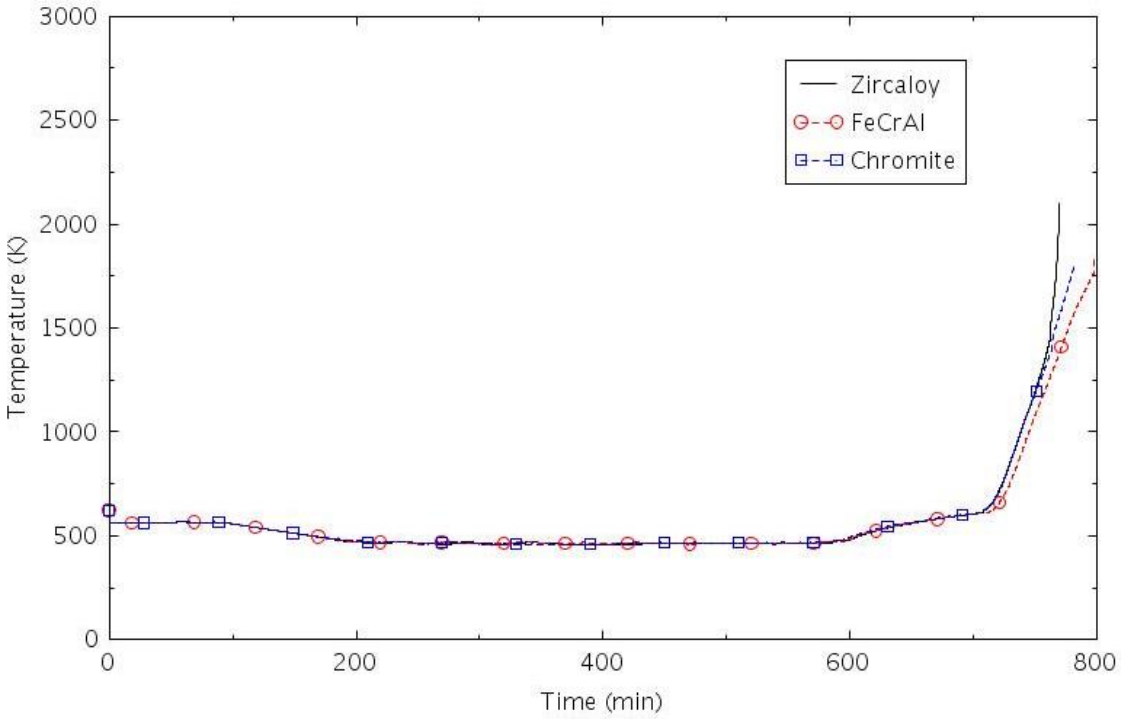

Figure 2-178. Maximum cladding temperature (LOSC-182a).

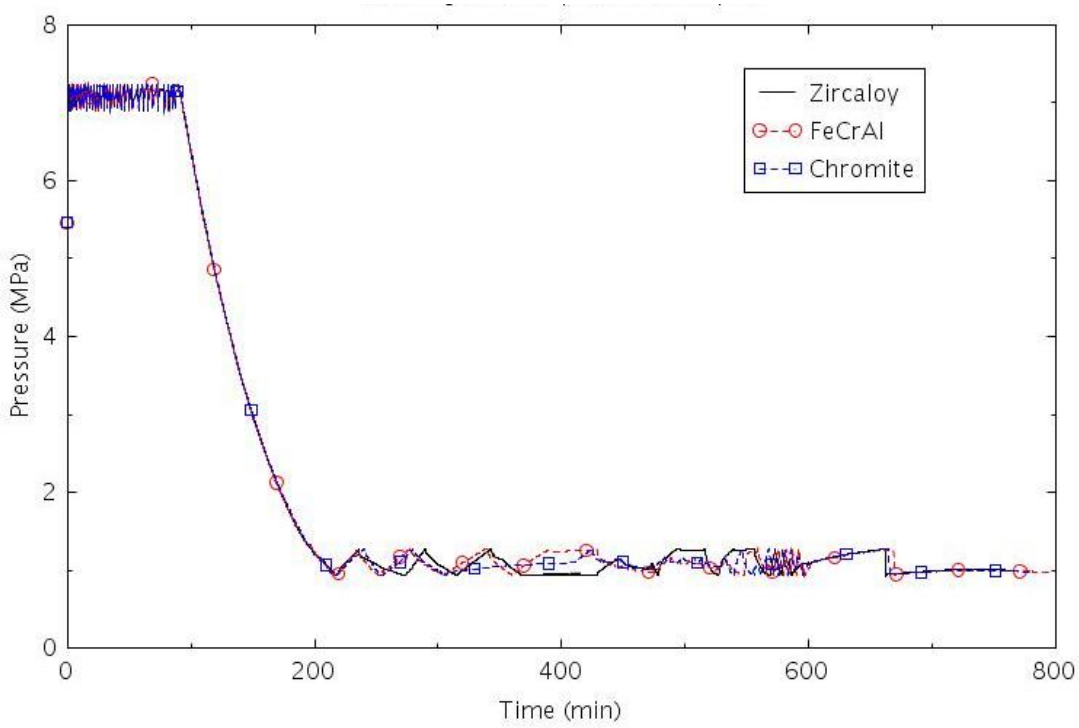

Figure 2-179. Pressure in SG B (LOSC-182a).

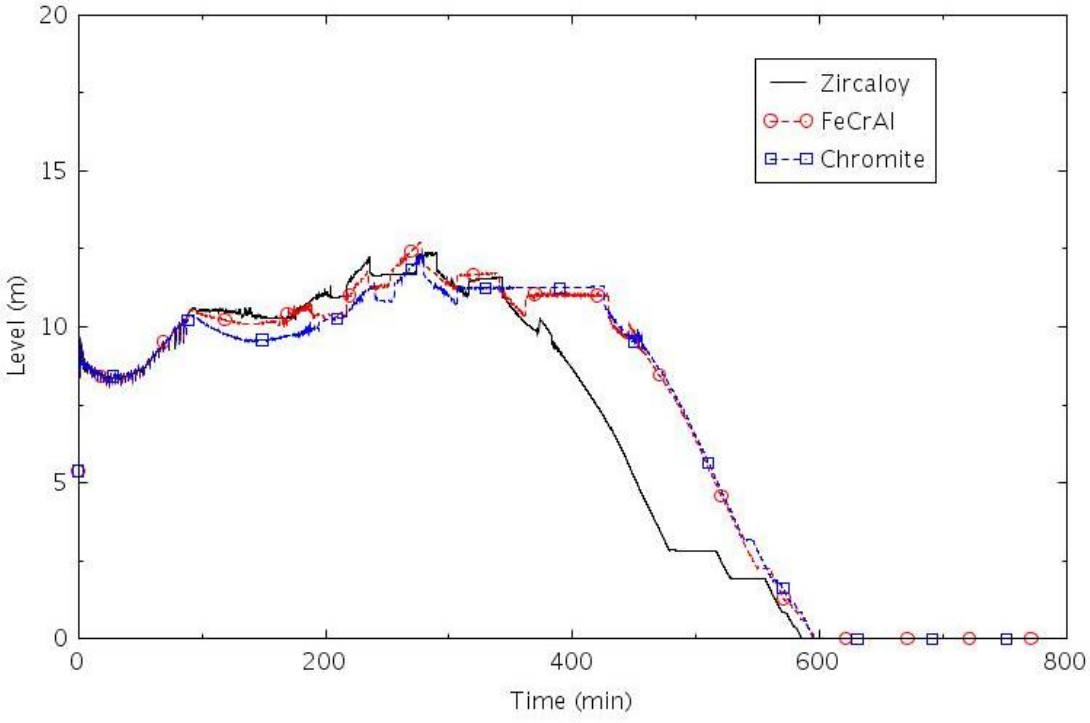

Figure 2-180. Collapsed liquid level in SG B (LOSC-182a).

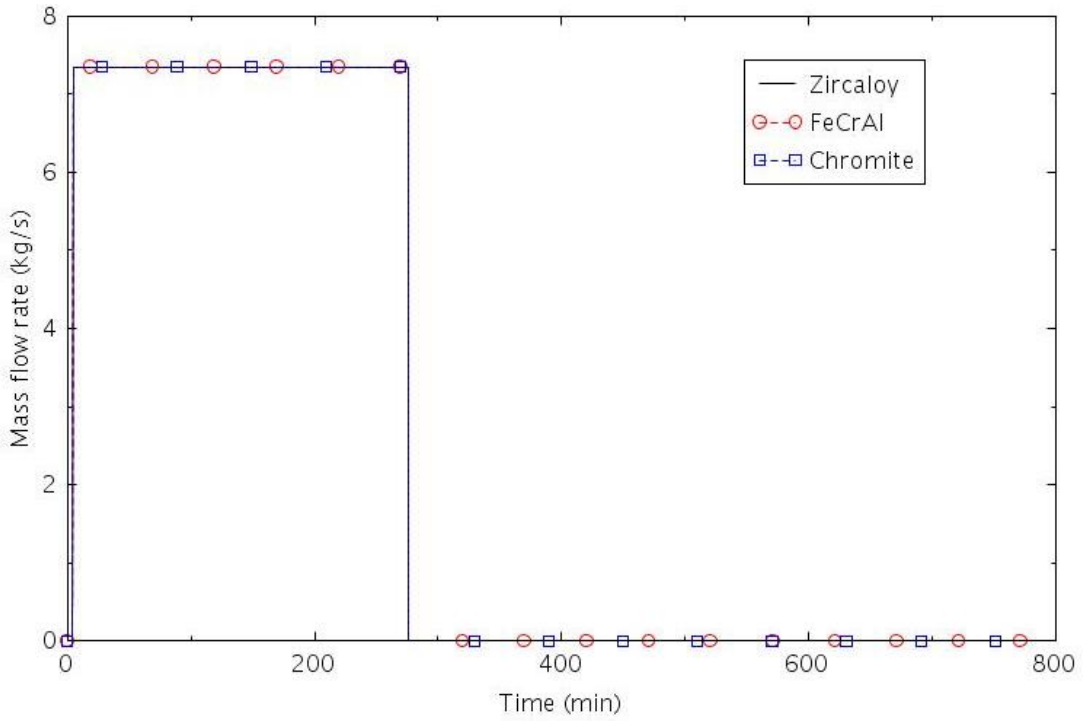

Figure 2-181. AFW flow rate to SG B (LOSC-182a).

2.3.3.5 LOSC-182b

This scenario assumes that one motor-driven AFW pump is available, that the RCP pump seals fail, and that no high-pressure injection is available. The pump seal failures produce an initial leakage of 0.011 m^3/s (182 gpm) per pump. Since power is available in this scenario, the cause of the seal failure is not mechanistic due to overheating, as is generally modeled in an SBO. The seal failure was assumed to conservatively occur simultaneously with the turbine trip.

The calculated sequences of events are shown in Table 2-35. The event was initiated by the turbine trip at 0.0 s, which caused the TSVs to close and a direct reactor trip. The first lift of the SG PORVs occurred within 30 s. The SIAS occurred at 4 minutes on low reactor pressure and the AFW was initiated 30 seconds later. The HPSI was assumed to fail. The RCPs were tripped at 52 minutes. The RCS coolant inventory decreased continuously due to flow through the ruptured pump seals and lack of HPSI. The core began to uncover near 8 hours. The AFW was terminated shortly thereafter because the ECST was depleted. Core damage occurred near 10 hours. The differences between calculations were generally negligible before the core began to uncover. The time between when the core began to uncover and core damage occurred was 83 minutes with Zircaloy, 94 minutes with FeCrAl, and 88 minutes with Chromite. The calculated amount of hydrogen produced during the transients varied significantly between claddings. The amount of hydrogen produced was 2.1 kg for FeCrAl, 8.9 kg for Chromite, and 30.3 kg for Zircaloy.

Table 2-35. Sequence of Events for Scenario LOSC-182b.

	Time (hr:min)		
Event	**Zircaloy**	**FeCrAl**	**Chromite**
Turbine trip	0:00	0:00	0:00
SIAS	0:04	0:04	0:04
AFW initiated	0:04	0:04	0:04
RCPs tripped	0:52	0:52	0:52
Core begins to uncover	8:14	8:19	8:16
AFW terminated	8:19	8:19	8:19

0.5 kg H_2 generation	9:14	9:54	9:25
First cladding rupture	9:20	9:20	9:21
Core damage	9:37	9:54	9:44

The following figures illustrate the effects of the cladding on various parameters. The mass flow through the seals in RCP B is illustrated in Figure 2-182. The fluid going out through the pump seals was mostly liquid before 110 minutes and mostly vapor afterwards. Pressurizer pressure is shown in Figure 2-183. The LOCA initiated by the rupture of the pump seals caused the pressure to decrease until the RCS and SG pressures were nearly the same after 15 minutes. The collapsed liquid level in the pressurizer is shown in Figure 2-184. The LOCA caused the pressurizer to empty within 10 minutes.

The LOCA caused some voiding in the core within a few minutes of the start of the transient as shown in Figure 2-185. The collapsed level remained nearly constant between 100 and 490 minutes, when the level began to decrease sharply. The core began to heat up a few minutes later as shown in Figure 2-186.

The pressure in SG B is shown in Figure 2-187. The pressure was generally between the open and close setpoints of the SG PORVs. The collapsed liquid level in SG B is shown in Figure 2-188 and the AFW flow is shown in Figure 2-189. Although the AFW flow was initiated at 4 minutes, the collapsed liquid level did not increase significantly until after the RCPs were tripped at 52 minutes. The levels then increased until the AFW was manually shut off near 200 minutes. The collapsed levels then decreased until about 320 minutes when the AFW was manually restarted. The AFW was terminated near 500 minutes because the ECST was depleted of liquid.

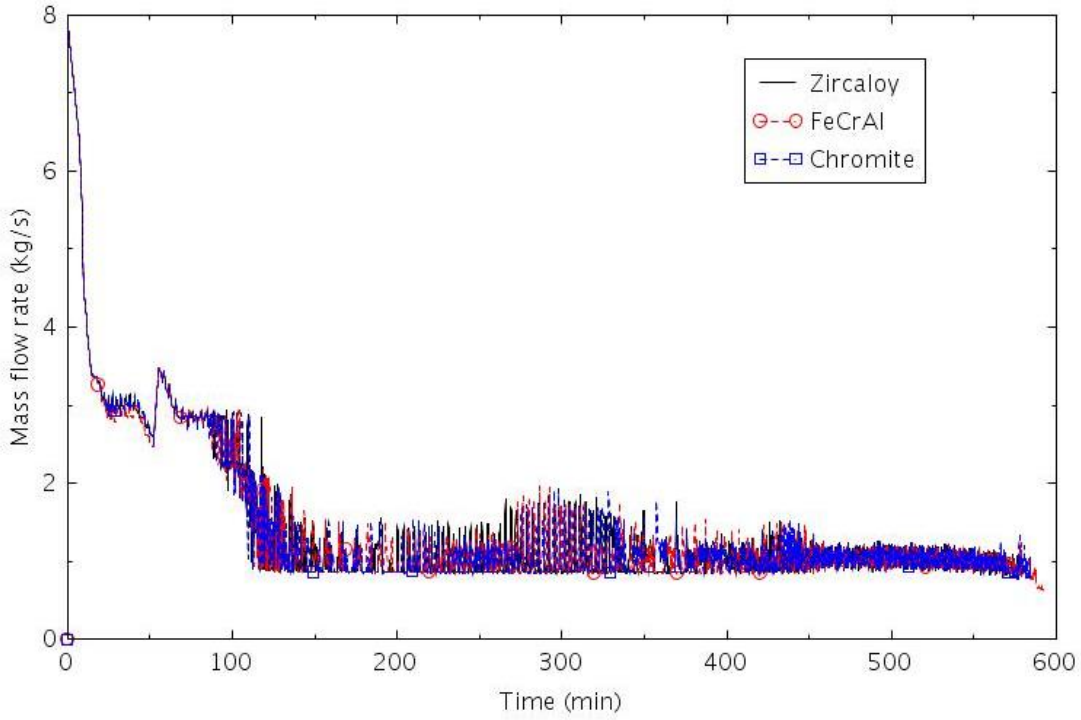

Figure 2-182. Mass flow rate through the seals of RCP B (LOSC-182b).

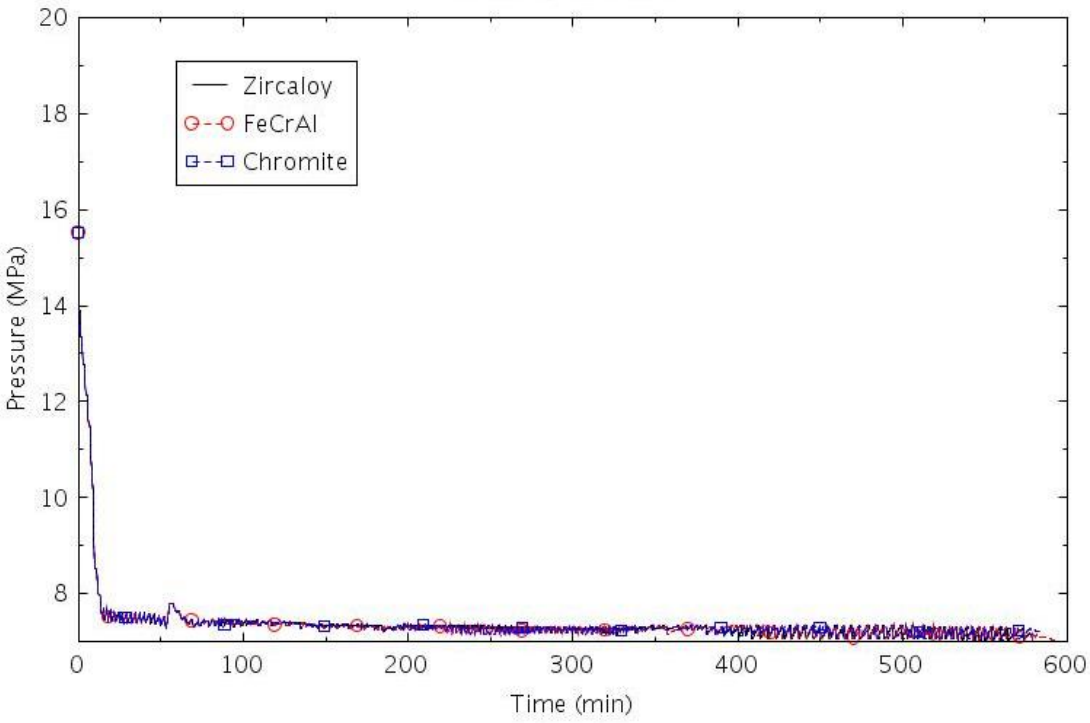

Figure 2-183. Pressure in the pressurizer (LOSC-182b).

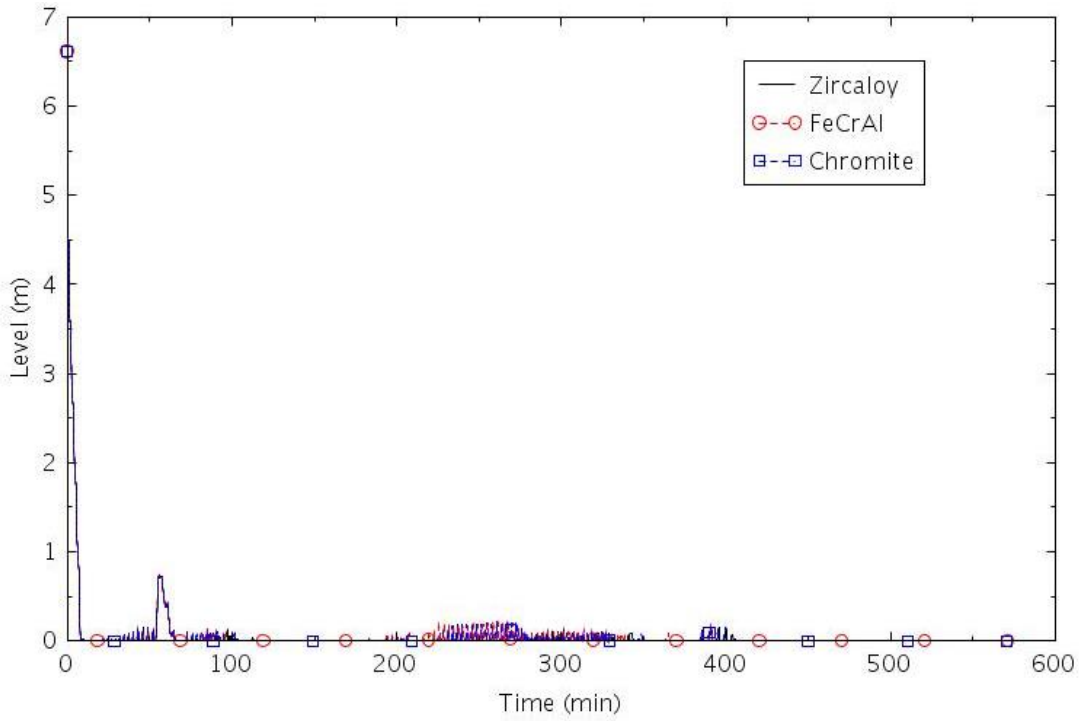

Figure 2-184. Collapsed liquid level in the pressurizer (LOSC-182b).

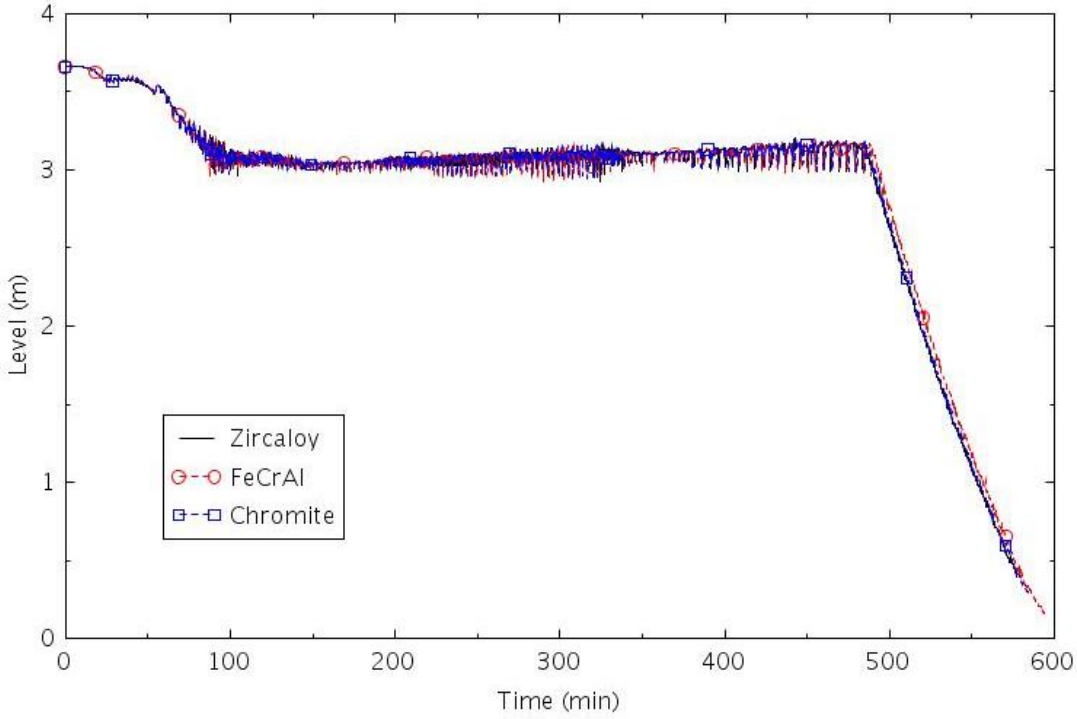

Figure 2-185. Collapsed liquid level in the central core channel (LOSC-182b).

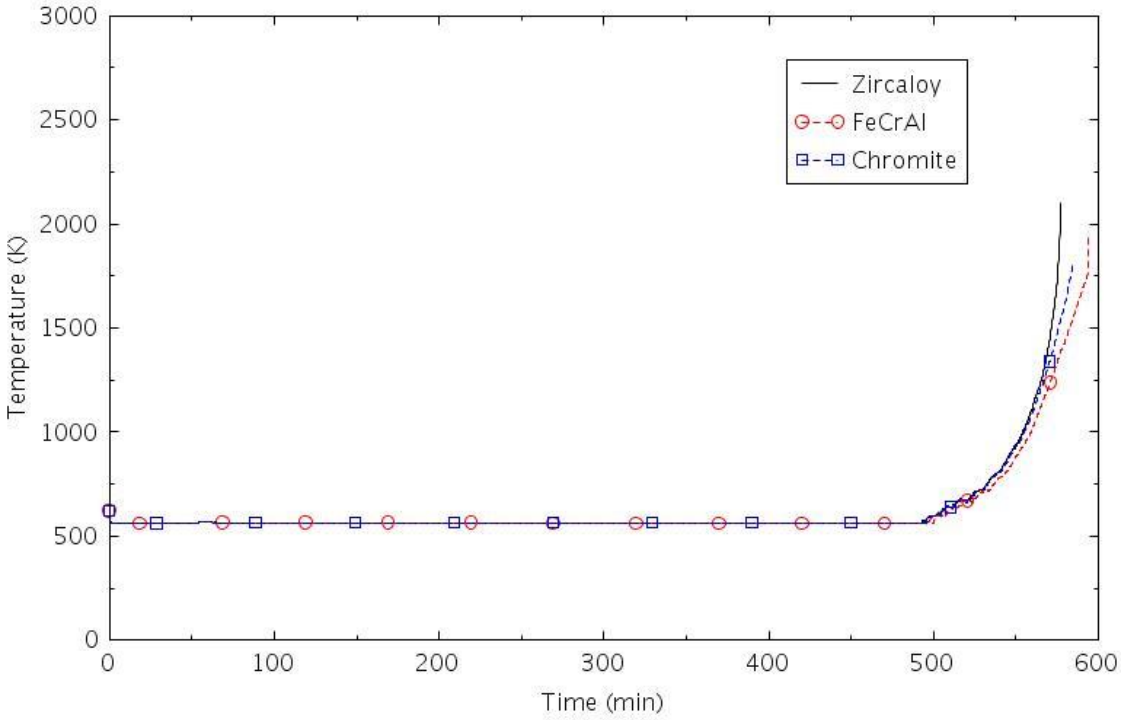

Figure 2-186. Maximum cladding temperature (LOSC-182b).

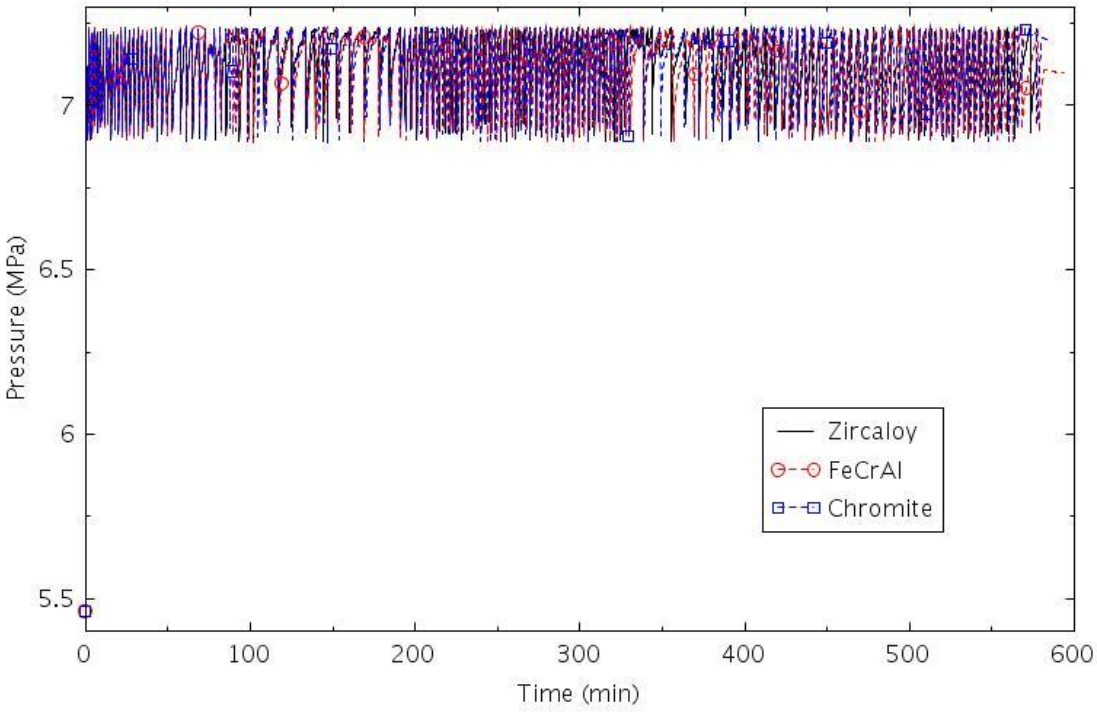

Figure 2-187. Pressure in SG B (LOSC-182b).

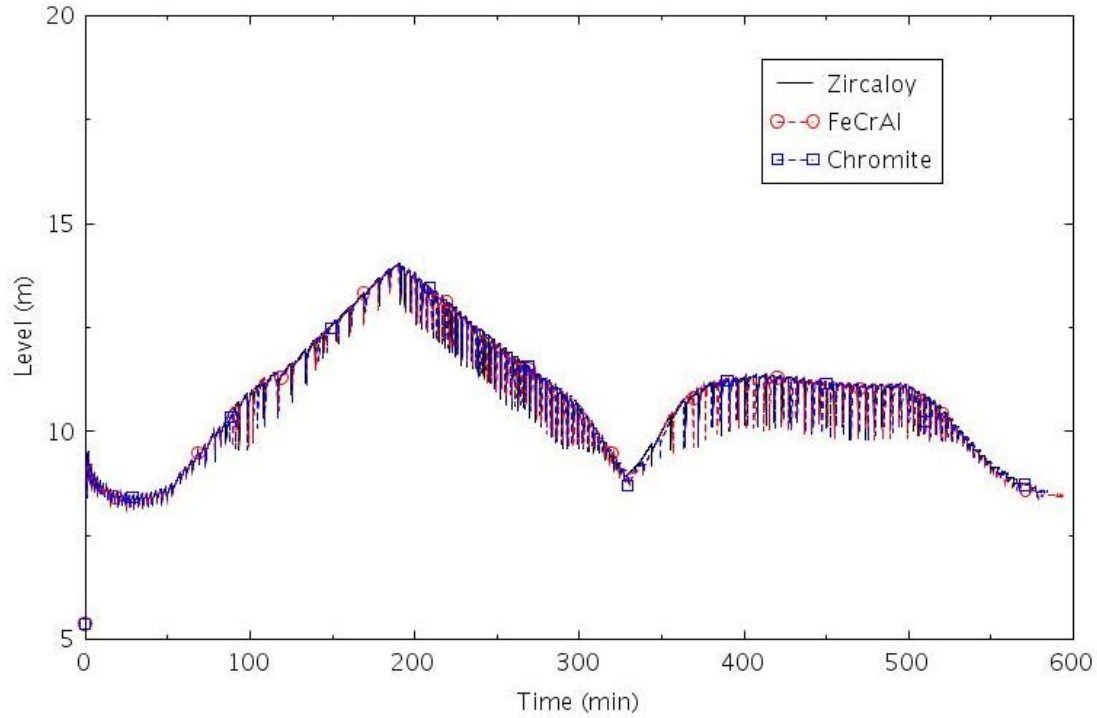

Figure 2-188. Collapsed liquid level in SG B (LOSC-182b).

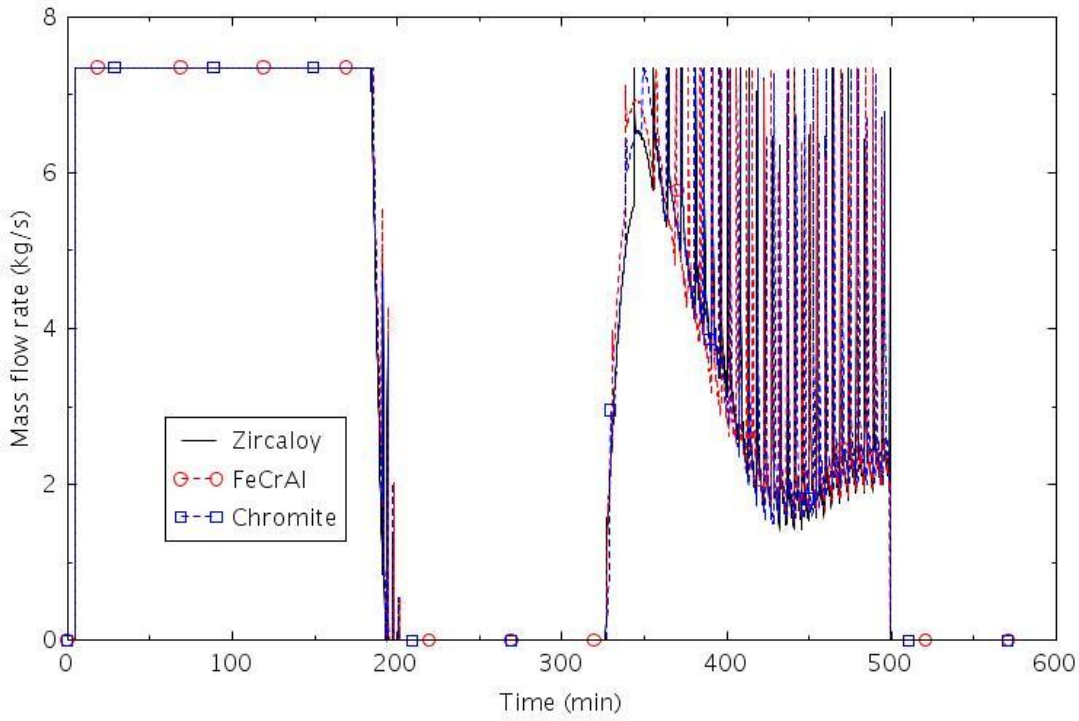

Figure 2-189. AFW flow rate to SG B (LOSC-182b).

2.3.3.6 LOSC-76

This scenario assumes that one motor-driven AFW pump is available, that the RCP pump seals fail, that no high-pressure injection is available, and that the operators manually initiate SSC at 1.5 hours, the same time as assumed in Section 3.1.4.1 of (NRC, 2012). The pump seal failures produce an initial leakage of 0.0048 m^3/s (76 gpm) per pump. Since power is available in this scenario, the cause of the seal failure is not mechanistic due to overheating, as is generally modeled in an SBO. The seal failure was assumed to conservatively occur simultaneously with the turbine trip. The PORVs were opened as necessary to obtain a 56°C/hr (100°F/hr) cooldown rate in the steam generators. The cooldown was terminated when the SGs reached 0.93 MPa (134.7 psia), so that the turbine-driven AFW pumps would be available if needed. Thereafter, the PORVs opened as needed to control the SG pressure between 0.93 MPa (134.7 psia) and 1.27 MPa (184.7 psia).

The calculated sequences of events are shown in Table 2-36. The event was initiated by the turbine trip at 0.0 s, which caused the TSVs to close and a direct reactor trip. The first lift of the SG PORVs occurred within 30 s. The RCP pump seals were assumed to fail simultaneously with the turbine trip. The SIAS occurred at about 9 minutes on low reactor pressure and the AFW was initiated 30 seconds later. The HPSI was assumed to fail. The RCS coolant inventory decreased continuously due to flow through the ruptured pump seals and lack of HPSI. The RCPs were tripped at 115 minutes. The operators were assumed to manually initiate a controlled cooldown of the SGs beginning at 90 minutes. The resulting depressurization of the RCS resulted in accumulator injection near 130 minutes. The AFW was terminated near 5 hours, because the ECST was depleted. The SGs were empty near 9 hours. The core began to uncover near 12 hours. The differences between calculations were generally small before the core began to uncover. The time between when the core began to uncover and core damage occurred was 70 minutes with Zircaloy, 87 minutes with FeCrAl, and 78 minutes with Chromite. The calculated amount of hydrogen produced during the transients varied significantly between claddings. The amount of hydrogen produced was 2.7 kg for FeCrAl, 6.2 kg for Chromite, and 83.3 kg for Zircaloy.

Table 2-36. Sequence of Events for Scenario LOSC-76.

	Time (hr:min)		
Event	**Zircaloy**	**FeCrAl**	**Chromite**
Turbine trip	0:00	0:00	0:00
SIAS	0:09	0:09	0:10
AFW initiated	0:10	0:10	0:10
SSC begins	1:30	1:30	1:30
RCPs tripped	1:45	1:45	1:45
Accumulator flow initiated	2:11	2:11	2:11
SSC ends	3:33	3:33	3:33
AFW terminated	4:42	4:42	4:42
Accumulator flow terminated	7:26	7:51	7:29
All SGs empty	9:14	9:13	9:24
Pressurizer PORV begins to cycle	11:23	11:21	11:22
PRT rupture disk opens	11:24	11:22	11:23
Core begins to uncover	11:50	11:48	11:50
0.5 kg H_2 generation	12:22	13:08	13:04
First cladding rupture	12:55	12:56	13:03
Core damage	13:00	13:15	13:08

The following figures illustrate the effects of the cladding on various parameters. The mass flow through the seals in RCP B is illustrated in Figure 2-190. The increase in mass flow near 560 minutes was due to an increase in RCS pressure. The leakage was small enough that mostly liquid passed through the seals until about 700 minutes. Pressurizer pressure is shown in Figure 2-191. The LOCA initiated by the rupture of the pump seals caused the pressure to decrease until the RCS and SG pressures were nearly the same near 30 minutes. The decrease in pressure at 90 minutes was due to the SSC. The RCS and SG pressures were closely coupled until all the SGs were empty near 560 minutes. Thereafter, boiling in the core caused the pressure to increase until the pressurizer PORV began to cycle near 680 minutes. As shown in Figure 2-192, the pressurizer completely filled with liquid shortly before the PORV began to cycle. The pressurizer then began to drain again and was empty by the end of the calculation.

The LOCA caused some voiding in the core within 20 minutes of the start of the transient, as shown in Figure 2-193. The onset of accumulator injection near 130 minutes eventually refilled the core. The level decreased somewhat after accumulator injection was terminated near 450 minutes. The level decreased sharply near 700 minutes. The core began to heat up near 710 minutes, as shown in Figure 2-194.

The pressure in SG B is illustrated in Figure 2-195. The pressure was generally between the open and close setpoints of the SG PORVs until 90 minutes, when the manual SSC was initiated. After the cooldown was terminated near 200 minutes, the operators were assumed to open and close the PORVs as necessary to maintain the pressure between 0.93 MPa (134.7 psia) and 1.27 MPa (184.7 psia).

The collapsed liquid level in SG B is shown in Figure 2-196 and the AFW flow is shown in Figure 2-197. The collapsed levels decreased after AFW flow was terminated near 280 min.

Scenario LOSC-76 was identical to Scenario LOSC-182a, except that there was less leakage through the pump seals. A comparison of Table 2-34 and Table 2-36 shows that the core uncovered only about 5 minutes later, on average, with the smaller leakage. This unexpected result can be explained as follows: The smaller leakage in Scenario LOSC-76 resulted in less energy removal through the break, which required additional heat transfer to the SGs in order to remove core decay heat and cool down the RCS. Consequently, the SGs were empty about 40 minutes earlier, on average, in Scenario LOSC-76. The earlier dryout of the SGs resulted in an earlier pressurization of the RCS and more RCS mass lost out the PORV near the end of the calculation in Scenario LOSC-76.

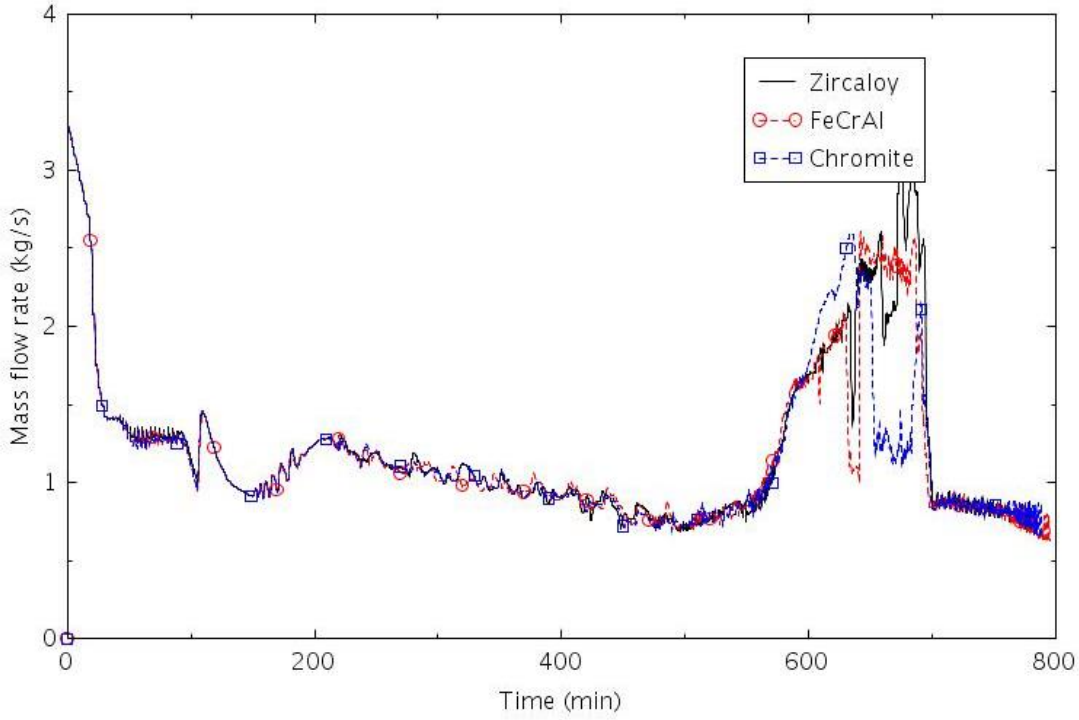

Figure 2-190. Mass flow rate through the seals of RCP B (LOSC-76).

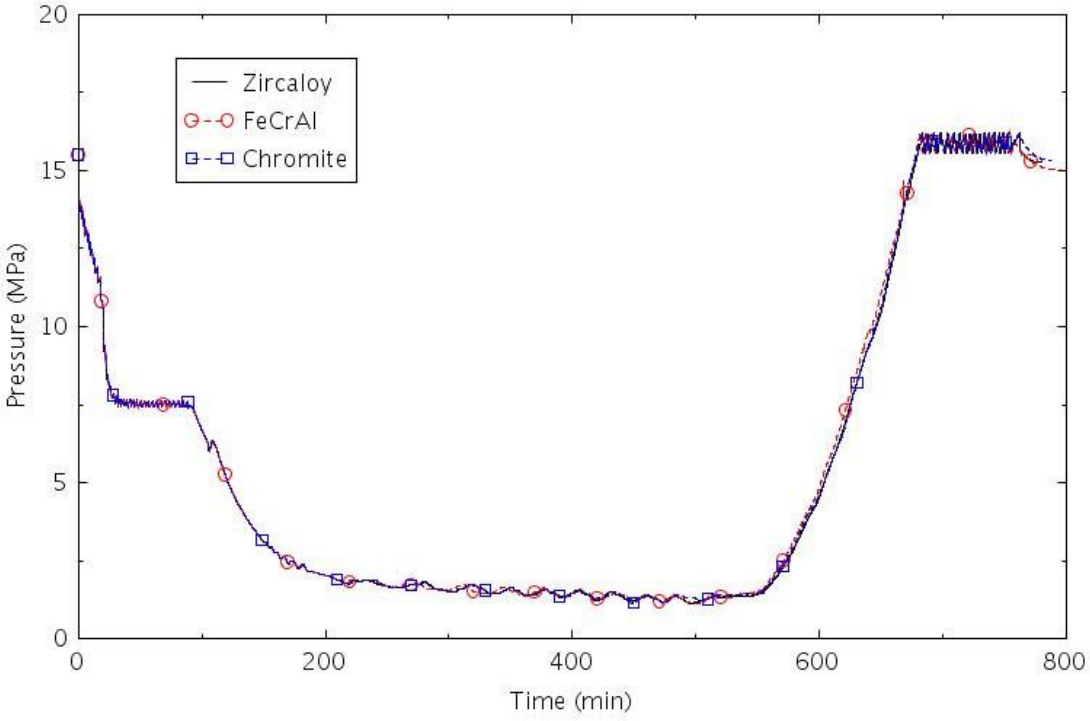

Figure 2-191. Pressure in the pressurizer (LOSC-76).

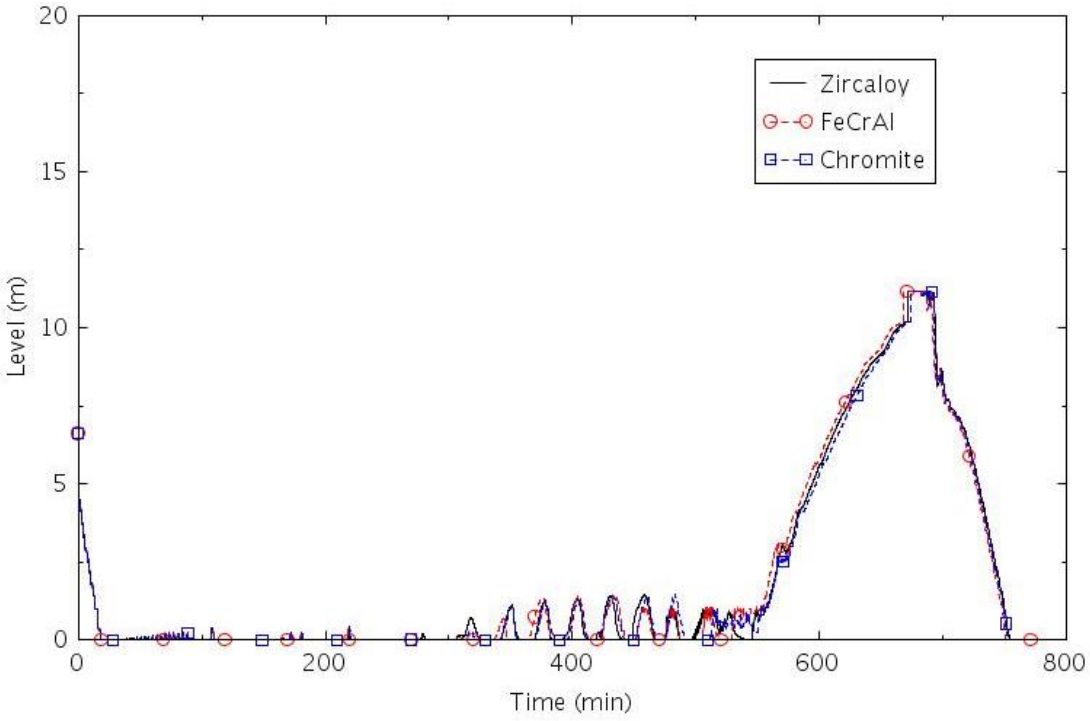

Figure 2-192. Collapsed liquid level in the pressurizer (LOSC-76).

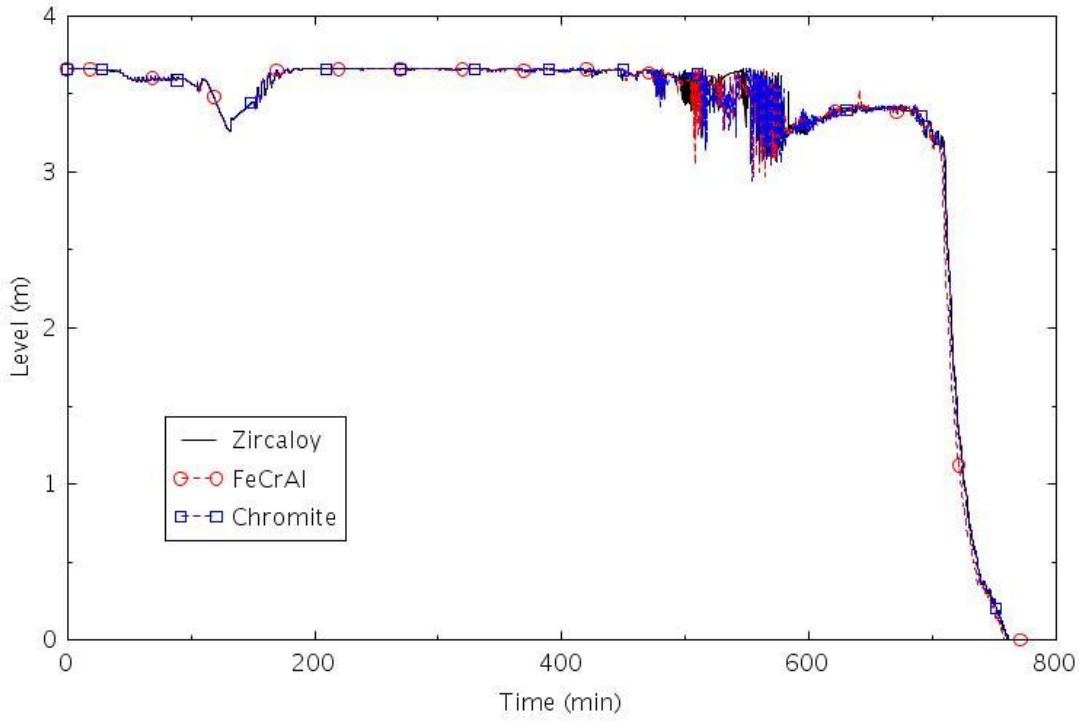

Figure 2-193. Collapsed liquid level in the central core channel (LOSC-76).

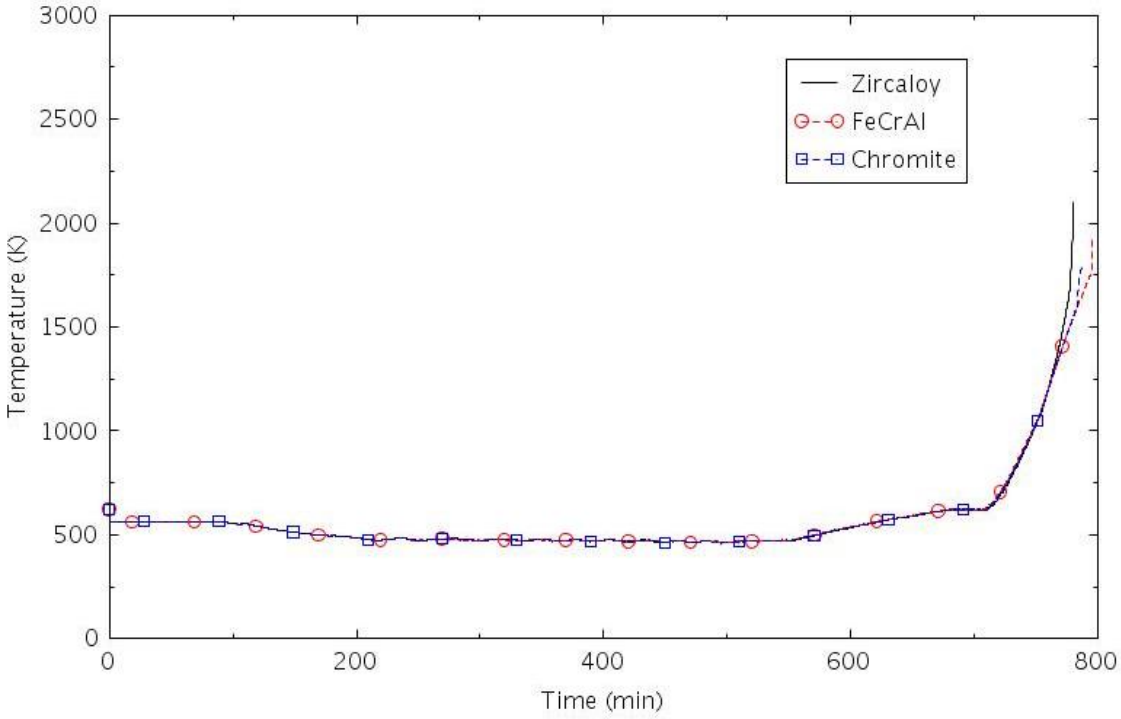

Figure 2-194. Maximum cladding temperature (LOSC-182a).

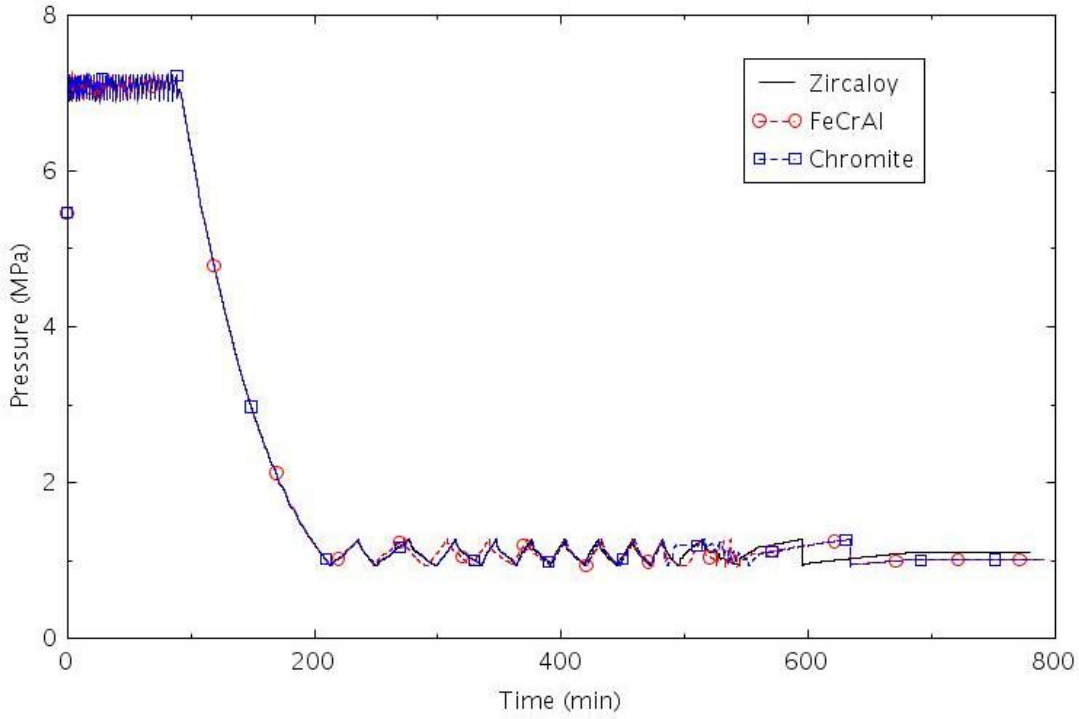

Figure 2-195. Pressure in SG B (LOSC-76).

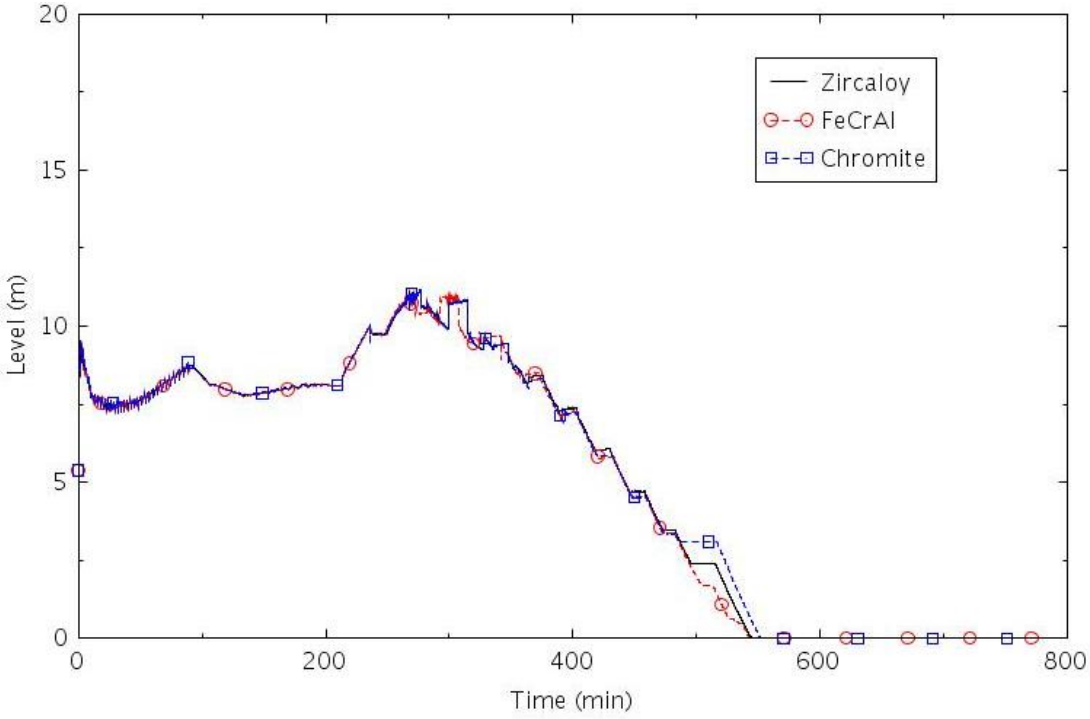

Figure 2-196. Collapsed liquid level in SG B (LOSC-76).

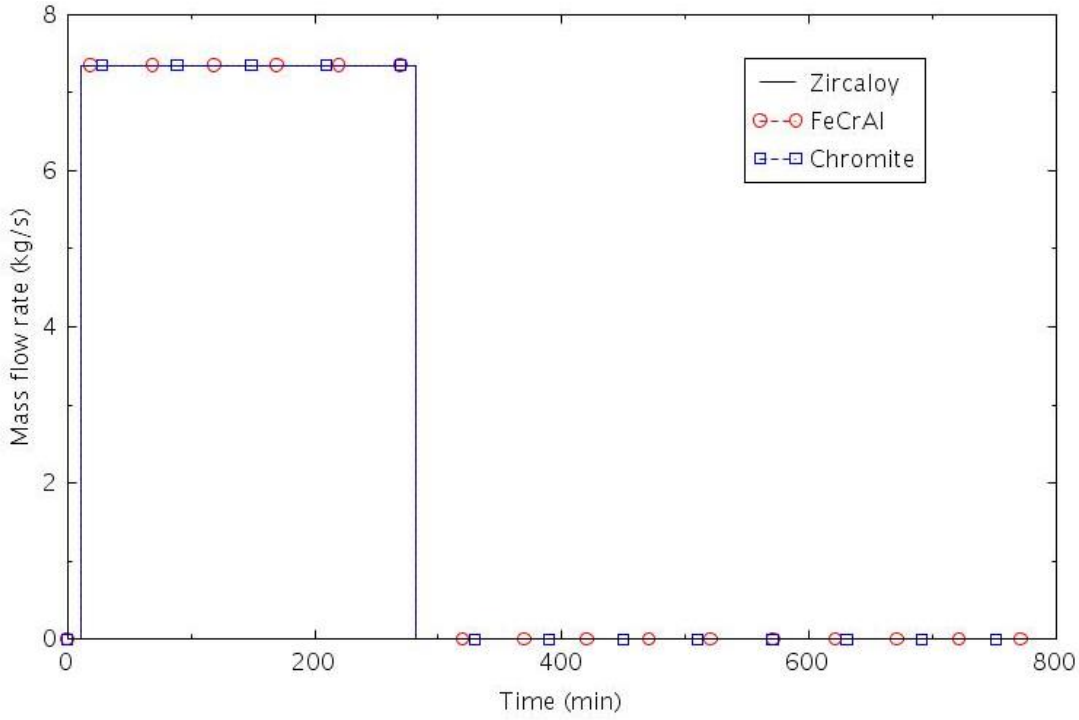

Figure 2-197. AFW flow rate to SG B (LOSC-76).

2.3.3.7 LOSC-480

This scenario assumes that one motor-driven AFW pump is available, that the RCP pump seals fail, that no high-pressure injection is available, and that the operators manually initiate SSC. The pump seal failures produce an initial leakage of 0.030 m^3/s (480 gpm) per pump. Since power is available in this

scenario, the cause of the seal failure is not mechanistic due to overheating, as is generally modeled in an SBO. The seal failure was assumed to conservatively occur simultaneously with the turbine trip. The SSC was assumed to begin at 1.5 hours, the same time as assumed in Section 3.1.4.1 of (NRC, 2012). The PORVs were opened as necessary to obtain a 56°C/hr (100°F/hr) cooldown rate in the steam generators. The cooldown was terminated when the SGs reached 0.93 MPa (134.7 psia), so that the turbine-driven AFW pumps would be available if needed. Thereafter, the PORVs opened as needed to control the SG pressure between 0.93 MPa (134.7 psia) and 1.27 MPa (184.7 psia).

The calculated sequences of events are shown in Table 2-37. The event was initiated by the turbine trip at 0.0 s, which caused the TSVs to close and a direct reactor trip. The first lift of the SG PORVs occurred within 30 s. The RCP pump seals were assumed to fail simultaneously with the turbine trip. The SIAS occurred at about 1minute on low reactor pressure and the AFW was initiated 30 seconds later. The HPSI was assumed to fail. The RCPs were tripped at 18 minutes. The RCS coolant inventory decreased continuously due to flow through the ruptured pump seals and lack of HPSI. The operators were assumed to manually initiate a controlled cooldown of the SGs beginning at 90 minutes. The resulting depressurization of the RCS resulted in accumulator injection at 131 minutes. The accumulators emptied near 205 minutes. The AFW flow was terminated near 5 hours, because the ECST was depleted. However, the SGs were not empty at the end of the calculations. The core began to uncover near 5 hours. The calculations were terminated by either high cladding temperature or severe fuel rod ballooning at the top of the core. The differences between calculations were negligible before the SSC ended, and were generally small afterwards. The increased variability after the SSC ended was more likely due to numerical issues than to the differences between claddings. The calculations with the Zircaloy and Chromite claddings were terminated due to severe cladding ballooning in the middle core channel. Consequently, the cladding in those calculations did not reach temperatures as high as obtained in the previous calculations and less hydrogen was produced. The amount of hydrogen produced was 0.2 kg for Chromite, 0.7 kg for FeCrAl, and 1.0 kg for Zircaloy.

Table 2-37. Sequence of Events for Scenario LOSC-480.

	Time (hr:min)		
Event	**Zircaloy**	**FeCrAl**	**Chromite**
Turbine trip	0:00	0:00	0:00
SIAS	0:01	0:01	0:01
AFW initiated	0:02	0:02	0:02
RCPs tripped	0:18	0:18	0:18
SSC begins	1:30	1:30	1:30
Accumulator flow initiated	2:11	2:11	2:11
Accumulator flow terminated	3:25	3:26	3:25
SSC ends	3:37	3:38	3:38
AFW terminated	5:02	4:41	4:40
Core begins to uncover	5:13	4:51	4:53
First cladding rupture	5:53	NA	5:39
0.5 kg H_2 generation	5:59	6:17	6:01[a]
Core damage	6:03	6:17	5:46

a. Estimated.

The following figures illustrate the effects of the cladding on various parameters. The mass flow through the seals in RCP B is illustrated in Figure 2-198. The flow rate increased after accumulator flow was initiated near 130 minutes. The accumulators emptied near 205 minutes and the mass flow decreased shortly thereafter.

Pressurizer pressure is shown in Figure 2-199. The LOCA initiated by the rupture of the pump seals caused the pressure to decrease until the RCS and SG pressures were nearly the same near 5 minutes. The decrease in pressure at 90 minutes was due to the SSC. The RCS and SG pressures were closely coupled for the remainder of the calculations. The collapsed liquid level in the pressurizer is shown in Figure 2-200. The LOCA caused the pressurizer to empty within a few minutes.

The LOCA caused some voiding in the core within a few minutes of the start of the transient, as shown in Figure 2-201. The core did not begin to heat up until about 300 minutes, as shown in Figure 2-202. The cladding did not reach the termination temperatures of 2099 K for Zircaloy and 1804 K for Chromite before the calculations were terminated, due to severe ballooning of the cladding that reduced the flow area of the middle channel to near zero.

The pressure in SG B is illustrated in Figure 2-203. The pressure was generally between the open and close setpoints of the SG PORVs until 90 minutes, when the manual SSC was initiated. After the cooldown was terminated near 220 minutes, the operators were assumed to open and close the PORVs as necessary to maintain the pressure between 0.93 MPa (134.7 psia) and 1.27 MPa (184.7 psia).

The collapsed liquid level in SG B is shown in Figure 2-204 and the AFW flow is shown in Figure 2-205. Even though the AFW flow was initiated at 2 minutes, the collapsed liquid level decreased until the unaffected RCPs were tripped near 20 minutes. The level then increased until the SSC was initiated at 90 minutes. The levels remained nearly constant until the SSC ended near 220 minutes. The levels then increased until AFW was terminated near 290 minutes. The collapsed levels then generally decreased, although there was considerable variation in the calculated levels within a single SG. The break was big enough in all these calculations that the SGs were not empty when the calculations were terminated.

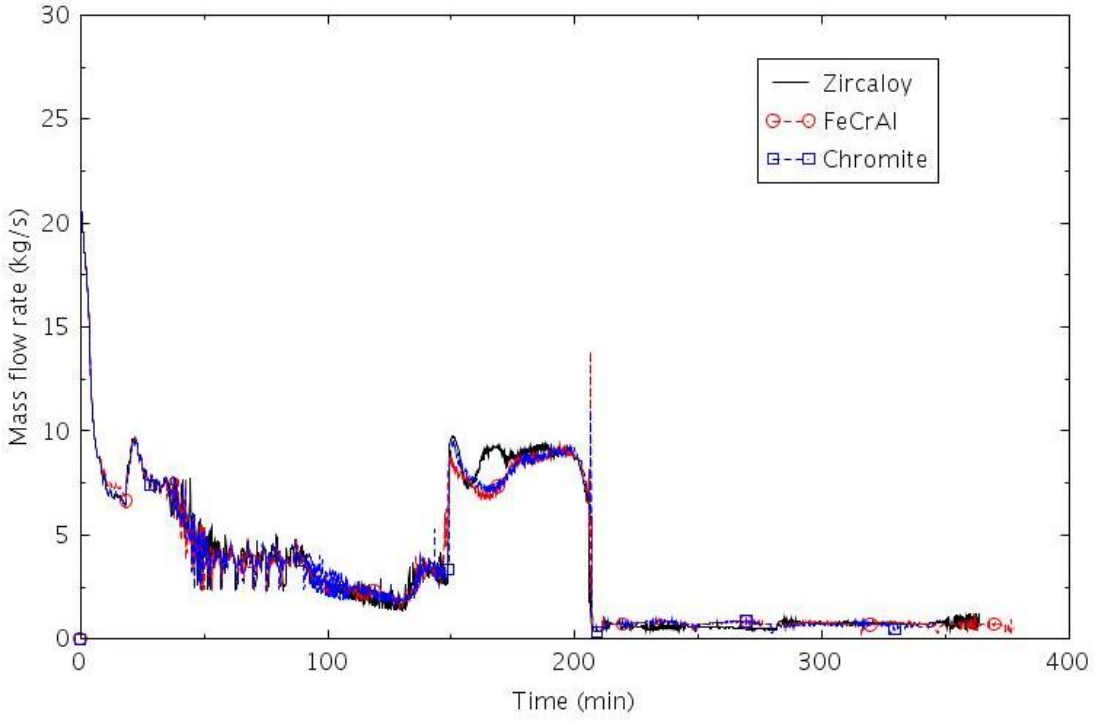

Figure 2-198. Mass flow rate through the seals of RCP B (LOSC-480).

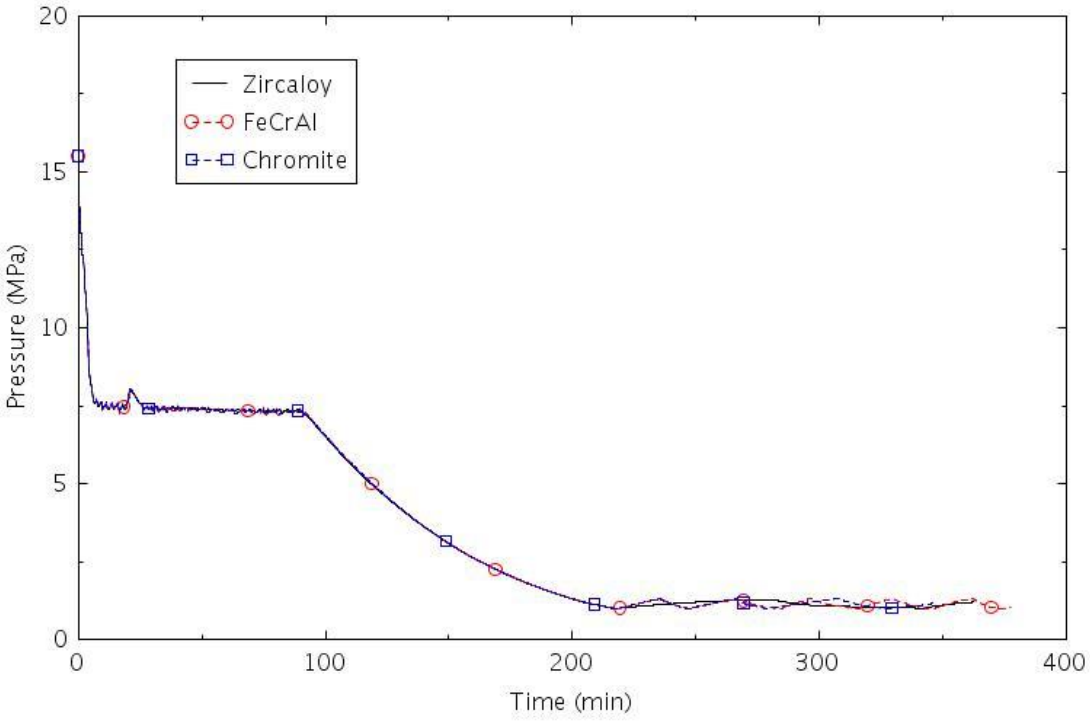

Figure 2-199. Pressure in the pressurizer (LOSC-480).

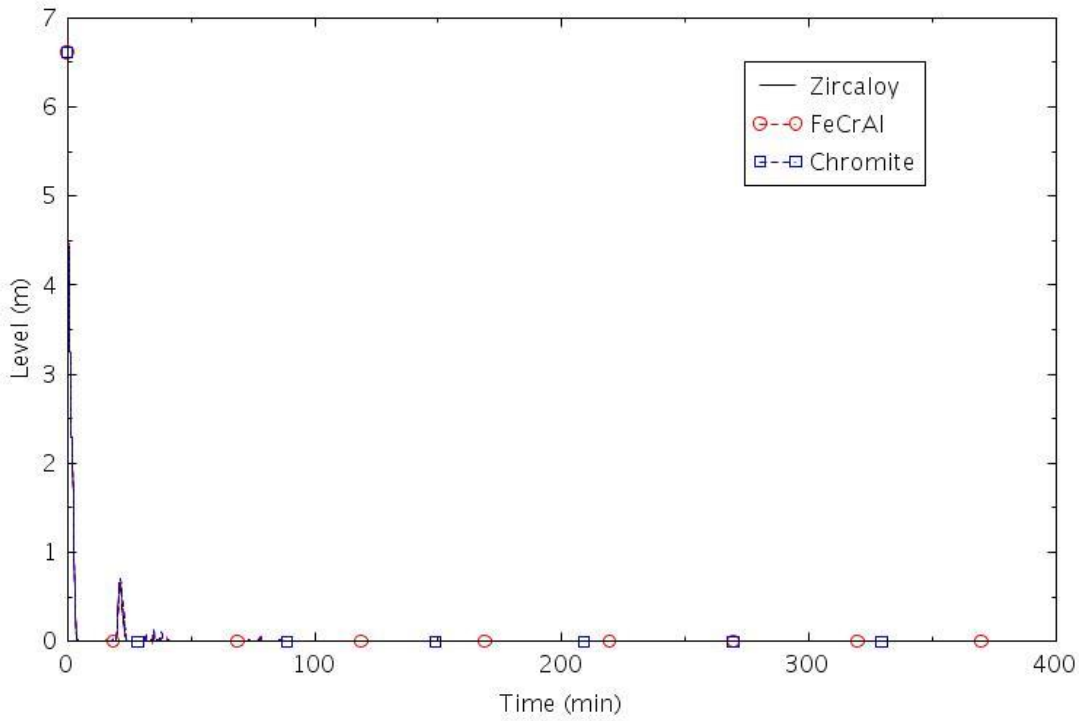

Figure 2-200. Collapsed liquid level in the pressurizer (LOSC-480).

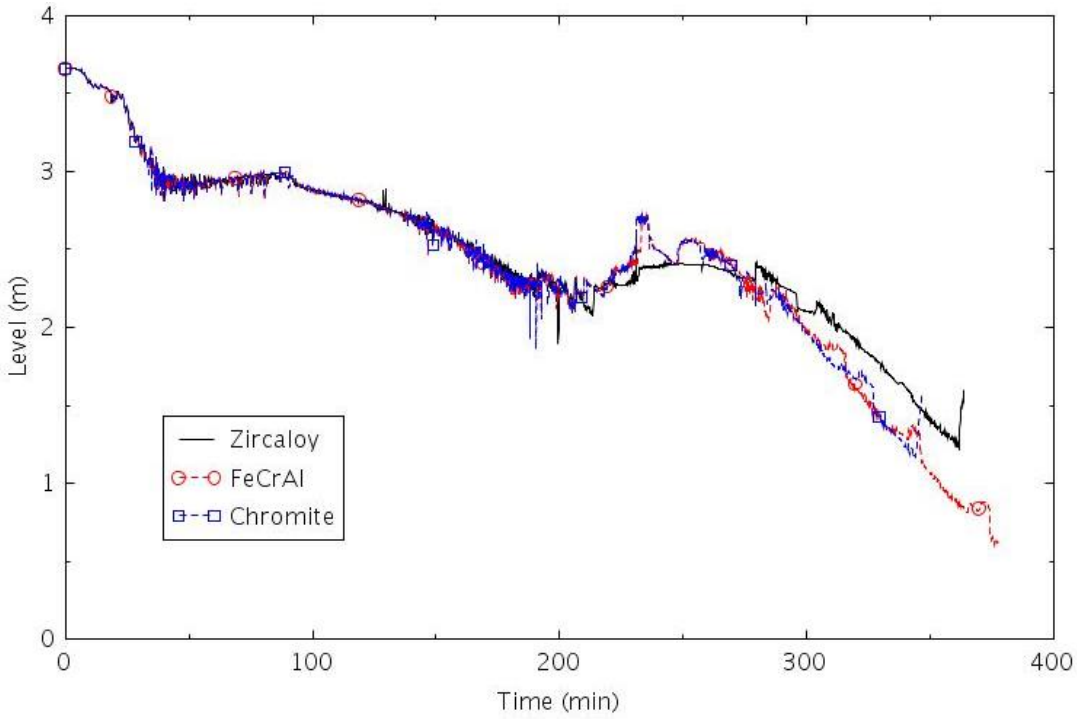

Figure 2-201, Collapsed liquid level in the central core channel (LOSC-480).

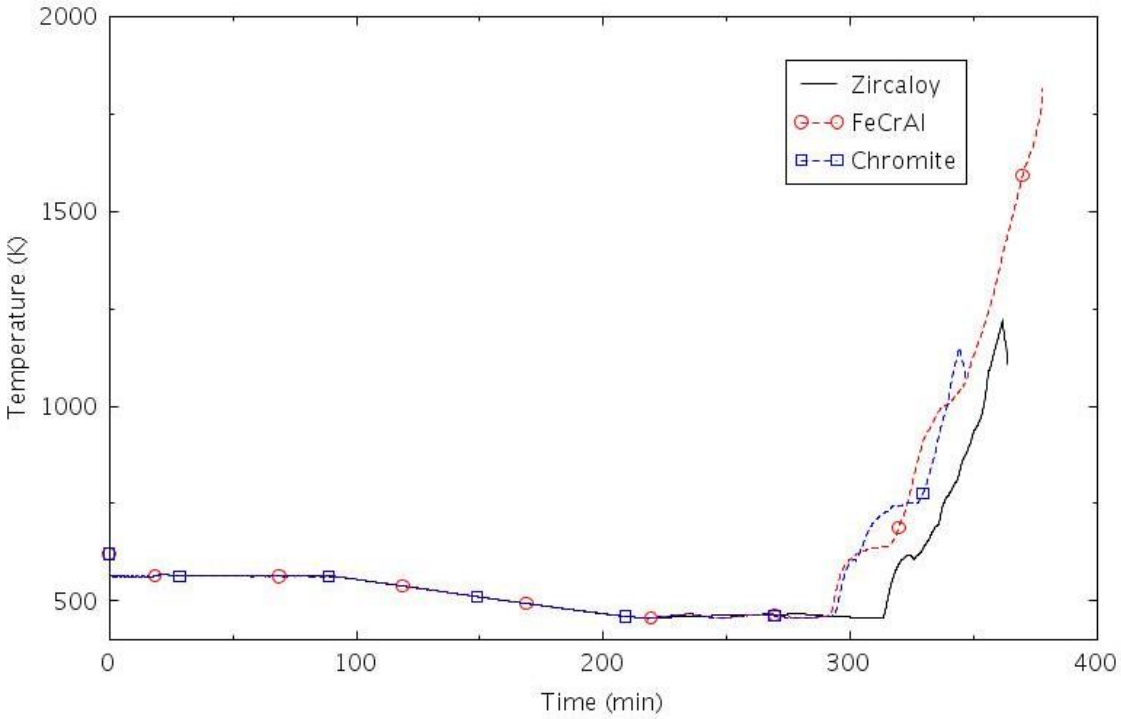

Figure 2-202. Maximum cladding temperature (LOSC-480).

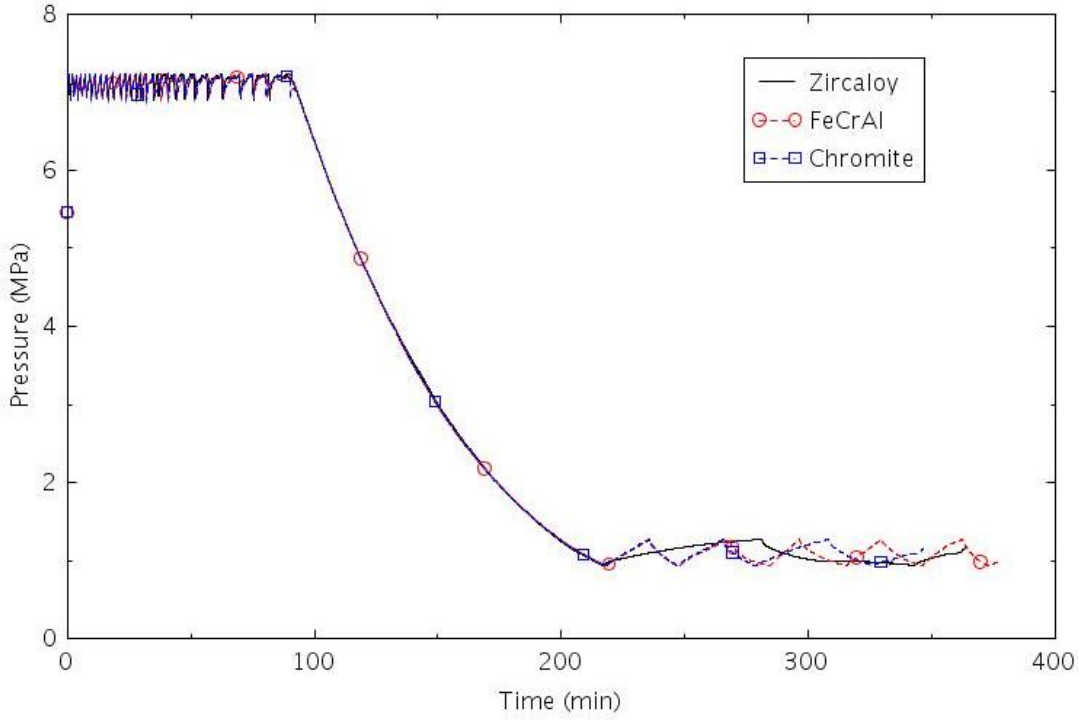

Figure 2-203. Pressure in SG B (LOSC-480).

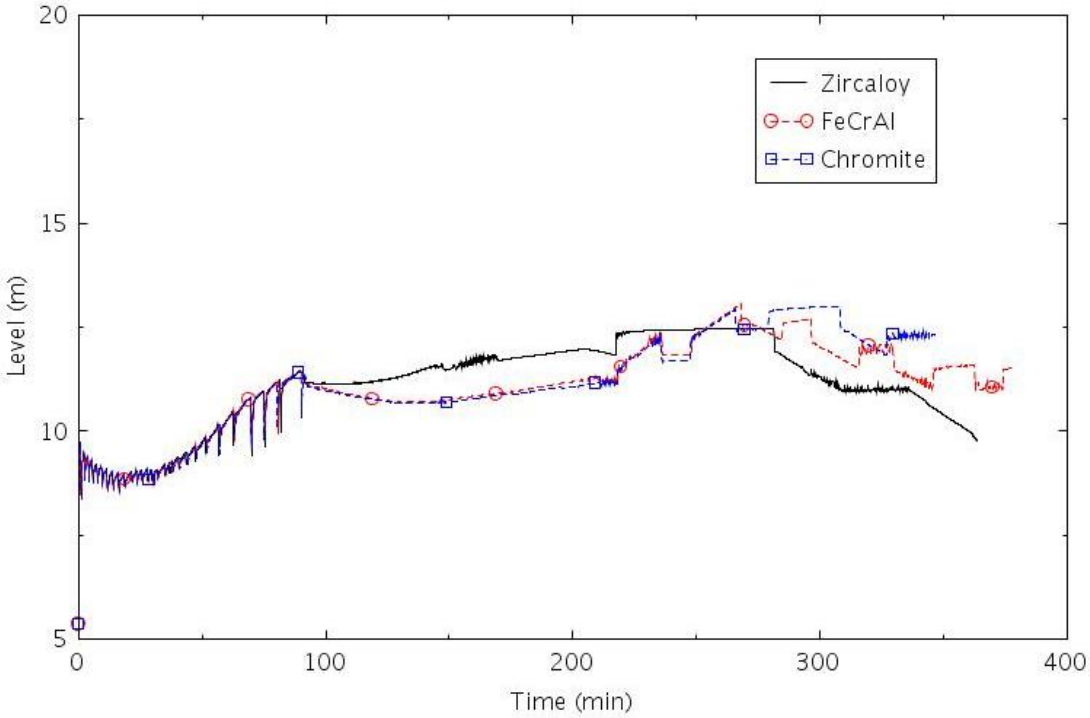

Figure 2-204. Collapsed liquid level in SG B (LOSC-480).

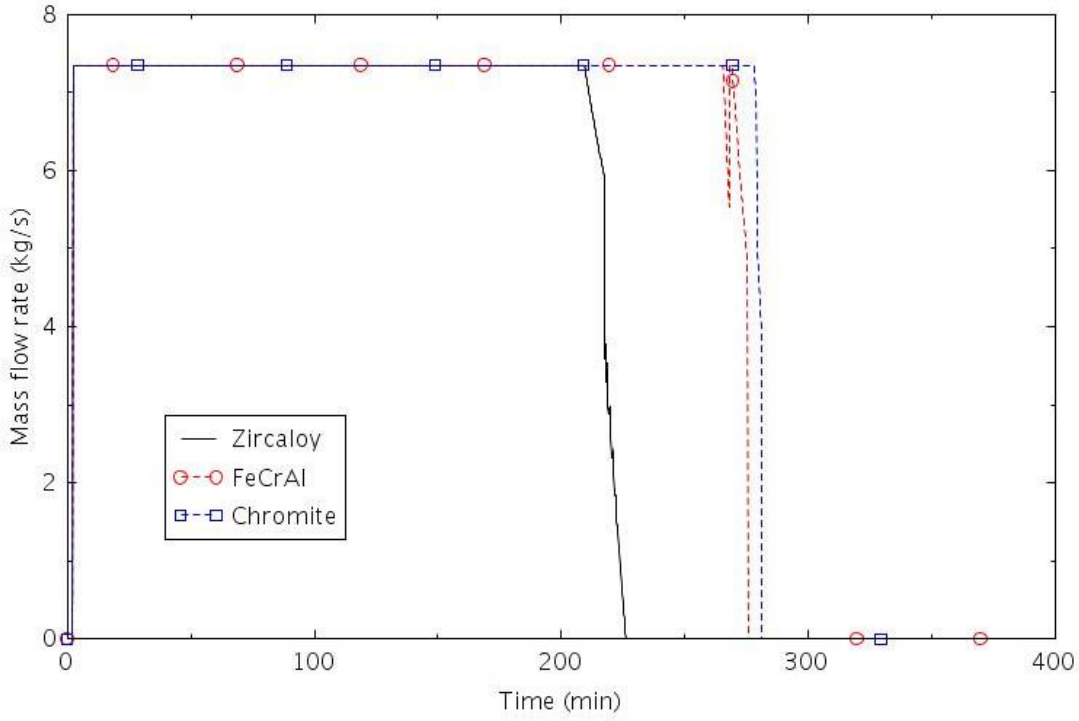

Figure 2-205. AFW flow rate to SG B (LOSC-480).

2.3.4 Turbine Trip Analysis Results

Table 2-38 presents a summary of the RELAP5-3D results for time to core uncovery, time to 0.5 kg of hydrogen production, and time to core damage for turbine trip scenarios with Zircaloy and ATF claddings. The most severe scenarios in terms of the shortest time to core damage are PORV-1, in which AFW is available but a PORV LOCA occurs without safety injection; and TRANS-1, in which there is no feedwater and no safety injection.

Table 2-38. Summary of RELAP5-3D Time Results for Turbine Trip Scenarios with Zircaloy and ATF Claddings.

Scenario	Time to core uncovery (hr:min)			Time to 0.5 kg H_2 (hr:min)			Time to core damage (hr:min)		
	Zircaloy	FeCrAl	Chromite	Zircaloy	FeCrAl	Chromite	Zircaloy	FeCrAl	Chromite
TRANS-1	1:46	1:46	1:46	2:00	2:29	2:26	2:25	2:32	2:27
TRANS-2	13:40	13:19	13:06	14:09	14:36	14:25	14:51	14:49	14:25
PORV-1	2:36	2:35	2:35	3:01	3:23	3:06	3:14	3:23	3:16
LOSC-182a	11:47	11:53	11:48	12:16	13:10	12:44	12:49	13:17	13:01
LOSC-182b	8:14	8:19	8:16	9:14	9;54	9:25	9:37	9:54	9:44
LOSC-76	11:50	11:48	11:50	12:22	13:08	13:04	13:00	13:15	13:08
LOSC-480	5:13	4:51	4:53	5:59	6:17	6:01	6:03	6:17	5:46

Table 2-39 compares the times to core damage for the ATF designs with those for the existing design with Zircaloy cladding in different turbine trip scenarios. On average, the gain in coping time is about 13 minutes for FeCrAl. For Chromite, the average loss in coping time is about 2 minutes, but this difference is likely due to numerical causes. A better estimate of the gain in coping time can be obtained by subtracting the time to core uncovery from the time to core damage in Table 2-38 and averaging. Using this metric, the gain in coping time increases to about 18 minutes for FeCrAl and 6 minutes for Chromite. The gain in coping time with the ATF designs is modest for the turbine trip scenarios.

With the above relatively small increase of the time to core damage from the RELAP5-3D simulation results, a change to the general transient PRA model (event tree, fault tree, success criteria, or human reliability analysis) is not warranted. The risk benefit on behalf of the CDF brought by the ATF designs would be very small and is not conducted in this analysis.

However, the RELAP5-3D results show a clear benefit in adopting the ATF designs as much less hydrogen is produced at the time of core damage. Table 2-40 compares the hydrogen production for the ATF designs with those for the existing Zircaloy-clad design in different turbine trip scenarios. The hydrogen production is generally significantly smaller with the ATF claddings. The one exception is Scenario LOSC-480, where the hydrogen production with FeCrAl is 75% of that with Zircaloy. However, this result is atypical, because the calculation with Zircaloy was terminated due to severe cladding ballooning rather than maximum cladding temperature. Consequently, the Zircaloy cladding did not reach temperatures as high as those with FeCrAl, which resulted in less hydrogen production than typical for Zircaloy. Excluding Scenario LOSC-480, the average hydrogen production with FeCrAl was 4.1% of that with Zircaloy. The average hydrogen production with Chromite was 16.9% of that with Zircaloy.

Table 2-39. Time to Core Damage Comparisons for Turbine Trip Scenarios with ATF Designs.

Section	Scenario	Description	Time to core damage (hr:min)				
			Zircaloy	FeCrAl	Δt (FeCrAl)	Chromite	Δt (Chromite)
2.3.3.1	TRANS-1	General transient, no FW, no HPSI	2:25	2:32	0:07	2:27	0:02
2.3.3.2	TRANS-2	General transient, no FW, HPSI	14:51	14:49	-0:02	14:25	-0:26
2.3.3.3	PORV-1	PORV LOCA with AFW	3:14	3:23	0:09	3:16	0:02
2.3.3.4	LOSC-182a	RCP seal LOCA, 182 gpm, AFW, SSC	12:49	13:17	0:28	13:01	0:12
2.3.3.5	LOSC-182b	RCP seal LOCA, 182 gpm, AFW, no SSC	9:37	9:54	0:17	9:44	0:07
2.3.3.6	LOSC-76	RCP seal LOCA, 76 gpm, AFW, SSC	13:00	13:15	0:15	13:08	0:08
2.3.3.7	LOSC-480	RCP seal LOCA, 480 gpm, AFW, SSC	6:03	6:17	0:14	5:46	-0:17

Table 2-40. H2 Production Comparisons for Turbine Trip Scenarios with ATF Designs.

Section	Scenario	Description	Total H_2 (kg)			H_2 %	
			Zircaloy	FeCrAl	Chromite	FeCrAl	Chromite
2.3.3.1	TRANS-1	General transient, no FW, no HPSI	90.1	1.5	1.8	1.7	2.0
2.3.3.2	TRANS-2	General transient, no FW, HPSI	100.6	2.7	2.3	2.7	2.3
2.3.3.3	PORV-1	PORV LOCA with AFW	18.9	1.4	5.9	7.3	31.0
2.3.3.4	LOSC-182a	RCP seal LOCA, 182 gpm, AFW, SSC	57.3	1.7	16.6	3.0	29.0
2.3.3.5	LOSC-182b	RCP seal LOCA, 182 gpm, AFW, no SSC	30.3	2.1	8.9	6.9	29.4
2.3.3.6	LOSC-76	RCP seal LOCA, 76 gpm, AFW, SSC	83.3	2.7	6.2	3.2	7.5
2.3.3.7	LOSC-480	RCP seal LOCA, 480 gpm, AFW, SSC	1.0	0.7	0.2	75.0	17.7

2.4 MSLB Scenario Analysis

2.4.1 MSLB PRA Model and Scenarios

The generic SAPHIRE PWR model does not include MSLB event due to its general low risk significance. The MSLB scenarios in the following analysis were developed based on information from deterministic safety analysis report instead of PRA inputs.

2.4.2 MSLB RELAP5-3D Model

The same RELAP5-3D IGPWR model as in (Ma, et al., 2018) was used in this analysis. The details of this are described in (Parisi, et al., 2016). To properly model the MSLB transient, several new features were introduced in the IGPWR nodalization, which are summarized below.

- Nodalization for an MSLB on SG C was introduced. As shown in Figure 2-206, a broken main steam line was assumed at the exit of the SG C, before the MSIV and inside the containment. Both sides of the breaks were connected with the containment, in order to simulate the containment pressurization. The SG break area was set to 1.4 ft^2, simulating the SG flow restrictor. Standard Ransom-Trapp choked model (RELAP5-3D Code Development Team, 2018) was activated during all the calculations.

As shown in

- Figure 2-207, a check-valve component was added on each steam line, before the steam-dump header. The function of the check valve is to avoid backflow from the unbroken SGs.
- Core nodalization was modified by adding two independent thermal-hydraulic (T-H) channels, one modeling a single (hot) fuel assembly (FA) and the other one a single (hot) fuel rod. These new T-H channels are interconnected with the rest of the core, using multiple junctions for simulating core and assembly cross-flows. Each channel has a dedicated heat structure simulating 203 and 1 fuel rod, respectively. The peaking factors for the hot FA and the hot rod are reported in Table 2-41. The peaking factors were derived from Surry FSAR (Dominion, 2007), referring to the 15 by 15 LOPAR FA geometry.
- A 0-D neutron kinetics model was added, implementing Doppler, moderator and boron reactivity coefficients. Two core states were simulated, the no-load (hot zero power, HZP) condition and the full-load (hot full power, HFP) condition.
- Dedicated RELAP5-3D control variables for the automatic calculation of the departure from nucleate boiling ratio (DNBR) were added. The control variables were used in calculating the critical heat flux and the DNBR, according to the W-3 correlation (Tong, 1968). DNBR was calculated for the hot rod, at level 5 (core midplane) and at level 7 (core upper part).

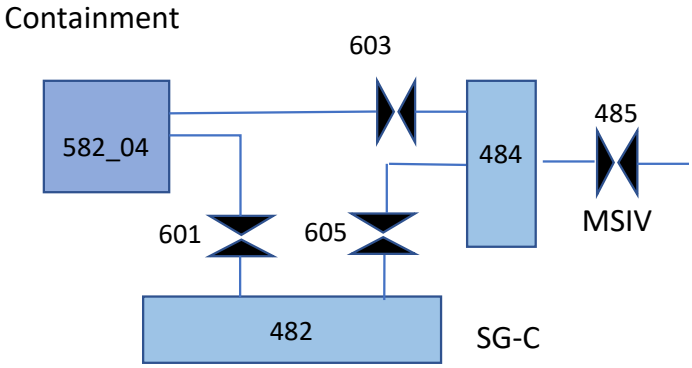

Figure 2-206. Modeling of MSLB on SG C.

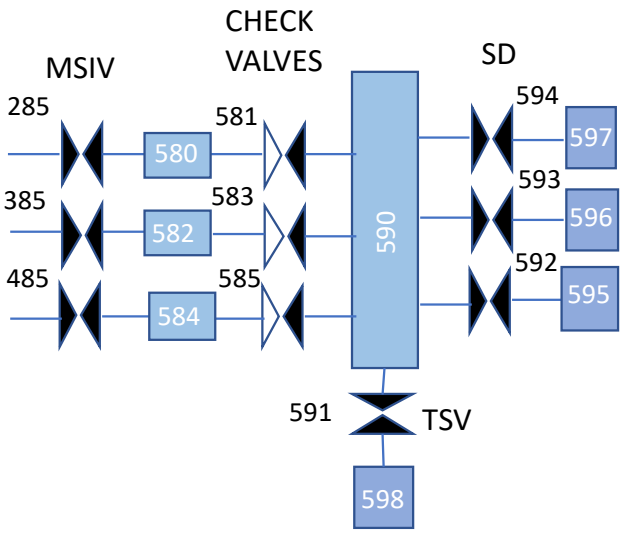

Figure 2-207. Steam line nodalization for MSLB transient.

Table 2-41. Peaking Factors for HZP and HFP.

Parameters	HZP	HFP
Hot FA Enthalpy Rise	1.465	1.465
Hot Channel Enthalpy Rise	1.620	1.580
Hot Channel Peaking Factor	2.397	2.338

2.4.3 MSLB RELAP5-3D Analysis

Before introducing the simulation of detailed MSLB sequences, a MSLB base case is presented below to show the nominal plant responses to a MSLB event.

The MSLB sequence starts with a break of a main steam pipe, or a pipe that carries steam from the SG to the main turbine. The steam release causes an increase in steam flow and a SG depressurization. Depending on the break position, the steam can be released inside or outside the containment. As the SG pressure falls, the steam flow at the break decreases. The depressurization of the SG causes a temperature decrease of the primary coolant, which in turn causes an insertion of positive reactivity due to the positive moderator temperature feedback.

In case the most reactive control rod assembly (CRA) is stuck in its fully withdrawn position, there could be a decrease of the shutdown margin with a possible core re-criticality. The safety injection of borated water by the emergency core cooling system (ECCS) guarantees the final shutdown on the core.

Therefore, a MSLB safety analysis has to demonstrate that: (i) assuming the most reactive CRA stuck and a single failure of the ESF, there is no core and/or primary system damage; (ii) there is no departure from nucleate boiling (DNB), with associated clad rupture; (iii) the energy released to the containment from the worst MSLB scenario does not cause containment failure.

The following systems provide protection against a MSLB: (i) actuation of the ECCS for high steam flow and low RCS average temperature or low main steam line pressure, or high containment pressure signal or manual intervention; (ii) overpower reactor trips and reactor trip upon actuation of the ECCS; (iii) redundant isolation of the feedwater lines; (iv) trip of fast-acting MSIV; (v) flow restrictor installed on each SG at the SG outlet.

The analyses have been performed using best-estimate approach; therefore, choked flow models were used and no additional failures of equipment were considered.

As such, the set of analyses reported hereafter partially follow the approach used in Surry Power Station FSAR (Dominion, 2007), where a predefined set of boundary conditions were identified for maximizing the safety challenges for the reactor fuel.

In particular, three scenarios where investigated: (1) MSLB at HFP (MSLB-HFP); (2) MSLB at HZP, with loss of external power (MSLB-HZP-1); (3) MSLB at HZP, with no loss of external power (MSLB-HZP-2). The calculated results for these MSLB scenarios are summarized in the following sections.

2.4.3.1 MSLB-HFP

The MSLB-HFP scenario was assumed to be initiated by a MSLB on SG C at 1.01 seconds. The steam was discharged into the containment while the SG C was being depressurized. Since there was a lack of information on the safety injection signal control logic, the signal was assumed to be actuated 0.5 second after the initiating event. The actuation of the SI signal generated the following actuations:

(1) Reactor scram, with insertion of -3.5 dollars of negative reactivity by the CRAs. The scram value considers the most reactive CRA stuck out of the core
(2) Immediate trip of the MFW pumps on all three SGs
(3) Immediate trip of the main coolant pump (MCP)
(4) Closure of the MSIV in 10 seconds
(5) Start of one HPI pump for delivering borated water to the core. The HPI was assumed to start 30 seconds after the SI signal, and the borated water was supposed to arrive at the core 200 seconds after starting the HPI. This delay in the boron injection was introduced considering the flushing of the un-borated water in the pipelines between the HPI pump and the cold legs.

The sequence of events is summarized in Table 2-42. The main parameters of the transient are reported in Figure 2-208 through Figure 2-216. No DNB conditions were reached during the transient, and the fuel clad experienced only a small temperature surge, which is not of safety concern.

Table 2-42. Sequence of Events for Scenario MSLB-HFP.

Event	Time (hr:min:ss)
SG-C MSLB	00:00:01
SI signal	00:00:06
MCPs trip. FW trip. Reactor Scram	00:00:06
MSIV close	00:00:16
HPI pump #1 injection	00:00:36
Reactivity peak	00:02:13
Calculation terminated	25:00:00

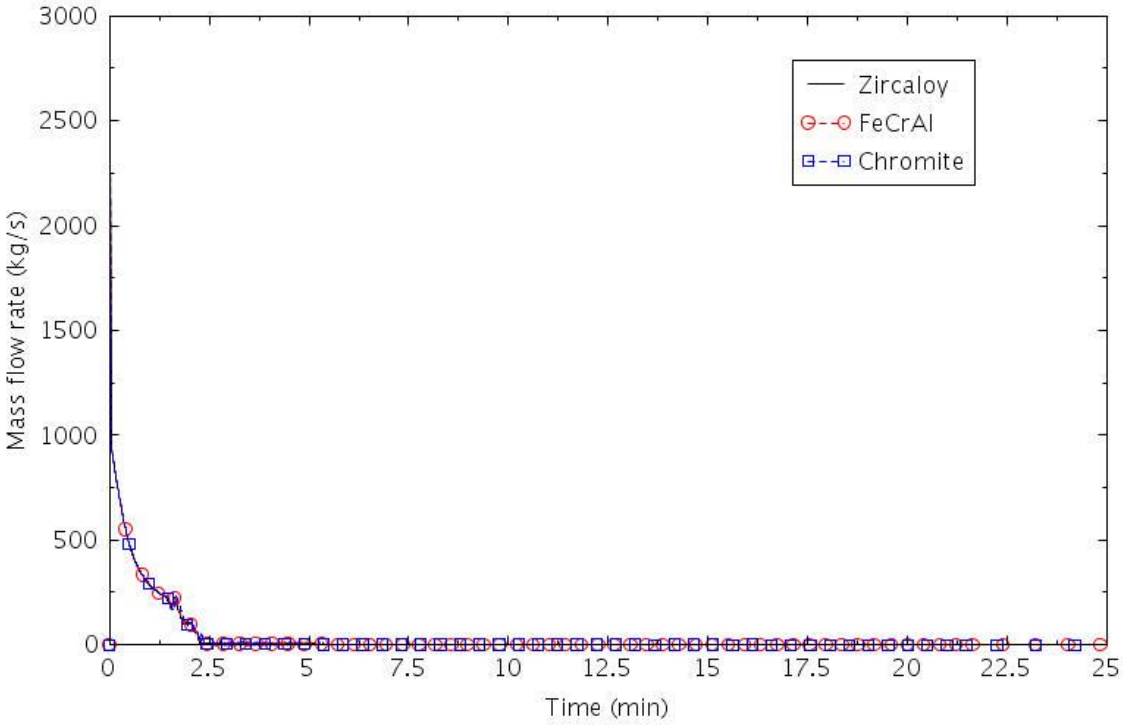

Figure 2-208. Total mass flow at the break (MSLB-HFP).

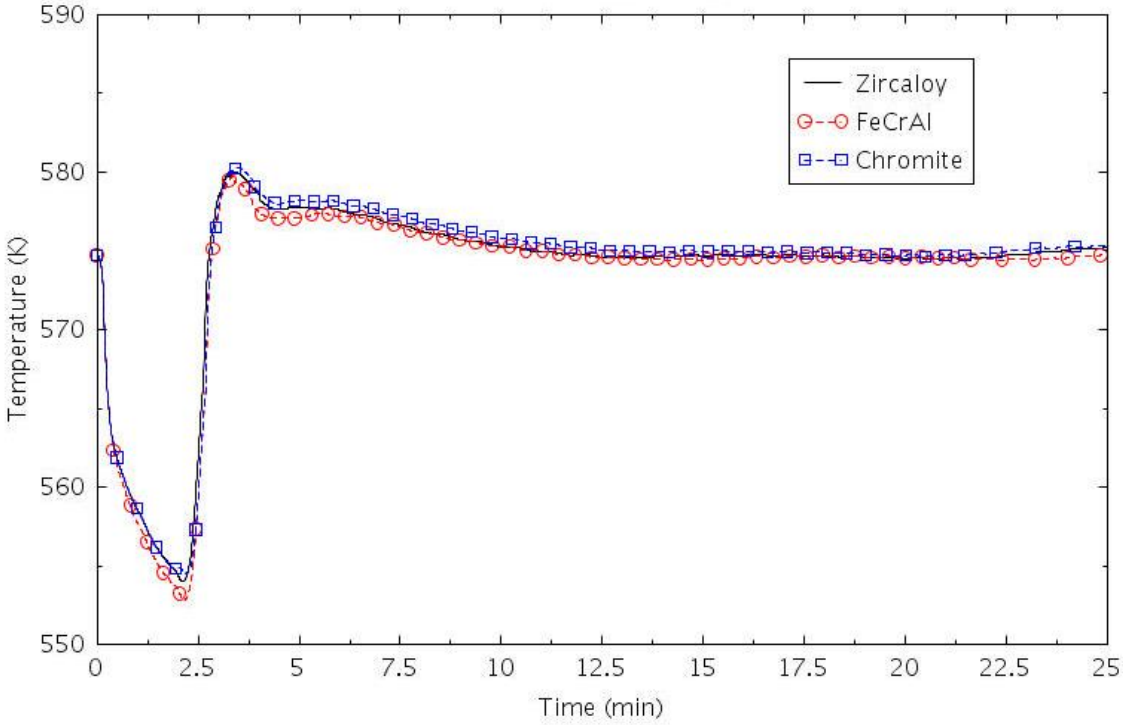

Figure 2-209. RCS average temperature (MSLB-HFP).

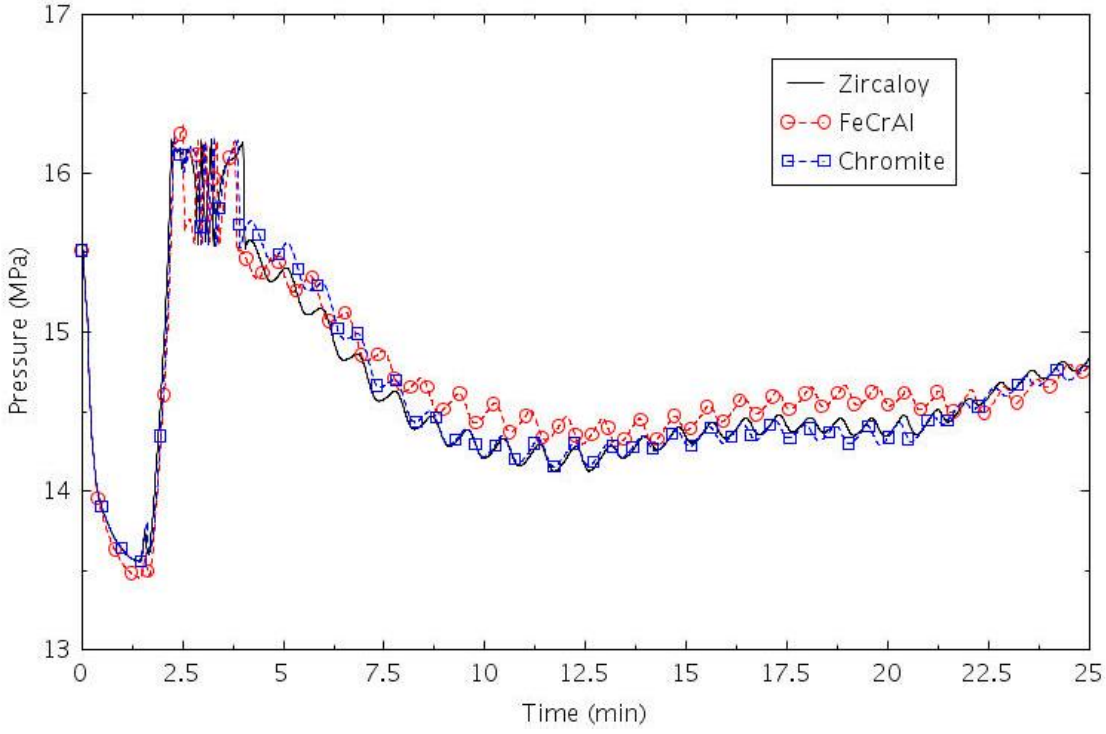

Figure 2-210. PRZ pressure (MSLB-HFP).

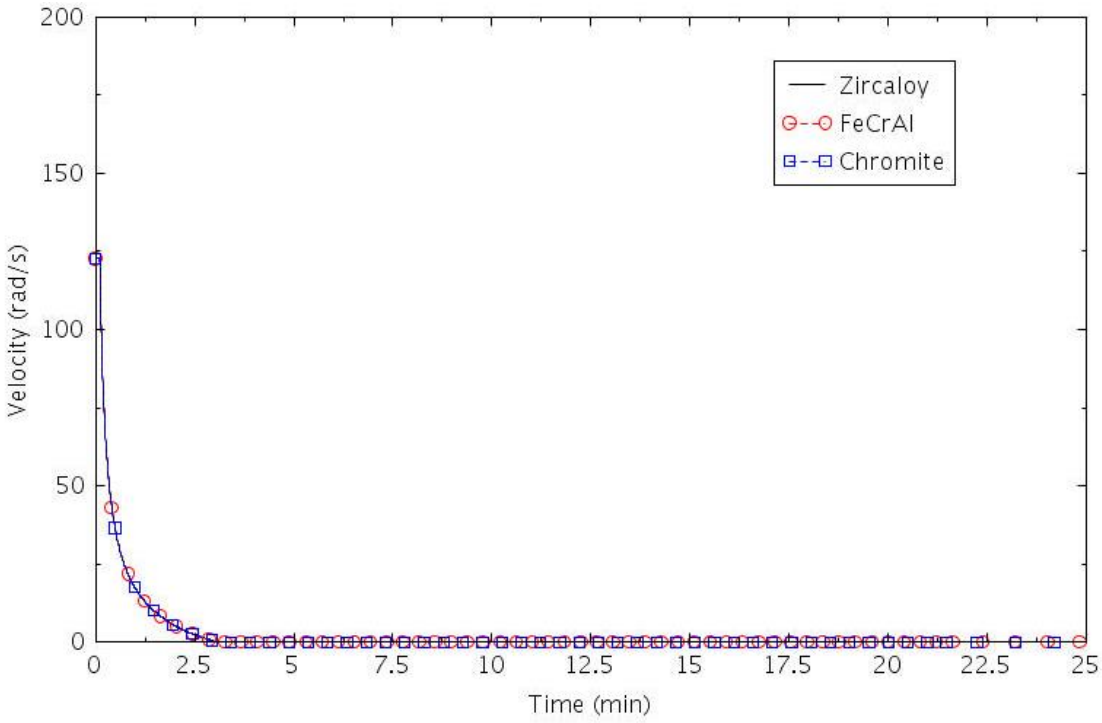

Figure 2-211. RCP-A velocity (MSLB-HFP).

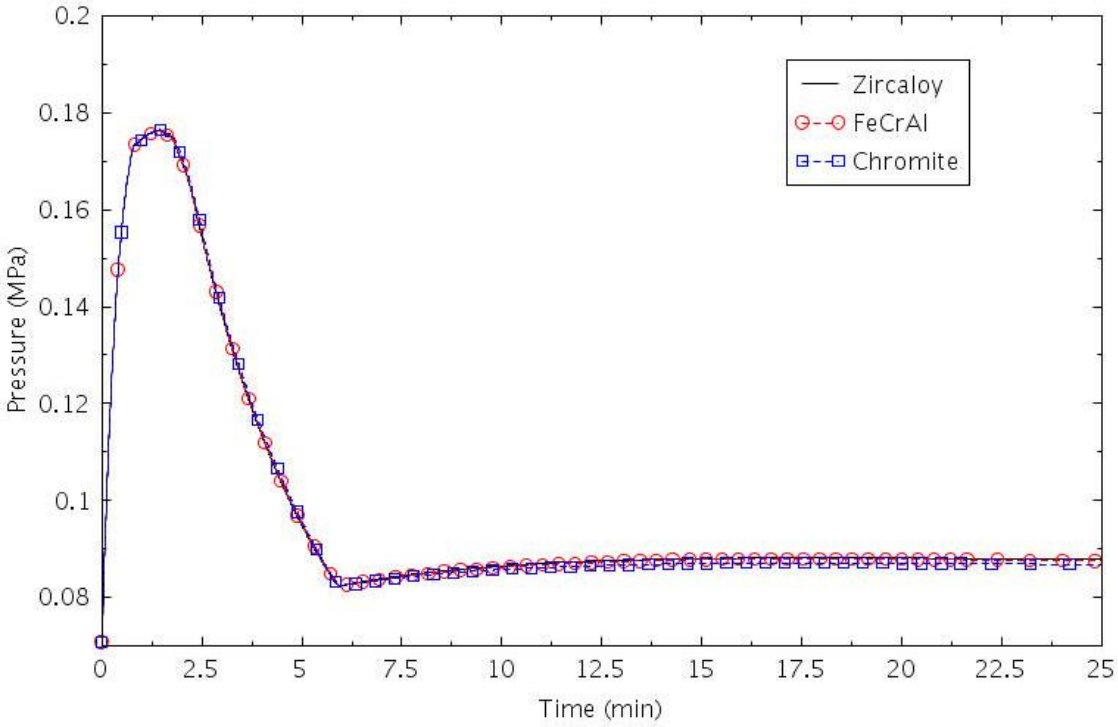

Figure 2-212. Containment pressure (MSLB-HFP).

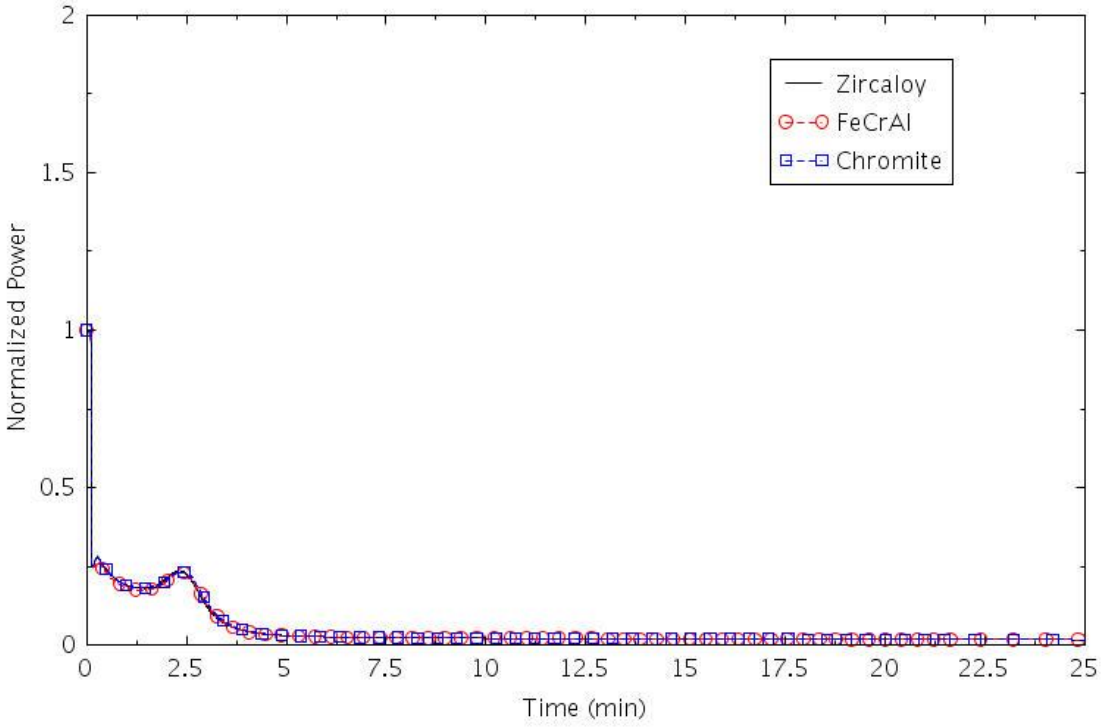

Figure 2-213. Normalized power (MSLB-HFP).

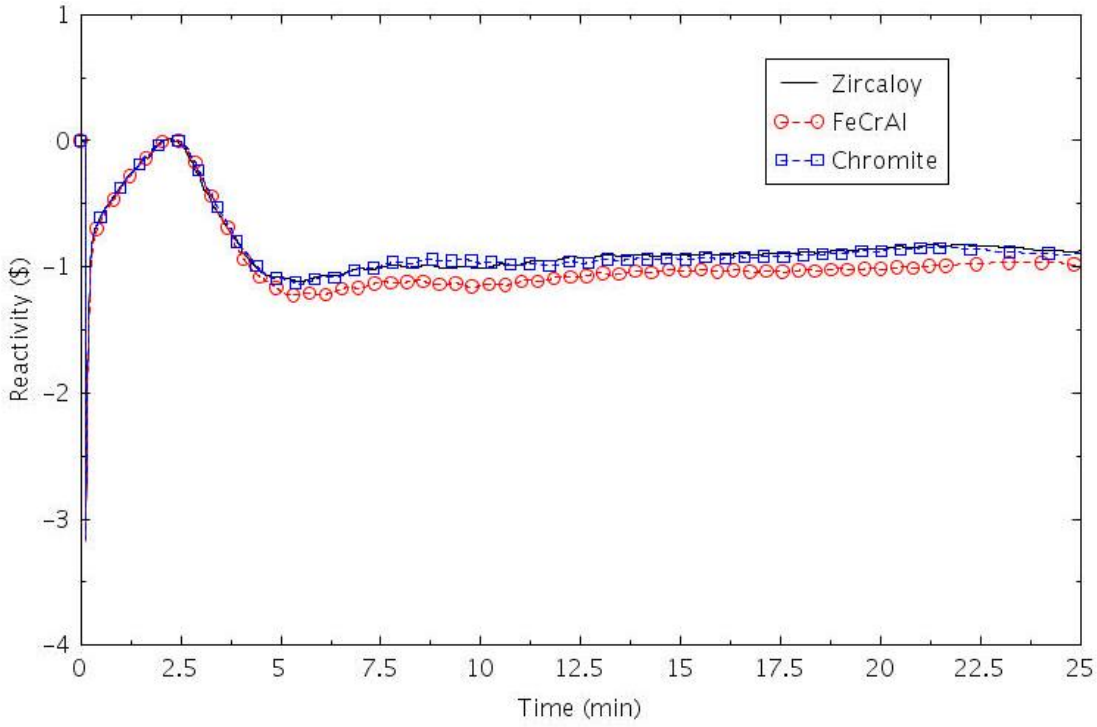

Figure 2-214. Reactivity (MSLB-HFP).

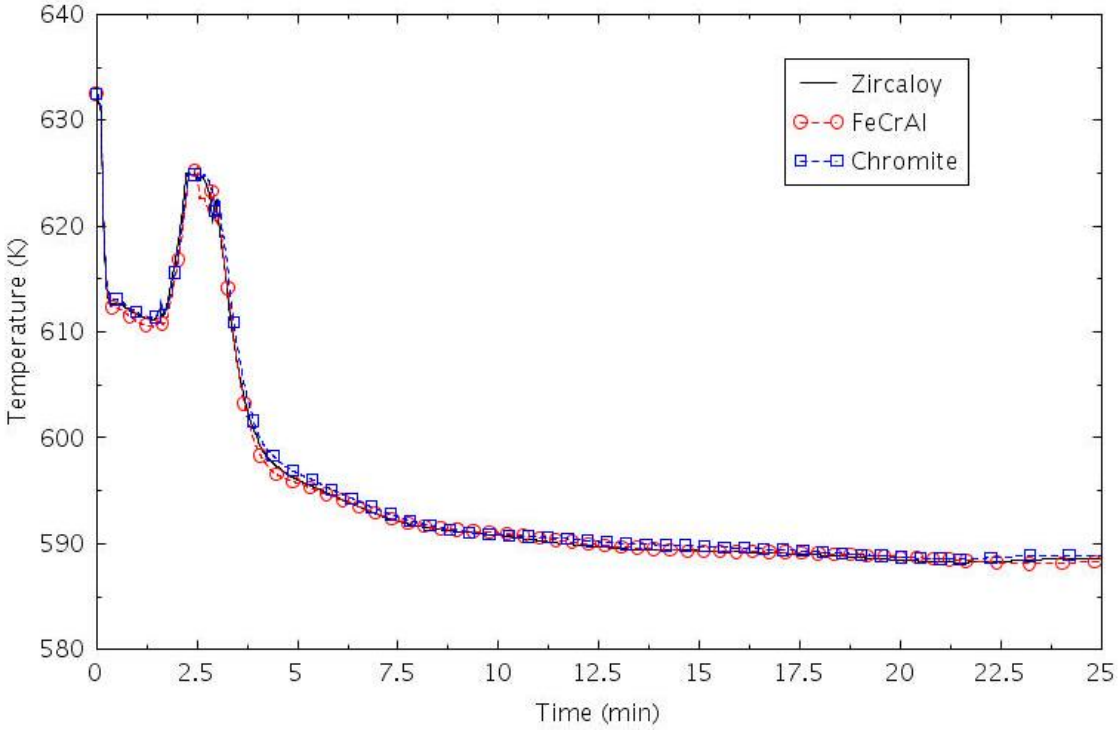

Figure 2-215. Maximum clad temperature (MSLB-HFP).

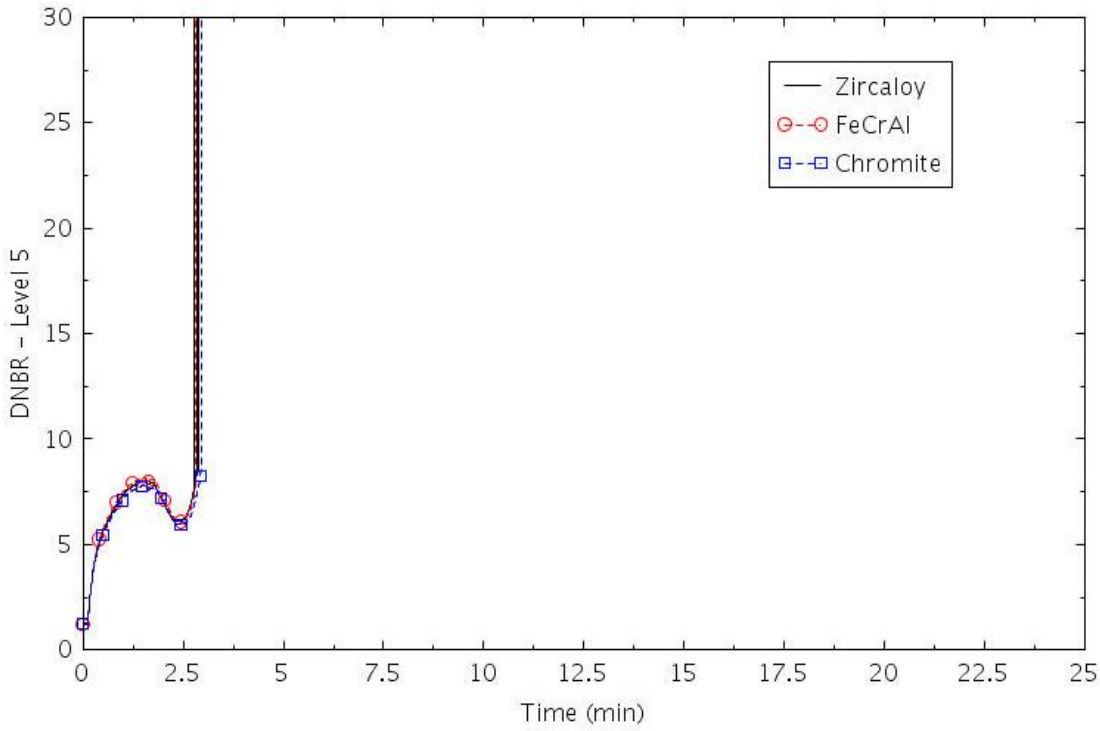

Figure 2-216. Hot rod DNBR at level 5 (MSLB-HFP).

2.4.3.2 MSLB-HZP-1

The MSLB-HZP-1 scenario was assumed to start at no-load conditions with a MSLB on SG C at 1.01 seconds. The following RCS parameters were assumed for the no-load conditions:

(1) Uniform coolant temperature, 559.3 K
(2) Reactor power at 2.546 MW (0.1% $P_{nominal}$)
(3) Reactor sub-critical, with -3.2 dollars of negative reactivity inserted. This reduced subcriticality value considers the most reactive RCA stuck out of the core
(4) MSIV open, TSV closed, steam discharged by the steam dump valves
(5) RCPs operating.

The MSLB-HZP-1 assumed a MSLB with a coincident loss-of-load that caused the RCPs rundown. The steam was discharged into the containment while the SG C was being depressurized. Since there was a lack of information on the safety injection signal control logic, the signal was assumed to be actuated 0.5 second after the initiating event. The actuation of the SI signal generated the following actuations:

(1) Immediate trip of the MFW pumps on all three SGs
(2) Closure of the MSIV in 10 seconds
(3) Start of one HPI pump for delivering borated water to the core. The HPI was assumed to start 30 seconds after the SI signal, and the borated water is supposed to arrive into the core 200 seconds after starting the HPI. This delay in the boron injection is introduced considering the flushing of the un-borated water in the pipelines between the HPI pump and the cold legs.

The sequence of events is summarized in Table 2-43. The main parameters of the transient are reported in Figure 2-217 through Figure 2-225. No DNB conditions were reached during the transient, and the fuel clad experienced only a small temperature surge, which is not of safety concern.

Table 2-43. Sequence of Events for Scenario MSLB-HZP-1.

Event	Time (hr:min:ss)
SG-C MSLB + loss of load. RCPs rundown.	00:00:01
SI signal	00:00:06
FW trip.	00:00:06
MSIV close	00:00:16
HPI pump #1 injection	00:00:36
First borated water reaches the core	00:03:44
Reactivity peak	00:15:48
Calculation terminated	25:00:00

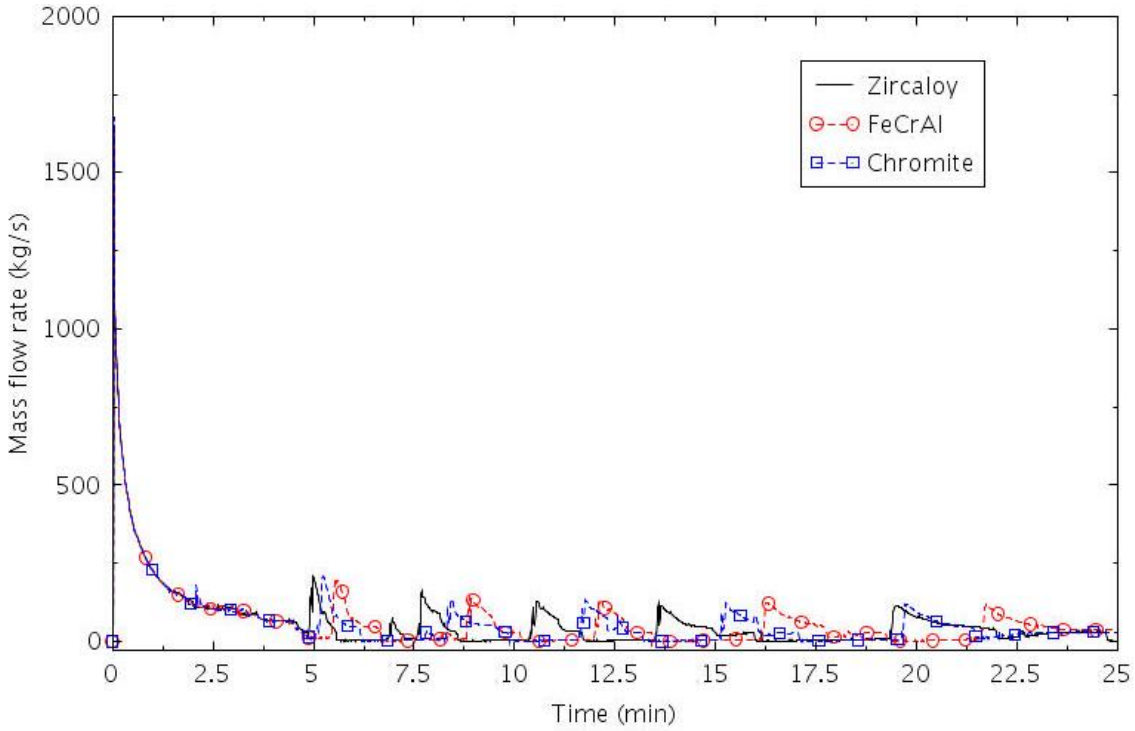

Figure 2-217. Total mass flow at the break (MSLB-HZP-1).

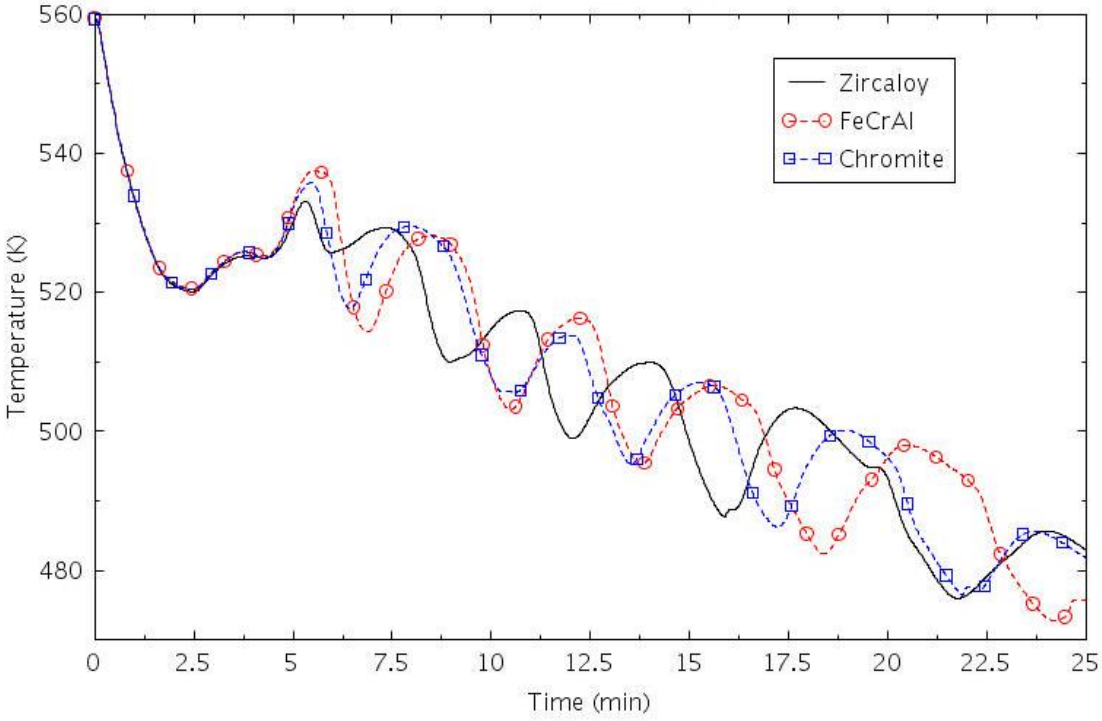

Figure 2-218. RCS average temperature (MSLB-HZP-1).

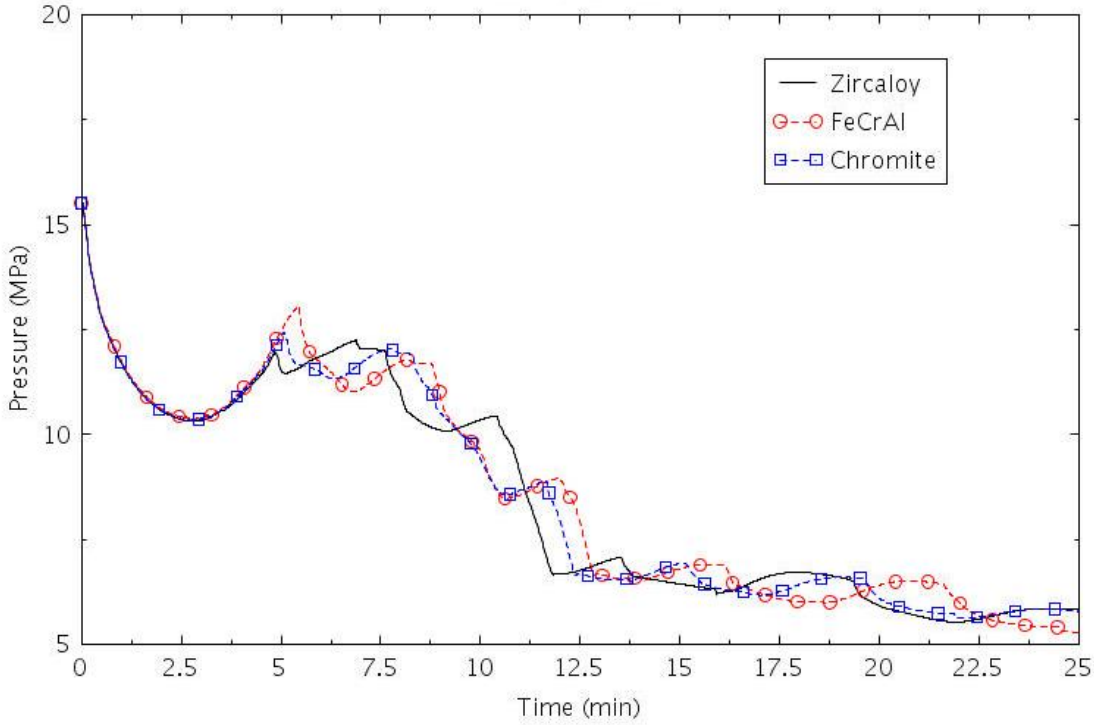

Figure 2-219. PRZ pressure (MSLB-HZP-1).

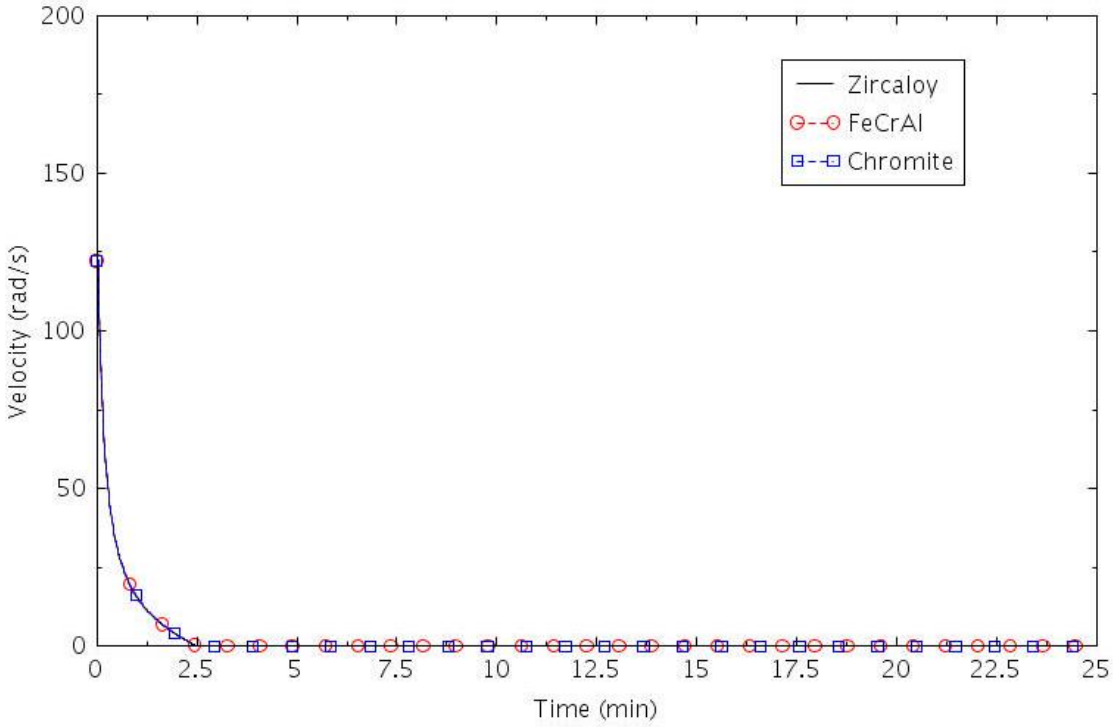

Figure 2-220. RCP-A velocity (MSLB-HZP-1).

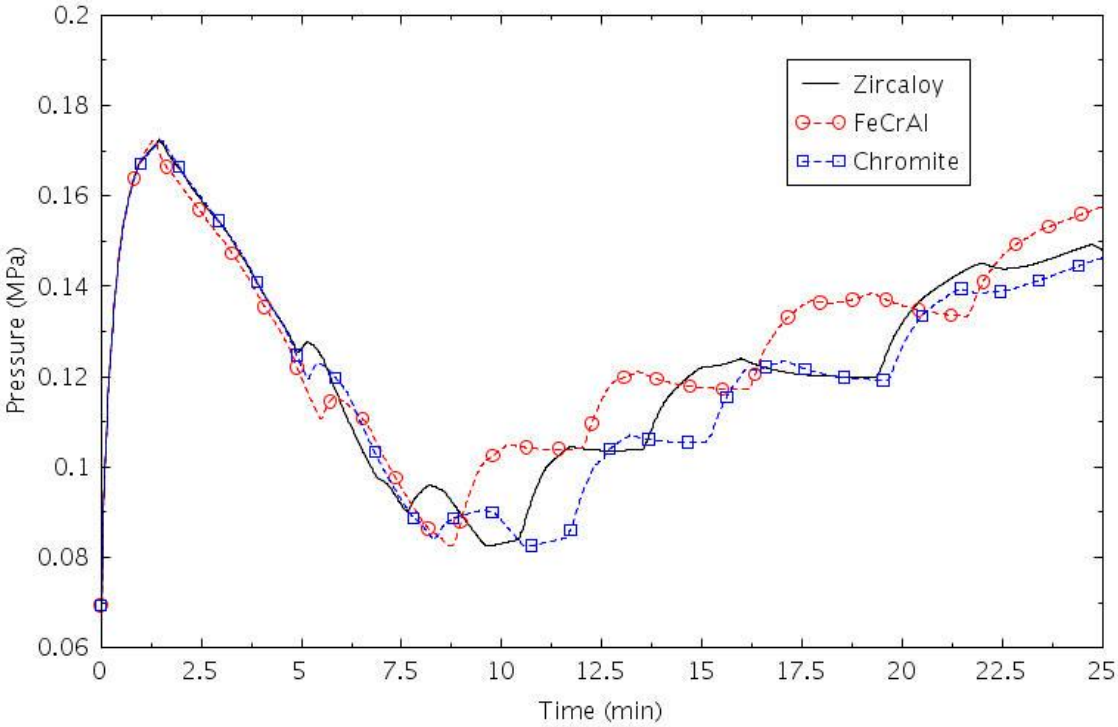

Figure 2-221. Containment pressure (MSLB-HZP-1).

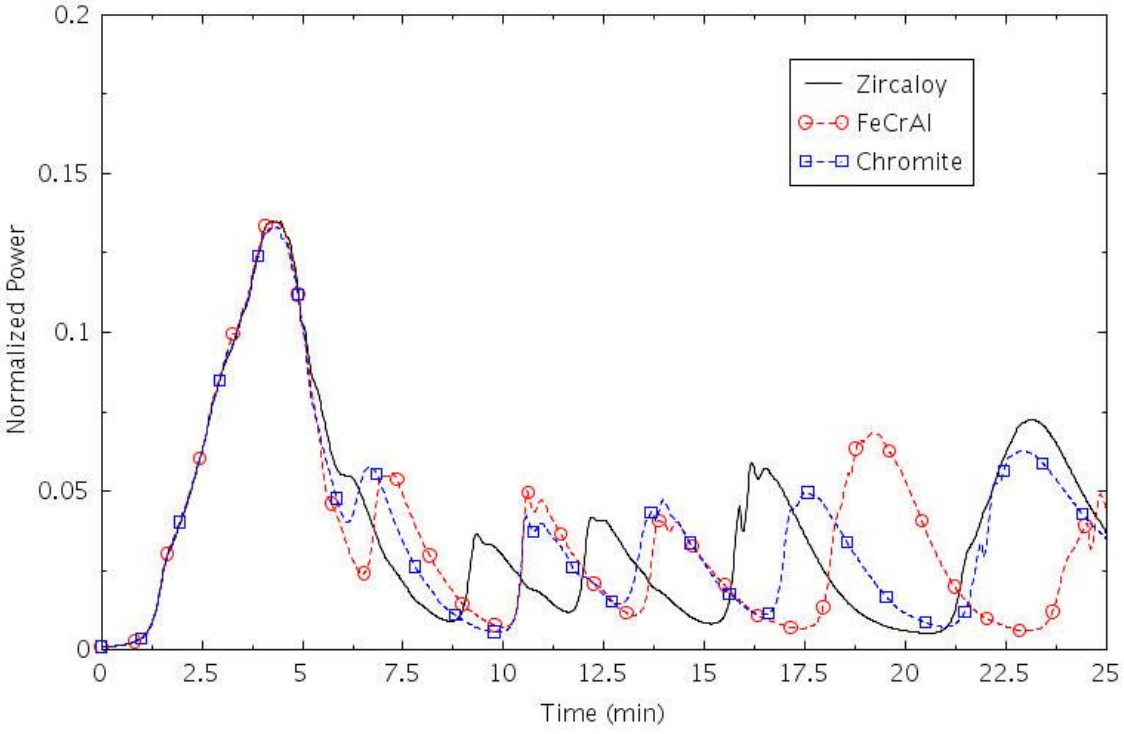

Figure 2-222. Normalized power (MSLB-HZP-1).

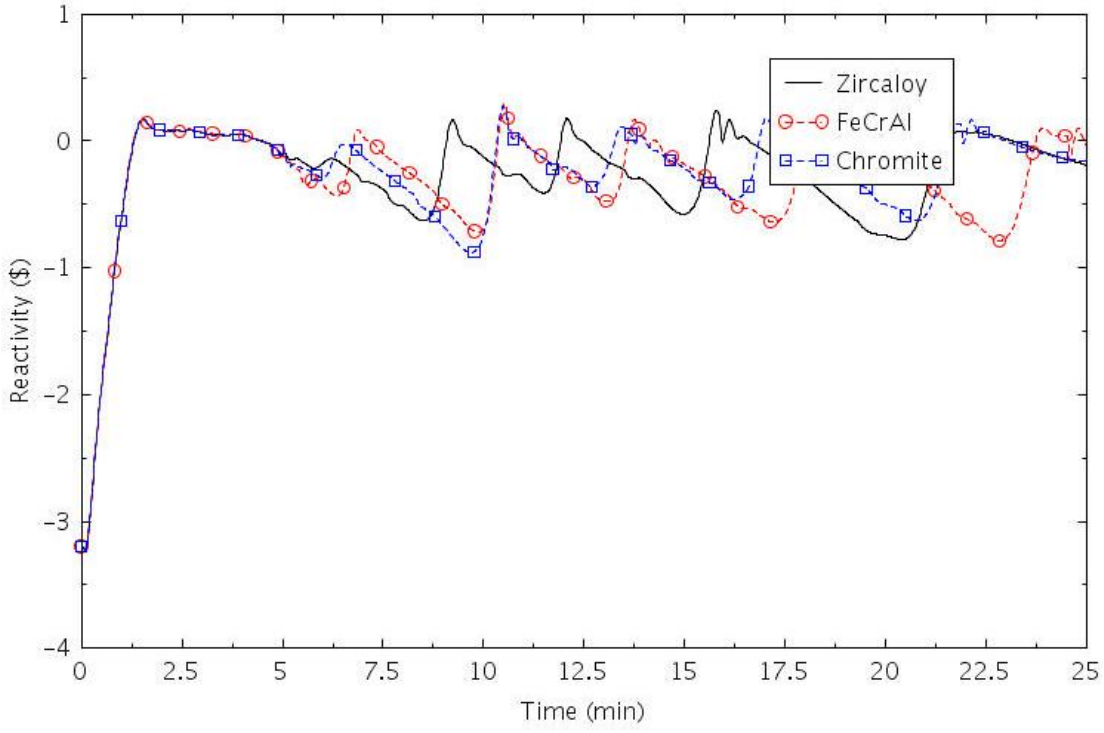

Figure 2-223. Reactivity (MSLB-HZP-1).

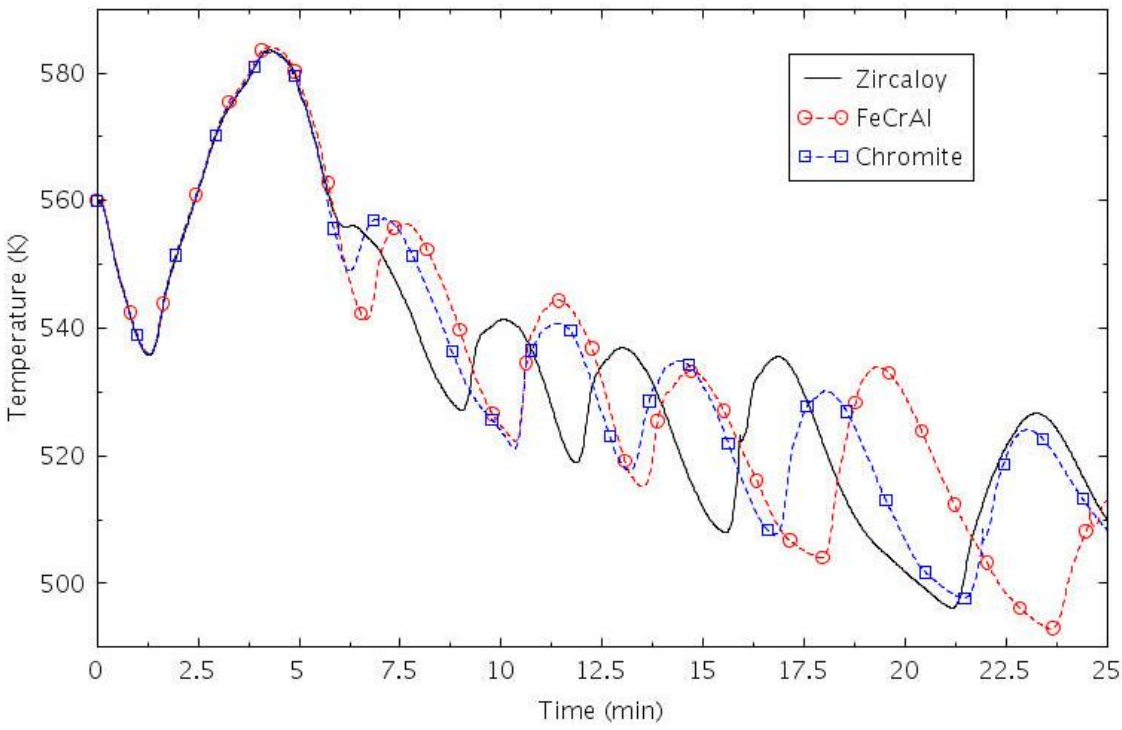

Figure 2-224. Maximum clad temperature (MSLB-HZP-1).

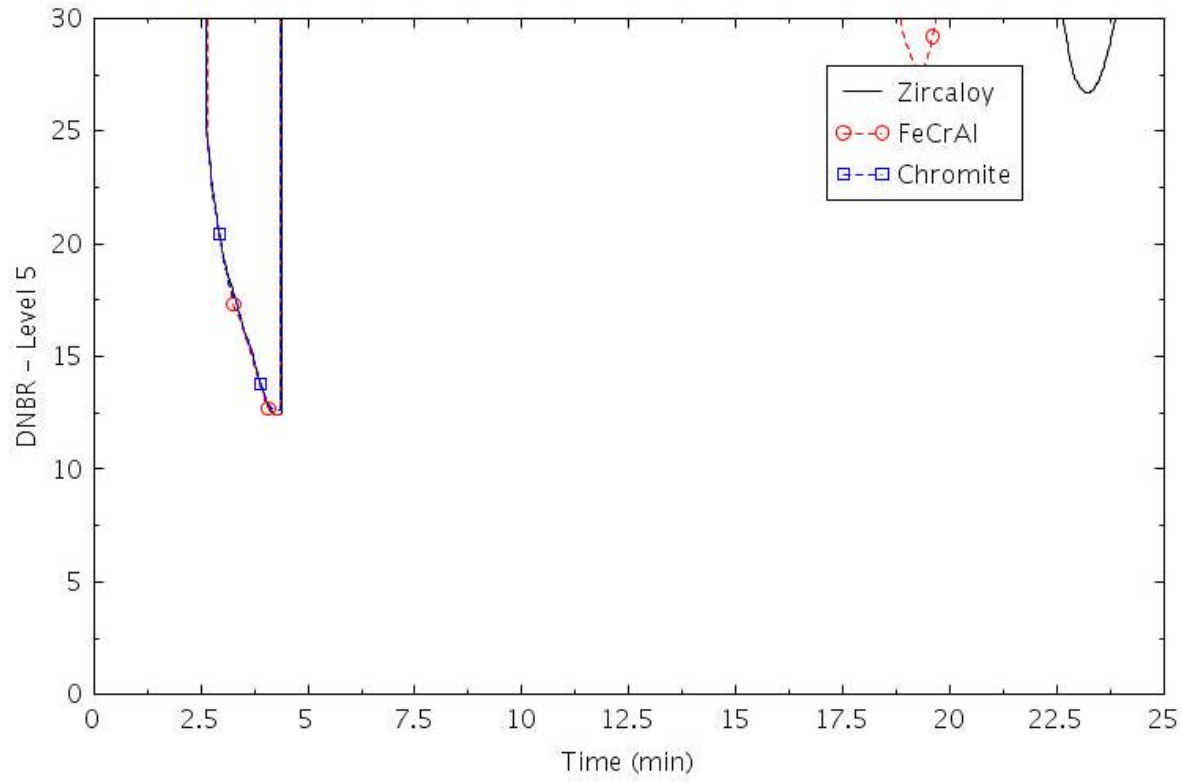

Figure 2-225. Hot rod DNBR at level 5 (MSLB-HZP-1).

2.4.3.3 MSLB-HZP-2

The MSLB-HZP-2 scenario was assumed to start at no-load conditions with a MSLB on SG C at 1.01 seconds. The same RCS parameters used for MSLB-HZP-1 were assumed here.

The MSLB-HZP-2 assumed a continuous run of the MCP during the accident. The steam was discharged in the containment while the SG C was being depressurized. Since there was a lack of information on the safety injection signal control logic, the signal was assumed to be actuated 0.5 second after the initiating event. The actuation of the SI signal generated the same actuations as MSLB-HZP-1, which are introduced in Section 2.4.3.2.

The sequence of events is summarized in Table 2-44. The main parameters of the transient are reported in Figure 2-226 through Figure 2-234. No DNB conditions were reached during the transient, and the fuel clad experienced only a small temperature surge that is not of safety concern.

Table 2-44. Sequence of Events for Scenario MSLB-HZP-2.

Event	Time (hr:min:ss)
SG-C MSLB + loss of load.	00:00:01
SI signal	00:00:06
FW trip.	00:00:06
MSIV close	00:00:16
HPI pump #1 injection	00:00:36
First borated water reaches the core	00:03:29
Reactivity peak	00:21:43
Calculation terminated	25:00:00

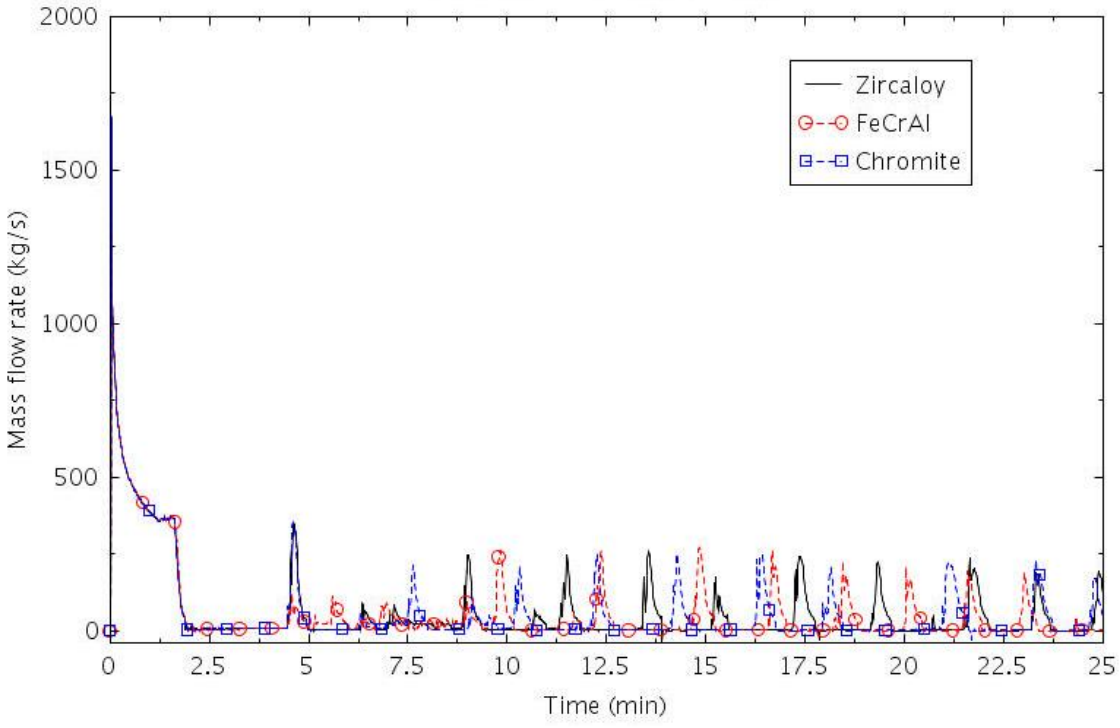

Figure 2-226. Total mass flow at the break (MSLB-HZP-2).

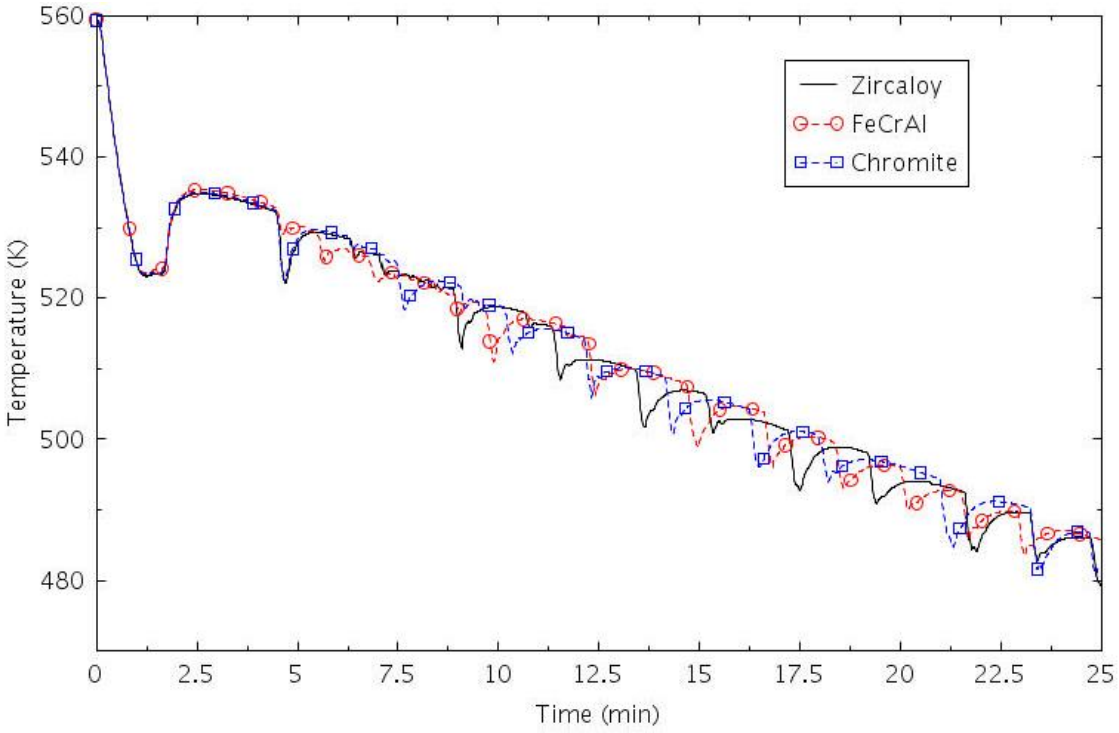

Figure 2-227. RCS average temperature (MSLB-HZP-2).

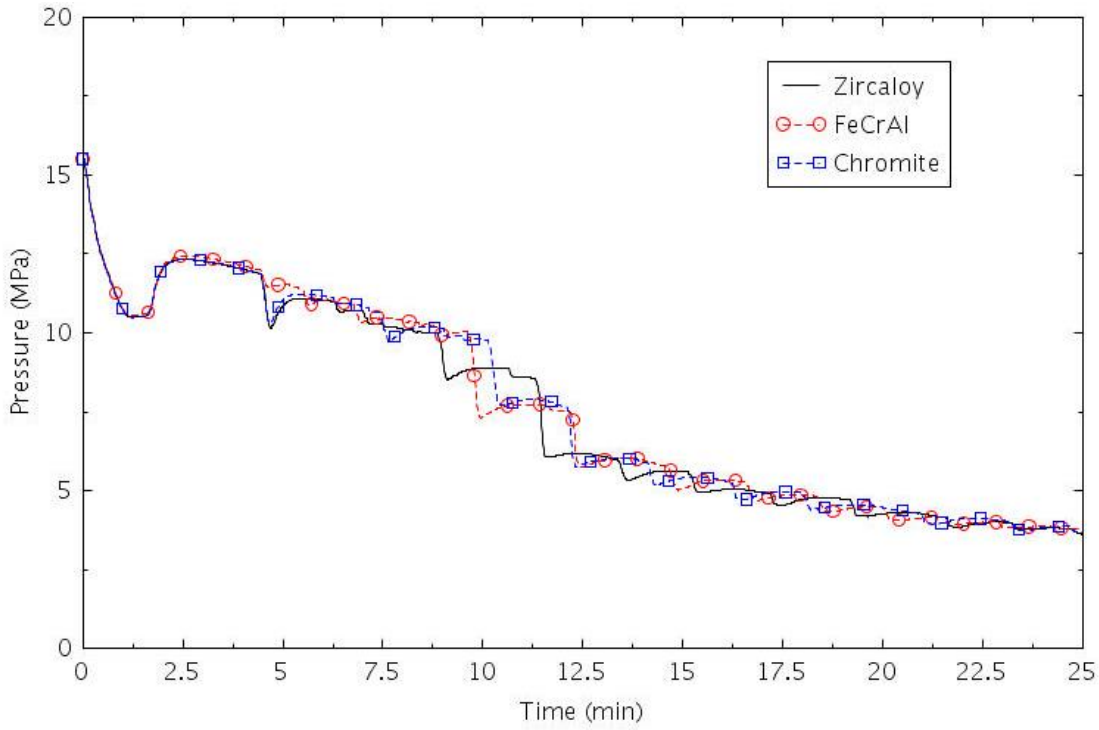

Figure 2-228. PRZ pressure (MSLB-HZP-2).

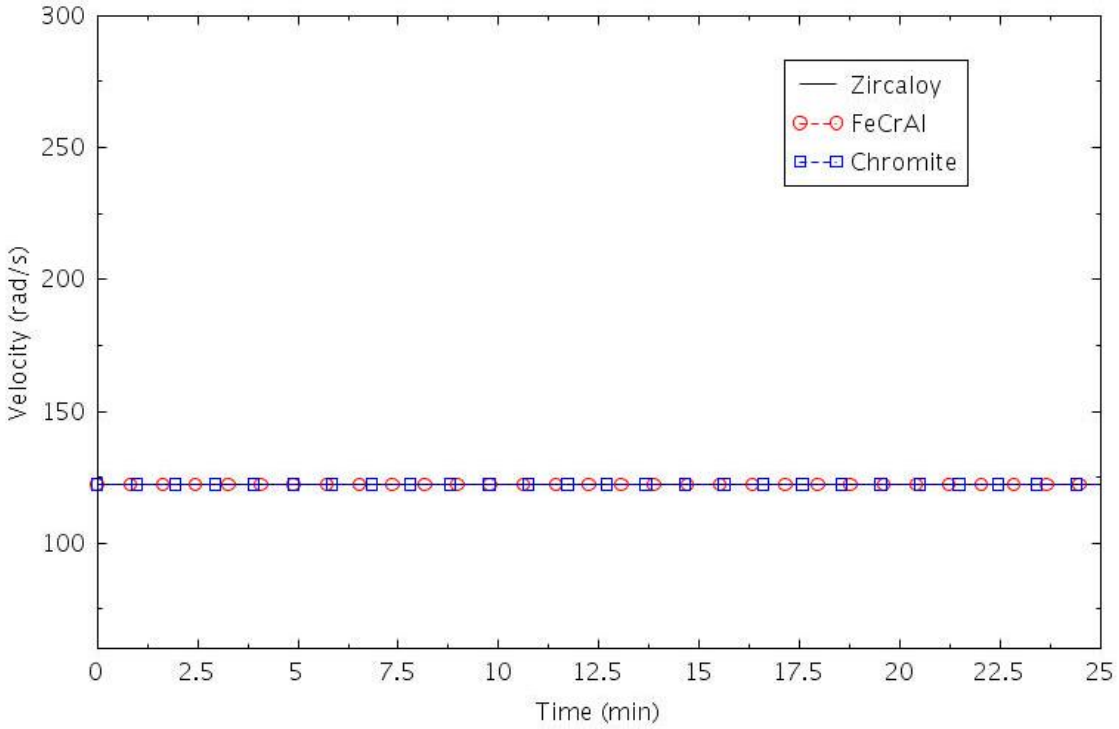

Figure 2-229. RCP-A velocity (MSLB-HZP-2).

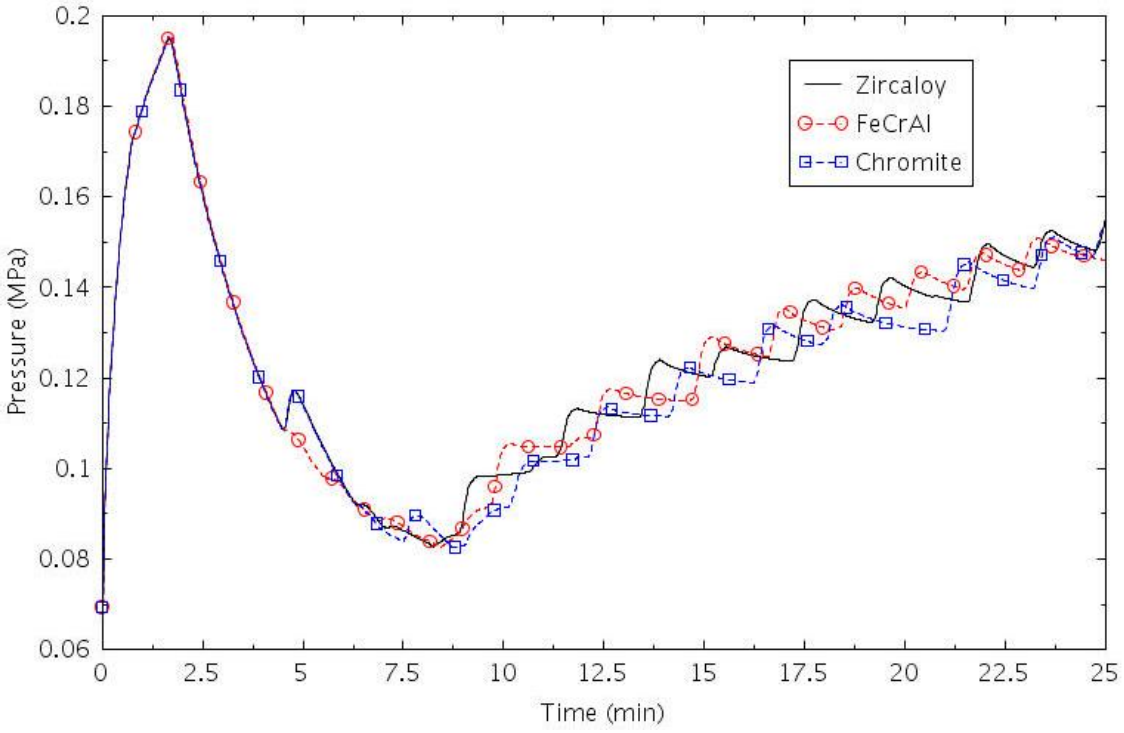

Figure 2-230. Containment pressure (MSLB-HZP-2).

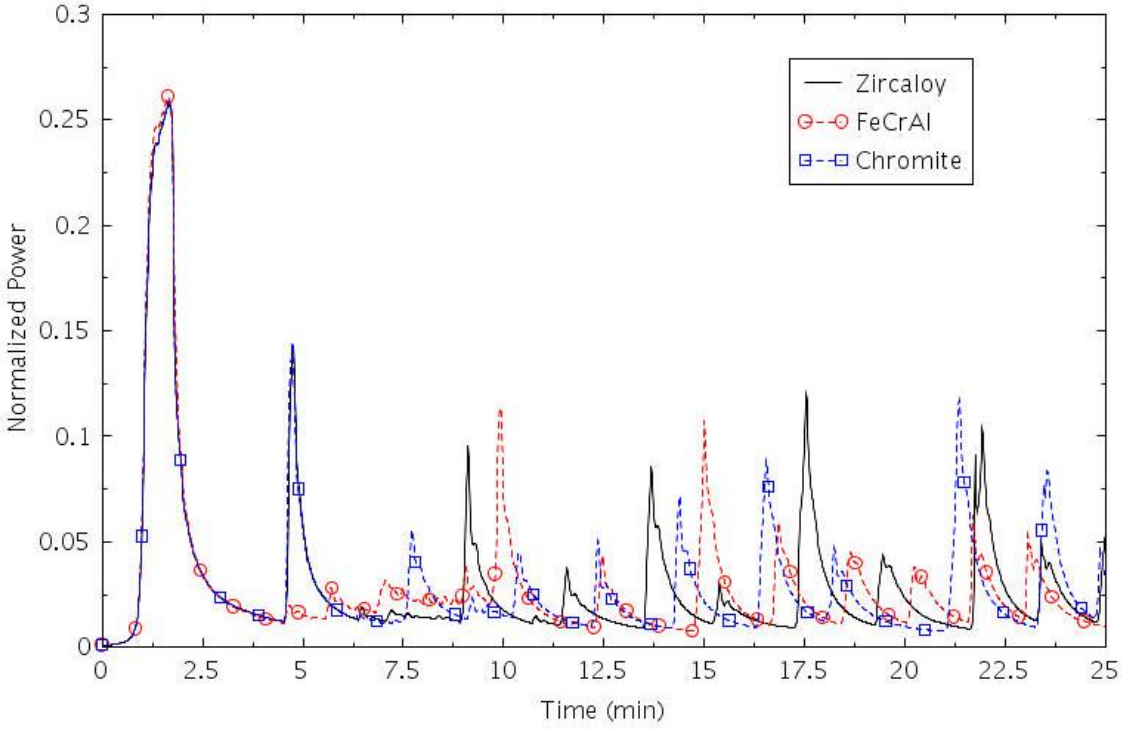

Figure 2-231. Normalized power (MSLB-HZP-2).

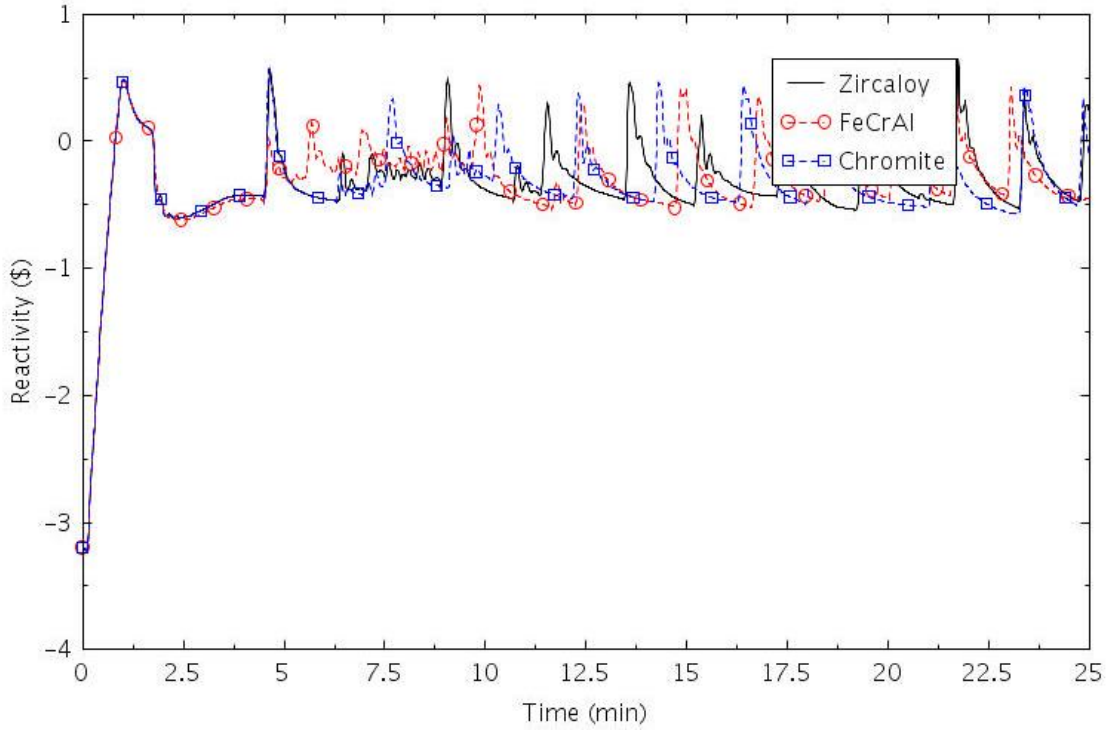

Figure 2-232. Reactivity (MSLB-HZP-2).

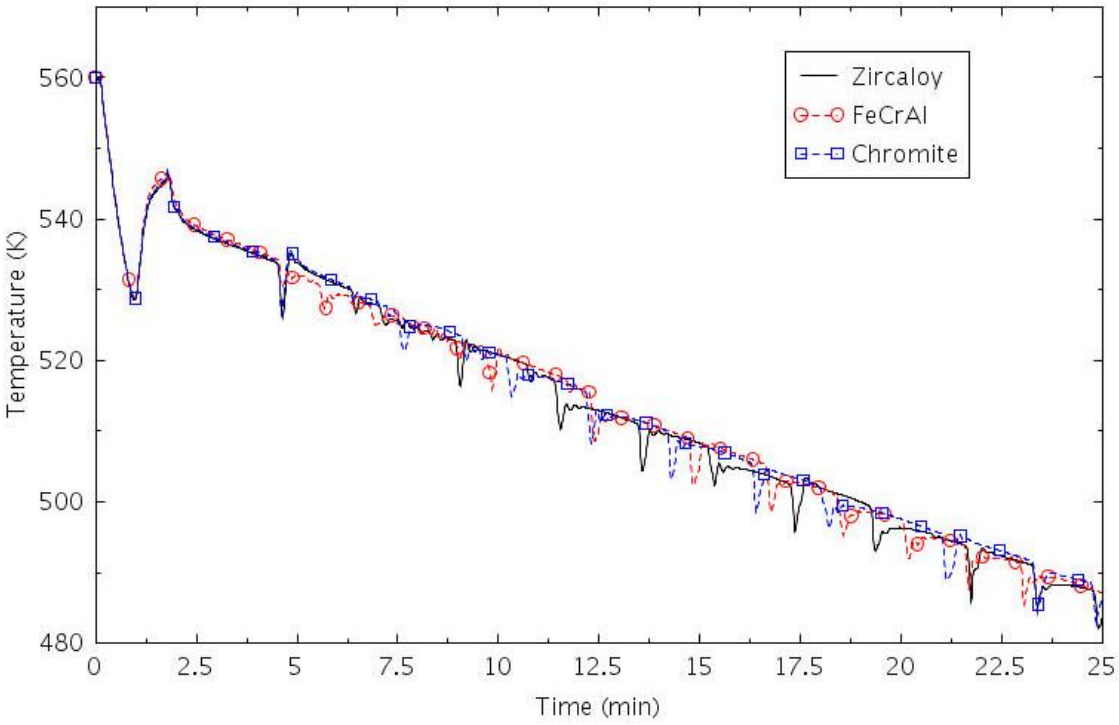

Figure 2-233. Maximum clad temperature (MSLB-HZP-2).

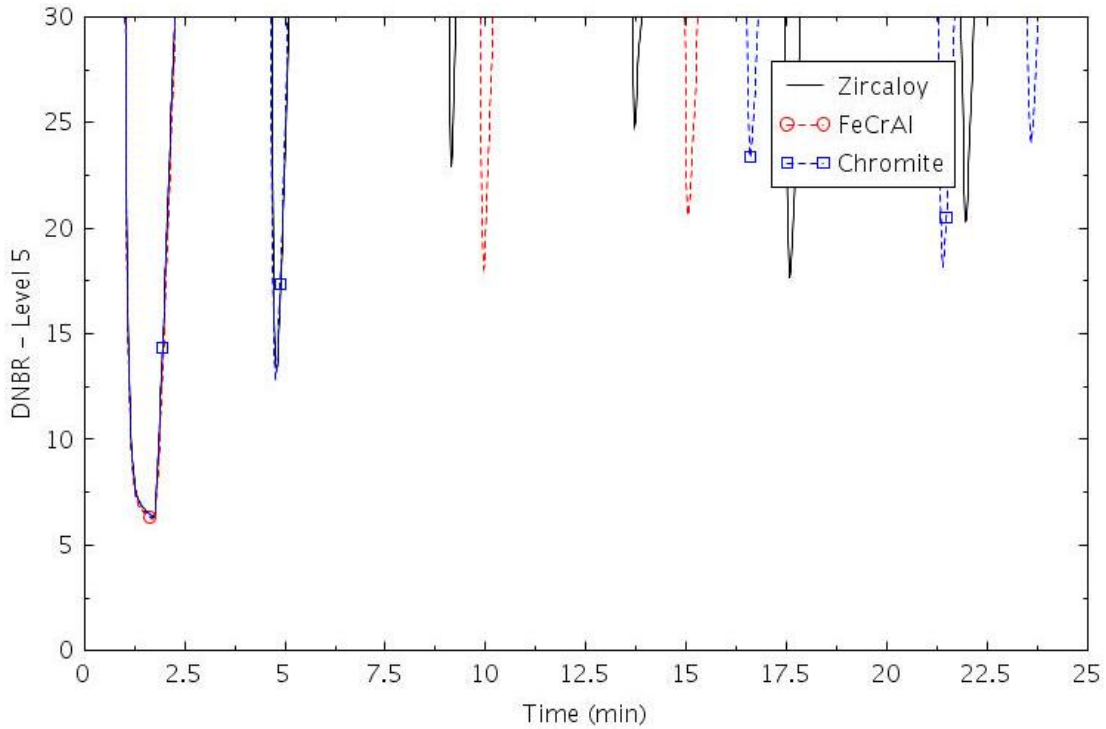

Figure 2-234. Hot rod DNBR at level 5 (MSLB-HZP-2).

2.4.4 MSLB Analysis Results

The analysis of the three different MSLB accident scenarios, at HFP and HZP conditions, showed that no safety thresholds were violated for all the three different types of claddings (Zircaloy, FeCrAl, Cr-coated). Both the DNBR and the clad temperature of the hot rod clad were well below the safety limits. Therefore, no differences have been found in terms of MSLB safety performance between the standard Zircaloy clad and the other near-term ATF claddings.

2.5 Benchmark Calculations between RELAP5-3D and MELCOR

This section presents benchmark calculations conducted by University of Wisconsin to compare ATF analysis results between RELAP5-3D and MELCOR for the performances of Zircaloy and near-term ATF cladding designs under the postulated severe accident scenarios. Three SBO scenarios were selected from (Ma, et al., 2018) as a common ground for the benchmark calculations. The details of the benchmark calculations are documented in (Dailey, Wang, & Corradini, 2019).

2.5.1 SBO MELCOR Model

The MELCOR code is a fully integrated engineering-level systems code, which models the development of severe accidents in nuclear power plants (NPPs) (Humphries, Beeny, Gelbard, Louie, & Phillips, 2017). MELCOR models all related plant systems, plant phenomena, and generating transients in a wide-range system: thermal hydraulic performance, thermo-mechanical interactions, and chemical interactions.

One objective of ATF materials and associated designs is to minimize clad oxidation that causes hydrogen and heat generation resulting from zirconium-steam reactions by either replacing zirconium with another material altogether, or by coating it with one that has more favorable oxidation properties. The modeling of such alternative cladding and duplex coated claddings is facilitated using the User-Defined Generalized Coating version of MELCOR 1.8.6, which includes recent extensions to the oxidation and material property models made by INL (Humrickhouse & Merrill, 2018).

A MELCOR model divides the core into a number of radial rings and axial levels, and a particular ring and level identify a core cell. Each cell contains some number of components, which may be fuel pellets, cladding, canisters, supporting structure, non-supporting structure, or other structure. Each component in a core cell is made up of different materials, which are specified in user input.

The MELCOR model in this analysis is based on Surry plant which is a Westinghouse three-loop PWR. The nodalization scheme is shown in Figure 2-235 (Wang, Jo, & Corradini, 2018) and mimics that used in (NRC, 2012). As seen in this figure, the core of this PWR plant is separated into 5 rings in the radial direction, and 10 nodes in an axial direction. The lower plenum and dome are also divided into several nodes. In the top dome, some nodes are coincident. This situation will influence the results of the reactor pressure vessel water level. Only one loop is displayed in the figure as a representative for the three SG loops in the plant.

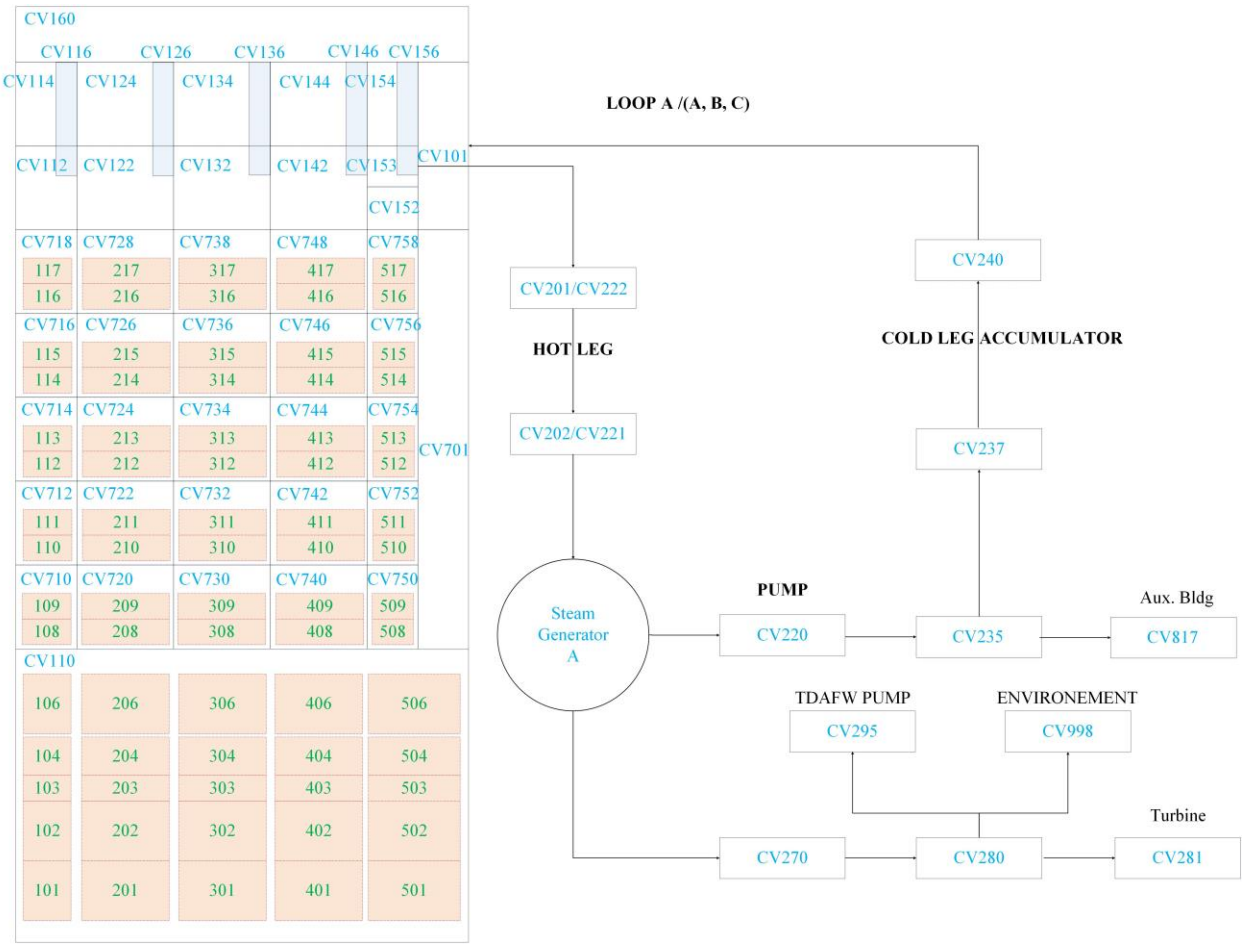

Figure 2-235. Nodalization of Surry Plant (a Westinghouse three-loop PWR) by MELCOR.

2.5.2 SBO MELCOR Analysis

In this analysis, two broad categories of accident scenario are investigated: long-term SBO (LTSBO) and short-term SBO (STSBO). Both of these accident scenarios can be initiated by the same type of event; however, a short-term station blackout represents more coincident equipment failures.

STSBOs, which are characterized by the near-complete failure of reactor safety systems, tend to have the most severe damage simulated for the reactor vessel. In the severe accident scenario, a large seismic event could result in the complete loss of offsite power (LOOP) and onsite emergency alternating current (AC) power due to significant damage to diesel generators. While the reactor can still be shut down in this scenario, supporting systems are left disabled. Notable among the disabled systems are the direct current (DC) batteries, which are assumed to not be available from the start of this accident scenario. Loss of DC power translates into the loss of control and assumed failure of the turbine-drive auxiliary feedwater (TDAFW) system, as well as the control and operation of the automatic safety relief valves (e.g., secondary-side PORVs). In this analysis, Case SBO 7.0 refers to a short-term SBO scenario selected from (Ma, et al., 2018).

LTSBOs are similar to short-term SBOs but operate under the assumption that the DC batteries will be available and not deplete for a period of time. While DC power is available, direct control and operability of the TDAFW and PORV systems is possible, which can significantly extend the ability to cool the reactor core under these conditions. For this analysis, two battery-failure times were assumed: 4 hours (Case SBO 1.0) and 8 hours (Case SBO 1.3), based on (Ma, et al., 2018). Finally, the accident causes the primary system coolant to reach saturation conditions, and this can cause additional leakage from the primary system

RCP seals. In this analysis, the leak rate is assumed based on (NRC, 2012). The assumptions as to the initial system conditions are shown in Table 2-45.

Table 2-45. SBO Scenarios for MELCOR Analysis.

Parameter	SBO 1.0	SBO 1.3	SBO 7.0
Reactor Thermal Power	2546 MW	2546 MW	2546 MW
TDAFW Operable	0-4 hours	0-8 hours	0
PORV Operable	0-4 hours	0-8 hours	0
RCP Leakage Per Loop	21 gpm	21 gpm	21 gpm

A total of nine simulation cases were performed with MELCOR to be consistent with RELAP5 analyses of SBO cases 7.0, 1.0, 1.3 respectively, using Zircaloy cladding, Cr-coated cladding, and FeCrAl cladding. The key events from these simulations are shown in Table 2-46.

Table 2-46. Key Event List of MELCOR Analysis.

Event	Time to Event (hr)								
	1.0 Base	1.0 Cr	1.0 FeCrAl	1.0 Base	1.0 Cr	1.0 FeCrAl	1.0 Base	1.0 Cr	1.0 FeCrAl
Blackout Initiation	0	0	0	0	0	0	0	0	0
SG Dry out	10.37	10.53	10.13	16.23	16.5	16.43	1.34	1.22	1.36
SG Depressurized	1.5	1.5	1.5	1.5	1.5	1.5	-	-	-
Steam Formation	1.57	1.57	1.57	1.57	1.57	1.57	1.83	1.84	1.83
Water at Top of Fuel	12.27	12.27	12.27	18.40	18.40	18.40	2.32	2.31	2.31
Hydrogen > 0.5kg	12.83	13.77	14.03	19.03	20.33	20.53	2.66	3.11	2.96
Fission Prod. Release	13.79	13.93	14.17	20.55	20.87	20.79	3.07	3.01	3
Creep Rupture C-Loop	14.72	14.86	15.4	21.64	22.10	16.84	3.99	3.9	3.88
Accumulators Discharge	2.41	2.41	2.41	2.41	2.41	2.41	4	3.91	3.88
Accumulators Empty	14.73	14.86	15.41	21.65	22.11	21.92	4	3.91	3.89
Core Supp. Plate Fails	15.97	-	16.82	22.74	-	23.22	4.97	5.2	5.5

2.5.2.1 SBO-7.0

The first set of results focus on the STSBO scenario (Case 7.0) as simulated by MELCOR. They represent a "worst-case" accident, with multiple failures in key safety systems. Each simulation was run for 8 hours for the three different cladding material types. Key events can be found in Table 2-46. In addition, the accident progression history is shown for the following parameters: pressurizer pressure, SG secondary-side pressure, collapsed water level in the RPV, peak clad/debris temperature, and hydrogen mass generated by clad oxidation. For these cases, most key parameters did not experience significant changes under the influence of different clad material choices, apart from the notable delay of hydrogen generation due to the ATF clad materials. Given the rapid progression of this accident scenario, the difference between each cladding material oxidation rate kinetic is apparent. Zircaloy tended to see the highest production of hydrogen, while significant hydrogen generation for FeCrAl and Cr-coated Zircaloy were delayed by more than an hour and with lower total amount of hydrogen generation.

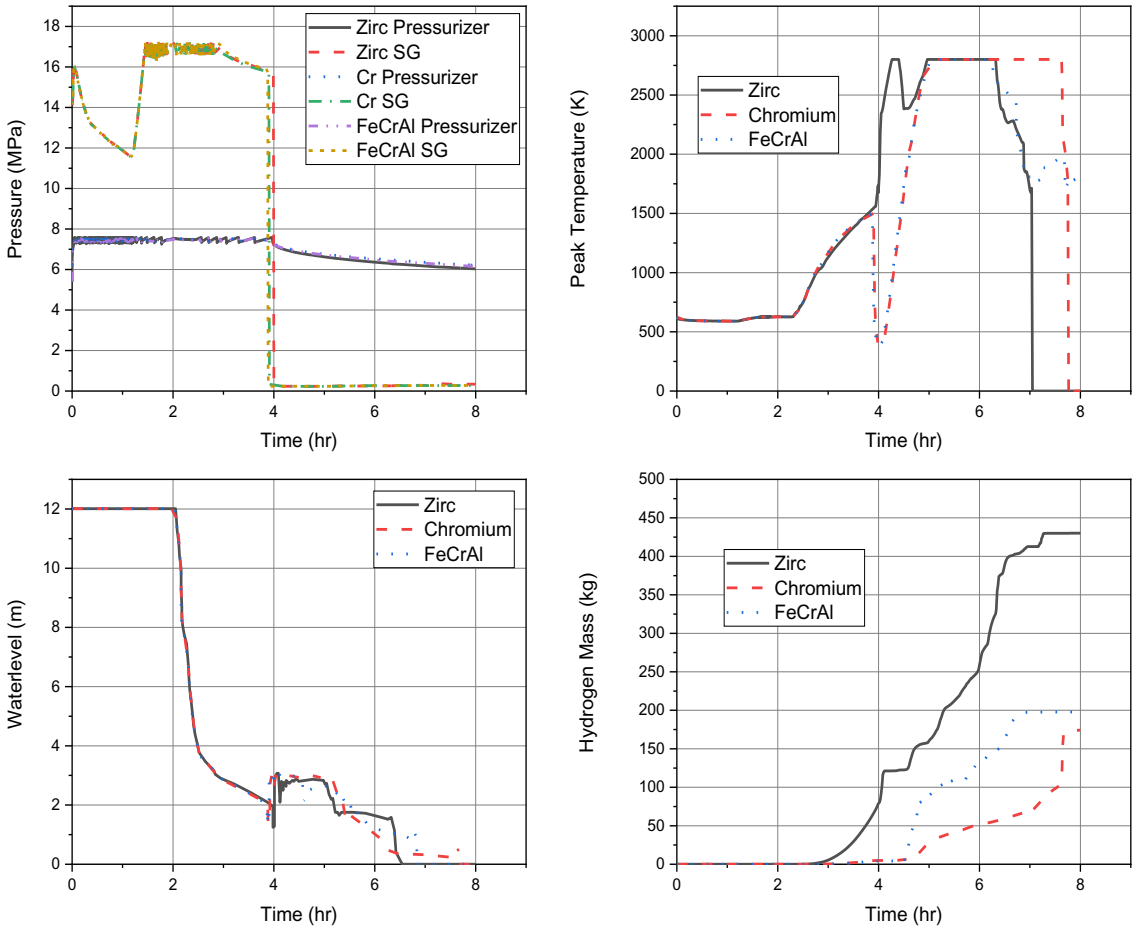

Figure 2-236. MELCOR thermal hydraulic outputs with three cladding options (SBO 7.0).

2.5.2.2 SBO-1.0

The SBO Case 1.0 results focus on an LTSBO scenario, as simulated by MELCOR. In these cases, TDAFW operation and relief valve operation are available for 4 hours with DC batteries available. This has the effect of delaying the accident progression and slowing the system response, due to the reduced core decay heat output as the core is first cooled by TDAFW operation. Each case was simulated for 20 hours.

Operation of the TDAFW system delays removed the core decay heat and delayed the onset of accident consequences significantly. The accident progression is again similar for all three cases, with the exception of hydrogen generation. In this accident scenario, significant hydrogen generation was still delayed a couple of hours for ATF cladding materials.

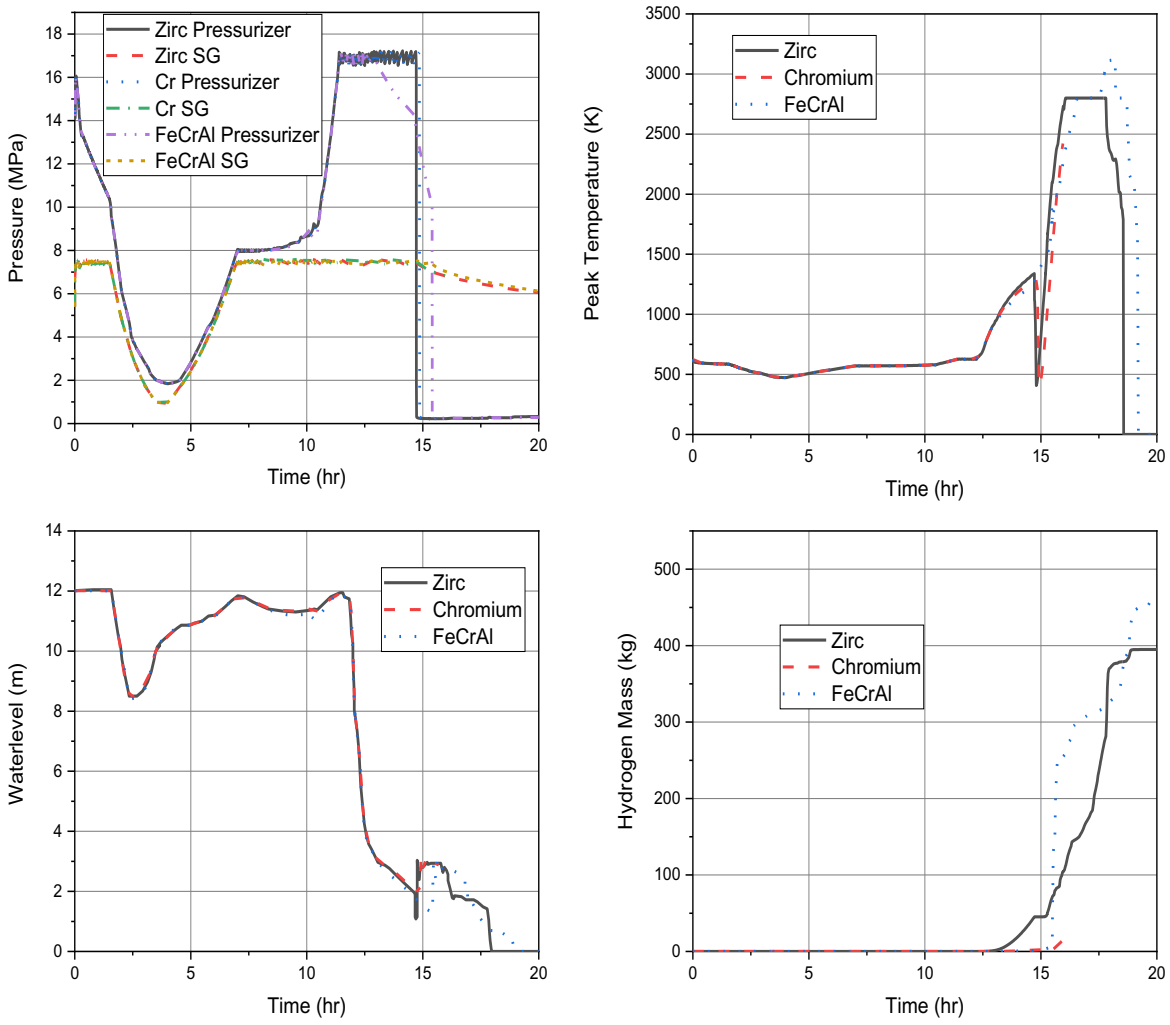

Figure 2-237. MELCOR thermal hydraulic outputs with three cladding options (SBO 1.0).

2.5.2.3 SBO-1.3

Similar to the SBO Case 1.0, the SBO Case 1.3 features extended AFW operation. In this case, the AFW functions for 8 hours. Once again accident consequences are delayed significantly. Hydrogen generation in all cases was delayed to nearly 20 hours, with ATF materials (FeCrAl and Cr-coated Zr) showing a delay of more than a couple of hours in hydrogen generation when compared against Zircaloy.

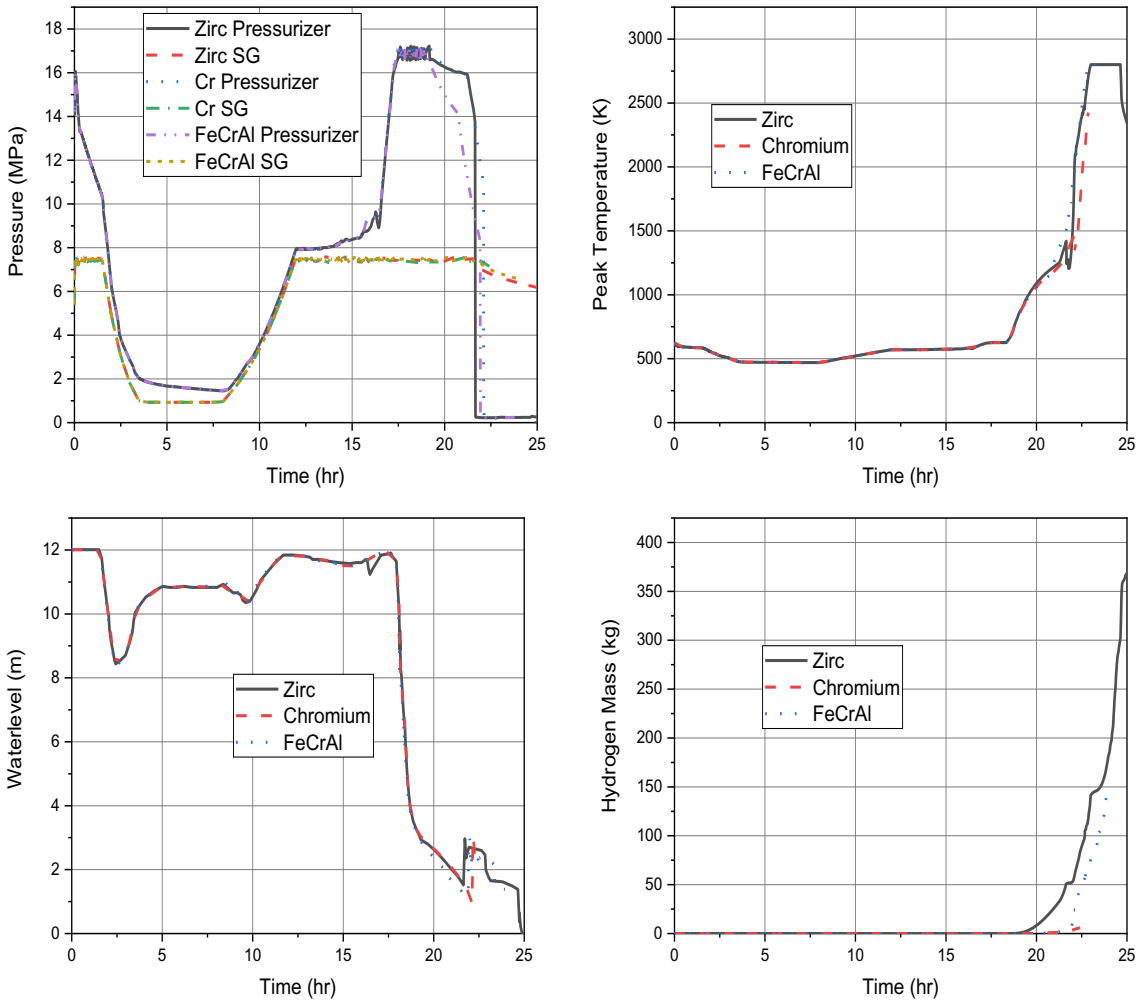

Figure 2-238. MELCOR thermal hydraulic outputs with three cladding options (SBO 1.3).

2.5.3 Comparison between RELAP5-3D and MELCOR Results

2.5.3.1 Comparison of Key Event Lists

To show differences between RELAP5-3D and MELCOR simulations, the key events for Zircaloy cladding are compared in Table 2-47.

Table 2-47. Key Event List Comparison between RELAP5-3D and MELCOR.

Event	SBO 1.0 (hr:min)		SBO 1.3 (hr:min)		SBO 7.0 (hr:min)	
	RELAP5-3D	MELCOR	RELAP5-3D	MELCOR	RELAP5-3D	MELCOR
Initiating event – LOOP and failure of the onsite emergency AC power systems	0:00	0:00	0:00	0:00	0:00	0:00
Reactor trip, MSIVs close, RCP seals initially leak at 21 gpm/pump (~1 kg/s)	0:00	0:00	0:00	0:00	00:00	0:00

TDAFW auto initiates at full flow	0:01	0:00	0:01	0:00	N/A	N/A
Operators control AFW to maintain level	0:15	0:15	0:15	0:15	N/A	N/A
First SG SRV opening	0:25	0:04	0:25	0:04	00:06	0:03
Operator performs controlled cooldown of secondary at ~100 F/hr (~55.5 C/hr)	1:30	1:30	1:30	1:30	N/A	N/A
Accumulators begin to inject	2:30	2:25	2:30	2:25	N/A	3:42
Secondary pressure reduced to ~0.9 MPa	3:40	3:46	3:40	3:46	N/A	N/A
DC batteries depleted	4:00	4:00	8:00	8:00	N/A	N/A
SG water depletion	8:16	10:22	12:57	16:14	1:06	1:20
System re-pressurize, pressurizer SRV opens	9:01	11:20	13:34	17:14	1:16	N/A
RPV water level decreases with core uncovery	9:30	12:16	14:28	18:24	1:53	2:19
Core Damage	10:32	15:58	15:40	22:44	2:34	4:58

2.5.3.2 Comparison of Different Scenarios for Zircaloy

SBO 7.0: The first MELCOR and RELAP5-3D comparison was made for the case SBO 7.0, which does not feature AFW injection or other active systems. The five parameters chosen for comparison include primary and secondary pressures, core peak temperature, reactor core water level, and hydrogen generation. For these comparisons, it should be noted that the MELCOR simulations were continued much further into the accident progression than for RELAP5-3D. It should also be noted that for the peak reactor core temperature, MELCOR provided both the peak debris and cladding temperature, which displays the maximum between these two parameters, while RELAP5-3D results provided peak cladding temperatures.

From Figure 2-239 it can be seen that MELCOR and RELAP5-3D produced different timing results for certain parameters; e.g., core water level. It is likely that there exists a difference in certain initial conditions that affects these results. In addition, the observed could also be due to differences between the system code models themselves. Based on the timing behavior of key events (SG water depletion and pressure, core water level), it is surmised that the differences exist in the initial SG inventory, SG heat transfer, as well as flow out of the safety relief valves. Such differences can likely lead to notable differences in the timing of core heatup, peak clad temperatures, and the start of rapid hydrogen generation, and so on. To be able to ascertain the root cause of the differences, more information on the RELAP5-3D results need to be acquired and analyzed.

SBO 1.0: As previously noted, SBO1.0 assumes that AFW is operable for 4 hours after accident initiation. The comparison of RELAP5-3D and MELCOR of SBO 1.0 are shown in Figure 2-240. The T-H parameter histories, including pressures, core water level, peak cladding temperature, and hydrogen mass were quite similar before 8 hours. This is because of the cooling from secondary side is still similar and the events are mostly affected by the accident assumptions. Following the 4-hour window of operability, the differences first arise in the system pressures and then core water inventory. This again leads to the surmise of differences in initial conditions and the system code model differences in flow from the safety relief valves and core and steam generator heat transfer.

SBO 1.3: This case is similar to SBO 1.0, except that AFW is operable for 8 hours. As shown in Figure 2-241, the events were also similar before 12 hours, when the secondary side can still provide cooling. After this point, RELAP5-3D and MELCOR simulation timing of events diverged for the same key parameters. RELAP5-3D predicted that key events (pressure rise, core water depletion) occurred two to three hours earlier than those predicted by MELCOR (see the event list in Table 2-47). Similar to the SBO 1.0 case, the SBO 1.3 case sees RELAP5-3D predicting core heatup and degradation earlier than in the simulation compared to MELCOR.

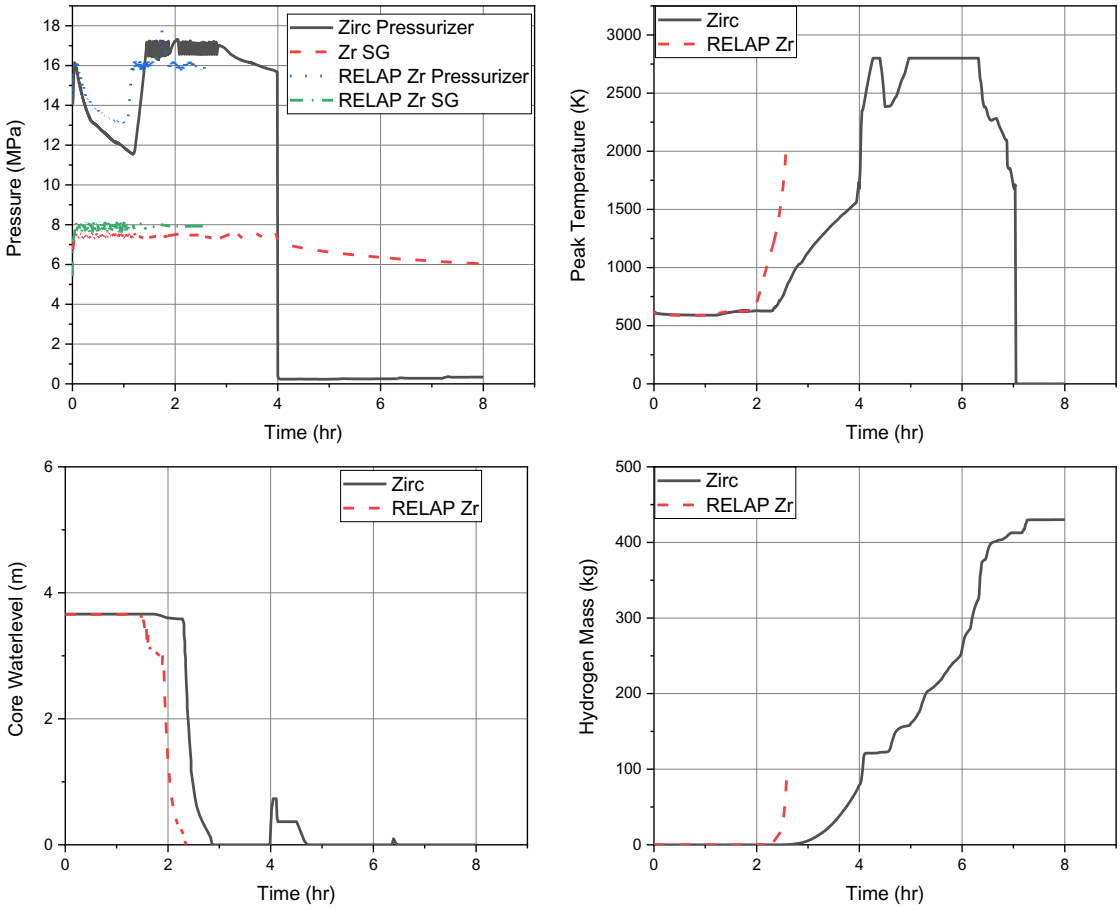

Figure 2-239. Comparison between RELAP5-3D and MELCOR – Zircaloy cladding (SBO 7.0).

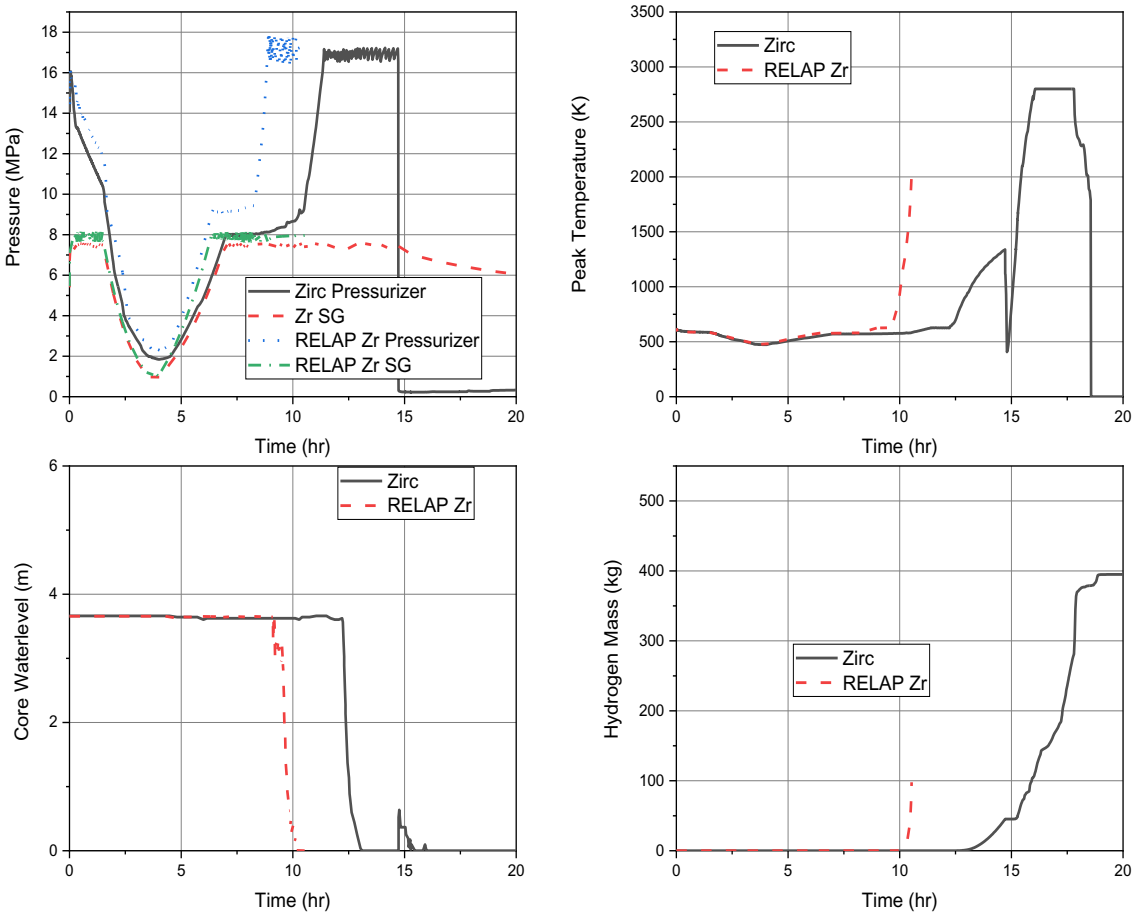

Figure 2-240. Comparison between RELAP5-3D and MELCOR – Zircaloy cladding (SBO 1.0).

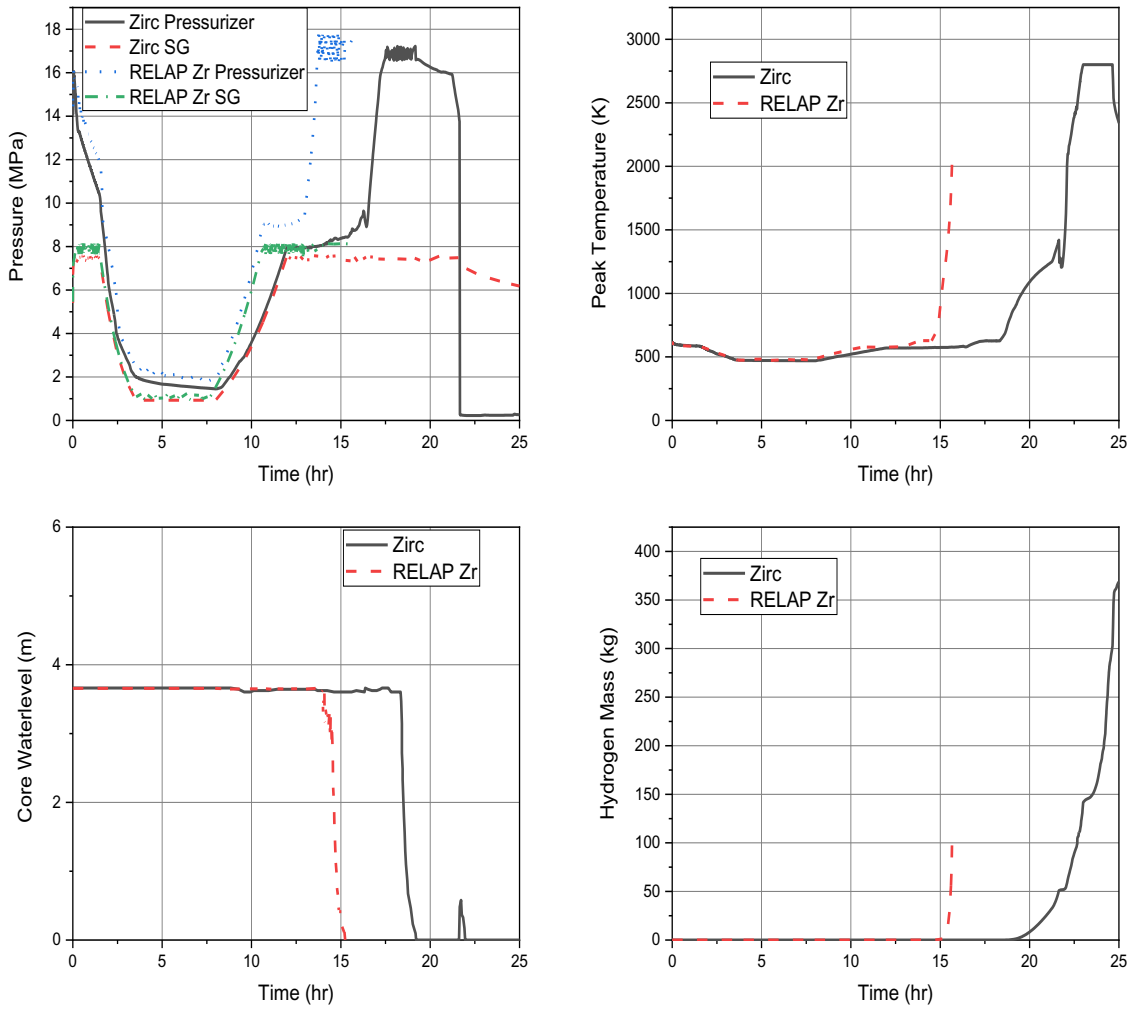

Figure 2-241. Comparison between RELAP5-3D and MELCOR – Zircaloy cladding (SBO 1.3).

2.5.3.3 Comparison of a Single Scenario for Three Cladding Designs

Finally, a comparison of the three cladding material options are compared between RELAP5-3D and MELCOR specifically for SBO 7.0. As expected, the histories of thermal hydraulic parameters, such as primary pressure, secondary-side pressure, core water level, and peak cladding temperature were initially similar but there are some differences, particularly in the timing of the core water level and the rate of hydrogen generation. The core water level in the RELAP simulations began to fall below the top of active fuel sooner, resulting in earlier hydrogen generation production. Since no safety systems operate, the rate of water loss from the safety relief valves in the primary system is likely different between the two codes. This needs to be investigated further, and seems to drive the later behavior.

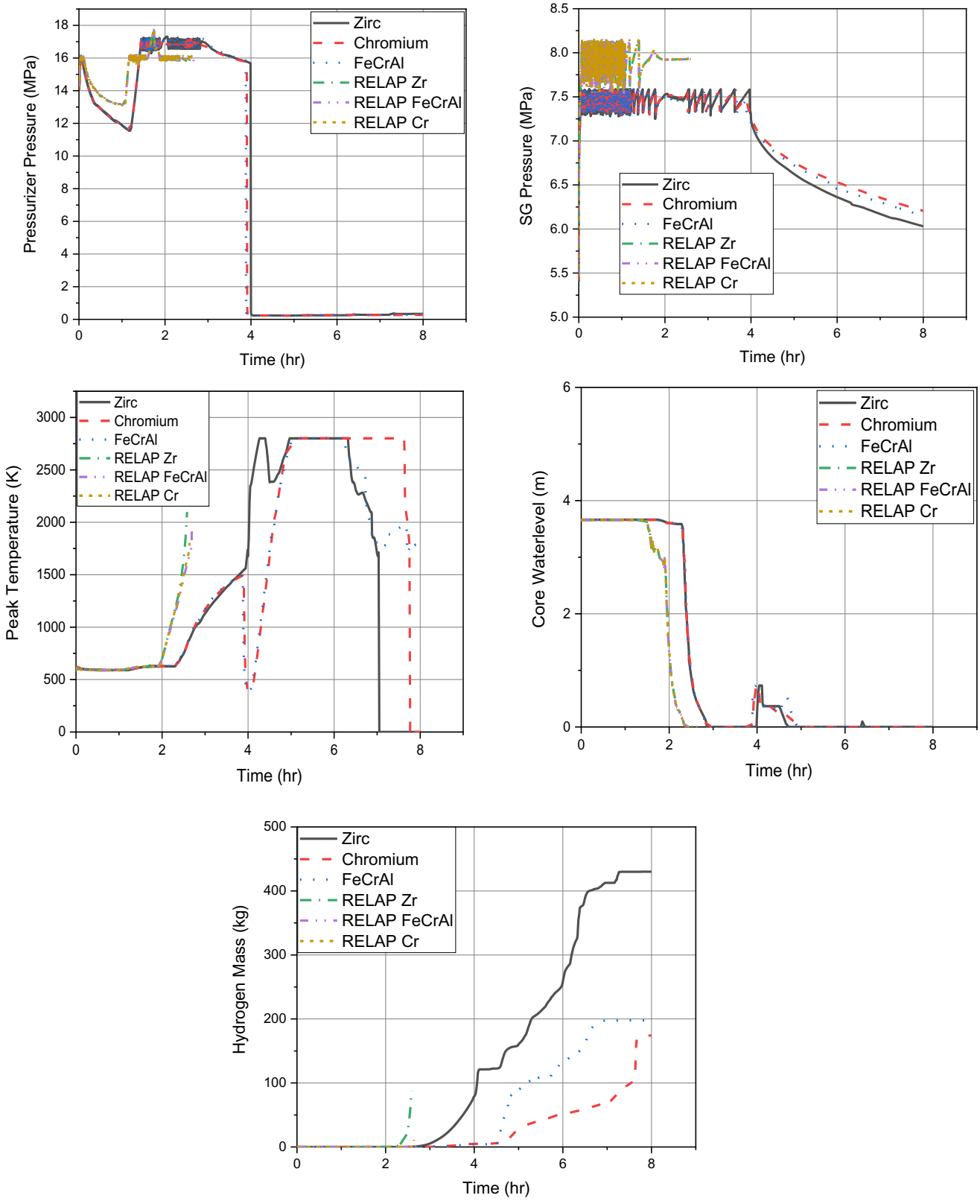

Figure 2-242. Comparison between RELAP5-3D and MELCOR – three cladding options (SBO 7.0).

2.5.3.4 Summary

The SBO cases of 1.0, 1.3, and 7.0 are simulated by MELCOR in order to compare to previous severe accident simulations using RELAP5-3D (Ma, et al., 2018). These simulations involved a sensitivity analysis of standard Zircaloy cladding compared to different ATF clad materials, i.e., FeCrAl cladding, and Cr-coated cladding. Certain cases are then directly compared with the simulation results using RELAP5-3D, to compare simulation results and help reveal particular model differences. When comparing these results, it is noted that there exist noticeable differences in timing of water depletion on the secondary-side of the SGs, as well as the associated depletion of the primary system core water inventory. These differences cause an earlier predicted temperature rise of the core clad temperatures and associated rapid hydrogen generation using RELAP5-3D. Further investigation and comparison of simulation results are needed to ascertain the source of these observed differences. The RELAP5-3D and MELCOR simulations need to be compared in more detail, specifically the SG initial water mass, the heat transfer models for the SG and core region, and the AFW injection rate and control logic as well as the coolant flow models for the relief valves when actuated for pressure control.

3. FLEX EVALUATION

This section presents the risk impact and benefit evaluation of FLEX. The evaluation is based on the same generic PWR plant SAPHIRE PRA model including the FLEX modeling as in INL/EXT-19-53556, but examines the risk impact and benefits of FLEX on NPPs from an additional perspective, i.e., the impact on significance determination process (SDP) results.

3.1 Overview of FLEX PRA

For reference purpose, this section provides a summary of the FLEX and its modeling in PRA as described in (Ma, et al., 2019).

After the Fukushima Dai-ichi nuclear accident, attentions have been drawn to prevention and mitigation capabilities of NPPs for beyond-design-basis external events (BDBEEs). Diverse and flexible coping strategies (FLEX) is proposed by the U.S. nuclear industry to enhance defense-in-depth (DID) for BDBEE scenarios and address concurrent extended loss of alternating power (ELAP) and loss of normal access to the ultimate heat sink (LUHS) (NEI, 2016).

Besides its designed functions, the FLEX implementation has a potential in bringing additional safety and economic benefits to NPP through risk reductions and a variety of risk-informed decision-making processes, e.g., SDP, notices of enforcement discretion (NOED) for allowed discretion time, risk-informed technical specifications (RITS) for increased limiting condition for operation (LCO), and categorization and treatment for structures, systems, and components. The risk-informed FLEX analysis under the ERP research intends to seek for and evaluate such benefits. The safety benefits through baseline risk reduction is presented in (Ma, et al., 2019), while this report intends to demonstrate the safety benefits through SDP.

As the basis for SDP analysis, the following paragraph in this section intends to summarize the FLEX PRA conducted for the generic PWR plant SAPHIRE PRA model, as well as the FLEX risk impact on the plant baseline CDF (i.e., the CDF estimated from all the IEs in the PRA model). More details of FLEX PRA can be found in (Ma, et al., 2019).

Two types of FLEX equipment (i.e., portable 480V AC diesel generator (DG) and SG makeup pump), and the associated human actions are credited in the PRA model by adding new top events into the existing LOOP/SBO event trees and developing fault trees for the newly-added top events. Three new top events are added, including FLEX-SBO-4 (operator failing to deploy FLEX equipment), FLEX-DGN-480 (whether the FLEX 480V DG could be functional), and FLEX-SGP (whether the SG makeup pump could provide secondary cooling to SG). Two redundant FLEX 480V DG trains and two redundant FLEX SG makeup pump trains are assumed. For these FLEX equipment, different failure modes (e.g., failure to start [FTS], and failure to run [FTR]), unavailability due to test and maintenance, and associated human actions are included in the PRA model.

Several topics related to FLEX PRA modeling still need further exploration, including FLEX equipment reliability data, FLEX common cause failure (CCF), and FLEX HRA. The assumptions made for the current FLEX PRA model are explained as follows:

FLEX reliability data: Assume that the FTS probability of portable FLEX equipment is 10 times the industry-average estimates for permanently-installed equipment; the FTS rate of portable FLEX equipment is assumed the same as the industry-average estimates for permanently-installed equipment.

FLEX CCF: Only the CCFs of the redundant portable FLEX equipment (e.g., two redundant FLEX SG pumps) are modeled; the CCFs of portable FLEX equipment and permanently-installed equipment are not modeled at this stage.

FLEX HRA: A scoping value of 0.1 is used as the human error probability (HEP) in the current model.

As indicated by the PRA quantification results, the implementation of FLEX could reduce the plant risk by 5.93E-7 per year, about 26% reduction of the LOOP CDF without FLEX (2.28E-6 per year).

3.2 FLEX Risk Impact – SDP Case

3.2.1 Overview of SDP

Compared to the analysis in Section 3.1, the analysis in this section also utilizes risk insights but examines the risk impacts and benefits of FLEX from another angle, i.e., how the FLEX implementation affects the SDP results and associated actions. The SDP is a risk-informed process, which assists the NRC staff in determining safety or security significance of inspection findings by assessing their impacts on plant risk (NRC, 2016). The SDP could provide inputs for another risk-informed process, i.e., Reactor Oversight Process (ROP), in which the NRC staff determine the appropriate responses to the inspection findings based on their safety or security significances (NRC, 2018). For an inspection finding, its safety or security significance is represented by one of four colors with qualitative descriptions and quantitative thresholds as shown in Table 3-1 (NRC, 2016) (NRC, 2018).

Table 3-1. SDP Color versus Safety Significance and NRC Action Matrix.

	Color			
	Green	**White**	**Yellow**	**Red**
Incremental Conditional Core Damage Probability (ICCDP)	≤1.0E-6	>1.0E-6 & ≤1.0E-5	>1.0E-5 & ≤ 1.0E-4	>1.0E-4
Safety Significance	Very low	Low to moderate	Substantial	High
NRC Action Matrix	Column I	Column II	Column III	Column IV
NRC Increased Oversight/Inspection	n/a	Special inspection	Augmented inspection	Incident investigation

Based on (NRC, 2016), the significance of an inspection finding (e.g., the unavailability of equipment as a degraded condition) can be calculated with ICCDP or Delta CDF annual, which are two different concepts with probability versus frequency but are equivalent to each other:

ICCDP = Delta CDF annual = (CDF new annual – CDF baseline annual).

CDF new annual = (CDF degradation * fraction of year of degradation exposure time) + (CDF baseline * fraction of year of non-degradation exposure time).

The CDF given the equipment in an unavailable state (denoted as "CDF degradation" in the above equations) is calculated with the equipment unavailable, while the calculation of the baseline CDF (denoted as "CDF baseline" in the above equations) considers the equipment as available.

3.2.2 FLEX SDP Analysis

This section provides a case study of FLEX SDP analysis. An emergency diesel generator (EDG), denoted as EDG-A, is assumed failed to start and being inoperable from May 10, 2019, 9:00 am, to May 19, 2019, 9:00 am, for nine days. In the baseline PRA model, the FTS probability of EDG-A is 2.86E-3; in the PRA model for estimating "CDF degradation," the EDG-A is set at a "failed" state. The FLEX SDP analysis results are shown in Table 3-2.

Table 3-2. FLEX SDP Analysis Results.

Metric	Without FLEX	With FLEX	ΔCDF (w/ – w/o FLEX)	ΔCDF% (ΔCDF/CDF baseline)
CDF baseline (per year)	3.12E-5	3.06E-5	-5.90E-7	-2.0%
CDF degradation (per year)	8.64E-5	6.86E-5	-1.78E-5	-21.0%
Duration (day)	9	9		
ICCDP	1.36E-6	9.38E-7		
SDP Color	White	Green		

Based on the results in Table 3-2, the maximum days of being inoperable to remain within SDP color zone thresholds are calculated and shown in Table 3-3.

Table 3-3. Max Days of Being Inoperable to Remain Within SDP Color Zone Thresholds (FLEX).

SDP Color Zone	Without FLEX	With FLEX	Delta
White	7	10	3
Yellow	66	96	30

As shown in Table 3-3, by implementing FLEX strategies, 3 additional days could be gained before crossing the white zone threshold (1E-6), and 30 additional days could be gained before crossing the yellow zone threshold (1E-5). Such gains could allow more time for plant staff to repair or replace the inoperable equipment and keep the safety significance of this degradation condition in a level as low as possible. The gains could lead to both safety and economic benefits: if not entering a more severe SDP color zone, the plant can be maintained at a safer state while substantial regulatory efforts and associated costs in inspection and investigation can be avoided.

4. PASSIVE COOLING SYSTEM EVALUATION

This section presents the risk impact and benefit evaluation of a passive cooling system, specifically the dynamic natural convection (DNC) system designed by DYNAC Systems. INL/EXT-19-53556 (Ma, et al., 2019) includes the RELAP5-3D analysis of the DNC system in selected SBO scenarios and the risk impact analysis of the DNC system on baseline risk of NPPs. This report examines the risk impacts and benefits of the DNC system from an additional perspective, i.e., the impact on SDP results.

4.1 Overview of DNC System PRA

As a basis for the DNC system SDP analysis, this section summarizes the DNC system design and PRA, and more details can be found in (Ma, et al., 2019).

As shown in Figure 4-1 (Ma, et al., 2019), the DNC system relies on a passive condensing jet ejector that generates a pumping action (pressure differential) via condensation of saturated steam through the ejector that subsequently draws secondary cooling water into the steam mixture downstream of the ejector nozzle. This results in a continuous return flow to the steam generator. The system takes steam from the main steam line and mixes it with cooling water from a heat exchanger (HX) in a passive jet ejector to supply water to the feedwater line of an SG. The passive jet ejector can generate sufficient head to cause natural circulation for mixed steam and water flow through the system. The HX is connected to a water pool or tank that contains water to remove decay heat for several days.

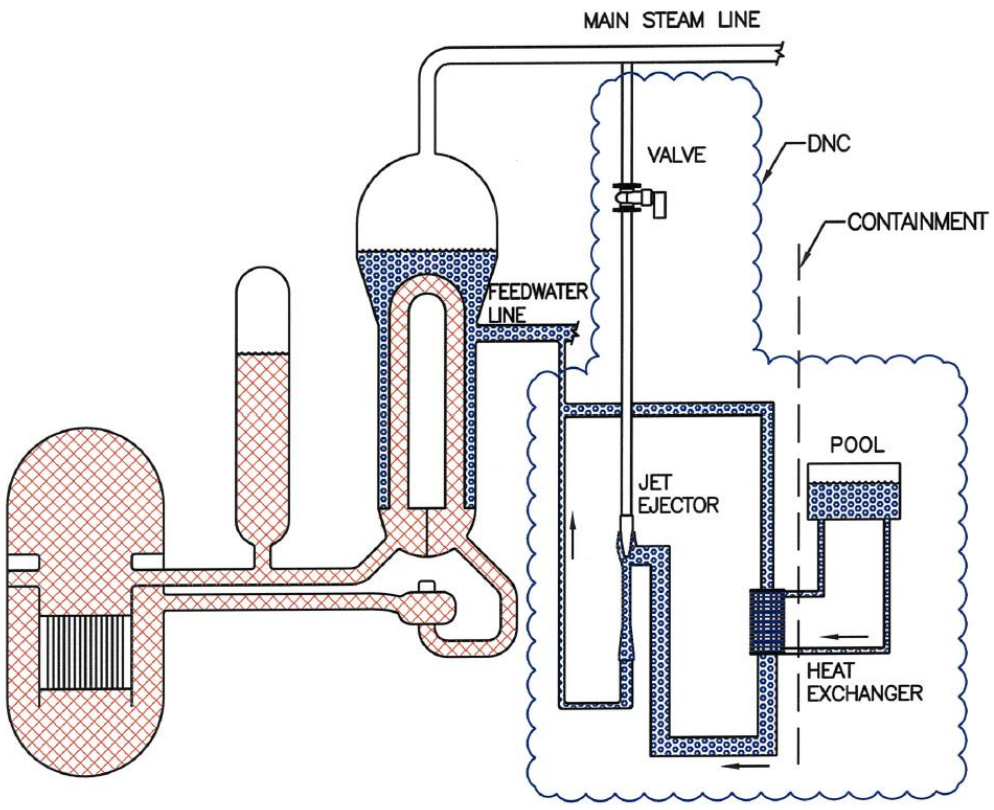

Figure 4-1. Schematic of the DNC system.

In the PRA, the DNC system is assumed to be able to replace AFW to provide secondary cooling safety function after an IE is occurred. The original AFW fault tree was revised to add the DNC system model, with a house event, DNC-HE, as the switch to turn on or off the DNC system in the PRA model with the benefit that event trees are not needed to change in order to incorporate the DNC. As a passive system, the DNC system has fewer failure modes with fewer components to be modeled, including DNC starting steam valves, heat exchangers, jet ejectors, and condensate tank. For these DNC equipment, different failure modes, unavailability due to test and maintenance, and common cause failures are included in the PRA model, using the latest nuclear industry-average parameter estimates (NRC, 2017).

As indicated by the PRA quantification results, the implementation of the DNC system could reduce the LOOP CDF from 2.28E-6 per year to 9.79E-7 per year (or about 57% reduction), and reduce plant total CDF from 3.17E-5 per year to 2.34E-5 per year (or about 25% reduction).

4.2 DNC System Risk Impact – SDP Case

The analysis in this section examines the risk impact of the DNC system through SDP analysis based on the calculation method introduced in Section 3.2.1 and the same SDP case for FLEX analysis. An emergency diesel generator (EDG), denoted as EDG-A, is assumed failed to start and being inoperable from May 10, 2019, 9:00 am, to May 19, 2019, 9:00 am, for nine days. In the baseline PRA model, the FTS probability of EDG-A is 2.86E-3; in the PRA model for estimating "CDF degradation," the EDG-A is set at a "failed" state. The DNC system SDP analysis results are shown in Table 4-1.

Table 4-1. DNC System SDP Analysis Results.

Metric	Without DNC	With DNC	ΔCDF (w/ – w/o DNC)	ΔCDF% (ΔCDF/CDF baseline)
CDF baseline (per year)[1]	3.12E-5	2.28E-5	-8.34E-6	-27.0%
CDF degradation (per year)	8.64E-5	4.51E-5	-4.13E-5	-48.0%
Duration (day)	9	9		
ICCDP	1.36E-6	5.48E-7		
SDP Color	White	Green		

Based on the results in Table 4-1, the maximum days of being inoperable to remain within SDP color zone thresholds are calculated and shown in Table 4-2.

Table 4-2. Max Days of Being Inoperable to Remain Within SDP Color Zone Thresholds (DNC).

SDP Color Zone	Without DNC	With DNC	Delta
White	7	16	10
Yellow	66	164	98

As shown in Table 4-2, by replacing the AFW with the DNC system, 10 additional days are gained before crossing the white zone threshold (1E-6), and 98 additional days are gained before crossing the yellow zone threshold (1E-5). Similar to the implications from the FLEX SDP results, such gains could lead to both safety and economic benefits, i.e., allowing more time for repair or replacement of the inoperable equipment, and avoiding the regulatory efforts in inspection and investigation as well as associated costs.

[1] The plant total CDF values in Table 4-1 (3.12E-5 without DNC and 2.28E-5 with DNC) are slightly different from those in INL/EXT-19-53556 and Section 4.1 (3.17E-5 without DNC and 2.34E-5 with DNC). The CDF values in this table represent the core damage end state quantification results by SAPHIRE, while the CDF values in INL/EXT-19-53556 and Section 4.1 are the sum of plant internal event tree CDFs from SAPHIRE. In general, core damage end state results would better reflect plant risk.

5. CONCLUSIONS AND FUTURE WORK

This report, along with report INL/EXT-19-53556 (Ma, et al., 2019) published in August 2019, documents the FY 2019 activities on ERP R&D. These activities continued the investigation of integrated evaluation approaches that combine the plant PRA models with multi-physics best estimate analyses and perform detailed risk and benefit assessments of ATF designs, FLEX, and passive cooling system designs for current nuclear power plants. These studies will help achieve both safety and operational performance enhancements.

Compared with (Ma, et al., 2019), this report is an "add-on" project report that includes additional accident scenarios for risk-informed ATF analysis, and examines the risk impacts of FLEX and passive cooling system on NPPs from additional perspectives. The same analysis process, risk analysis approaches, and analysis tools as in FY 2018 were used for near-term ATF cladding designs under the SBLOCA including SBLOCA with ATWS scenarios, two types of general transients (locked rotor and turbine trip) including locked rotor with ATWS scenarios, and MSLB scenarios.. Benchmark calculations for ATF analysis using RELAP5-3D and MELCOR are also presented. In addition, based on the generic probabilistic risk assessment (PRA) model, the risk impacts of FLEX and the DNC system on NPPs are evaluated through a risk-informed SDP.

In the ATF analysis under different accident scenarios, the RELAP5-3D simulation results show that there are various modest gains of coping time, or the delay of time to core damage due to the ATF designs. The risk benefits on behalf of the CDF brought by the ATF designs would be very small and they are not conducted in this analysis. However, the RELAP5-3D simulation results show a clear benefit in adopting ATFs with much less hydrogen produced at the time of core damage.

In the benchmark calculations between RELAP5-3D and MELCOR, it is noted that there exist noticeable differences in timing of water depletion on the secondary-side of the SGs, as well as the associated depletion of the primary system core water inventory. These differences cause an earlier predicted temperature rise of the core clad temperatures and associated rapid hydrogen generation using RELAP5-3D. Further investigation and comparison of simulation results are needed to ascertain the source of these observed differences. The RELAP5-3D and MELCOR simulations need to be compared in more detail, specifically the SG initial water mass, the heat transfer models for the SG and core region, and the AFW injection rate and control logic, as well as the coolant flow models for the relief valves when actuated for pressure control.

In the SDP case study for FLEX, the results show that 3 additional days could be gained before crossing the white zone threshold (1E-6), and 30 additional days could be gained before crossing the yellow zone threshold (1E-5). Such gains could allow more time for plant staff to repair or replace the inoperable equipment and keep the safety significance of this degradation condition in a level as low as possible. The gains could lead to both safety and economic benefits: if not entering a more severe SDP color zone, the plant can be maintained at a safer state while substantial regulatory efforts and associated costs in inspection and investigation can be avoided.

In the case study of the DNC system analysis, the results show that 10 additional days could be gained before crossing the white zone threshold (1E-6), and 98 additional days could be gained before crossing the yellow zone threshold (1E-5). Similar to the implications from the FLEX SDP results, such gains could lead to both safety and economic benefits, i.e., allowing more time for repair or replacement of the inoperable equipment, and avoiding the regulatory efforts in inspection and investigation as well as associated costs.

For future work, we recommend the following activities for the ERP research which are similar to those recommended in INL/EXT-19-53556 except the ATF industry collaboration work in the 2nd bullet:

- Develop generic BWR SAPHIRE Level 1 model and perform ERP risk analyses for selected boiling water reactor (BWR) accident scenarios
- Collaborate with the industry to provide necessary plant-specific ATF analysis in order to support implementation of ATF technology
- Continue to investigate approaches that could maximize the benefits from the industry investment of FLEX and collaborate with industry to conduct plant-specific FLEX analysis

- Collaborate with the industry to work on the FLEX HRA
- Collaborate with the industry to conduct plant-specific dynamic natural convection system analysis
- Investigate other passive cooling system designs including Terry turbine, and their impact on enhancing plant resilience.

6. REFERENCES

Dailey, R., Wang, J., & Corradini, M. 2019. "Benchmark calculations between RELAP5 and MELCOR."

Dominion. 2007. "Surry Power Station Units 1 and 2. Updated Final Safety Analysis Report. Rev. 39." Virginia Electric and Power Company (Dominion). Washington, DC: US NRC.

Fletcher, D., Bolander, M., Waterman, M., Burtt, J., Stitt, B., Kullberg, C., . . . Ogden, D. 1985. "Thermal-hydraulic analyses of pressurized thermal shock sequences for the H. B. Robinson Unit 2 Pressurizer Water Reactor." (NUREG/CR-3977).

Humphries, L., Beeny, B., Gelbard, F., Louie, D., & Phillips, J. 2017. "MELCOR Computer Code Manuals." Sandia National Laboratories.

Humrickhouse, P. W., & Merrill, B. J. 2018. "Modifications to MELCOR 1.8.6 for modeling accident tolerant fule in boiling water reactors." Idaho National Laboratory.

INL. 2018. "Light Water Reactor Sustainability Program Integrated Program Plan." Idaho National Laboratory.

Ma, Z., Parisi, C., Davis, C., Park, J., Boring, R., & Zhang, H. 2019. "Risk-Informed Analysis for an Enhanced Resilient PWR with ATF, FLEX, and Passive Cooling."

Ma, Z., Parisi, C., Zhang, H., Mandelli, D., Blakely, C., Yu, J., . . . Anderson, N. 2018. "Plant-Level Scenario-Based Risk Analysis for Enhanced Resilient PWR – SBO and LBLOCA." Idaho National Laboratory.

NEI. 2016. "Diverse and Flexible Coping Strategies (FLEX) Implementation Guide." NEI 12-06, Rev. 4.

NRC. 2011. "Confirmatory Thermal-hydraulic Analysis to Support Specific Success Criteria in the Standardized Plant Analysis Risk Models – Surry and Peach Bottom." NUREG-1953.

NRC. 2012. "State-of-the-Art Reactor Consequence Analyses Project / Volume 2: Surry Integrated Analysis." Nuclear Regulatory Commission.

NRC. 2016. "NRC Inspection Manual Chapter 0308 Attachment 3 - Significance Determination Process Technical Basis."

NRC. 2017. "Industry Average Parameter Estimates 2015 Update." Nuclear Regulatory Commission. Retrieved from Reactor Operational Experience Results and Databases. https://nrcoe.inl.gov/resultsdb/AvgPerf/

NRC. 2018. "NRC Inspection Manual, Chapter 0308 - Reactor Oversight Process Basis Document."

Parisi, C., Prescott, S. R., Szilard, R. H., Coleman, J. L., Spears, R. E., & Gupta, A. 2016. "Demonstration of External Hazards Analysis." Idaho National Laboratory.

RELAP5-3D Code Development Team. 2018. "RELAP5-3D Code Manual, Volume I." Idaho National Laboratory.

Smith, C. L., & Wood, S. T. 2011. Systems Analysis Programs for Hands-on Integrated Reliability Evaluations (SAPHIRE). Idaho National Laboratory. Idaho Falls: US NRC.

Tong, L. S. 1968. "An Evaluation of the Departure from Nucleate Boiling in Bundles of Reactor Fuel Rods." Nuclear Science and Engineering. 7-15.

Wang, J., Jo, H. J., & Corradini, M. L. 2018, October. "Potential recovery actions from a severe accident in PWR: MELCOR analysis of a station blackout scenario." Nuclear Technology, 204, 1-14.